UNIVERSITY OF OKLAHOMA

GRADUATE COLLEGE

PHOTOGRAMMETRIC SAND GRAINSIZE ANALYSIS OF A CIRCUMNAVIGATIONAL SAMPLING OF BEACHES OF THE BIG ISLAND OF HAWAII: POSSIBLE INSIGHT INTO CONTROLLING PROCESSES AND PROVENANCE

A THESIS

SUBMITTED TO THE GRADUATE FACULTY

in partial fulfillment of the requirements for the

Degree of

MASTER OF SCIENCE

By

Kurt Crandall

Norman, Oklahoma

2021

PHOTOGRAMMETRIC SAND GRAINSIZE ANALYSIS OF A CIRCUMNAVIGATIONAL SAMPLING OF BEACHES OF THE BIG ISLAND OF HAWAII: POSSIBLE INSIGHT INTO CONTROLLING PROCESSES AND PROVENANCE

A THESIS APPROVED FOR THE

SCHOOL OF GEOSCIENCES

BY THE COMMITTEE CONSISTING OF

Dr. John D. Pigott, Chair

Dr. Kulwadee L. Pigott

Dr. Shannon Dulin

Acknowledgements

I would first like to thank my wonderful committee, Kulwadee Pigott and Shannon Dulin for their expertise and guidance. I also would like to especially thank my advisor Dr. John Pigott for aiding and guiding me through my thesis research, providing me with an immensely interesting project and logistical help. I am especially grateful for his helpful nature and willingness to adapt and help me adapt in this unprecedented time of Covid. I'd also like to acknowledge and thank my wife Jennifer for motivating and supporting me in this endeavor.

Abstract

A circumnavigational photogrammetric sampling of the sands on the island of Hawai'I was done using the photogrammetry program pyDGS. The island of Hawai'i provides a perfect landscape to test the viability of pyDGS since it is a small island whose beaches are accessible, and which are subject to predictable weather and climate effects. A total of 18 beaches were chosen, taking photographs of transects at each beach. After calibrating standards and comparing them to the sands on Hawaii, this study found that pyDGS is a viable alternative to conventional grain-size analysis techniques, when correctly tuned and adjusted. Moreover, key findings conclude that weather and climate are driving factors in sand distribution, grain size, beach slope, sorting, skewness, and kurtosis on the island, with each statistical moment offering insight into weather and energy effects. Compositional and mineralogical data showed differences in sands throughout several beaches accounting for the large diversity of color ranging from black (basaltic) to green sand (volcanic) to tan (volcaniclastic-carbonate mixed) and white sands (carbonate). These compositional differences also affect grain size distributions, and several survey locations exhibiting bimodal distributions. To further test pyDGS, four photographs from Mars taken by the Curiosity Rover were applied and compared to previously published data.

Table of Contents

1 Introduction

1.1 Introduction

Grain size is widely known and accepted to be the principal and fundamental property of sediment textural analysis that governs entrainment, transport, and deposition thereby yielding more information such as genesis, climate controls, modes of transportation, energies, and more (Folk and Ward, 1957; Blott and Pye, 2001). Many sediment analysis techniques have been developed in order to better understand both fluvial and non-fluvial processes concerning and regarding grain size (Moberley et al., 1965; Cheng and Liu, 2015). Established analyses and techniques consist of both descriptive and quantitative or statistical approaches (Buscombe et al., 2010). Descriptive types of analysis are used to describe, distinguish, and categorize distinct sedimentary environments (Folk and Ward, 1957). Qualitative descriptors can include and range from transportation, age, composition, size, roundness, sorting, provenance, and response to external forces such as wind or water. Additionally, quantitative descriptors and parameters are employed to also understand and differentiate environments in a statistical manner and can often aid in the categorization and description of environment and grouping.

Descriptive methods account for controlling environmental factors that lead to physical attributes. In a seminal paper, Folk and Ward (1957) delineated principles and guidelines that have since broadly become standard methods in geology and sedimentology. Such descriptive qualities yield information that can be sorted and grouped into distinct environments. Sorting and roundness are characteristics that are optically described and interpreted to be of certain environments and transportation depending on what side of the spectrum they are on. Other characteristics such as composition and age can be tested through optical and mineralogical identifications or using instruments such as and XRF. These kinds of details can shed light onto source provenance and other important sedimentary process and environmental characterizations.

Widely accepted statistical methods usually employ some sort of numerical and mathematical analyses that can be applied to grains (Inman, 1952). Inman (1952) provided four statistical modes or moments that directly aid in quantifying grain size distribution, namely the four statistical moments: mean diameter, variance (standard deviation), skewness, and kurtosis. Size-frequency curves have often been used to group distributions, and those curves

become more symmetrical and readable when the logarithm of the diameter is plotted instead of the diameter alone (Inman, 1952; Blott and Pye, 2001). The conventionally accepted grouping of sand sediment size classes uses phi notation of Krumbien (1936) which calculates phi as $\phi = -\log_2$ of the diameter in millimeters. Then, after this logarithmic transform, mean diameter is taken as an overall average of size represented. Variance, or standard deviation, is a calculated value to measure dispersion in a distribution. It is calculated by obtaining one-half the distance between the 16th and 84th percentiles of a distribution (Inman, 1954; Krumbian, 1938).

$$Variance\ (standard\ deviation):\ \sigma_I = \frac{\phi_{84} - \phi_{16}}{2}$$

Skewness is the measurement of the asymmetry of a distribution or displacement of the median from the mean and is calculated using the 5th, 16th, 50th, 84th, and 95th percentiles. It can be graphically represented, normally categorized as neutral (without skew or lopsided tails), positive (tail on the right of the main body), or negative (tail on the left of the main body).

$$Skewness:\ SK_I = \frac{\phi_{16} + \phi_{84} - 2\phi_{50}}{2\,(\phi_{84} - \phi_{16})} + \frac{\phi_5 + \phi_{95} - 2\phi_{50}}{2\,(\phi_{95} - \phi_5)}$$

Kurtosis is a measurement of the "tails" in a distribution curve, or in other words relating to grain size analysis, is a comparison of main body sorting to the sorting in the tails (Folk and Ward, 1957). It is calculated using the 5th, 25th, 75th, and 95th percentiles. Descriptors, depending on the calculated value, range from mesokurtic (even distribution), leptokurtic (concentrated distribution), and platykurtic (broad distribution).

$$Kurtosis:\ K_G = \frac{\phi_{95} - \phi_5}{2.44\,(\phi_{75} - \phi_{25})}$$

The different statistical moments are calculable in nature and provide a mathematical analysis of the overall distribution that yield information for descriptors. These moments can be calculated graphically, but this process can be very laborious. Several computer programs have been created in order to calculate these moments more rapidly, such as the widely used and accepted GRADISTAT program developed and published by Blott and Pye (2001). This program calculates the moments arithmetically, geometrically, and logarithmically and provides descriptors for associated numerical values (Blott and Pye, 2001).

(a) Arithmetic method of moments

Mean	Standard deviation	Skewness	Kurtosis
$\bar{x}_a = \frac{\Sigma f m_m}{100}$	$\sigma_a = \sqrt{\frac{\Sigma f (m_m - \bar{x}_a)^2}{100}}$	$Sk_a = \frac{\Sigma f (m_m - \bar{x}_a)^3}{100\sigma_a{}^3}$	$K_a = \frac{\Sigma f (m_m - \bar{x}_a)^4}{100\sigma_a{}^4}$

(b) Geometric method of moments

Mean	Standard deviation	Skewness	Kurtosis
$\bar{x}_g = \exp \frac{\Sigma f \ln m_m}{100}$	$\sigma_g = \exp \sqrt{\frac{\Sigma f (\ln m_m - \ln \bar{x}_g)^2}{100}}$	$Sk_g = \frac{\Sigma f (\ln m_m - \ln \bar{x}_g)^3}{100 \ln \sigma_g{}^3}$	$K_g = \frac{\Sigma f (\ln m_m - \ln \bar{x}_g)^4}{100 \ln \sigma_g{}^4}$

(c) Logarithmic method of moments

Mean	Standard deviation	Skewness	Kurtosis
$\bar{x}_\phi = \frac{\Sigma f m_\phi}{100}$	$\sigma_\phi = \sqrt{\frac{\Sigma f (m_\phi - \bar{x}_\phi)^2}{100}}$	$Sk_\phi = \frac{\Sigma f (m_\phi - \bar{x}_\phi)^3}{100\sigma_\phi{}^3}$	$K_\phi = \frac{\Sigma f (m_\phi - \bar{x}_\phi)^4}{100\sigma_\phi^4}$

(d) Logarithmic (original) Folk and Ward (1957) graphical measures

Mean	Standard deviation	Skewness	Kurtosis
$M_Z = \frac{\phi_{16} + \phi_{50} + \phi_{84}}{3}$	$\sigma_I = \frac{\phi_{84} - \phi_{16}}{4} + \frac{\phi_{95} - \phi_5}{6{\cdot}6}$	$Sk_I = \frac{\phi_{16} + \phi_{84} - 2\phi_{50}}{2(\phi_{84} - \phi_{16})} + \frac{\phi_5 + \phi_{95} - 2\phi_{50}}{2(\phi_{95} - \phi_5)}$	$K_G = \frac{\phi_{95} - \phi_5}{2{\cdot}44(\phi_{75} - \phi_{25})}$

(e) Geometric (modified) Folk and Ward (1957) graphical measures

Mean	Standard deviation
$M_G = \exp \frac{\ln P_{16} + \ln P_{50} + \ln P_{84}}{3}$	$\sigma_G = \exp \left(\frac{\ln P_{16} - \ln P_{84}}{4} + \frac{\ln P_5 - \ln P_{95}}{6{\cdot}6} \right)$

Skewness	Kurtosis
$Sk_G = \frac{\ln P_{16} + \ln P_{84} - 2(\ln P_{50})}{2(\ln P_{84} - \ln P_{16})} + \frac{\ln P_5 + \ln P_{95} - 2(\ln P_{50})}{2(\ln P_{25} - \ln P_5)}$	$K_G = \frac{\ln P_5 - \ln P_{95}}{2{\cdot}44(\ln P_{25} - \ln P_{75})}$

Table 1.1.1: The formulae for the statistical moments including arithmetic (a), geometric (b), logarithmic (c) and also the Folk and Ward (1957) adjusted calculations for logarithmic (d) and geometric (e). *f* is the frequency in percent, *m* is the mid-point of each interval in metric (m_m) or phi (m_φ) units, P_x and φ_x are grain diameters in metric or phi units, and *x* is the cumulative percentile values. Table modified and adjusted from Blott and Pye (2001).

Folk and Ward (1957) have provided tweaked calculations for both the geometric and logarithmic methods of each moment to help when relating the statistical moments to sedimentology. All five of these equations can be seen in *Table 1.1.1*. In geology, the Folk and Ward (1957) equations are mainly used and will be employed in this study for comparison. The

results for sorting, skewness, and kurtosis can then be classified or described based on their value. The terms or descriptors were coined by Folk and Ward (1957) and can be seen in *Table 1.1.2*. In order to carry out a calculation of moments, an entire distribution, meaning the spread between the start and finish points, must be known (Blott and Pye, 2001).

Sorting (σ_1)		Skewness (Sk_1)		Kurtosis (K_G)	
Very well sorted	<0·35	Very fine skewed	$^{+}$0·3 to $^{+}$1·0	Very platykurtic	<0·67
Well sorted	0·35–0·50	Fine skewed	$^{+}$0·1 to $^{+}$0·3	Platykurtic	0·67–0·90
Moderately well sorted	0·50–0·70	Symmetrical	$^{+}$0·1 to $^{-}$0·1	Mesokurtic	0·90–1·11
Moderately sorted	0·70–1·00	Coarse skewed	$^{-}$0·1 to $^{-}$0·3	Leptokurtic	1·11–1·50
Poorly sorted	1·00–2·00	Very coarse skewed	$^{-}$0·3 to $^{-}$1·0	Very leptokurtic	1·50–3·00
Very poorly sorted	2·00–4·00			Extremely leptokurtic	>3·00
Extremely poorly sorted	>4·00				

Table 1.1.2: Descriptors from Folk and Ward (1957) for the calculated moments. Table adapted from Blott and Pye (2001).

A complete analysis on samples should include both a descriptive and statistical approach. Since sand or grains can occur in a variety of different sources such as aqueous or subaerial dunes, riverbeds, or in this case, beaches, different techniques and reasons for analysis exist; however, most conventional processes can be demanding and time consuming, usually including sample extraction, laboratory sieving and sorting, and manual calculations and classification.

Although several methods have been developed to analyze grains and beds in-situ (Wolman, 1954; Fehr, 1987), these processes are still time consuming, require many measurements and manual calculations, and can be very robust and inaccurate. Moreover, many conventional techniques require sample extraction, which may not always be feasible or realistic given remote locations, dangerous or aqueous environments, or sheer quantity needed for a thorough study. New and emerging techniques have been developed and are currently being revised and refined in order to do a grain size analysis more quickly with better precision and less of a hassle.

One such technique is called photogrammetry. Photogrammetry is simply, by definition, making measurements by using photographs (Landen, 1959). This method has many applications ranging from large scale mapping to microscale environment analysis. On a grainsize scale, several software and procedures have been created for a variety of

environments such as riverbeds (Rüther et al., 2013) to smaller, non-cohesive, sand-size grains (Buscombe, 2013; Cheng and Liu, 2015) and even to cemented sandstones of a tsunamiite (Moreland, et al, 2019).

Buscombe et al. (2010) classifies two categories of photogrammetry: geometrical and statistical. Geometrical calculations and methodology use segmentation thereby isolating and measuring visible grains. These methods assume and need void spaces in between grains to calculate grain edges, which can cause problems for real-world and in-situ photographs where grains are overlapping and stacked. Statistical methods are more sensitive to texture, and some methods employ a spatial autocorrelation (Rubin, 2004). In other words, these types of methods, according to Rubin (2004), correlate the intensity of the pixels with each other, or the observed values with the predicted values. The main downfall of these types of methods is that they require calibration and therefore each method needs to be correlated to its specific site.

Since neither the geometrical nor statistical methods are completely satisfactory on their own, Buscombe (2013) proposes a duality approach, meaning a combination of the two. This type of method would look at both discrete individual grains as well as continuous features and textures. Such a methodology would employ a continuous wavelet transform looking at both a spatial and spectral resolution. This means that a continuous wavelet transform application would assess or divide an image into variance or energy per pixel while also providing and delineating grain boundaries based off those peaks and troughs or differing intensities. Such a method requires little to no calibration therefore rendering it universal in its applications and capabilities.

The grainsize analysis photogrammetry method outlined by Buscombe et al. (2010) and refined by Buscombe and Rubin (2012b) and Buscombe (2013) requires high resolution imagery, where the smallest grain is represented by at least several pixels. These images should have more than 1000 distinguishable grains. Additionally, converting the image to an 8-bit grayscale ensures higher accuracy as it helps translate the varying degrees of energy in each pixel to one common spectrum. Buscombe (2013) has developed both a MATLAB and Python code for his method and has named this program pyDGS.

Through pyDGS, one can input pictures and yield the geometric statistical moments through photogrammetric analysis. Buscome (2010) employs the Folk and Ward (1957) geometric statistical analysis, which is the most accepted and thoroughly applicable method for a sedimentological study. These outcomes can be compared to standards or real sieved samples to ensure accuracy, and the program can thereafter be tweaked in order to insure preciseness.

1.2 Study Area: The Island of Hawaii

The Hawaiian Islands are part of the 6000-kilometer-long Hawaiian-Emperor archipelago comprised of large shield volcanoes protruding out of the Pacific Ocean and include over 100 major volcanoes (Macdonald and Abbott, 1983; Walker, 1990). The source for the island creations is a mantle-sourced hotspot that continues in place as the overlying lithosphere moves due to tectonic activity (Macdonald and Abbott, 1983). The oldest and earliest known creation from the hotspot is a sea mount dated to be around 80 ma (Walker, 1990) and the youngest volcano is on the island of Hawai'i, also known as the "Big Island", and is still on-again off-again active with the ongoing eruption that started up again in early 2021. The "Big Island" flows are of both of a Pahoehoe (smooth and ropy) and A'a (rough and rubbly) variety offering a combination of both surfaces throughout the island and is composed mainly mafic minerals such as olivine and pyroxenes (Macdonald and Abbott, 1983; Walker, 1990).

The island of Hawaii is made up of five shield volcanoes, namely Kilauea, Mauna Loa, Mauna Kea, Hualalai, and Kohala (*Figure 1.2.1*). Because of the shear thickness of the volcanoes and extensive subsidence, it is unclear when exactly the island of Hawai'i began forming, but some estimates and K-Ar dating have been done showing ages of at least the oldest exposed flows. Kilauea is the youngest and is currently erupting into the South-Eastern part of the island. The oldest dates for eruptions from this volcano date to around 0.1 ma (Clague and Darymple, 1987). Mauna Loa is the largest on the island and the oldest dated eruption puts it at 0.54 ma (Clague and Darymple, 1987). The oldest flow from the Western-most volcano Hualalai has been dated to 0.4 ma and the oldest flow from the Northern most volcano Kohala has been dated to 0.43 ma (Clague and Darymple, 1987). The second largest volcano on the island Mauna Kea has the oldest dated flow being around 0.6 ma, though the oldest volcano on the island is

actually thought to be Kohala. Despite the age, each volcano has had at least one eruption within the last 4000 years with the exception of Kohala, whose last eruption was 60,000 years ago.

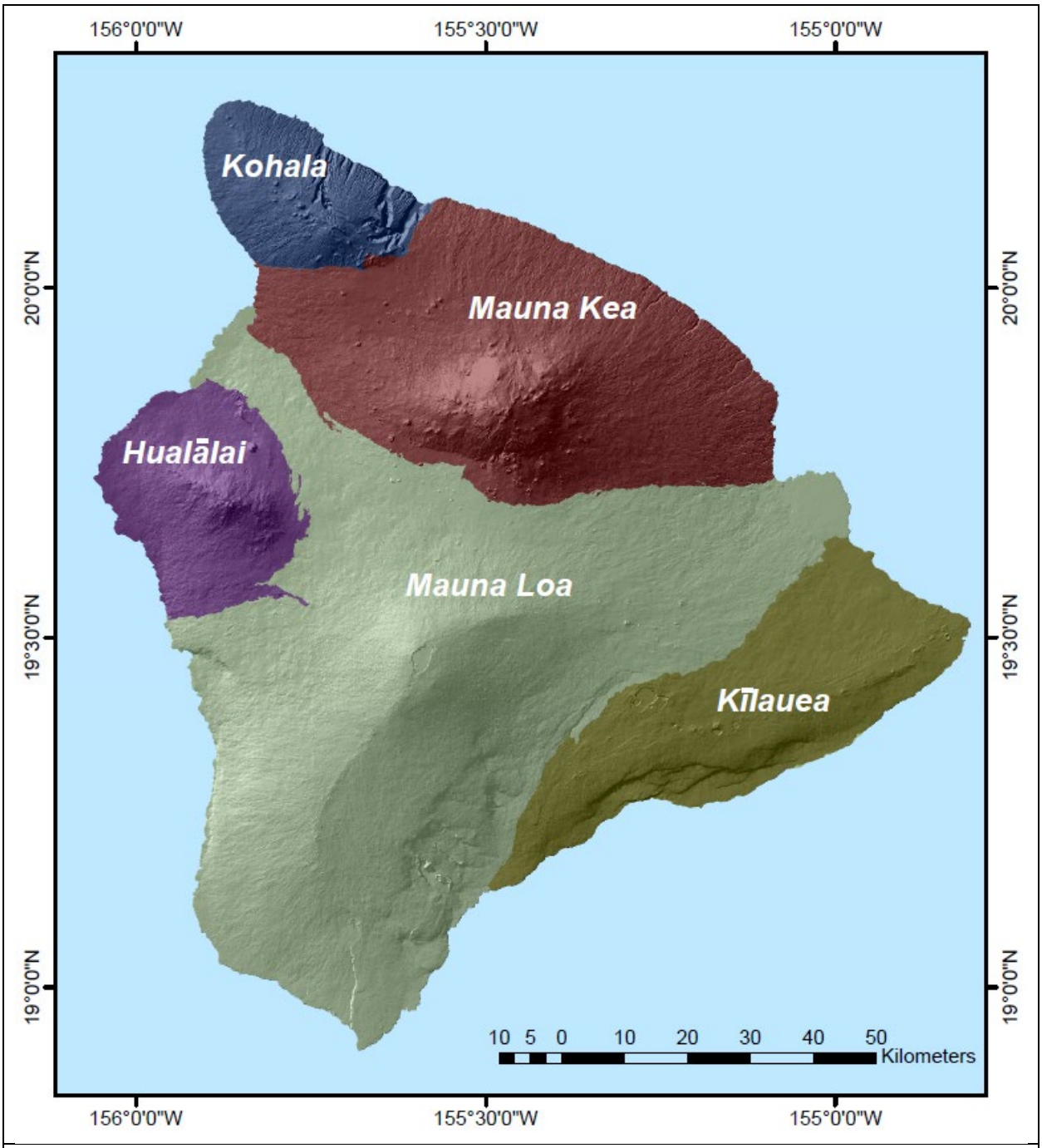

Figure 1.2.1: A map of the Island of Hawaii showing the five different volcanoes and the extent of their lava flows. (Richmond et al., 2008).

The island of Hawaii is still regularly active with ongoing and recurring eruptions, the most recent of which started again in late 2020. Despite the large size of the island and height of the tall volcano mountains, the island itself is estimated to have subsided a total of 1.2 km at a rate of about 2.6mm/year over the last 450,000 years (Richmond et. al, 2008; Zhong and Watts, 2002). Because of the active island creation happening and the relatively young age of the island, it is always undergoing isostatic adjustment and tectonic subsidence. Under the immense weight of the large shield volcanoes on top of oceanic crust, some estimates put subsidence from 2 km to 6 km (Moberly and McCoy, 1966). Many fault scarps within the volcanic deposits as well as submarine landslides and offshore terraces are continually growing.

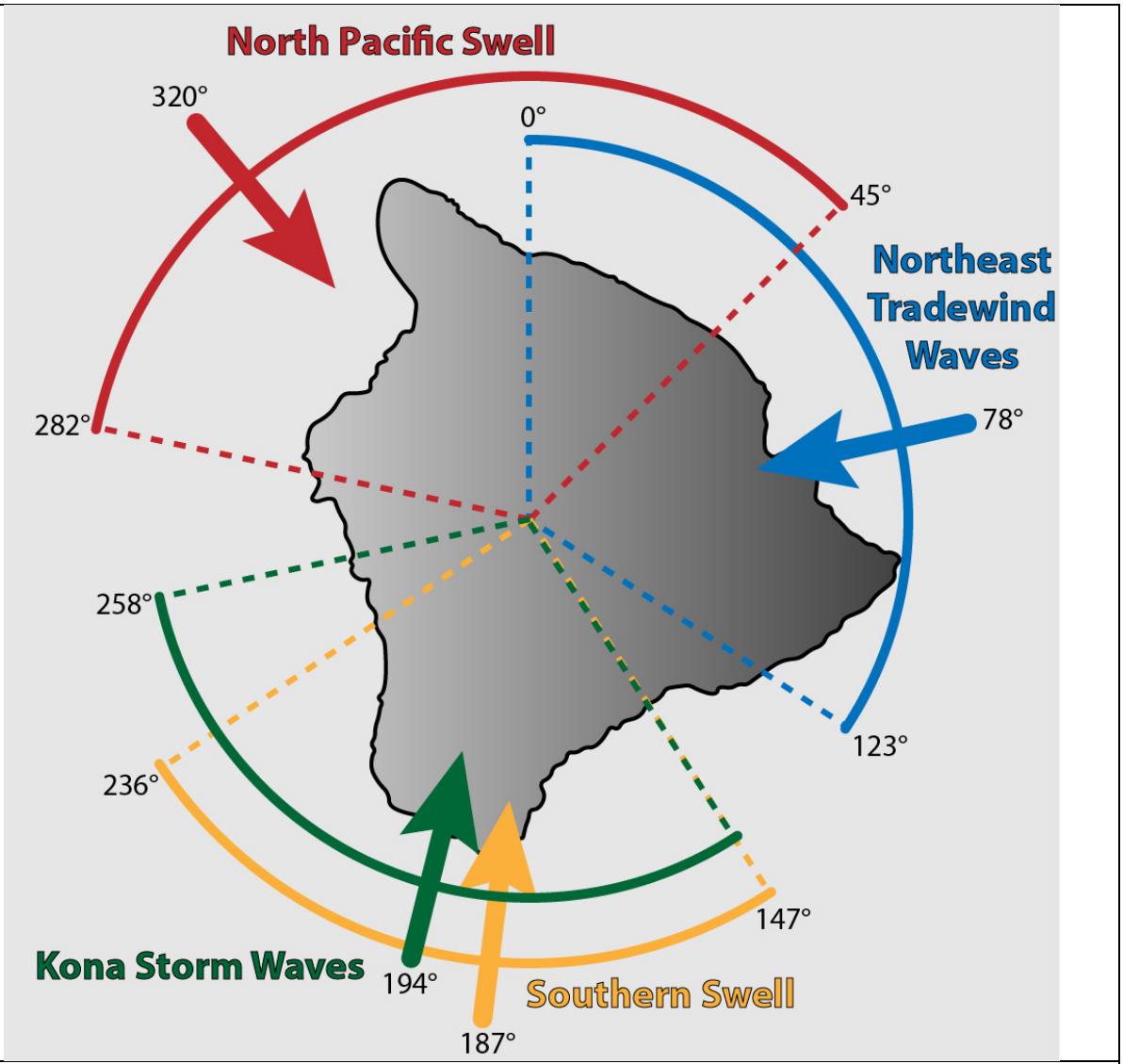

Figure 1.2.2: A diagram (adapted from Moberly and Chamberlain, 1964) showing the island of Hawaii and the predominant wave energy regime.

Additionally, seasonal weather and currents play a role in erosion and the everchanging landscape of the island. The island of Hawai'i is the last and South-Easternmost Island in the archipelago and thereby is subject to frequent and generally predictable Northern Pacific and Southern swells as well as local storms (Moberly et al., 1965) (*Figure 1.2.2*). The North Pacific Swell occurs throughout the year but is strongest normally from October through May. Some of the largest waves in Hawaii are caused by the North Pacific Swell, ranging in height from about 2.7 m – 6 m with a period of 10 sec – 15 sec (Richmond et. al, 2008). The Northeast Trade Winds occur throughout the year but are strongest from April through November. They create waves by the trade winds blowing on the open ocean, generating wave heights of about 1.3 m – 4 m with periods of 5 sec – 8 sec (Richmond et. al, 2008). The Southern Swell is generated in the southern and Indian oceans throughout the year, but largest during the months of April through October. The swell can generate waves of about 0.3 m – 1.3 m with periods ranging from 14 sec – 22 sec (Richmond et. al, 2008). The Kona Storm waves are inconsistent, usually occurring during the winter and are generated by local fronts or extra-tropical lows. These waves generally are 3.3 m – 5 m with periods of 8 sec – 10 sec (Richmond et. al, 2008).

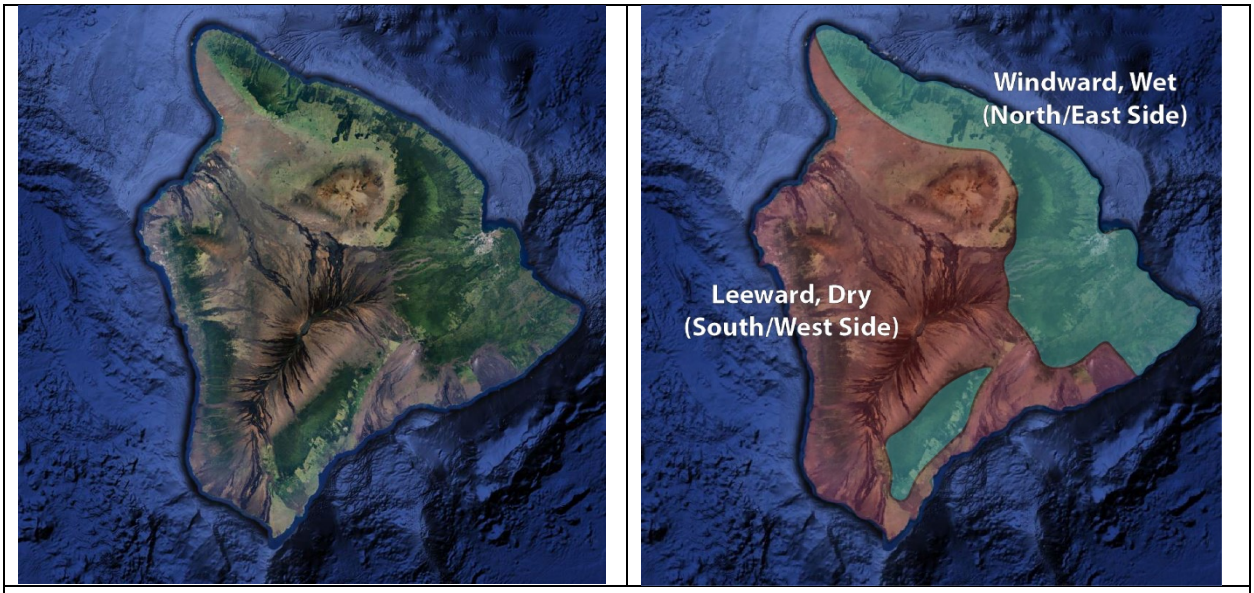

Figure 1.2.3: (*left*) The unlabeled island of Hawaii and (*right*) a labelled picture showing the windward and leeward sides of the island where rainfall greatly varies; as can be seen by the relative density of vegetation cover in the left image.

Moreover, there is a distinct difference in erosion and rates of erosion between the wet, windward side (North/East side) of the island and the dry, leeward side (South/West side) of the island (*Figure 1.2.3*) (Richmond et. al, 2008). The wetter, North/East side (and a pocket in

the South) of the island can, on average, receive up to 300 inches of rain annually (range: about 100 inches – 300 inches) and therefore is much more subject to higher rates of erosion manifested by the presence of large canyons and rivers (*Figure 1.2.4*) (Frazier et. al, 2016). As opposed to windward side, the leeward side is the dry side of the island where drier conditions account for lower amounts of rain (range: about 8 inches – 80 inches) and lower rates of erosion (*Figure 1.2.4*) (Richmond et. al, 2008; Frazier et. al, 2016). The island of Hawai'i is different than the other islands because it has active volcanism, and as such, local weathering and beach position within a weathering epicenter play a larger role in the sorting of grains. Also, unlike the other islands, the "Big Island" has most reefs and widest beaches located on the Southern and Eastern side of the island. Beach morphology on the "Big Island" is largely controlled by lava flow morphology. It is also important to note that Hawai'i has in the past and can be in the future affected by tsunamis. Several tsunamis within the last century have deeply affected beach morphology and the geologic record (Chagué et al., 2018).

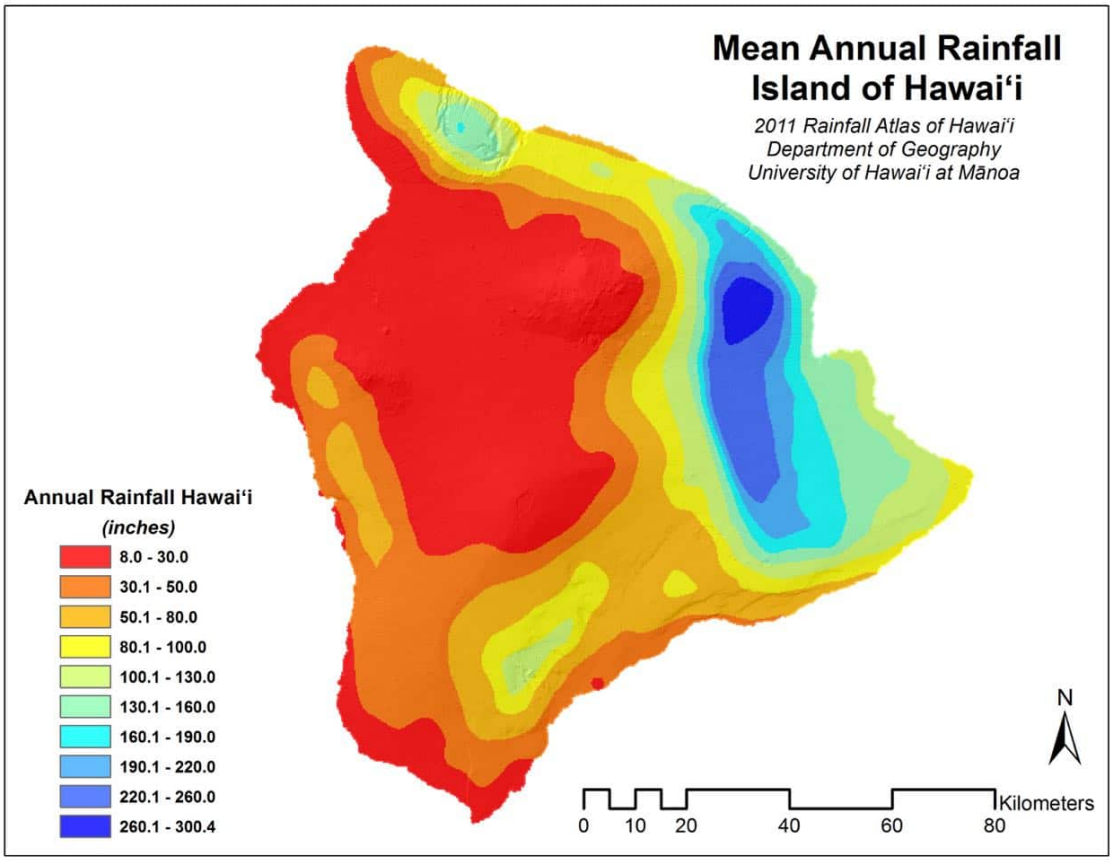

Figure 1.2.4: Mean annual rainfall on the Island of Hawaii (Figure from Frazier et al., 2016).

Over the history of the island, sea level has affected island morphology and subsequent beach creation and erosion. During the mid to late Holocene there was a high stand and low stand sea level, being +1m – 2 m and -1 m – 2 m current sea level. Geologic records show coastal planes regressing in several spots on the Island of Kauai showing a migrating sea level (Calhoun and Fletcher, 1995). Moreover, several radiocarbon dates have been analyzed of ancient berms from a high standing sea-level during the mid to late Holocene (Harney et al., 2000). Nonetheless, sea-level and rate of sea-level rise or subsidence can affect greatly many factors of a beach including morphology, grainsize, and sorting (see *Figure 1.2.5* for typical beach morphology).

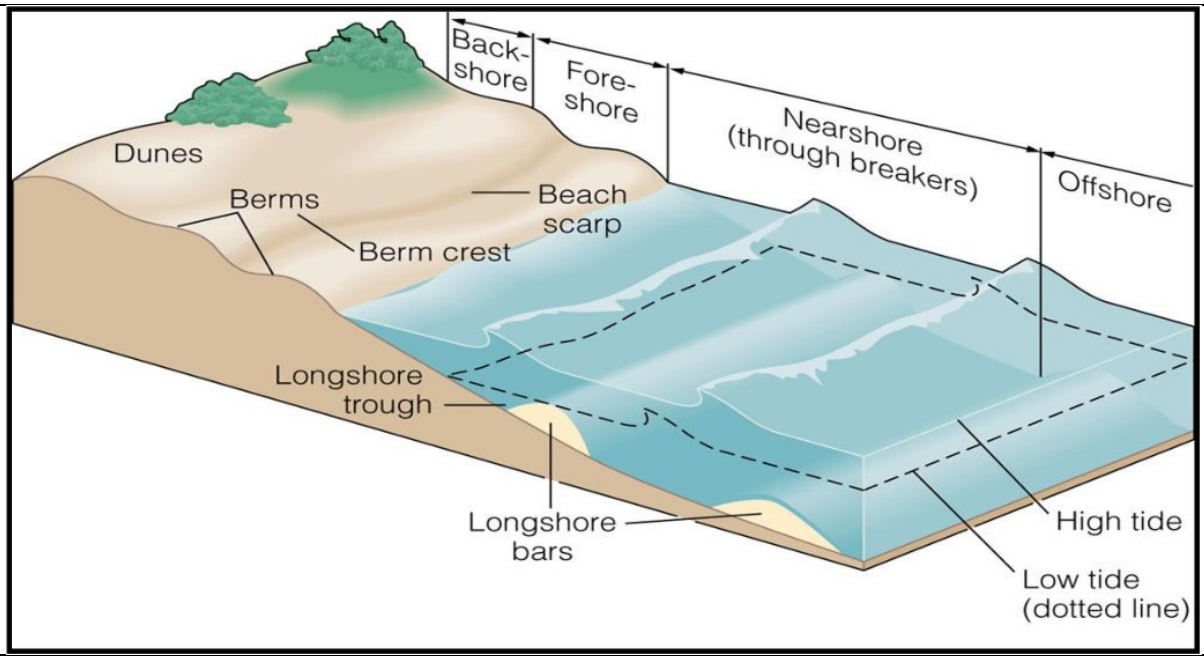

Figure 1.2.5: A schematic of typical beach morphology (Fadil, 2018).

Sand and the creation of sand in Hawaii are largely based on environmental factors and proximity to active volcanism. Because the Island of Hawai'i is still active, it can be assumed that the beaches are also relatively young. Moberly and Chamberlin (1964) estimated that some organic, detrital beaches on the island of Oahu have a turn-over rate of about 50 – 100 years, however, more recent studies and dating of organic grains show an actual turnover rate to be about 1500 years at those same beaches (Resig, 2004). That being said, other radiocarbon studies have dated other beaches on Oahu as being around 5000 years old (Harney et al., 2000). In contrast, other carbonate or white/tan beaches are known to have higher turnover

rates. For example, Magic Sands beach on the Island of Hawai'i is known to periodically gain and lose its sand entirely. During high surf times, usually during the winter and other storm seasons, the beach can lose all of its sand within a day or two (Clark, 1985). Normal wave action will then replenish the beach sand within a few months following the storm or high surf (Clark, 1985).

Beaches in the Hawaiian Islands are in fact very dynamic and continuously changing. Some studies have shown beach erosion occurring as fast as 1.28m/yr (Campbell and Hwang, 1982). Intuitively, beaches are also growing in many parts of the Hawaiian Islands. For comparison, some studies have shown that certain beaches on is island of Oahu grow at 0.5m/yr, with small fluctuations throughout the year reacting to seasons and storms (Norcross et al., 2002). The behavior observed in this study showed that longshore rather than cross-shore transport is more important in long-term time (Norcross et al., 2002). Mainly, sand transport and beach sand morphology and accumulation were seen to depend on topography of respective offshore reefs. Topography may provide important context in learning and understanding how beaches throughout the Hawaiian Islands react and are created.

The earliest studies and extensive sampling of Hawaiian beaches began in the 1960s (Moberly et al., 1965; Moberly and Chamberlain, 1964). These studies found that Hawaiian littoral sand, or swash zone to beach sand, was generally comprised of detrital basaltic and organic grains. The relative abundance within the mixture depends on the proximity to active volcanism and weathering as well as location and setting of organic growth namely coral reefs (Moberly et al., 1965). On the island of Hawaii, the sand ranges from white and brown organic grains to black and green olivine/pyroxene grains. This accounts for white sand, black sand, grey sand, brown sand, and even green sand beaches. Moreover, there is a range of grain size from detritus-like particles to large boulders.

Relative to the other islands in general, coral reefs are absent on the island (Richmond et al., 2008). This is mainly due to the active volcanism and local sea-level rise (Richmond et al., 2008). Also, because the Hawaiian Islands are isolated within the Pacific Ocean, the reefs have a low species diversity comparatively with other reefs around the world (Fletcher et al., 2008). Main reef builders and biological components on the Hawaiian Islands generally are *Porites*

(species *lobata* and *compressa*), *Montipora* (species *patula* and *capitula*), *Porolithon* (species *gardineri*), *Hydrolithon* (species *onkods*), as well as *Halimeda* (species *discoidea* and *incrassate*) and other minor builders (Fletcher et al., 2008). Where there are reefs and beaches found together, there are carbonate sands. Studies on other beaches on different Hawaiian Islands such as Oahu have found similar biological components to those found on the Big Island (Harney et al., 1999).

The island of Hawaii provides an optimal setting for a photogrammetric grain-size study because of its relatively young age, large size, and diverse compositional beaches throughout all sides of the island due to active volcanic activity and low latitudinal location. Although some may know the "Big Island" as being the island without beaches, this simply is not true. According to Moberly and Chamberlain (1964), the island of Hawaii has an estimated 1,300,000 m3 of beach-sand reservoir and a beach-sand volume of coastline of 3,000 m3/km (Richmond et al., 2008).

1.3 Problem Definition

The Island of Hawaii is an ideal place to perform a photogrammetric grain-size study because it is an everchanging island/environment, has diverse beaches located in diverse microclimates, and virtually no studies have been done concerning beach sand on the island regarding geology or sedimentology. Many studies have focused on Oahu and can thereby be compared or contrasted to our study creating a broader impact. However, this investigation will be a reconnaissance study and sampling of the entire island allowing circumnavigational comparisons to differing seasonal wave energies, currents, and micro-climate controls on the Big Island's beaches and beach sands.

The aim of this study is to first asses the viability of calibrated photogrammetry as an alternative to a sieve sampling and subsequently tune the method to be able to calculate statistical moments to a satisfactory degree of precision. Next, one can proceed with an initial reconnaissance analysis of each beach and cross sections within the Hawaiian beaches, determining how these preliminary samples differ in size, sorting, composition, regional climate, geographic location, and provenance. After this analysis, preliminary conclusions can

be drawn about composition/grain size reactions to wave energy, beach reactions to regional climate and weather, beach and sand feedback to ocean currents, among others.

1.4 Study Sites: Mars

As an additional site for testing the proposed procedure of photogrammetric sediment size analysis, one may examine some locations on the planet Mars. Since sand is important in understanding weather and climate, it is of great interest to geologists to study and learn about the sand on Mars, as well as other planets, to comprehend planetary processes both above the surface in terms of climate but also underneath in terms of geological and climate history. There currently are satellites around the planet that have been sent to take high resolution photographs of the surface. These photographs are helpful when studying large-scale sand migration and other geological implications, however, these types of photographs lack resolution enough to study the sand on a smaller scale.

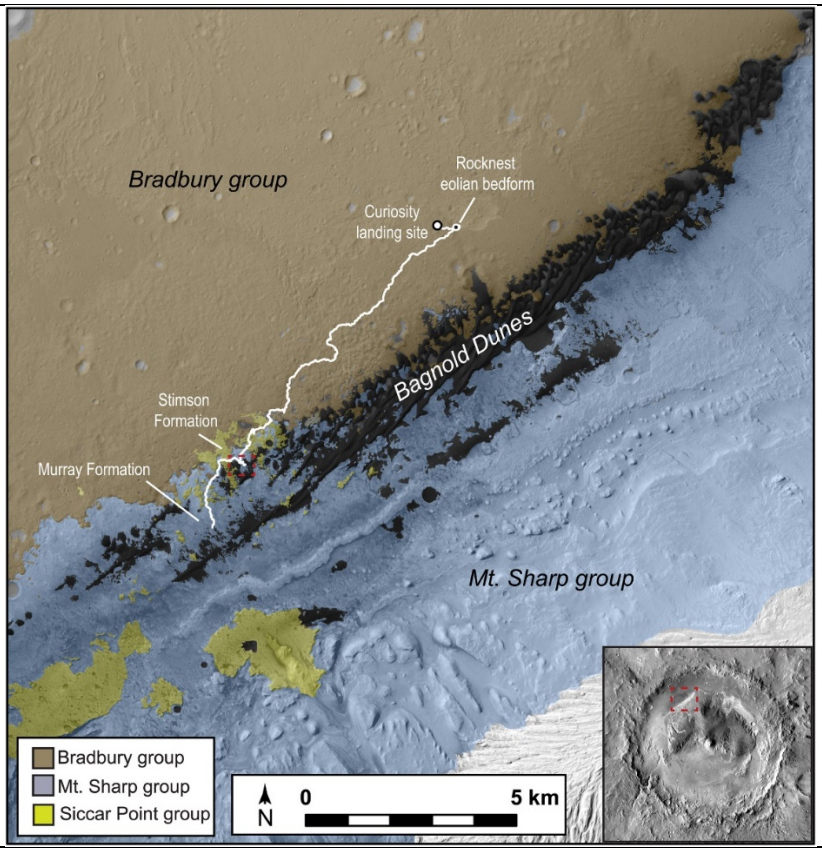

Figure 1.4.1: Map from Ehlmann et al. (2018) showing the location and path of the Curiosity Rover on Mars.

To further study the sand on Mars, NASA, along with many other instruments, included a small scoop shovel and sieve on the Curiosity rover that is capable of scraping the surface and collecting a small sample. The Collection and Handling for In-Situ Martian Rock Analysis, or CHIMRA, is attached to the end of a robotic arm and is able to collect, sieve, and analyze chemistry and mineralogy (Anderson et al., 2012). The sieves on the Curiosity rover are capable of sieving grains <150 µm, 150 µm to 1mm, and >1mm. The distribution of grains has not been looked at and the sieves are used primarily for chemical and mineralogical analysis instead of studying the sand distribution itself. Another tool useful for photogrammetry interpretation is the Mars Hand Lens Imager, or MAHLI, that is capable of taking high resolution pictures of sediment at a close range with an accurate, laser-measured scale.

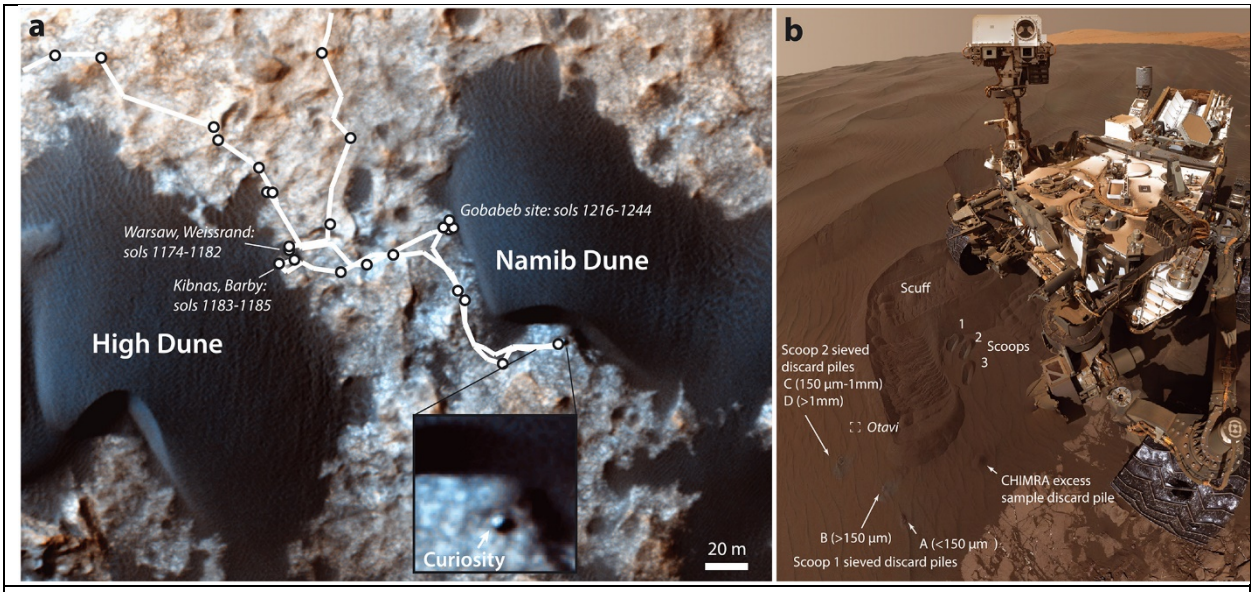

Figure 1.4.2: Map from Ehlmann et al. (2018) showing the location and path of the Curiosity Rover on Mars and the two visited dunes: High Dune and Namib Dune.

One particular area of interest that could be useful for comparison to sands from Hawai'i are on the Bagnold Dunes that are located in the Gale Crater on Mars (*Figure 1.4.1*). Here the rover Curiosity has extensively studied from November 2015 to April 2017 (Bridges and Ehlmann, 2018). In this crater, photographs of sand from these dunes, namely the High Dune and Namib Dune (*Figure 1.4.2*), can be used to analyze and test photogrammetry, comparing it to the research published by Ehlmann et al. (2018), which provides only a little amount of grain size analysis while focusing mainly on compositional components of the sand.

There are four sites, two at each dune, where the MAHLI took pictures of undisturbed sediment from the dunes; the sites from High Dune are named Barby and Kibnas and the sites from the Namib Dune are named Otavi and Wheel. A picture of these sands can be seen in *Appendix B.19.1*.

Ehlmann et al. (2018) described the photograph site Barby as being an undisturbed ripple crest with grains ranging from 150µm to 600µm with few larger grains. The Kibnas photograph site is described as an undisturbed trough with grains ranging in size from 50µm to 400µm with one large 1mm grain. From the other site, Namib Dune, Ehlmann et al. (2018) describes the photograph site Otavi as having grains ranging from 60µm to 450µm and the photograph site Wheel as being sediment mixed by the wheel of the Curiosity rover and having grains ranging in size from 80µm to 350µm. They published that generally the Namib Dune was better sorted but provide no numerical findings.

The mineralogy of these sites shows that grains are typical of basalt with the dominant crystalline phases being Na,Ca-feldspar (~37 wt %), olivine (26 wt %), and two pyroxenes (22 wt % augite and 11 wt % pigeonite) (Ehlmann et al., 2018). These dunes were found to lack a lot of aeolian dust that is common around other sites on Mars most likely due to winds blowing dust away (Bridges and Ehlmann, 2018).

2. Methods

2.1 Sampling Locations

For a circumnavigational sampling of the island of Hawai'i, tourists and state maps were consulted to pick beaches to sample (Clague and Dalrymple, 1987; Clark, 1985; Fletcher et al., 2008). Eighteen beaches were selected throughout the entirety of the island, and the locations of these beaches can be seen in *Figure 2.1.1*. Because of geographic and island climate, there are parts of the island where there are large areas of cliffs that have no beaches present (north-eastern part) and areas with ongoing lava eruption and cliffs that also have no beaches (south-eastern part). There are more beaches present on the west, dry side of the island and less on the east, wet side of the island. The selection of beaches also includes a large variety of different sands, including white, black, grey, brown, and green. Additionally, the selection

includes a variety of grain sizes, ranging from silty to cobble-like boulders. There are 18 beaches chosen and are namely (beginning with the north and moving clockwise) Pololu beach, Honoli'I beach, Pohoiki beach, Punalu'u beach, Green Sand beach, Miloli'I beach, Pebble beach Ho'okena beach, Kahalu'u beach, Magic Sands beach, Pahoehoe Beach Park, Old Kona Airport Park, Mahai'ula beach, Manini'owali beach, Waialea beach, Hapuna beach, Mauna Kea beach, and Spencer beach. The locations of each beach in relationship to weather events as well as

Figure 2.1.1: The island of Hawaii with the 18 beaches sampled.

rainfall can be seen in *Figure 2.1.2* and *Figure 2.1.3* respectively.

At each beach, a cross section would be measured including distance from swash zone to a berm which would be anywhere from 15 to 50 ft. At intervals, the slope would be measured, and a high-resolution photograph would be taken at a distance of 1.5 ft above the sand (on a tripod) with a Sony α6400 camera with a 16-50mm lens and a laser-etched scale to ensure accuracy. At least one cross-section was recorded at each beach, and some beaches

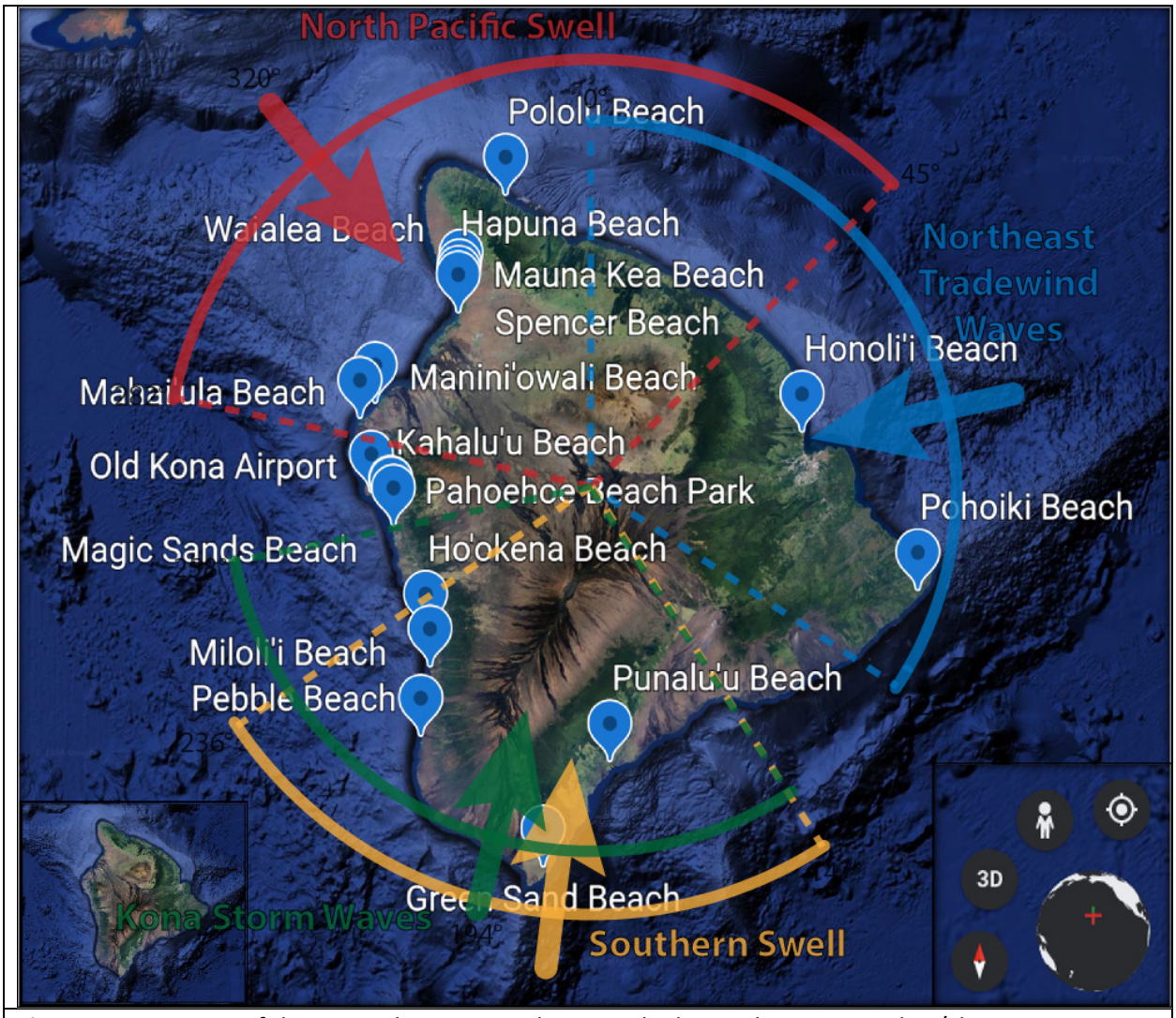

Figure 2.1.2: A map of the survey locations with an overlaid map showing weather/climate subjugation.

included multiple cross-sections to compare different measurements along a bay's exposed shoreline. Starting in the North and moving counterclockwise, Pololu Beach had 3 transects and 14 survey points (A 1-4, B 1-3, and C 1-7), Spencer Beach had 1 transect, 3 survey points (A 1-3), Mauna Kea Beach had 1 transect and 1 survey point (A 1), Hapuna Beach had 1 transect and 3 survey points (A 1-3), Waialea Beach had 3 transects and 6 survey points (A 1-3, B1 1-2, B2 1), Manini'owali had 3 transects and 7 survey points (A 1-3, B 1-2, and C 1-2), Mahai'ula Beach had 6 transects and 18 survey points (A1 1-2, A2 1-2, A3 1-7, A4 1-3, A5 1-2, and B1 1-2), Old Kona Airport Beach had 1 transect and 2 survey points (A 1-2), Pahoehoe Beach Park had 1 transect and 5 survey points (A1-5), Magic Sands Beach had 1 transect and 2 survey points (A 1-2), Kahalu'u Beach had 1 transect and 4 survey points (A 1-4), Ho'okena Beach had 1 transect

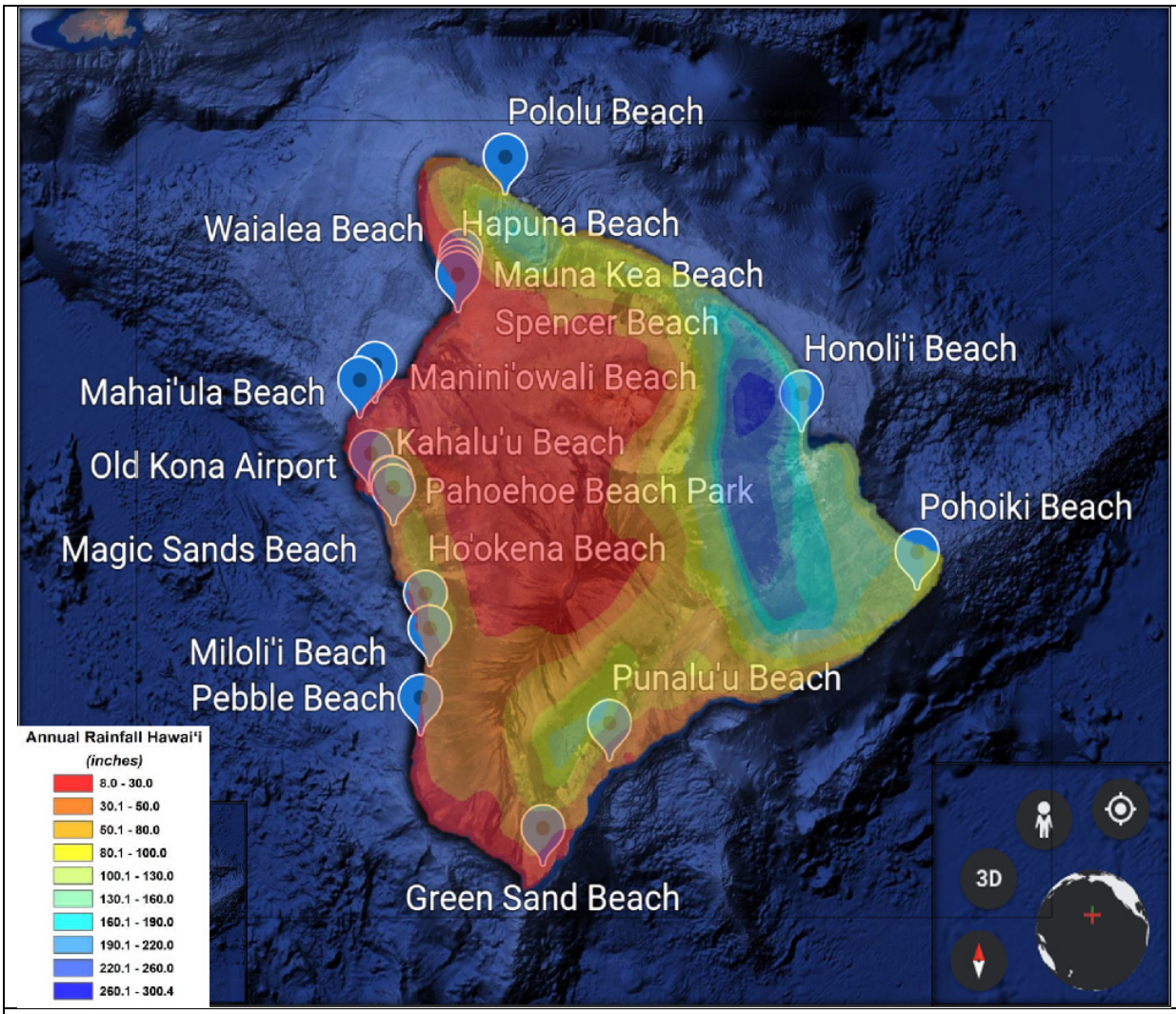

Figure 2.1.3: A map of the survey locations with an overlaid map showing rainfall subjugation.

and 3 survey points (A 1-3), Pebble Beach had 1 transect and 4 survey points (A 1-4), Miloli'I Beach had 1 transect and 3 survey points (A 1-3), Green Sand Beach had 1 transect and 4 survey points (A 1-4), Punalu'u Beach had 5 transects and 17 survey points (A 1-4, B 1-3, C 1-3, D 1-3, E 1-4), Pohoiki Beach had 1 transect and 5 survey points (A 1-5), and Honoli'i Beach had 2 transects and 6 survey points (A 1-3, B 1-3). Each beach and the labelled transects can be seen in *Appendix A* and each individual transect with the measuring tape and survey site photographs can be seen in *Appendix B*.

2.2 Photogrammetric Calibrations

To ensure accuracy in the photogrammetry computer program, a series of sand standards from around the world were measured and sieved out. Those samples are from Brown's Cay Bahamas, Santa Lucia, Barbados, Yallahs, Galveston, San Juan Puerto Rico,

Mahaiula, New Providence Nassau, Los Cabos, Dry Tortugas, Hua Hin Thailand, Eritrea Red Sea, Punaluu, Papakulea, Algeria, White Sands New Mexico, Cancun, Bali, Newfoundland, and Isla Baru Colombia. As sand sieving for more than 10 minutes gives the least variation in results (Roman An-Sierra, et al., 2013) these sands were sieved for 25 minutes each in a Gilson Inc Model: SS-15 Sieve Shaker. The sieve mesh sizes ranged in size from -2ϕ to 4ϕ with a pan underneath and increment at each 1/2 ϕ. Each sieved size was subsequently weighed and photographed.

A total of six physical sand samples were taken for examination and comparison from Hawai'i. The small samples were taken from Pololu Beach, Green Sand Beach, Mauna Kea Beach, Spencer Beach, Mahai'ula Beach, and Punalu'u Beach. These samples represent the diversity of sand across the island and include both small and large grains, organic and volcanic grains, and tan, green, black, white, and pepper-colored sand. The samples were about 10 – 40g in weight. After sieving both the standards and the six samples from Hawai'i, the weights were recorded and run through GRADISTAT to create distribution and cumulative curve graphs, all of which can be found in *Appendix C*.

Buscombe's (2013) program requires only three inputs in addition to the photograph, namely: resolution (mm/pixel), maxscale (the maximum grainsize to be considered in pixels), and an area-by-number to volume-by-number conversion dubbed 'x'. To measure mm/pixel, an extension on MATLAB called imtool was used, which measures pixels in a drawn line. Because each image had a millimeter scale, it was possible to measure how many pixels were in a millimeter using this tool. Buscombe (2013) gives a default value for the maxscale input, and states that it only needs to change in extenuating circumstances, such as not wanting larger particles to be counted. Buscombe (2013) also explains that the area-by-number to volume-by-number conversion otherwise known as 'x' can instead be used as a tuning factor since environments can be variable. This program has several outputs, including spectral frequency, statistics (including the statistical moments, but not as according to the Folk and Ward (1957) method), and percentiles at 5, 10, 16, 25, 50, 75, 84, 90, and 95 in millimeters. The outputted percentiles are most useful for this study, as they can be converted first to ϕ units, used to create distribution (as a %) and cumulative curve graphs, and then used to calculate the

statistical moments according to the Folk and Ward (1957) method (see *Table 1.1.1* for calculations).

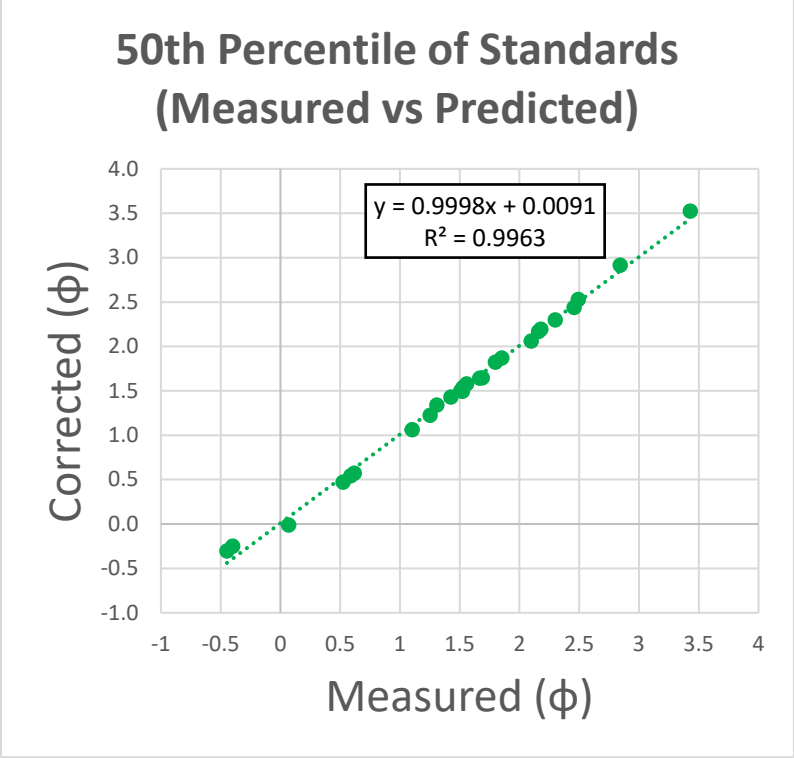

Figure 2.2.1: The 50th percentile data points from the standards. The program accurately predicts the 50th percentile.

After the physical standard samples as well as the Hawai'i samples were weighed out and graphed, the photographs of each were run through the Buscombe (2013) program to compare the measured (sieve) results to the predicted (modelled) results. The resulting predicted data points at the 10th, 50th, and 90th phi percentiles are plotted against the measured phi percentiles and the overall slope measured. For the program to be correct, the measured data points should be the same as the predicted points; however, the predicted percentiles of the standards, similar to findings by Buscombe (2013), underestimated at the 10th percentile and overestimated at the 90th percentile, while the measured and predicted for the 50th percentiles were statistically the same requiring no calibration (*Figure 2.2.1*). Since the relationships at the percentiles are linear, the slope equation is $y = m_o x + B_o$. To calculate the corrections, the slope and y-intercept from the predicted data points must be compared to the standard slope and y-intercept, $y_s = m_s x + B_s$, as is represented in the example schematic in

Figure 2.2.2. The change, or delta of the slopes is calculated by subtracting the predicted from the standard ($\Delta m = m_s - m_o$) and the change of the y-intercepts is also calculated by subtracting the predicted from the standard ($\Delta B = B_s - B_o$). For the 10th percentiles, the equation before corrections is y = 0.62 x – 0.03 yielding a Δm of 0.38 and a ΔB of 0.03. For the 90th percentile, the equation before corrections is y = 1.34 x – 0.12 yielding a Δm of -0.34 and a ΔB of 0.12. These correction factors were applied, generating the new slopes and y-intercepts seen in *Figure 2.2.3*, showing the post-corrected equation for the 10th percentile to be y = 0.99 x – 0.002 and 90th percentile to be y = 1.001 x + 0.006. The 50th percentile equation is seen in *Figure 2.2.1* and is y = 0.99 x + 0.009.

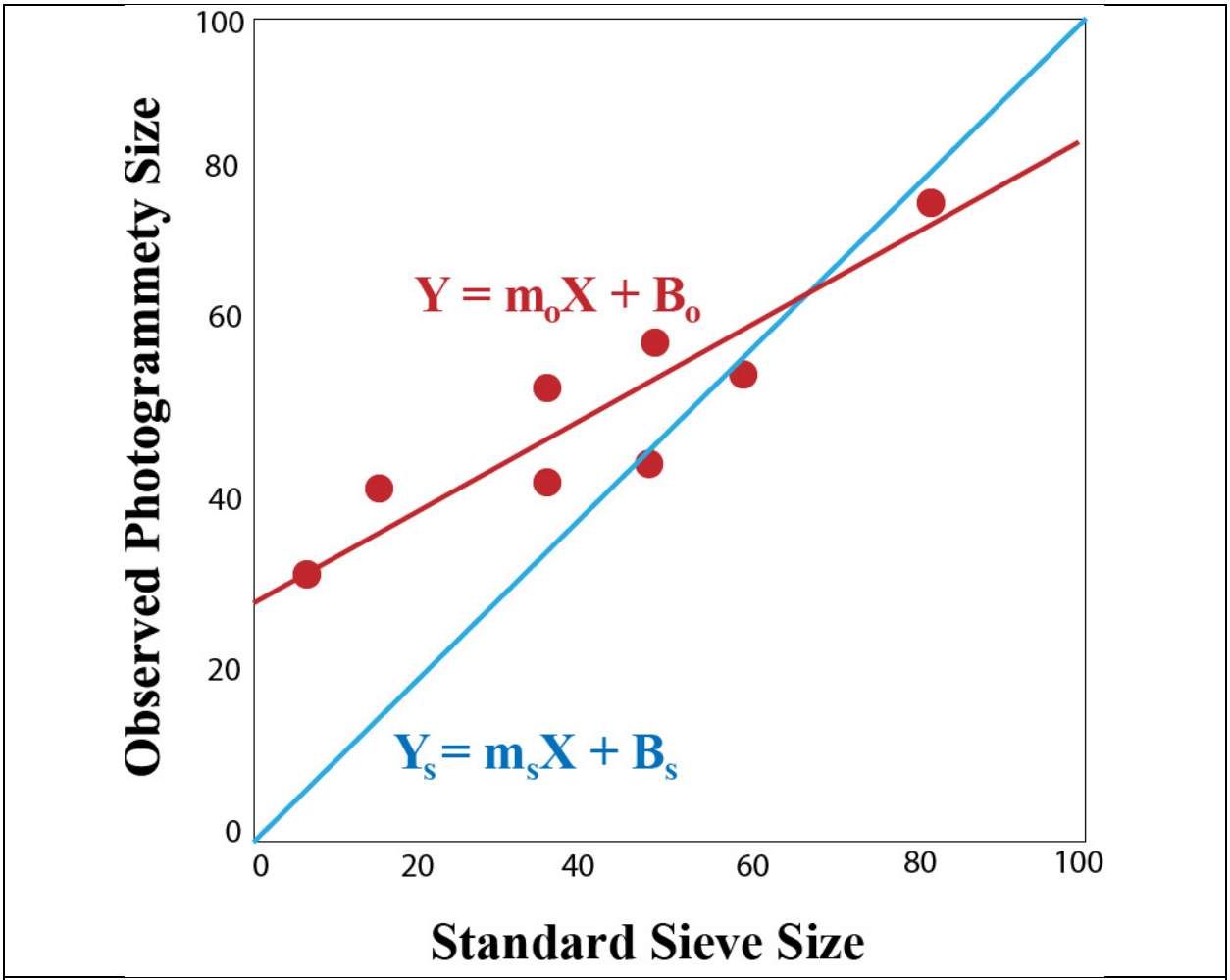

Figure 2.2.2: A schematic example of how the predicted (modelled) data points compare and can be corrected to the measured (sieved) data points.

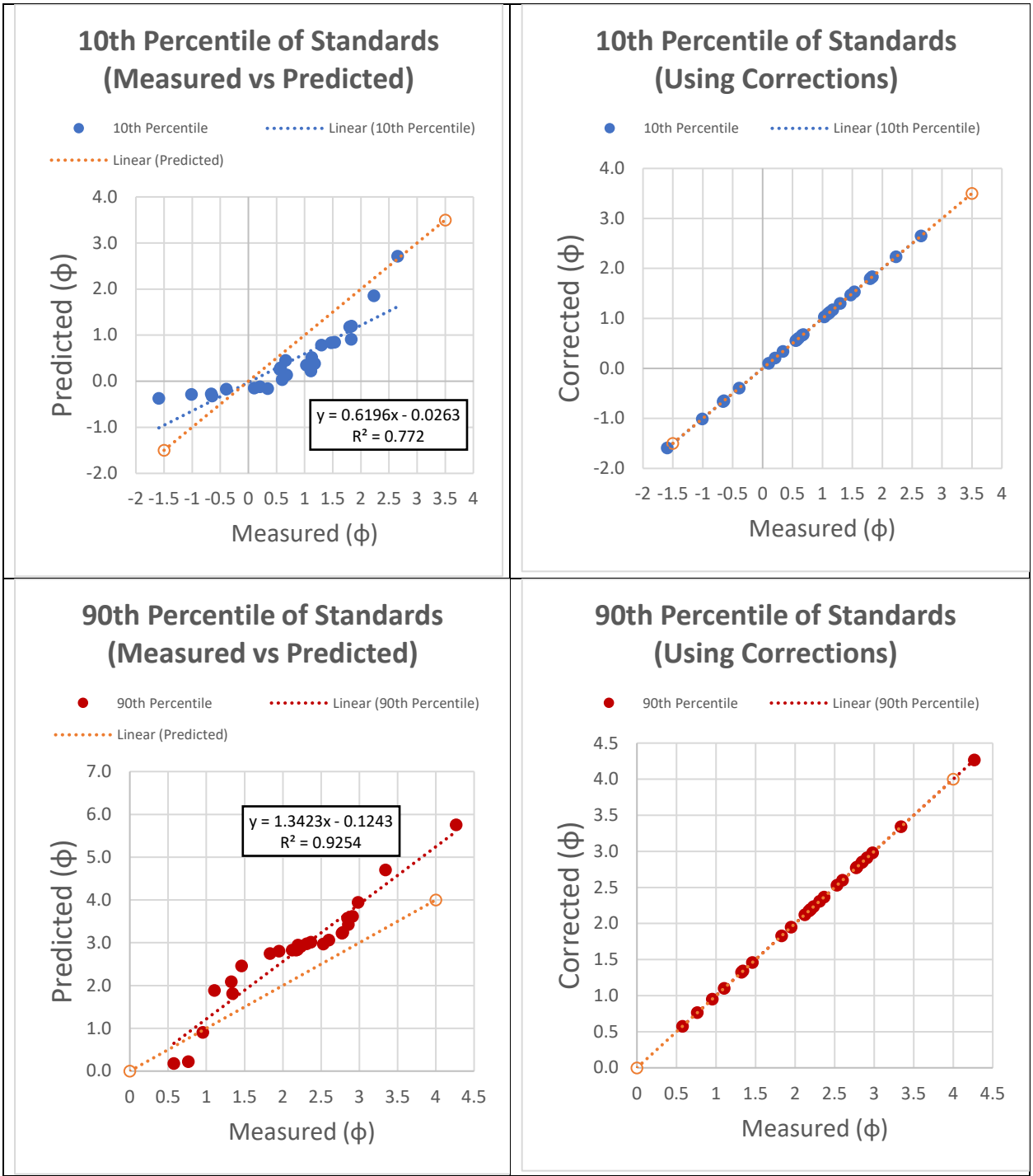

Figure 2.2.3: (*top*) The 10th percentile data points for the standards before (*top-left*) and after (*top-right*) corrections were applied. (*bottom*) The 90th percentile data points for the standards before (*bottom-left*) and after (*bottom-right*) corrections were applied.

Each of the six physical samples were also tested for composition using the XRF. The instrument used was the Thermo Fisher Scientific Niton Analyzer model XL3 Analyzer which is a

portable XRF device mounted on a desk casing for laboratory tests. Each sand sample was loaded into an XRF designated sample bag and ran for 5 minutes. For this study, it was determined that the principle compositional components of interest were aragonite, olivine, and labradorite, or in other words, carbonate, olivine, and feldspar. Laboratory standards of each of these minerals was used to compare and calculate percentages via a program coded by John D. Pigott (personal communication, 2021).

3. Results

3.1 Grain Size Distribution and Statistics

The numerical results from running each of the 116 survey points at all 18 beaches with their labels, distance from water (measuring point), slope, calculated percentile in mm and ϕ, statistical moments and descriptors, distribution and cumulative curve graphs, and height profiles can be seen in *Appendix D*.

The north most beach, Pololu Beach, is subject to the effects of the North Pacific Swell. As the distance from the water increases on the beach, all three transects decrease in sorting, digressing from well sorted to very poorly sorted in Transect A, very well sorted to well sorted in Transect B, and well sorted to poorly sorted in Transect C. Skewness also decreased with distance from water varying in all three transects from very coarse skewed to coarse skewed. Coarse skewness likely comes from an addition of larger grains during a storm and the subtraction of finer grains with decreasing wave energy. Kurtosis also decreased in all three transects going from extremely leptokurtic to platykurtic. On all three transects, the median migrates first to finer particles and then to larger particles. All survey point distribution graphs for Pololu Beach can be seen grouped by transect in *Figures 3.1.1 – 3.1.3*.

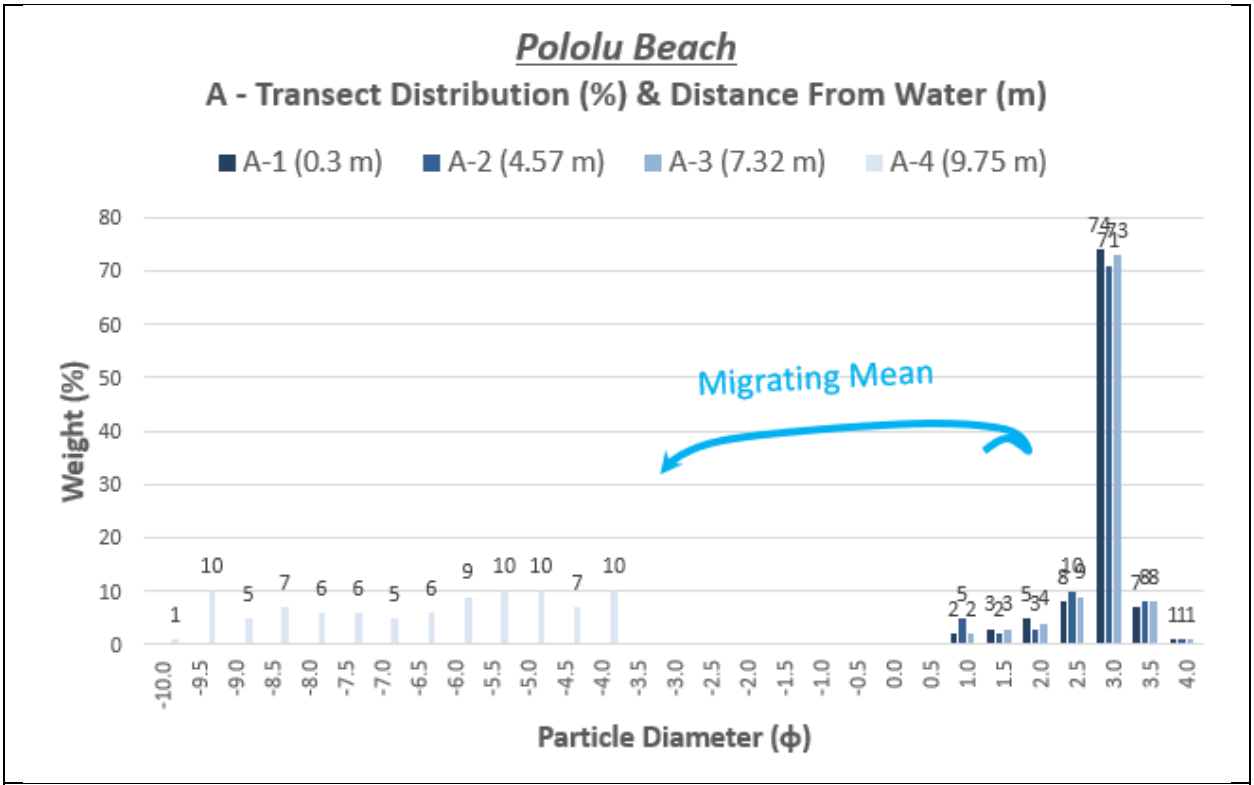

Figure 3.1.1: Pololu Beach distribution graph (% of whole) for transect A. See *Appendix A.1.1* for location photo and transect locations.

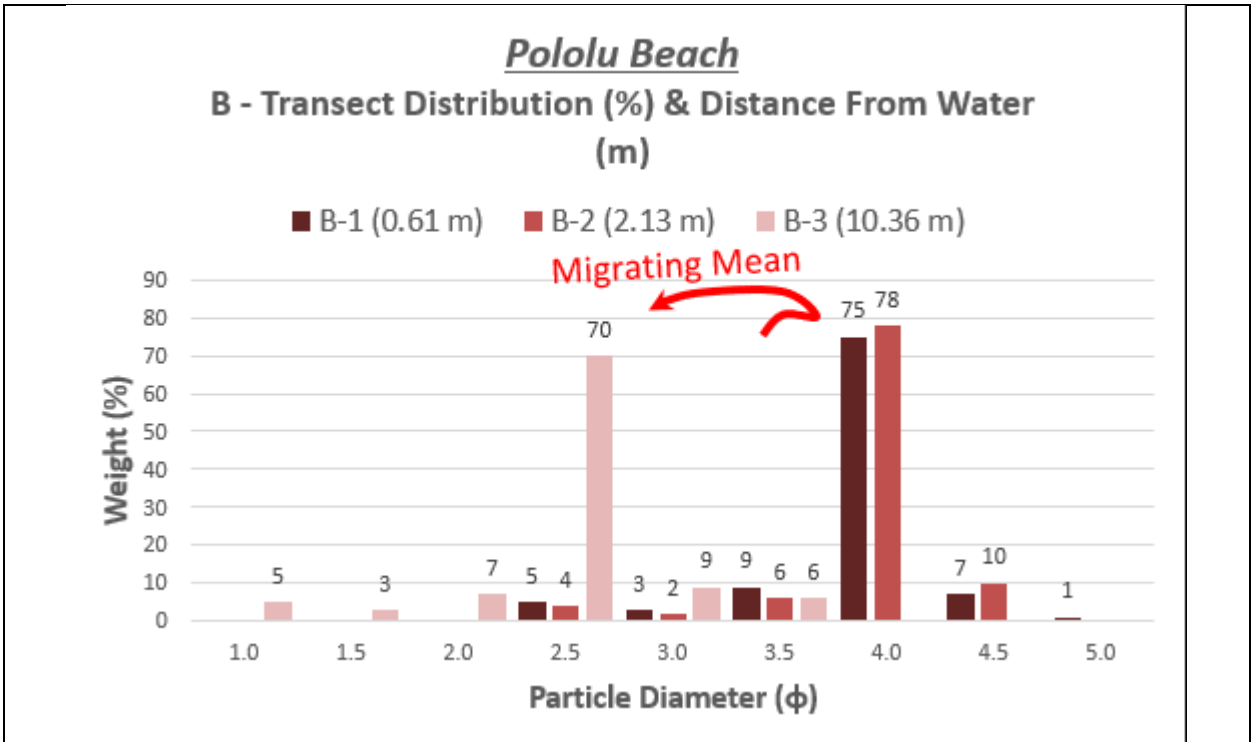

Figure 3.1.2: Pololu Beach distribution graph (% of whole) for transect B. See *Appendix A.1.1* for location photo and transect locations.

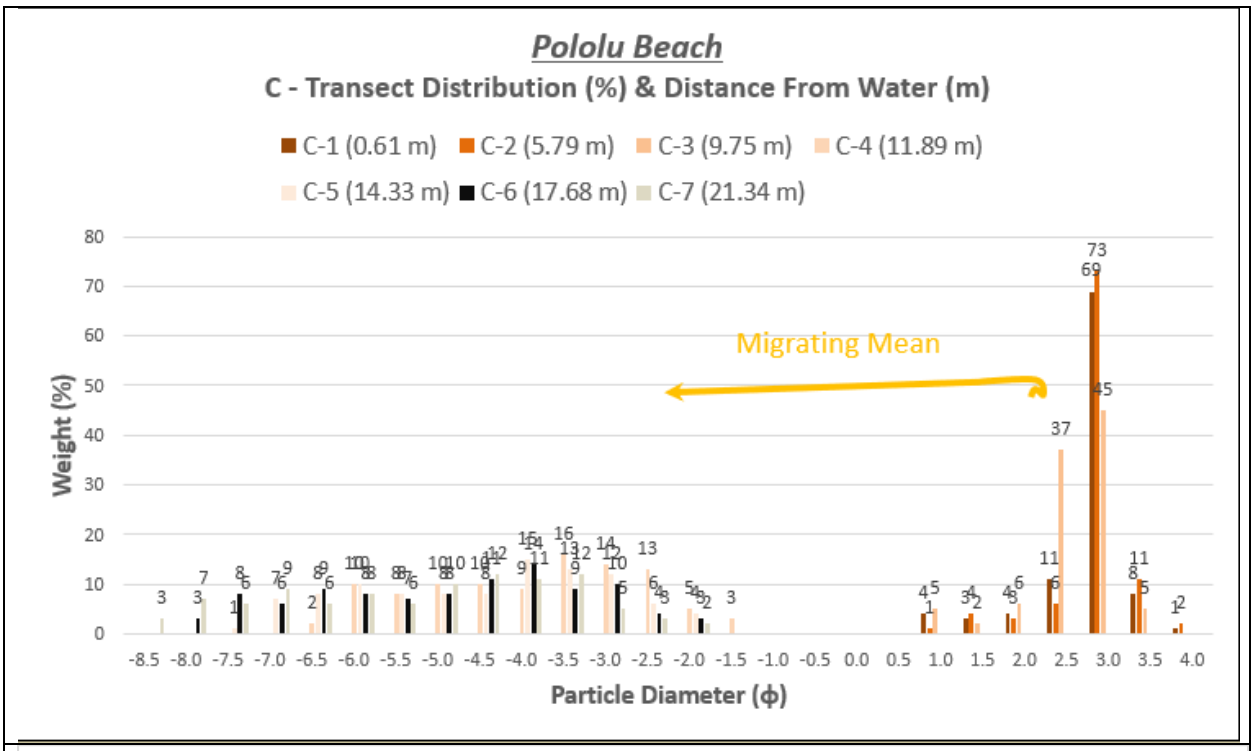
Pololu Beach
C - Transect Distribution (%) & Distance From Water (m)
C-1 (0.61 m)
C-2 (5.79 m)
C-3 (9.75 m)
C-4 (11.89 m)
C-5 (14.33 m)
C-6 (17.68 m)
C-7 (21.34 m)
Migrating Mean
Weight (%)
Particle Diameter (ϕ)

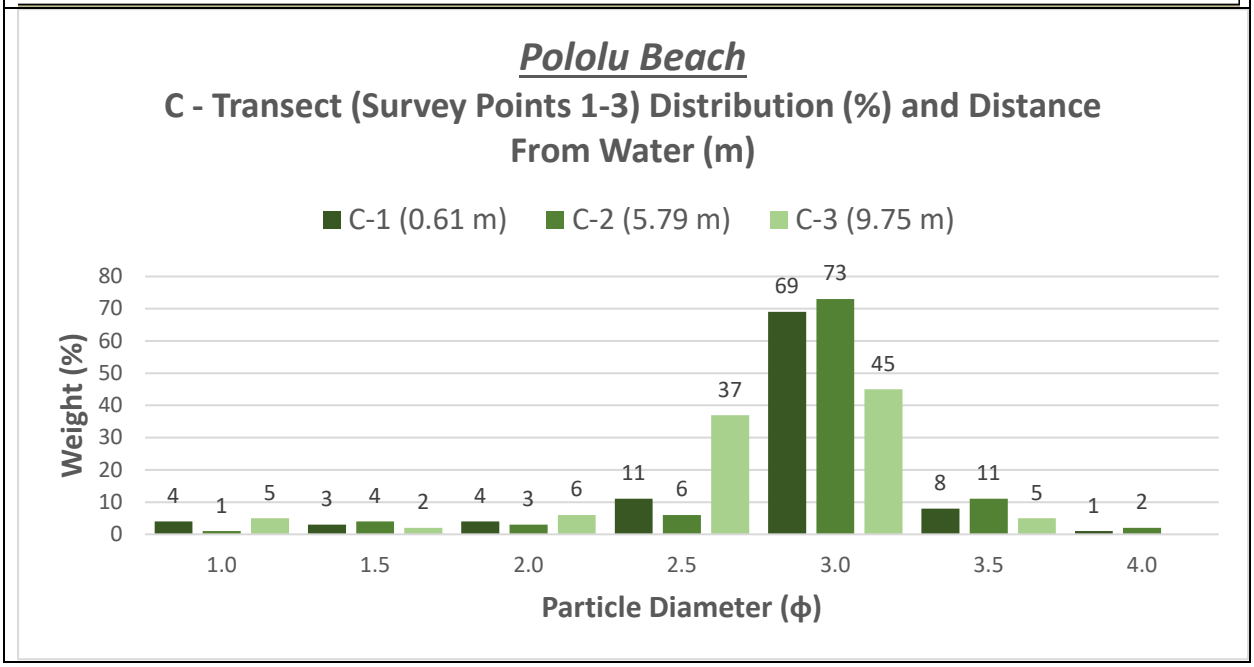
Pololu Beach
C - Transect (Survey Points 1-3) Distribution (%) and Distance From Water (m)
C-1 (0.61 m)
C-2 (5.79 m)
C-3 (9.75 m)
Weight (%)
Particle Diameter (ϕ)

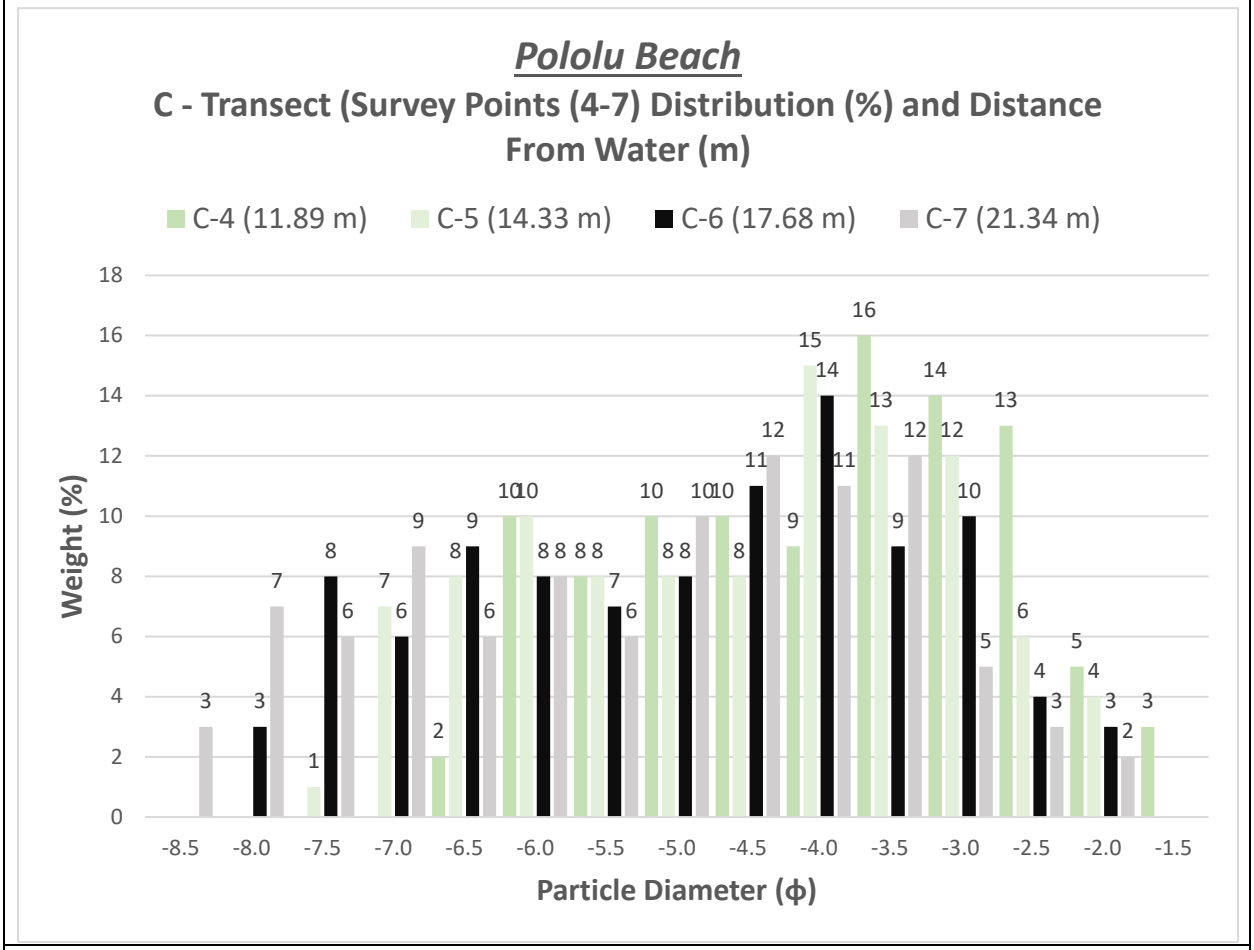

Figure 3.1.3: Pololu Beach distribution graphs (% of whole) for all survey points in Transect C (*top*), survey points 1 – 3 (*middle*), and survey points 4 – 7 (*bottom*). See *Appendix A.1.1* for location photo and transect locations.

Spencer Beach is also subject to the effects of the North Pacific Swell and as distance from the water increases, the sorting or standard deviation increases from moderately well sorted to well sorted. Skewness slightly decreases, maintaining very coarse skewed. Because of the intensity of the North Pacific Swell, it is likely that larger grains were deposited due to the higher energy and finer grains were winnowed away through decreasing energy. Kurtosis increases from very leptokurtic to extremely leptokurtic as distance from the water increases. The median migrates slightly to finer particles as distance increases. The survey point distribution graph for Spencer Beach can be seen grouped by transect in *Figures 3.1.4*.

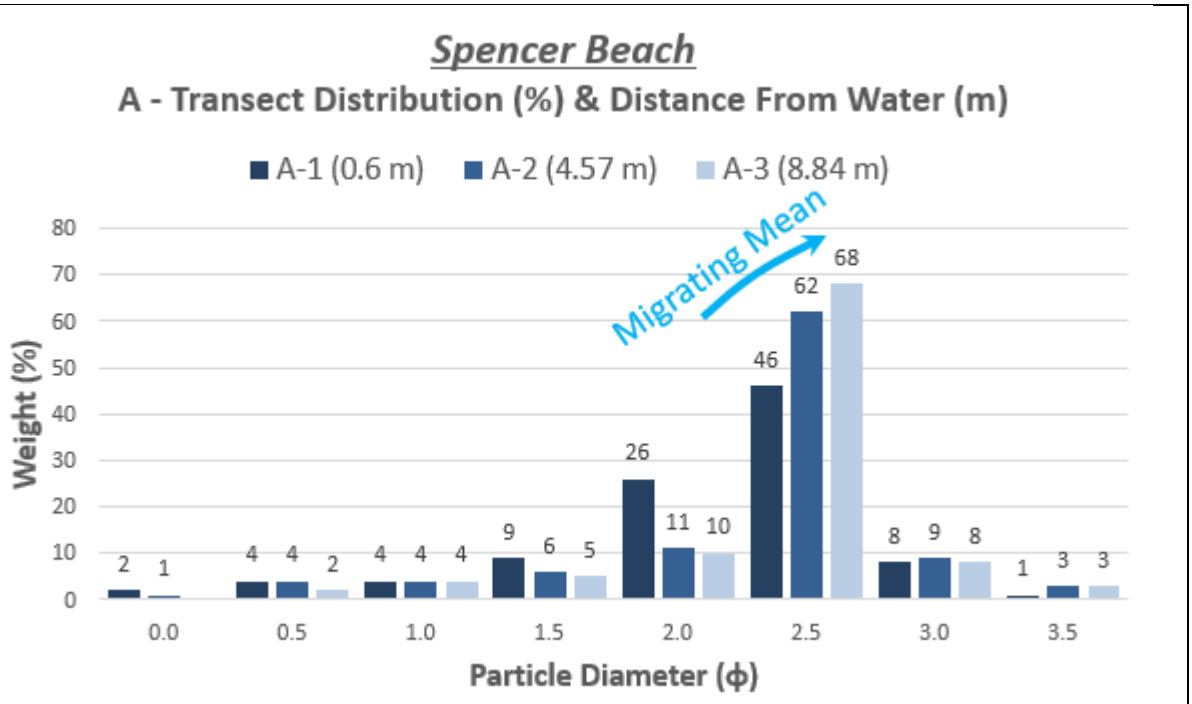

Figure 3.1.4: Spencer Beach distribution graph (% of whole) for all survey points in Transect A. See *Appendix A.1.2* for location photo and transect locations.

Mauna Kea Beach is subject to the North Pacific Swell and only has one survey point. The survey showed that the sand is moderately well sorted, very coarsely skewed, and leptokurtic. Since Mauna Kea Beach is subject to the North Pacific Swell, it is likely that larger grains were deposited during higher energy times and the finer grains winnowed away during decreasing energy. The distribution graph can be seen in *Figure 3.1.5*.

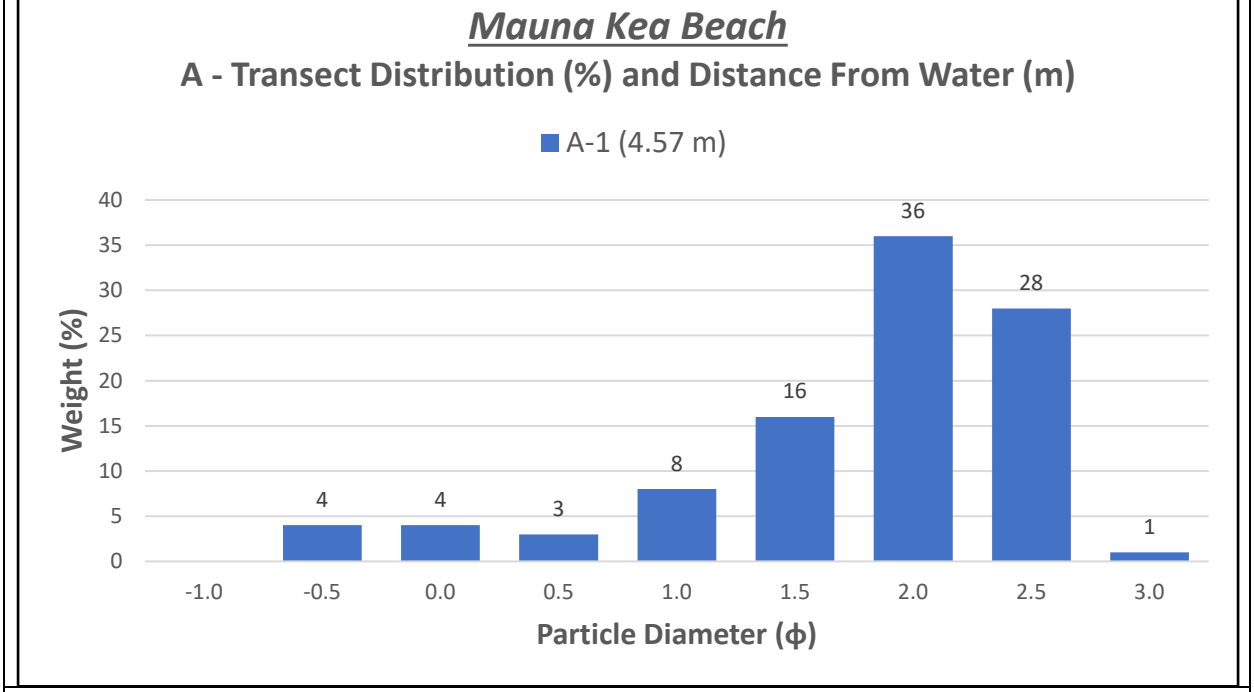

Figure 3.1.5: Mauna Kea Beach distribution graph (% of whole) for the survey point in Transect A. See *Appendix A.1.3* for location photo and transect locations.

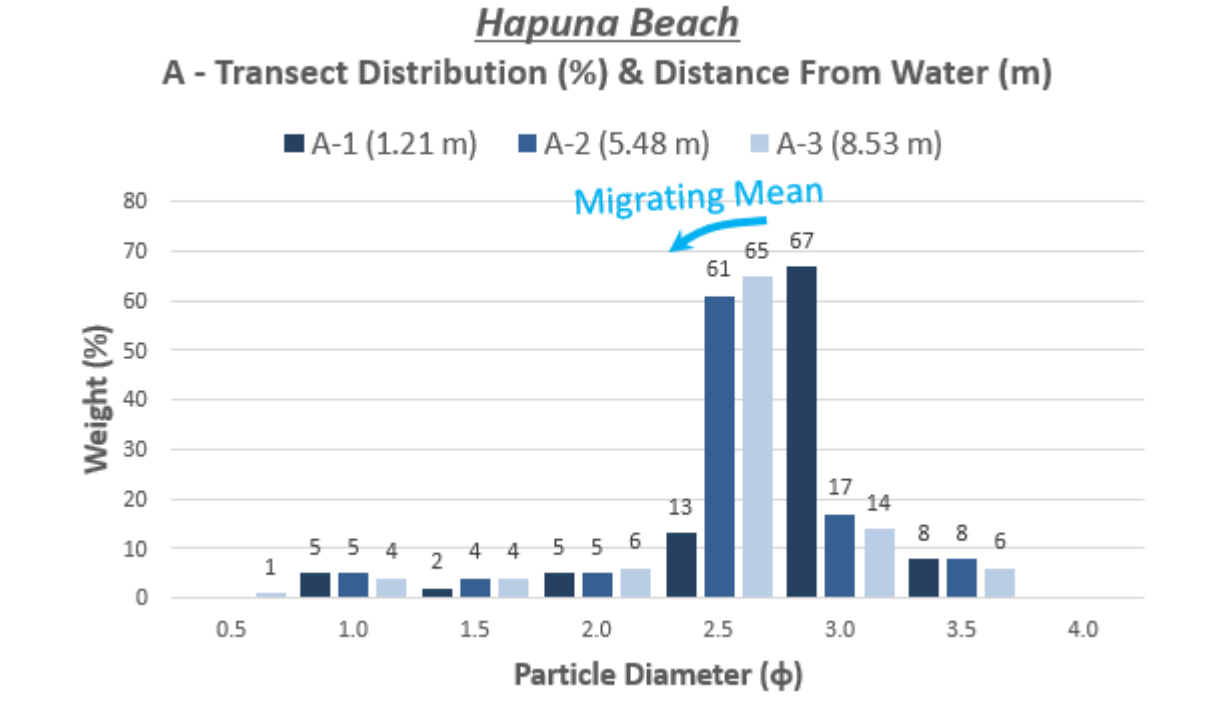

Figure 3.1.6: Hapuna Beach distribution graph (% of whole) for all survey points in Transect A. See *Appendix A.1.4* for location photo and transect locations.

Hapuna Beach is subject to the North Pacific Swell and as distance from the water increases, sorting slightly decreases from very well sorted to well sorted, skewness slightly decreases maintaining very coarse skewed, and kurtosis slightly increases maintaining extremely leptokurtic. It is likely that higher energy times during the North Pacific Swell deposited larger grains while a decreasing energy depleted finer grains accounting for the skewness. A distribution graph for all survey points for Hapuna Beach can be seen in *Figure 3.1.6* all grouped by the transect.

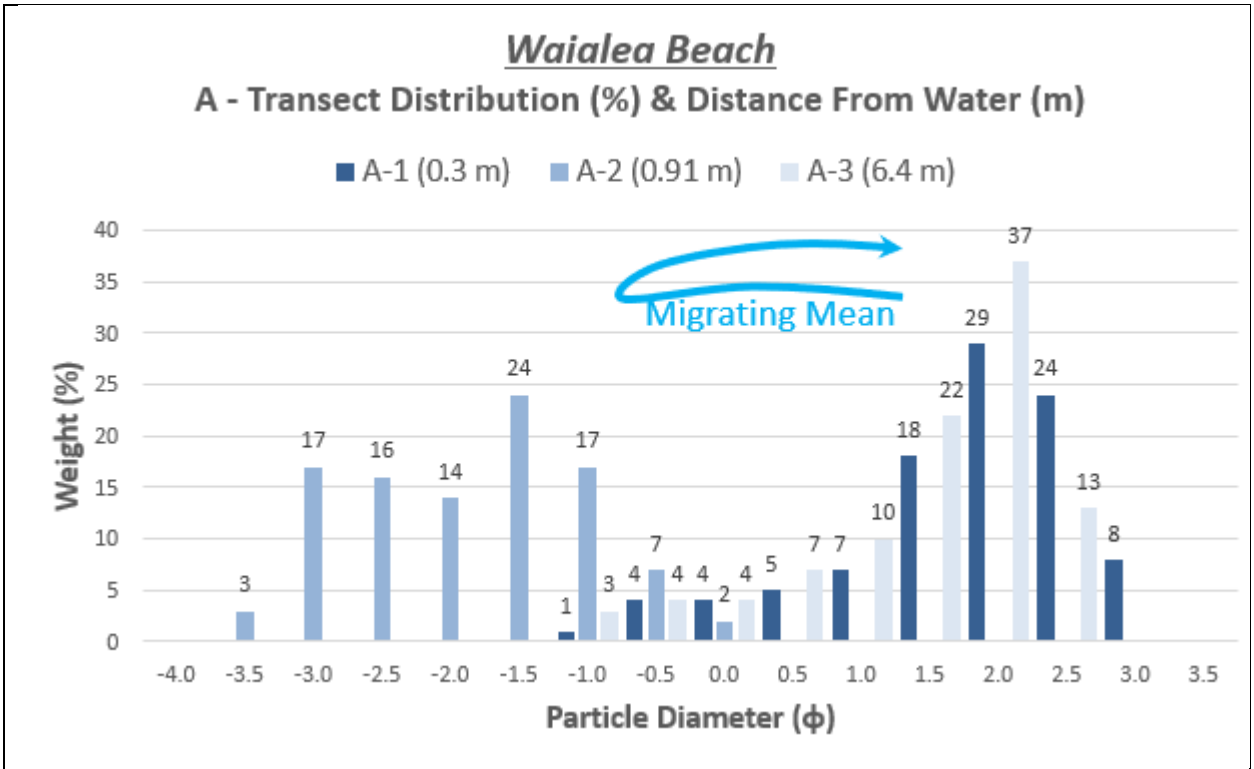

Figure 3.1.7: Waialea Beach distribution graph (% of whole) for all survey points in Transect A. See *Appendix A.1.5* for location photo and transect locations.

Waialea Beach is also affected by the North Pacific Swell and as distance from the water increases, sorting slightly increases at Transect A, all staying moderately sorted, and slightly decreases at Transect B1, staying well sorted at all survey points. Skewness slightly increases overall for Transect A and Transect B1, all survey points being very coarse skewed (with the exception of survey point A-2 which is coarse skewed). The coarse skewness and skewness trend can be explained by larger grains being deposited during higher energy times, especially with the North Pacific Swell, and a winnowing of the finer grains as wave energy decreases. Kurtosis generally decreases in Transect A starting and ending being leptokurtic. Transect B1

slightly decreases kurtosis from extremely leptokurtic to very leptokurtic. The median values for Transect A migrate first to larger particles, then to finer particles. The median grain size at Transect B1 tends toward finer particles. Waialea Beach distribution graphs for each survey grouped by transects can be seen in *Figure 3.1.7 – 3.1.9*.

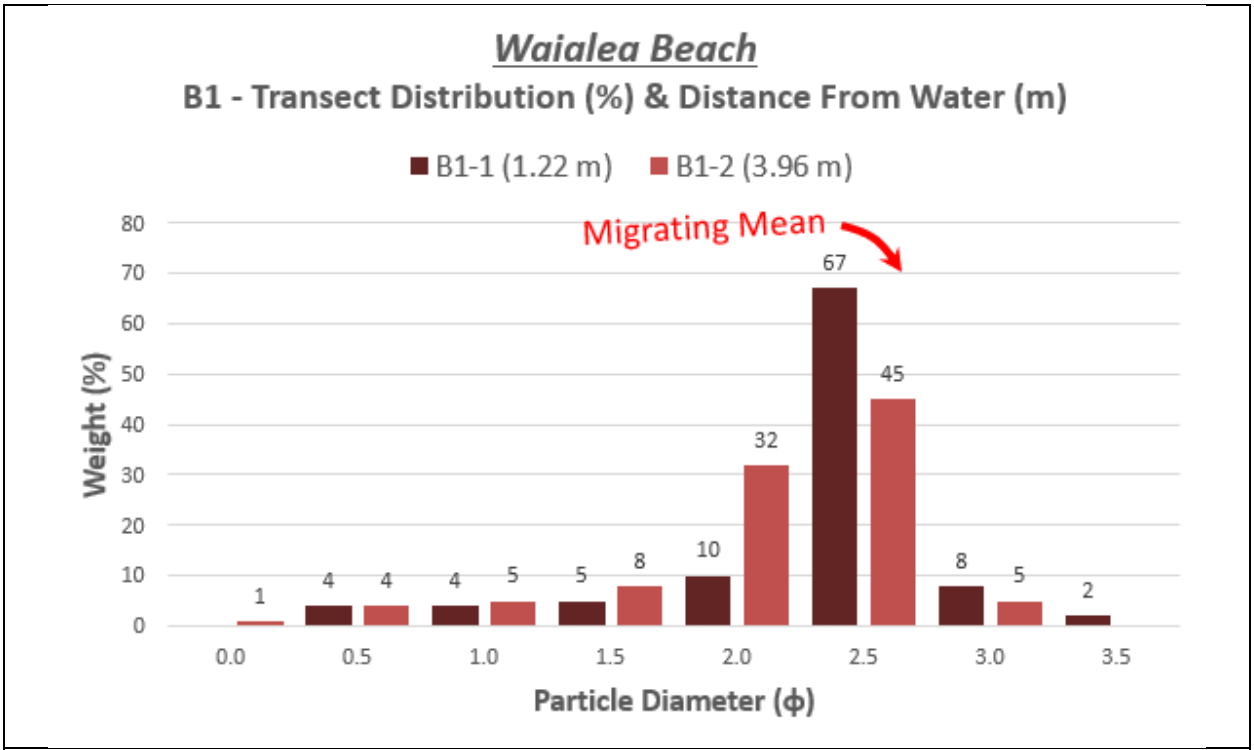

Figure 3.1.8: Waialea Beach distribution graph (% of whole) for all survey points in Transect B. See *Appendix A.1.5* for location photo and transect locations.

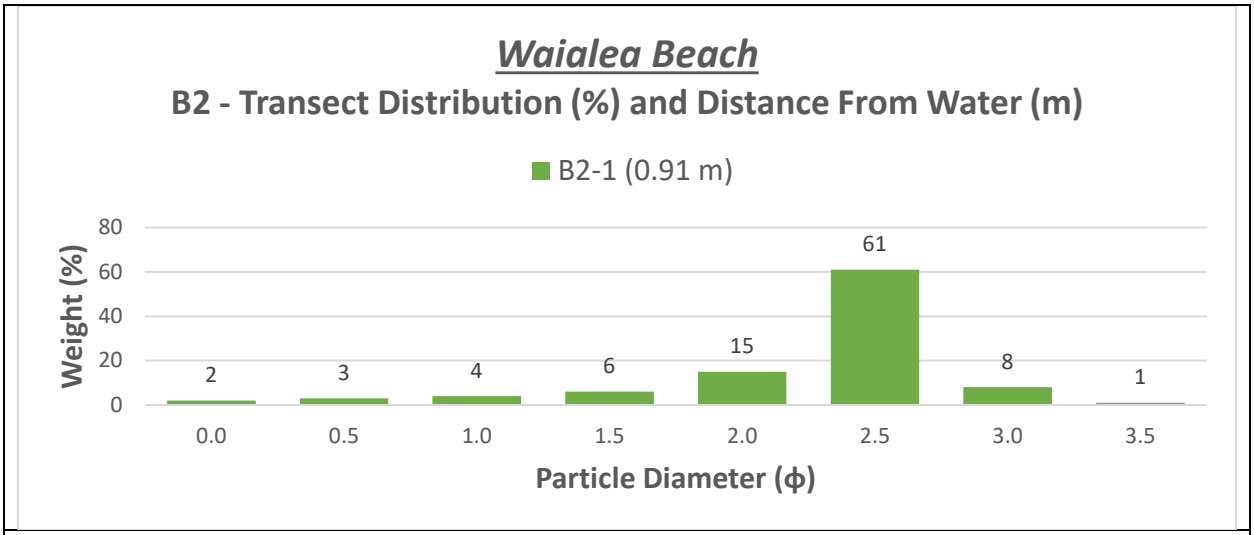

Figure 3.1.9: Waialea Beach distribution graph (% of whole) for the survey point in Transect C. See *Appendix A.1.5* for location photo and transect locations.

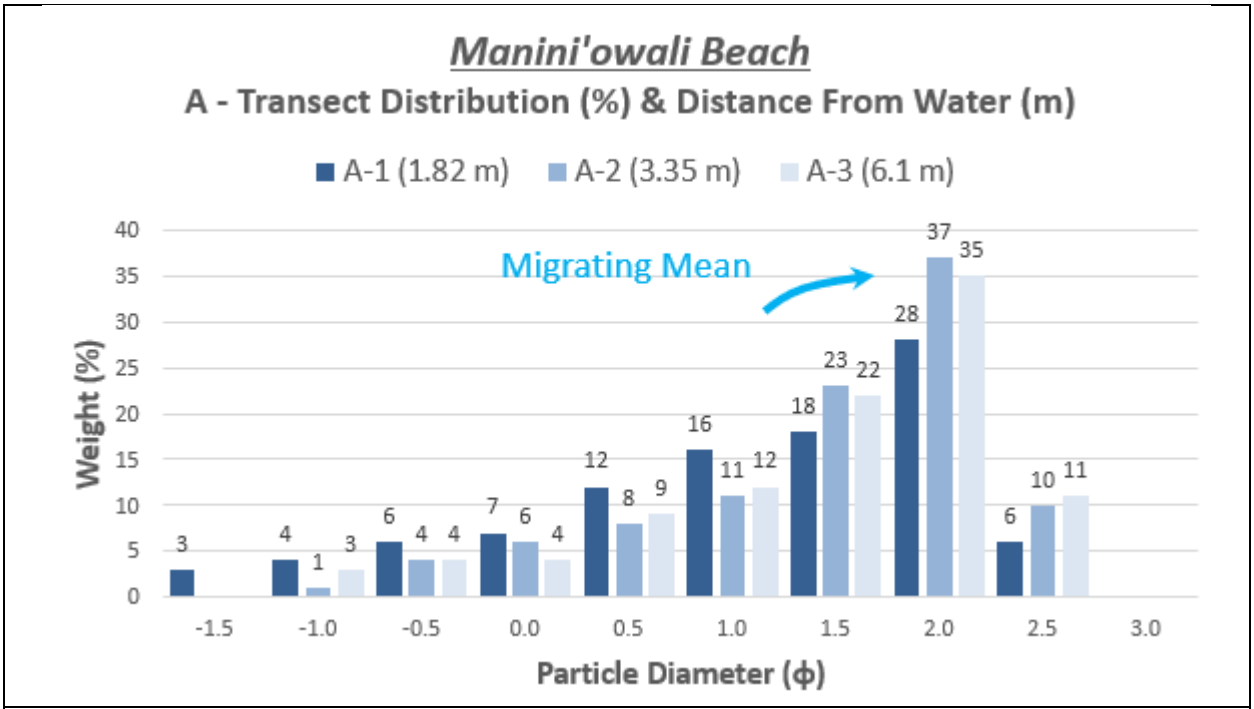

Figure 3.1.10: Manini'owali Beach distribution graph (% of whole) for all survey points in Transect A. See *Appendix A.1.6* for location photo and transect locations.

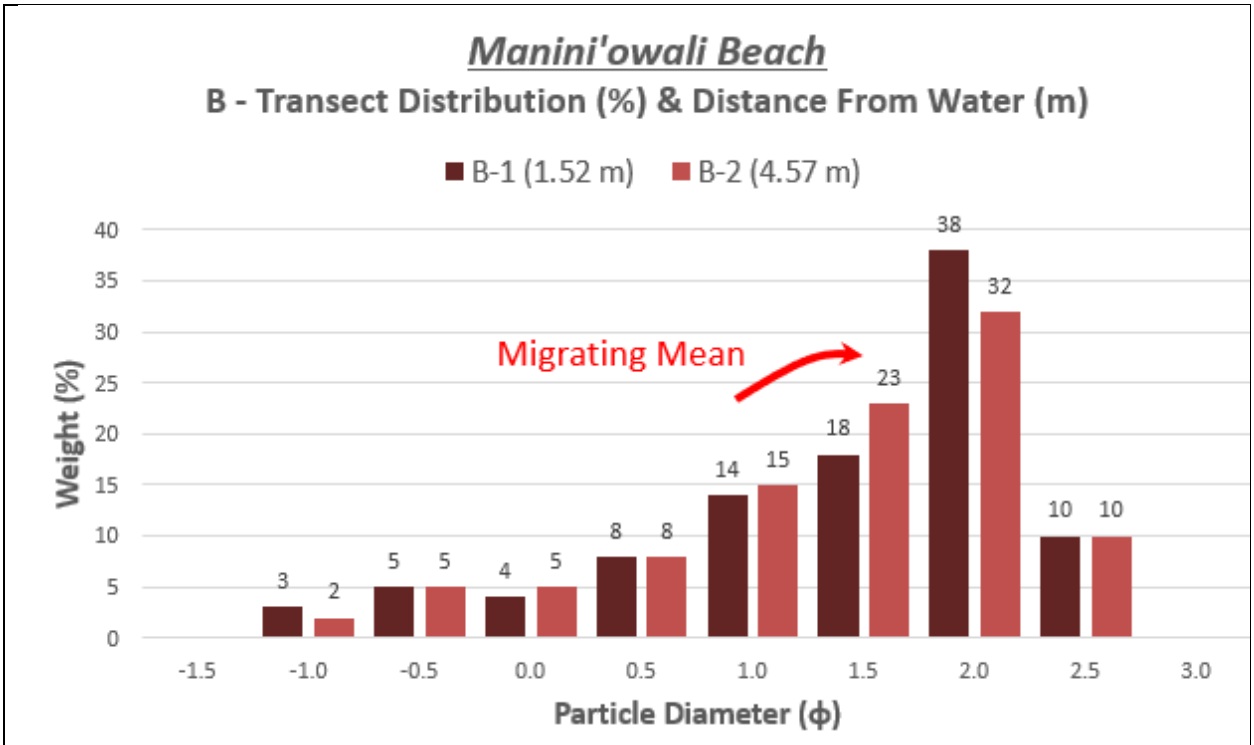

Figure 3.1.11: Manini'owali Beach distribution graph (% of whole) for all survey points in Transect B. See *Appendix A.1.6* for location photo and transect locations.

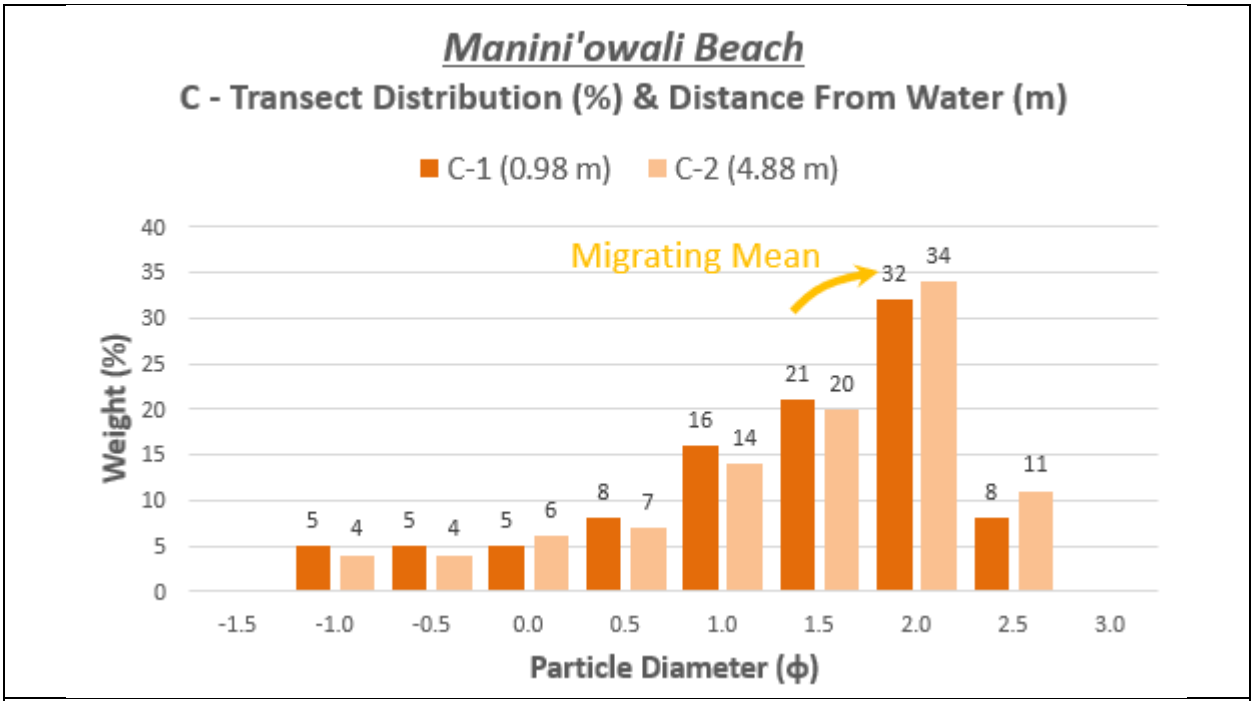

Figure 3.1.12: Manini'owali Beach distribution graph (% of whole) for all survey points in Transect C. See *Appendix A.1.6* for location photo and transect locations.

Manini'owali Beach is affected by the North Pacific Swell and as distance from water increases, sorting increases for all transects, going from poorly sorted to moderately sorted. Skewness increases for Transect A and decreases for Transects B and C, all survey points being very coarse skewed. Since the North Pacific Swell is a high energy climate/weather event, it is likely that larger grains were deposited during a high energy and finer grains were depleted as energy decreased accounting for the skewness trend. As distance from the water increases, kurtosis increases in Transect A and decreases for Transects B and C, being all platykurtic. The median tends toward finer particles as distance from the water increases. A distribution graph for each survey point can be seen grouped together by transect in *Figure 3.1.10 – 3.1.12*.

Mahai'ula Beach is also affected by the North Pacific Swell, and as distance from the water increases, sorting also increases, going from moderately sorted to well sorted. Skewness decreases overall with some staying in coarse skewed and others going toward symmetrical. Mahai'ula Beach is the last beach affected by the North Pacific Swell and is on the edge of the climate/weather effect meaning that the effects seen on this beach may be less than the

others. Because of the beach location and less exposure to the North Pacific Swell, skewness trends more toward symmetrical. Kurtosis slightly increases in all transects as distance increases, all being platykurtic. The median for all transects migrates toward finer particles as the distance from the water increases. A distribution graph for each survey point can be seen grouped together by transect in *Figure 3.1.13 – 3.1.18*.

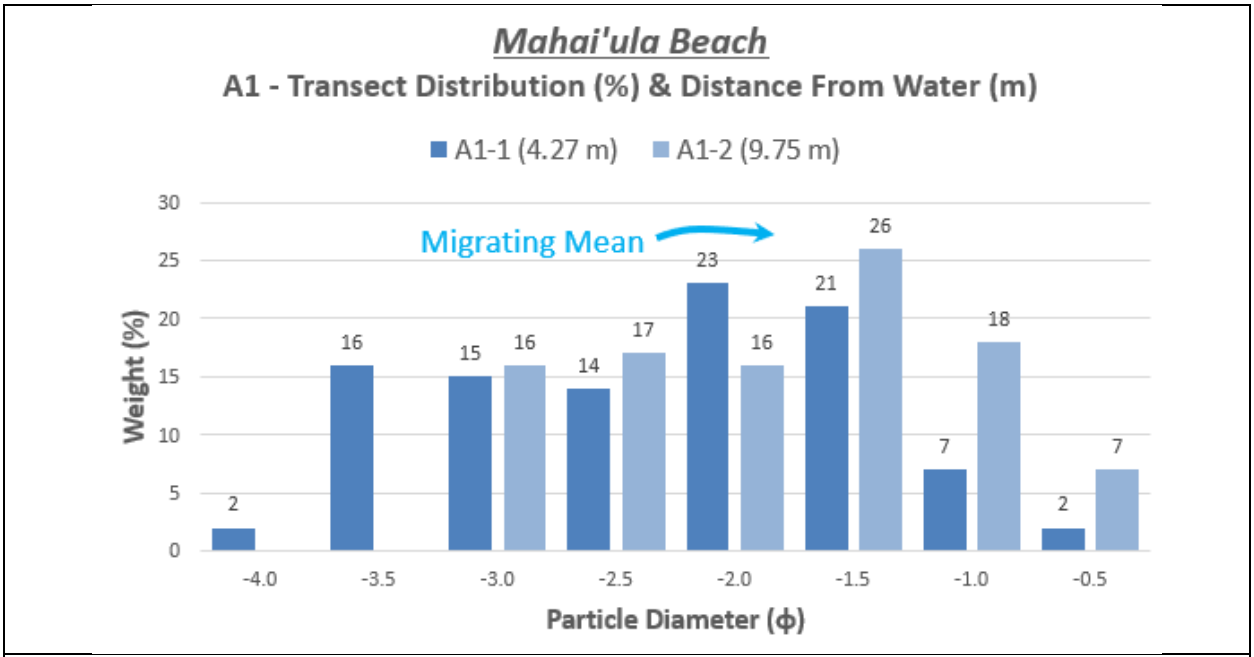

Figure 3.1.13: Mahai'ula Beach distribution graph (% of whole) for all survey points in Transect A1. See *Appendix A.1.7* for location photo and transect locations.

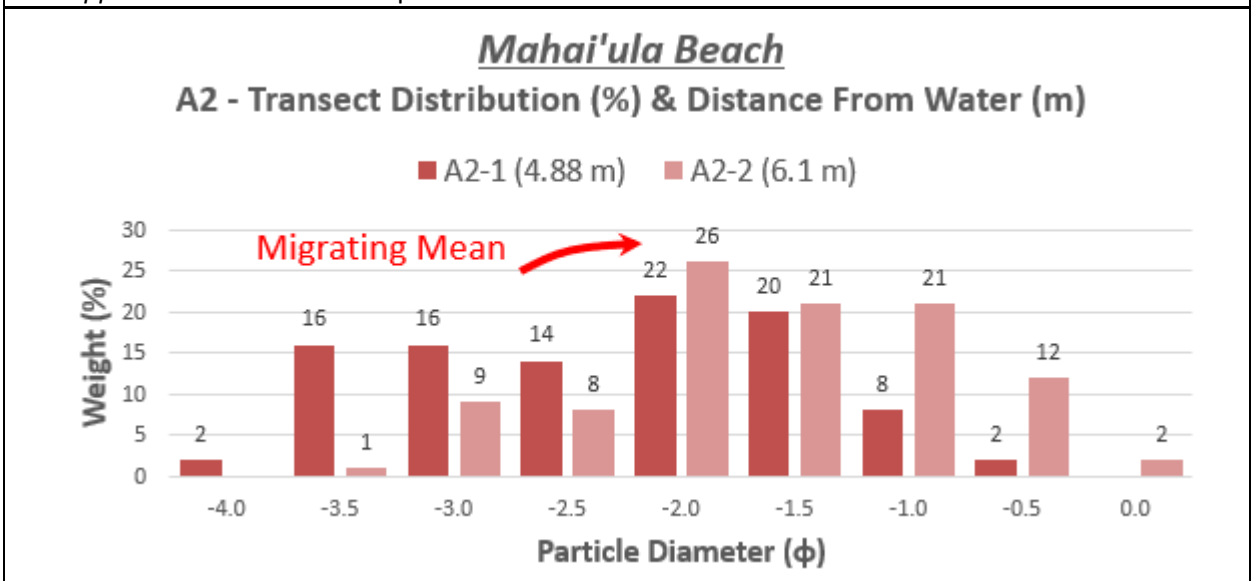

Figure 3.1.14: Mahai'ula Beach distribution graph (% of whole) for all survey points in Transect A2. See *Appendix A.1.7* for location photo and transect locations.

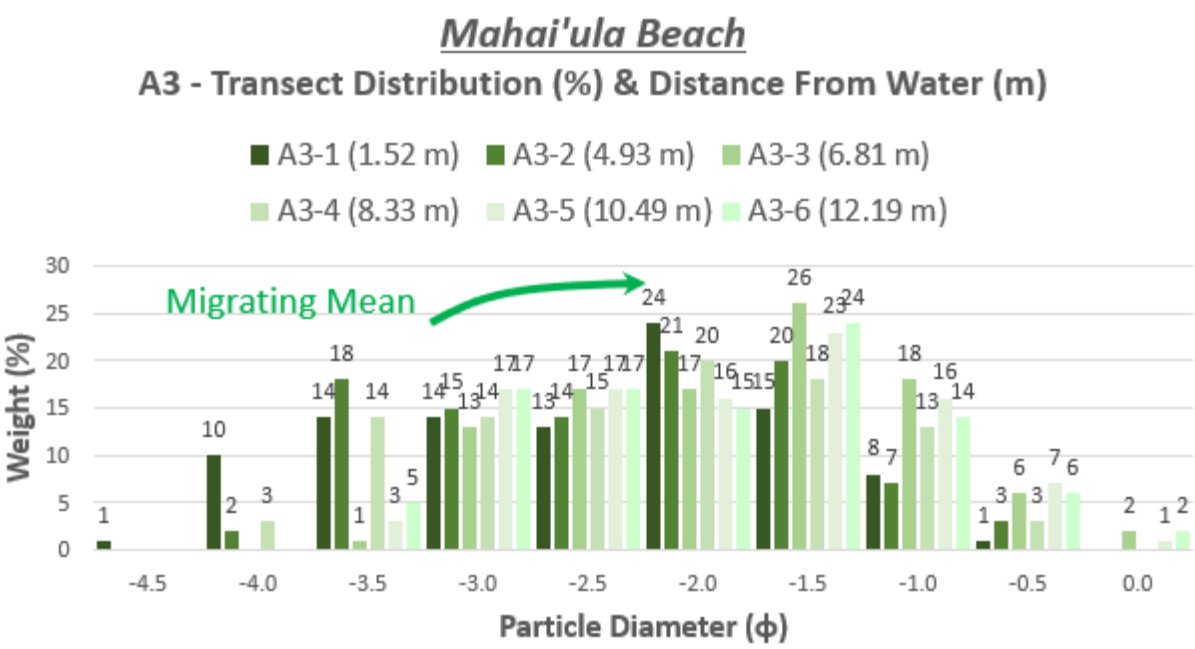

Figure 3.1.15: Mahai'ula Beach distribution graph (% of whole) for all survey points in Transect A3. See *Appendix A.1.7* for location photo and transect locations.

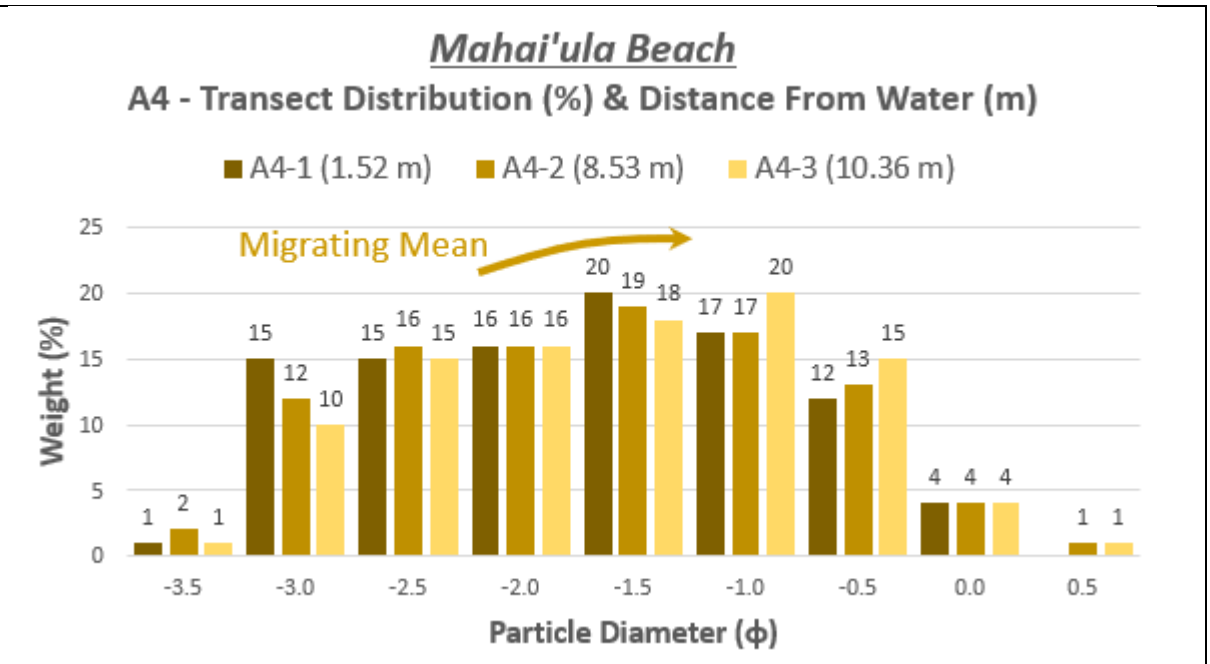

Figure 3.1.16: Mahai'ula Beach distribution graph (% of whole) for all survey points in Transect A4. See *Appendix A.1.7* for location photo and transect locations.

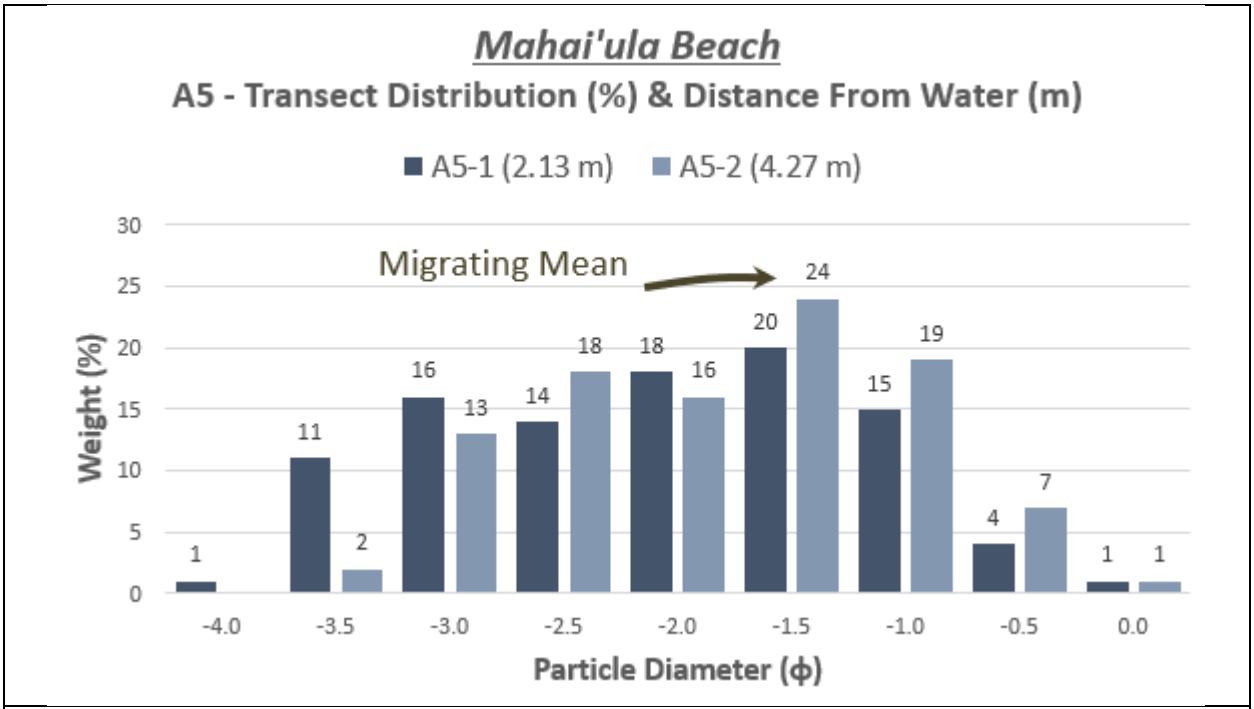

Figure 3.1.17: Mahai'ula Beach distribution graph (% of whole) for all survey points in Transect A5. See *Appendix A.1.7* for location photo and transect locations.

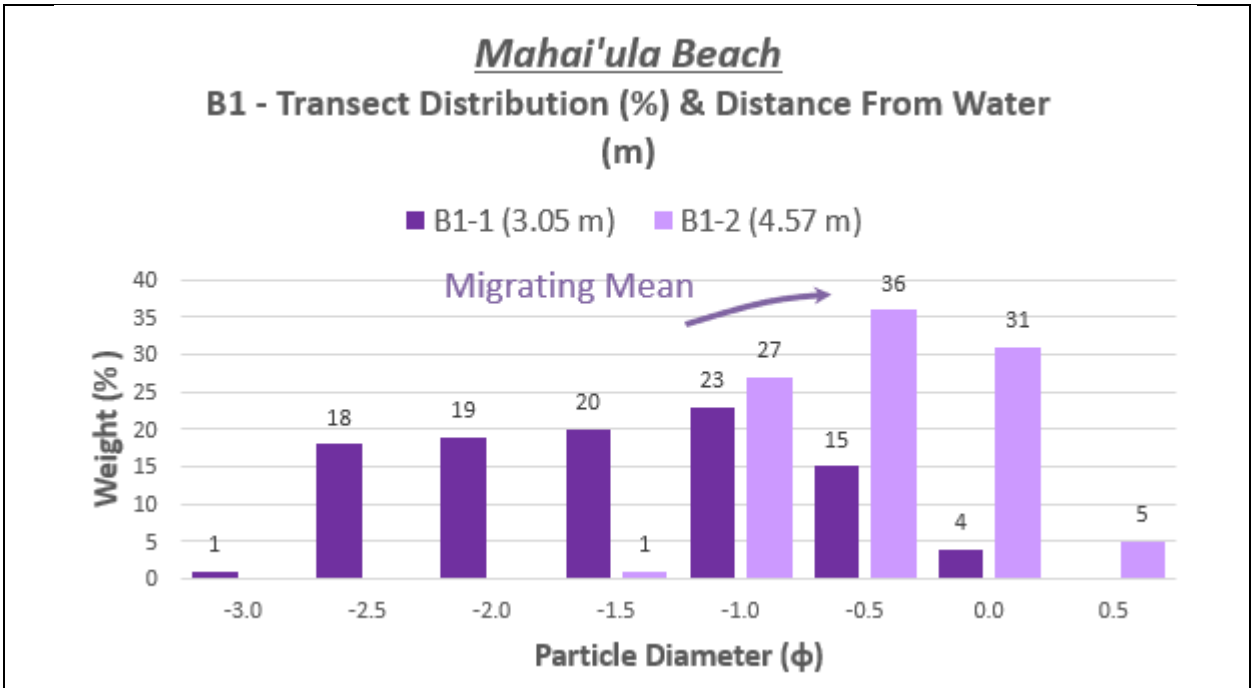

Figure 3.1.18: Mahai'ula Beach distribution graph (% of whole) for all survey points in Transect B1. See *Appendix A.1.7* for location photo and transect locations.

Old Kona Airport Beach is the first beach going counterclockwise that is outside the predicted weather/climate effects (see Figure 2.1.2). As distance from the water increases, sorting slightly increases, staying moderately sorted, skewness slightly decreases, staying symmetrical, and kurtosis slightly increases staying platykurtic. The median grain size migrates toward finer particles as the distance from the water increases. A distribution graph for each survey point can be seen grouped together by transect in *Figure 3.1.19*.

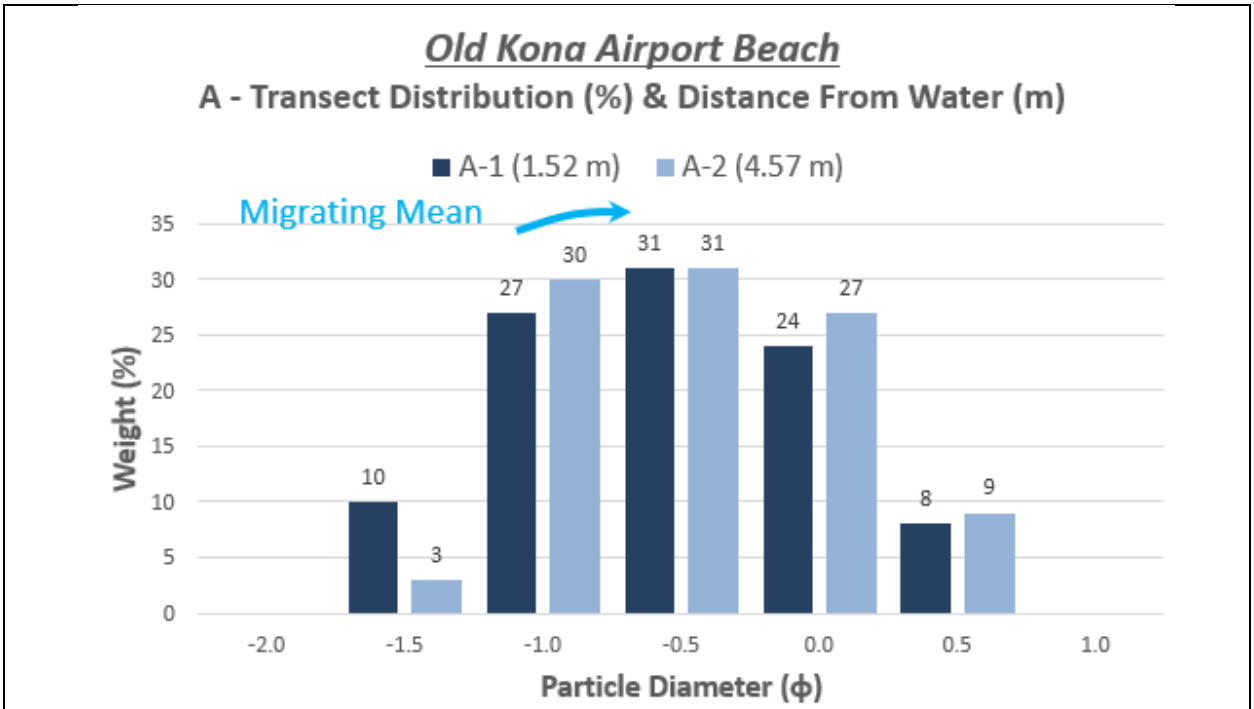

Figure 3.1.19: Old Kona Airport Beach distribution graph (% of whole) for all survey points in Transect A. See *Appendix A.1.8* for location photo and transect locations.

Pahoehoe Beach Park is also outside the predicted weather/climate effects, and as distance from the water increases, sorting slightly increases and then decreases going from moderately well sorted to well sorted to poorly sorted. Skewness varies slightly at all survey sites maintaining symmetrical until the final survey site, which is coarse skewed. The symmetrical skewness is expected since the beach is outside any predicted weather/climate effects; however, the coarse skewness site may be explained by an increase in energy depositing larger grains and a then a winnowing of the finer grains as energy decreases perhaps due to a local storm. Kurtosis slightly decreases, all sites being platykurtic. Like sorting, the median grain size migrates toward finer particles until the last survey site, which includes the

largest grains. A distribution graph for each survey point can be seen grouped together by transect in *Figure 3.1.20*.

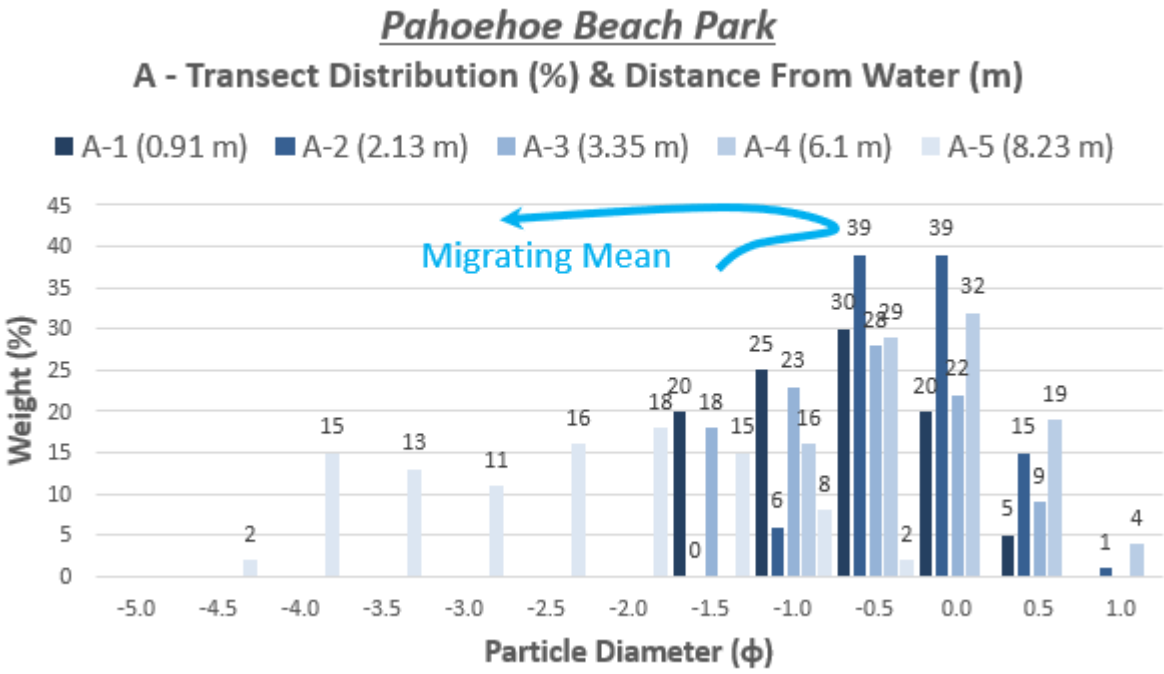

Figure 3.1.20: Pahoehoe Beach Park distribution graph (% of whole) for all survey points in Transect A. See *Appendix A.1.9* for location photo and transect locations.

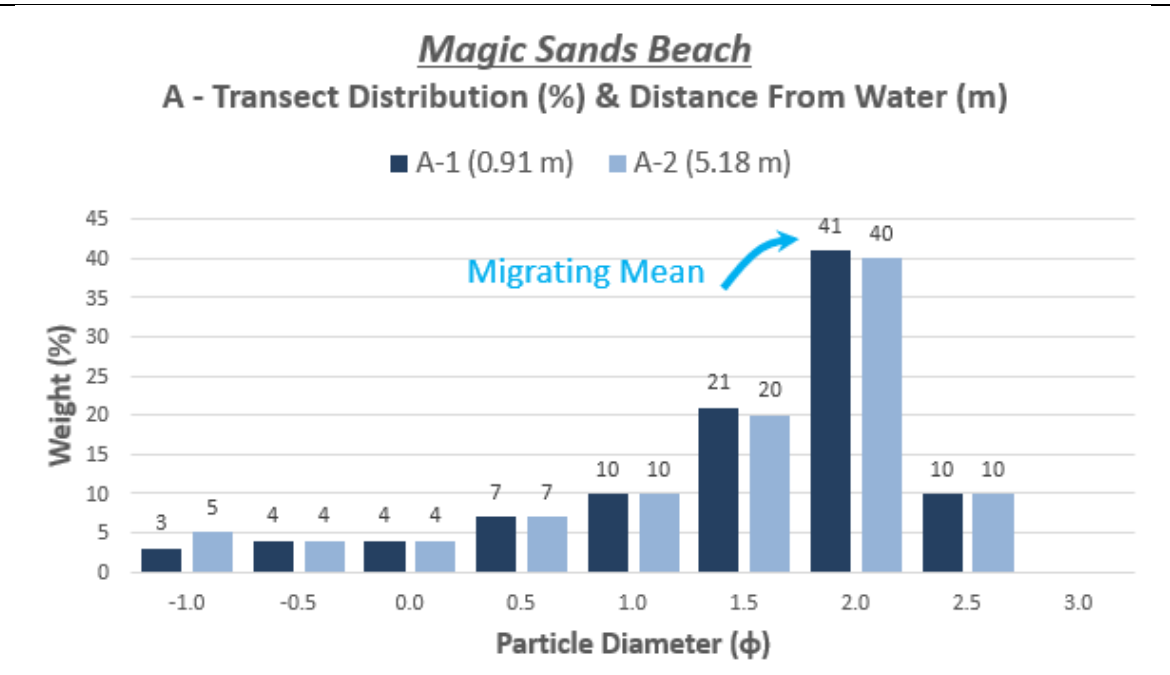

Figure 3.1.21: Magic Sands Beach distribution graph (% of whole) for all survey points in Transect A. See *Appendix A.1.10* for location photo and transect locations.

Magic Sands Beach is outside the predicted weather/climate effects, and as the distance from the water increases, sorting slightly decreases staying moderately well sorted through the transect. Skewness also slightly decreases, being very coarse skewed throughout. Since Magic Sands Beach is known to periodically disappear or erode away during times of high energy such as local storms, the deposited sand skewness may be explained by a winnowing of finer grains as wave energy decreases. Kurtosis slightly decreases being leptokurtic. As the distance from the water increases, the median grain size migrates toward finer particles. A distribution graph for each survey point can be seen grouped together by transect in *Figure 3.1.21*.

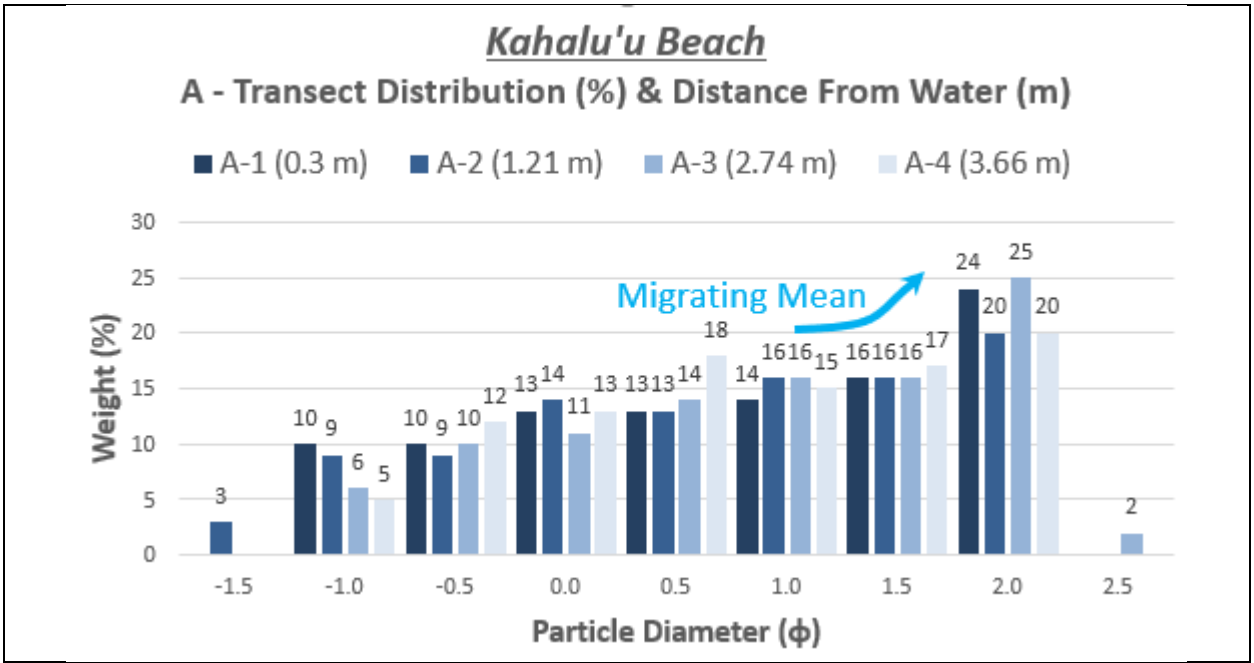

Figure 3.1.22: Kahalu'u Beach distribution graph (% of whole) for all survey points in Transect A. See *Appendix A.1.11* for location photo and transect locations.

Kahalu'u Beach is outside the predicted weather effects and as the distance from the water increases, sorting increases from poorly sorted to moderately sorted. Skewness also increases from coarsely skewed to symmetrical. The skewness trend toward symmetrical can be explained by initial high wave energy depositing large grains while finer grains are depleted as energy decreases, such as is seen as distance from the water increases. Kurtosis slightly increases all being platykurtic. As the distance from the water increases, the median grain size

migrates to finer particles. A distribution graph for each survey point can be seen grouped together by transect in *Figure 3.1.22*.

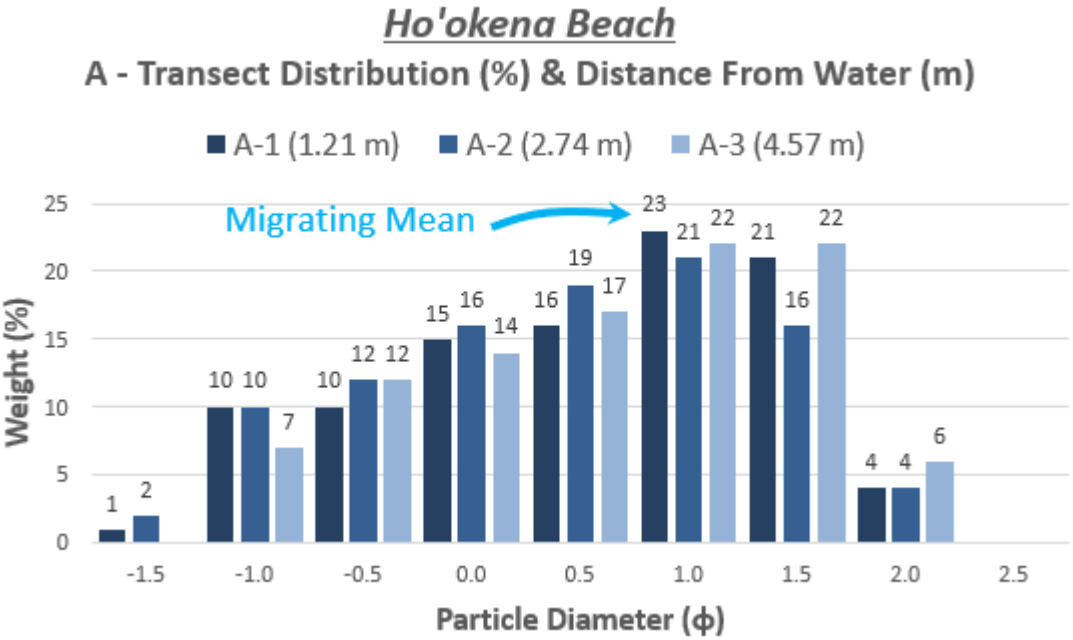

Figure 3.1.23: Ho'okena Beach distribution graph (% of whole) for all survey points in Transect A. See *Appendix A.1.12* for location photo and transect locations.

Ho'okena Beach is the first beach surveyed on the east side of the island that is affected by both the Kona Storm Waves and the Southern Swell. It was found that as distance from the water increases, sorting also slightly increased, all survey sites being moderately sorted. Skewness and kurtosis slightly decreased generally, with all survey sites being coarsely skewed and platykurtic respectively as distance from the water increased. The coarse skewness may be due to storms and higher energy events such as the Kona Storm Waves or Southern Swell depositing larger grains on the beach while finer grains are winnowed away. The median grain size in the transect tends toward finer particles as the distance from the water increased. A distribution graph for each survey point can be seen grouped together by transect in *Figure 3.1.23*.

Pebble Beach is affected by both the Kona Storm Waves and Southern Swell and as the distance from the water increases, sorting decreases going from moderately sorted to poorly sorted. In the same period, skewness and kurtosis slightly decrease being coarsely skewed and

platykurtic respectively at all survey points. Since Pebble Beach is affected by the Kona Storm Waves and the Southern Swell, it is likely that the coarse skewness can be explained through a winnowing of the finer grains. The median grain size in the transect tends toward larger grains as the distance from the water increases. A distribution graph for each survey point can be seen grouped together by transect in *Figure 3.1.24*.

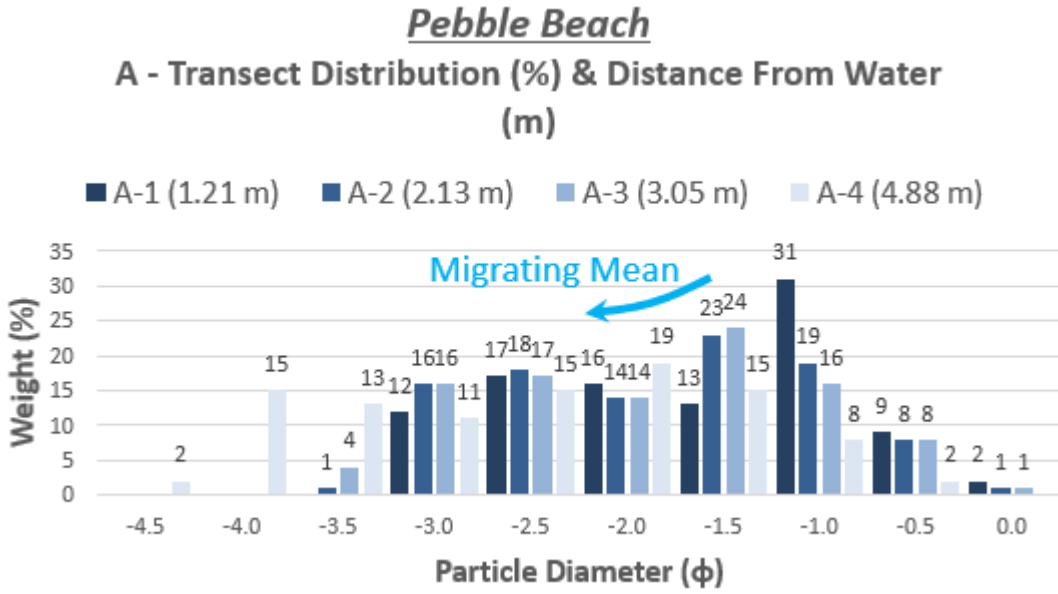

Figure 3.1.24: Pebble Beach distribution graph (% of whole) for all survey points in Transect A. See *Appendix A.1.13* for location photo and transect locations.

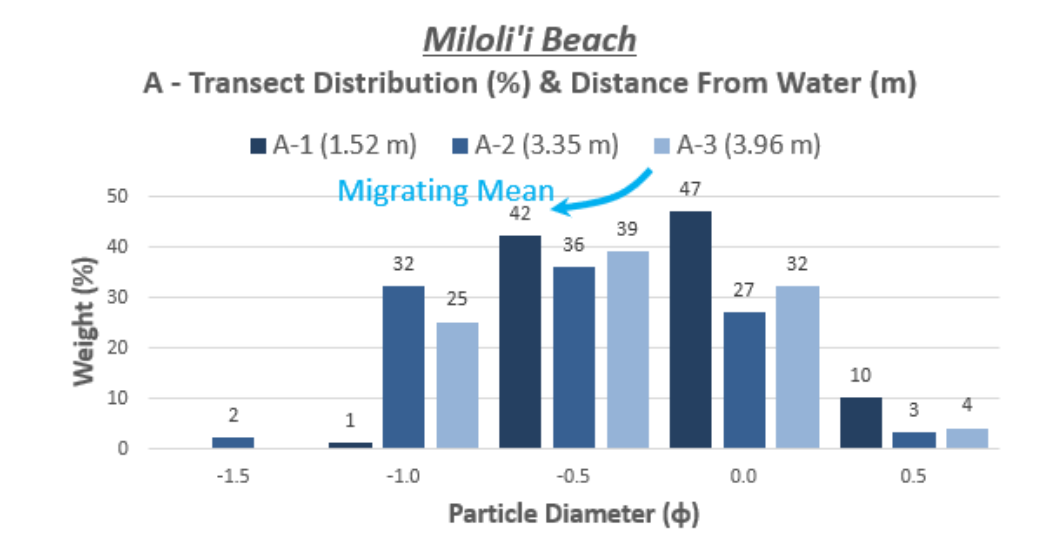

Figure 3.1.25: Miloli'i Beach distribution graph (% of whole) for all survey points in Transect A. See *Appendix A.1.14* for location photo and transect locations.

Miloli'I Beach is affected by the Kona Storm Waves and the Southern Swell. As distance from the water increases, sorting slightly decreases all being well sorted. In the same period, skewness and kurtosis both slightly decrease being symmetrical and platykurtic respectively. The median grain size tends toward larger grains as the distance from the water increases. A distribution graph for each survey point can be seen grouped together by transect in *Figure 3.1.25*.

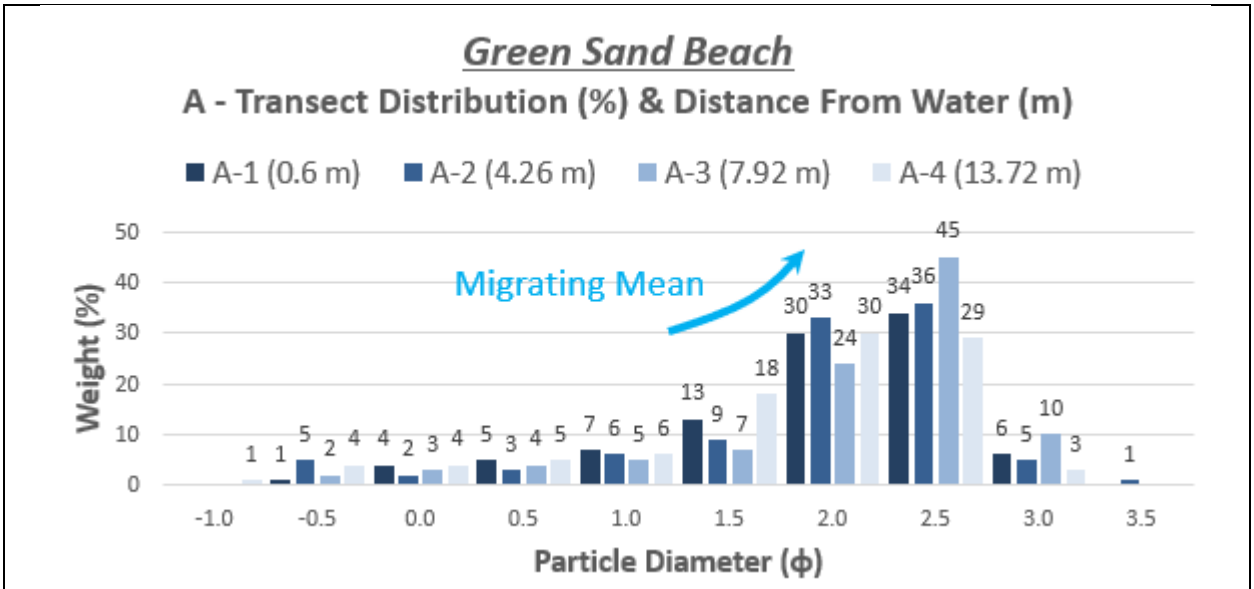

Figure 3.1.26: Green Sand Beach distribution graph (% of whole) for all survey points in Transect A. See *Appendix A.1.15* for location photo and transect locations.

Green Sand Beach is affected by both the Kona Storm Waves and the Southern Swell. As distance from the water increases, sorting slightly decreases from moderately well sorted to moderately sorted. In the same period, skewness slightly decreases and kurtosis slightly increases, being very coarsely skewed and leptokurtic respectively. Since Green Sand Beach is the Southern-most beach and is on the Southern-most part of the island, it is exposed and subject to high energy weather and climate, likely explaining the coarse skewness where larger grains would be deposited and finer grains winnowed away. As distance from the water increases, the median grain size tends toward finer particles. A distribution graph for each survey point can be seen grouped together by transect in *Figure 3.1.26*.

Punalu'u Beach is affected by both the Kona Storm Waves and the Southern Swell. As distance from the water increases, sorting increases in all transects, from moderately sorted to

moderately well sorted in Transects A, B, and C, moderately sorted in all in Transect D, and poorly sorted to moderately well sorted in Transect E. Skewness increases for Transects A, B, C, and D, going from coarsely skewed to symmetrical in Transects A and B and maintaining coarse skewed in Transect B and symmetrical in Transect D. Skewness in Transect E slightly decreased going from being coarsely skewed to being symmetrical. The angular morphology of this beach, as well as the exposure to the Kona Storm Waves and the Southern Swell, likely explain the skewness trends, where coarse skewness is due to higher wave energy and the depositing of larger grains and the symmetrical skewness where wave energy is depleted. Kurtosis slightly increased in all transects with all survey sites being platykurtic. The median grain size tends toward larger particles for Transects B, C, and D as the distance from the water increases. The median grain size for Transect A seems to vary, first decreasing toward finer particles and then increasing toward larger grains. In the same period, the median grain size for Transect E first tended towards larger grains, and then toward finer grains. A distribution graph for each survey point can be seen grouped together by transect in *Figure 3.1.27 – Figure 3.1.31*.

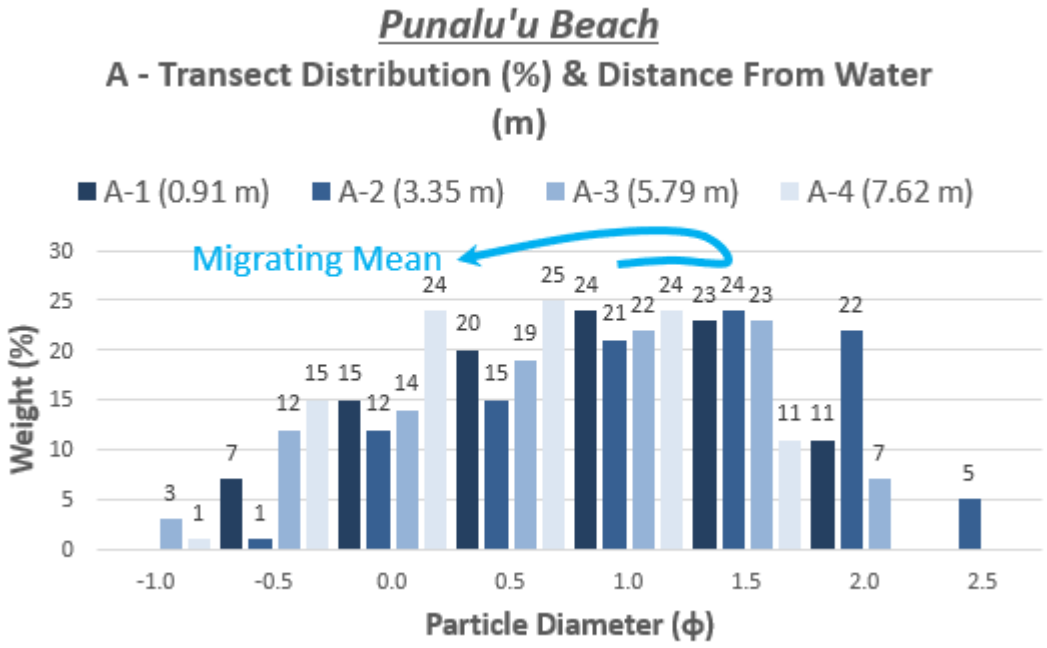

Figure 3.1.27: Punalu'u Beach distribution graph (% of whole) for all survey points in Transect A. See *Appendix A.1.16* for location photo and transect locations.

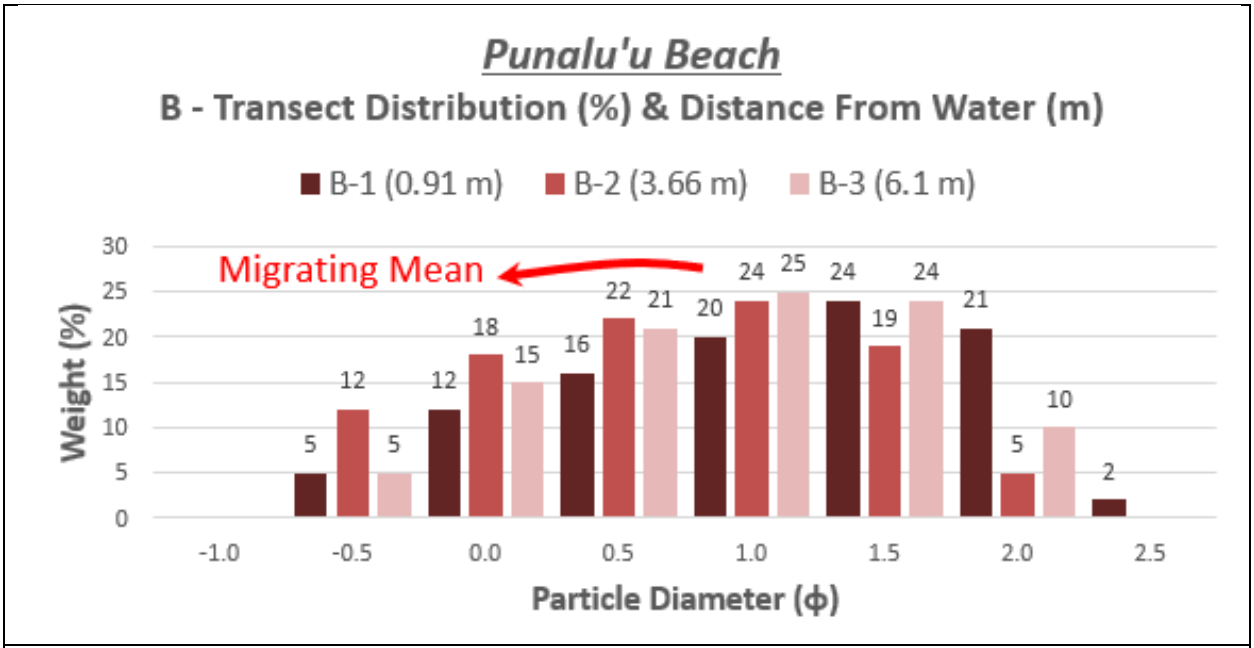

Figure 3.1.28: Punalu'u Beach distribution graph (% of whole) for all survey points in Transect B. See *Appendix A.1.16* for location photo and transect locations.

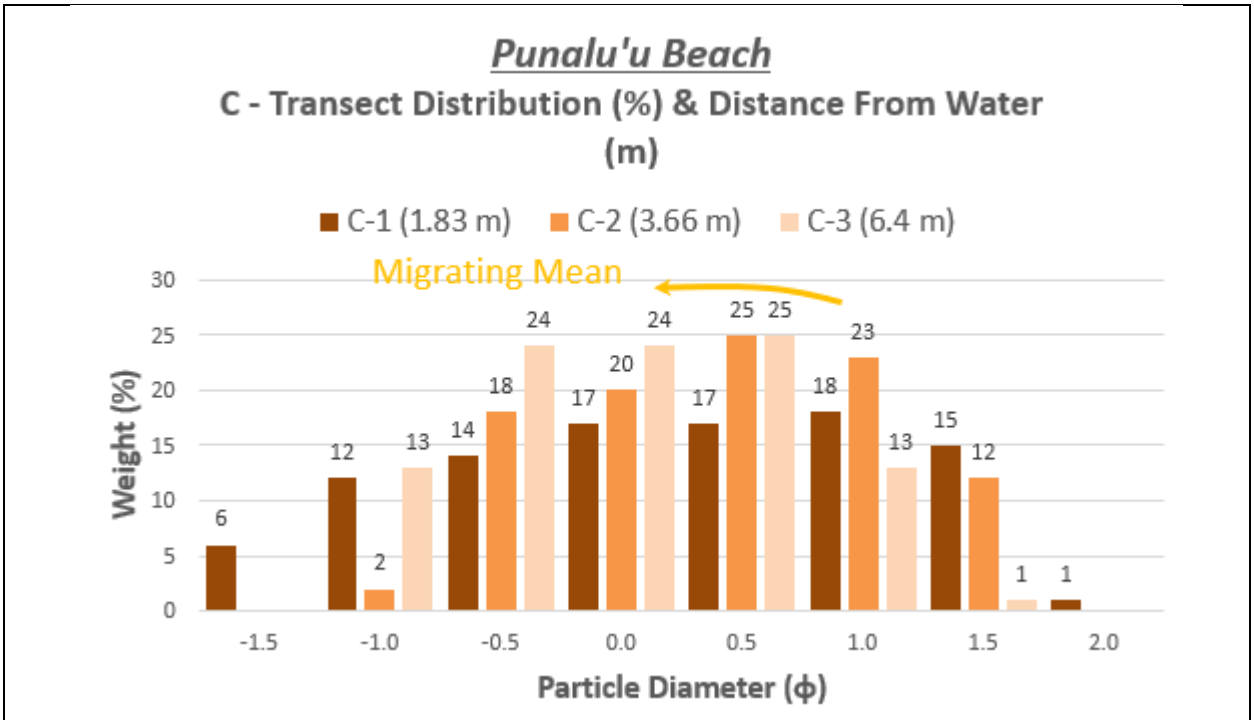

Figure 3.1.29: Punalu'u Beach distribution graph (% of whole) for all survey points in Transect C. See *Appendix A.1.16* for location photo and transect locations.

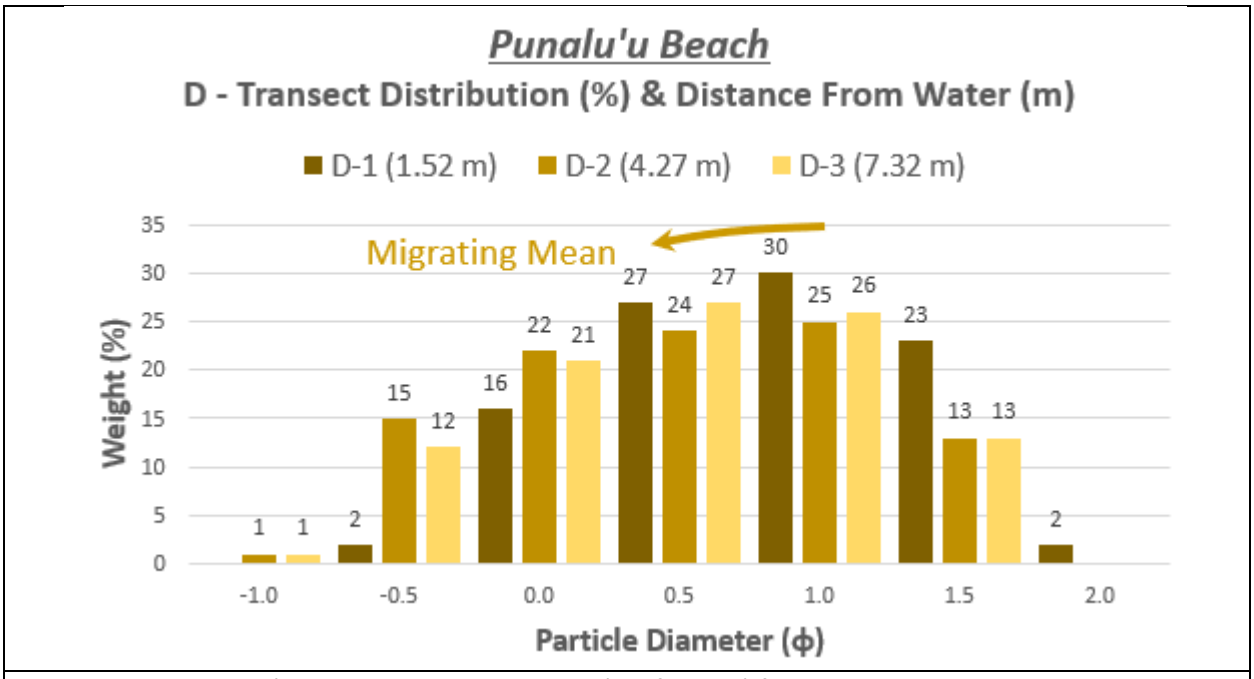

Figure 3.1.30: Punalu'u Beach distribution graph (% of whole) for all survey points in Transect D. See *Appendix A.1.16* for location photo and transect locations.

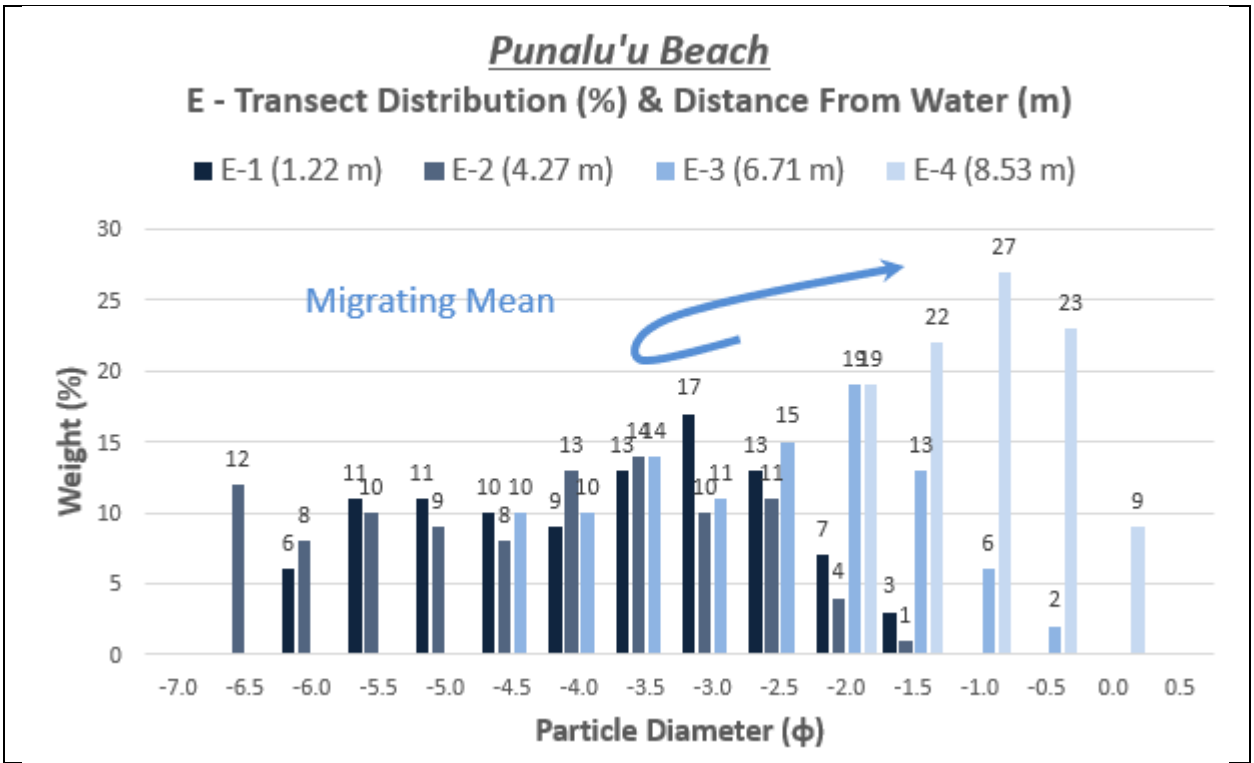

Figure 3.1.31: Punalu'u Beach distribution graph (% of whole) for all survey points in Transect E. See *Appendix A.1.16* for location photo and transect locations.

Pohoiki Beach is subject to the Northeast Tradewind Waves and as distance from the water increases, sorting generally decreased from moderately sorted to poorly sorted. In the same period, skewness and kurtosis both slightly decrease being coarsely skewed and platykurtic respectively. The coarse skewness can be explained by a depositing of larger material during high energy such as waves from the Northeast Tradewind while finer material is subsequently winnowed away. The median grain size overall tends toward larger particles as the distance from the water increases. A distribution graph for each survey point can be seen grouped together by transect in *Figure 3.1.32*.

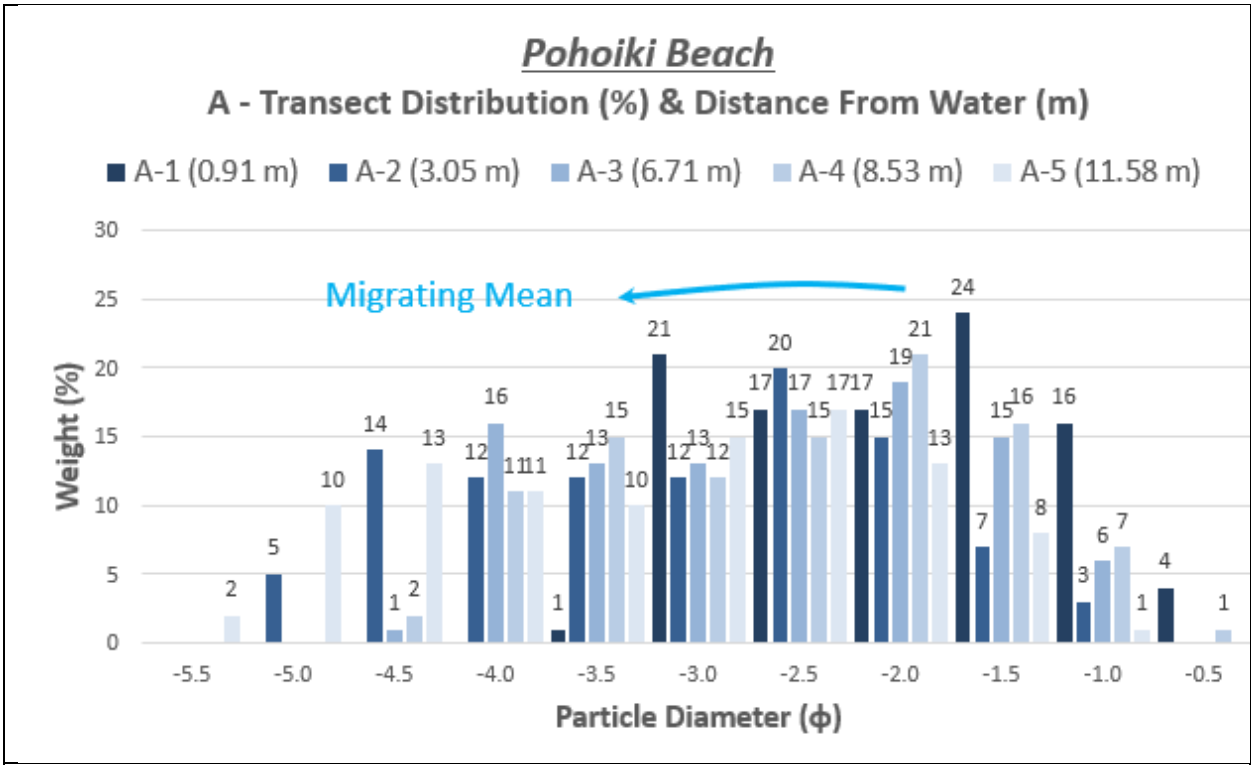

Figure 3.1.32: Pohoiki Beach distribution graph (% of whole) for all survey points in Transect A. See *Appendix A.1.17* for location photo and transect locations.

Honoli'I Beach is affected by the Northeast Tradewind Waves and as the distance from the water increases, sorting increases from moderately sorted to moderately well sorted. In the same period, skewness and kurtosis both slightly increase being symmetrical and platykurtic respectively. As the distance from the water increases, the median grain size for Transect A tends toward finer particles and tends toward larger particles for Transect B. A distribution

graph for each survey point can be seen grouped together by transect in *Figure 3.1.33 – Figure 3.1.34*.

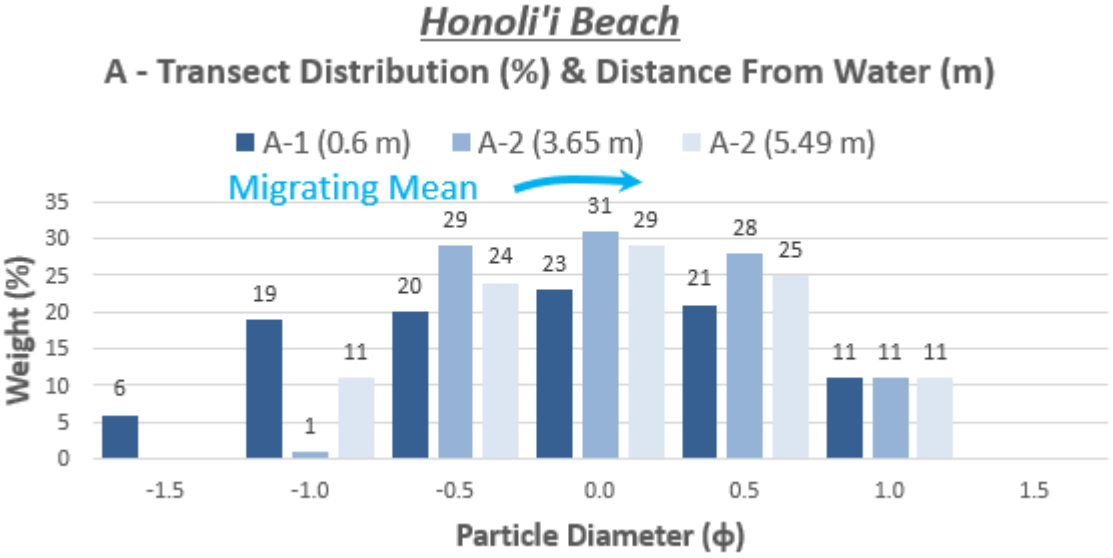

Figure 3.1.33: Honoli'i Beach distribution graph (% of whole) for all survey points in Transect A. See *Appendix A.1.18* for location photo and transect locations.

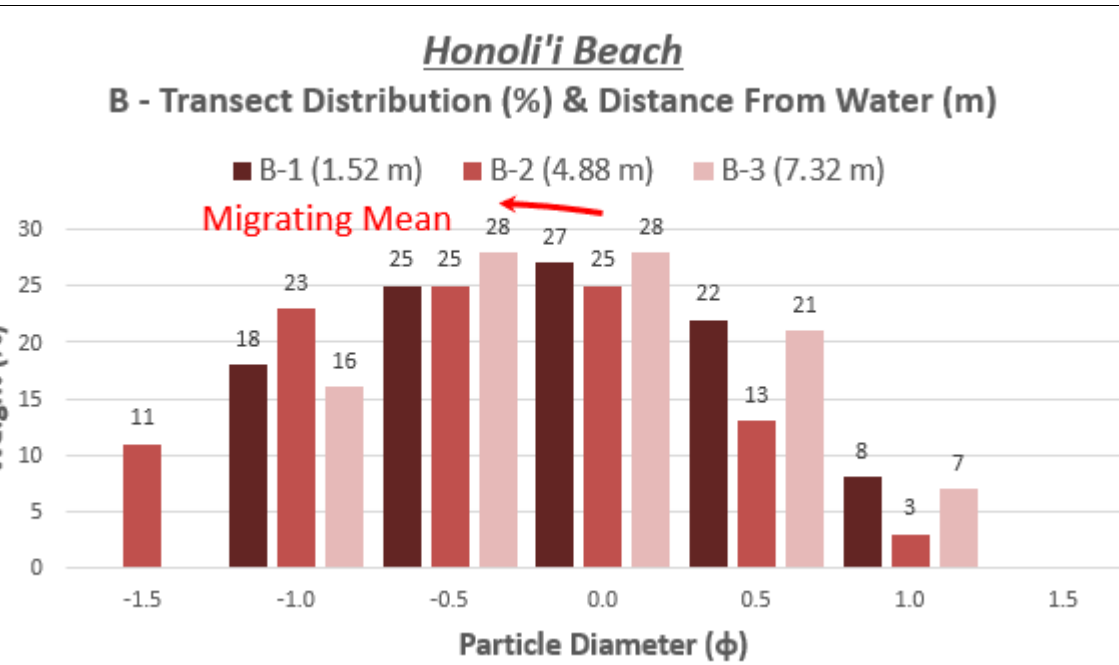

Figure 3.1.34: Honoli'i Beach distribution graph (% of whole) for all survey points in Transect B. See *Appendix A.1.18* for location photo and transect locations.

3.2 Mars Sands

The Bagnold Dunes distribution graphs can be seen grouped by the two dunes namely the High Dune and the Namib Dune in *Figure 3.2.1 – Figure 3.2.2*. The Namib Dune is better sorted than the sands at the High Dune; Namib Dunes being well sorted and High Dunes being moderately well sorted. High Dune sands are coarsely skewed, and Namib Dune sands are very coarsely skewed. The skewness is explained by a winnowing of finer materials due to winds in the dunes, as is observed by Ehlmann et al. (2018). All sites at both the High Dunes and Namib Dunes are platykurtic except for the Otavi site which is mesokurtic.

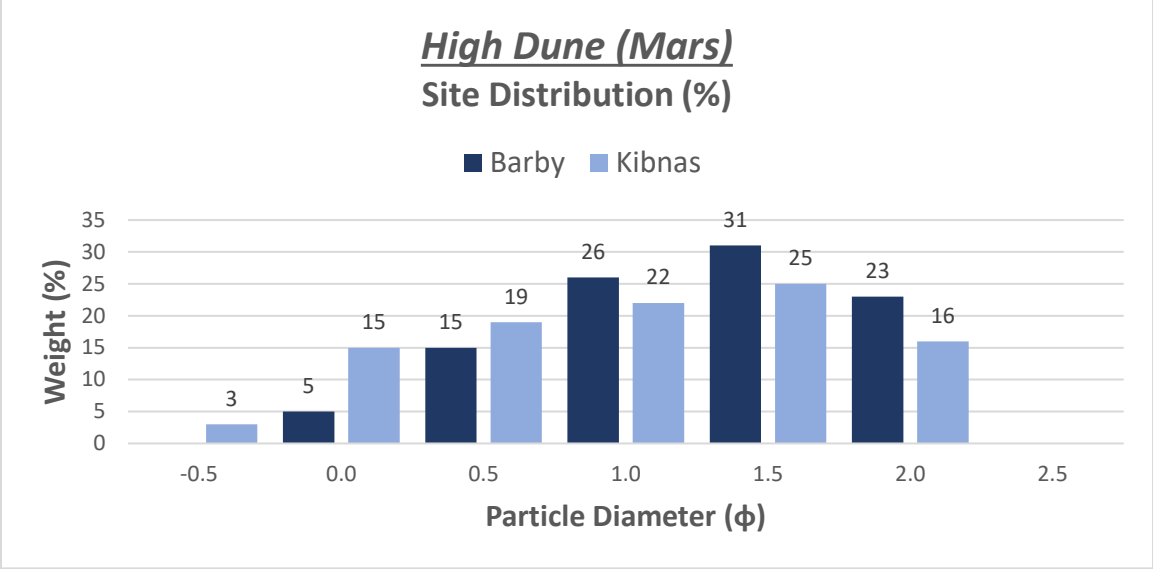

Figure 3.2.1: High Dune distribution graph (% of whole) for both the Barby and the Kibnas sites.

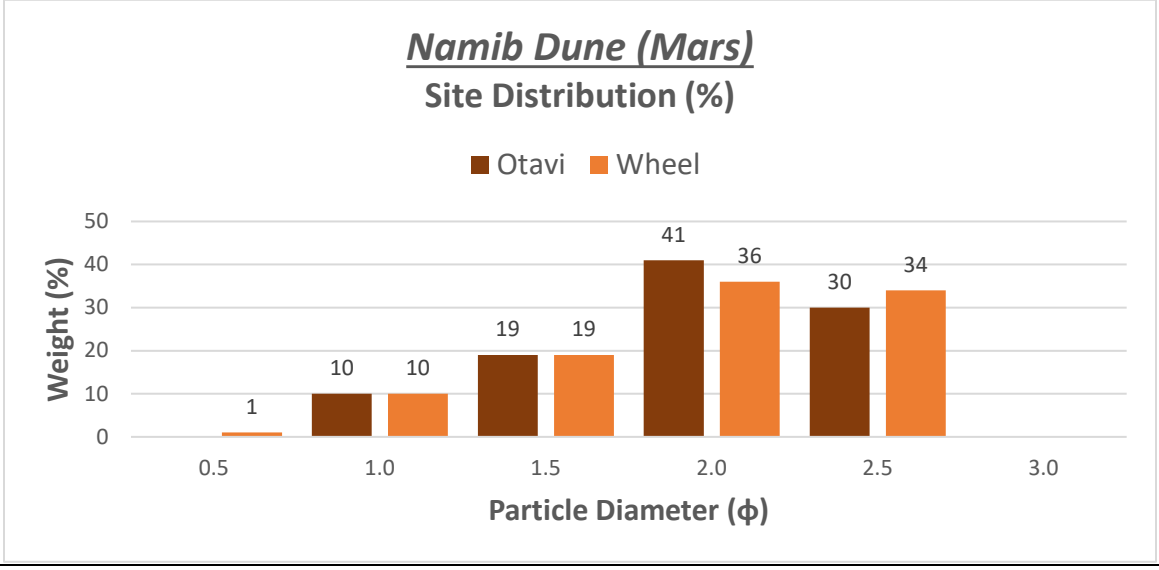

Figure 3.2.2: Namib Dune distribution graph (% of whole) for both the Otavi and the Wheel sites.

3.3 Weather Effects

As seen in *Figure 2.1.2*, each of the 18 beaches can be categorized by what weather effects they are subject to. By categorizing the beaches, it becomes apparent as to what effects the weather/climate has on each beach. That being said, it should be noted that one of the two beaches affected by the Northeast Tradewind Waves is very young (Pohoiki Beach) and a lava flow covered the existing beach in 2018. Nevertheless, there are some telling results from said categorization and the statistical moments can be seen in *Table 3.3.1*.

	Average				
	50th % (ϕ)	**Slope**	**Std Dev.**	**Skewness**	**Kurtosis**
NPS	0.02	-7.08	0.762	-0.329	4.247
KSWandSS	-0.24	-10.74	0.770	-0.175	0.902
NTW	-1.45	-11.09	0.788	-0.080	0.796
OPE	-0.07	-5.77	0.770	-0.156	0.859

Table 3.3.1: The average for the statistical moments, including the slope for the beaches associated with each weather/climate effects, those being the North Pacific Swell Beaches (NPS), Kona Storm Waves and Southern Swell Beaches (KSWandSS), Northeast Tradewind Wave Beaches (NTW), and those beaches outside predicted effects (OPE).

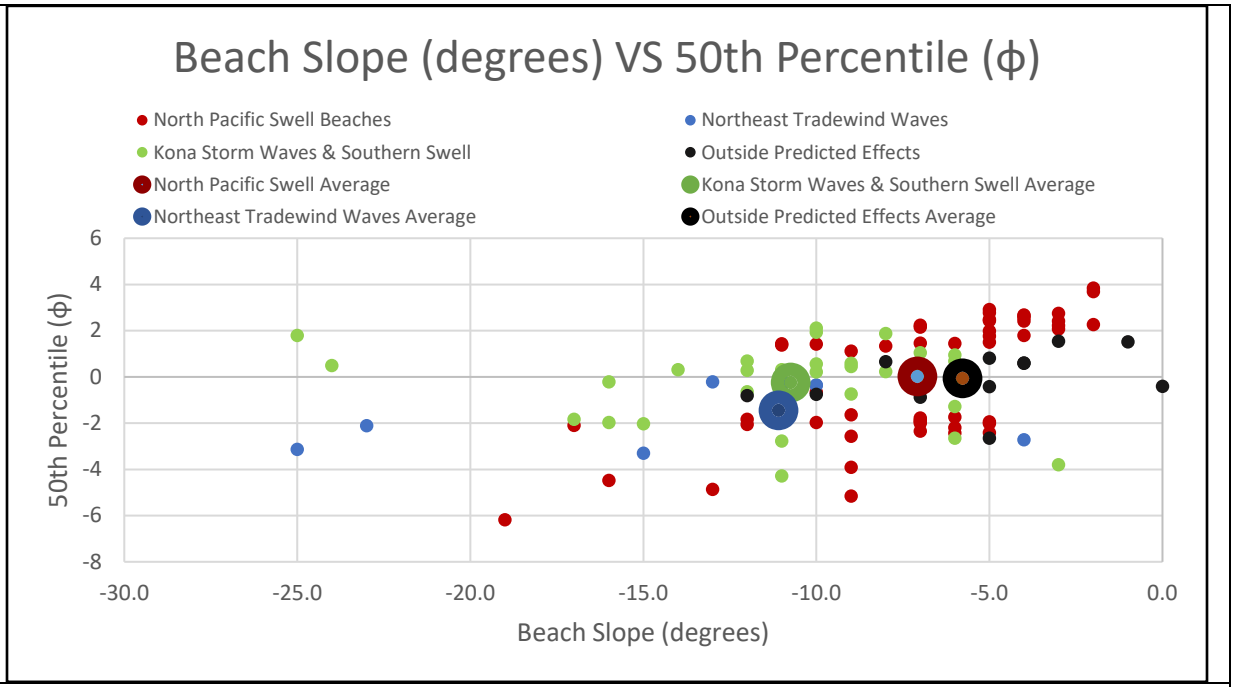

Figure 3.3.1: Beach Slope vs 50th Percentile showing the averages and the relationship between the two.

The average 50th percentile for each beach can be seen in *Table 3.3.1* and shows that the beaches subject to the North Pacific Swell tend to have the smallest grain sizes (average of

0.02 ϕ) while those effected by the Northeast Tradewind Waves have the largest grain sizes (-1.45 ϕ); though it should be noted that this statistic could be skewed due to recent lava flows. It also should be noted that the steepest beaches seem to be those subject to the Kona Storm Waves, Southern Swell, and the Northeast Tradewind Waves (*Figure 3.3.1*). Standard deviation, or sorting, also shows a relationship; as the distance from the water increases, sorting also increases on those beaches affected by the Kona Storm Waves, Southern Swell, and those outside the predicted effects and actually decreases on those beaches affected by the North Pacific Swell and the Northeast Tradewind Waves (*Figure 3.3.2*).

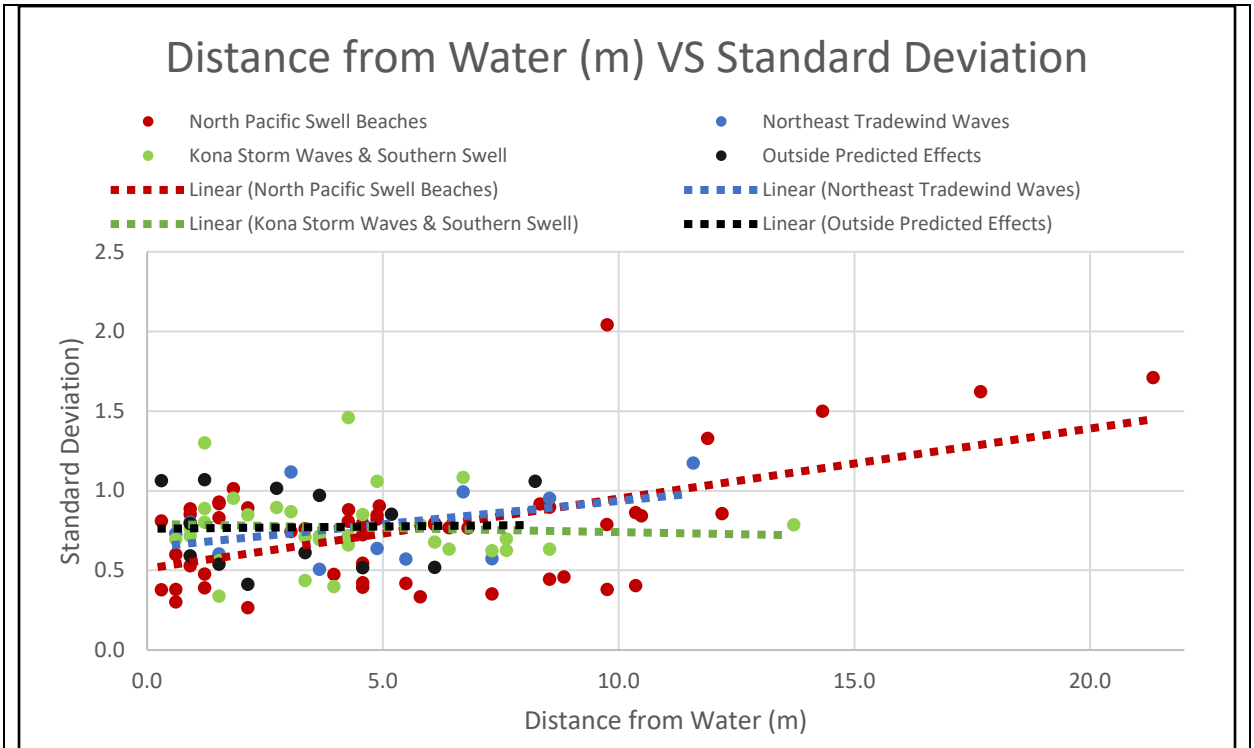

Figure 3.3.2: Distance from water vs Standard Deviation (sorting) graph showing a positive relationship for those beaches subject to the North Pacific Swell and Northeast Tradewind Waves and a negative relationship in those beaches affected by the Kona Storm Waves, Southern Swell, and those outside the predicted effects.

Skewness seems to have a relationship with the 50th percentile (*Figure 3.3.3*) and average skewness seems to be lowest (more finely skewed) on those beaches affected by the North Pacific Swell while those beaches affected by the other weather/climate effects have a higher skewness value (more coarsely skewed). Coarsely skewed relationships often indicate an addition of larger grains during higher energy times and a winnowing of finer materials as

energy decreases. Kurtosis is very similar on beaches affected by the Kona Storm Waves, Southern Swell, Northeast Tradewind Waves, and those outside the predicted effects, but is considerably higher on those beaches affected by the North Pacific Swell (*Figure 3.3.4*).

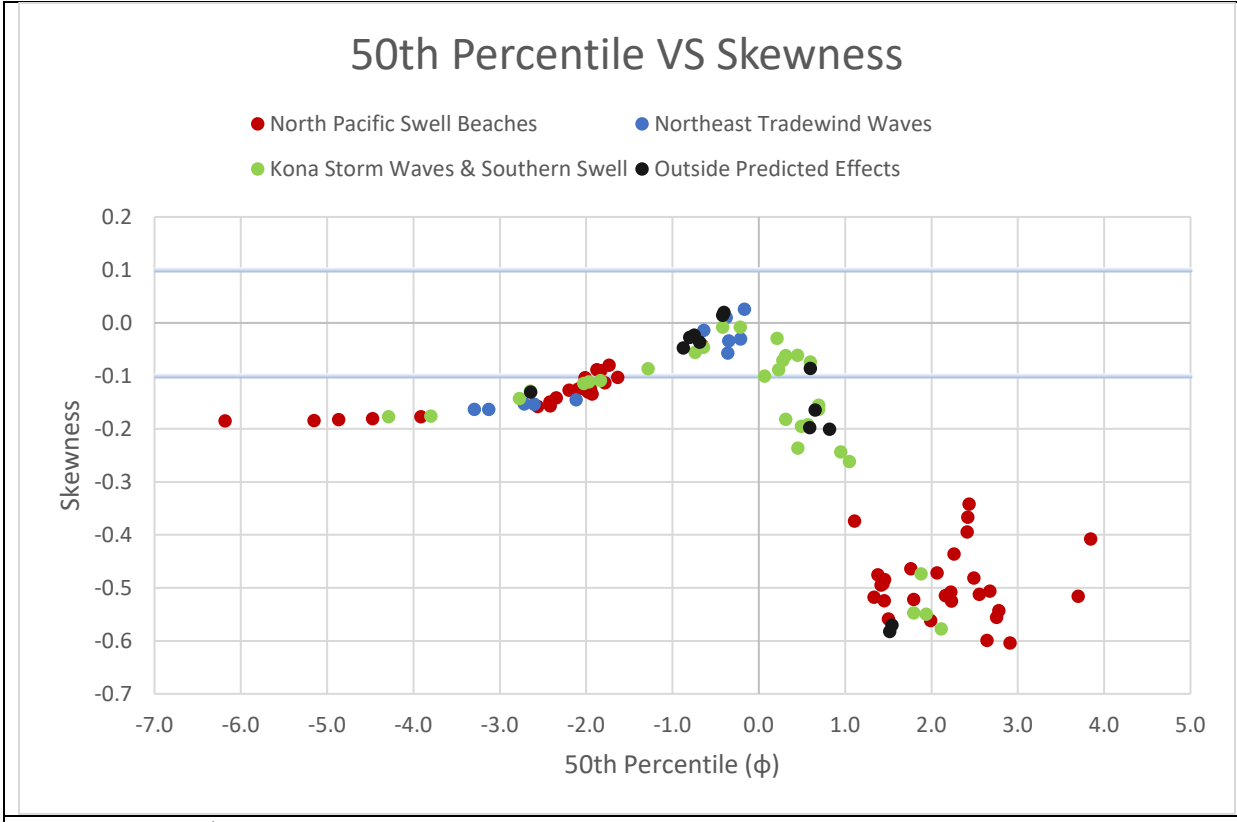

Figure 3.3.3: 50th Percentile graphed against Skewness showing the relationship between the two. Above the top blue line is described as fine skewed (0.1 – 0.3), in between both blue lines is described as symmetrical (-0.1 – 0.1), and below the last blue line is considered coarse skewed (-0.3 – -0.1).

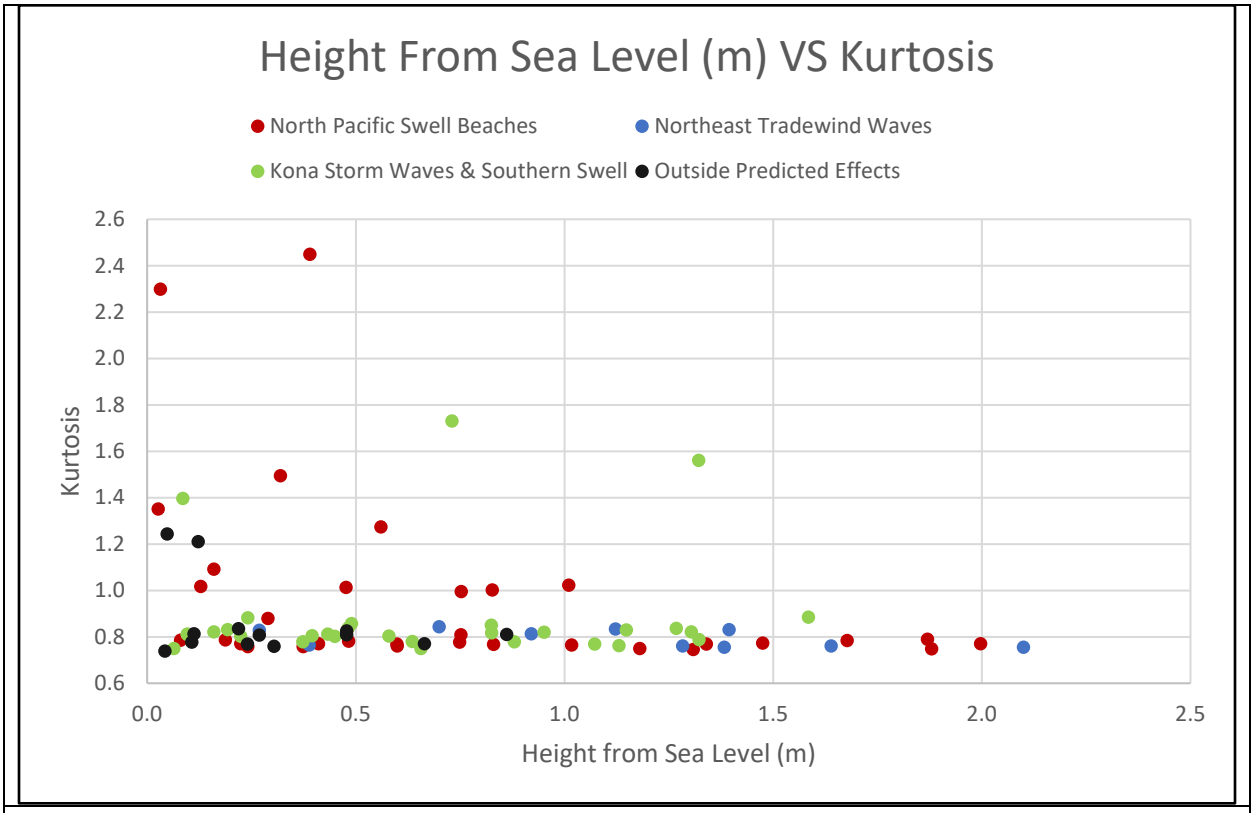

Figure 3.3.4: Height from sea level vs Kurtosis graph showing the relationship between the two.

3.4 Exposed Shorelines Within a Bay/Inlet Relationships

The transects surveyed were also directed to assess the effects and differences on an exposed shoreline within a bay or inlet on the outsides of the shoreline vs the inside or middle (see *Figure 3.4.0* for an example being Manini'owali Beach). Those beaches where bay/inlet shoreline surveys were possible are Pololu Beach, Waialea Beach, Manini'owali Beach, and Punalu'u Beach. Linear graphs were created to show the relationships and trends in the statistical moments and those can be seen in *Figure 3.4.1 – Figure 3.4.4*. The 50th percentile shows that smaller grains tend toward the middle of a bay/inlet shoreline (*Figure 3.4.1*). Standard deviation (sorting) showed a wider spread for the outsides of the bay and a smaller spread for the inside or middle of the bay, and the average is lower for the middle than the outsides of the bay meaning that the middle has better sorting than the outsides (*Figure 3.4.2*). Skewness was very similar for both the outsides and insides of the bay beaches, with the inside or middle having a slightly lower value (*Figure 3.4.3*). Kurtosis is also very similar for both the

outside and middle of the bay with the insides or middle having a slightly higher value than the outsides (*Figure 3.4.4*).

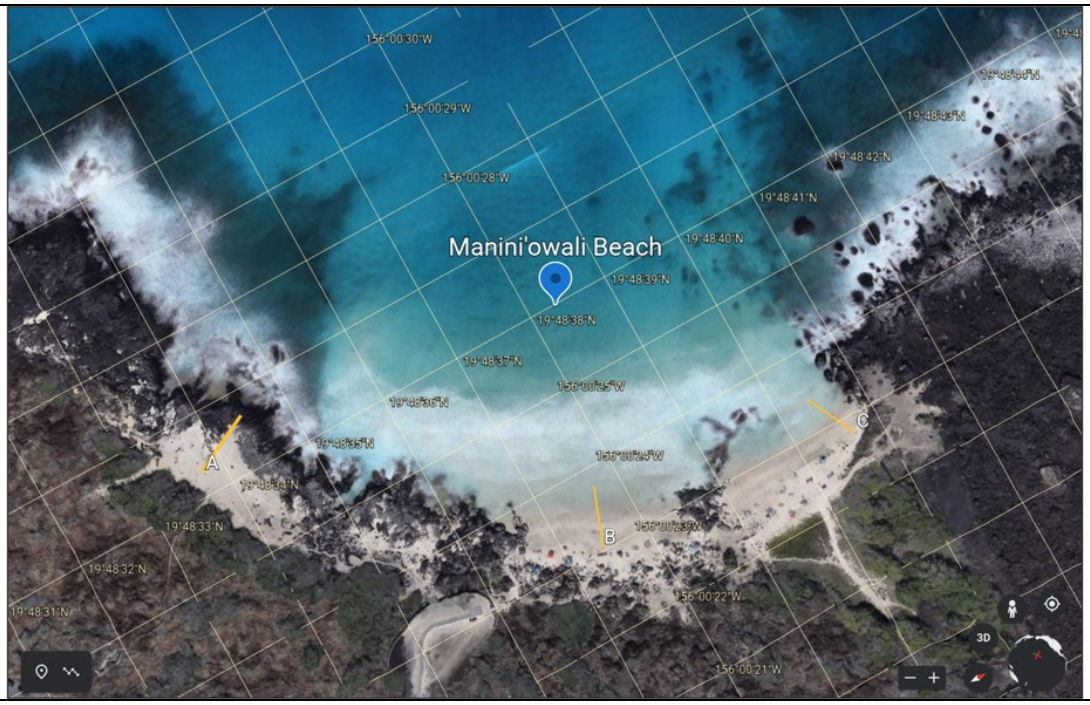

Figure 3.4.0: An example of one of the beaches where an exposed shoreline within an inlet was able to be sampled. This exposed beach is Manini'owali Beach.

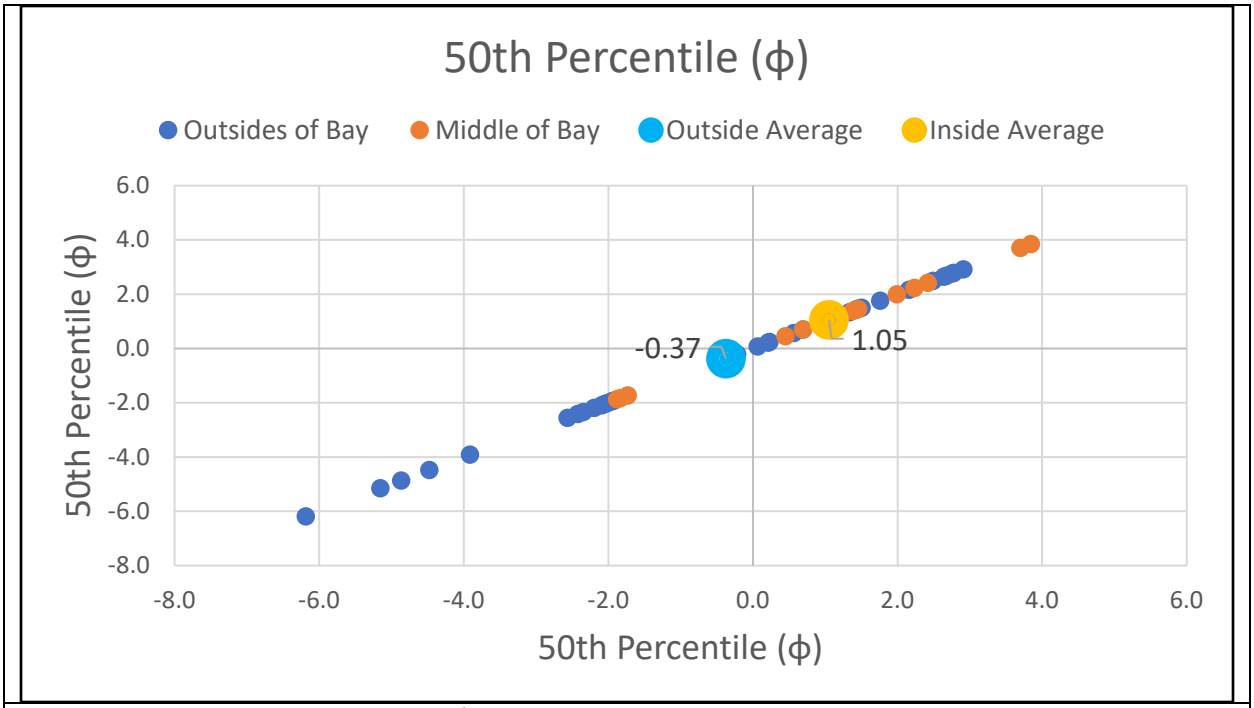

Figure 3.4.1: A linear graph of the 50th Percentile (ϕ) showing the differences between the outsides and inside of a bay or inlet.

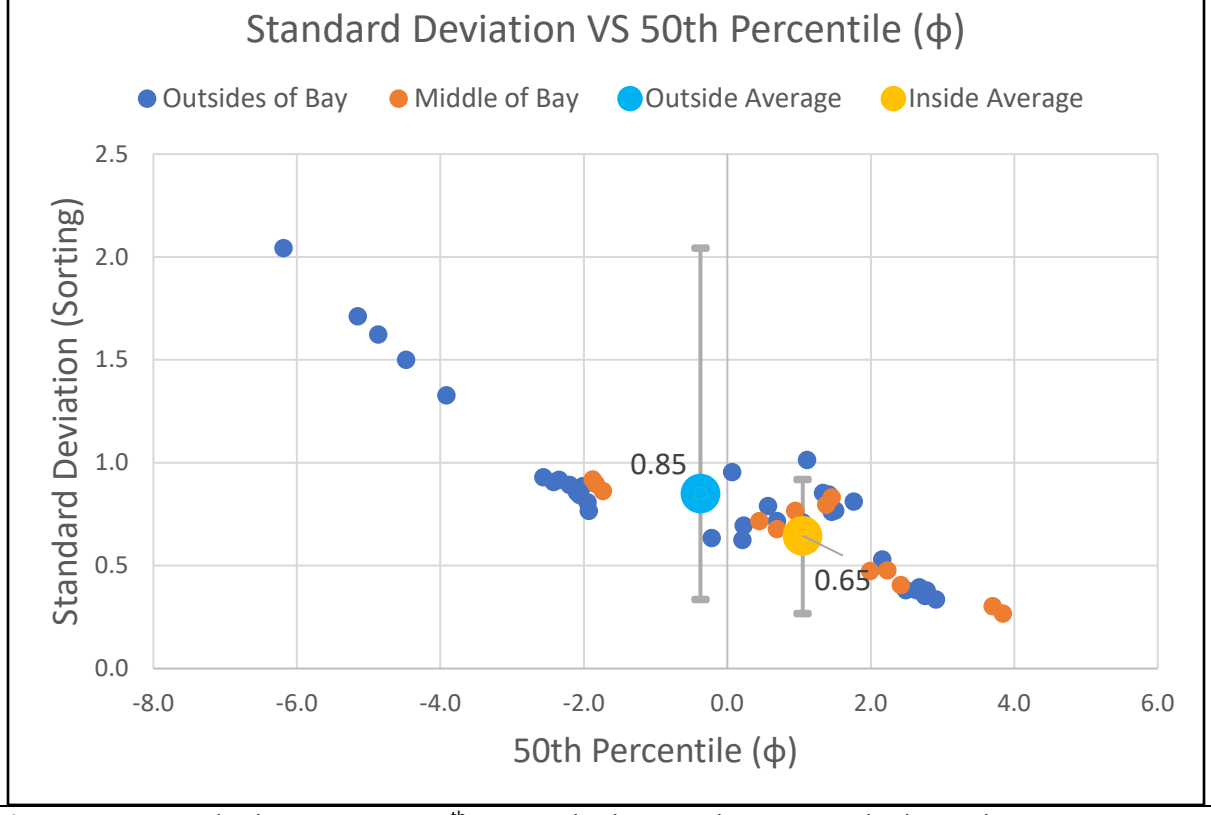

Figure 3.4.2: Standard Deviation vs 50th Percentile showing the range and relationship.

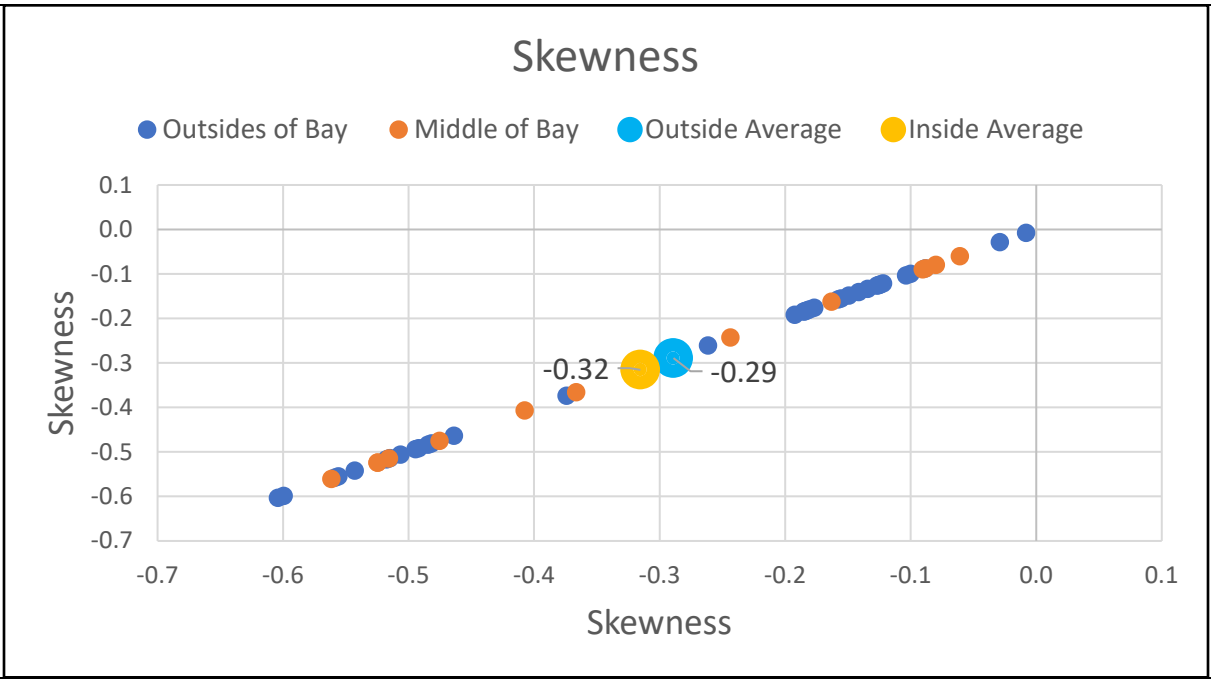

Figure 3.4.3: A linear graph of the skewness showing the differences between the outsides and inside of a bay or inlet.

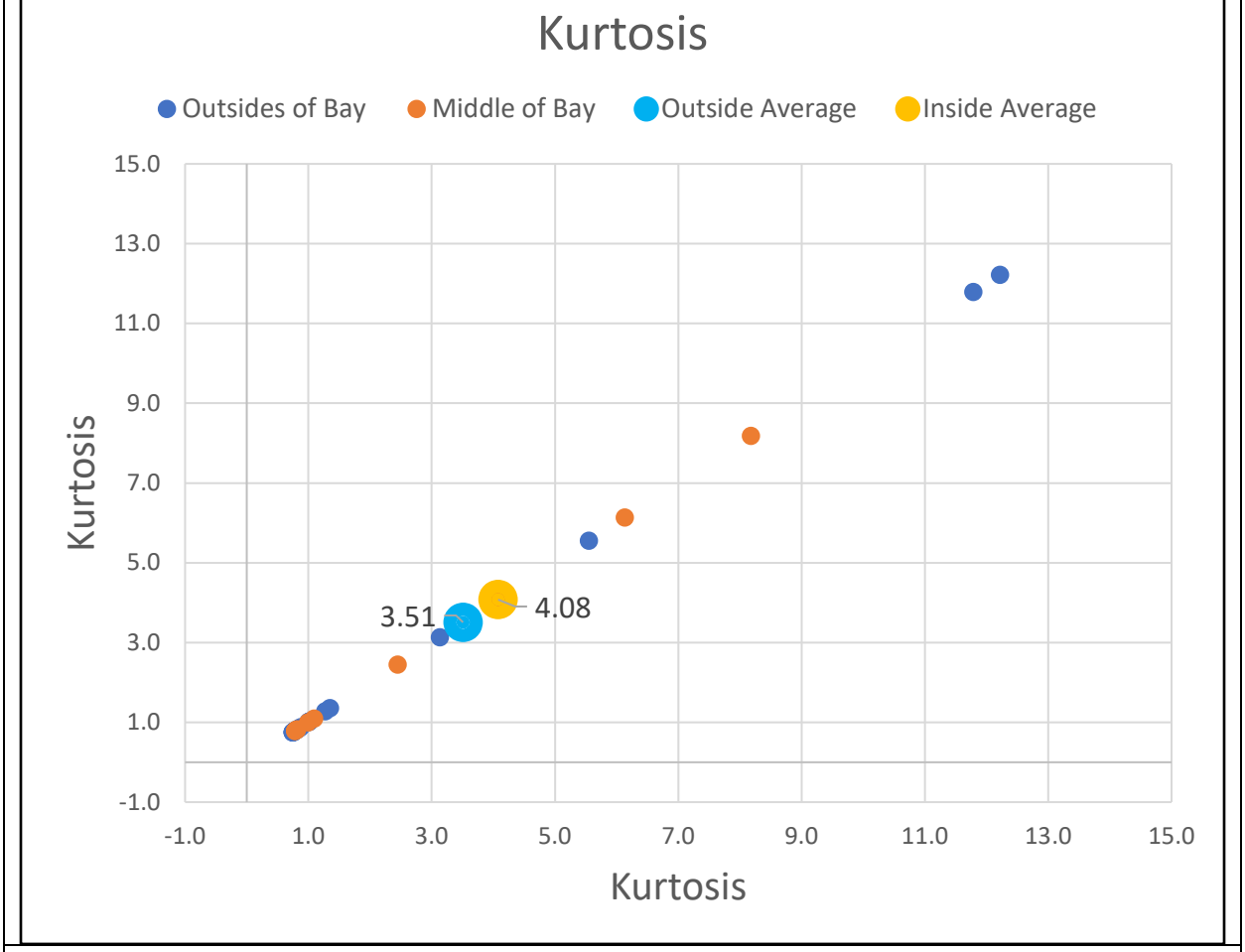

Figure 3.4.4: A linear graph of the kurtosis showing the differences between the outsides and inside of a bay or inlet.

3.5 XRF/Composition

The six sand samples tested for composition using the XRF were the Green Sand Beach, Mahai'ula Beach, Mauna Kea Beach, Pololu Beach, Punalu'u Beach, and Spencer Beach. The three principal components that were analyzed or sorted out were aragonite, pyroxene, and feldspar, or in other words, carbonate, olivine, and labradorite. The sands tested ranged in color from light tan to dark tan to green and to black. The tan/brown sands were taken from Mahai'ula Beach, Mauna Kea Beach, and Spencer Beach. These sands were thought to represent carbonate beaches. The other beaches tested, namely Punalu'u Beach, Pololu Beach, and Green Sand Beach were all black sand beaches with the exception of Green Sand Beach which had green olivine grains in addition to black sand grains.

The Green Sand Beach compositional distribution results for the three components tested can be seen in *Figure 3.5.1*. This sand was found to be 22.51% aragonite, 20.02% pyroxene, and 57.47% labradorite. The Mahai'ula Beach compositional distribution can be seen in *Figure 3.5.2* and is 88.45% aragonite, 0% pyroxene, and 11.55% labradorite. The Mauna Kea Beach compositional distribution can be seen in *Figure 3.5.3* and is 38.98% aragonite, 0% pyroxene, and 61.02% labradorite. The Pololu Beach distribution can be seen in *Figure 3.5.4* and is 11.12% aragonite, 12.45% pyroxene, and 76.43% labradorite. The Punalu'u Beach compositional distribution can be seen in *Figure 3.5.5* and is 11.6% aragonite, 12.43% pyroxene, and 75.97% labradorite. The Spencer Beach compositional distribution can be seen in *Figure 3.5.6* and is 98.13% aragonite, 0% pyroxene, and 1.87% labradorite.

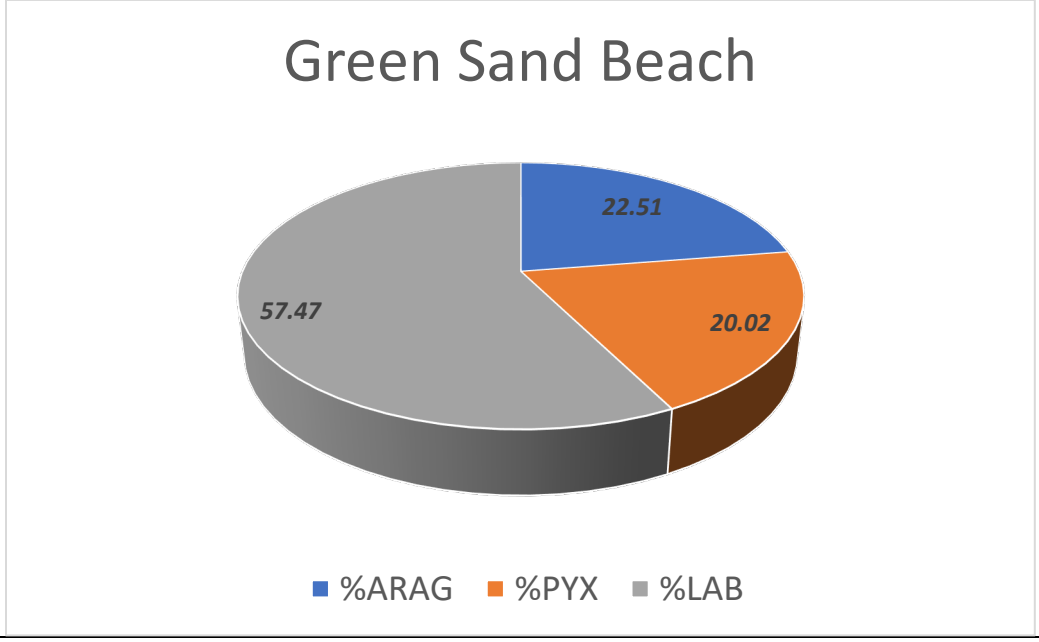

Figure 3.5.1: A pie chart representing the three compositional components tested for the sand sample from Green Sand Beach, namely aragonite (carbonate), pyroxene (olivine), and labradorite (feldspar).

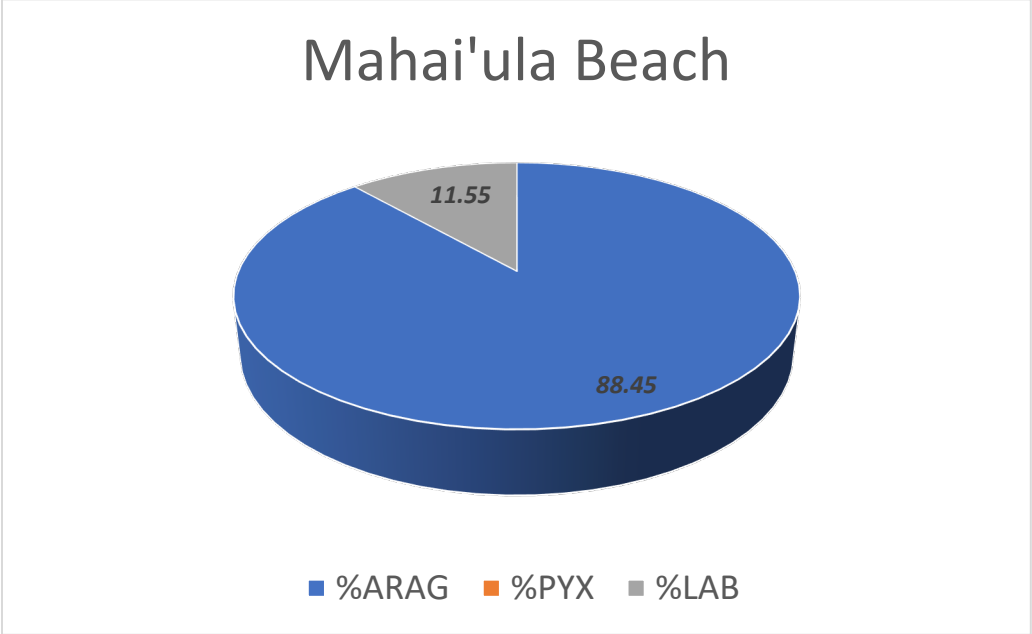

Figure 3.5.2: A pie chart representing the three compositional components tested for the sand sample from Mahai'ula Beach, namely aragonite (carbonate), pyroxene (olivine), and labradorite (feldspar).

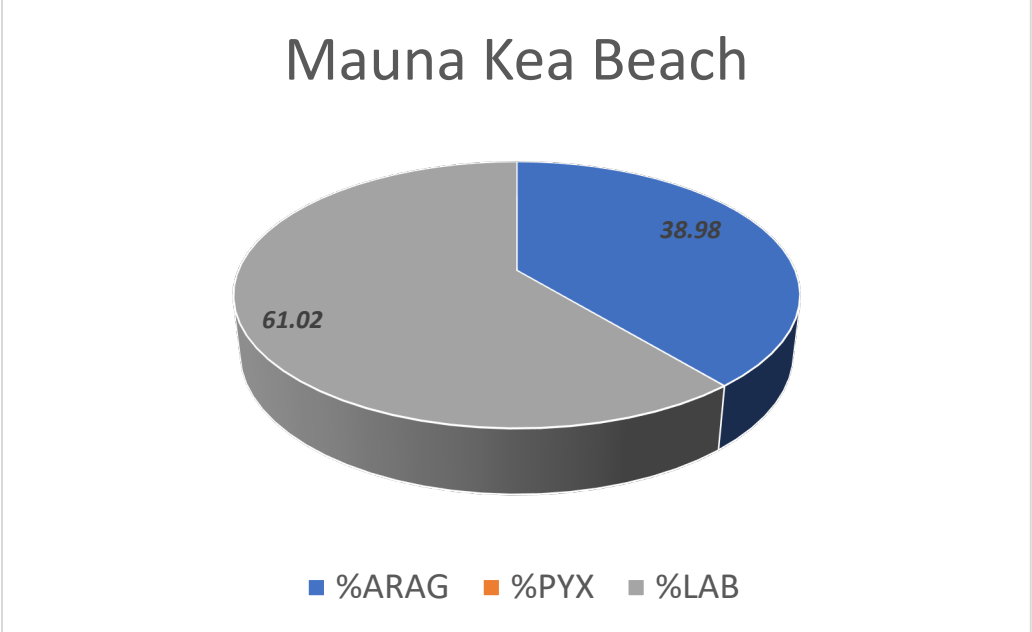

Figure 3.5.3: A pie chart representing the three compositional components tested for the sand sample from Mauna Kea Beach, namely aragonite (carbonate), pyroxene (olivine), and labradorite (feldspar).

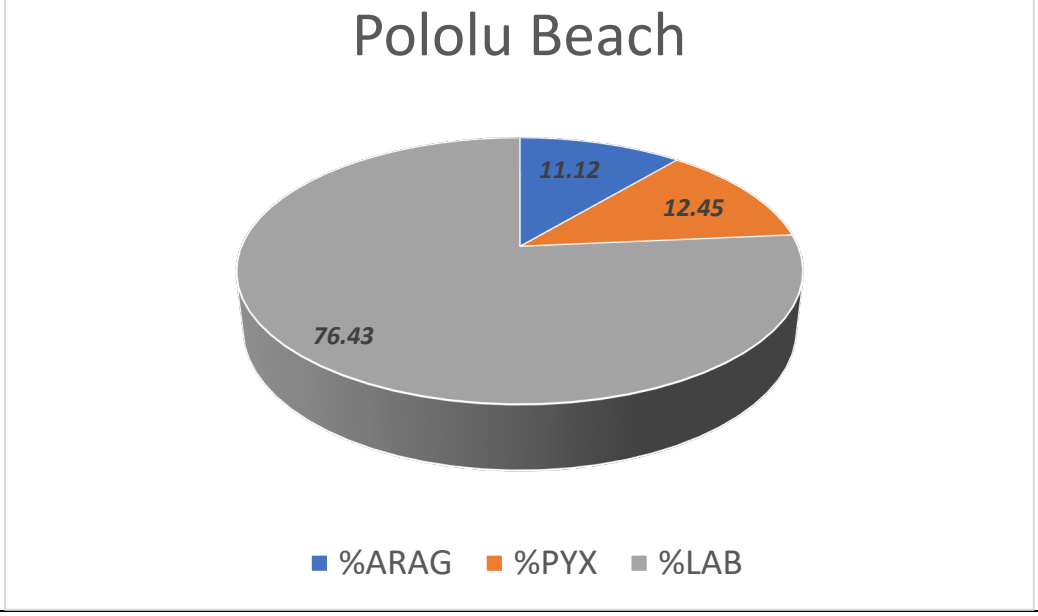

Figure 3.5.4: A pie chart representing the three compositional components tested for the sand sample from Pololu Beach, namely aragonite (carbonate), pyroxene (olivine), and labradorite (feldspar).

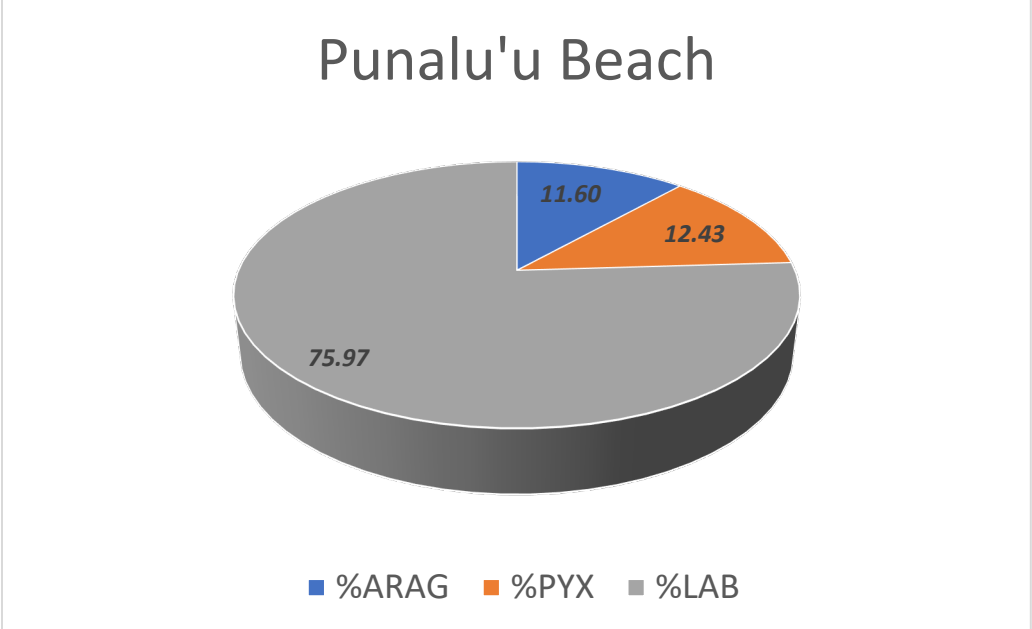

Figure 3.5.5: A pie chart representing the three compositional components tested for the sand sample from Punalu'u Beach, namely aragonite (carbonate), pyroxene (olivine), and labradorite (feldspar).

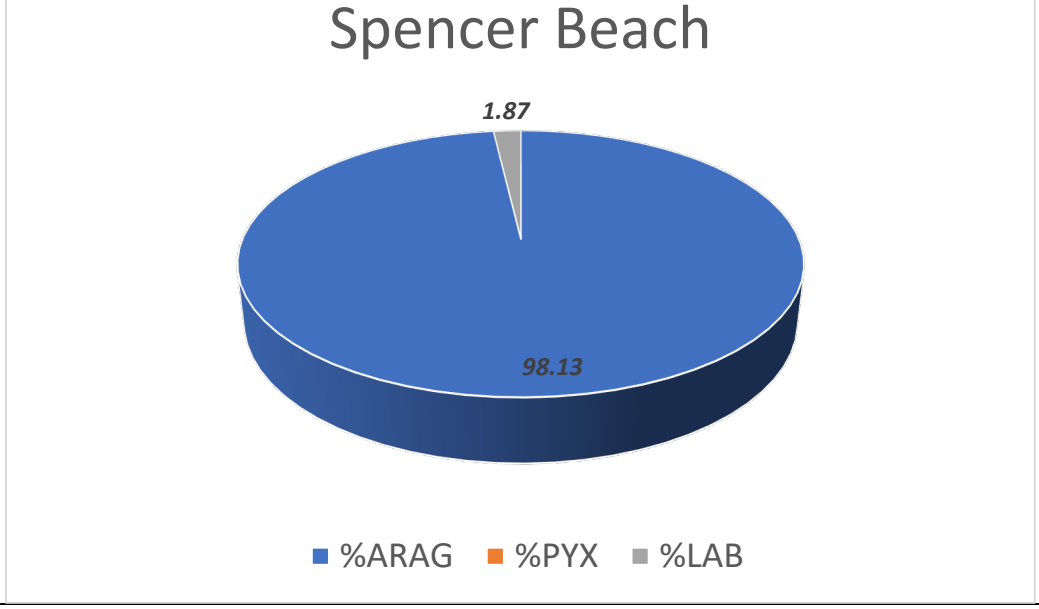

Figure 3.5.6: A pie chart representing the three compositional components tested for the sand sample from Spencer Beach, namely aragonite (carbonate), pyroxene (olivine), and labradorite (feldspar).

4. Discussion and Interpretations

Grain size distribution curves tend to show that known weather and climate in the Pacific Ocean and those specifically affecting the island of Hawai'i are controlling, or at least affecting to some degree, the overall trends of the statistical moments of mean, standard deviation, skewness, and kurtosis. Moreover, weather and climate may affect or have some control over 50th percentiles and beach slope.

The 50th percentiles calculated at each beach seem to fall within reasonable and expected ranges. The Northeast Tradewind Waves, the waves that affect the northeast and east part of the island, seem to have the beaches with the largest grains (such as Pohoiki Beach), however there were only two beaches sampled within this weather/climate effect and one of the two beaches was a relatively young beach with large grains and cobbles. Grain size is expected to relate to some degree with weather and climate generally (Gao et al., 1994). Also, steeper beaches seem to be located on the east to southeast part of the island, with those beaches being subject to both the Northeast Tradewind Waves and the Kona Storm Waves/Southern Swell (see *Figure 3.3.1*). Normally beaches that are subject to higher energies

experience coarser grains and narrower surf zones, concentrating wave energy (Komar, 1998), meaning that beaches that are actually subject to the North Pacific Swell should have generally steeper beaches. That may be the case on the island of Hawai'i, though it should be noted that neither swash to berm distance nor offshore to onshore gradient was always measured (and nor always possible due to manmade disturbances) and were not the primary focus of this study.

Standard deviation, or sorting, correlations show that all survey sites, when averaged for beaches, are very similar, all being moderately sorted. However, the survey sites on the beaches subject to the North Pacific Swell saw the extremes, being both very well sorted and poorly sorted. There are some interesting correlations when looking at beaches, weather and climate effects, and distance from the water. Through transect surveys, it was found that sorting increased generally as the distance from the water increased for those beaches subject to the North Pacific Swell and the Northeast Tradewind Waves. The opposite is true, and sorting seemed to slightly decrease as the distance from the water increased for those beaches subject to the Kona Storm Waves, Southern Swell, and those beaches outside the predicted weather and climate effects (*Figure 3.3.2*). It is important to note that the Kona Storm Waves are infrequent so the sorting may be due to a lack of higher energy weather/climate events.

Composition is also shown to affect in some capacity sorting (Folk and Robles, 1964). This is especially true for sands that are carbonate-rich, being composed of different carbonate biota (Folk and Robles, 1964). Although carbonate grains can be found throughout all the sand in the beaches on the island, there are several that are carbonate-dominant (>50% carbonate grains) and are brown, tan, or white in color. There are ten such beaches sampled, and they are, starting from the North and moving counterclockwise: Spencer Beach, Mauna Kea Beach, Hapuna Beach, Waialea Beach, Manini'owali Beach, Mahai'ula Beach, Old Kona Airport beach, Pahoehoe Beach Park, Magic Sands Beach, and Miloli'I Beach. On these beaches, some survey locations showed a bimodality (*Figure 3.1.14* and *Figure 3.1.15*), those being at Waialea Beach (A2) and Mahai'ula Beach (A1-1, A1-2, A2-1, A3-1, A3-2). Some of these sites however (Waialea A1 and Mahai'ula A1-1, A2-1, A3-1, and A3-2) are perhaps bimodal because these survey locations are heavily basalitic-grain rich thereby accounting for two grain sizes: one being

mainly composed of basaltic grains and the other being the carbonate grains. One site that showed a bimodality, A2-1, does have some mafic grains, but is more dominantly carbonate-grain rich, though the same factor of two grain sizes for detrital and organic grains may also apply at this site.

Most carbonate rich sand beaches were found to be better sorted than other beaches (*Figure 4.1.1*). Folk and Robles (1964) find that because of differing carbonate biota grains, sorting may be worse overall in carbonate rich sands, though the samples on Hawai'I have shown to be better sorted than other beaches. It should be noted that biota within carbonate grains were not specifically identified and therefore it may be possible that the contained biota reduces to the same size possibly resulting in a better sorting, following after the methodology and logic published in Folk and Robles (1964).

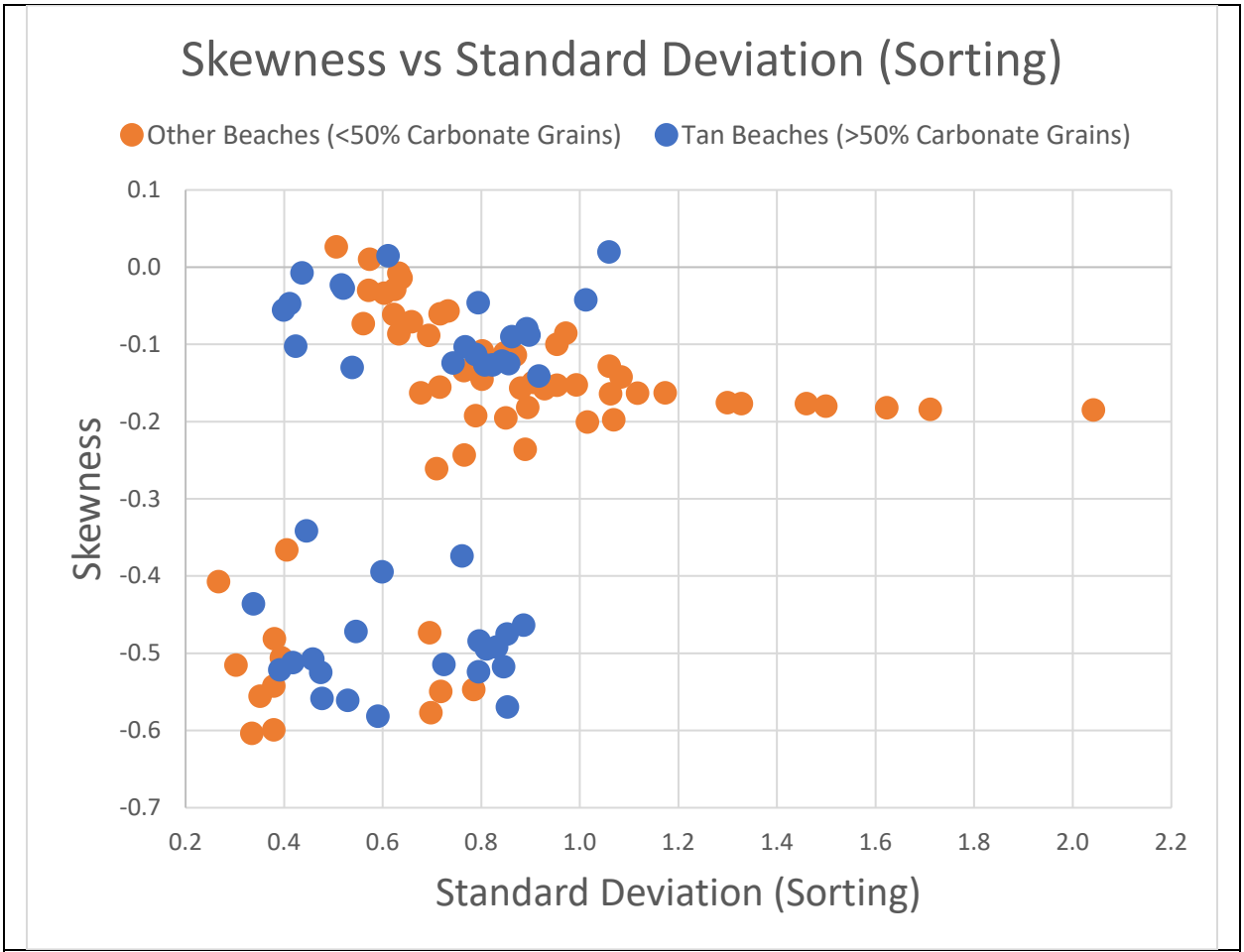

Figure 4.1.1: Relationships graphed between the skewness and standard deviation in carbonate-rich sands (>50% carbonate grains) vs other sands (<50% carbonate grains) throughout the island.

Weather and climate also seem to have some control over skewness, although it must be pointed out that the week of sampling was not a time of storms but culminating a summer of predominately calm weather. The beaches affected by the North Pacific Swell (highest energy weather/climate) have a noticeably lower skewness, or are more finely/positively skewed, whereas the other beaches have a higher skewness being more coarsely/negatively skewed. This trend seems to follow conventional theories that higher energy environment beaches are more positively skewed (Parrado Román and Achab, 1999).

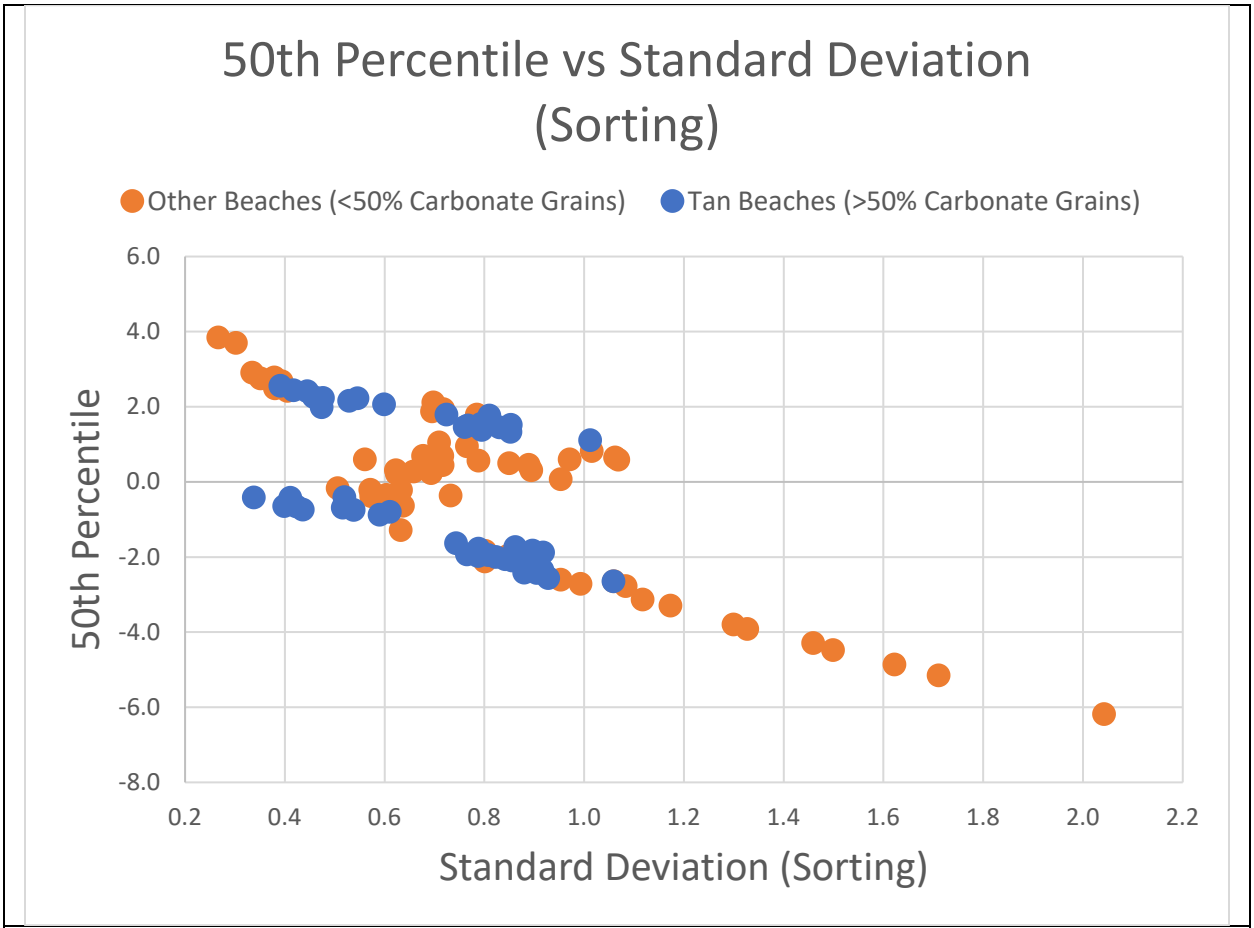

Figure 4.1.2: Relationships graphed between the 50th percentile and standard deviation in carbonate-rich sands (>50% carbonate grains) vs other sands (<50% carbonate grains) throughout the island.

Moreover, some studies suggest correlation between skewness and 50th percentile (Parrado Román and Achab, 1999; Folk and Robles, 1964, Folk and Ward, 1957). The results from this study show a very strong non-linear relationship between 50th percentile with the samples from the island of Hawai'i (*Figure 3.3.3*). This relationship is also noted in Folk and

Ward (1957) and Folk and Robles (1964) which identifies a sinusoidal relationship between grain size and skewness. Interestingly, Folk and Robles (1964) studied this relationship between mainly carbonate-rich sands, and this study found that relationship not exclusive to only carbonate-rich sands but also to sands that are comprised of < 50% carbonate grains. When carbonate-grain beaches are compared to other beaches (*Figure 4.1.2*), this relationship seems incomplete, most likely due to a low number of survey sites. Also, Folk and Robles (1964) note that this sinusoidal trend may not be seen when carbonate biota grains are close in size, meaning that there is not really a bimodality in the distribution. In this study, there was a combination of carbonate grains and basaltic grains which sometimes cause a bimodal distribution (*Figure 3.1.14* and *Figure 3.1.15*).

Skewness is also seen to be affected in some way by weather and climate events. Folk and Robles (1964) discuss that skewness, mainly negative skewness or being coarsely skewed, entails either an addition of larger grains or a subtraction of finer grains. Large energy events like storms or predictable weather/climate effects such as those discussed here can cause an addition of larger grains. It is also true that normal beach action or diminishing energy can cause a removal of finer grains (Folk and Robles, 1964). Such a grain spread can be visible through macro beach morphology as well as on a more micro level with smaller peaks and troughs of grains scattered through a beach. Normal waves throughout a given day will vary in size and larger waves will deposit larger grains farther up the shore while normal wave action will winnow away the finer materials below (Folk and Robles, 1964). On Hawai'I, some examples of these micro-level grain distributions were recorded (see Mahai'ula Beach Transect A1 (*Figure B.7.2*), Old Kona Airport Park (*Figure B.8.1*), and Pahoehoe Beach Park (*Figure B.9.2*)) and can be seen labelled on the photograph of Mahai'ula Beach in *Figure 4.1.3*. Micro scale peaks and troughs are also seen Pahoehoe Beach Park and were specifically samples at sites A1 and A2 (see *Figure B.9.2*). Here, survey sites A2 (7 ft) and A5 (27 ft) were sampled in an area where grains are visibly larger and have been deposited by a larger wave, whereas survey sites A1 (3 ft) and A3 (11 ft), were sampled in a trough where there is more fine material. At survey sites A2 and A5, the mean grain size is -0.4 ϕ and -2.8 ϕ respectively and the skewness is 0.015 and -0.13 respectively. Survey sites A1 and A3 have a mean grain size of -0.9 ϕ and -0.8 ϕ

respectively, and their skewness is -0.047 and -0.027 respectively. When comparing the two different distributions, although they are very similar, it is important to look at their differences in this context. The survey sites at the peaks are comprised of larger grains and is more positively skewed in the case of survey site A2, though only slightly, and more coarsely skewed at site A5. This convention seems to follow the recorded observations of Folk and Robles (1964) where larger grains are deposited up beach. The slightly more positive skewness in the A2 site may be explained by a regulation of grain size through normal winnowing.

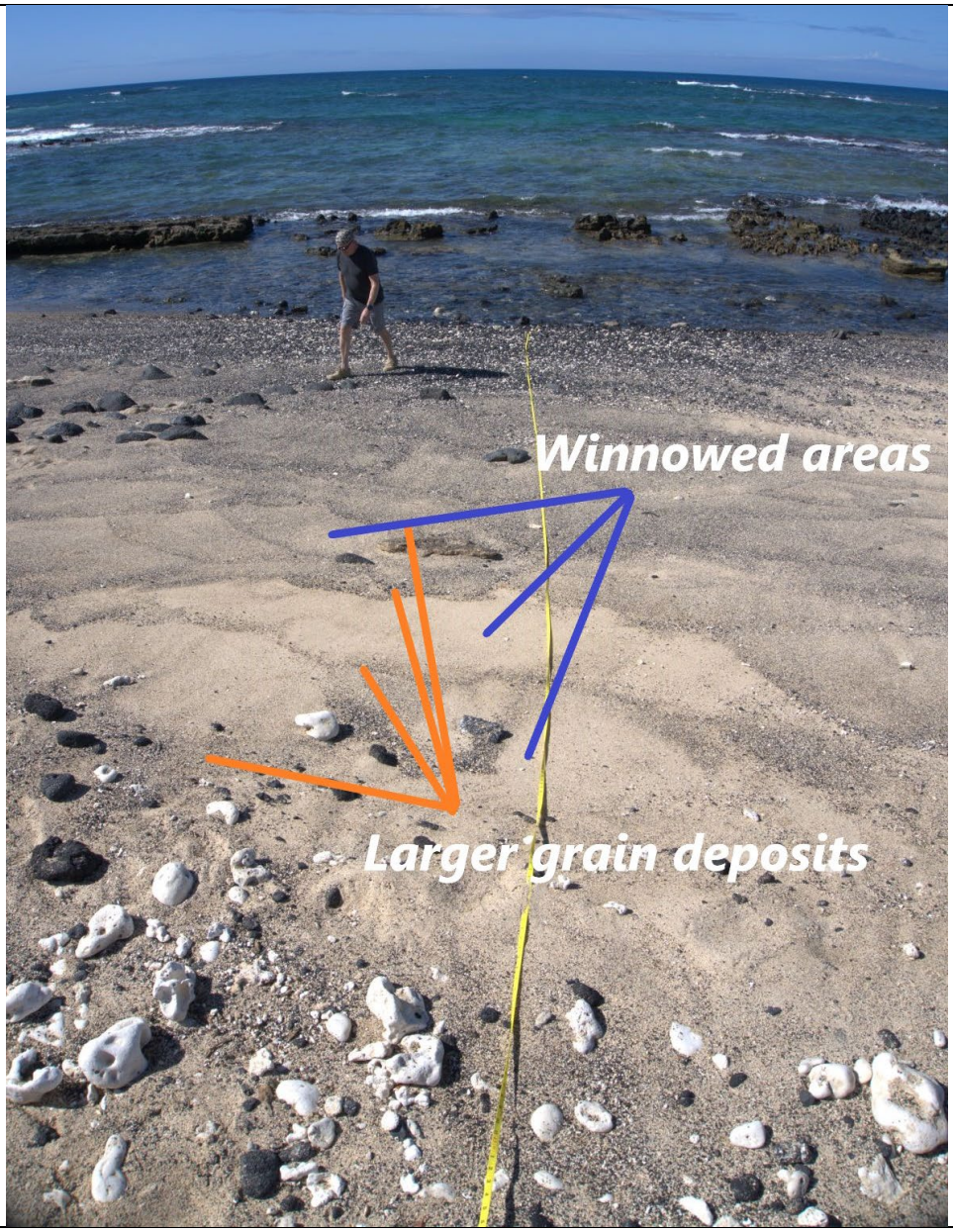

Figure 4.1.3: A labelled transect (Transect A1) from Mahai'ula Beach showing micro scale grain size differences where large grains have been deposited and finer grains have been winnowed away.

Kurtosis trends are more ambiguous when it comes to weather and climate effects on the survey sites and on the island as a whole. It has been found that an increase in the frequency of seasonal weather events could impact kurtosis (Nagalakshmi et al., 2018), though those beaches on Hawai'i subject to the North Pacific Swell, or the largest weather and climate effects, had the highest kurtosis being extremely leptokurtic overall. A possible lack of trends and correlation may be due to the failure or struggle of pyDGS to accurately predict the extremes of a distribution.

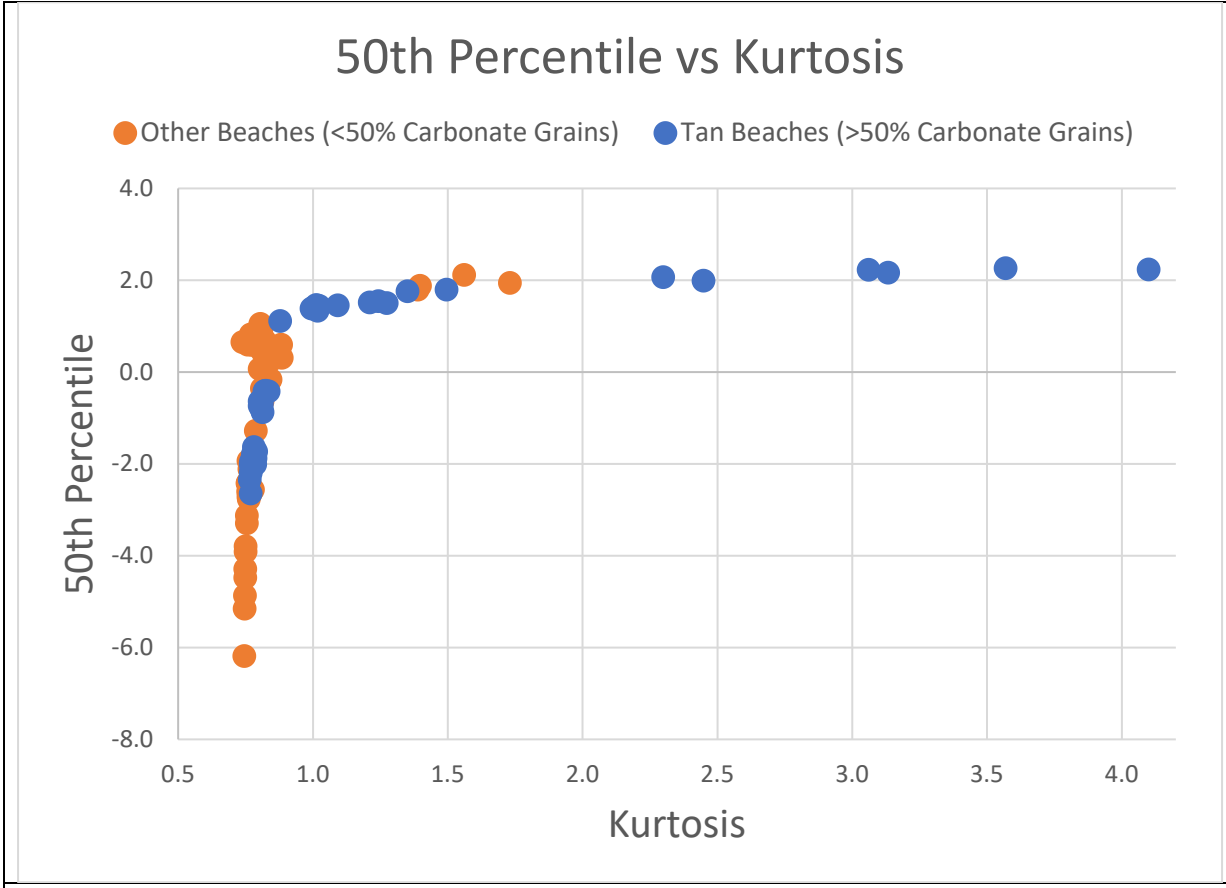

Figure 4.1.4: Relationships graphed between the 50th percentile and kurtosis in carbonate-rich sands (>50% carbonate grains) vs other sands (<50% carbonate grains) throughout the island.

It is also true that differing sizes of carbonate biota grains could potentially impact kurtosis (Folk and Robles, 1964). If there are differing sizes of carbonate biota, then survey sites would be more platykurtic, representing a larger spread of grain sizes, though Folk and Robles (1964) notes that a large presence of one grain size may drown out the other size modalities if it is large enough. As has been noted, a bimodality of grain sizes of carbonate grains has not

been seen on the island, and in fact, the opposite may be true for the carbonate beaches. If the opposite is true and the carbonate in grains is more uniform in size, it may explain why carbonate beaches on Hawai'I are actually more leptokurtic generally (*Figure 4.1.4*). Since there is a bimodality of grains on other beaches due to the presence of both basaltic and carbonate grains, this may explain the more platykurtic survey sites following the same theory outlined by Folk and Robles (1964).

Survey sampling at various beaches throughout the island allowed for an analysis of statistical moments on both the outside and inside on an exposed shoreline within bay. There were five locations where bay shoreline sampling was surveyed, namely Pololu Beach, Waialea Beach, Manini'owali Beach, Mahai'ula Beach, and Punalu'u Beach. Strong overall trends and relationships were delineated in all of the statistical moments. The 50^{th} percentile (ϕ) was found to be larger in the middle of a shoreline within a bay (smaller grains) as opposed to the outsides of the exposed shoreline (see *Figure 3.4.1*). This supports the observation that waves, as they approach a beach or a bay, are refracted on the outsides thereby diminishing the wave energy by the time it reaches the middle of the exposed shoreline accounting for finer grains. Standard deviation, or sorting, was generally found to be lower (better sorted) in the middle of a shoreline within a bay also supporting the previously discussed observation (see *Figure 3.4.2*). Skewness was found to be slightly lower in the middle of a bay's shoreline when compared to the outside shoreline values, though average values were very similar (see *Figure 3.4.3*). Kurtosis was found to be slightly lower on the outsides of a bay' shoreline than in the middle, both being extremely leptokurtic (see *Figure 3.4.4*), but again, this is possibly due to the failure of pyDGS to account for the extremes of a distribution.

Since five physical samples were taken from the circumnavigational survey of Hawai'i, they were able to be tested for their compositional distribution through XRF. Since the islands are volcanic, it is important to mainly look at distributional percent of three main components: aragonite (carbonate), pyroxene (olivine), and labradorite (feldspar). Those compositional distributions are seen in *Figure 3.5.1 – Figure 3.5.6*. It is found that the tan sand beaches (Spencer Beach, Mauna Kea Beach, and Mahai'ula Beach) are all carbonate beaches whereas

the black and green sand beaches (Green Sand Beach, Punalu'u Beach, and Pololu Beach) are all mafic/volcanic beaches.

Of the carbonate beaches, it is interesting to see that only Mahai'ula Beach and Spencer Beach are aragonite (carbonate) dominated. The other tan sand beach, Mauna Kea Beach, is actually labradorite (feldspar) rich. Though it is unknown exactly why this is, some possible explanations include proximity to a river runoff that would include weathering of rocks, a lack of nearby carbonate reefs, or possibly manmade infusions of sand due to its proximity to a large, popular tourist resort. The bimodal distribution explained by Folk and Robles (1964), which states that different grain sizes can be due to different sizes of carbonate biota, may explain distributions mainly in the Mahai'ula Beach sand. Although the sands at this beach are of a pepper color, being mixed with basalt and volcanic grains, Transect A4 is the transect with the least number of basaltic grains (*Figure B.7.9*). The survey points at this transect showed a more symmetrical skewness, perhaps due to the nature of the carbonate biota grains. It is likely that the carbonate grains and the volcanic grains differ in size and provide to some extent bimodality in the distribution. It should be noted that sands at the other two beaches tested compositionally had high amounts of carbonate biota grains and did not have a larger spread or representation of grain size. Though Miloli'I Beach sands were not tested compositionally, they were comprised of mostly visible carbonate biota grains (*Figure B.14.3*). This beach showed a distribution (*Figure 3.1.25*) similar to that from Transect A4 at Mahai'ula Beach, though the grains at this beach were predominantly carbonate (>50% carbonate grains) and although carbonate biota was not specifically identified, could potentially explain the bimodality.

Of the volcanic beaches, Pololu Beach and Punalu'u Beach are nearly identical in their compositional distribution, but the Green Sand Beach seems to be slightly different. The Green Sand Beach is seen to have a higher amount of both pyroxene and aragonite. It is important to note that this site is a small, cove-like steep beach. Leading to the water on the outcrop surrounding the beach are visible strata from ash and tuff from ancient eruptions (Walker, 1992). The ash and tuff from these eruptions are likely the source for some of the anomalies seen compositionally. Also, most of the grains comprising the Green Sand Beach sand are olivine (*Figure B.15.3*).

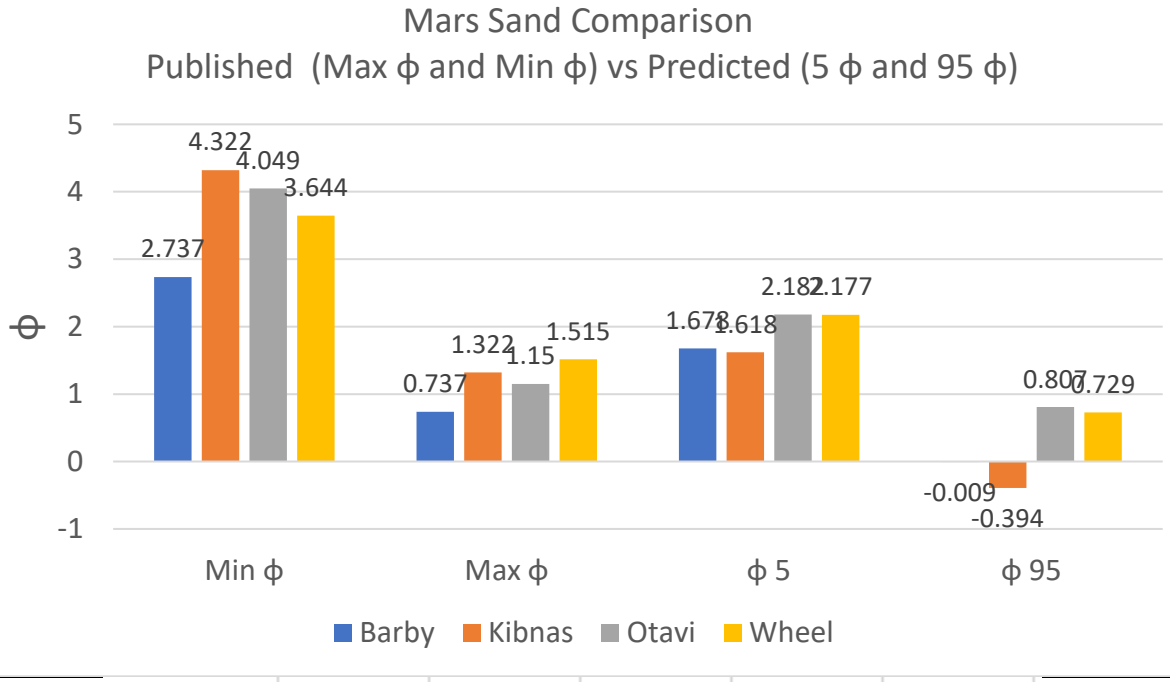

Mars Sands Comparison

		High Dune		*Namib Dune*	
		Barby	***Kibnas***	***Otavi***	***Wheel***
Published	***Min φ***	2.737	4.322	4.049	3.644
	Max φ	0.737	1.322	1.15	1.515
Predicted (Modelled)	***φ 5***	1.678	1.618	2.182	2.177
	φ 95	-0.009	-0.394	0.807	0.729

Figure 4.1.5: (*top*) Bar graph showing the published data points of the max and min phi values (Ehlmann et al., 2018) and the predicted values from pyDGS for the Mars sands. The values for the bar graph can be seen in the table on the *bottom*.

The data from the Mars sands pictures were similar to those studied and published by Ehlmann et al. (2018). Although statistical moments for these sands have not been published, Ehlmann et al. (2018) publishes the ranges for grain sizes to be for the High Dune site to be: Barby: 0.737ϕ – 2.737 ϕ and Kibnas: 1.322 ϕ – 4.322 ϕ and for the Namib Dune site to be: Otavi: 1.15 ϕ – 4.049 ϕ and Wheel: 1.515 ϕ – 3.644 ϕ (*Figure 4.1.5*). Although pyDGS does not give a max and min value, it does calculate a 5^{th} and 95^{th} percentile, which can be seen compared in *Figure 4.1.5*. Those values for the High Dune are: Barby: -0.009 ϕ – 1.678 ϕ and Kibnas: -0.394 ϕ – 1.618 ϕ and for the Namib Dune site: Otavi: 0.807 ϕ – 2.182 ϕ and Wheel:

0.729 ϕ – 2.177 ϕ. Through this figure, it is seen that pyDGS does a much better job at predicting the larger grains than the smaller grains, though both are different than the published data. The predicted values seemed to predict larger grains when compared to both the max and min published values. This could be due to the fact that pyDGS does not calculate a max and min value, however those values should be similar. Additionally, the smaller values are off by a few ϕ units, but it is important to remember that the phi scale is logarithmic and only account for a few microns.

Although the extremes of the distribution were slightly off, the overall distributional graphs and statistical moments were similar to published values (Ehlmann et al., 2018). Ehlmann et al. (2018) concluded that both the Otavi and Wheel sites within the Namib Dune were better sorted than the Barby and Kibnas sites within the High Dune. The predicted data from pyDGS also found this to be the case, with both sites in the Namib dune being well sorted as compared to the two other sites in High Dune which are moderately well sorted. Moreover, the predicted data showed that all four sites within the dunes are coarsely skewed (High dune sites Barby and Kibnas are coarse skewed and Namib dune sites Otavi and Wheel are very coarse skewed). This is supported by the observation that the dunes seem to lack finer silts and smaller grains that are otherwise seen throughout other explored areas on Mars (Ehlmann et al., 2018). The high winds throughout the dunes have most likely winnowed finer materials out causing a coarse skewness.

5. Conclusions

When correctly tuned and adjusted, pyDGS can serve as an alternative to conventional survey methods in calculating distribution and statistical moments. It has great potential and geological implications for future sedimentologists and field work, but there are several areas for improvement. First of all, the program can be very robust; as its author paper Buscombe (2013) states that the program has trouble identifying edges and fringes of the grain size distribution. Although those edges can be adjusted for and were for this study, the program could improve in identifying those grains without post-production corrections. Secondly, through this study, it became evident that the program struggled with porous rocks, namely

gravelly-sized grains with holes, as is common in basaltic and volcanic rocks. Through the distributions, it seems as though the program struggled with accounting for these grains (an example can be seen in *Figure 5.1*. Thirdly, it would be useful to include in the original code some additional calculations for other useful metrics such as roundness and automatic graphing. These kinds of features would not only save time post-production, but would also aid further investigations, especially for sands on other planets, and could yield more information into specific aeolian or water transport.

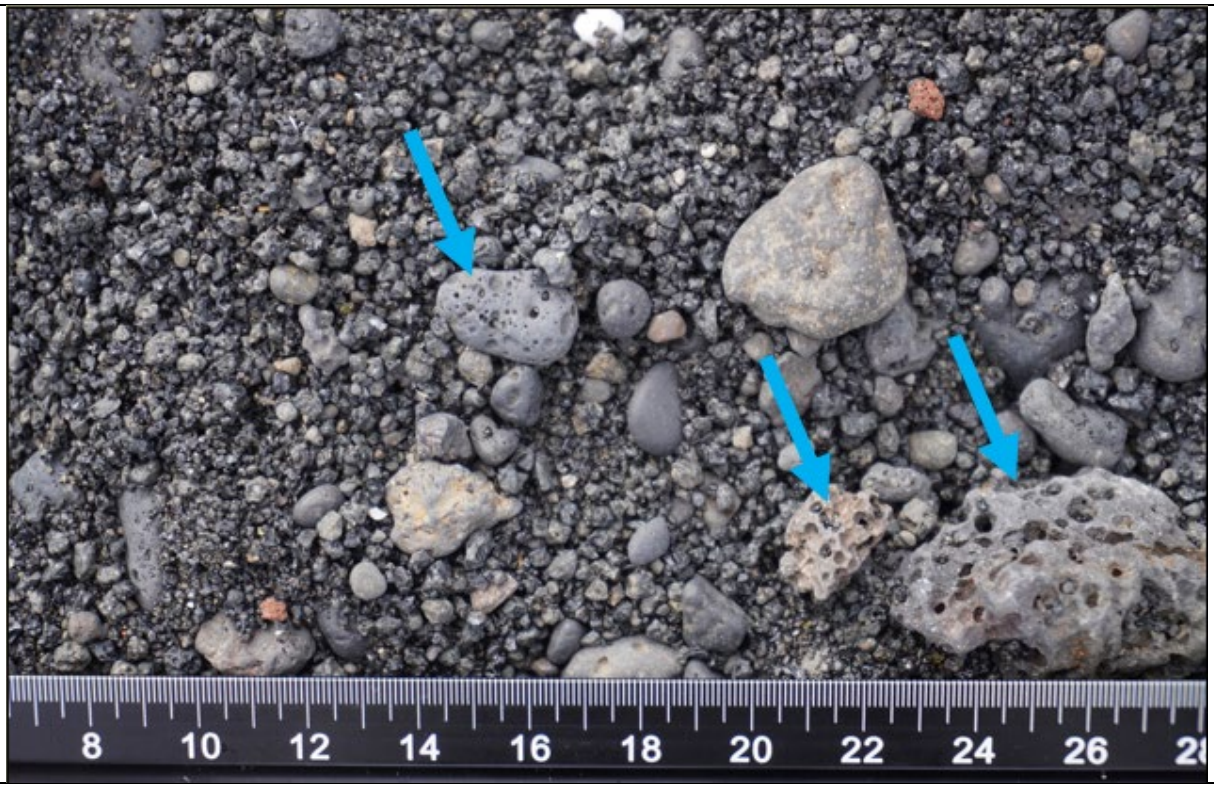

Figure 5.1: An example from Punalu'u Beach showing gravelly-sized grains with large pores that caused trouble in pyDGS.

In addition to preexisting geological features, weather and climate are driving factors in sand distribution, grain size, beach slope, sorting, skewness, and kurtosis on the island of Hawai'i. Overall, these surveys showed that on Hawai'i, the beaches subject to the North Pacific Swell meaning a higher energy (larger wind and waves), the higher the 50^{th} percentile (more positive ϕ or smaller grains), the lower the skewness (more coarsely skewed), and the higher the kurtosis (more leptokurtic). In this case, it may not be appropriate to overall generalize that a higher energy is equivalent to these conclusions; however, it is true for these specific weather

and climate energies that affect the island. Moreover, for higher energy beaches, the grain size seems to slightly increase as the distance from the water increases whereas the lower energy beaches seem to slightly decrease as the distance from the water increases. The sheer number of beaches are more present on the leeward, dry side of the island is due to the relative difference and lack of rain/erosion and to sea profiles are gentler in gradient. Where a bay's shoreline sampling was done (on the five mentioned beaches), it confirmed that the middle of the shoreline within a bay has smaller grains, is better sorted, is slightly more finely skewed, and is slightly more leptokurtic than the outsides of a bay.

Compositional data from the five samples indicate color and compositional relationships. Black and green sands are more volcanic and mafic, but in some cases, such as the Green Sand Beach, can yield more important information about surrounding geology and helps build a geologic story. On several beaches, a bimodal distribution can be explained by mineralogical differences. Several of the bimodal survey locations were comprised of both carbonate and basaltic grains. It is seen here that carbonate grains and basaltic grains generally were broken into two different sizes in some locations. Moreover, future investigations could yield even more information concerning different carbonate biota grains and how differing mineralogical grains account and affect grain size distribution. Future geomorphological studies could also yield more information about proximity to rivers, quantity and proximity to coral reefs, as well as possible associations to nearby specific lava flows.

The Mars sands that were sampled compared relatively well to the available published data further supporting the successful nature of pyDGS for grain size distribution (Ehlmann et al., 2018). Though, as previously noted, pyDGS failed to account for the smallest grains when compared to the published data. Overall, this program or others like it, if further developed, could prove to be impactful and priceless to future extraterrestrial missions. Future missions would be able to save precious space and weight replacing a sieve for a high-definition camera and could potentially save governments and companies thousands or millions of dollars in fuel, parts, engineering, and research.

It is important to note that sand and grainsize distribution can vary throughout the year and is greatly subject to not only seasonal climate and weather, but also local and concentrated

storm events. All samples were taken within a week's time and as such can only be used to generalize the sand distribution for that moment. Since this study showed that pyDGS and photogrammetric techniques generally can be applied and used to replicate and supplement or replace traditional ones, some future studies could be done to look deeper at daily and seasonal effects which would include daily or weekly sampling of the same beach.

7. References

Anderson, R. C., L. Jandura, A. B. Okon, D. Sunshine, C. Roumeloutis, L. W. Beegle, J. Hurowitz, B. Kennedy, D. Limonadi, S. McCloskey, M. Robinson, C. Seybold, K. Brown. 2012. Collecting samples in Gale Crater, Mars: An overview of the Mars Science Laboratory Sample Acquisition, Sample Processing and Handling System, *Space Sci. Rev.*

B. Ehlmann, K. S. Edgett, B. Sutter, C. N. Achilles, M. L. Litvak, M. G. A. Lapotre, R. Sullivan, A. A. Fraeman, R. E. Arvidson, D. F. Blake, N. T. Bridges, P. G. Conrad, A. Cousin, R. T. Downs, T. S. J. Gabriel, R. Gellert, V. E. Hamilton, C. Hardgrove, J. R. Johnson, S. Kuhn, P. R. Mahaffy, S. Maurice, M. McHenry, P.-Y. Meslin, D. W. Ming, M. E. Minitti, J. M. Morookian, R. V. Morris, C. D. O'Connell-Cooper, P. C. Pinet, S. K. Rowland, S. Schröder, K. L. Siebach, N. T. Stein, L. M. Thompson, D. T. Vaniman, A. R. Vasavada, D. F. Wellington, R. C. Wiens, A. S. Yen. 2017. Chemistry, mineralogy, and grain properties at Namib and High dunes, Bagnold dune field, Gale crater, Mars: A synthesis of Curiosity rover observations. JGR: Planets. Volume 122, Issue 12, p. 2510 – 2543.

Blott, S. J., Pye, K., 2001. Gradistat: A Grain Size Distribution And Statistics Package For The Analysis Of Unconsolidated Sediments. Earth Surface Processes and Landforms, 26, 1237 – 1248.

N. Bridges, B. Ehlmann. 2018. The Mars Science Laboratory (MSL) Bagnold Dunes Campaign, Phase I: Overview and introduction to the special issue. Journal of Geophysical Research: Planets. Volume 123, Issue 1. P. 3 – 19.

Buscombe, D., 2013. Transferable wavelet method for grain-size distribution from images of sediment surfaces and thin sections, and other natural granular patterns. Sedimentology 60 (7), 1709–1732.

Buscombe, D. and Rubin, D.M. (2012b) Advances in the simulation and automated measurement of well sorted granular material. Part 2: direct measures of particle properties. J. Geophys. Res., 117, F02002.

Buscombe, D., Rubin, D.M. and Warrick, J.A. (2010) A universal approximation to grain size from images of noncohesive sediment. J. Geophys. Res., 115, F02015.

Calhoun, R. S., Fletcher, C. H., 1995. Late Holocene Coastal Plain Stratigraphy and Sea-Level History at Hanalei, Kauai, Hawaiian Islands. Quaternary Research 45, 47-58 article no. 0005.

Campbell, J. F., Hwang, D. J., 1982. Beach Erosion at Waimea Bay, Oahu, Hawaii. Pacific Science (1982), vol. 36, no. 1.

Chagué, C., Sugawara, D., Goto, K., Goff, J., Dudley, W., Gadd, P., 2018. Geological evidence and sediment transport modeling for the 1946 and 1960 tsunamis in Shinmachi, Hilo, Hawaii. Sedimentary Geology 364 (2018) 319-333.

Cheng, Z., Liu, H., 2015. Digital grain-size analysis based on autocorrelation algorithm. Sedimentary Geology, 327, p. 21-31.

Clague, D. A., Dalrymple, G. B. 1987. Volcanism in Hawaii. The Hawaiian-Emporer volcanic charin. U>S Geologic Survey Professional Paper. 1350:5-54.

Clark, J., R., K., 1985. Beaches of the Big Island. Kolowalu Books.

Fadil, M., F., H. 2018. Assessment of beach morphological changes at Pantai Sepat. Environmental Science. V 2018 : 216.

Fehr, R. 1987. Geschiebeanalysen in Gebirgsflüssen (Grain Size Analysis in Torrents), Mitteilung Nr. 92, Versuchsanstalt für Wasserbau, Hydrologie und Glaziologie (VAW), ETH Zürich, Zürich (in German).

Fletcher, C., Bochicchio, C., Conger, C., Engles, M., Feirstein E., Frazer, N., Glenn, C., Grigg, R., Grossman, E., Harney, J., Isoun, E., Murray-Wallace, C., Rooney J., Rubin, K., Sherman, C., Vitousek, S. 2008. Geology of Hawaii Reefs in Coral Reefs of the USA. Springer Science Business Media B.V. p435-487.

Folk, R. L., 1959, Practical petrographic classification of limestones: Am. Assoc. Petroleum Geologists Bull., v. 43, no. 1, p. 1-38.

Folk, R. L., Robles, R. 1964. Carbonate Sands of Isla Perex, Alacran Reef Complex, Yucatan. The Journal of Geology. May 1964 v. 72:3. 255-292.

Folk, R.L. and Ward, W.C., 1957. Brazos River bar: A study in the significance of grain size parameters. *Journal of Sedimentary Petrology*, 27, 3-26.

Frazier, A. G., Giambelluca, T. W., Diaz, H. F. and Needham, H. L. (2016), Comparison of geostatistical approaches to spatially interpolate month-year rainfall for the Hawaiian Islands. Int. J. Climatol., 36(3), 1459-1470.

Gao, S ; Collins, M.B ; Lanckneus, J ; De Moor, G ; Van Lancker. 1994. Grain size trends associated with net sediment transport patterns: An example from the Belgian continental shelf. Marine geology, 1994, Vol.121 (3), p.171-185.

Harney, J. N., Grossman, E. E., Richmond, B. M., Fletcher, C., 1999. Age and Composition of Carbonate Shoreface Sediments, Kailua Bay, Oahu, Hawaii. Coral Reefs, 1 – 42.

Inman, D., L. 1952. Measures for describing the size distribution of sediments. Journal of Sedimentary Petrology, v. 22, 125-145.

J. M. Parrado Román, M. Achab. 1999. Grain-size trends associated with sediment transport patterns in Cadiz Bay (southwest Iberian Peninsula). Bol. Insti. Esp. Oceanogr. 15 (1-4). 1999:269-282.

K. Nagalakshmi, Madri Pramod Kumar, T. Lakshmi Prasad, N. Jayaraju, M. Lakshmanna and G. Sreenivasulu. 2018. A study on textural parameters of beach sands along some parts of the Nellore coast, east coast of India: Implications to Depositional Environment. J. Ind. Geophys. Union (September 2018) v.22, no.5, pp:558-567.

Komar, P. D. 1998. Beach processes and sedimentation. 2nd edition. Prentice Hall, New Jersey, USA.

Krumbein, W. C. (1936) Application of logarithmic moments to size frequency distribution of sediments: Journal of Sedimentary Petrology, vol. 6, pp. 35-47.

Landen, David. 1959. Impact of the Development of Photogrammetry upon Geology. Journal of the Washington Academy of Sciences, vol. 49, no. 7, p. 234-252.

Macdonald, G., A., Abbott, A., T. *Volcanoes in the Sea: the Geology of Hawaii*. University of Hawaii Press, 1983.

Moberly, T., Baver, L., Morrison, A. 1965. Source and variation of Hawaiian littoral sand. Journal of Sedimentary Petrology. Volume 4, 21-48.

Moberly, R., Jr. and Chamberlain, T., 1964, Hawaiian beach systems: Honolulu, University of Hawai'i, Hawai'i Institute of Geophysics, 95 p.

Moberly, R., Jr., McCoy, F., W., 1966. The Sea Floor North of the Eastern Hawaiian Islands. Marine Geology 4 (1966) 21-48.

Moreland, Travis, John Pigott, Fengyan Shi, and John Hornbuckle, 2019, Integration of reservoir characterization and numerical modeling to provide an alternative depositional style of the Middle Rader debris slide in the Delaware Basin, AAPG Southwest Section Dallas Spring Symposium 2019.

Norcross, Z. M., Fletcher, C. H., Merrifield, M., 2002. Annual and interannual changes on a reef-fringed pocket beach: Kailua Bay, Hawaii. Marine Geology 190 (2002) 553-580.

R. F. McLean and R. M. Kirk (1969) Relationships between grain size, sizesorting, and foreshore slope on mixed sand - shingle beaches, New Zealand Journal of Geology and Geophysics, 12:1, 138-155,

Resig, J., 2004. Age and Preservation of Amphistegina (foraminifera) in Hawaiian beach sand: implication for sand turnover rate and resource renewal. Marine Micropaleontology 50 (2004) 225-236.

Richmond, B., Gibbs, A., Cochran, S. 2008. Geologic Resource Evaluation of Kaloko-Honokohau National Historical Park, Hawai'I; Geology and Coastal Landforms. Open-File Report 1191.

Rubin, D.M. (2004) A simple autocorrelation algorithm for determining grain size from digital images of sediment. J. Sediment. Res., 74, 160–165.

Rüther, Nils and Huber, Sonja and Spiller, Stephan and Aberle, Jochen, 2013. Verifying a photogrammetric method to quantify grain size distribution of developed armor layers. Conference: 35th World Congress of IAHR.

Walker, G. 1990. Geology and Volcanology of the Hawaiin Islands. Pacific Science, vol. 44 no. 4: 315-347.

Walker, G. 1992. Puu Mahana Near South Point in Hawaii Is a Primary Surtseyan Ash Ring, Not a Sandhills-type Littoral Cone. Pacific Science (1992), vol. 46, no. 1:1-10.

Wolman, M.G. 1954.A method of sampling coarse river-bed material. Transactions American Geophysical Union 35, 951–956.

Wright, L.D. and Short, A.D., 1984. Morphodynamic variability of surf zones and beaches: A synthesis. Mar. Geol., 56: 93--118.

Zhong, S., and Watts, A.B., 2002, Constraints on the dynamics of mantle plumes from uplift of the Hawaiian Islands: Earth and Planetary Science Letters, v. 203, p. 105-116.

Mars sand pictures:

https://mars.nasa.gov/raw_images/300055/?site=msl

https://mars.nasa.gov/raw_images/300018/?site=msl

https://mars.nasa.gov/raw_images/310795/?site=msl

https://mars.nasa.gov/raw_images/308807/?site=msl

8. Figures

These Figures are included in the body of the text.

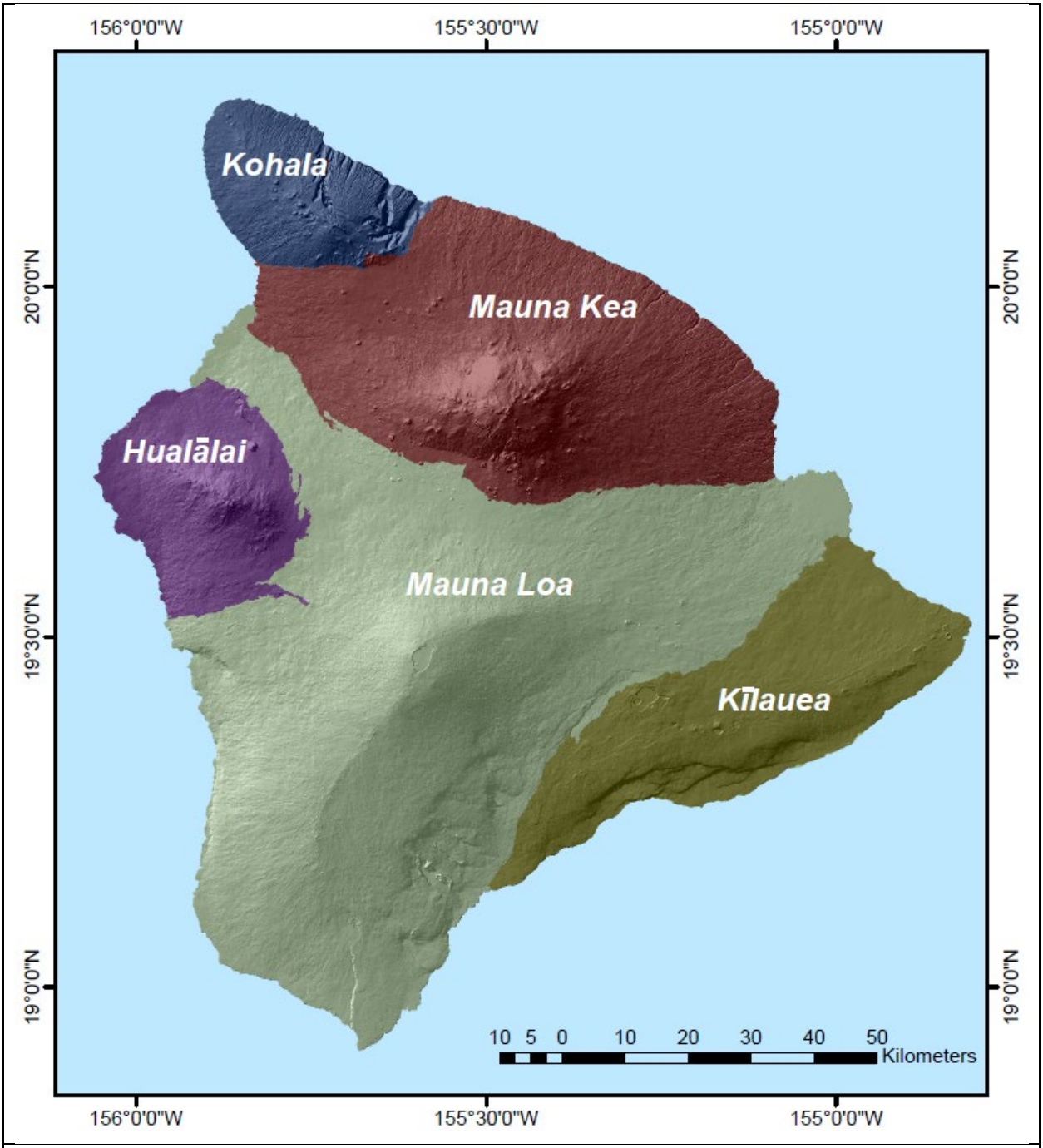

Figure 1.2.1: A map of the Island of Hawaii showing the five different volcanoes and the extent of their lava flows. (Richmond et al., 2008).

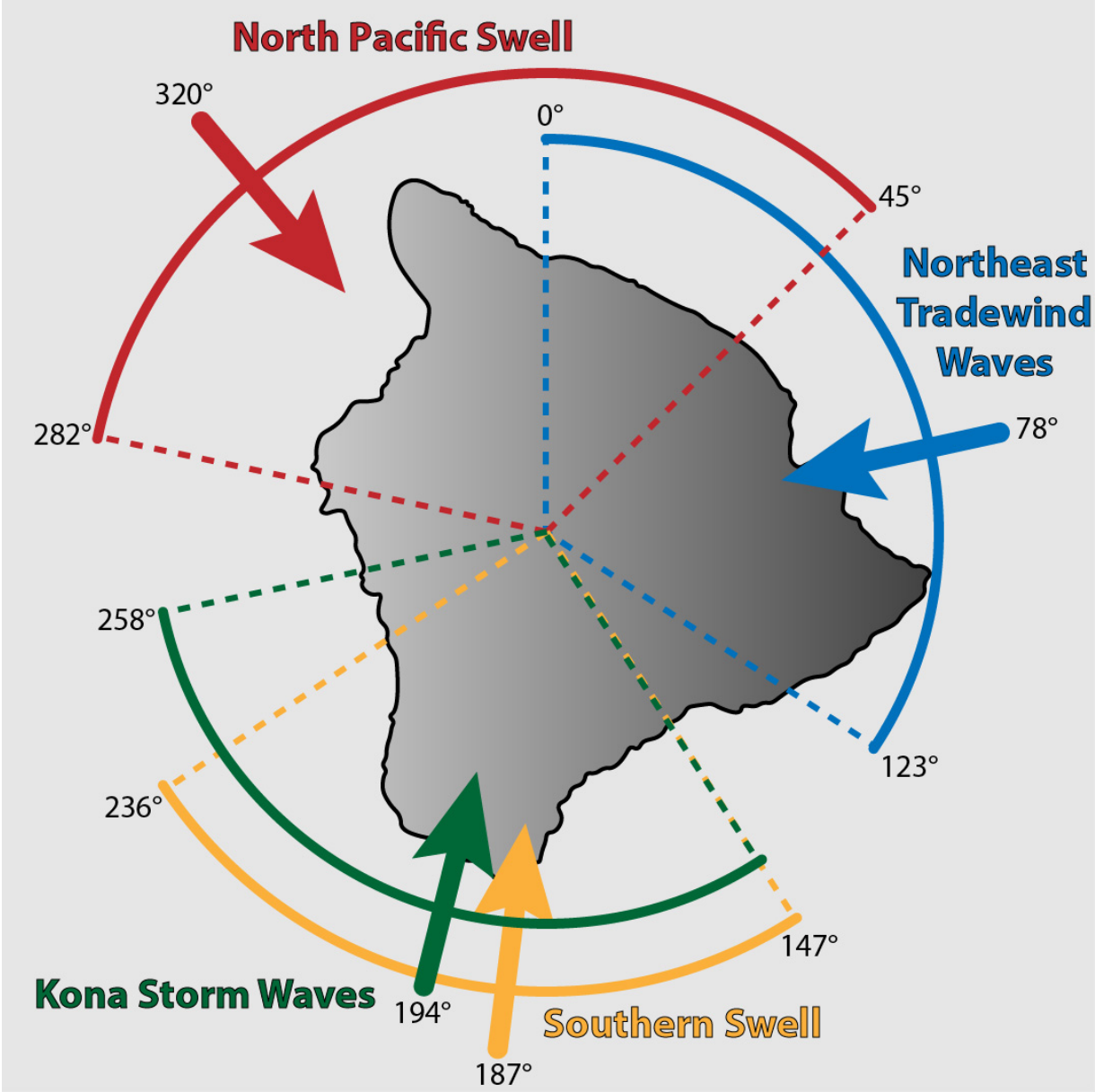

Figure 1.2.2: A diagram (adapted from Moberly and Chamberlain, 1964) showing the island of Hawaii and the predominant wave energy regime.

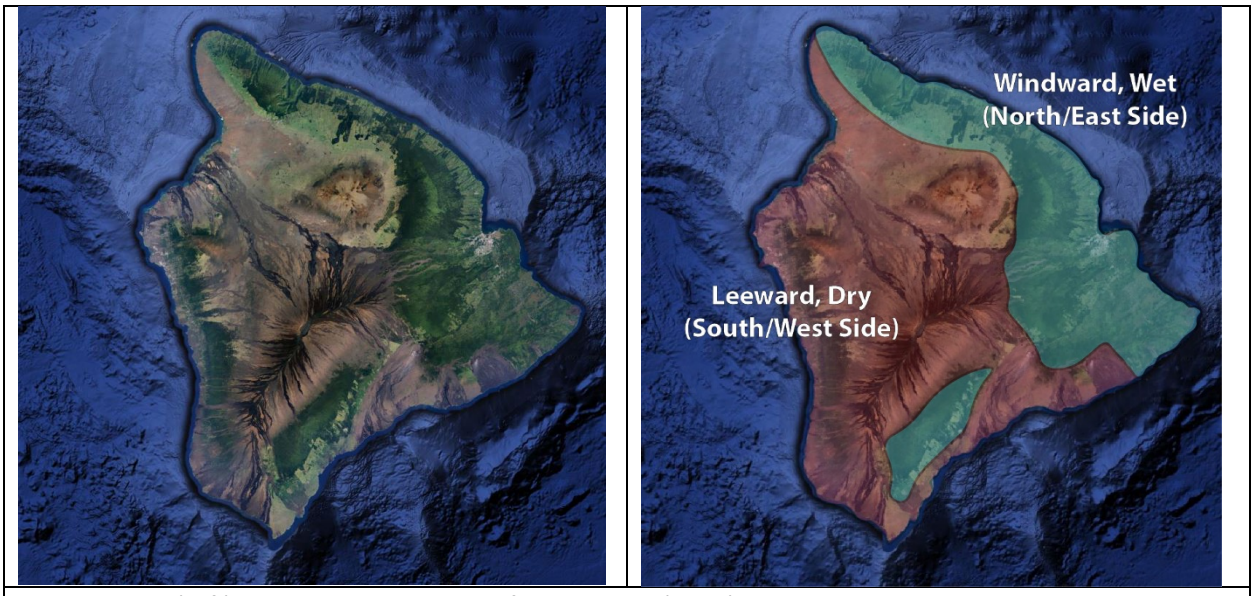

Figure 1.2.3: (*left*) The unlabeled island of Hawaii and (*right*) a labelled picture showing the windward and leeward sides of the island where rainfall greatly varies; as can be seen by the relative density of vegetation cover in the left image.

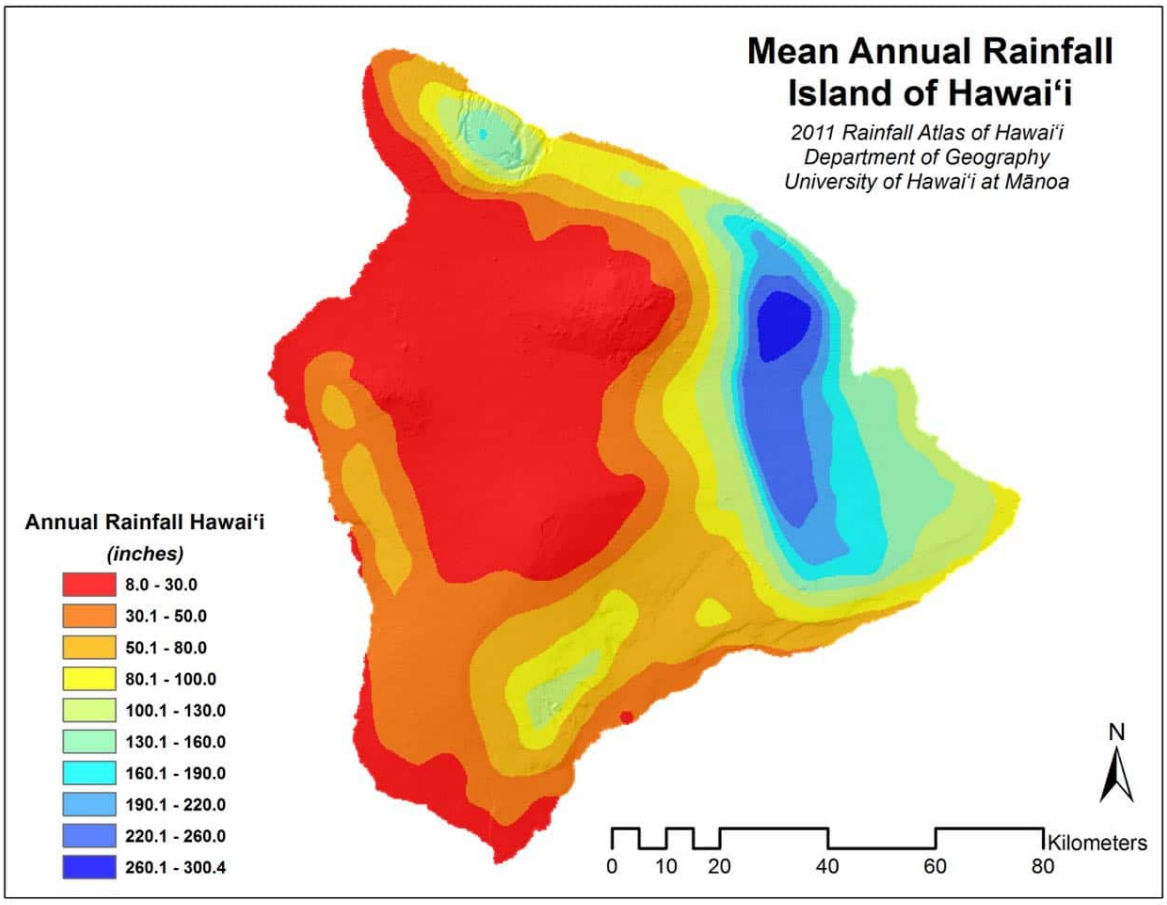

Figure 1.2.4: Mean annual rainfall on the Island of Hawaii (Figure from Frazier et al., 2016).

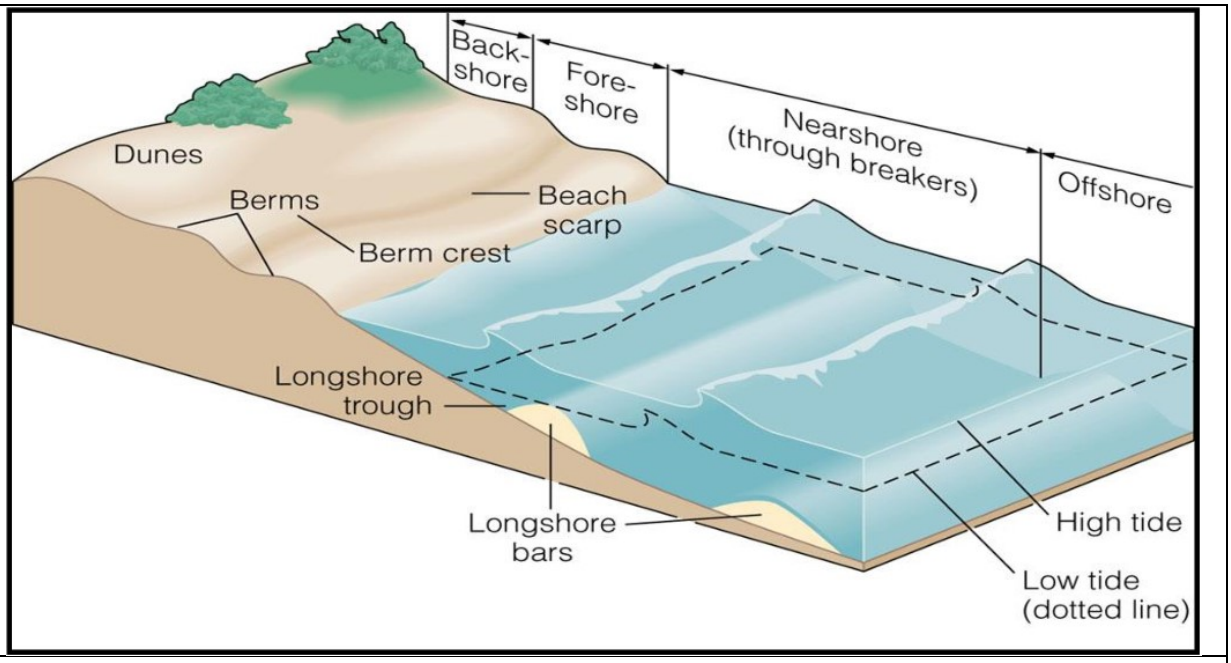

Figure 1.2.5: A schematic of typical beach morphology (Fadil, 2018).

(a) Arithmetic method of moments

Mean	Standard deviation	Skewness	Kurtosis
$\bar{x}_a = \frac{\Sigma f m_m}{100}$	$\sigma_a = \sqrt{\frac{\Sigma f (m_m - \bar{x}_a)^2}{100}}$	$Sk_a = \frac{\Sigma f (m_m - \bar{x}_a)^3}{100\sigma_a{}^3}$	$K_a = \frac{\Sigma f (m_m - \bar{x}_a)^4}{100\sigma_a{}^4}$

(b) Geometric method of moments

Mean	Standard deviation	Skewness	Kurtosis
$\bar{x}_g = \exp \frac{\Sigma f \ln m_m}{100}$	$\sigma_g = \exp \sqrt{\frac{\Sigma f (\ln m_m - \ln \bar{x}_g)^2}{100}}$	$Sk_g = \frac{\Sigma f (\ln m_m - \ln \bar{x}_g)^3}{100 \ln \sigma_g{}^3}$	$K_g = \frac{\Sigma f (\ln m_m - \ln \bar{x}_g)^4}{100 \ln \sigma_g{}^4}$

(c) Logarithmic method of moments

Mean	Standard deviation	Skewness	Kurtosis
$\bar{x}_\phi = \frac{\Sigma f m_\phi}{100}$	$\sigma_\phi = \sqrt{\frac{\Sigma f (m_\phi - \bar{x}_\phi)^2}{100}}$	$Sk_\phi = \frac{\Sigma f (m_\phi - \bar{x}_\phi)^3}{100\sigma_\phi{}^3}$	$K_\phi = \frac{\Sigma f (m_\phi - \bar{x}_\phi)^4}{100\sigma_\phi^4}$

(d) Logarithmic (original) Folk and Ward (1957) graphical measures

Mean	Standard deviation	Skewness	Kurtosis
$M_Z = \frac{\phi_{16} + \phi_{50} + \phi_{84}}{3}$	$\sigma_I = \frac{\phi_{84} - \phi_{16}}{4} + \frac{\phi_{95} - \phi_5}{6{\cdot}6}$	$Sk_I = \frac{\phi_{16} + \phi_{84} - 2\phi_{50}}{2(\phi_{84} - \phi_{16})} + \frac{\phi_5 + \phi_{95} - 2\phi_{50}}{2(\phi_{95} - \phi_5)}$	$K_G = \frac{\phi_{95} - \phi_5}{2{\cdot}44(\phi_{75} - \phi_{25})}$

(e) Geometric (modified) Folk and Ward (1957) graphical measures

Mean	Standard deviation
$M_G = \exp \frac{\ln P_{16} + \ln P_{50} + \ln P_{84}}{3}$	$\sigma_G = \exp\left(\frac{\ln P_{16} - \ln P_{84}}{4} + \frac{\ln P_5 - \ln P_{95}}{6{\cdot}6}\right)$
Skewness	**Kurtosis**
$Sk_G = \frac{\ln P_{16} + \ln P_{84} - 2(\ln P_{50})}{2(\ln P_{84} - \ln P_{16})} + \frac{\ln P_5 + \ln P_{95} - 2(\ln P_{50})}{2(\ln P_{25} - \ln P_5)}$	$K_G = \frac{\ln P_5 - \ln P_{95}}{2{\cdot}44(\ln P_{25} - \ln P_{75})}$

Table 1.1.1: The formulae for the statistical moments including arithmetic (a), geometric (b), logarithmic (c) and also the Folk and Ward (1957) adjusted calculations for logarithmic (d) and geometric (e). *f* is the frequency in percent, *m* is the mid-point of each interval in metric (m_m) or phi (m_φ) units, P_x and φ_x are grain diameters in metric or phi units, and *x* is the cumulative percentile values. Table modified and adjusted from Blott and Pye (2001).

Sorting (σ_1)		Skewness (Sk_1)		Kurtosis (K_G)	
Very well sorted	<0·35	Very fine skewed	$^{+}$0·3 to $^{+}$1·0	Very platykurtic	<0·67
Well sorted	0·35–0·50	Fine skewed	$^{+}$0·1 to $^{+}$0·3	Platykurtic	0·67–0·90
Moderately well sorted	0·50–0·70	Symmetrical	$^{+}$0·1 to $^{-}$0·1	Mesokurtic	0·90–1·11
Moderately sorted	0·70–1·00	Coarse skewed	$^{-}$0·1 to $^{-}$0·3	Leptokurtic	1·11–1·50
Poorly sorted	1·00–2·00	Very coarse skewed	$^{-}$0·3 to $^{-}$1·0	Very leptokurtic	1·50–3·00
Very poorly sorted	2·00–4·00			Extremely leptokurtic	>3·00
Extremely poorly sorted	>4·00				

Table 1.1.2: Descriptors from Folk and Ward (1957) for the calculated moments. Table adapted from Blott and Pye (2001).

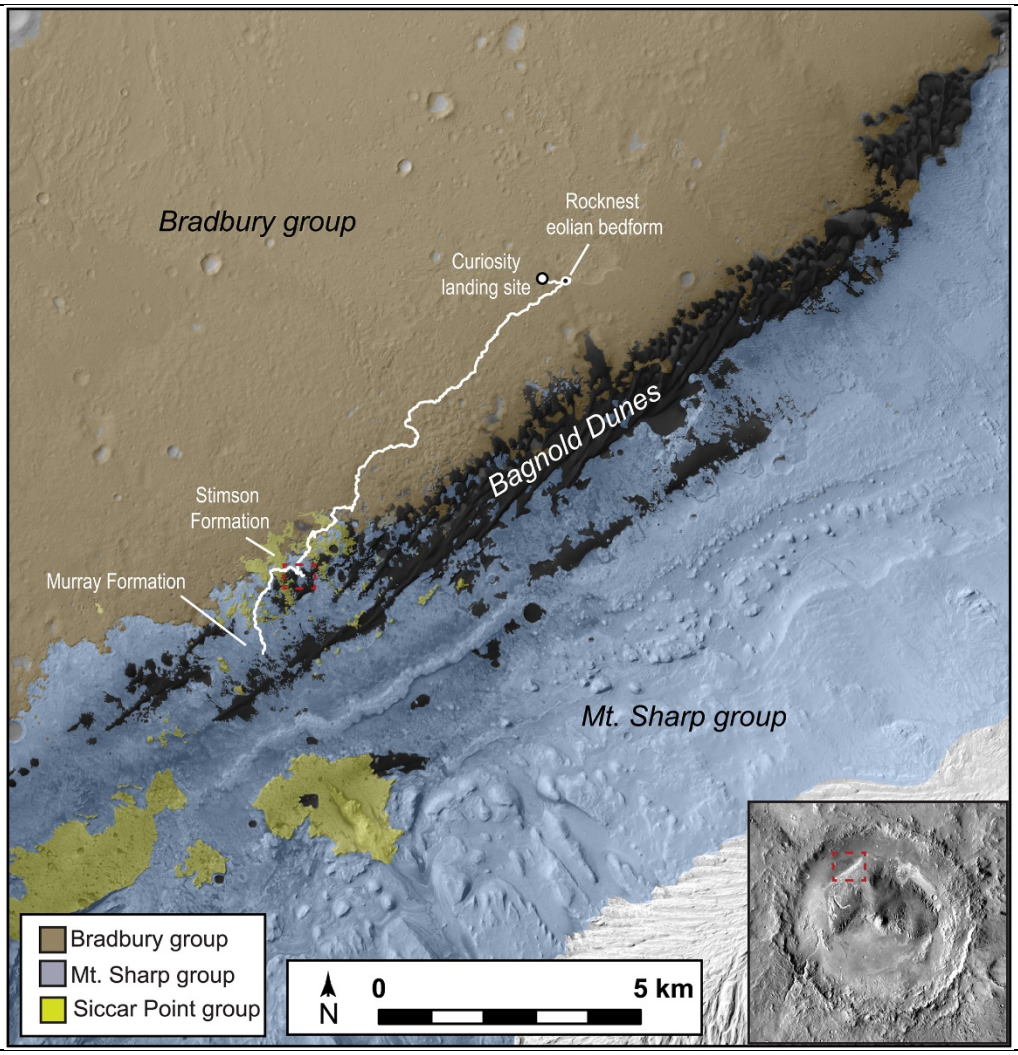

Figure 1.3.1: Map from Ehlmann et al. (2018) showing the location and path of the Curiosity Rover on Mars.

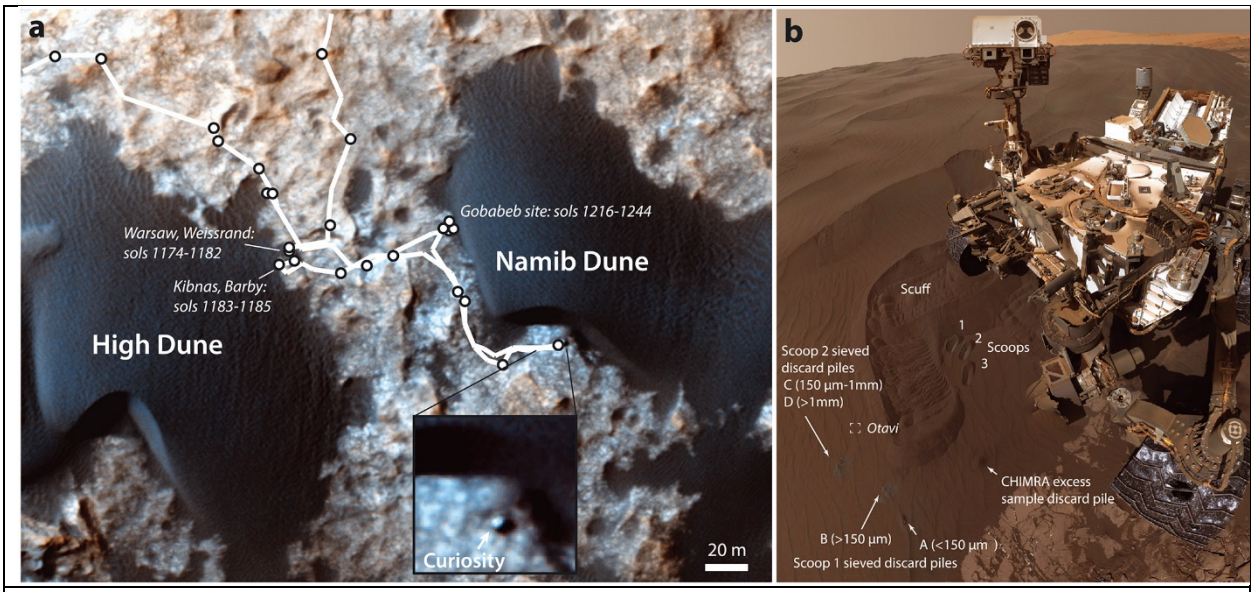

Figure 1.3.2: Map from Ehlmann et al. (2018) showing the location and path of the Curiosity Rover on Mars and the two visited dunes: High Dune and Namib Dune.

Figure 2.1.1: The island of Hawaii with the 18 beaches sampled.

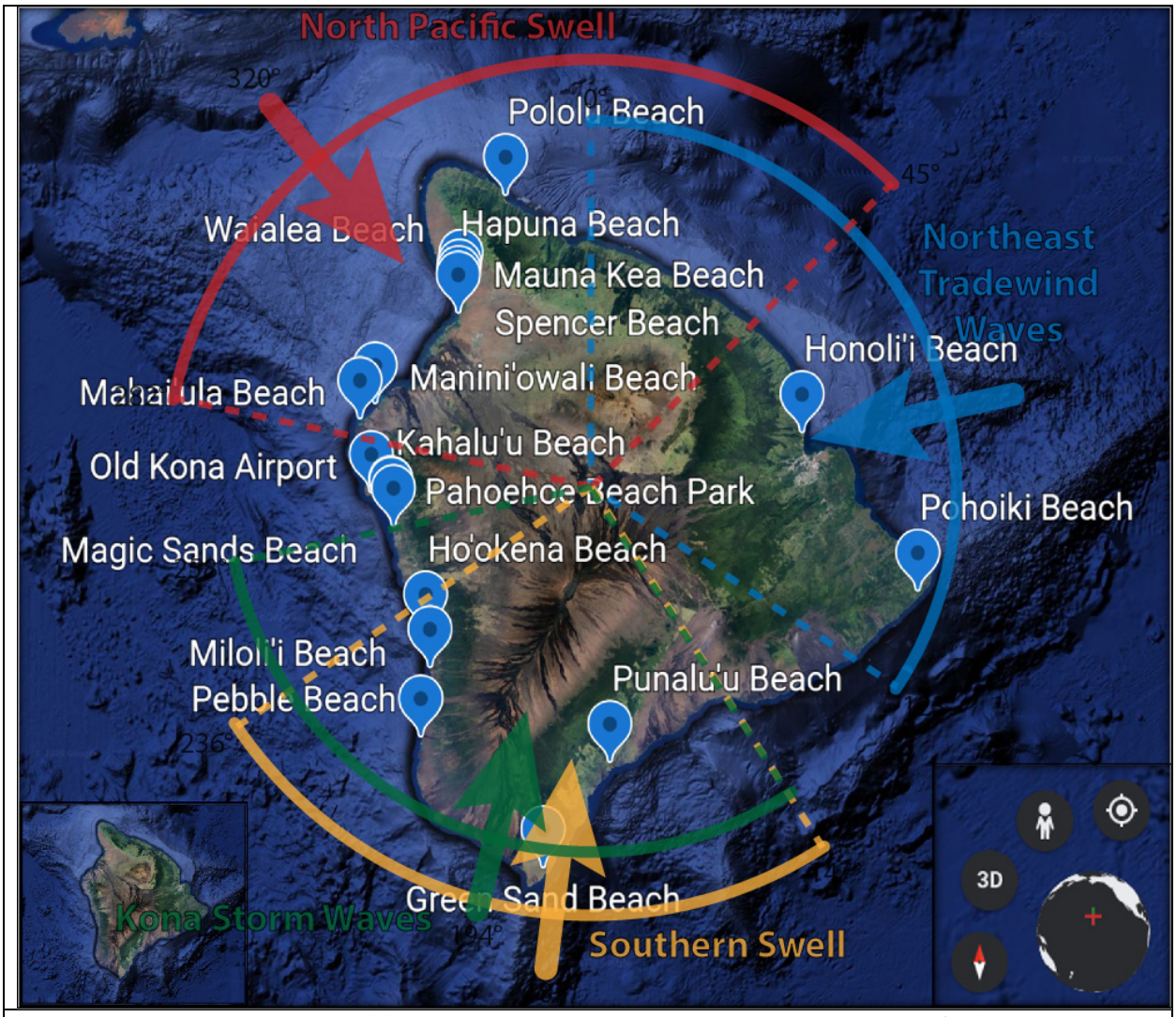

Figure 2.1.2: A map of the survey locations with an overlaid map showing weather/climate subjugation.

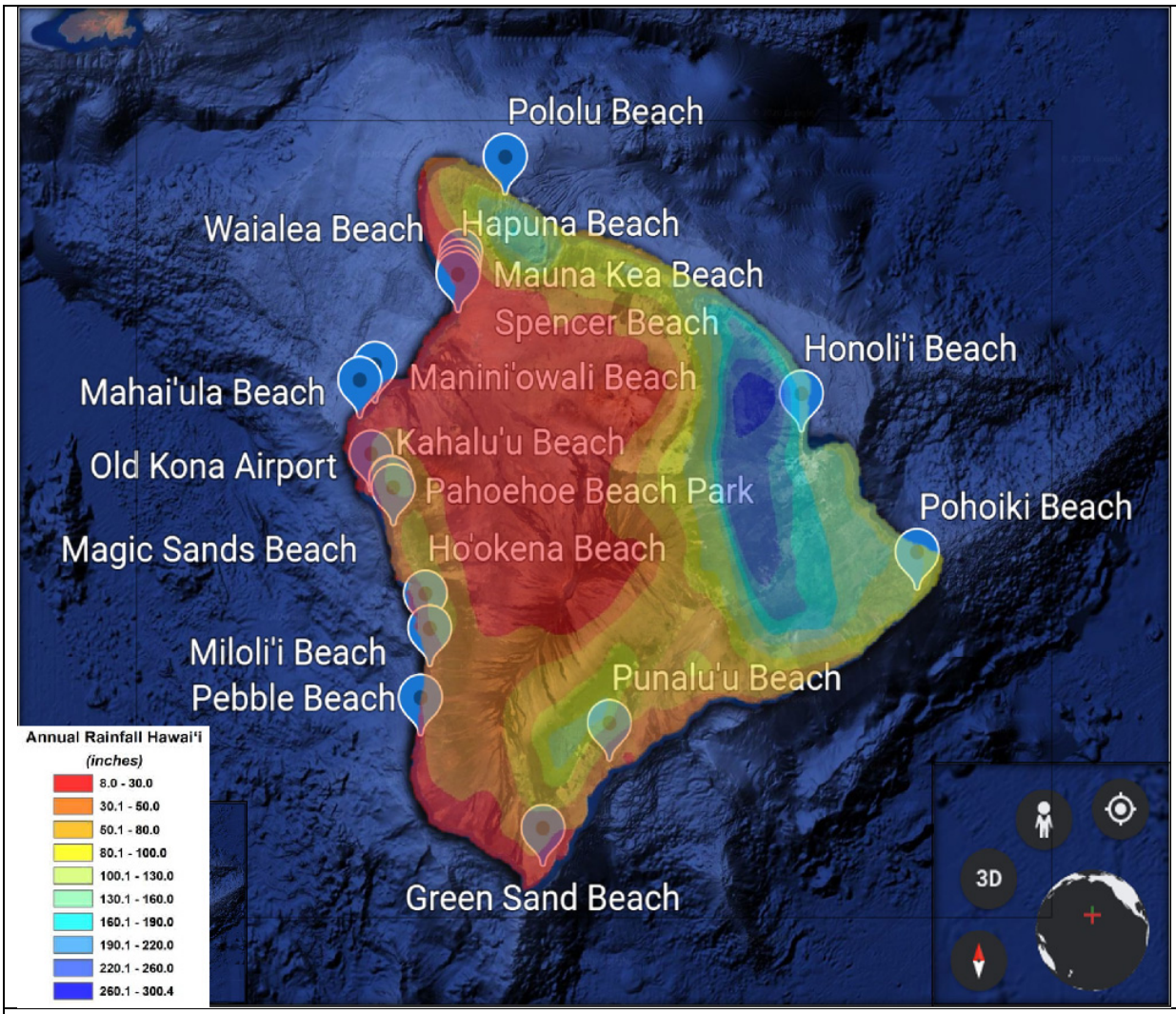

Figure 2.1.3: A map of the survey locations with an overlaid map showing rainfall subjugation.

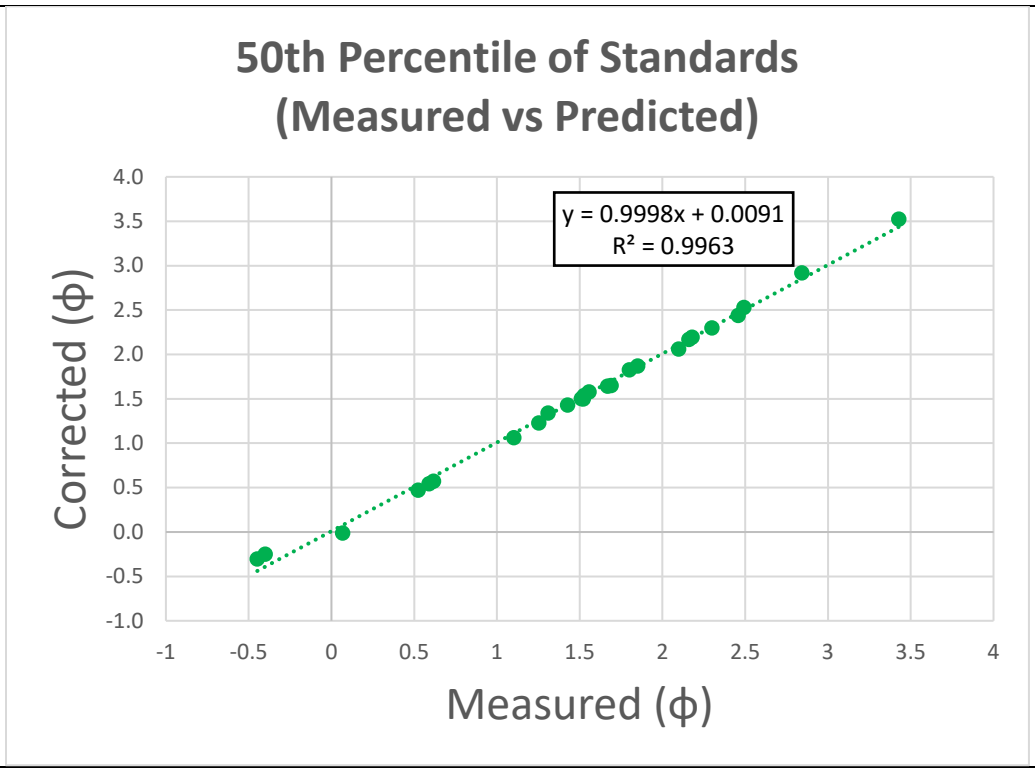

Figure 2.2.1: The 50th percentile data points from the standards. The program accurately predicts the 50th percentile.

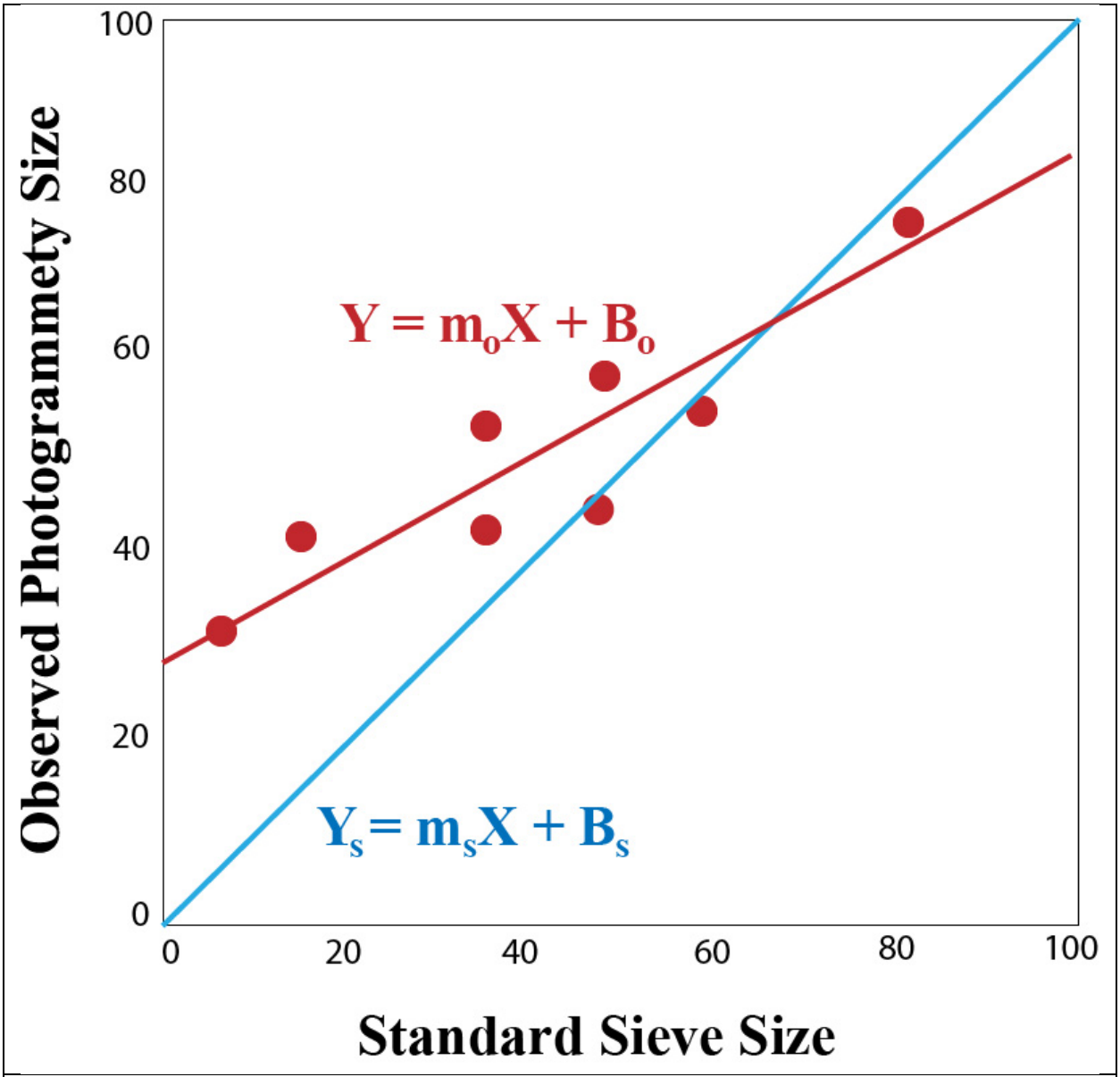

Figure 2.2.2: A schematic example of how the predicted (modelled) data points compare and can be corrected to the measured (sieved) data points.

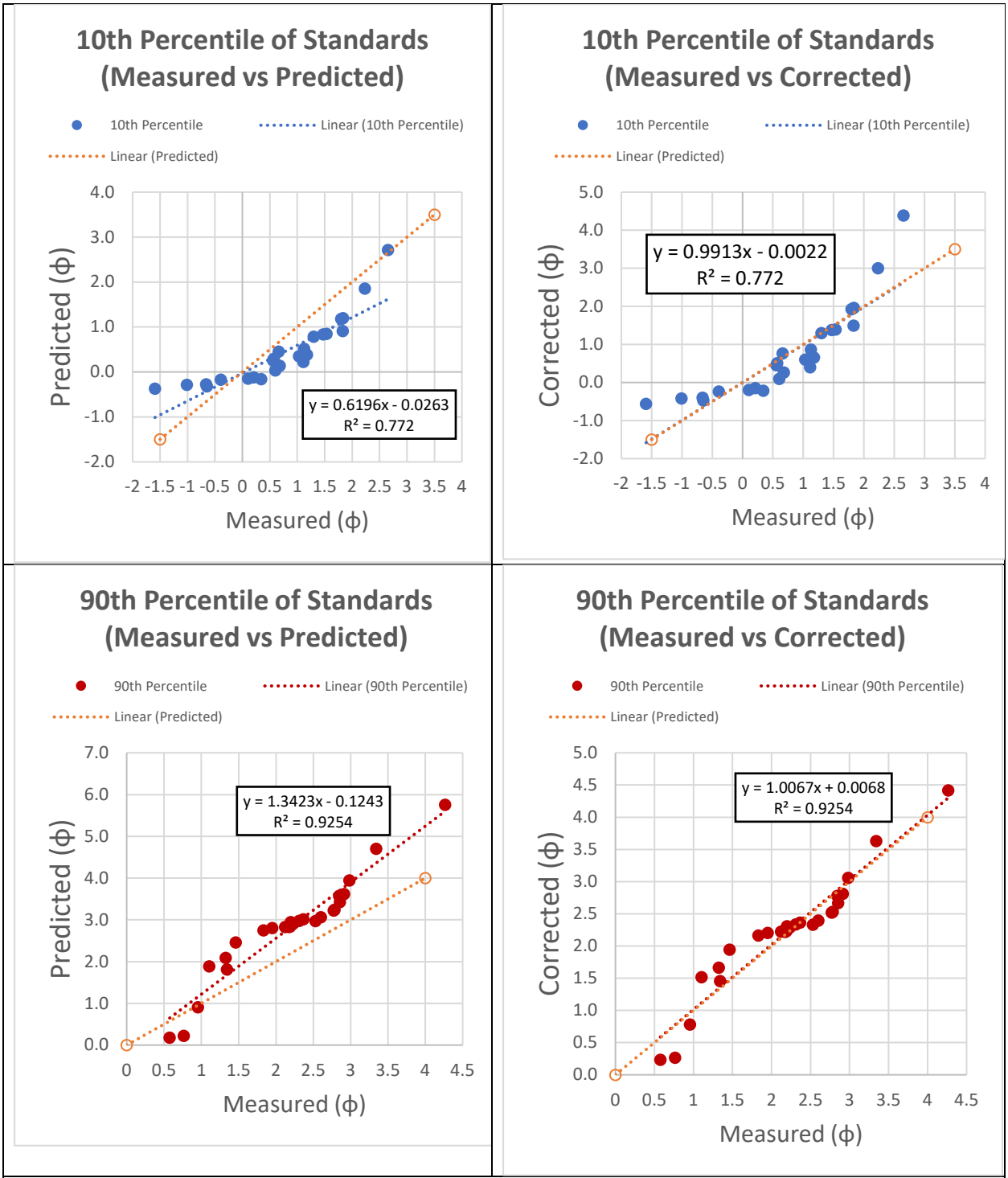

Figure 2.2.3: (*top*) The 10th percentile data points for the standards before (*top-left*) and after (*top-right*) corrections were applied. (*bottom*) The 90th percentile data points for the standards before (*bottom-left*) and after (*bottom-right*) corrections were applied.

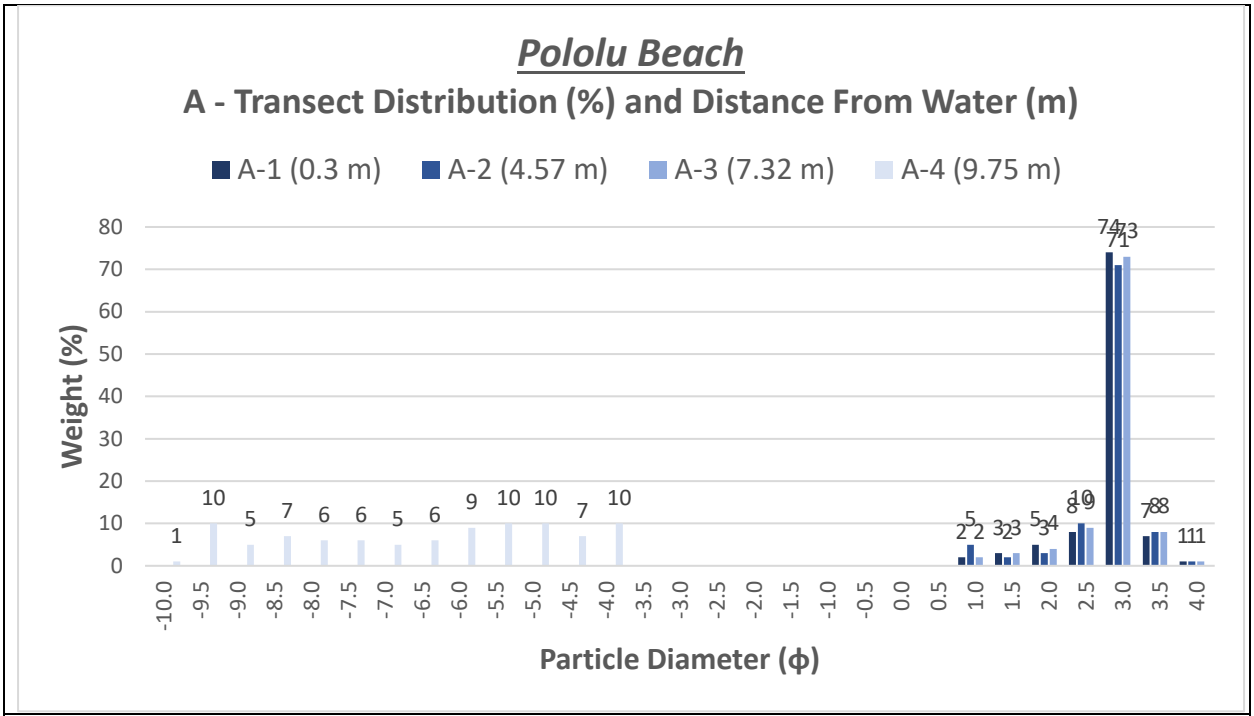

Figure 3.1.1: Pololu Beach distribution graph (% of whole) for transect A. See *Appendix A.1.1* for location photo and transect locations.

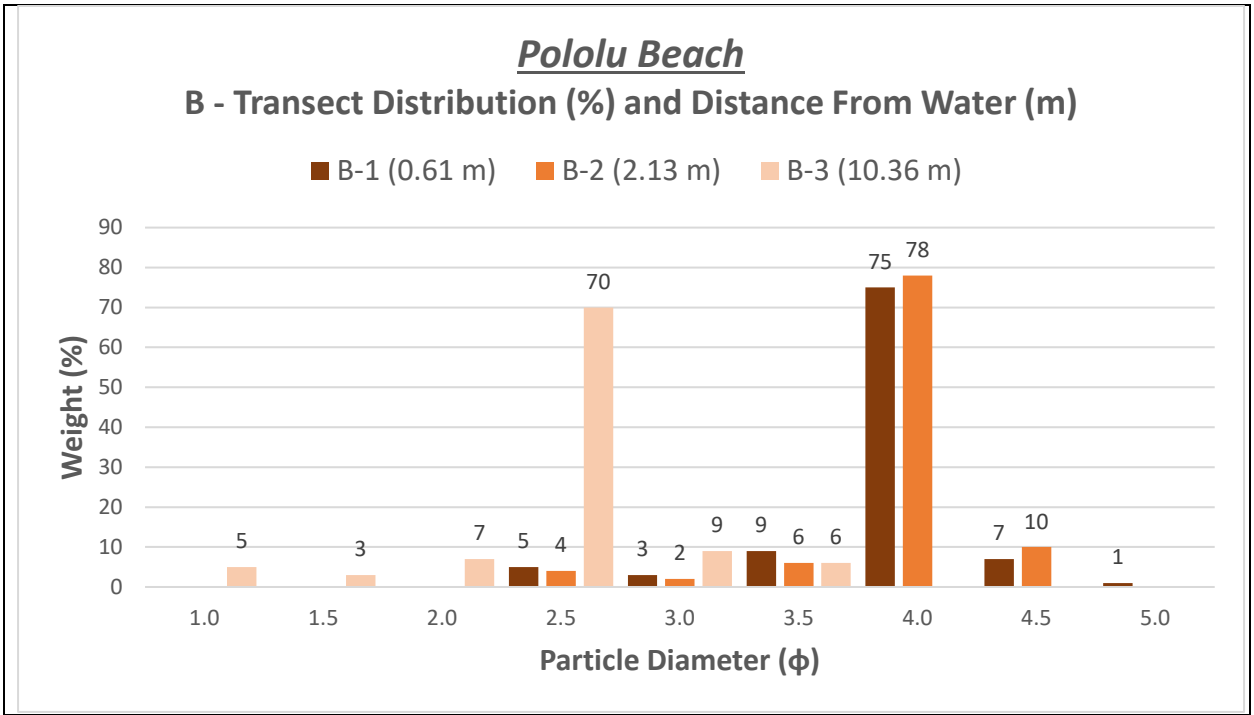

Figure 3.1.2: Pololu Beach distribution graph (% of whole) for transect B. See *Appendix A.1.1* for location photo and transect locations.

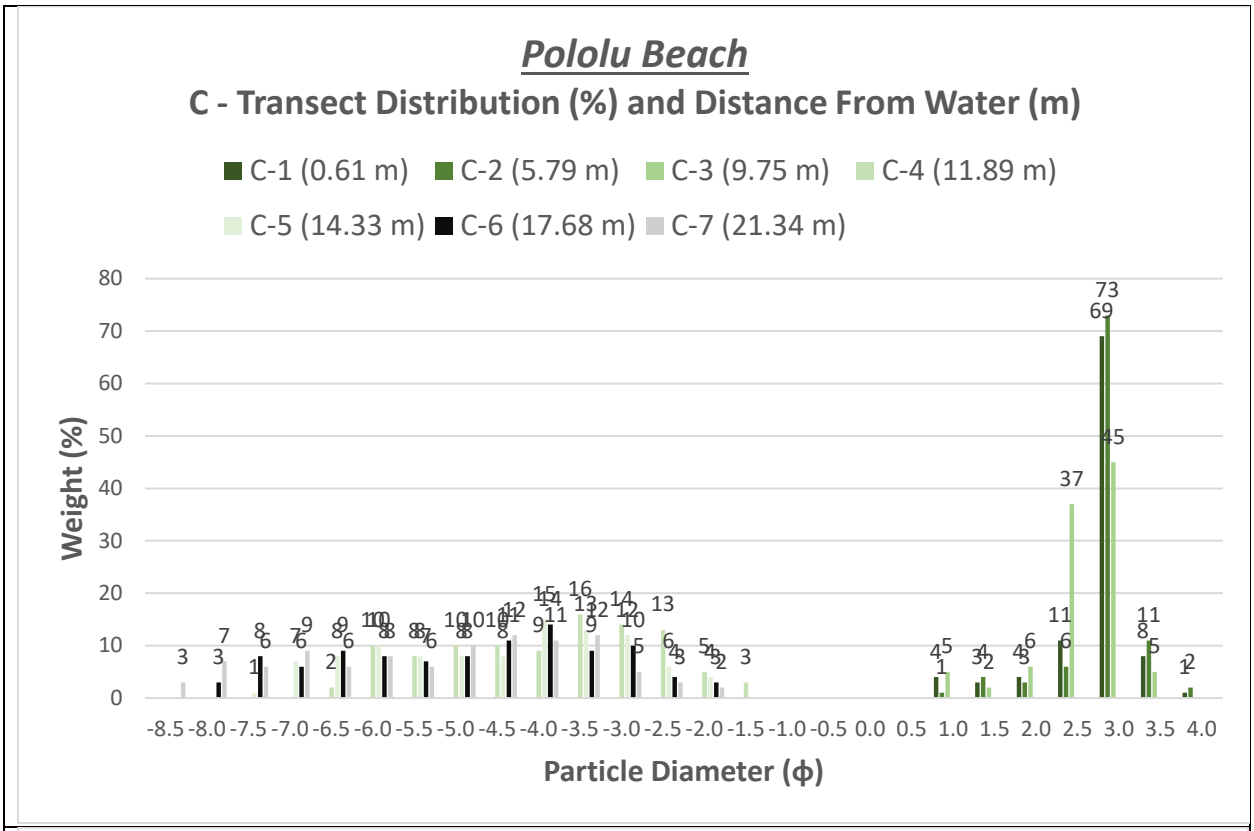
Pololu Beach
C - Transect Distribution (%) and Distance From Water (m)
C-1 (0.61 m)
C-2 (5.79 m)
C-3 (9.75 m)
C-4 (11.89 m)
C-5 (14.33 m)
C-6 (17.68 m)
C-7 (21.34 m)
Weight (%)
Particle Diameter (ϕ)

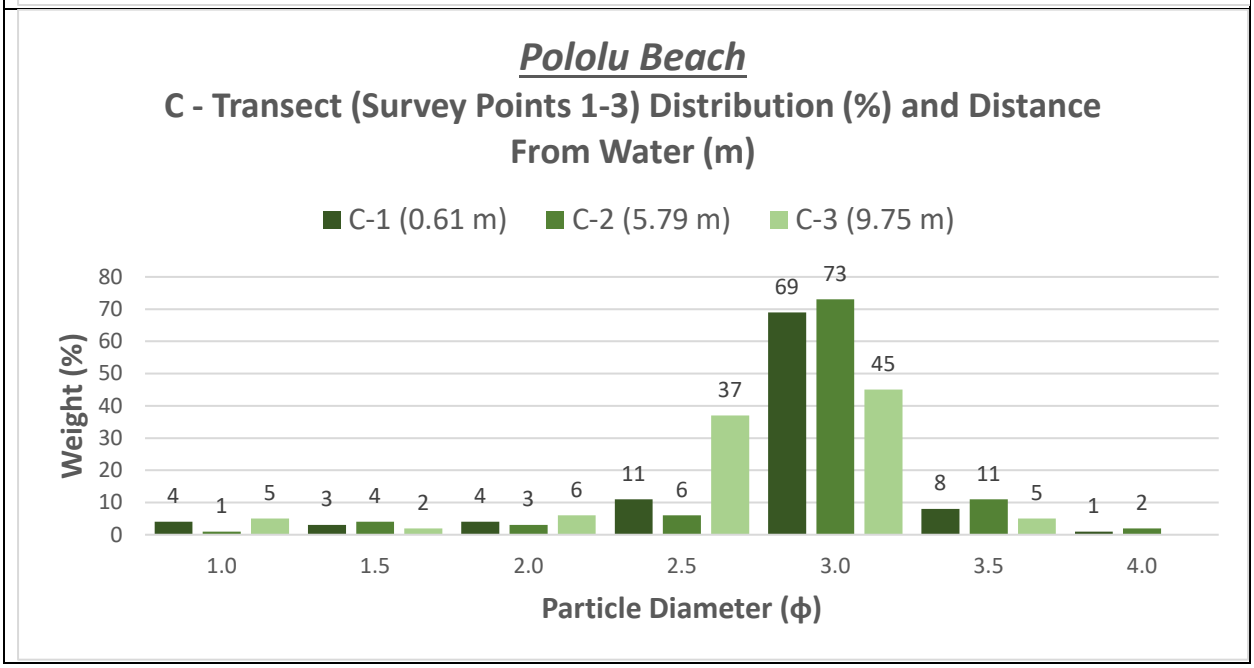
Pololu Beach
C - Transect (Survey Points 1-3) Distribution (%) and Distance From Water (m)
C-1 (0.61 m)
C-2 (5.79 m)
C-3 (9.75 m)
Weight (%)
Particle Diameter (ϕ)

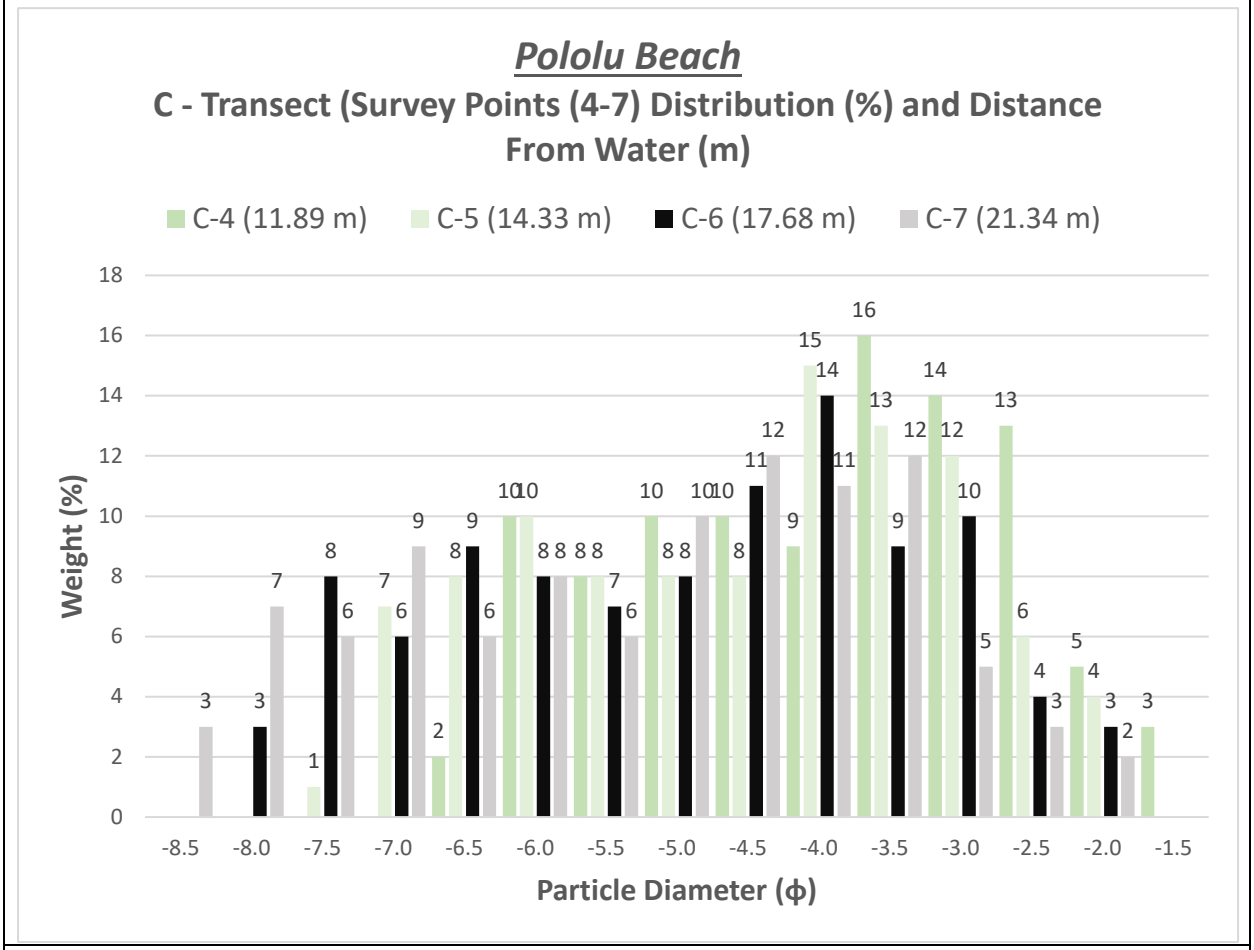

Figure 3.1.3: Pololu Beach distribution graphs (% of whole) for all survey points in Transect C (*top*), survey points 1 – 3 (*middle*), and survey points 4 – 7 (*bottom*). See *Appendix A.1.1* for location photo and transect locations.

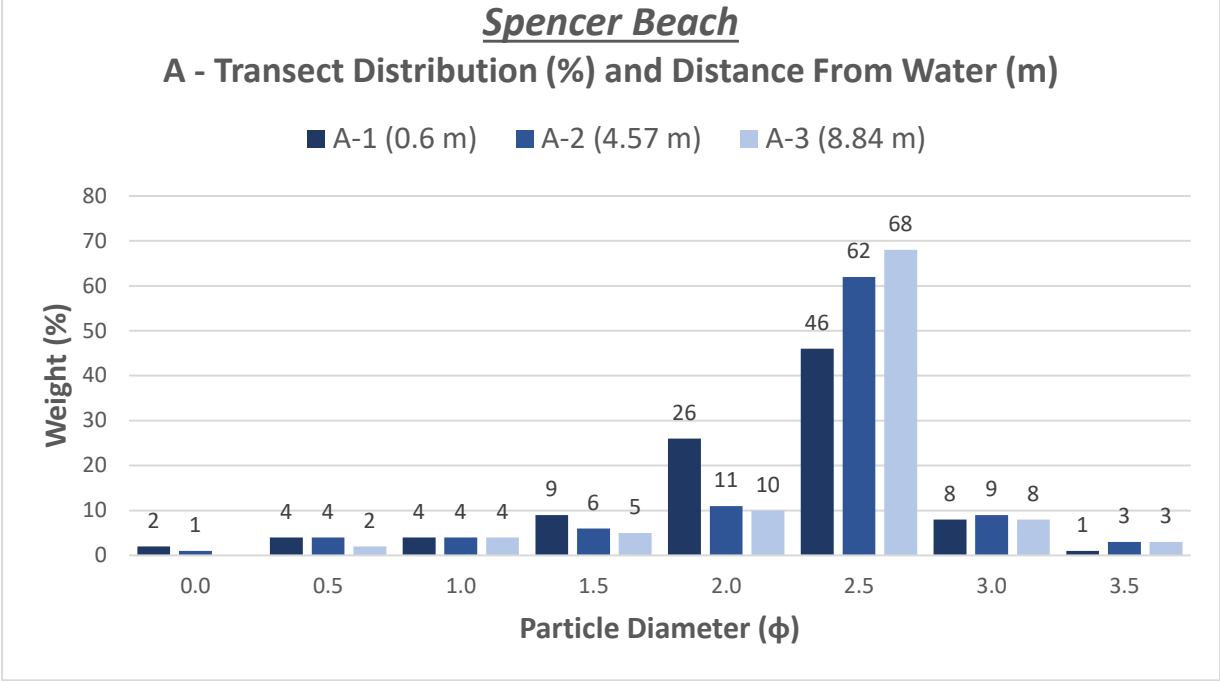

Figure 3.1.4: Spencer Beach distribution graph (% of whole) for all survey points in Transect A. See *Appendix A.1.2* for location photo and transect locations.

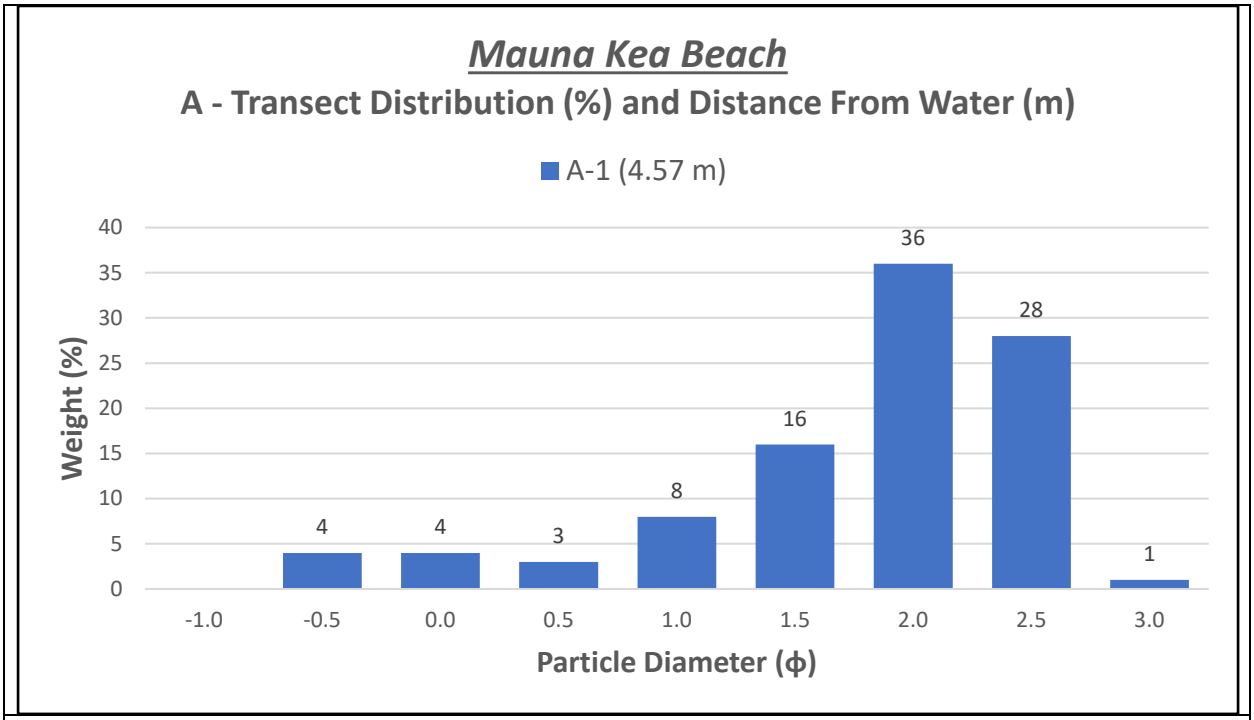

Figure 3.1.5: Mauna Kea Beach distribution graph (% of whole) for the survey point in Transect A. See *Appendix A.1.3* for location photo and transect locations.

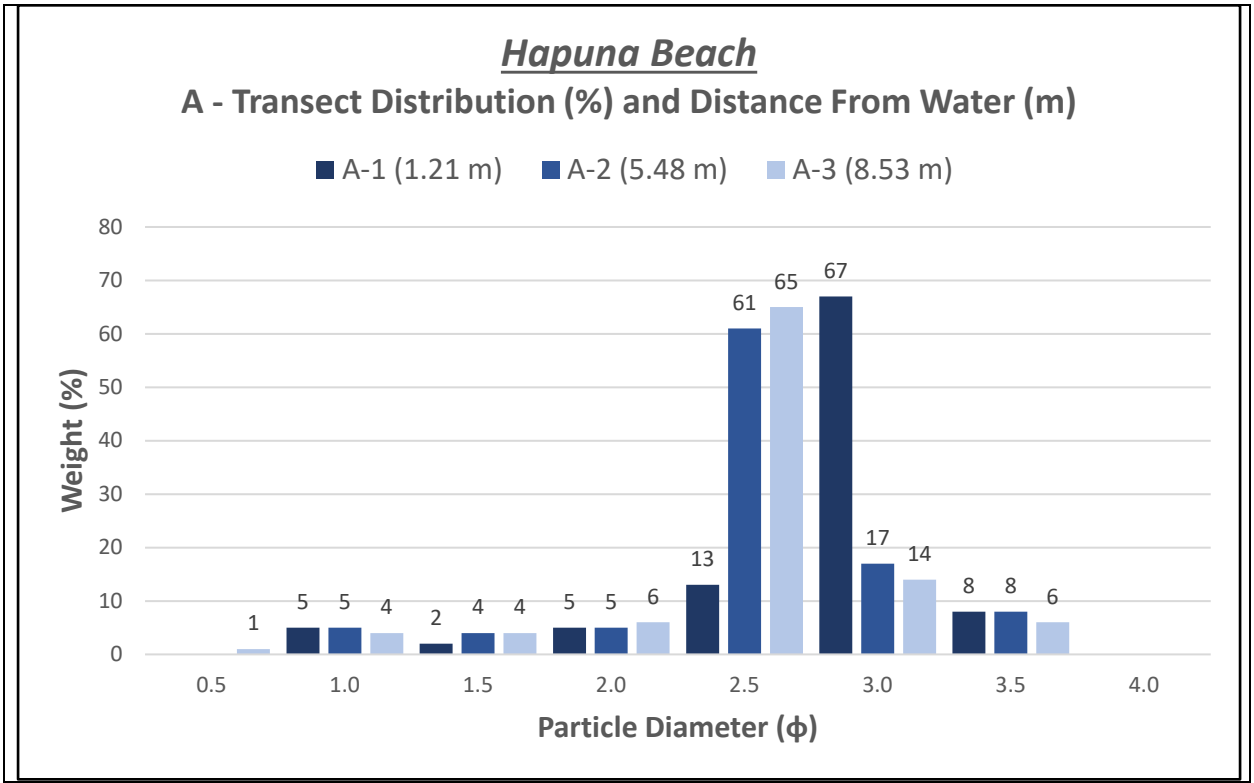

Figure 3.1.6: Hapuna Beach distribution graph (% of whole) for all survey points in Transect A. See *Appendix A.1.4* for location photo and transect locations.

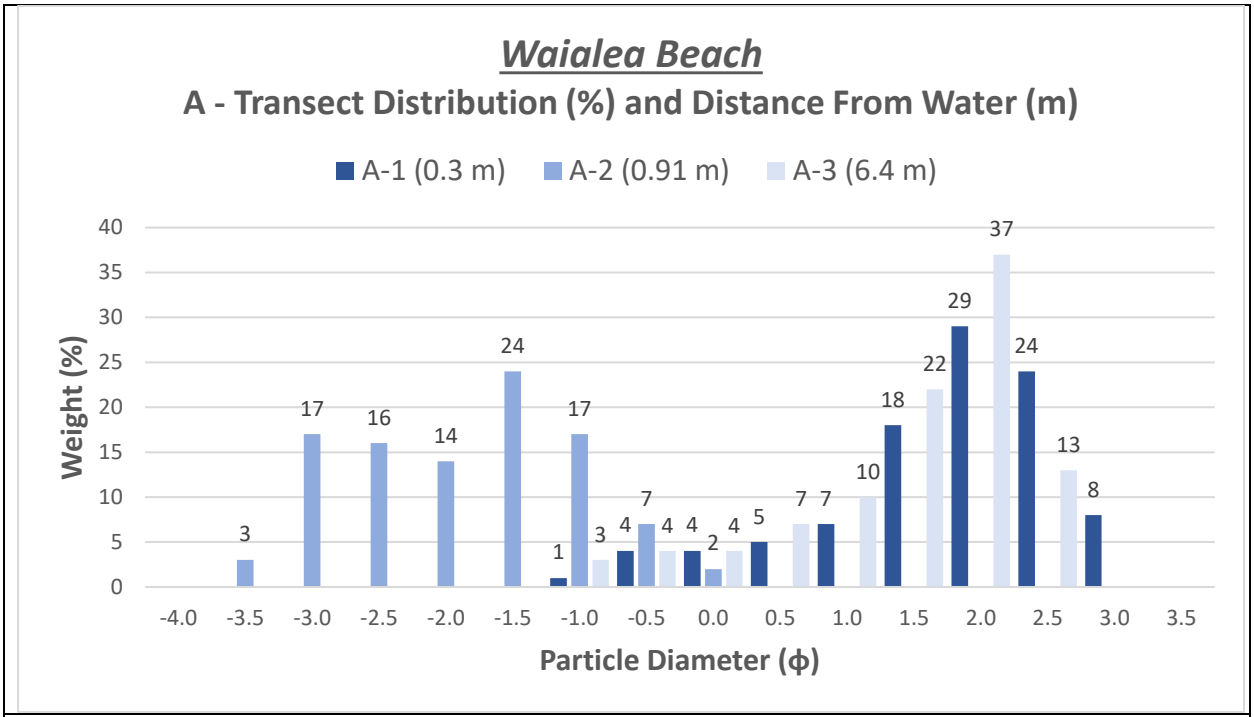

Figure 3.1.7: Waialea Beach distribution graph (% of whole) for all survey points in Transect A. See *Appendix A.1.5* for location photo and transect locations.

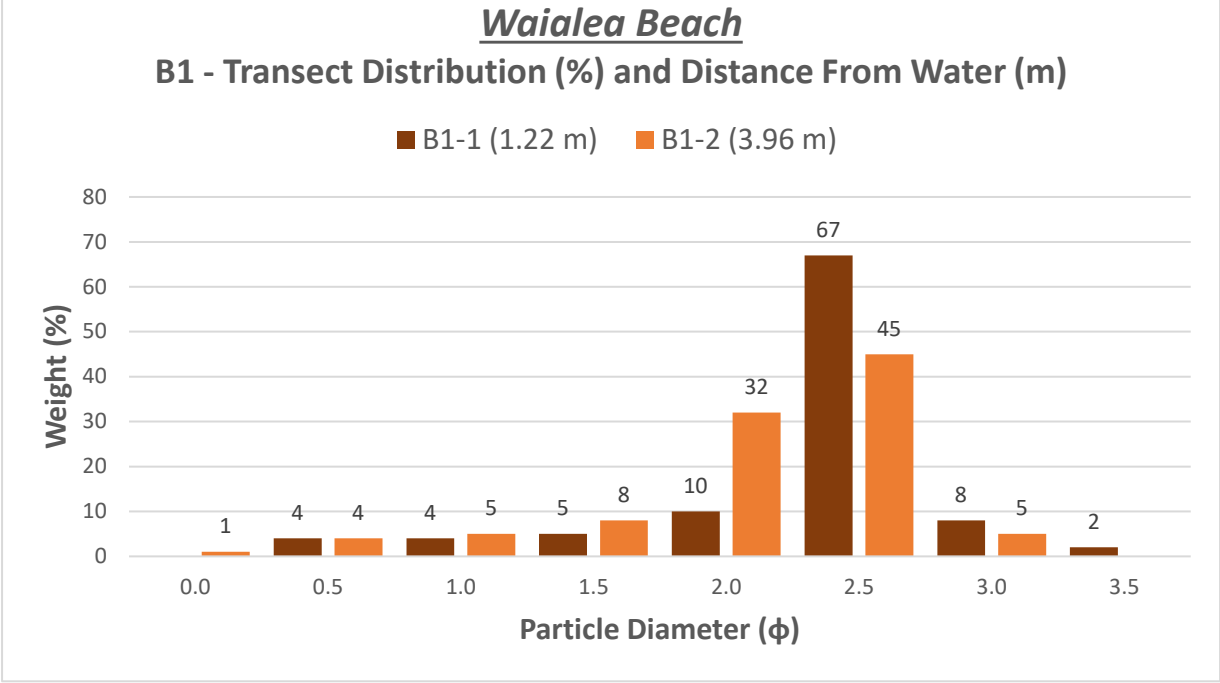

Figure 3.1.8: Waialea Beach distribution graph (% of whole) for all survey points in Transect B. See *Appendix A.1.5* for location photo and transect locations.

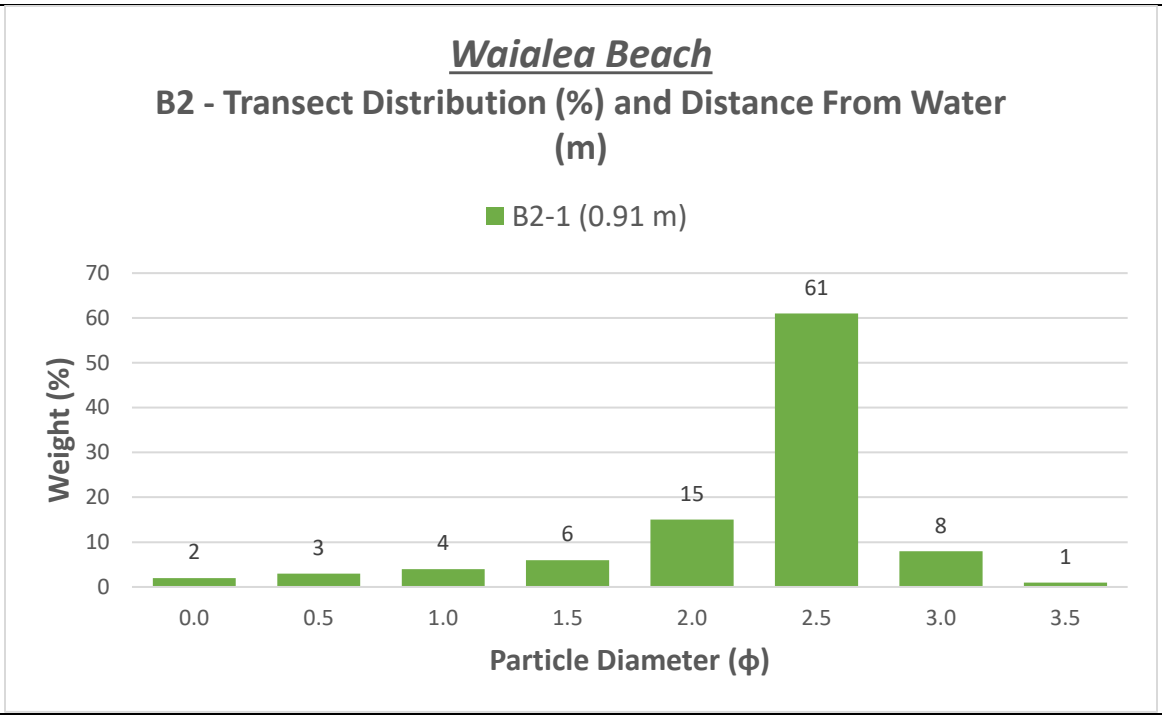

Figure 3.1.9: Waialea Beach distribution graph (% of whole) for the survey point in Transect C. See *Appendix A.1.5* for location photo and transect locations.

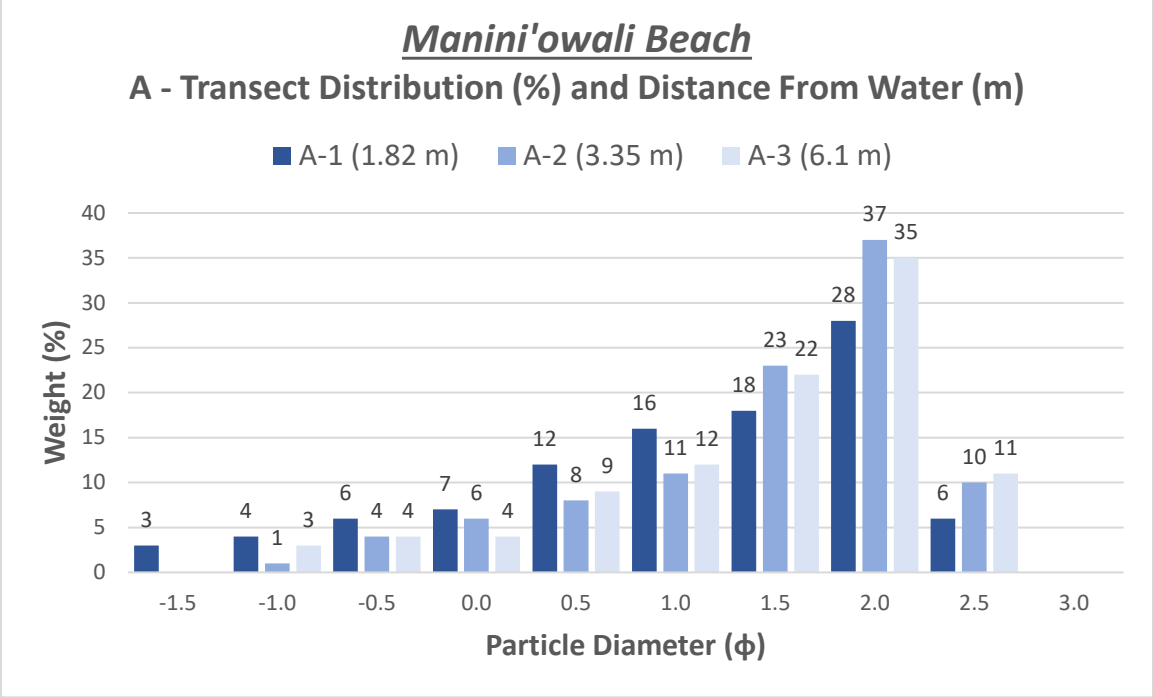

Figure 3.1.10: Manini'owali Beach distribution graph (% of whole) for all survey points in Transect A. See *Appendix A.1.6* for location photo and transect locations.

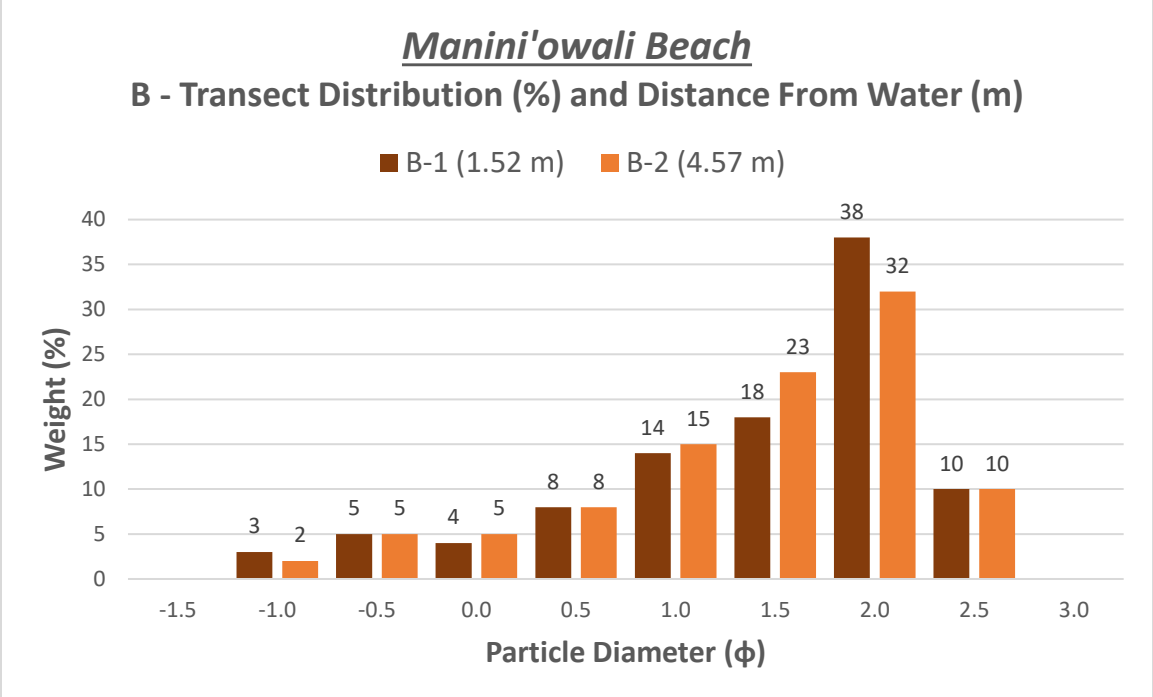

Figure 3.1.11: Manini'owali Beach distribution graph (% of whole) for all survey points in Transect B. See *Appendix A.1.6* for location photo and transect locations.

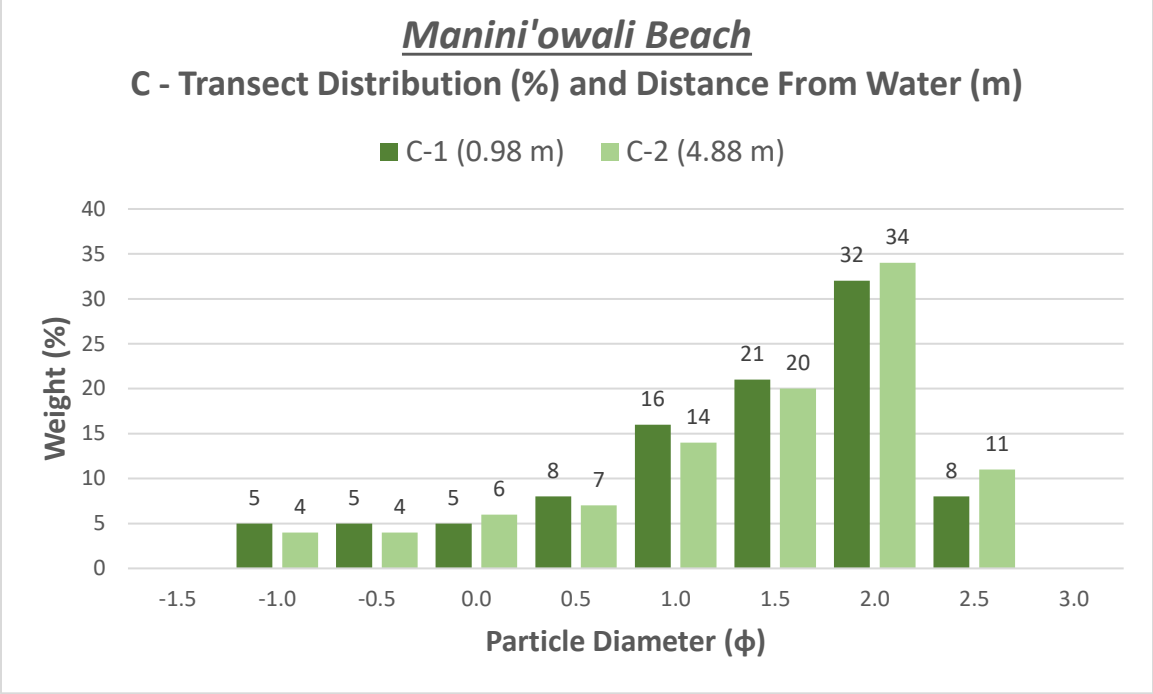

Figure 3.1.12: Manini'owali Beach distribution graph (% of whole) for all survey points in Transect C. See *Appendix A.1.6* for location photo and transect locations.

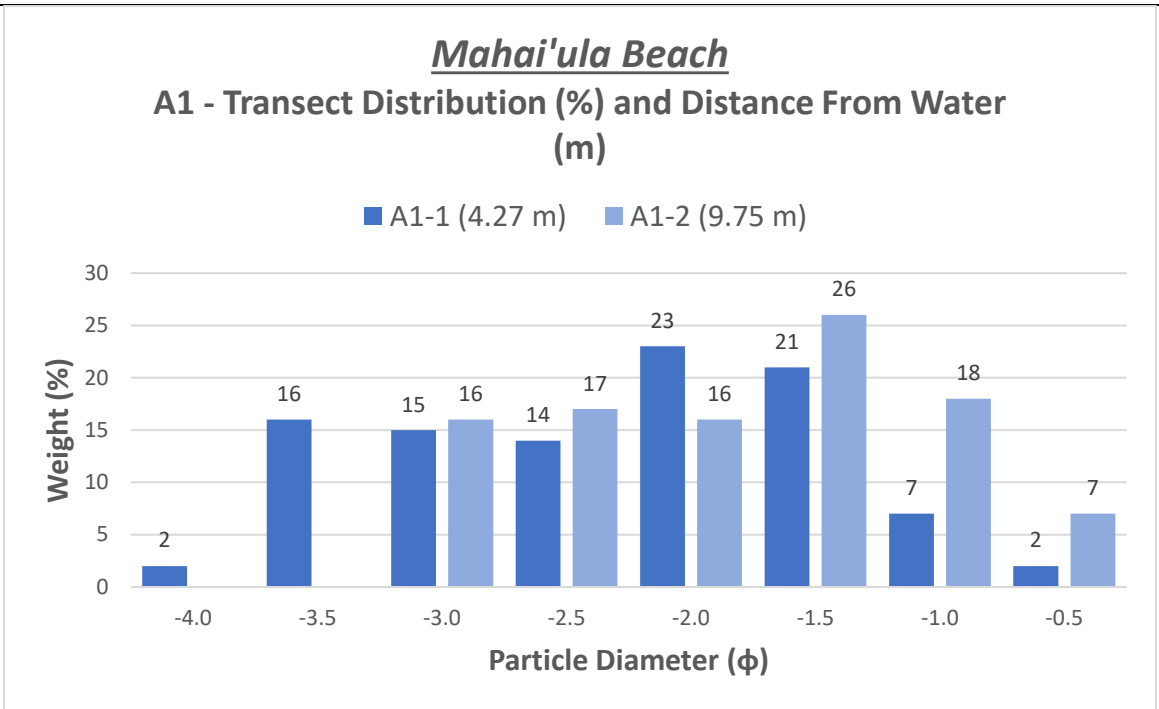

Figure 3.1.13: Mahai'ula Beach distribution graph (% of whole) for all survey points in Transect A1. See *Appendix A.1.7* for location photo and transect locations.

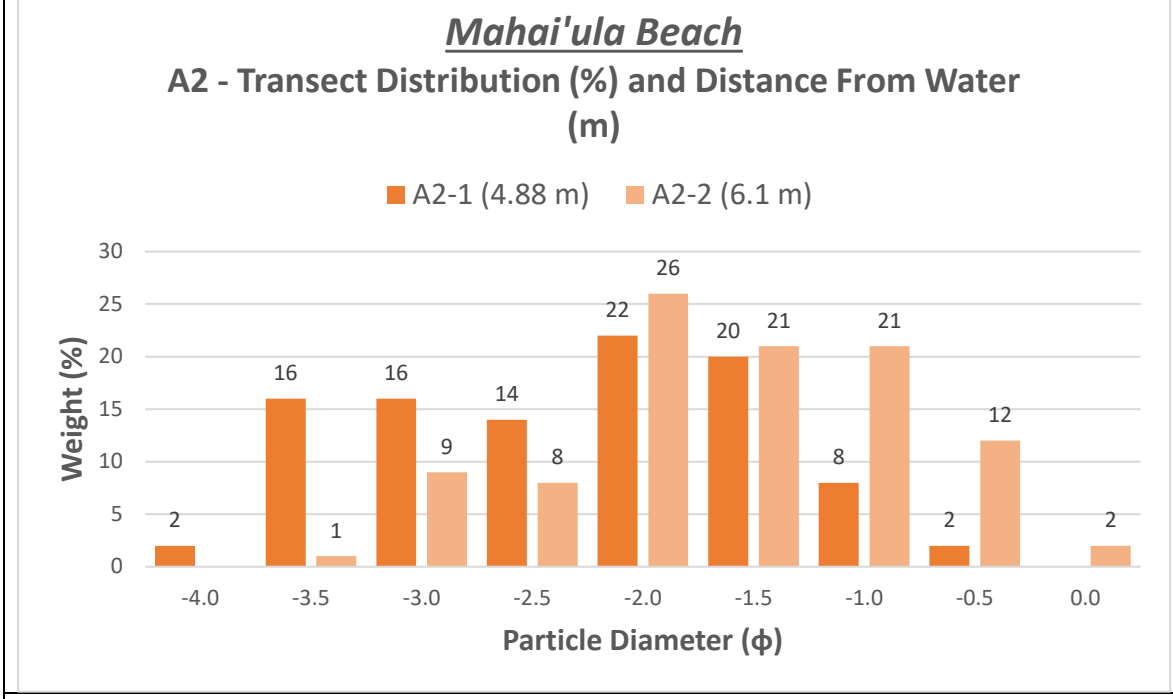

Figure 3.1.14: Mahai'ula Beach distribution graph (% of whole) for all survey points in Transect A2. See *Appendix A.1.7* for location photo and transect locations.

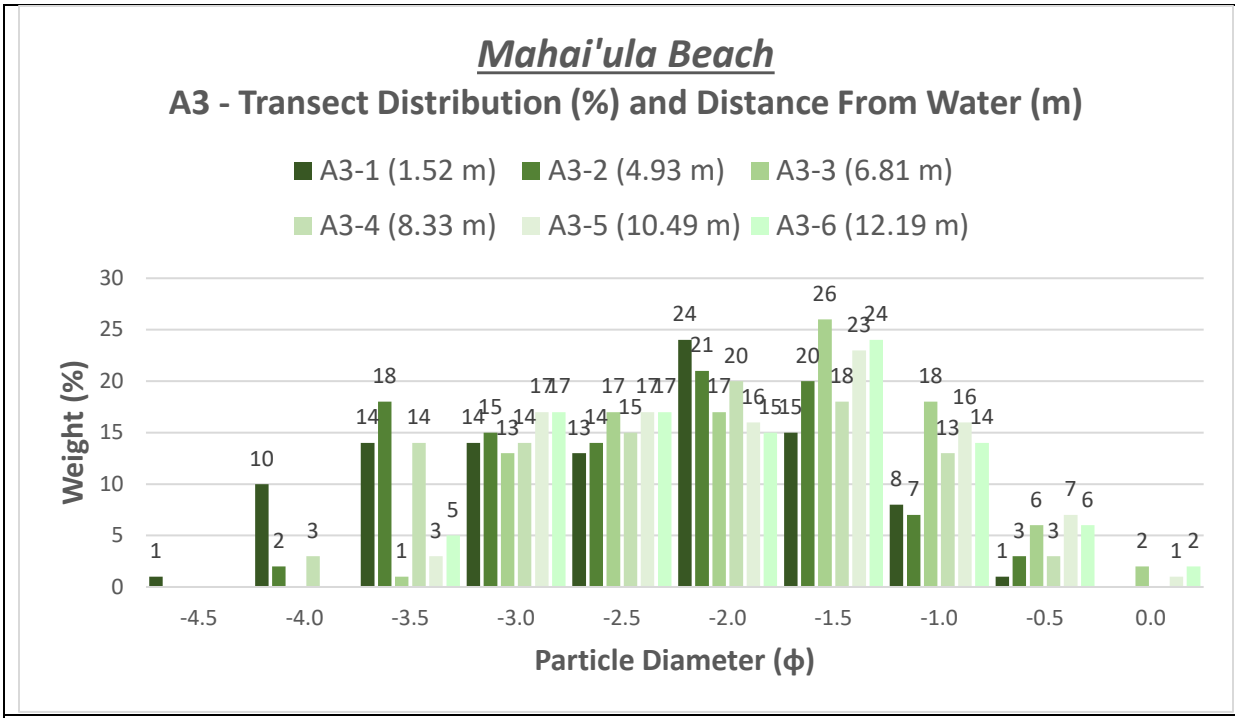

Figure 3.1.15: Mahai'ula Beach distribution graph (% of whole) for all survey points in Transect A3. See *Appendix A.1.7* for location photo and transect locations.

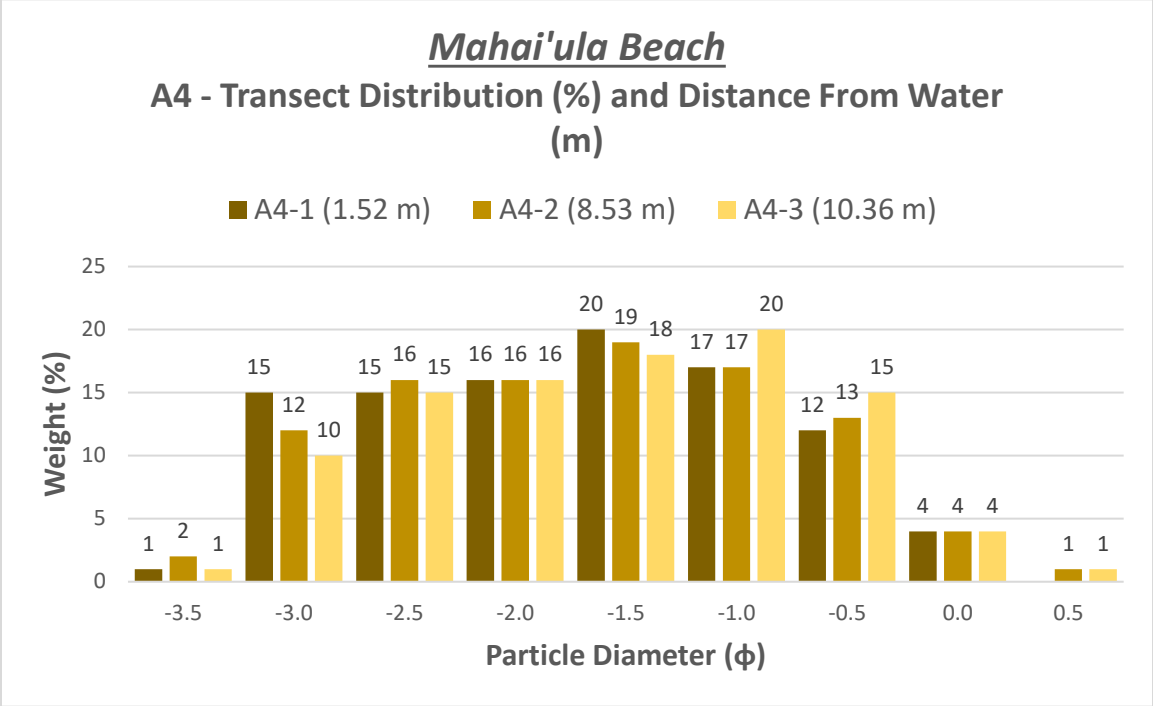

Figure 3.1.16: Mahai'ula Beach distribution graph (% of whole) for all survey points in Transect A4. See *Appendix A.1.7* for location photo and transect locations.

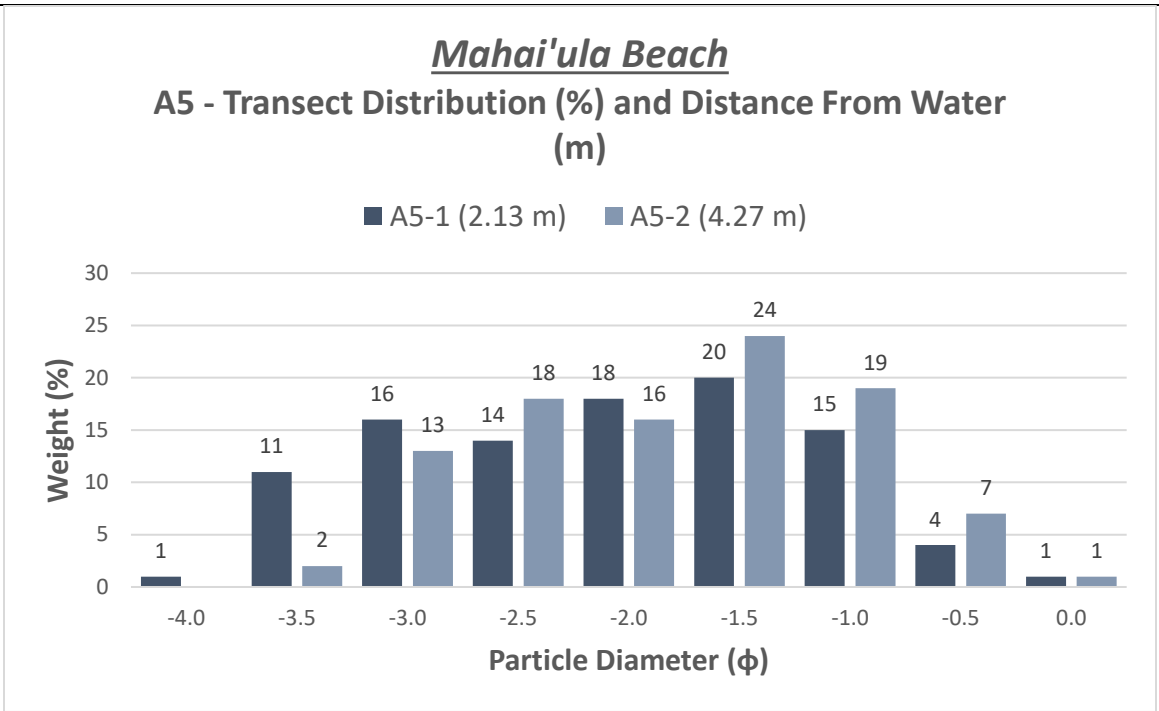

Figure 3.1.17: Mahai'ula Beach distribution graph (% of whole) for all survey points in Transect A5. See *Appendix A.1.7* for location photo and transect locations.

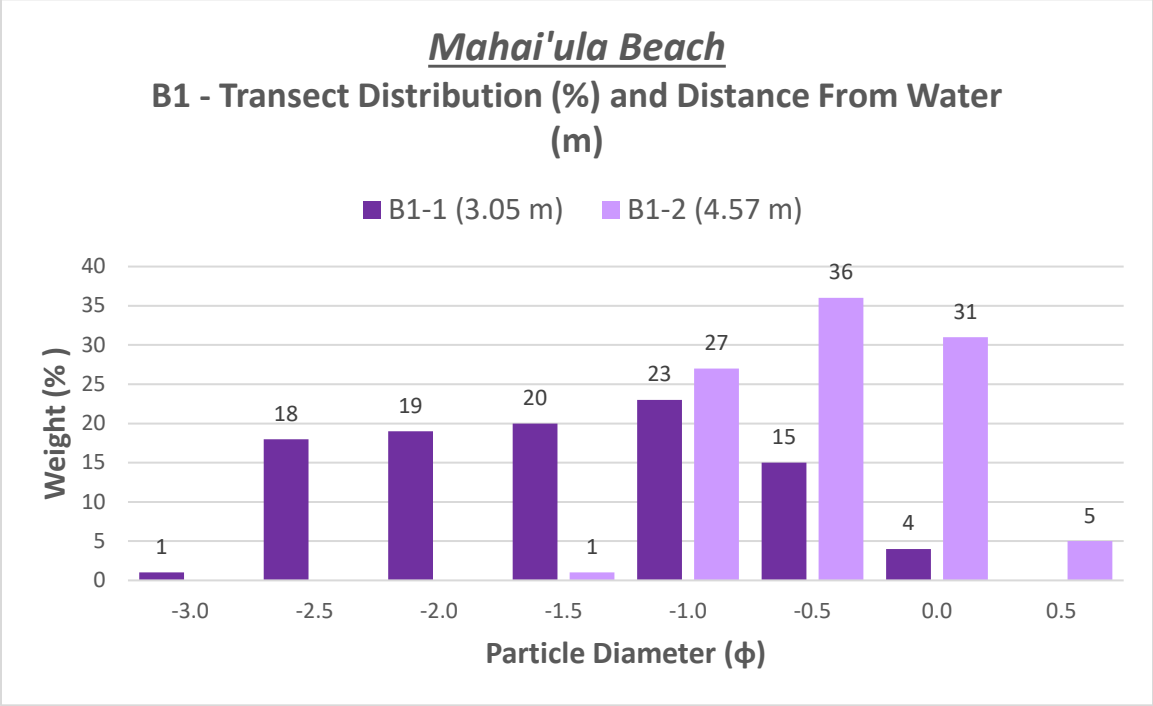

Figure 3.1.18: Mahai'ula Beach distribution graph (% of whole) for all survey points in Transect B1. See *Appendix A.1.7* for location photo and transect locations.

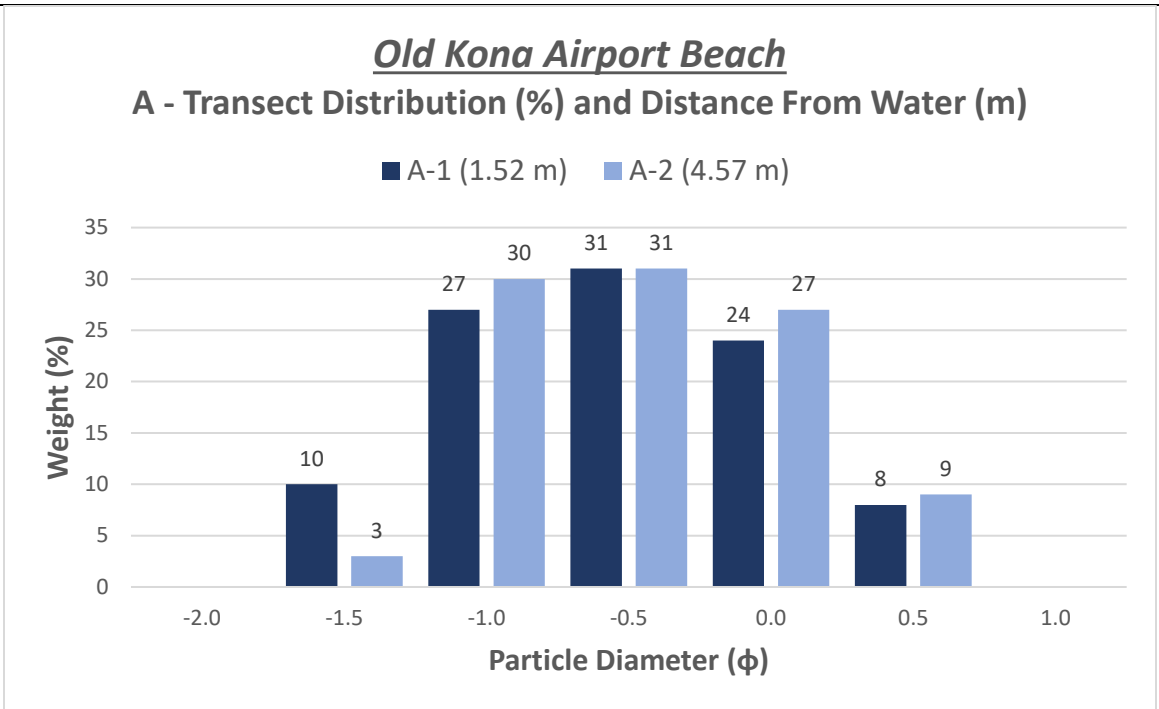

Figure 3.1.19: Old Kona Airport Beach distribution graph (% of whole) for all survey points in Transect A. See *Appendix A.1.8* for location photo and transect locations.

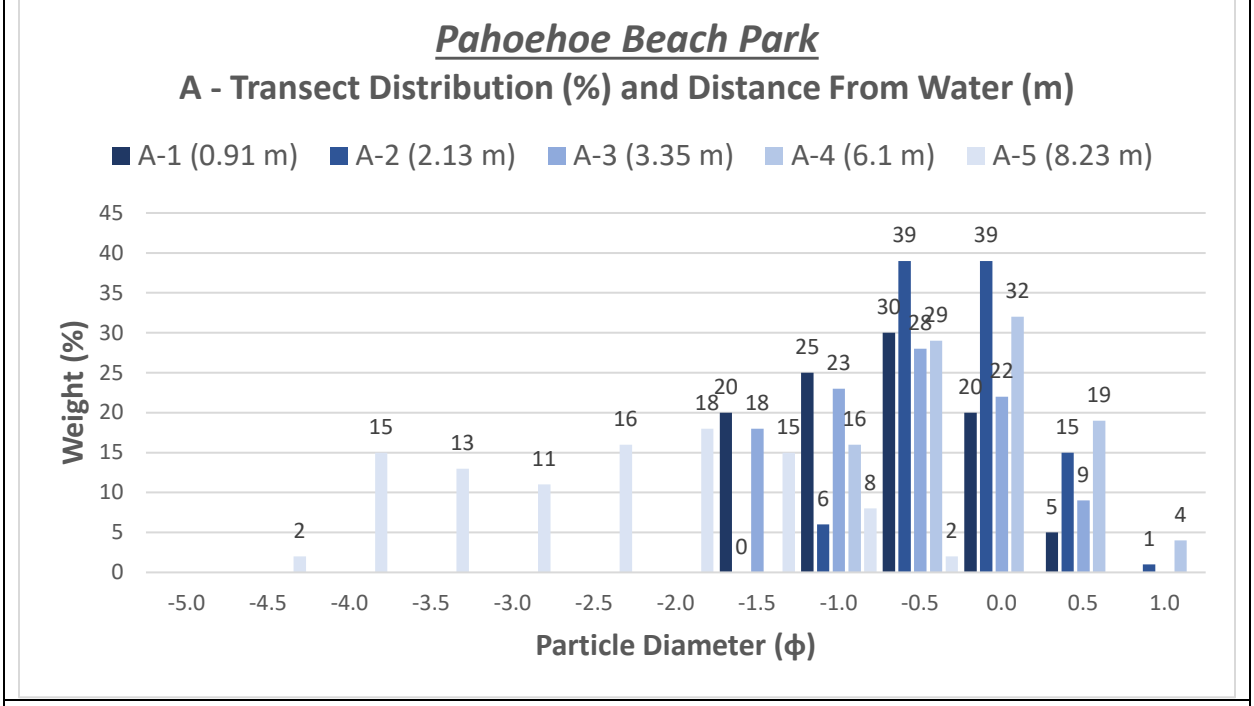

Figure 3.1.20: Pahoehoe Beach Park distribution graph (% of whole) for all survey points in Transect A. See *Appendix A.1.9* for location photo and transect locations.

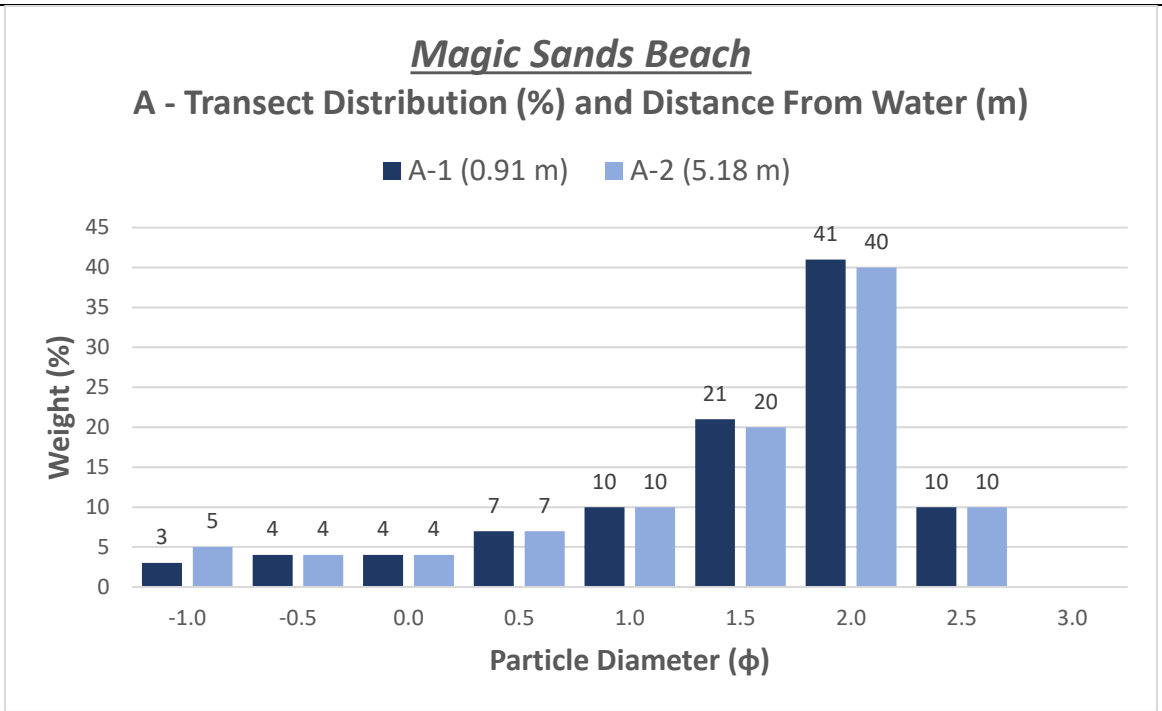

Figure 3.1.21: Magic Sands Beach distribution graph (% of whole) for all survey points in Transect A. See *Appendix A.1.10* for location photo and transect locations.

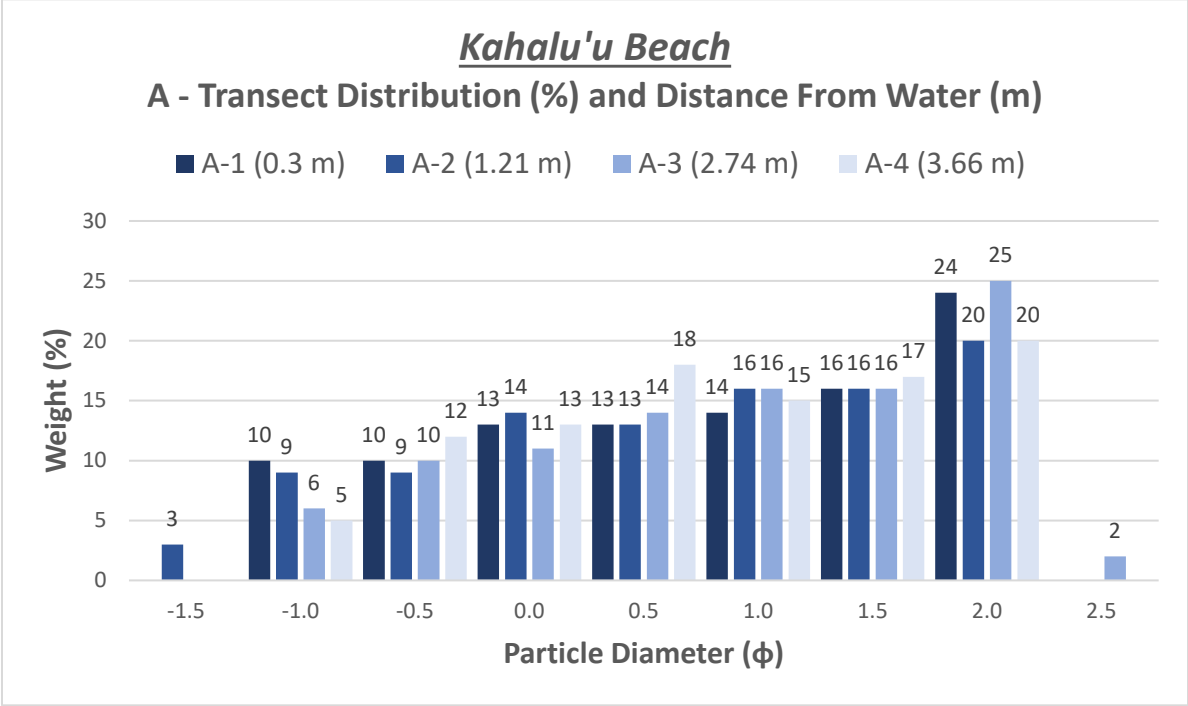

Figure 3.1.22: Kahalu'u Beach distribution graph (% of whole) for all survey points in Transect A. See *Appendix A.1.11* for location photo and transect locations.

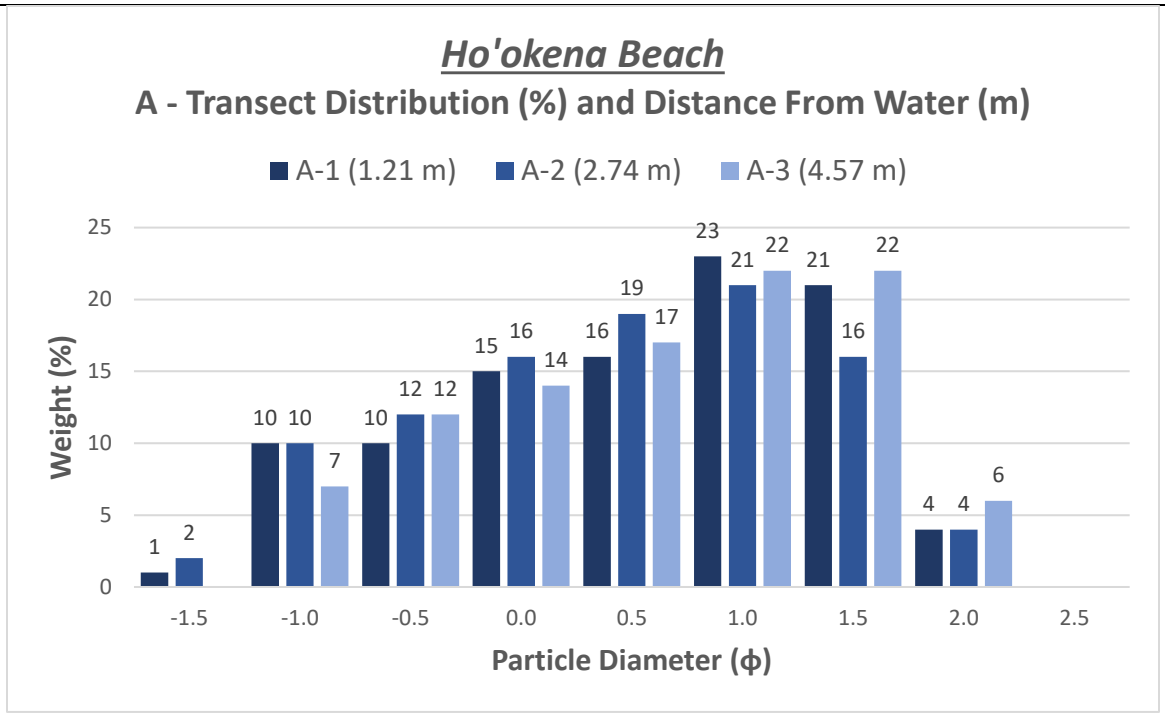

Figure 3.1.23: Ho'okena Beach distribution graph (% of whole) for all survey points in Transect A. See *Appendix A.1.12* for location photo and transect locations.

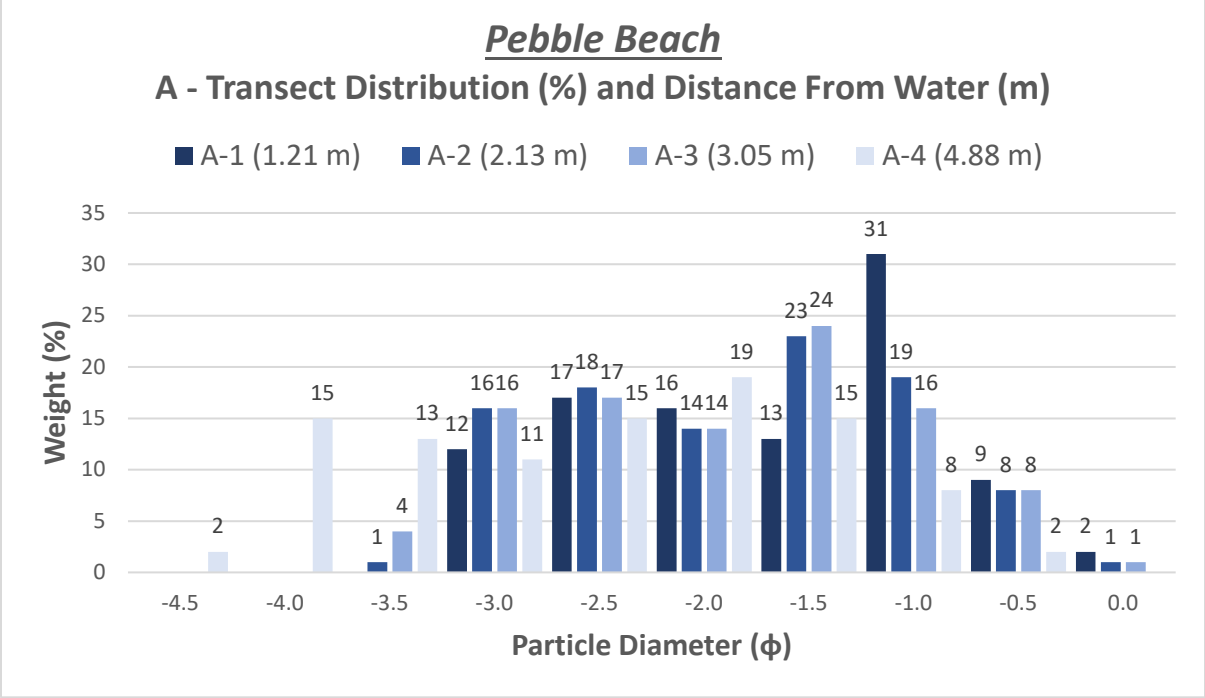

Figure 3.1.24: Pebble Beach distribution graph (% of whole) for all survey points in Transect A. See *Appendix A.1.13* for location photo and transect locations.

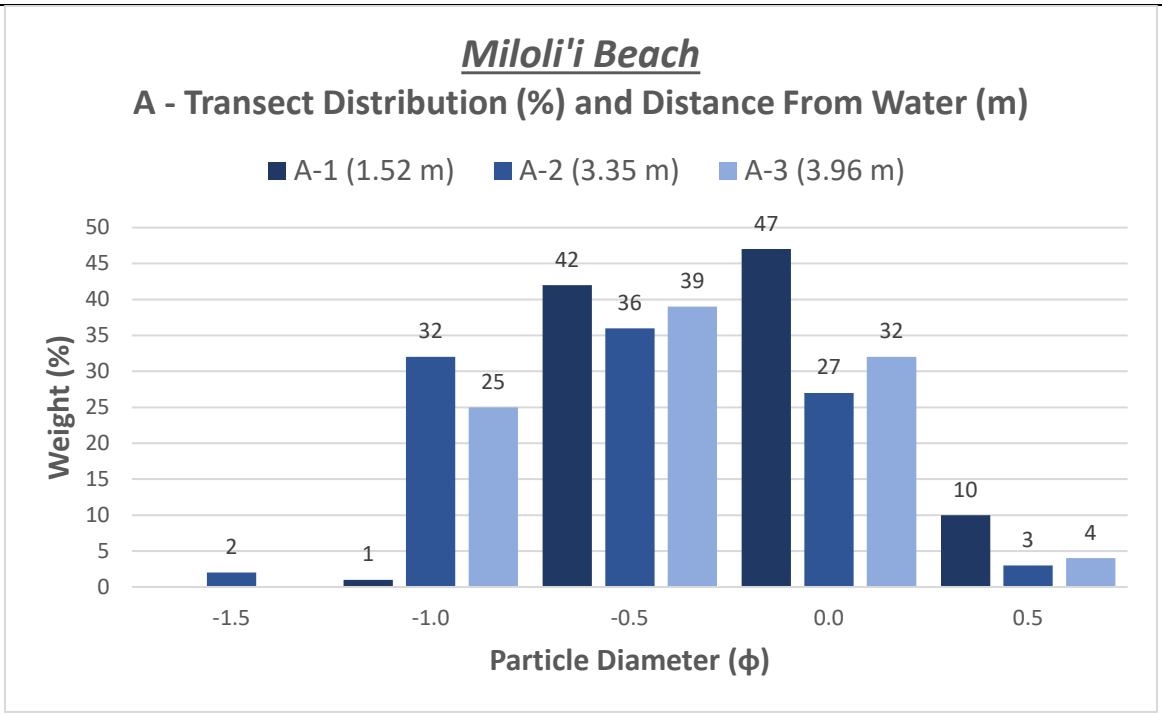

Figure 3.1.25: Miloli'i Beach distribution graph (% of whole) for all survey points in Transect A. See *Appendix A.1.14* for location photo and transect locations.

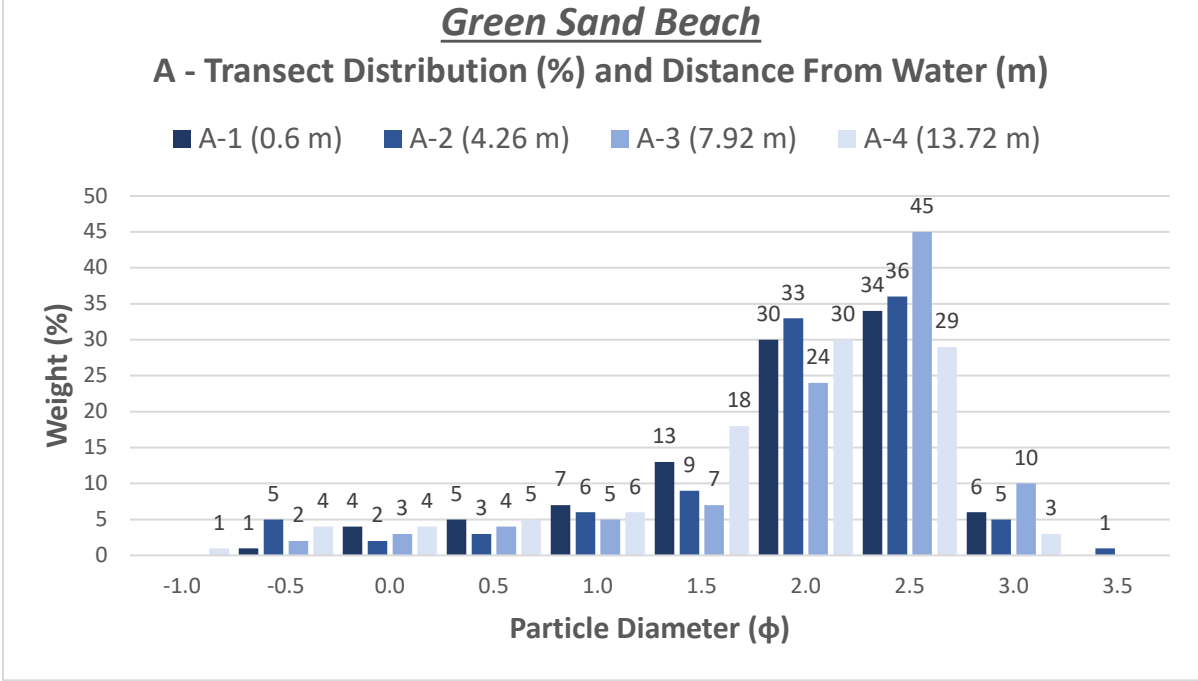

Figure 3.1.26: Green Sand Beach distribution graph (% of whole) for all survey points in Transect A. See *Appendix A.1.15* for location photo and transect locations.

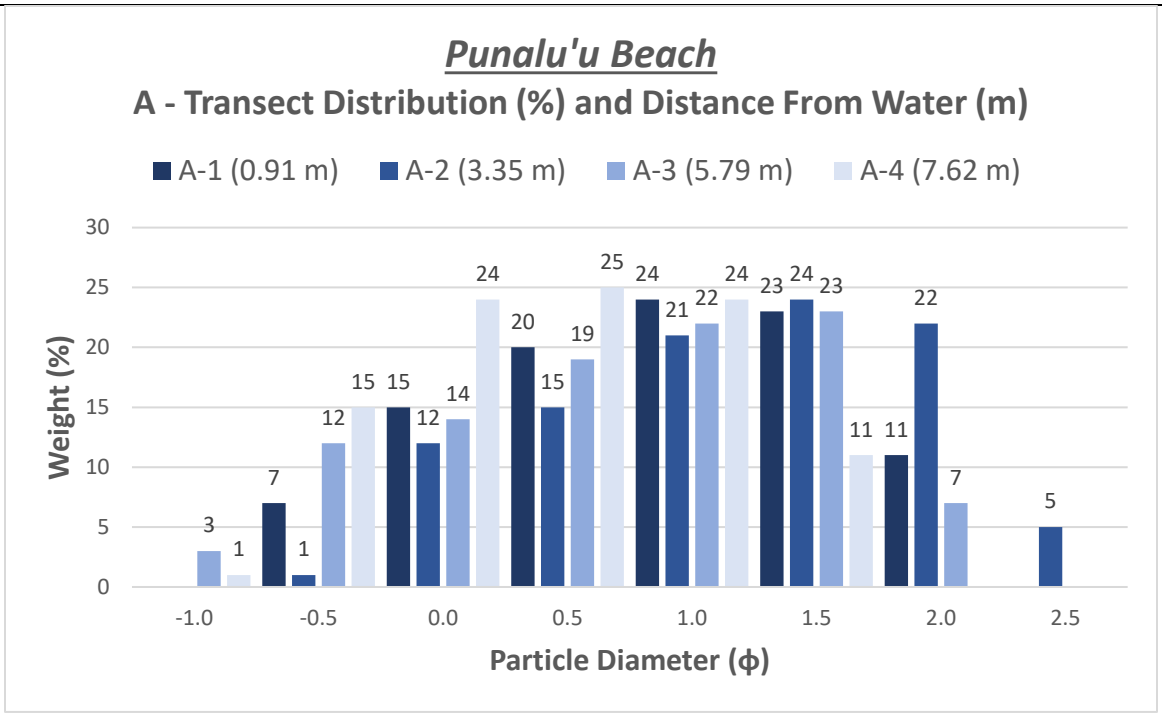

Figure 3.1.27: Punalu'u Beach distribution graph (% of whole) for all survey points in Transect A. See *Appendix A.1.16* for location photo and transect locations.

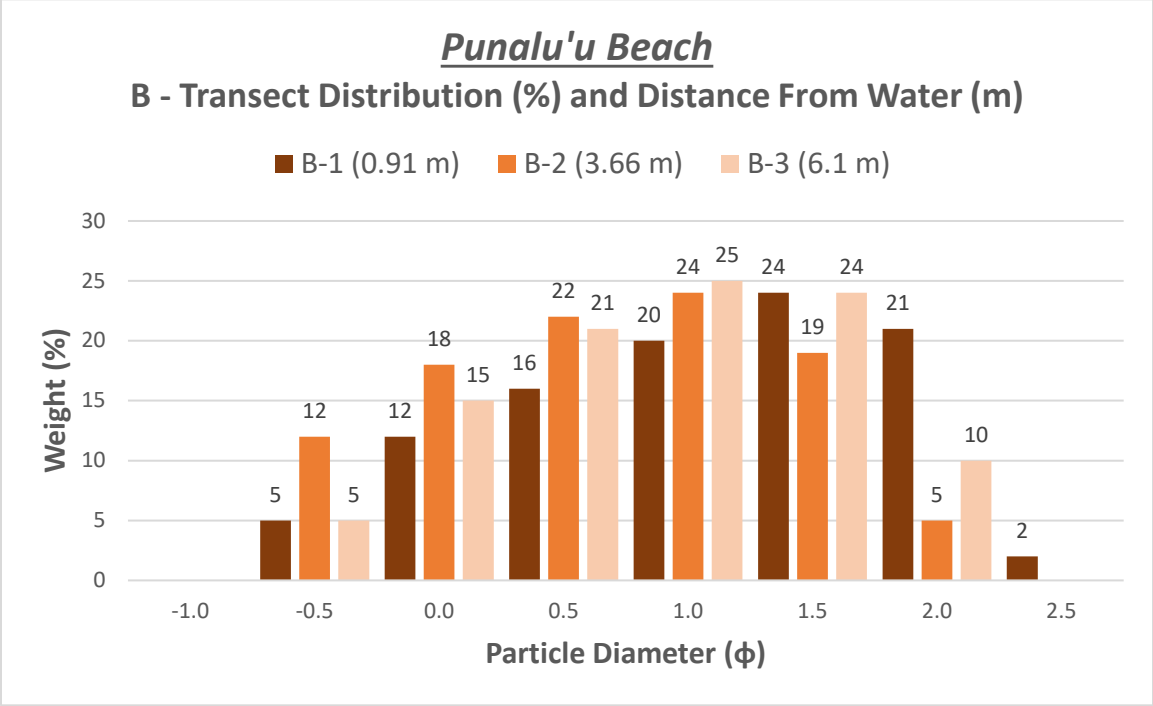

Figure 3.1.28: Punalu'u Beach distribution graph (% of whole) for all survey points in Transect B. See *Appendix A.1.16* for location photo and transect locations.

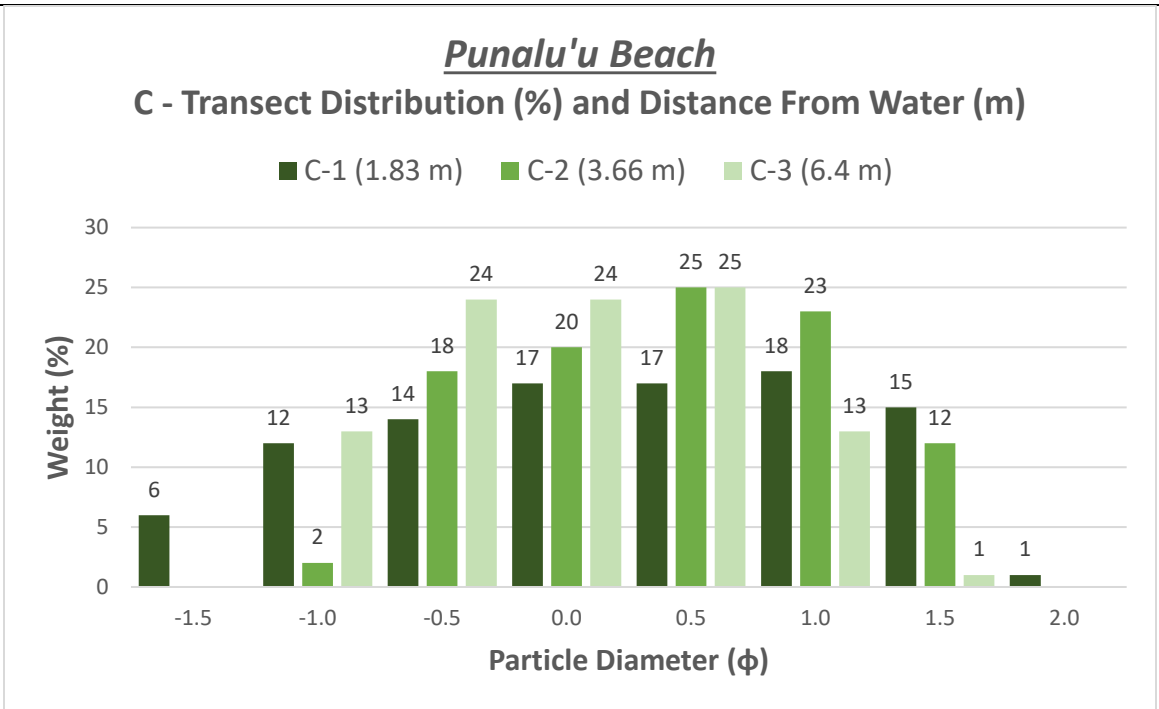

Figure 3.1.29: Punalu'u Beach distribution graph (% of whole) for all survey points in Transect C. See *Appendix A.1.16* for location photo and transect locations.

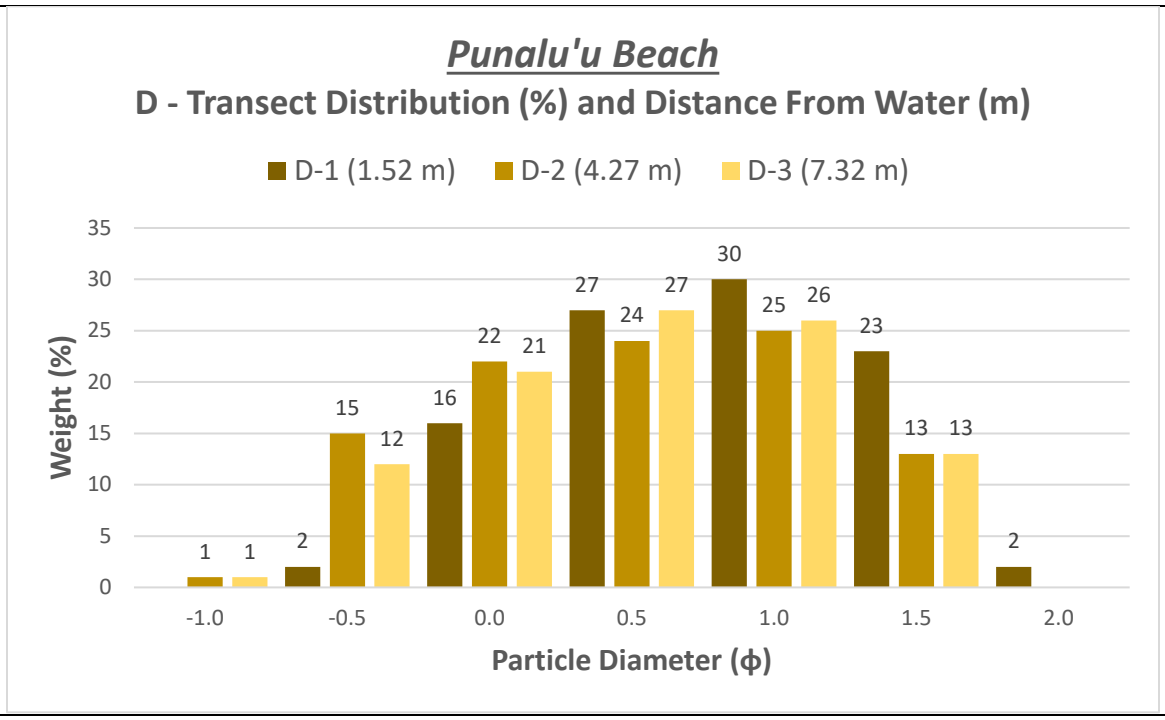

Figure 3.1.30: Punalu'u Beach distribution graph (% of whole) for all survey points in Transect D. See *Appendix A.1.16* for location photo and transect locations.

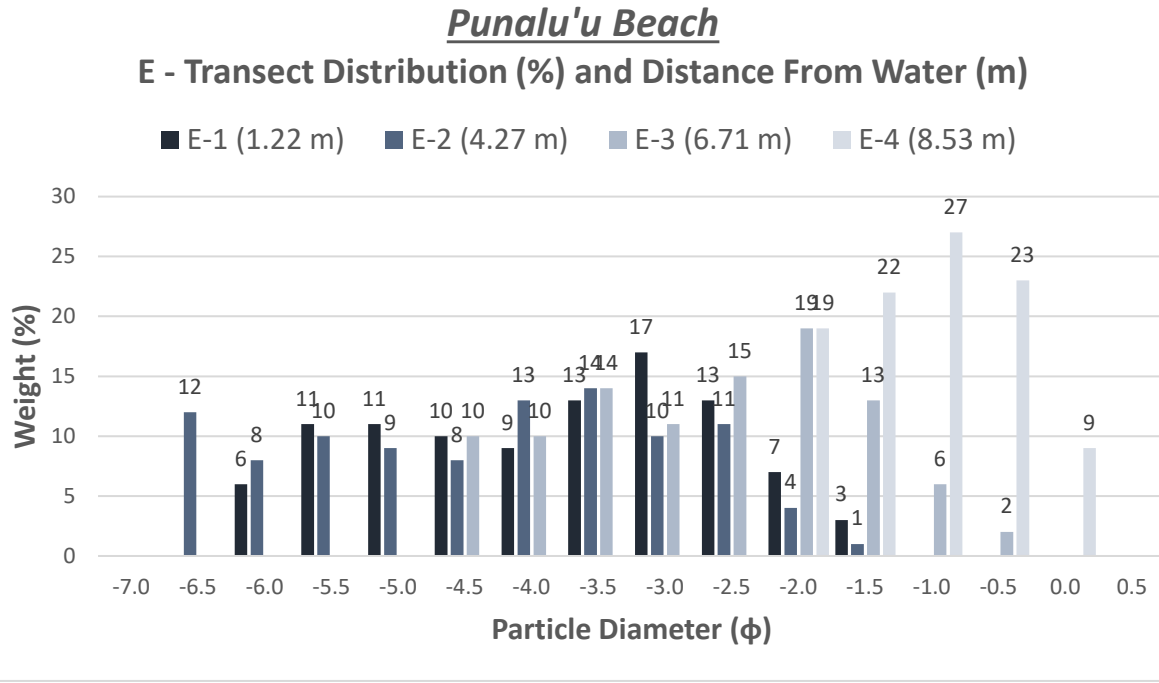

Figure 3.1.31: Punalu'u Beach distribution graph (% of whole) for all survey points in Transect E. See *Appendix A.1.16* for location photo and transect locations.

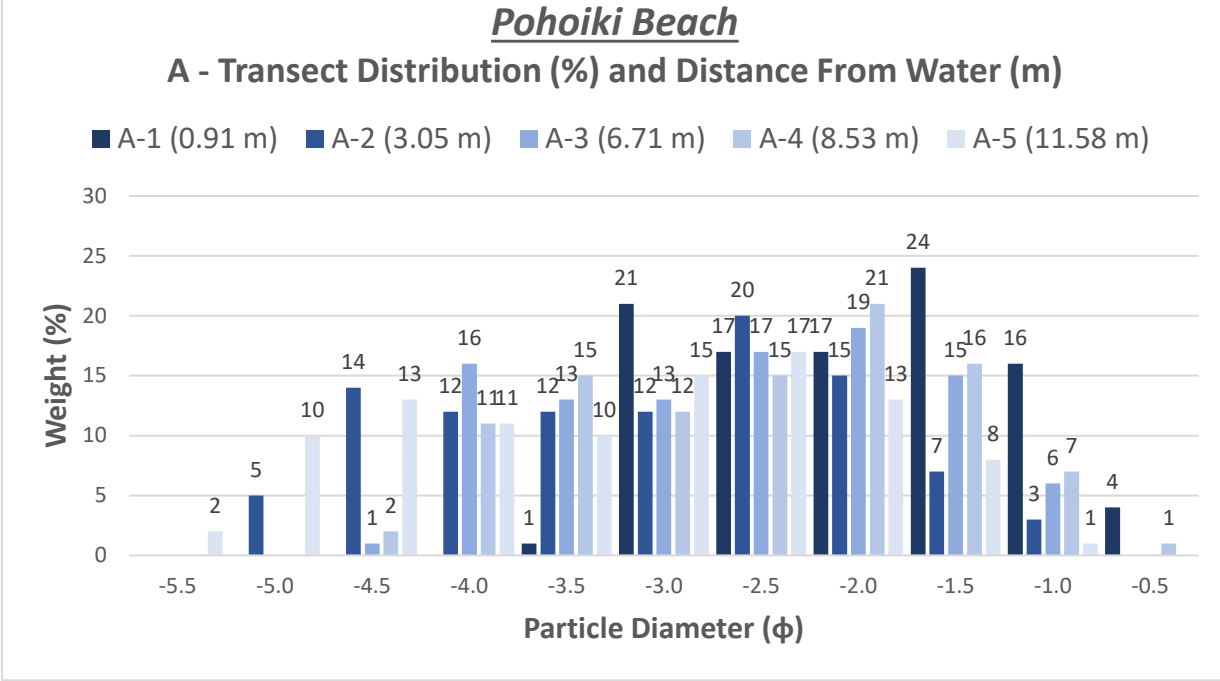

Figure 3.1.32: Pohoiki Beach distribution graph (% of whole) for all survey points in Transect A. See *Appendix A.1.17* for location photo and transect locations.

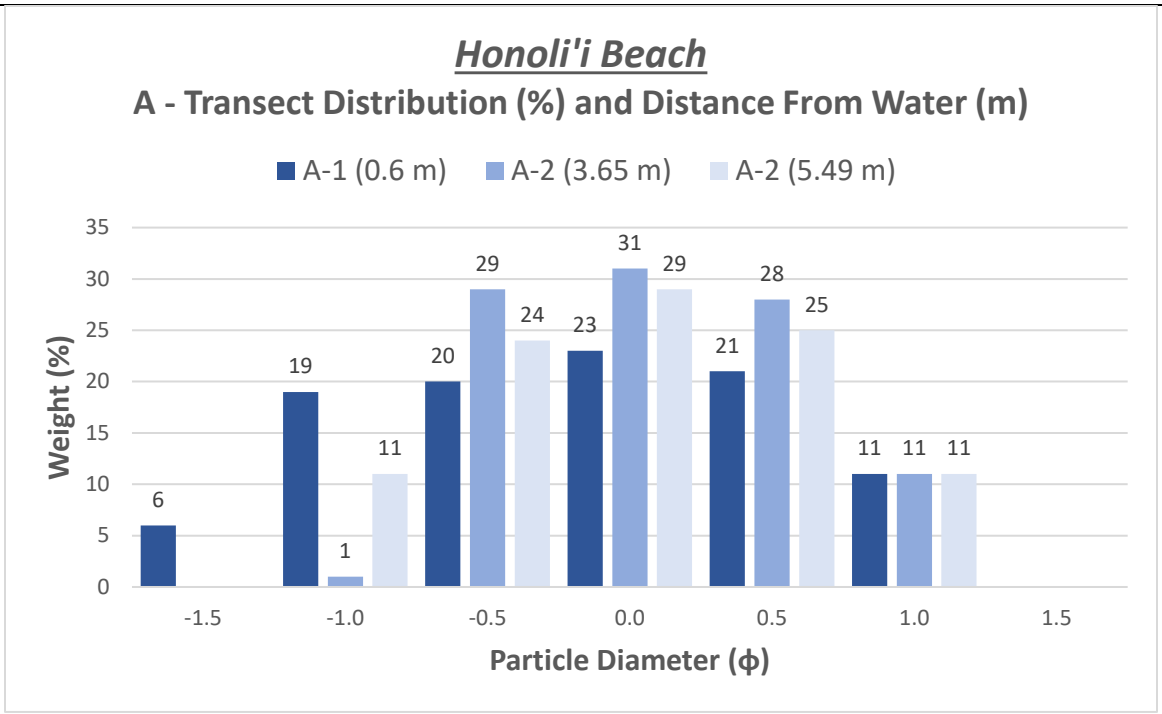

Figure 3.1.33: Honoli'i Beach distribution graph (% of whole) for all survey points in Transect A. See *Appendix A.1.18* for location photo and transect locations.

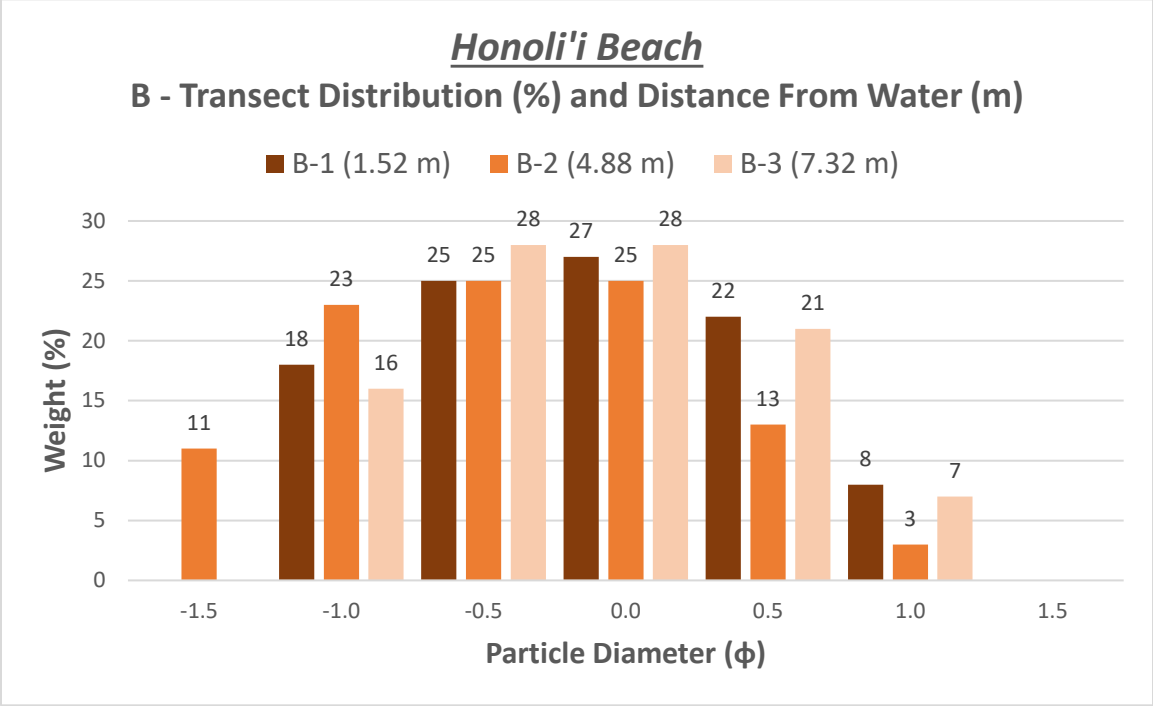

Figure 3.1.34: Honoli'i Beach distribution graph (% of whole) for all survey points in Transect B. See *Appendix A.1.18* for location photo and transect locations.

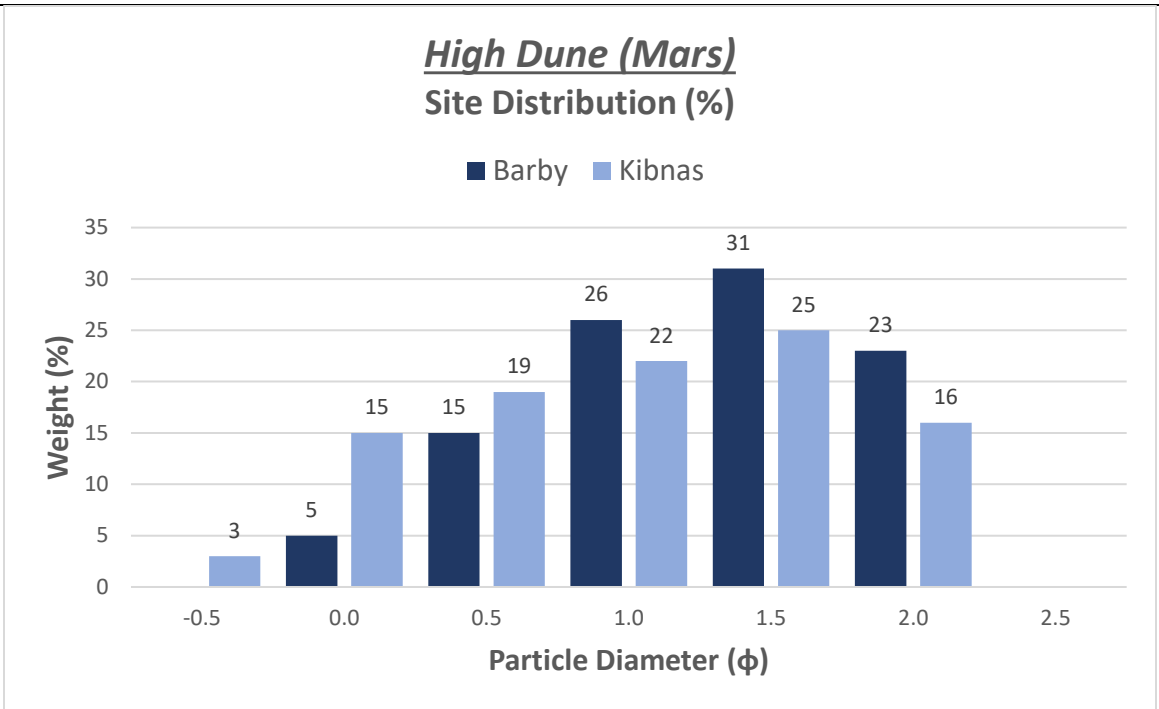

Figure 3.2.1: High Dune distribution graph (% of whole) for both the Barby and the Kibnas sites.

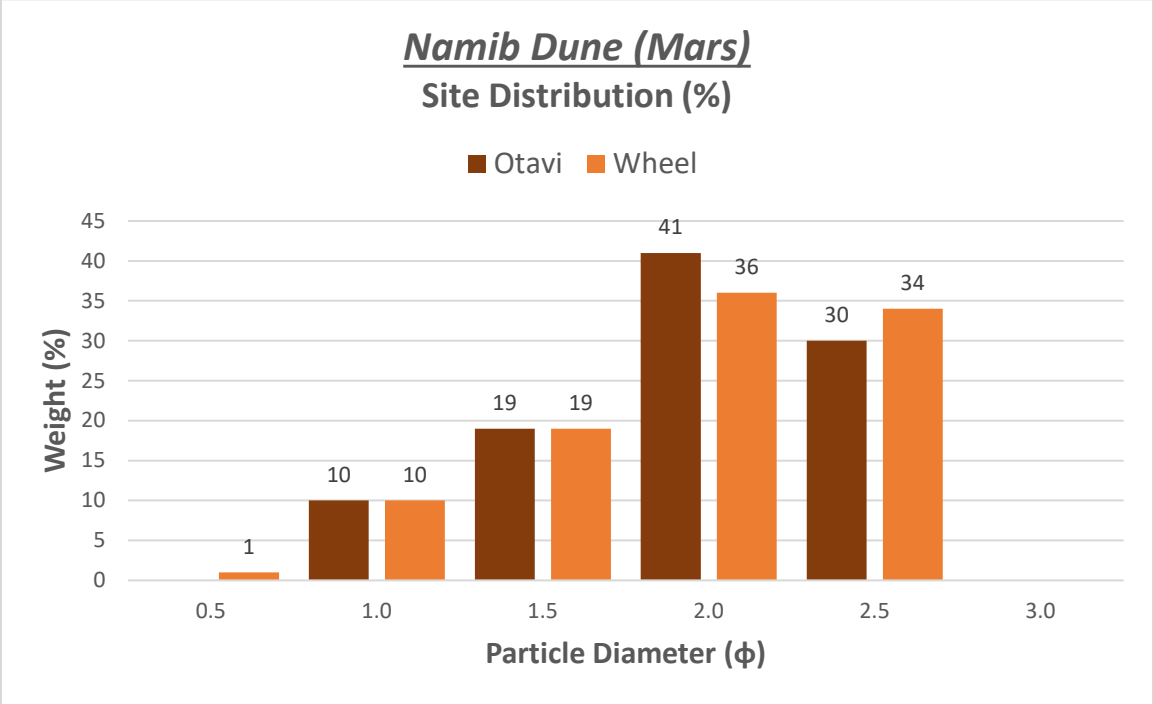

Figure 3.2.2: Namib Dune distribution graph (% of whole) for both the Otavi and the Wheel sites.

Average					
	50th % (ϕ)	**Slope**	**Std Dev.**	**Skewness**	**Kurtosis**
NPS	0.02	-7.08	0.762	-0.329	4.247
KSWandSS	-0.24	-10.74	0.770	-0.175	0.902
NTW	-1.45	-11.09	0.788	-0.080	0.796
OPE	-0.07	-5.77	0.770	-0.156	0.859

Table 3.3.1: The average for the statistical moments, including the slope for the beaches associated with each weather/climate effects, those being the North Pacific Swell Beaches (NPS), Kona Storm Waves and Southern Swell Beaches (KSWandSS), Northeast Tradewind Wave Beaches (NTW), and those beaches outside predicted effects (OPE).

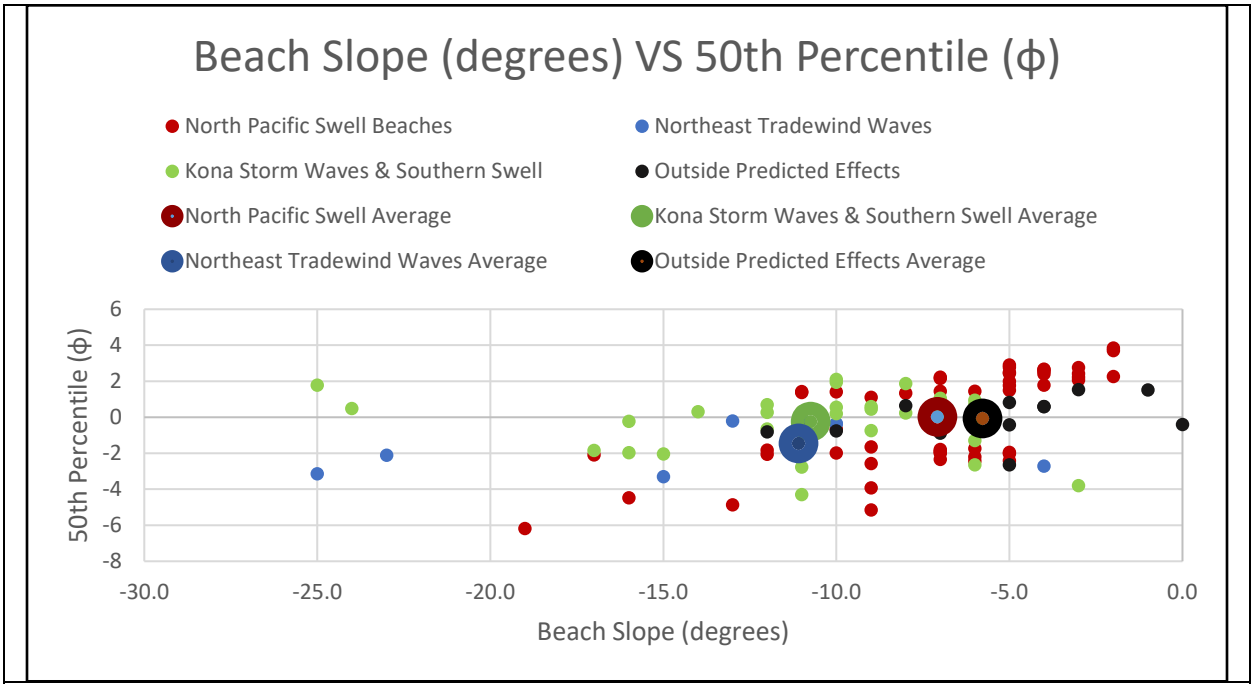

Figure 3.3.1: Beach Slope vs 50th Percentile showing the averages and the relationship between the two.

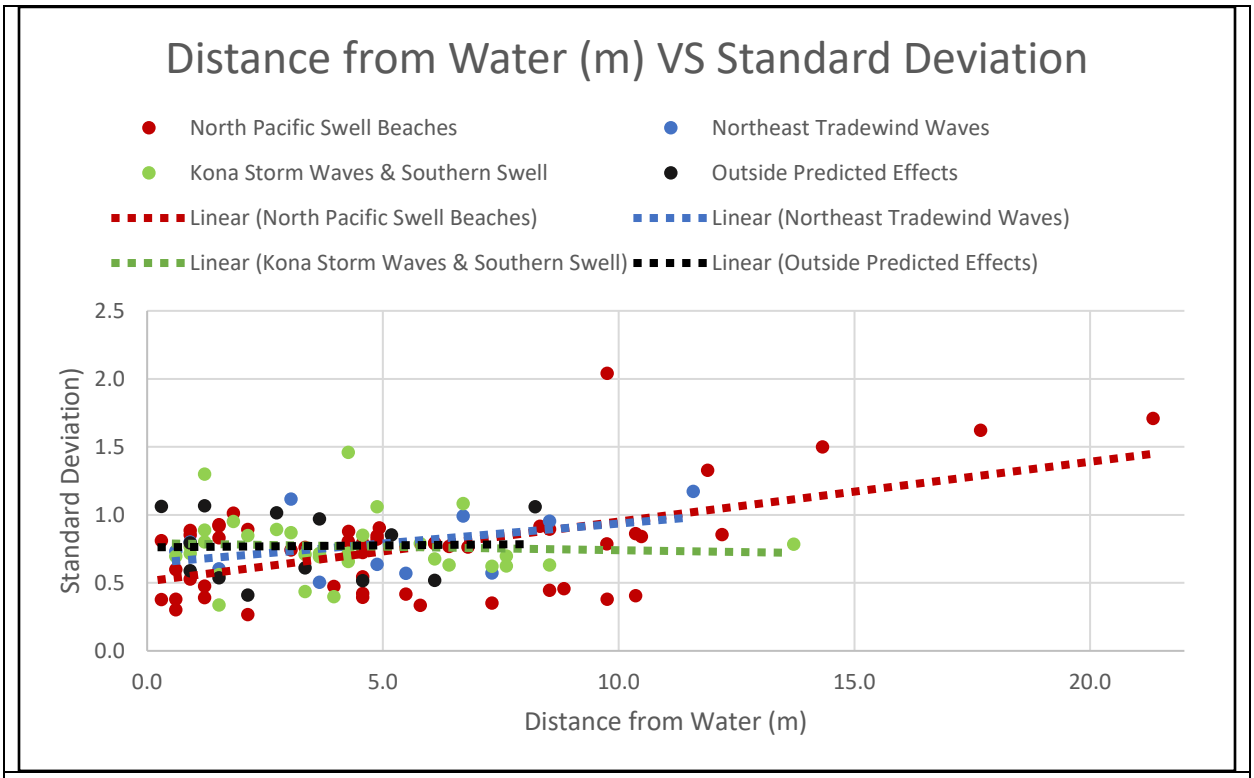

Figure 3.3.2: Distance from water vs Standard Deviation (sorting) graph showing a positive relationship for those beaches subject to the North Pacific Swell and Northeast Tradewind Waves and a negative relationship in those beaches affected by the Kona Storm Waves, Southern Swell, and those outside the predicted effects.

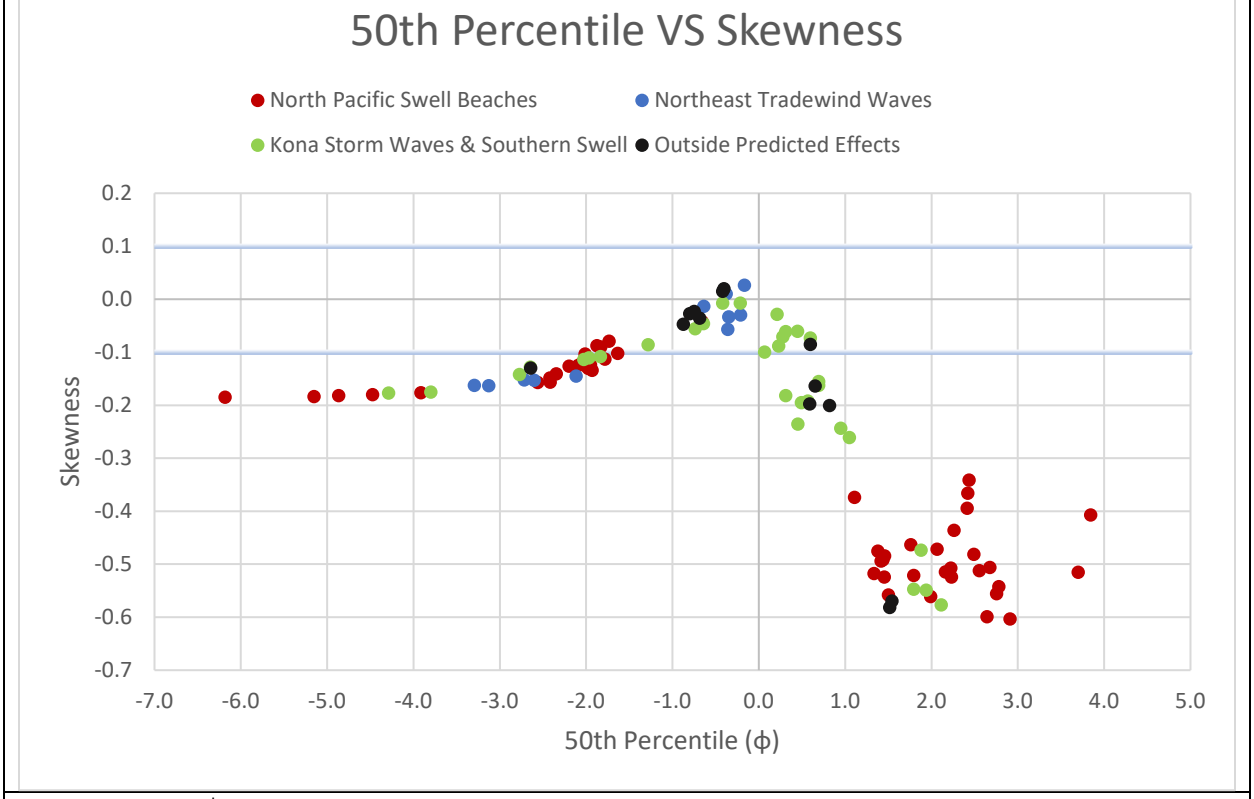

Figure 3.3.3: 50th Percentile graphed against Skewness showing the relationship between the two. Above the top blue line is described as fine skewed (0.1 – 0.3), in between both blue lines is described as symmetrical (-0.1 – 0.1), and below the last blue line is considered coarse skewed (-0.3 – -0.1).

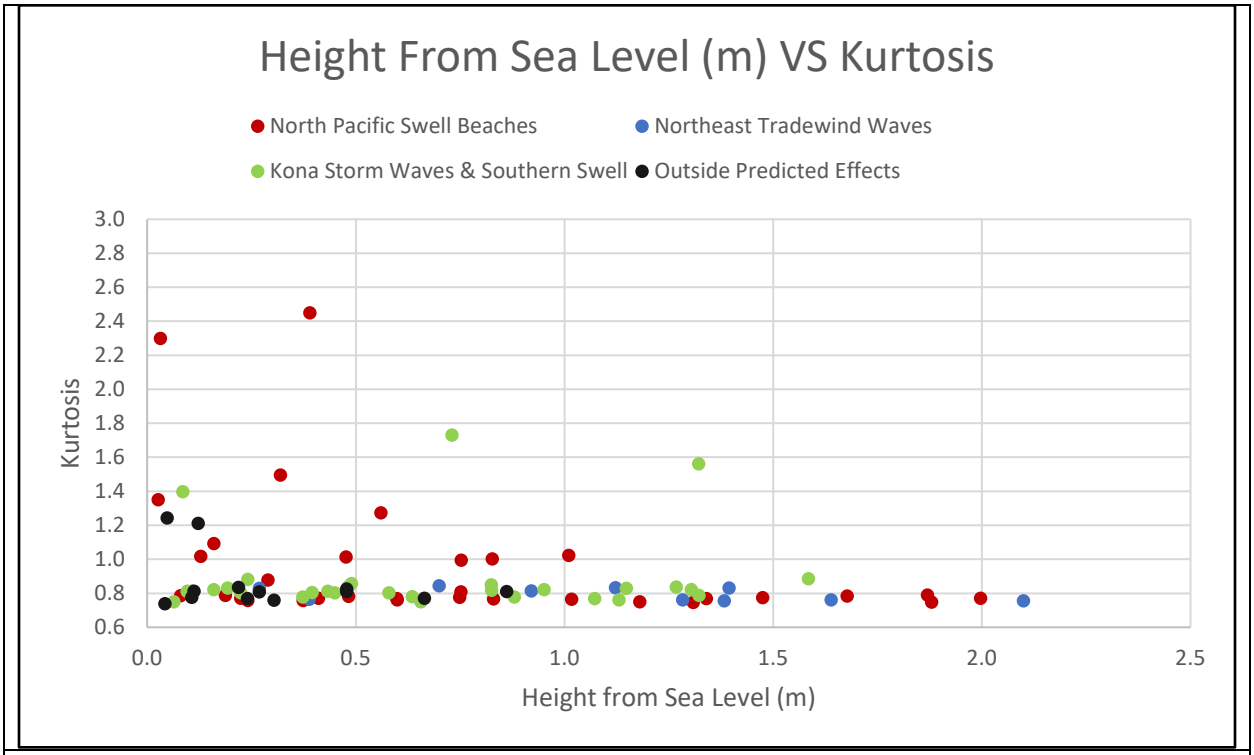

Figure 3.3.4: Height from sea level vs Kurtosis graph showing the relationship between the two.

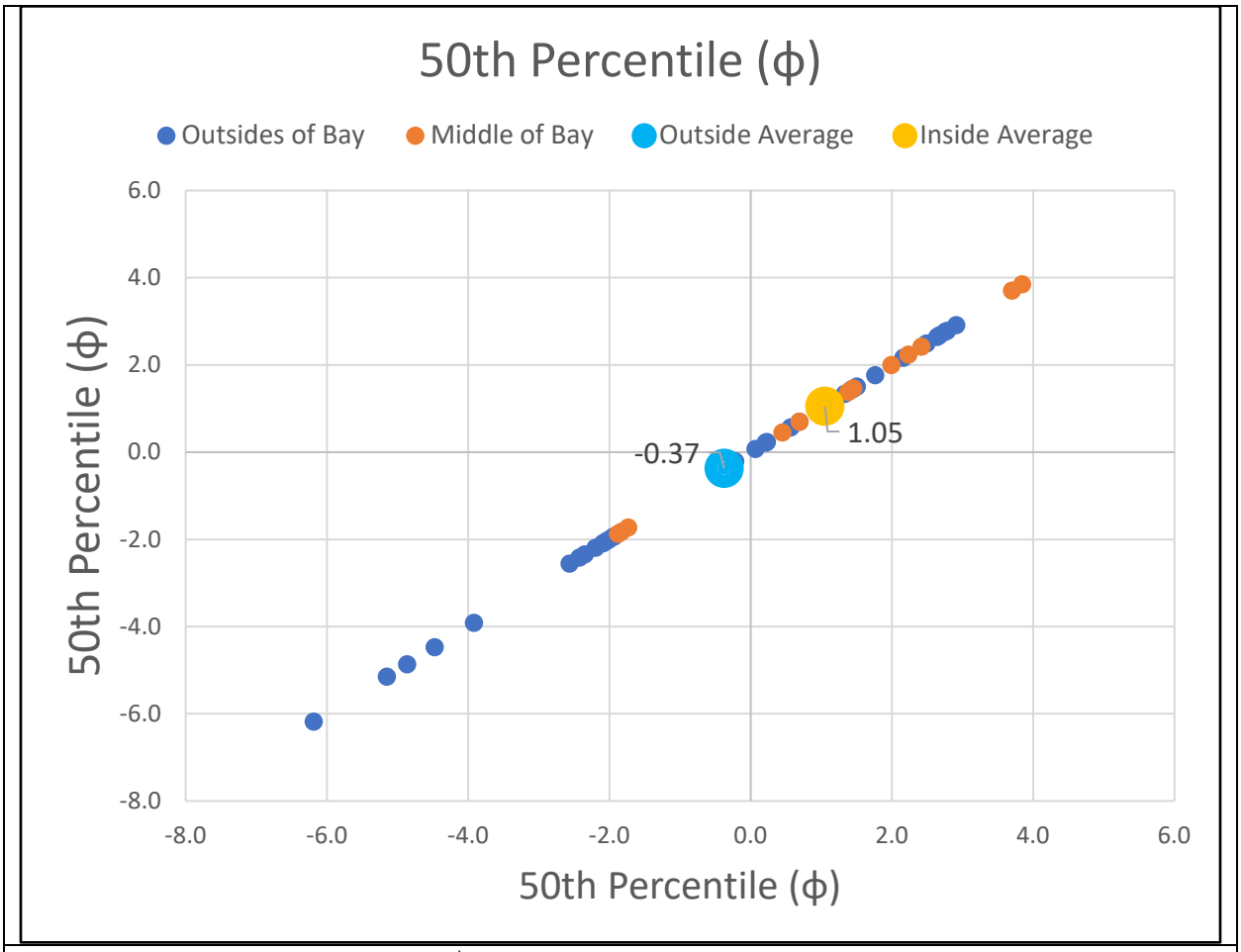

Figure 3.4.1: A linear graph of the 50th Percentile (ϕ) showing the differences between the outsides and inside of a bay or inlet.

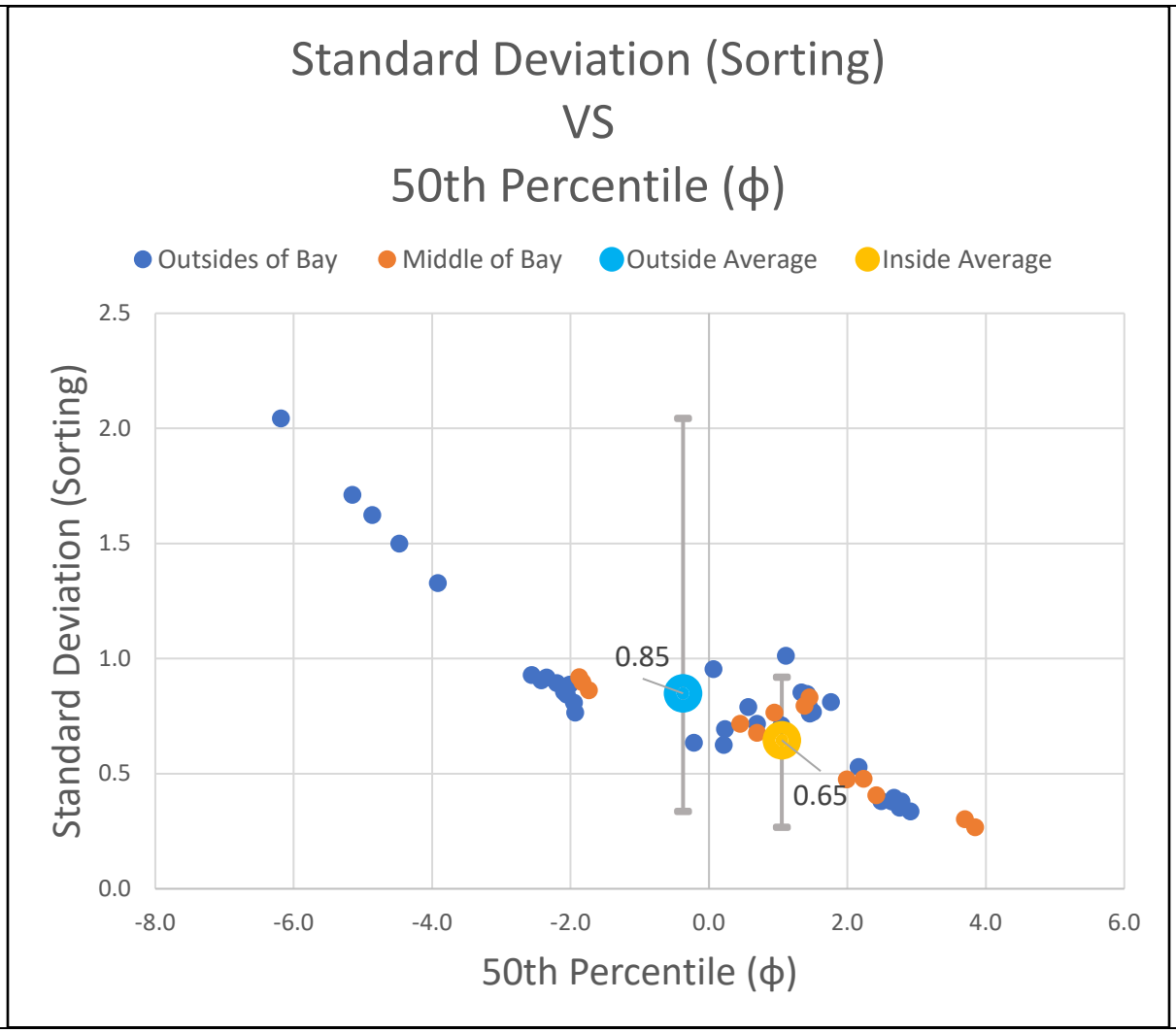

Figure 3.4.2: Standard Deviation vs 50th Percentile showing the range and relationship.

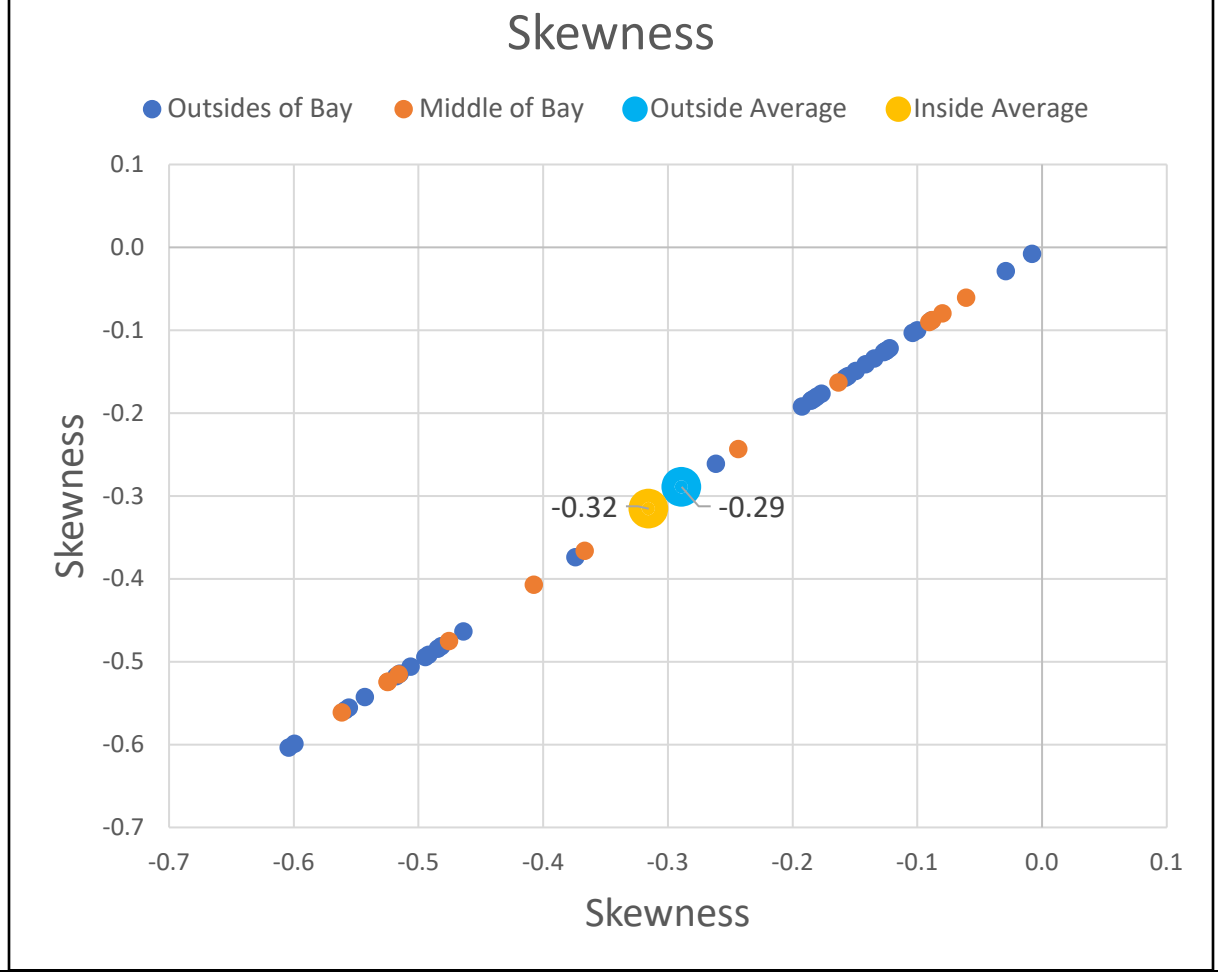

Figure 3.4.3: A linear graph of the skewness showing the differences between the outsides and inside of a bay or inlet.

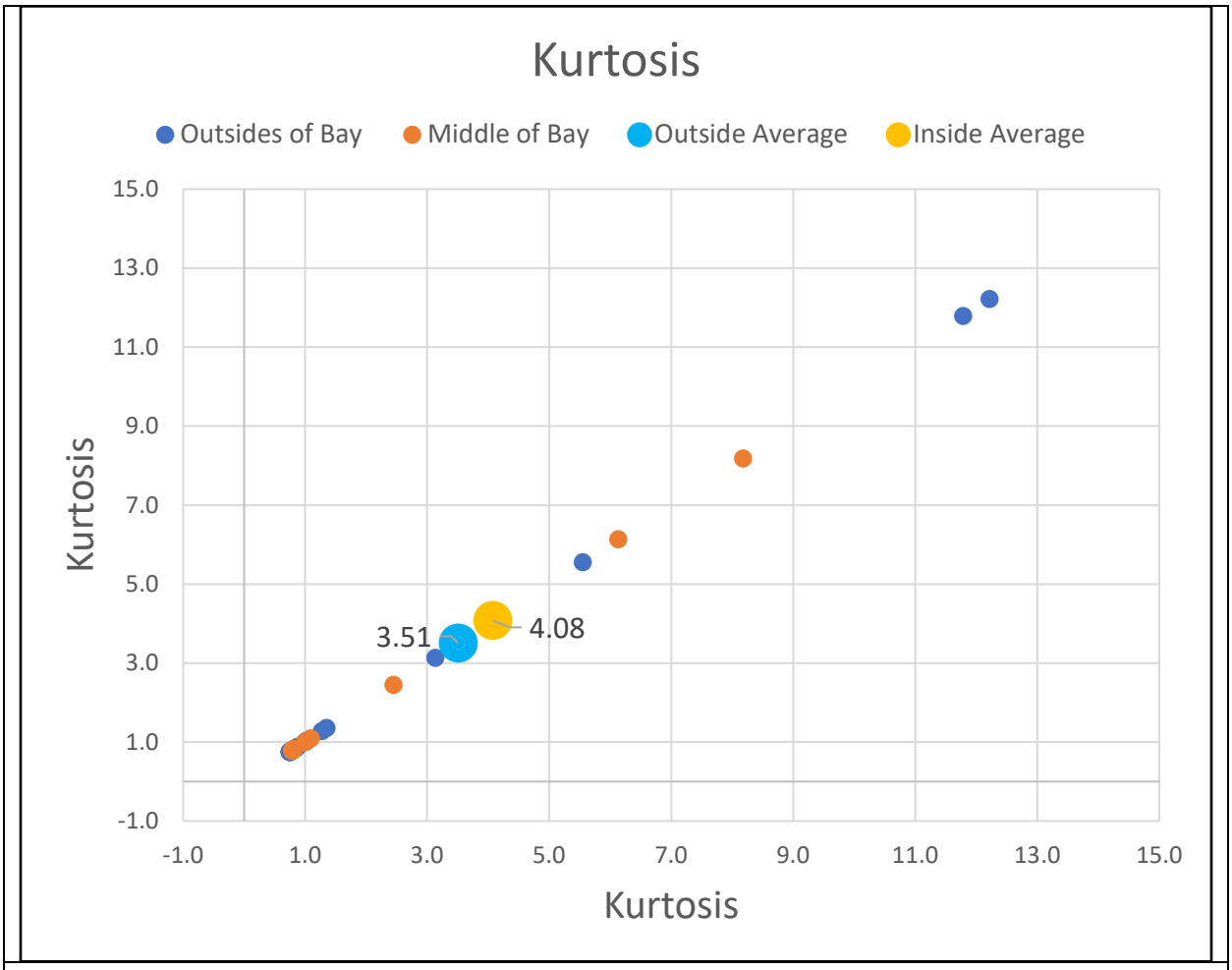

Figure 3.4.4: A linear graph of the kurtosis showing the differences between the outsides and inside of a bay or inlet.

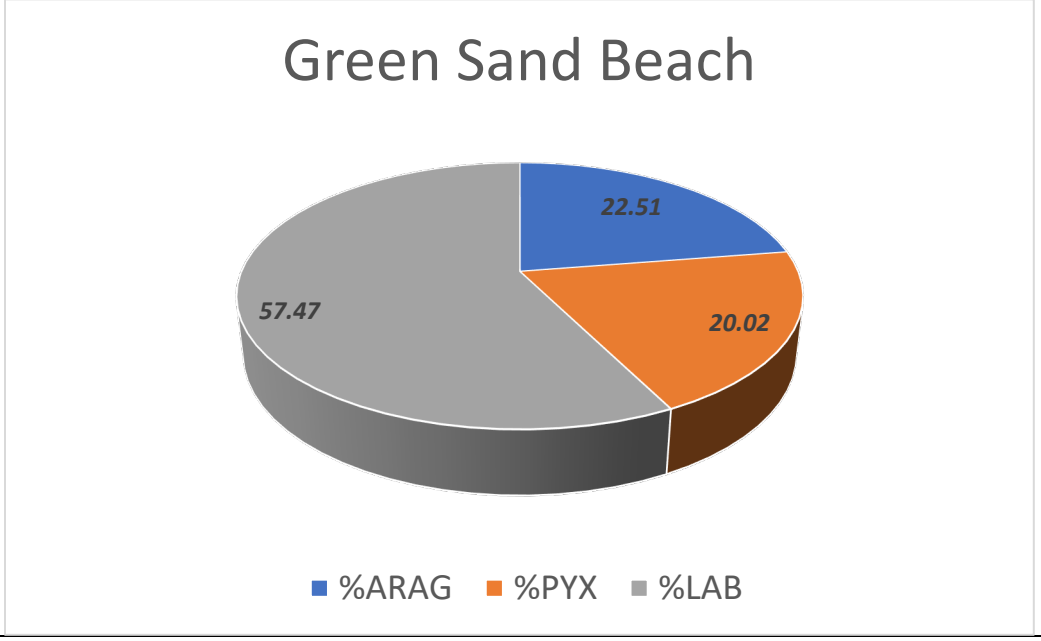

Figure 3.5.1: A pie chart representing the three compositional components tested for the sand sample from Green Sand Beach, namely aragonite (carbonate), pyroxene (olivine), and labradorite (feldspar).

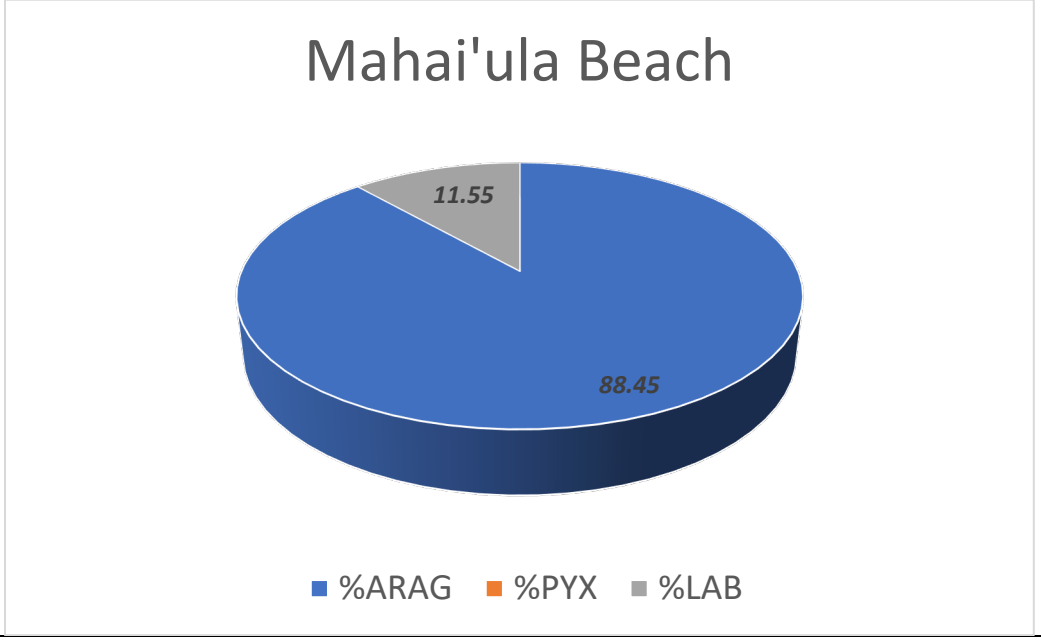

Figure 3.5.2: A pie chart representing the three compositional components tested for the sand sample from Mahai'ula Beach, namely aragonite (carbonate), pyroxene (olivine), and labradorite (feldspar).

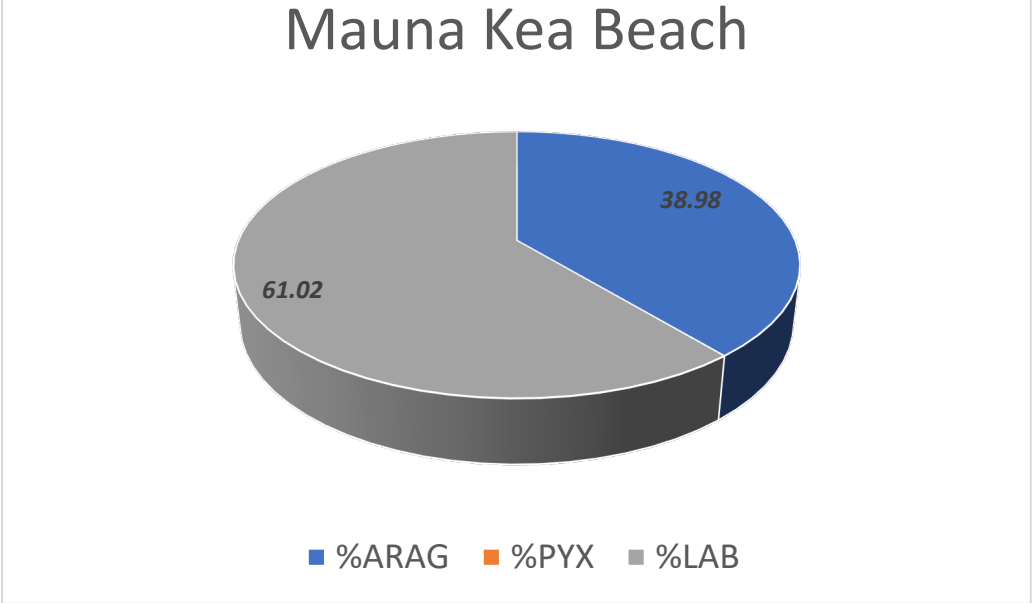

Figure 3.5.3: A pie chart representing the three compositional components tested for the sand sample from Mauna Kea Beach, namely aragonite (carbonate), pyroxene (olivine), and labradorite (feldspar).

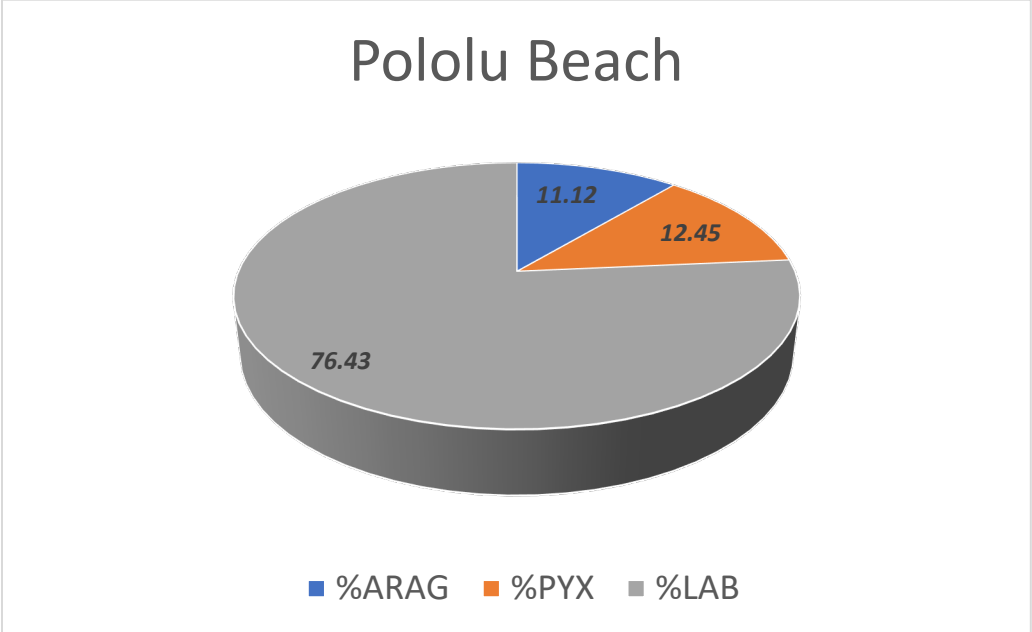

Figure 3.5.4: A pie chart representing the three compositional components tested for the sand sample from Pololu Beach, namely aragonite (carbonate), pyroxene (olivine), and labradorite (feldspar).

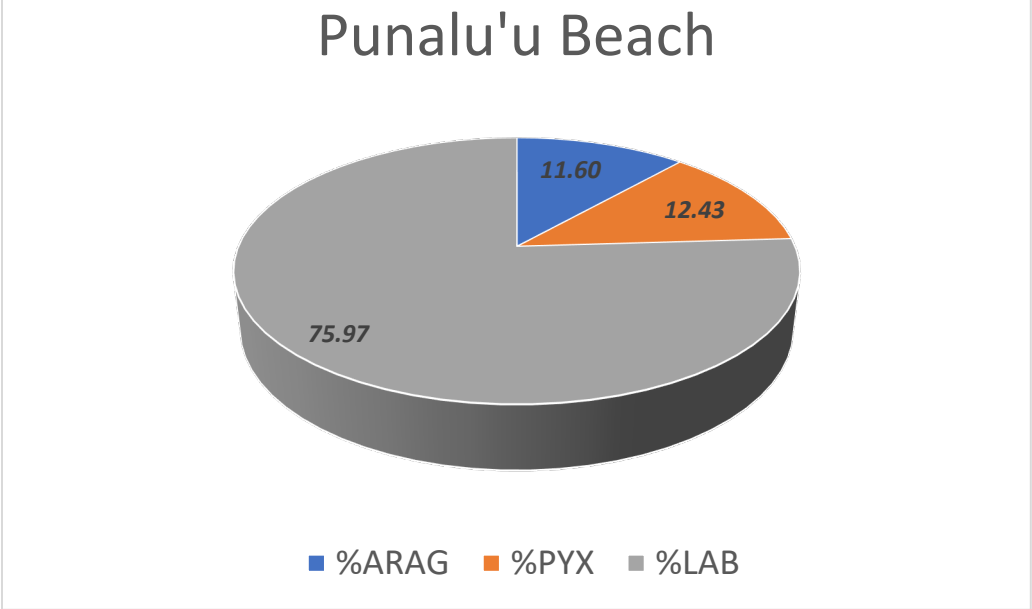

Figure 3.5.5: A pie chart representing the three compositional components tested for the sand sample from Punalu'u Beach, namely aragonite (carbonate), pyroxene (olivine), and labradorite (feldspar).

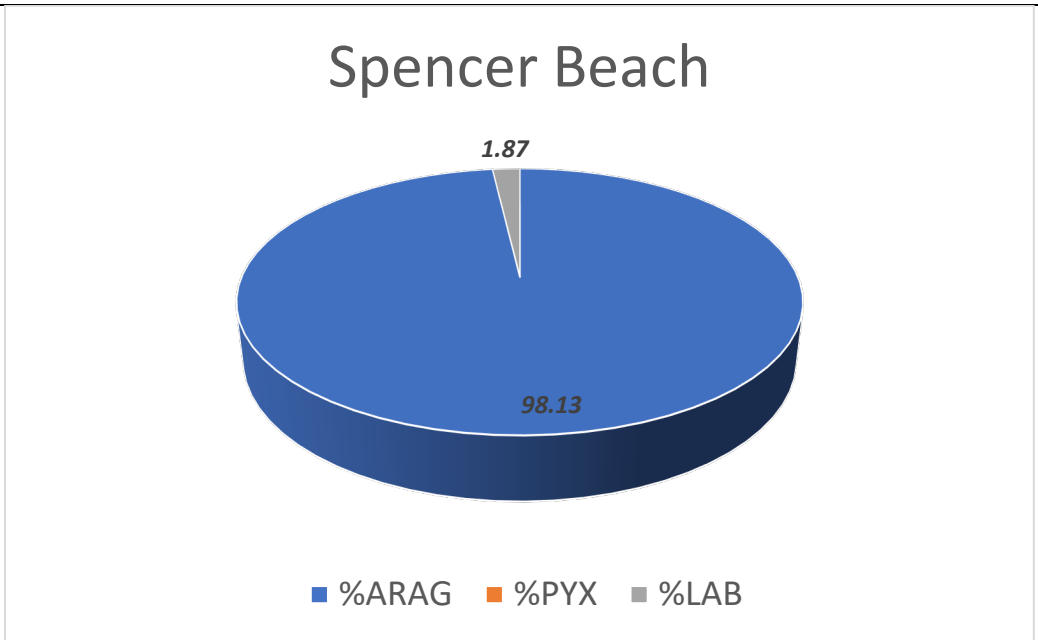

Figure 3.5.6: A pie chart representing the three compositional components tested for the sand sample from Spencer Beach, namely aragonite (carbonate), pyroxene (olivine), and labradorite (feldspar).

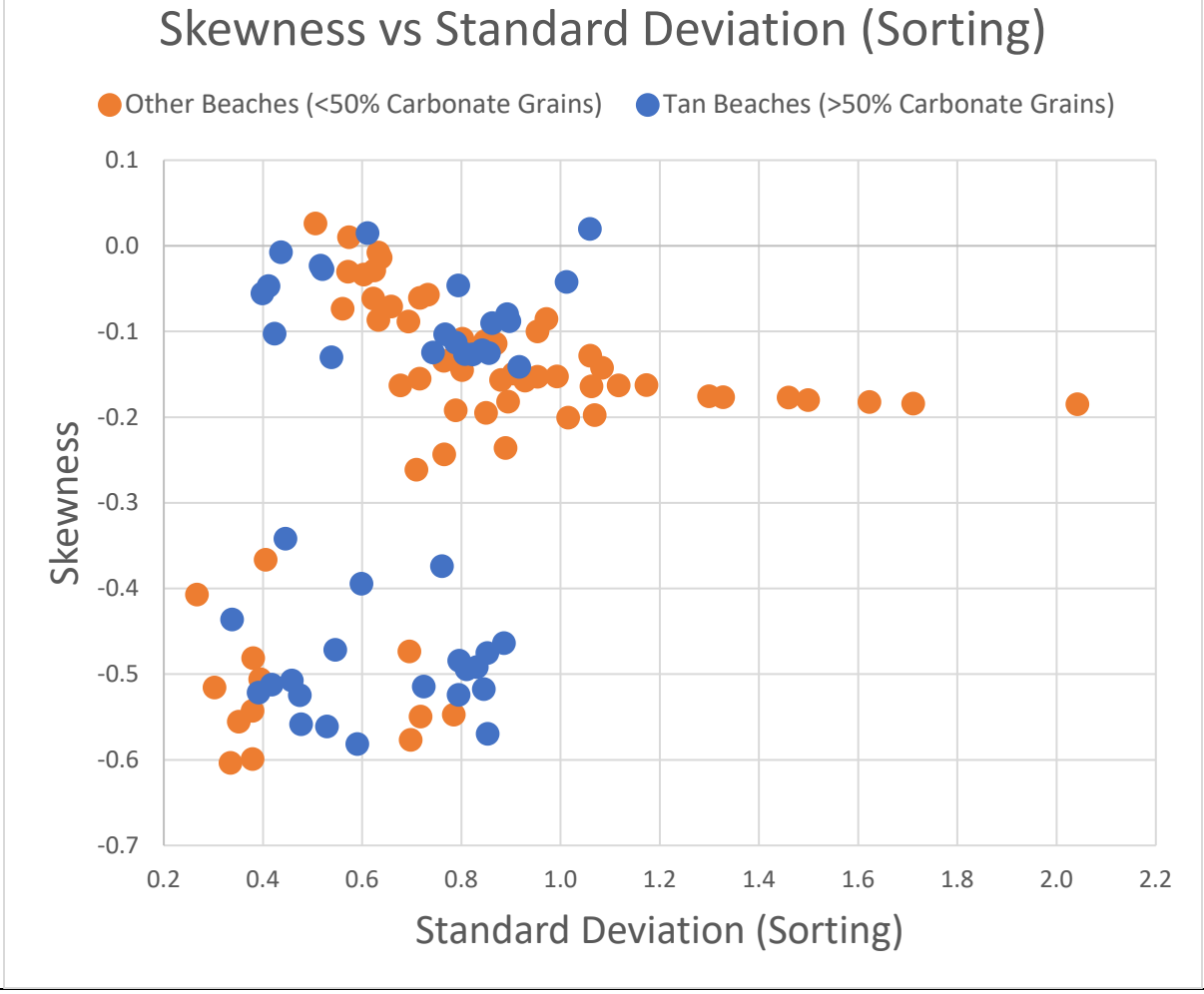

Figure 4.1.1: Relationships graphed between the skewness and standard deviation in carbonate-rich sands (>50% carbonate grains) vs other sands (<50% carbonate grains) throughout the island.

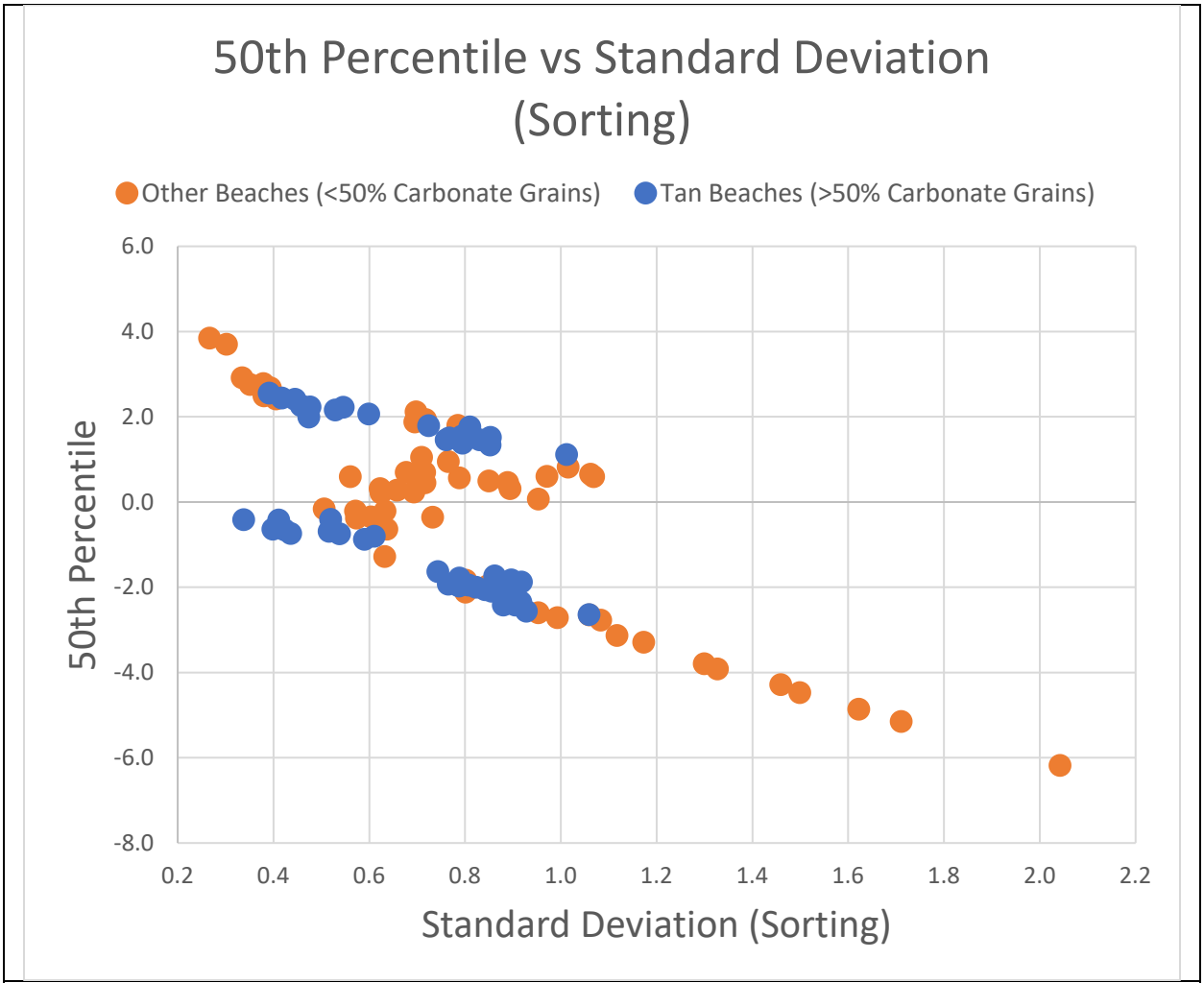

Figure 4.1.2: Relationships graphed between the 50th percentile and standard deviation in carbonate-rich sands (>50% carbonate grains) vs other sands (<50% carbonate grains) throughout the island.

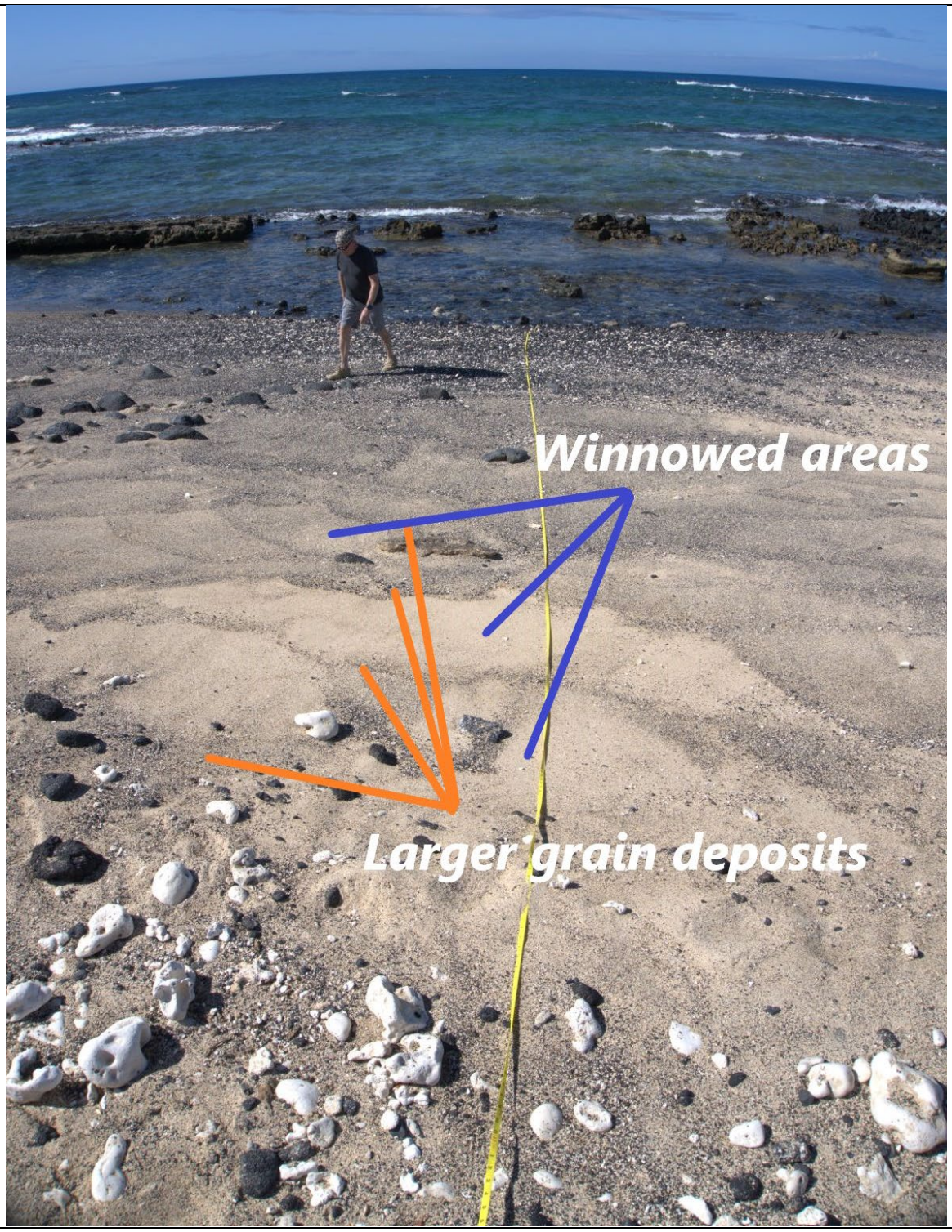

Figure 4.1.3: A labelled transect (Transect A1) from Mahai'ula Beach showing micro scale grain size differences where large grains have been deposited and finer grains have been winnowed away.

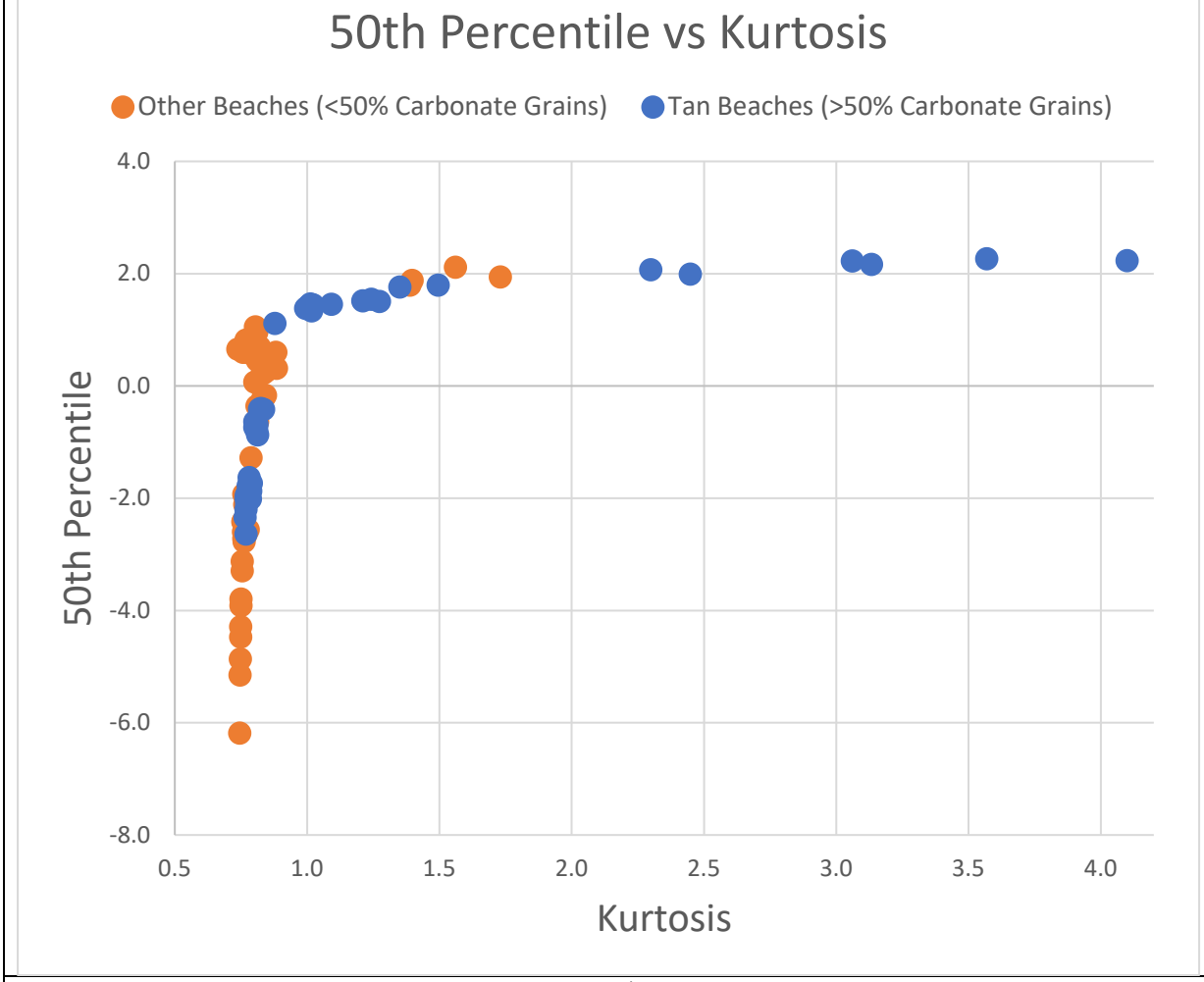

Figure 4.1.4: Relationships graphed between the 50th percentile and kurtosis in carbonate-rich sands (>50% carbonate grains) vs other sands (<50% carbonate grains) throughout the island.

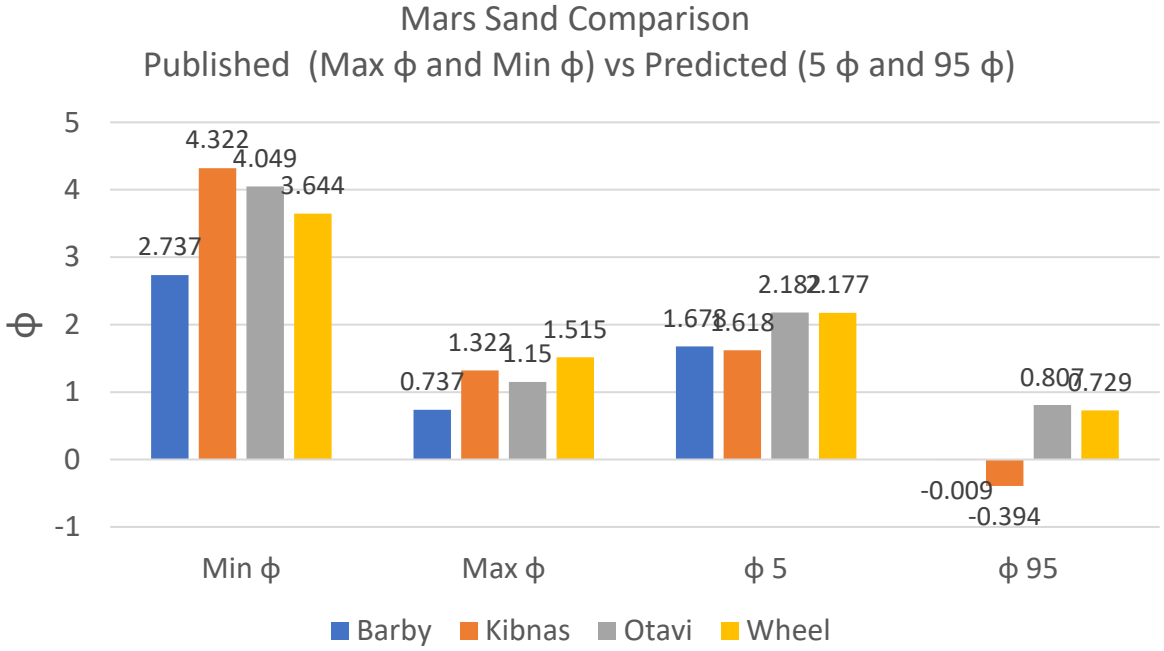

Mars Sands Comparison

		High Dune		*Namib Dune*	
		Barby	***Kibnas***	***Otavi***	***Wheel***
Published	***Min φ***	2.737	4.322	4.049	3.644
	Max φ	0.737	1.322	1.15	1.515
Predicted (Modelled)	***φ 5***	1.678	1.618	2.182	2.177
	φ 95	-0.009	-0.394	0.807	0.729

Figure 4.1.5: (*top*) Bar graph showing the published data points of the max and min phi values (Ehlmann et al., 2018) and the predicted values from pyDGS for the Mars sands. The values for the bar graph can be seen in the table on the *bottom*.

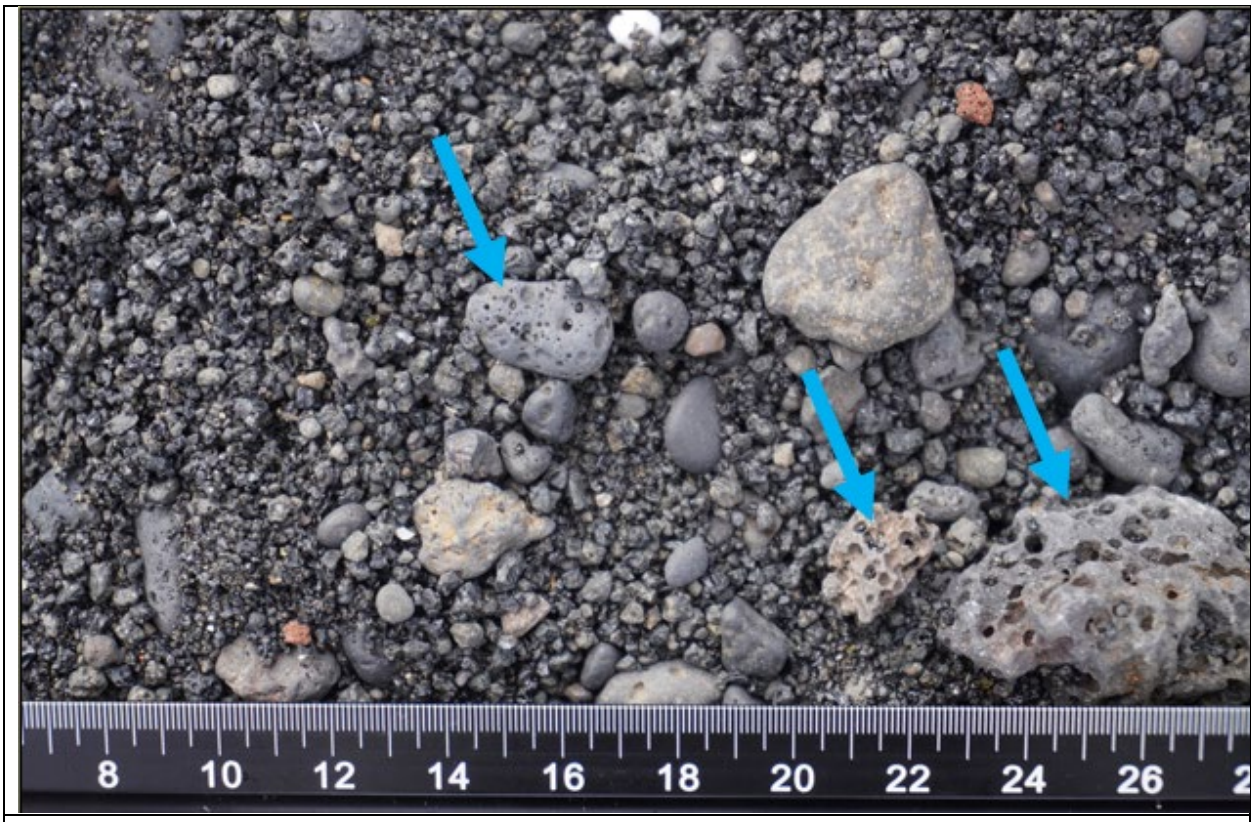

Figure 5.1: An example from Punalu'u Beach showing gravelly-sized grains with large pores that caused trouble in pyDGS.

Appendix A –

A.1 – Beach locations and corresponding labelled transects starting in the north and moving counter-clockwise through the island of Hawai'i.

A.2 – Beach/Transect height profiles.

A.1.1: Pololu beach with corresponding transect locations. Number of transects: 3. Number of surveys: 14; A(1-4), B(1-3), C(1-7).

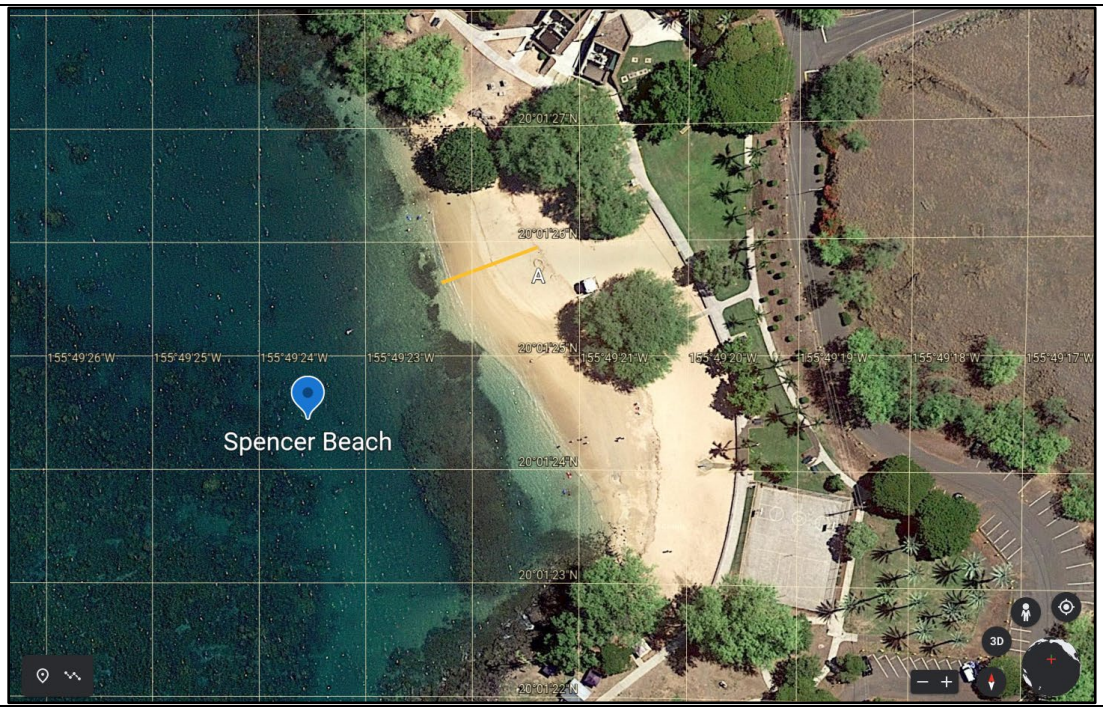

A.1.2: Spencer Beach with corresponding transect locations. Number of transects: 1. Number of surveys: 3; A(1-3).

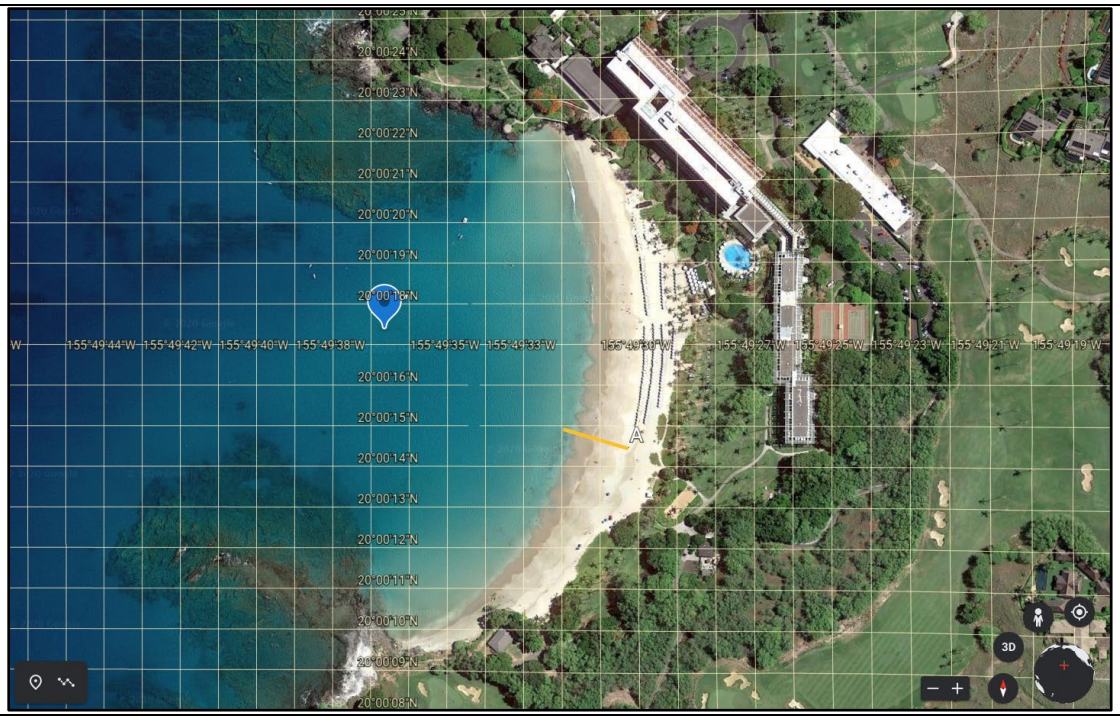

A.1.3: Mauna Kea Beach with corresponding transect location. Number of transects: 1. Number of surveys: 1; A(1).

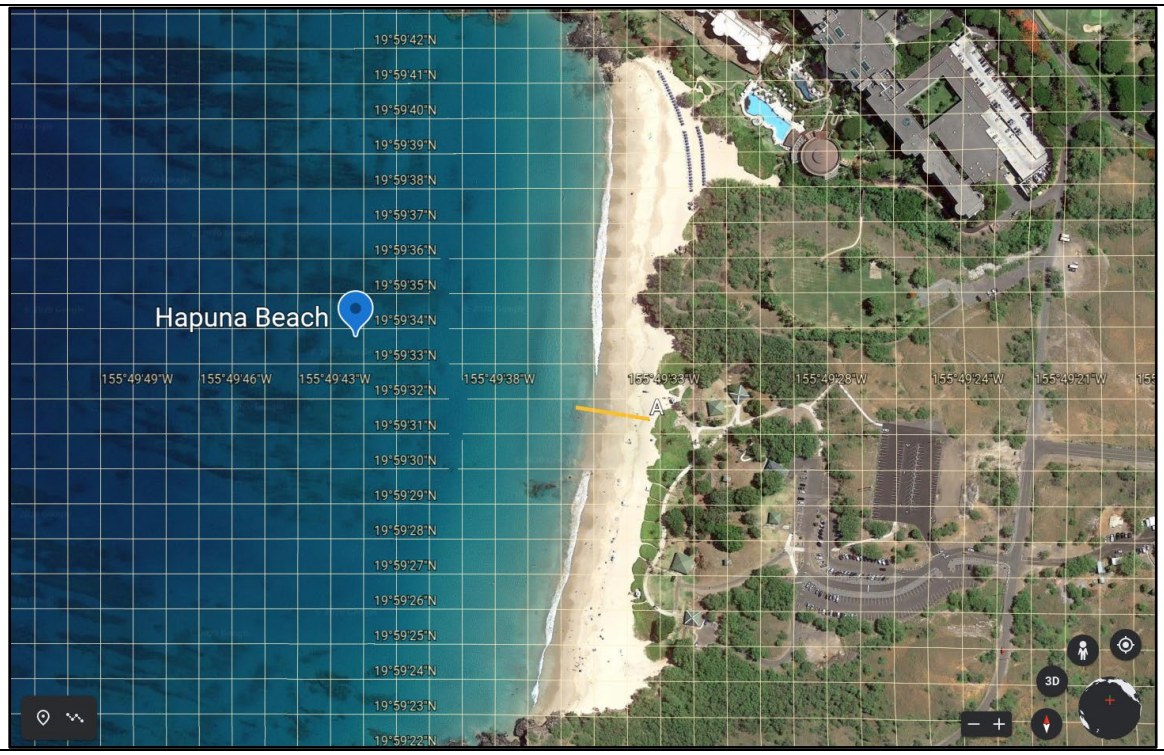

A.1.4: Hapuna Beach with corresponding transect location. Number of trnsects: 1. Number of surveys: 3; A(1-3).

A.1.5: Waialea Beach and corresponding transect locations. Number of transects: 3. Number of surveys: 6; A(1-3), B1(1-2), B2(1).

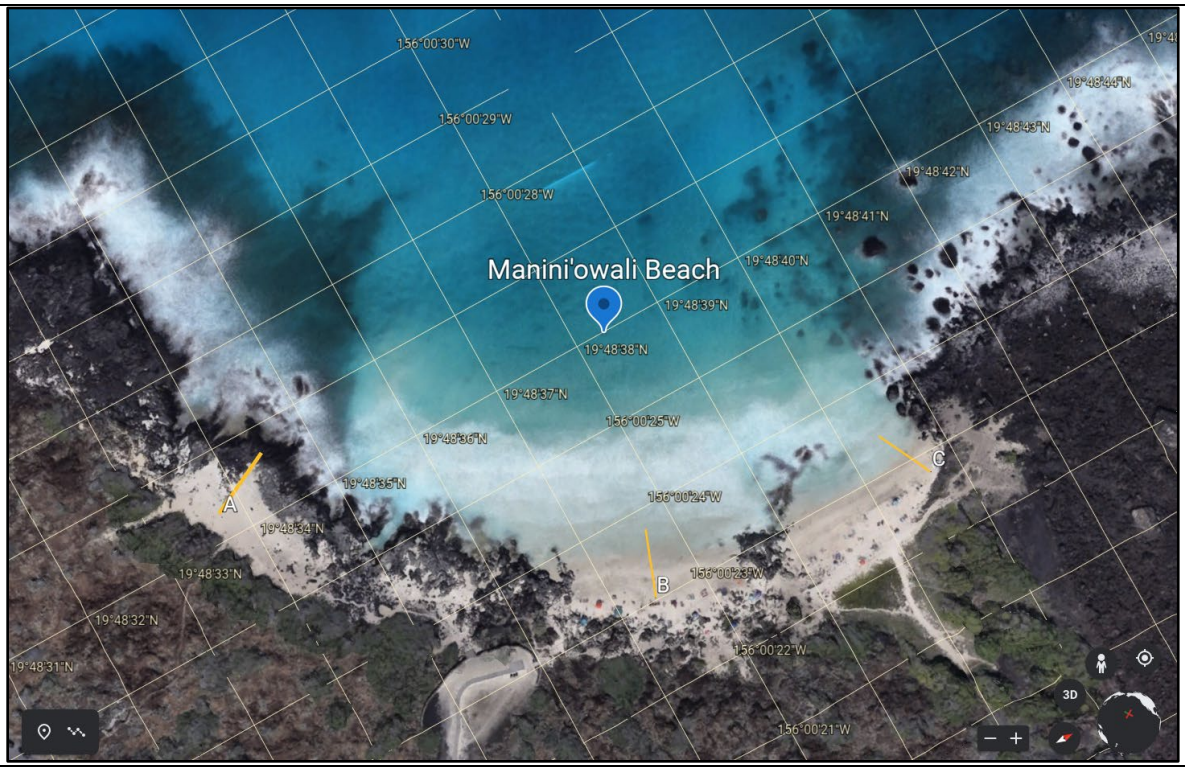

A.1.6: Manini'owali Beach and corresponding transect locations. Number of transects: 3. Number of surveys: 7; A(1-3), B(1-2), C(1-2).

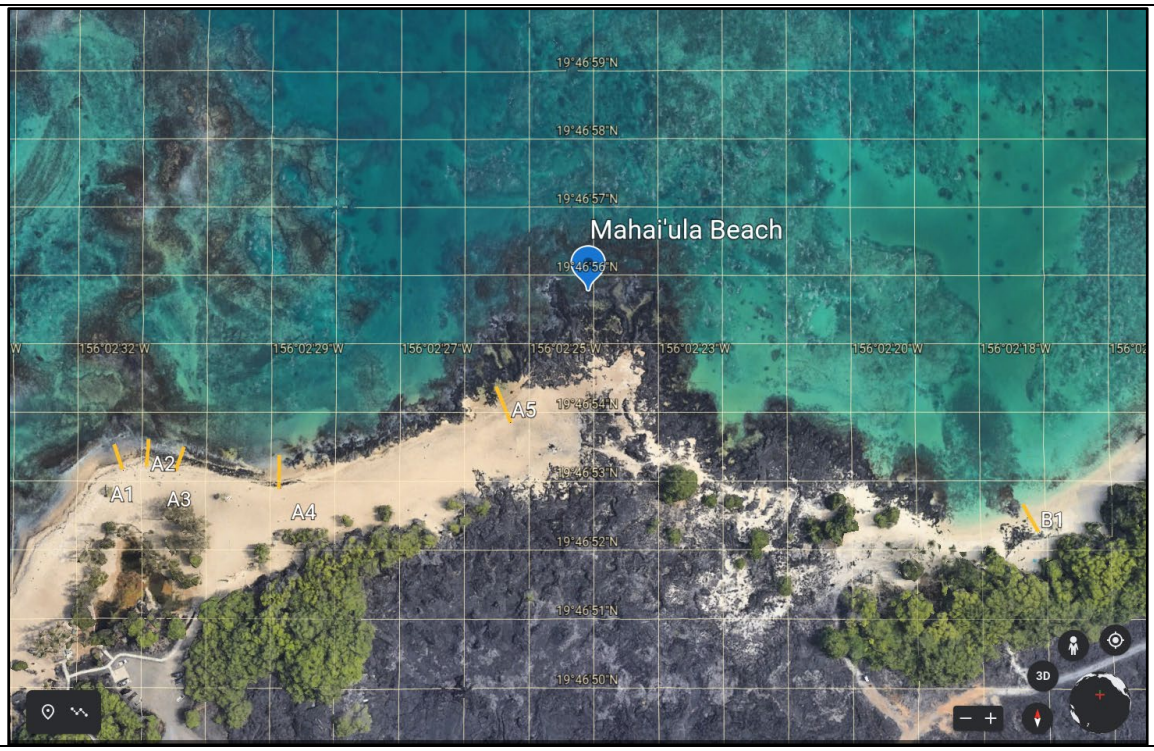

A.1.7: Mahai'ula Beach and corresponding transect locations. Number of transects: 6. Number of surveys: 18; A1(1-2), A2(1-2), A3(1-7), A4(1-3), A5(1-2), B1(1-2).

A.1.8: Old Kona Airport Beach and corresponding transect locations. Number of transects: 1. Number of surveys: 2; A(1-2).

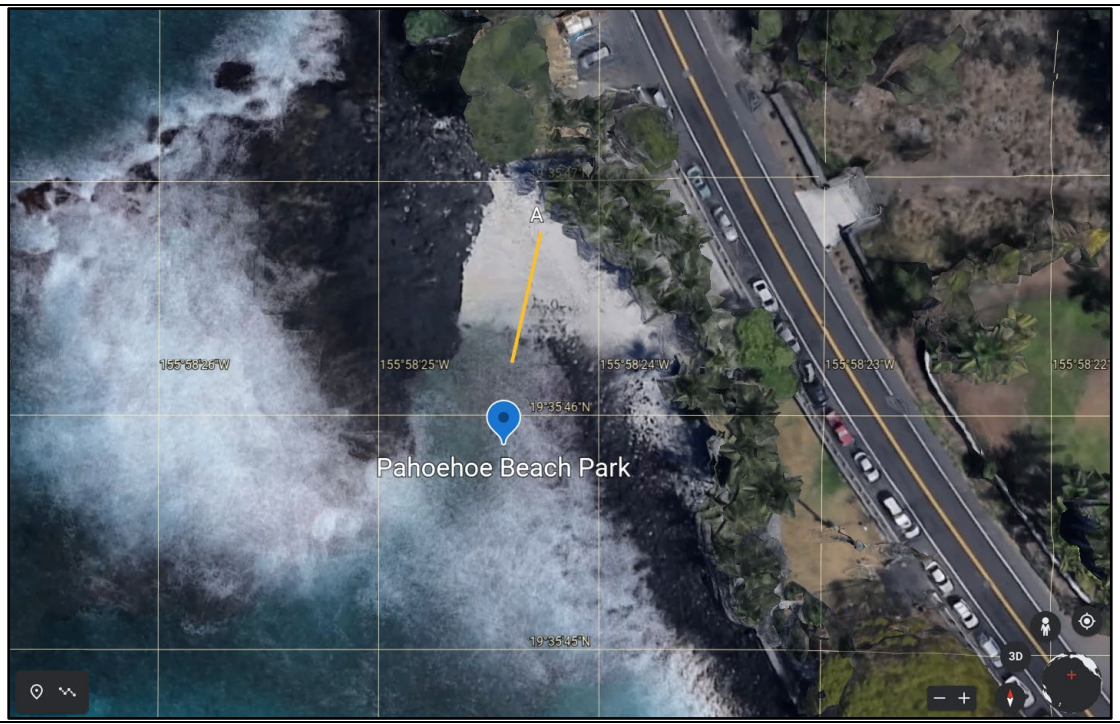

A.1.9: Pahoehoe Beach Park and corresponding transect location. Number of transects: 1. Number of surveys: 5; A(1-5).

A.1.10: Magic Sands Beach and corresponding transect location. Number of transects: 1. Number of surveys: 2; A(1-2).

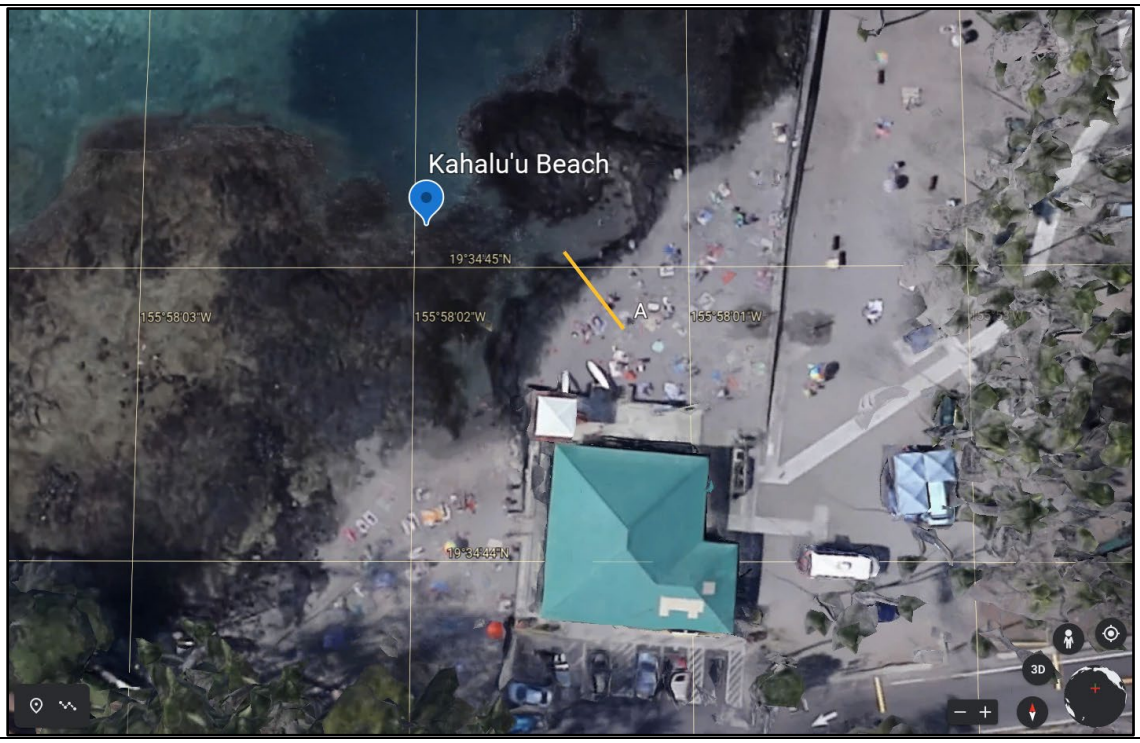

A.1.11: Kahalu'u Beach and corresponding transect location. Number of locations: 1. Number of surveys: 4; A(1-4).

A.1.12: Ho'okena Beach and corresponding transect location. Number of locations: 1. Number of surveys: 3; A(1-3).

A.1.13: Pebble Beach and corresponding transect location. Number of transects: 1. Number of surveys: 4; A(1-4).

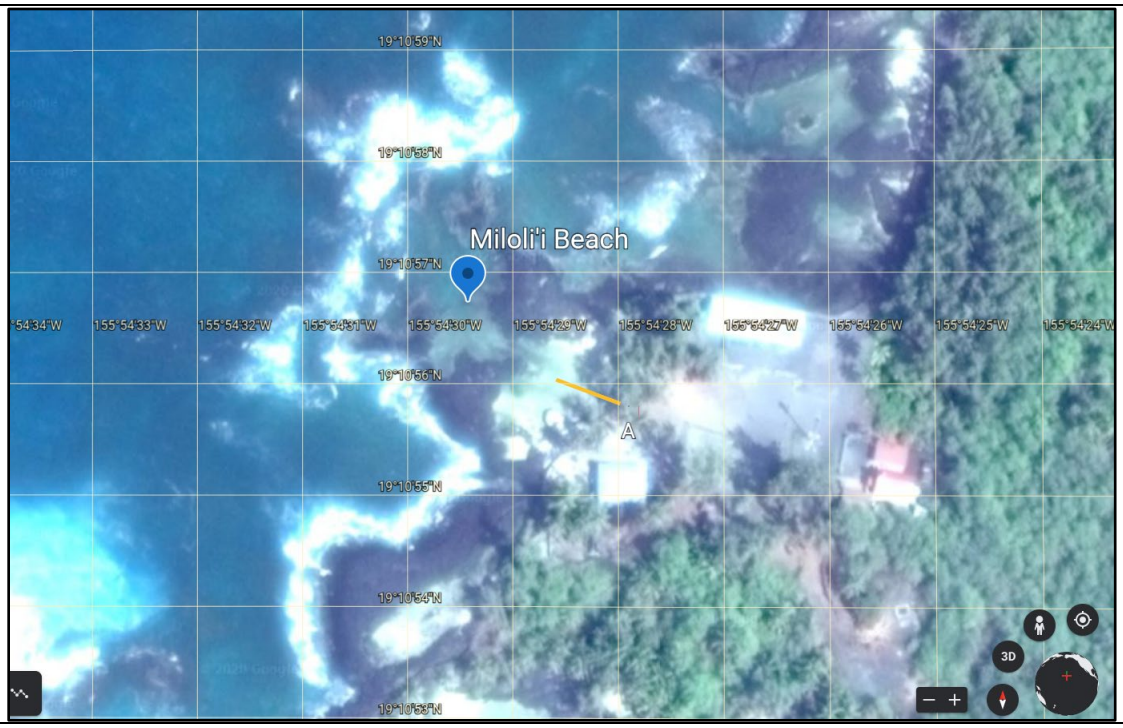

A.1.14: Miloli'I Beach and corresponding transect location. Number of transects: 1. Number of surveys: 3; A(1-3).

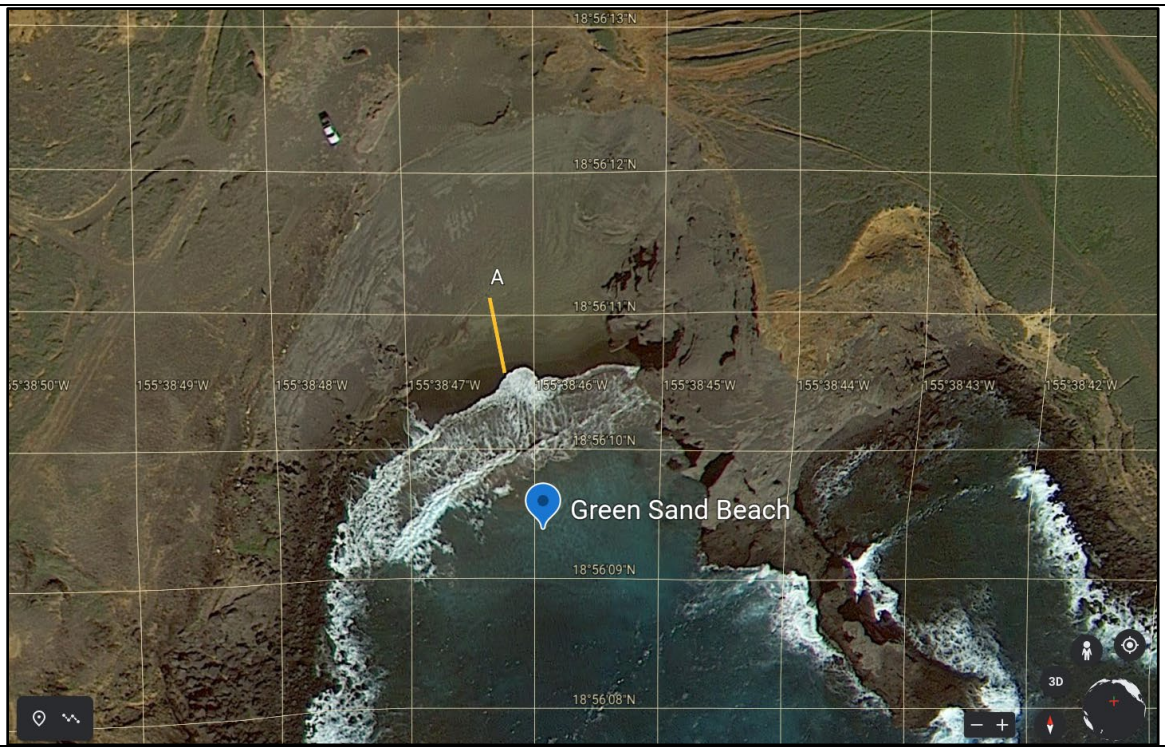

A.1.15: Green Sand Beach and corresponding transect location. Number of transects: 1. Number of surveys: 4; A(1-4).

A.1.16: Punalu'u Beach and corresponding transect locations. Number of transects: 5. Number of surveys: 17; A(1-4), B(1-3), C(1-3), D(1-3), E(1-4).

A.1.17: Pohoiki Beach and corresponding transect location. Number of transects: 1. Number of surveys: 5; A(1-5).

A.1.18: Honoli'I Beach and corresponding transect locations. Number of transects: 2. Number of surveys: 6; A(1-3), B(1-3).

Appendix B – Location, transect, and cropped sand pictures (used in pyDGS) beginning in the north and moving counter-clockwise.

B.1.1: Pololu Beach overview looking SE.

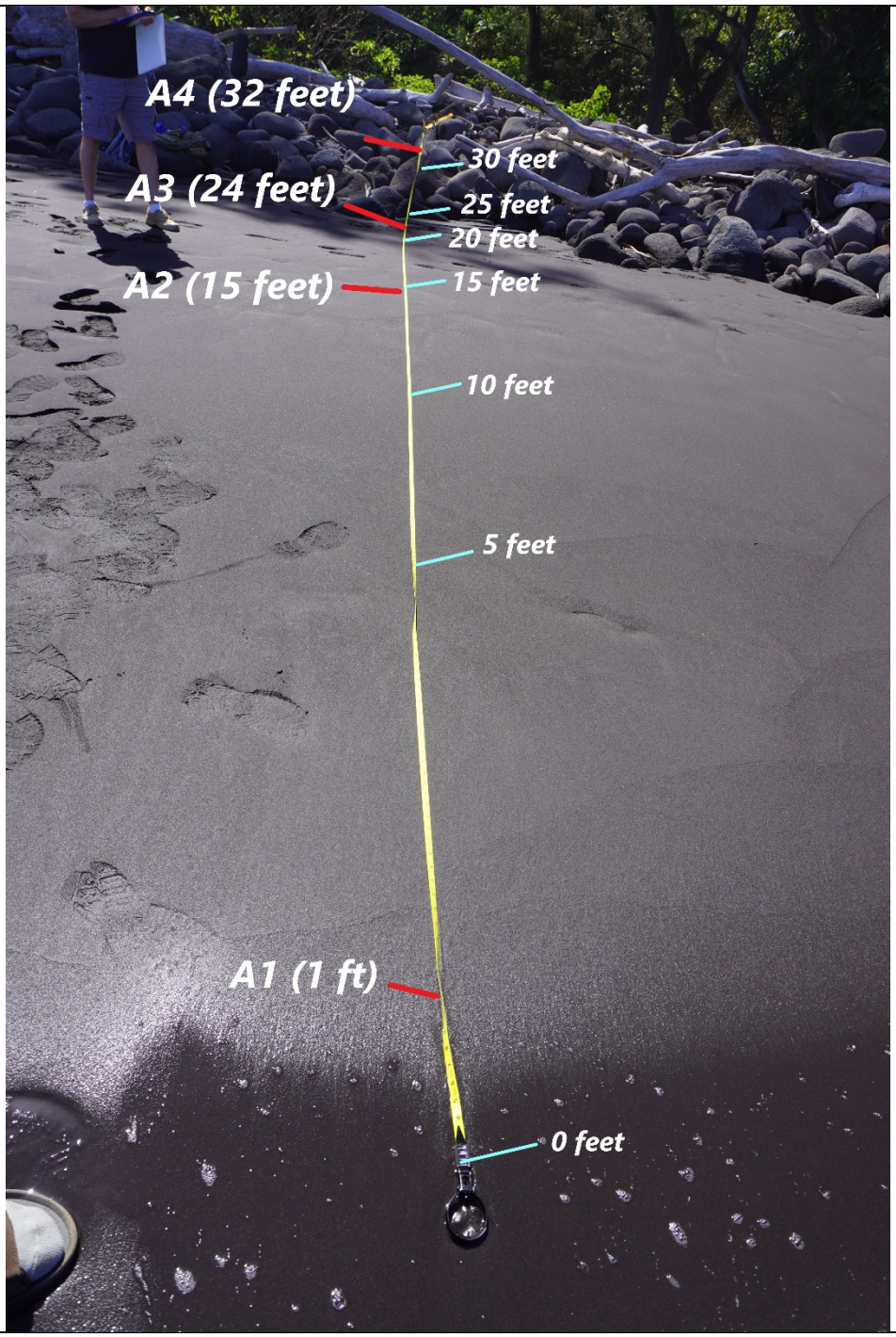

B.1.2: Pololu Beach Transect A, NW edge of bay, looking landward, with annotated survey locations.

A-1

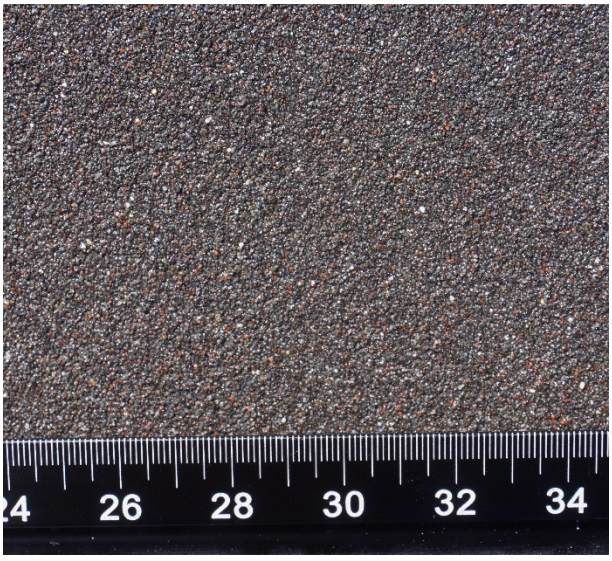

A-2

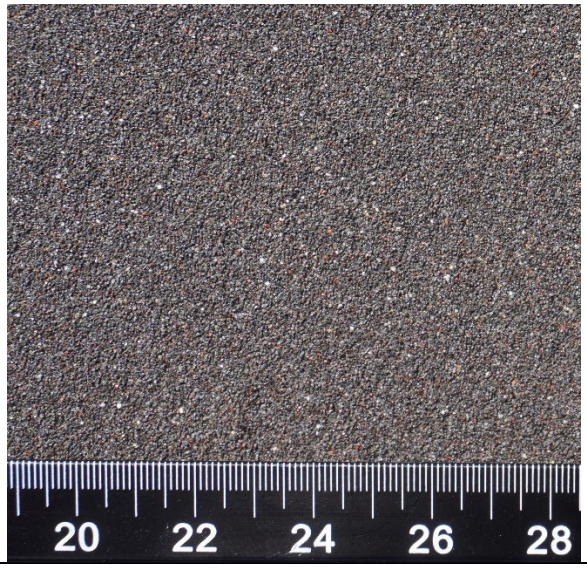

A-3

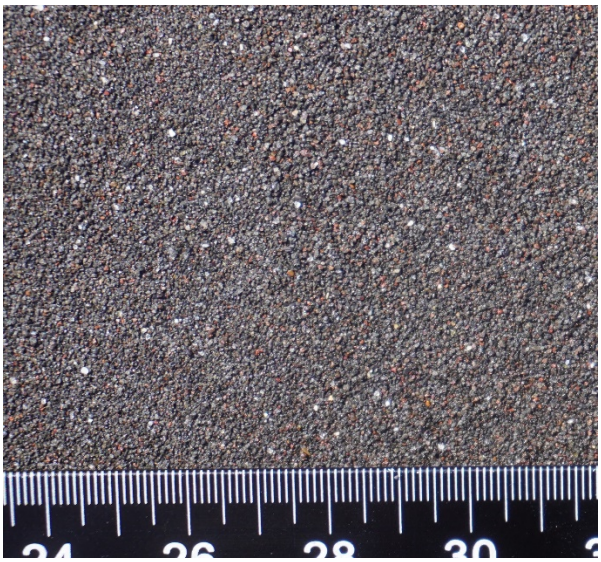

A-4

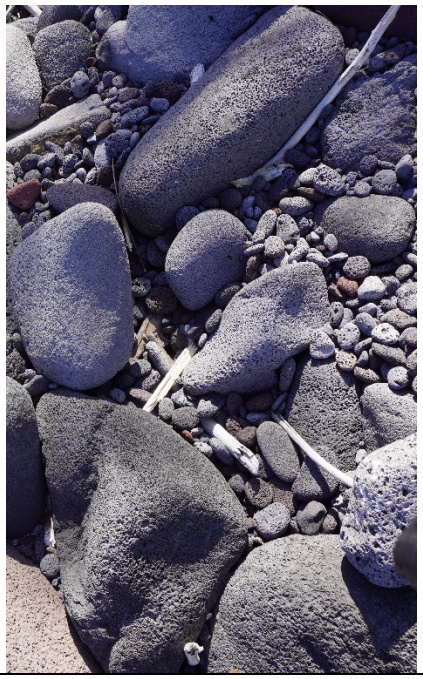

B.1.3: Pololu Beach Transect A survey site photographs with location labels. One inch is equal to 50 ticks (5 major scale units) on the laser-etched ruler.

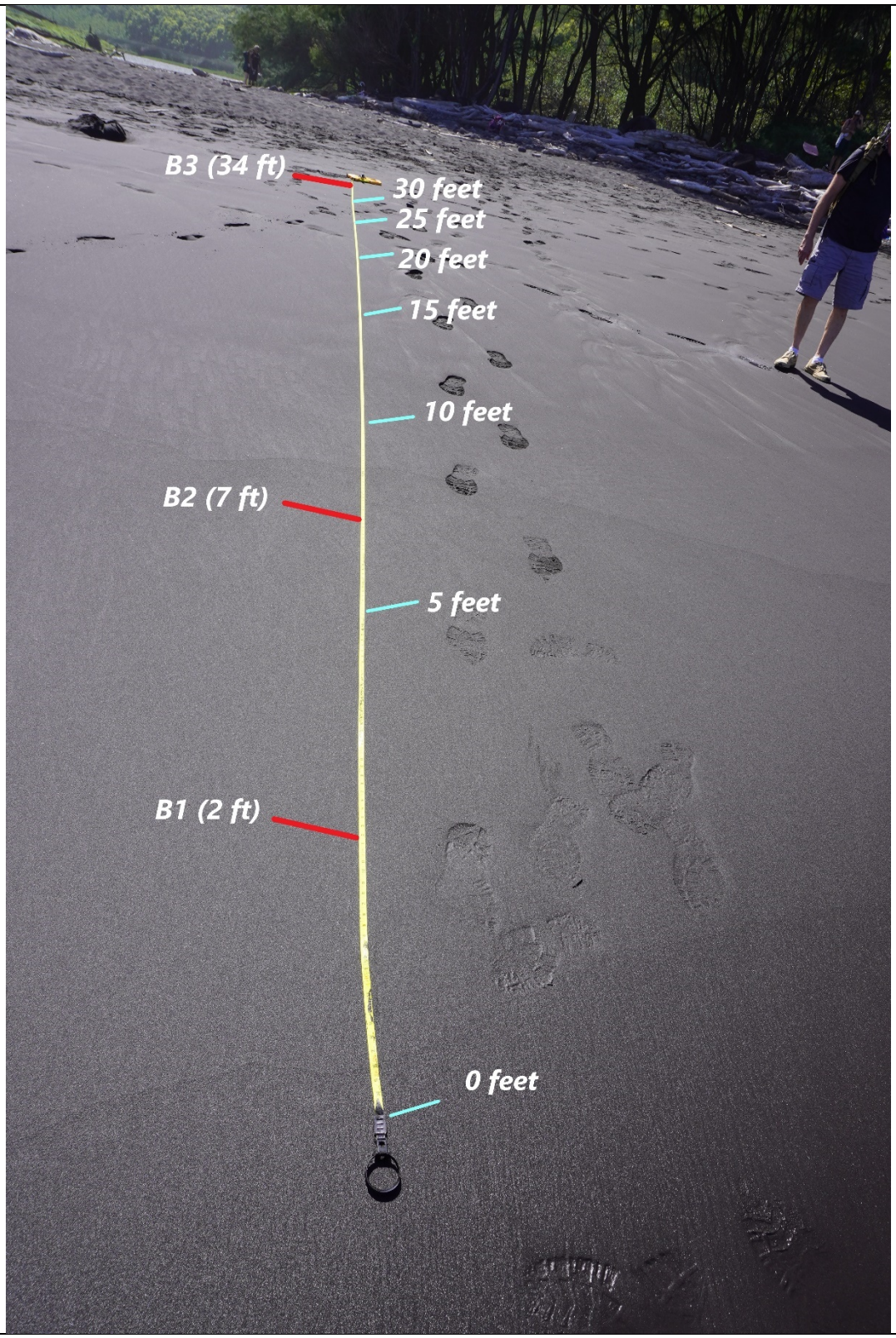

B.1.4: Pololu Beach Transect B, leading out from the river, middle of the bay, looking landward, with annotated survey locations.

B-1

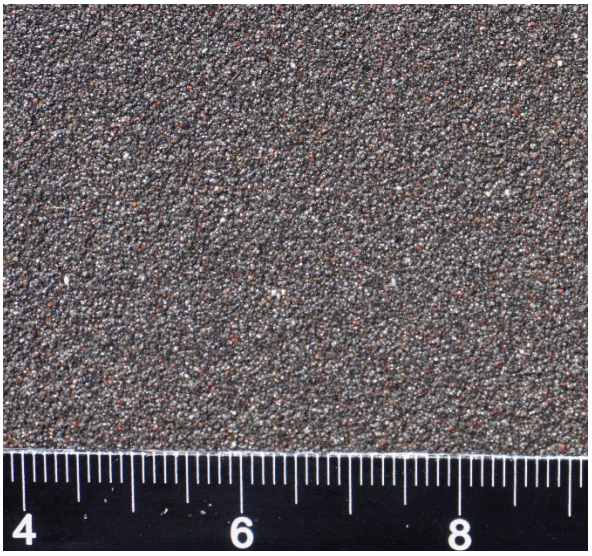

B-2

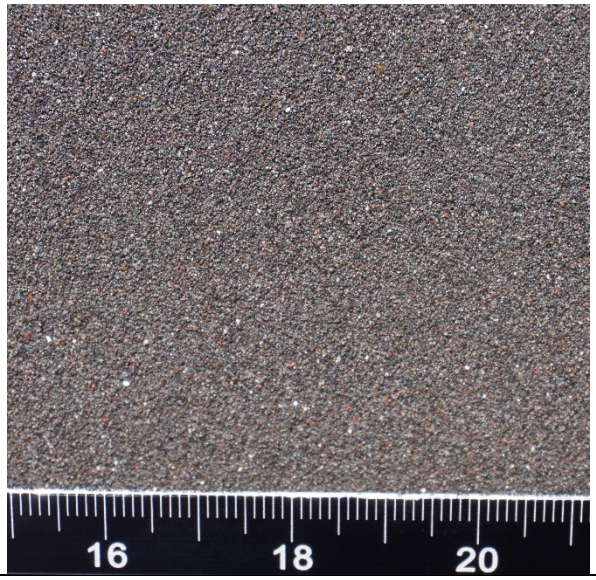

B-3

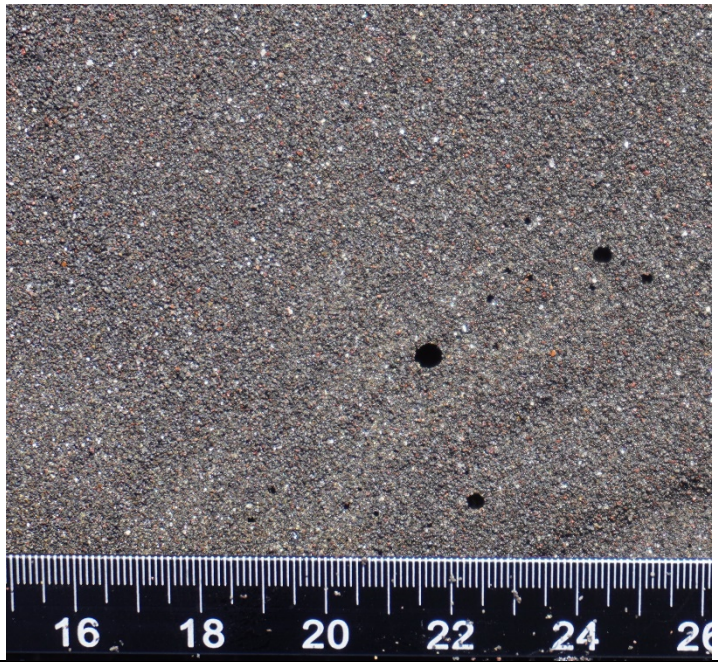

B.1.5: Pololu Beach Transect B survey site photographs with location labels. One inch is equal to 50 ticks (5 major scale units) on the laser-etched ruler.

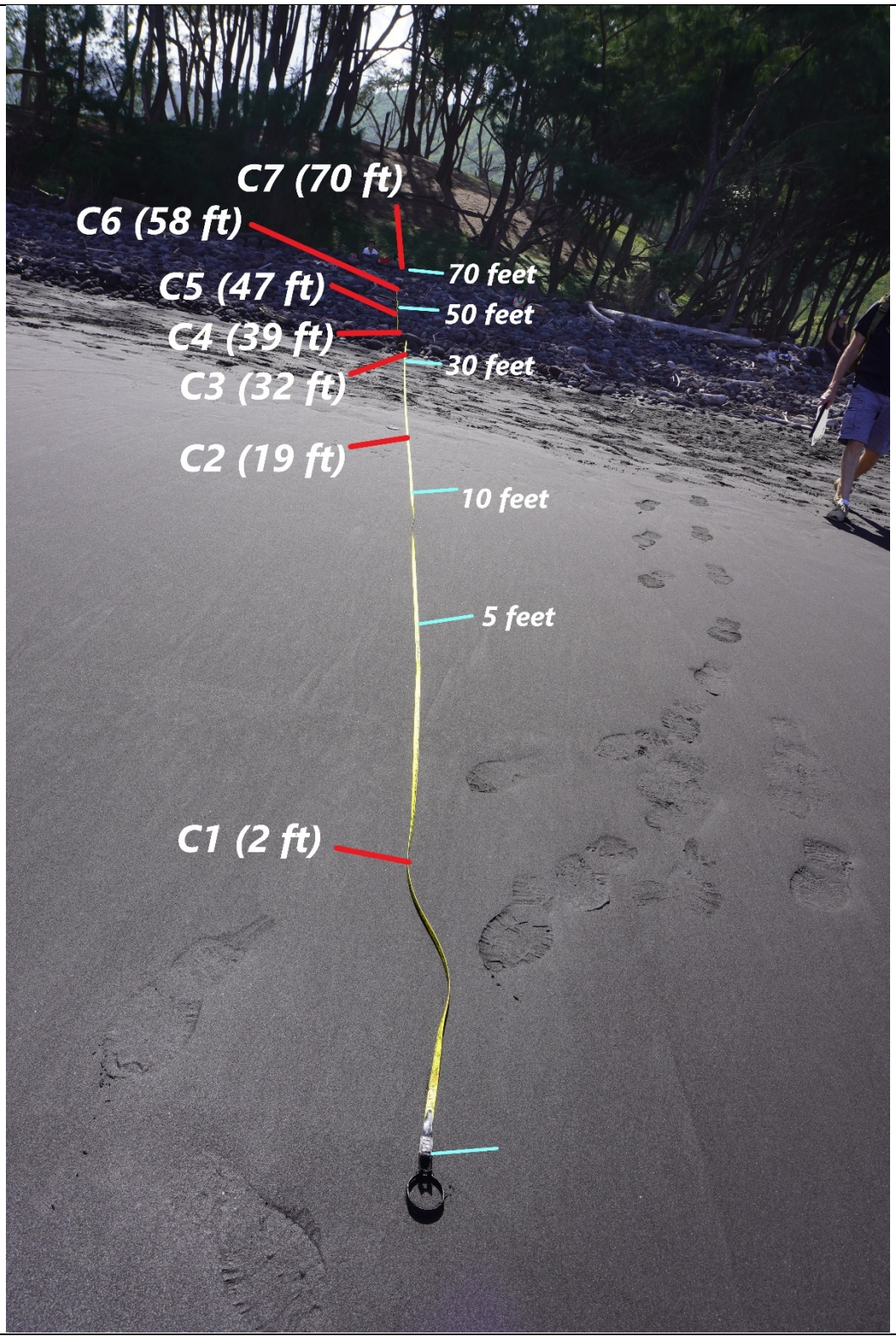

B.1.6: Pololu Beach Transect C, SE side of the bay, looking landward, goes onto cobbly berm, with annotated survey locations.


30
32
34
36


30
32
34
36

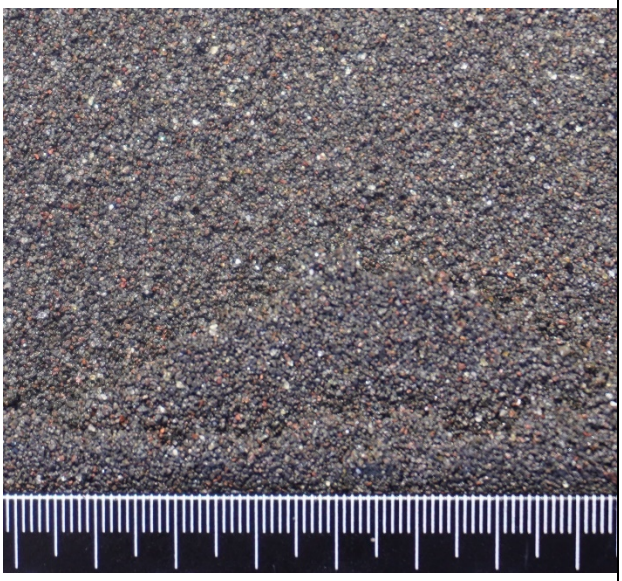

C-7

B.1.7: Pololu Beach Transect C survey point photographs with location labels. One inch is equal to 50 ticks (5 major scale units) on the laser-etched ruler. The units on the yellow tape are inches.

B.2.1: Spencer Beach overview photo taken from the NW corner looking SE.

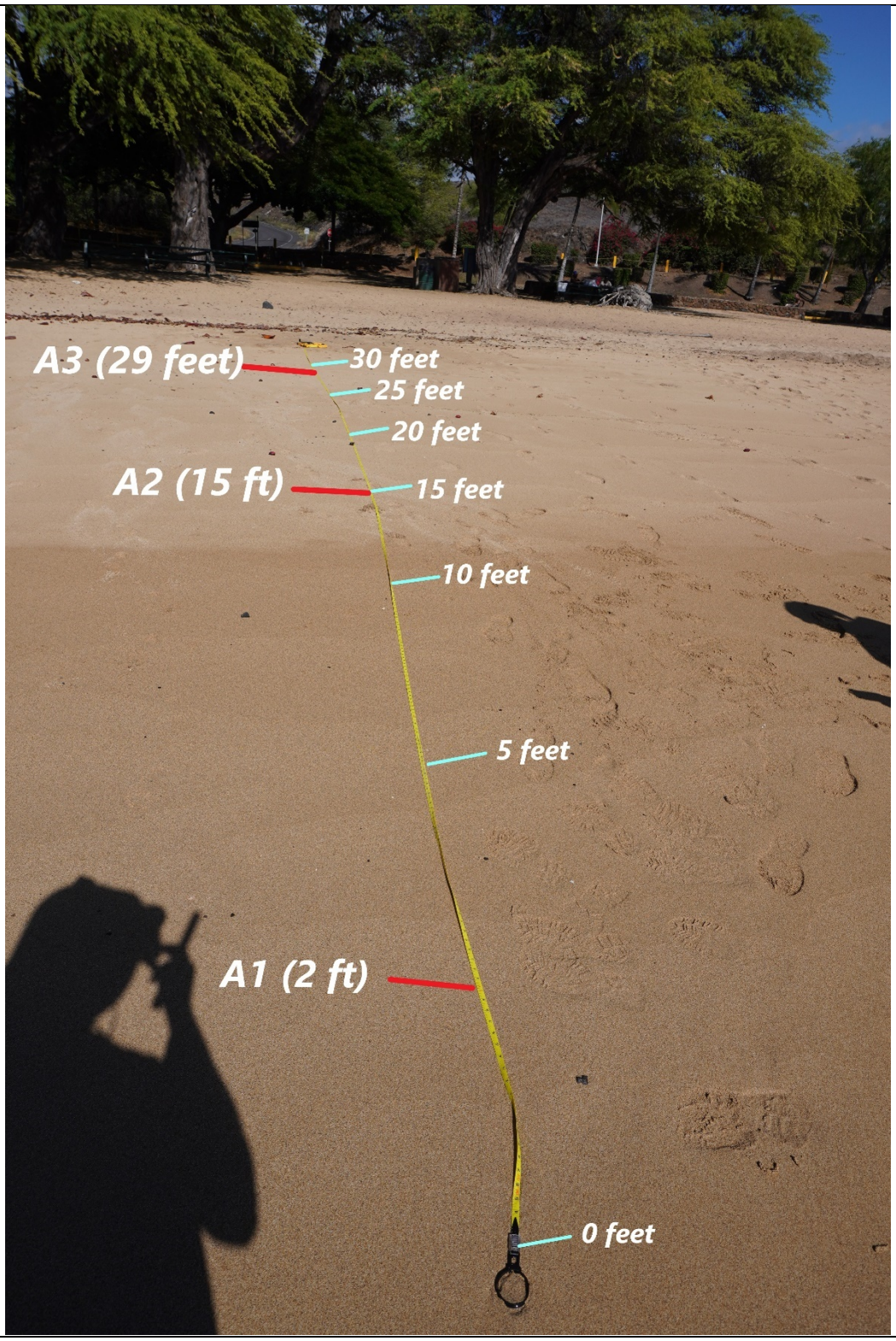

B.2.2: Spencer Beach Transect A looking landward, with annotated survey locations.

A-1

A-2

A-3

B.2.3: Spencer Beach Transect A survey site photographs with location labels. One inch is equal to 50 ticks (5 major scale units) on the laser-etched ruler.

B.3.1: Mauna Kea Beach overview looking N.

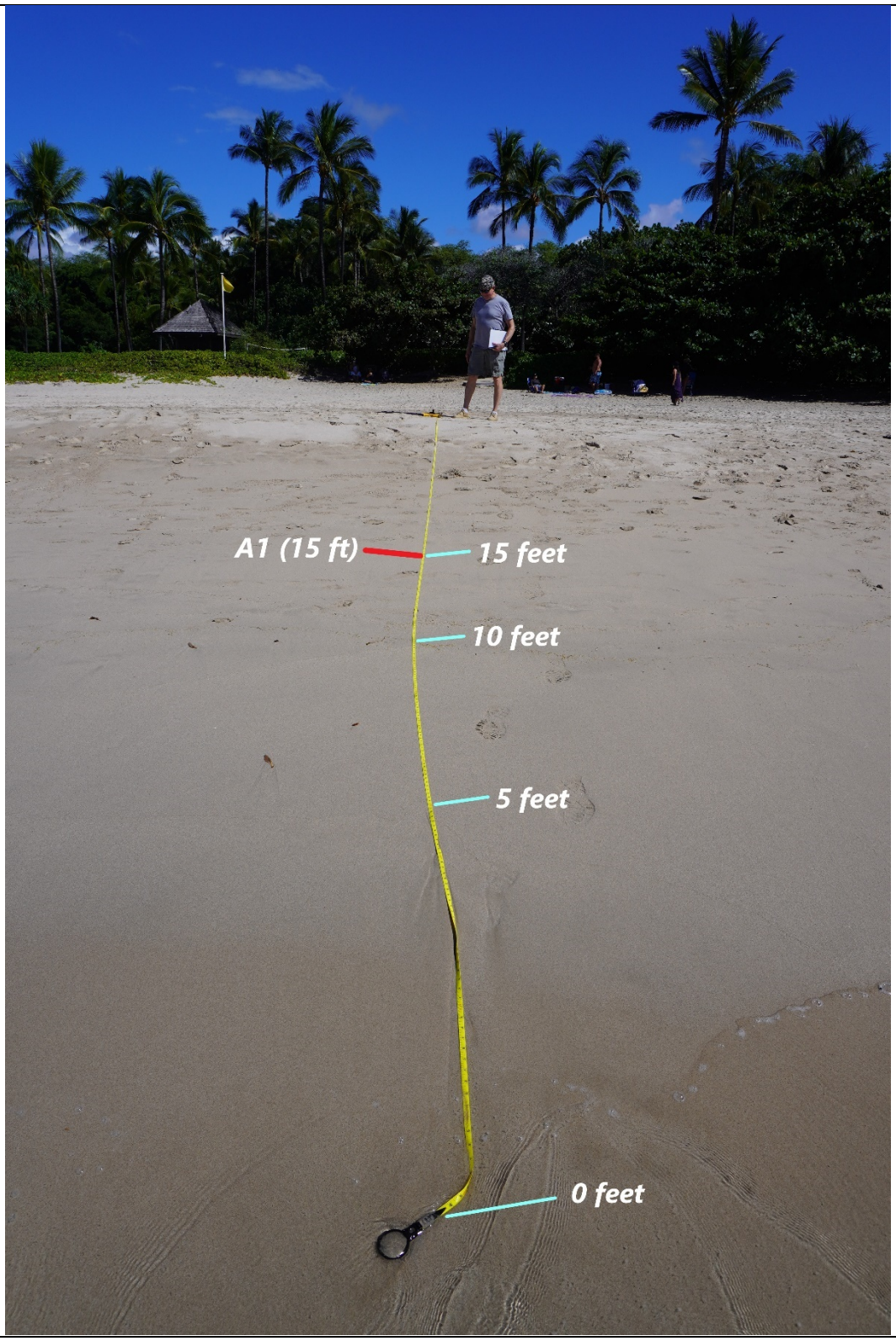

B.3.2: Mauna Kea Beach Transect A looking landward, with annotated survey locations.

A-1

B.3.3: Mauna Kea Beach Transect A survey site photograph with location label. One inch is equal to 50 ticks (5 major scale units) on the laser-etched ruler.

B.4.1: Hapuna Beach overview looking N.

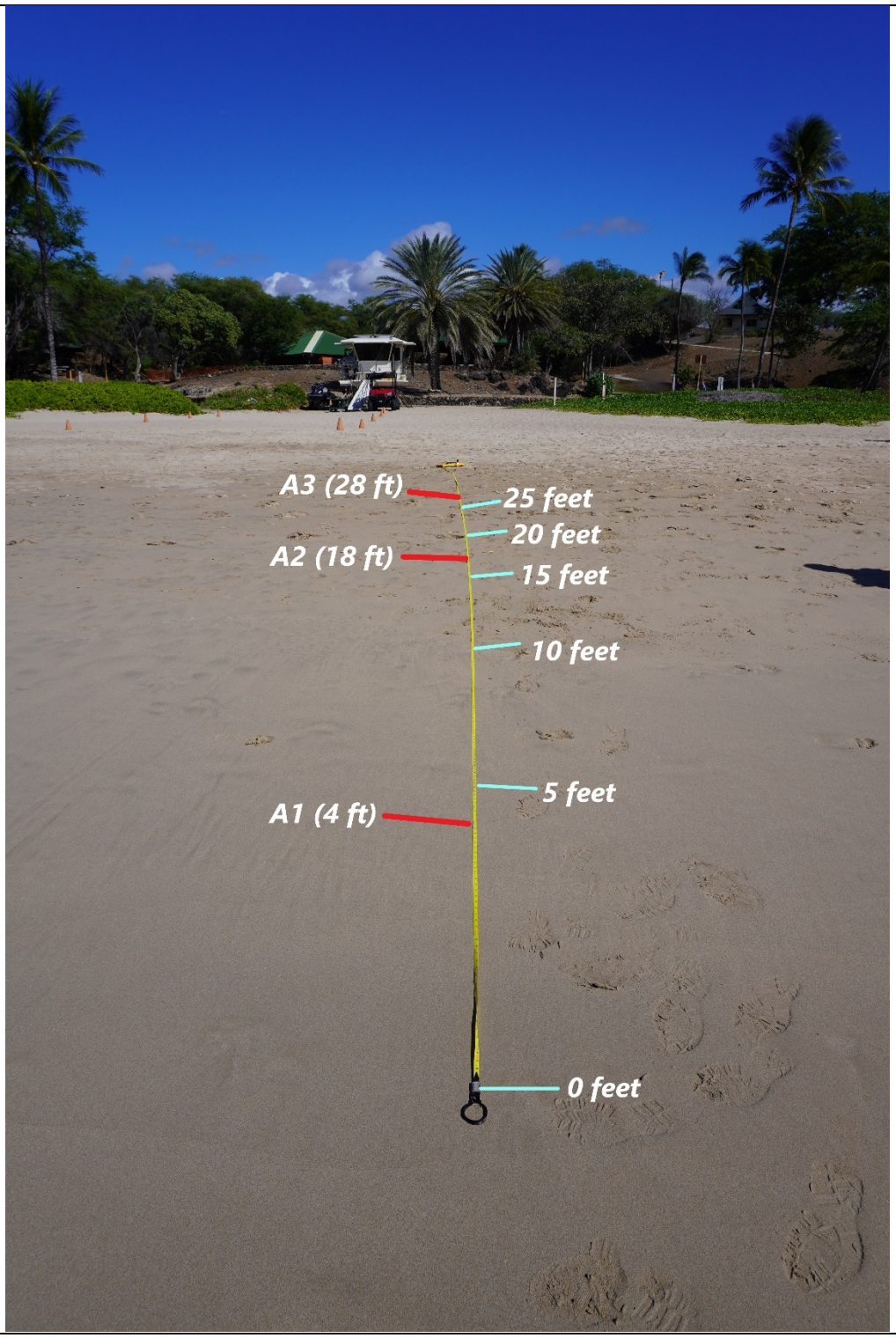

B.4.2: Hapuna Beach Transect A photograph looking landward, with annotated survey locations.

A-1

A-2

A-3

B.4.3: Hapuna Beach Transect A survey site photographs with location labels. One inch is equal to 50 ticks (5 major scale units) on the laser-etched ruler.

B.5.1: Waialea Beach overview photograph looking E.

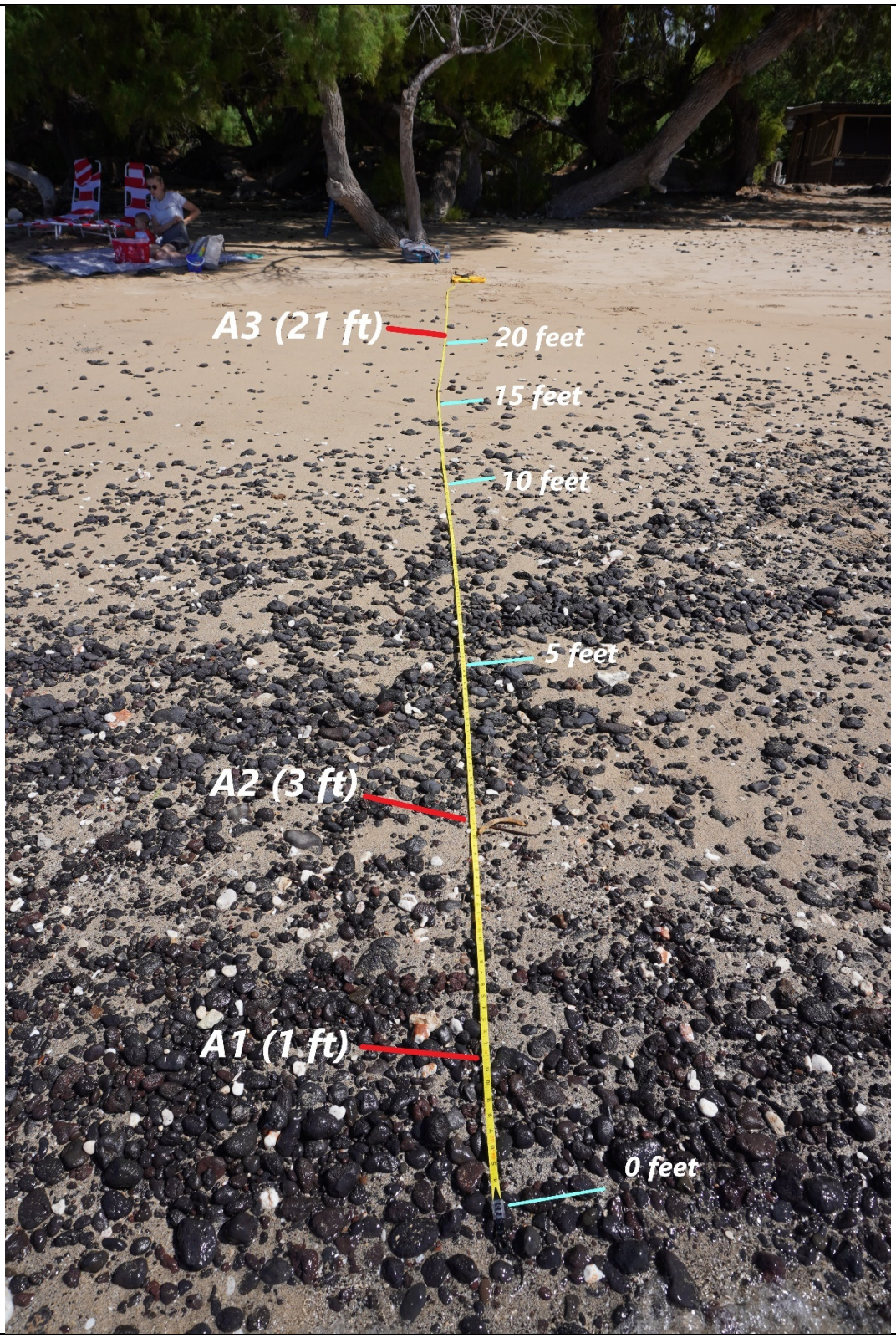

B.5.2: Waialea Beach Transcest A looking landward, with annotated survey locations.

A-1

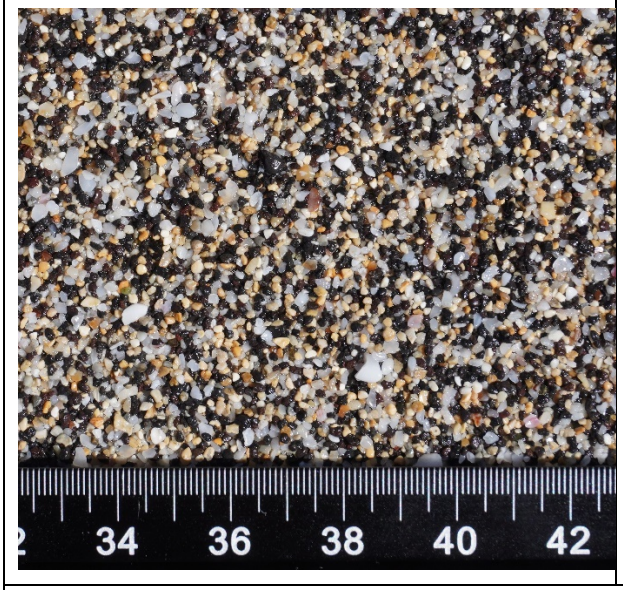

A-2

A-3

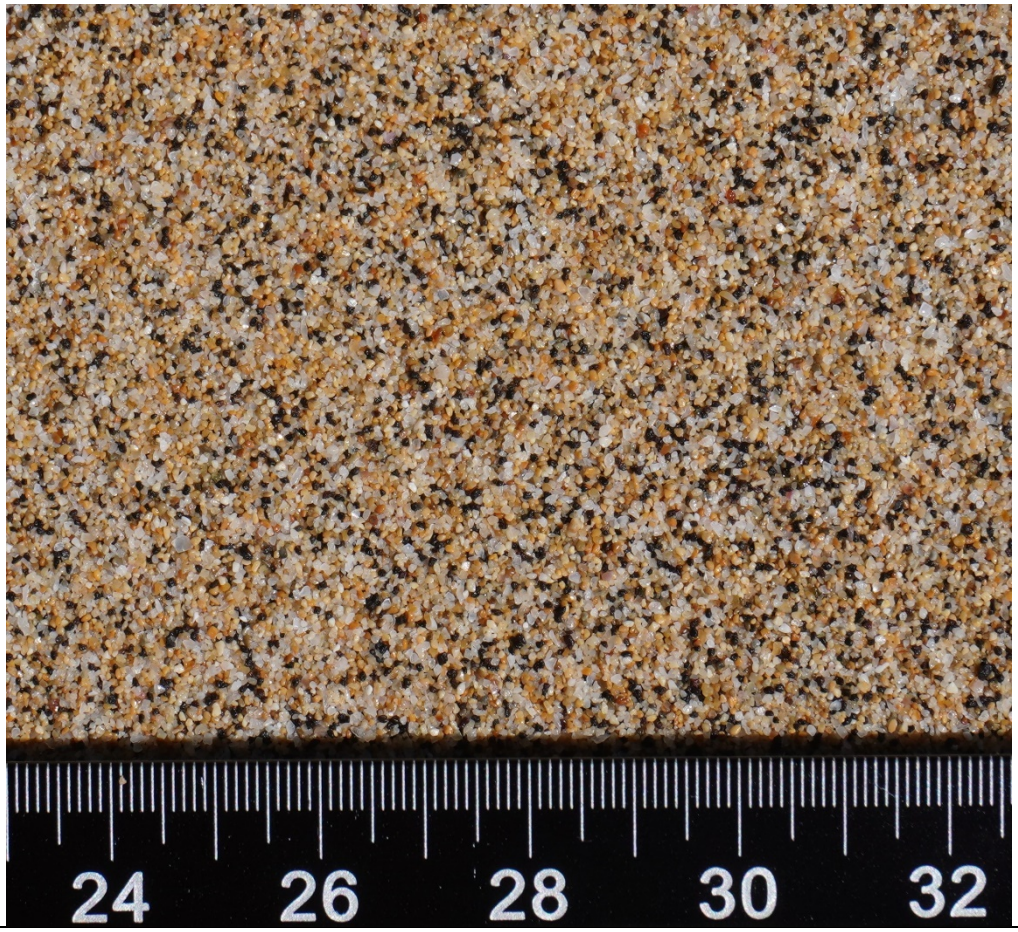

B.5.3: Waialea Beach Transect A survey site photographs with location labels. One inch is equal to 50 ticks (5 major scale units) on the laser-etched ruler.

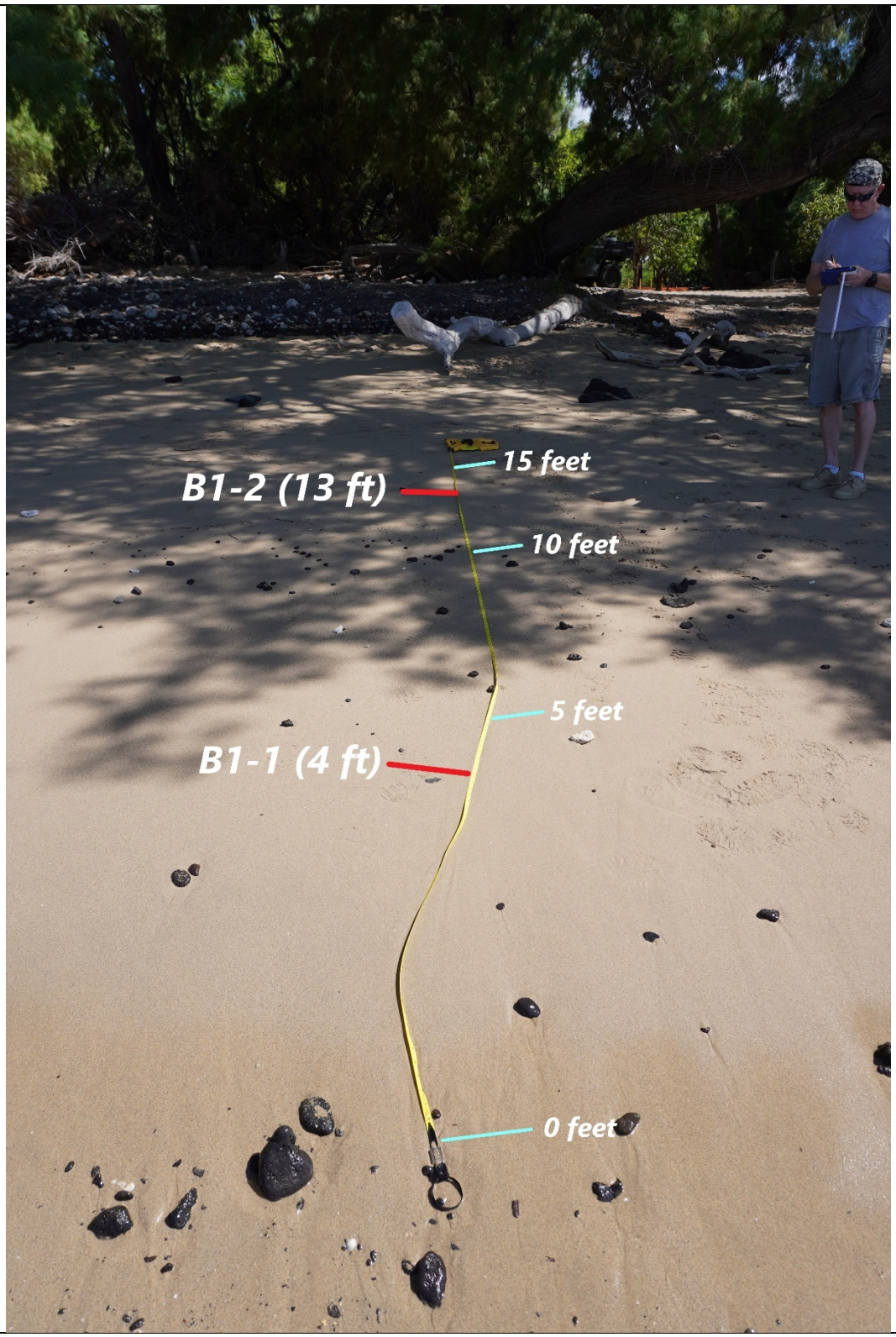

B.5.4: Waialea Beach Transect B1 photograph looking landward, with annotated survey locations.

B1-1

B1-2

B.5.5: Waialea Beach Transect B1 survey site photographs with location labels. One inch is equal to 50 ticks (5 major scale units) on the laser-etched ruler.

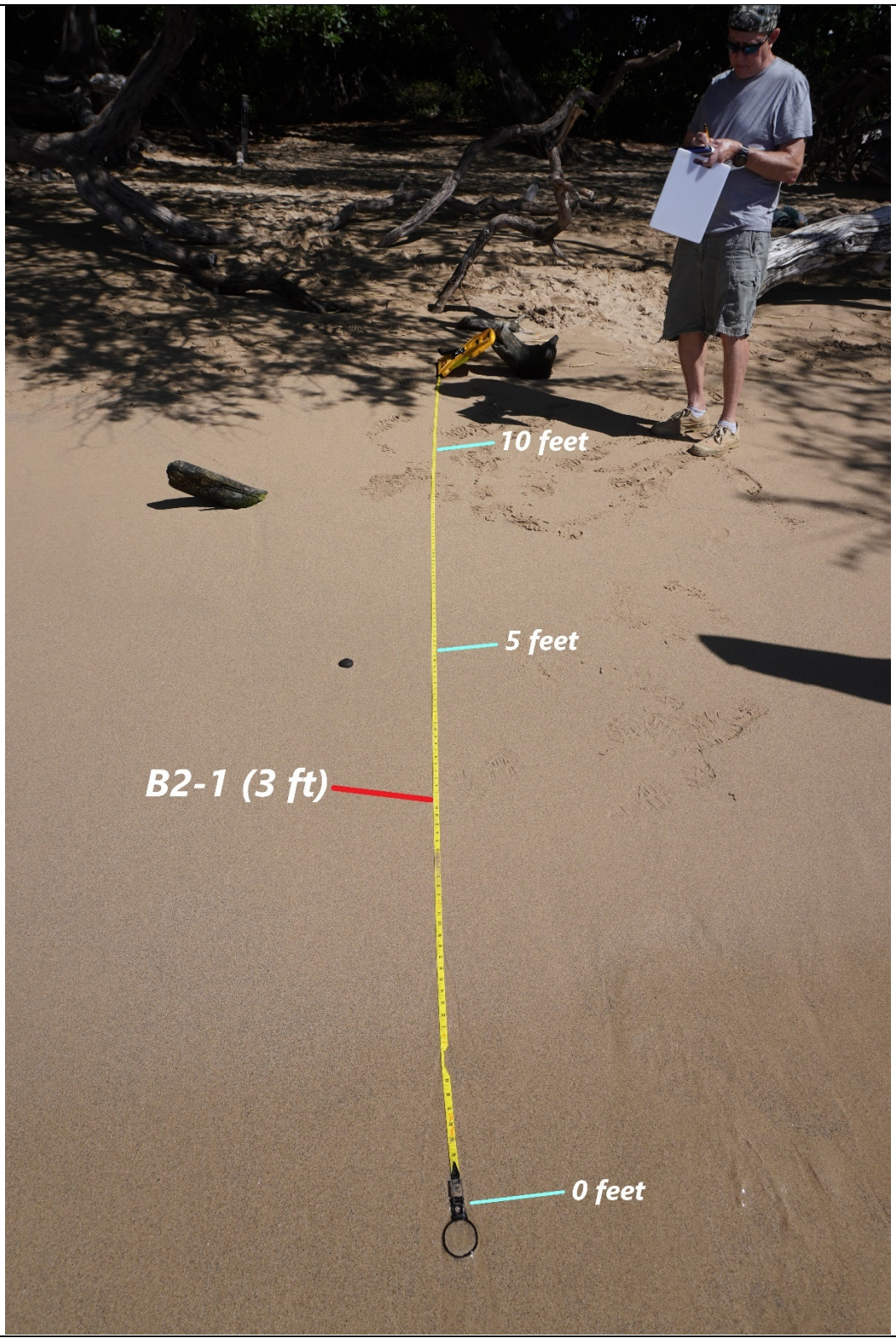

B.5.6: Waialea Beach Transect B2 looking landward, with annotated survey locations.

B2-1

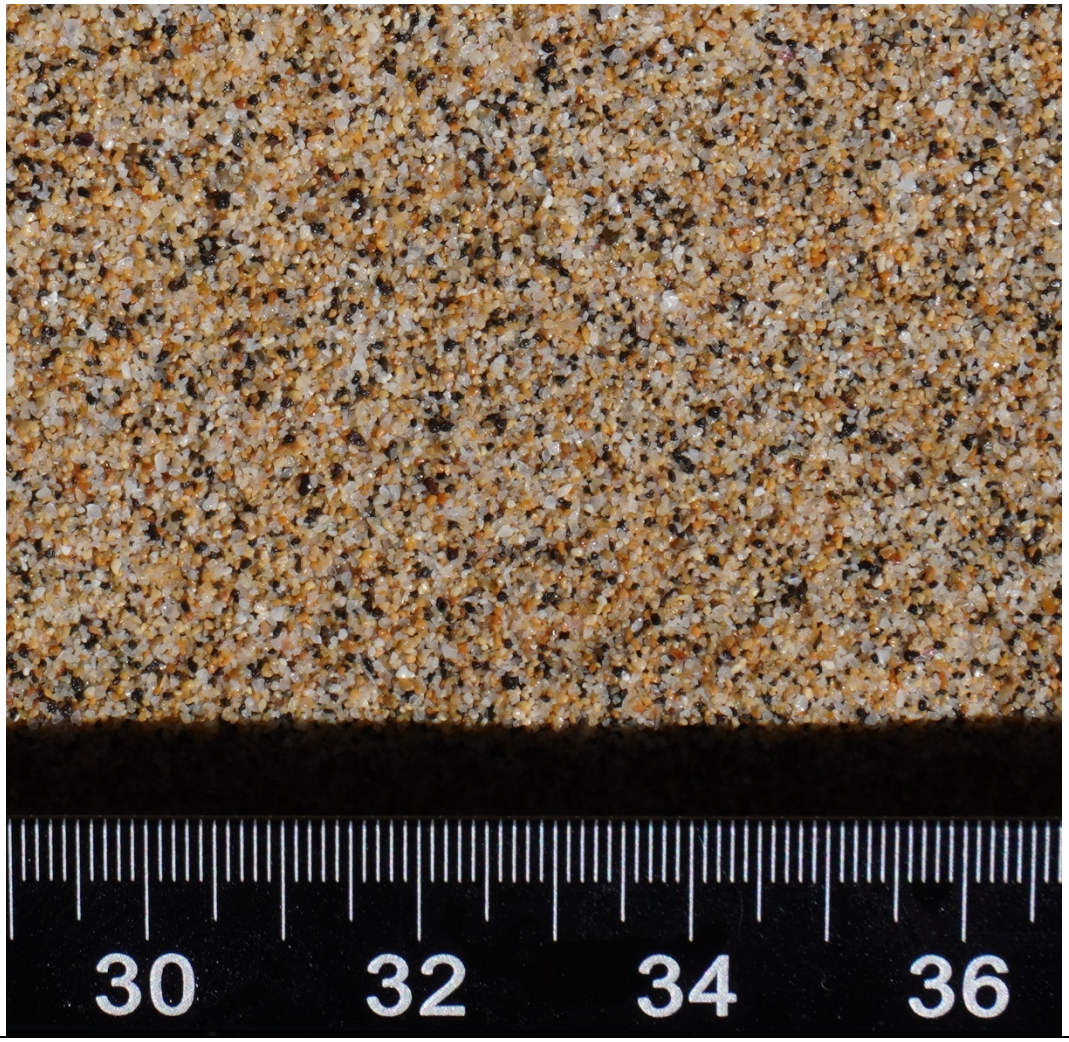

B.5.7: Waialea Beach Transect B2 survey site photograph with location label. One inch is equal to 50 ticks (5 major scale units) on the laser-etched ruler.

B.6.1: Manini’owali Beach overview photograph looking West.

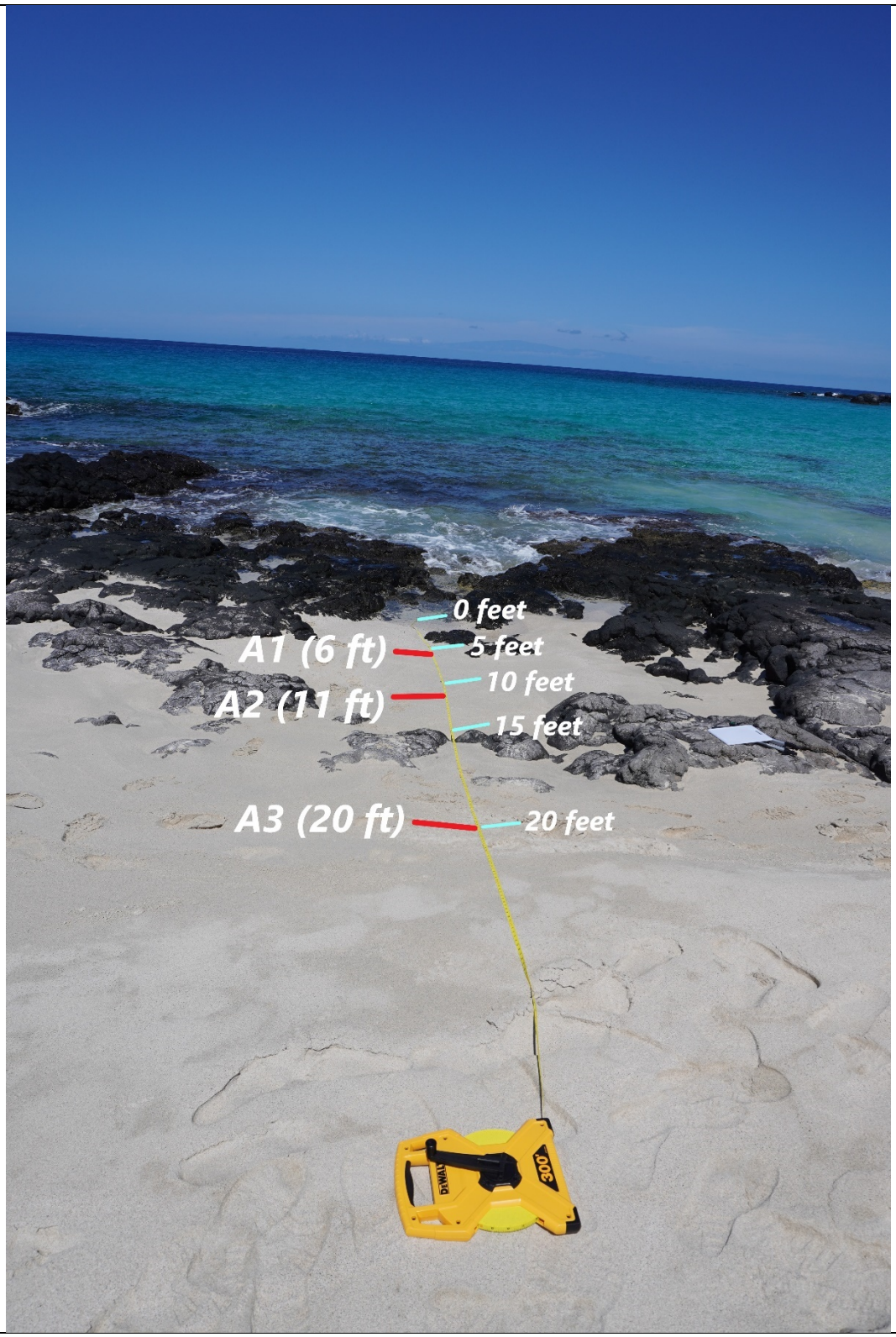

B.6.2: Manini'owali Beach Transect A photograph looking seaward, with annotated survey locations.

A-1

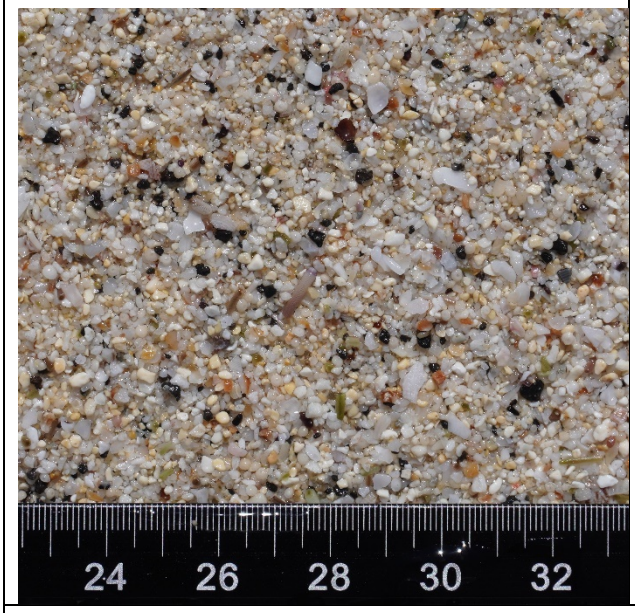

A-2

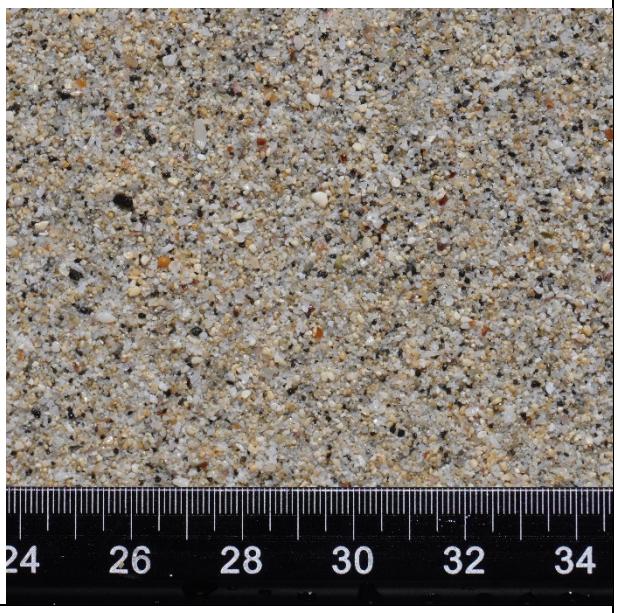

A-3

B.6.3: Manini'owali Beach Transect A survey site photographs with location labels. One inch is equal to 50 ticks (5 major scale units) on the laser-etched ruler.

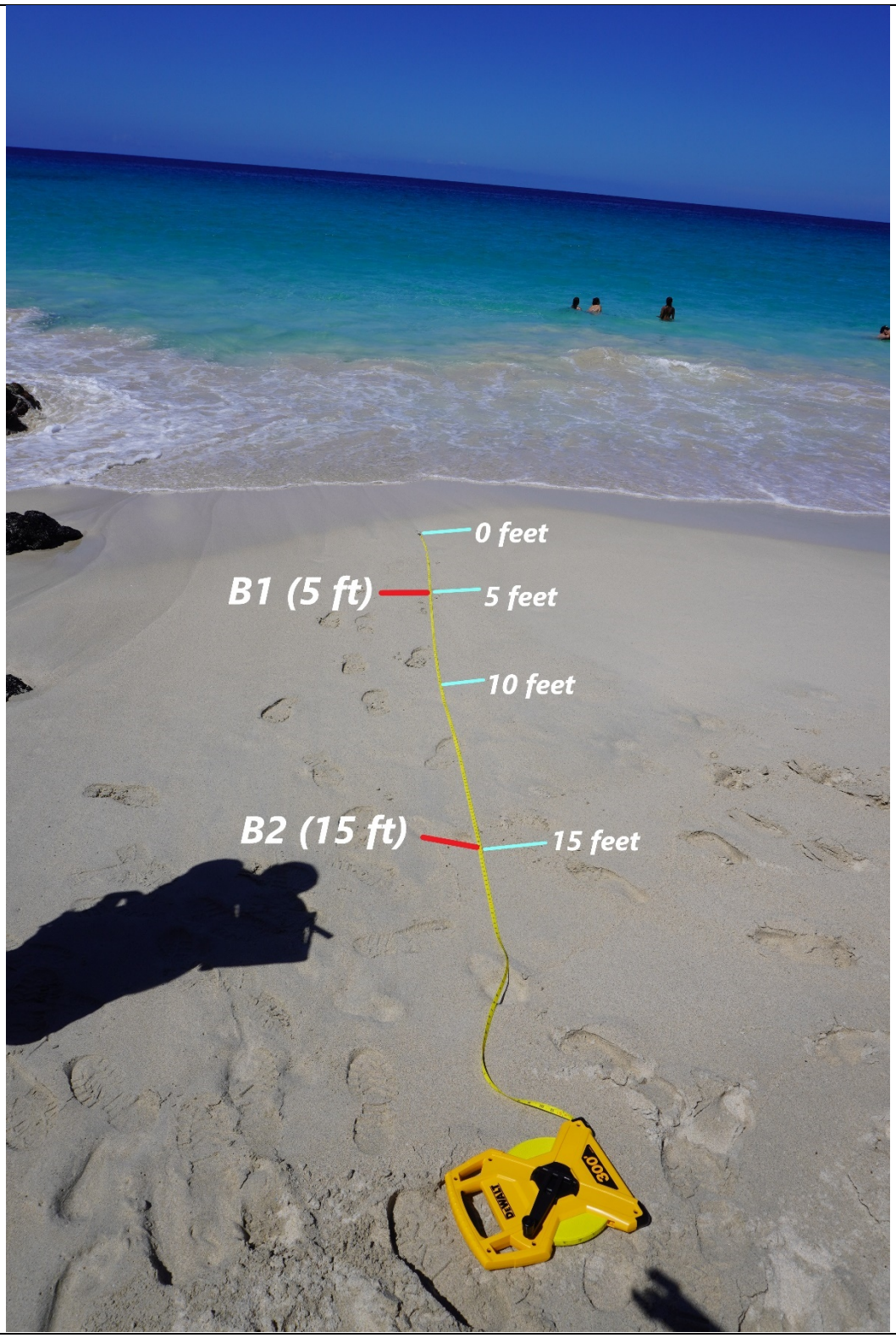

B.6.4: Manini'owali Beach Transect B photograph looking seaward, with annotated survey locations.

B-1

B-2

B.6.5: Manini'owali Beach Transect B survey site photographs with location labels. One inch is equal to 50 ticks (5 major scale units) on the laser-etched ruler.

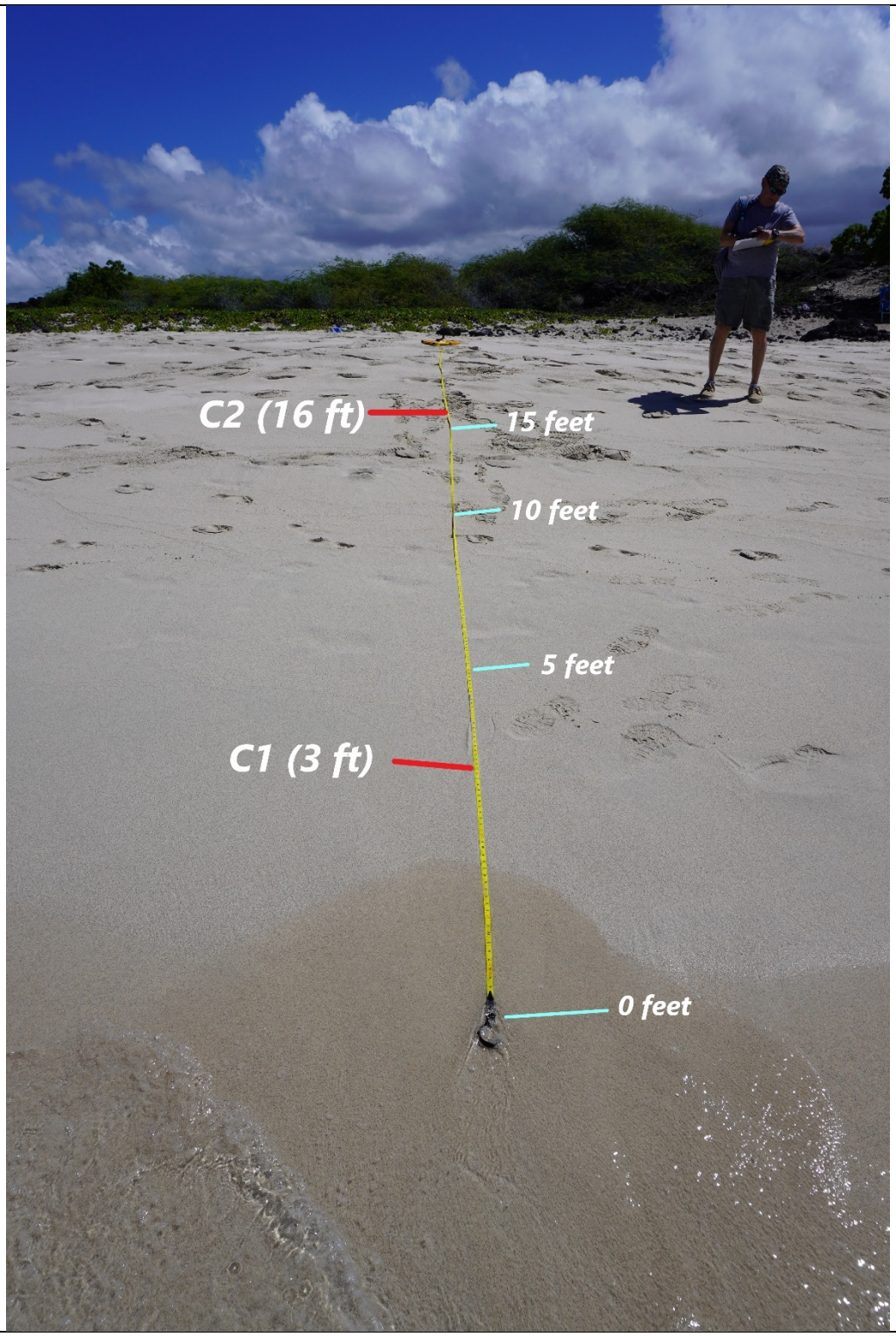

B.6.6: Manini'owali Beach Transect C looking landward, with annotated survey locations.

C-1

C-2

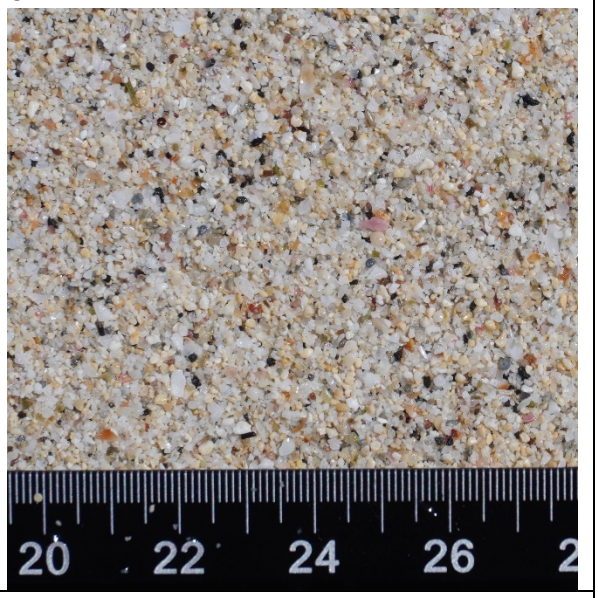

B.6.7: Manini'owali Beach Transect C survey sites with location labels. One inch is equal to 50 ticks (5 major scale units) on the laser-etched ruler.

B.7.1: Mahai'ula Beach overview photograph looking E.

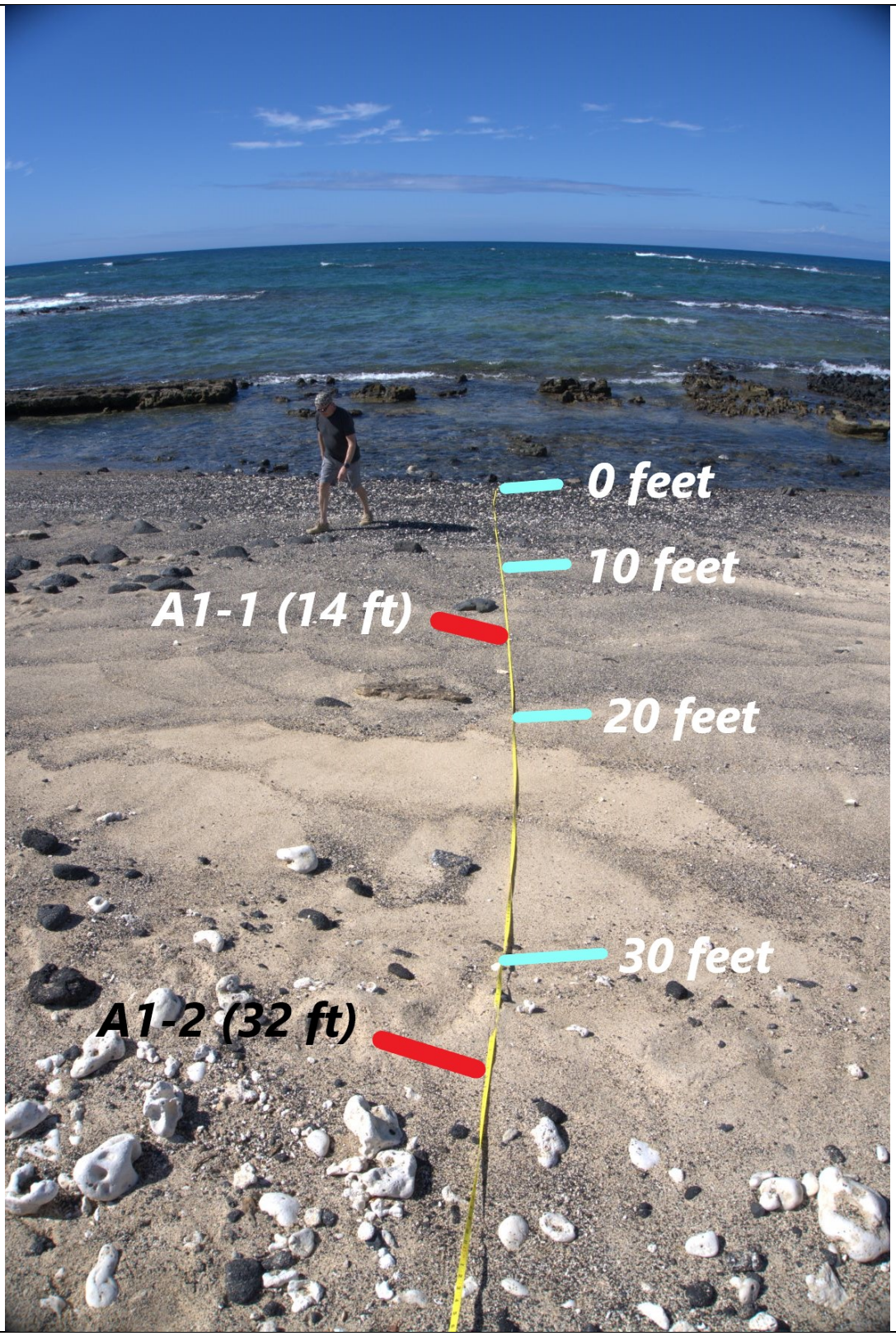

B.7.2: Mahai'ula Beach Transect A1 overview looking seaward, with annotated survey locations.

A1-1

A1-2

B.7.3: Mahai'ula Beach Transect A1 survey sites with location labels. One inch is equal to 50 ticks (5 major scale units) on the laser etched-ruler.

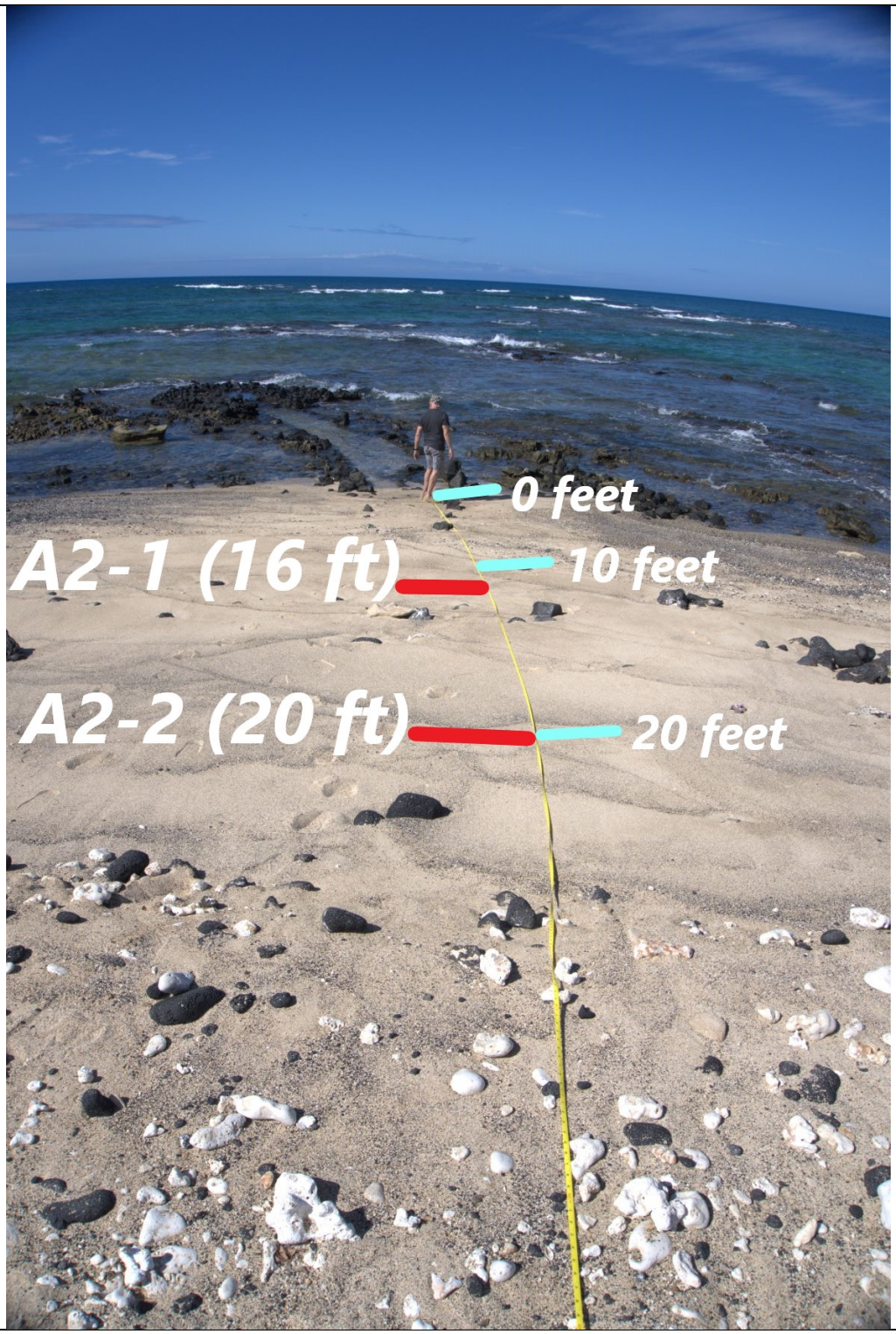

B.7.4: Mahai'ula Beach Transect A2 looking seaward, with annotated survey locations.

A2-1

A2-2

B.7.5: Mahai'ula Beach Transect A2 survey site photographs with location labels. One inch is equal to 50 ticks (5 major scale units) on the laser-etched ruler.

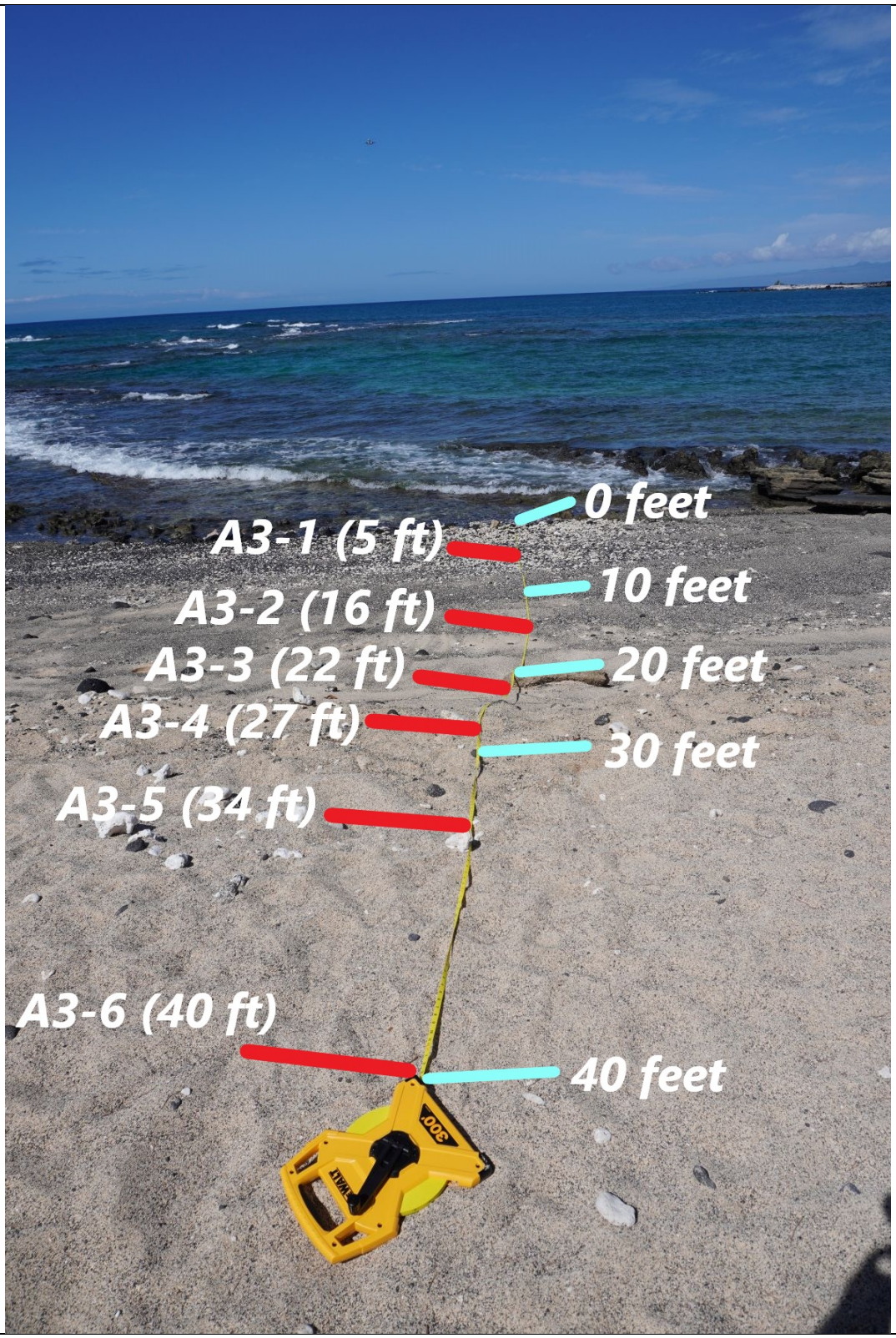

B.7.6: Mahai'ula Beach Transect A3 looking seaward, with annotated survey locations.


22 24 26 28 30 32 34 36 38 40 42 44 46 48 50


24 26 28 30 32 34 36 38 40 42 44 46


28 30 32 34 36 38 40 42 44 46 48 50


28 30 32 34 36 38 40 42 44 46 48 50

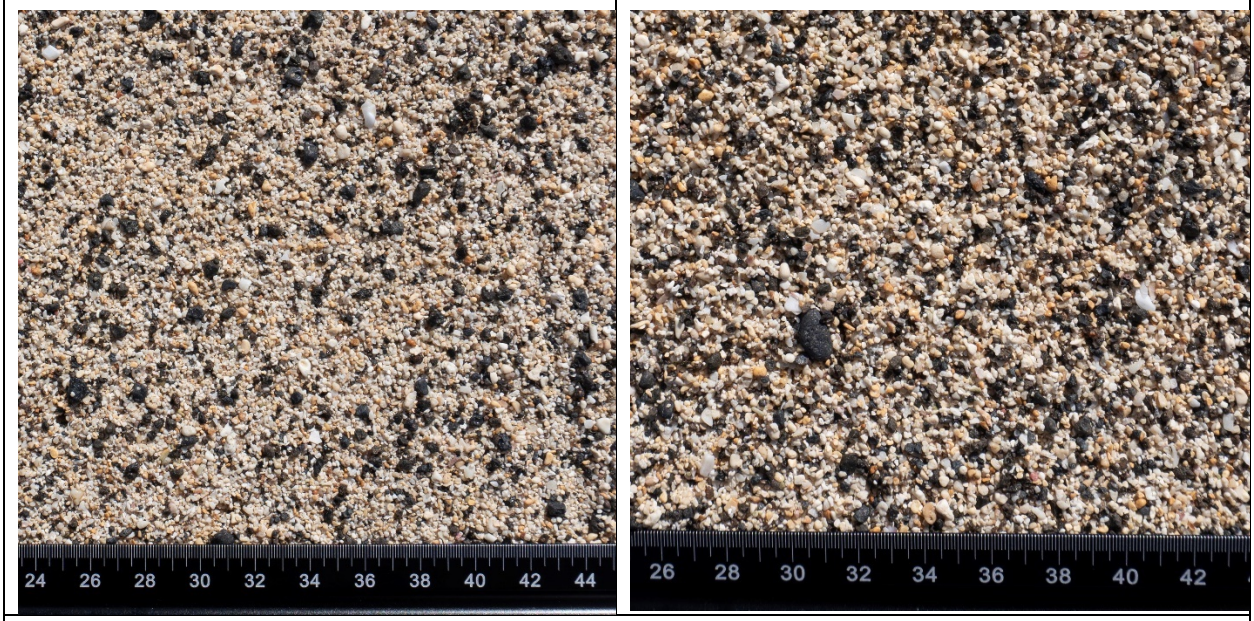

B.7.7: Mahai'ula Beach Transect A3 survey site photographs with location labels. One inch is equal to 50 ticks (5 major scale units) on the laser-etched ruler.

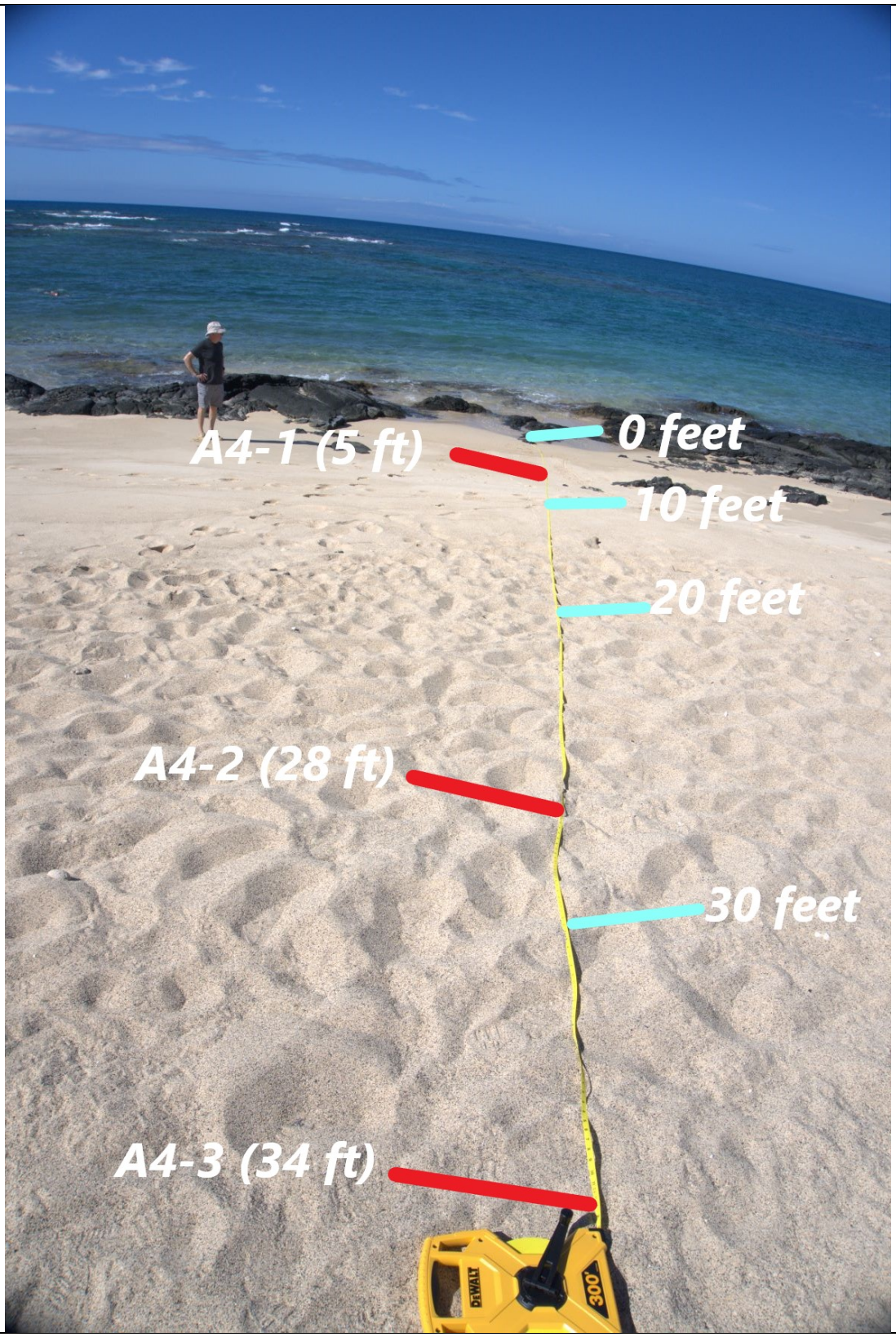

B.7.8: Mahai'ula Beach Transect A4 looking beachward, with annotated survey locations.

A4-1

A4-2

A4-3

B.7.9: Mahai'ula Beach Transect A4 survey site photographs with location labels. One inch is equal to 50 ticks (5 major scale units) on the laser-etched ruler.

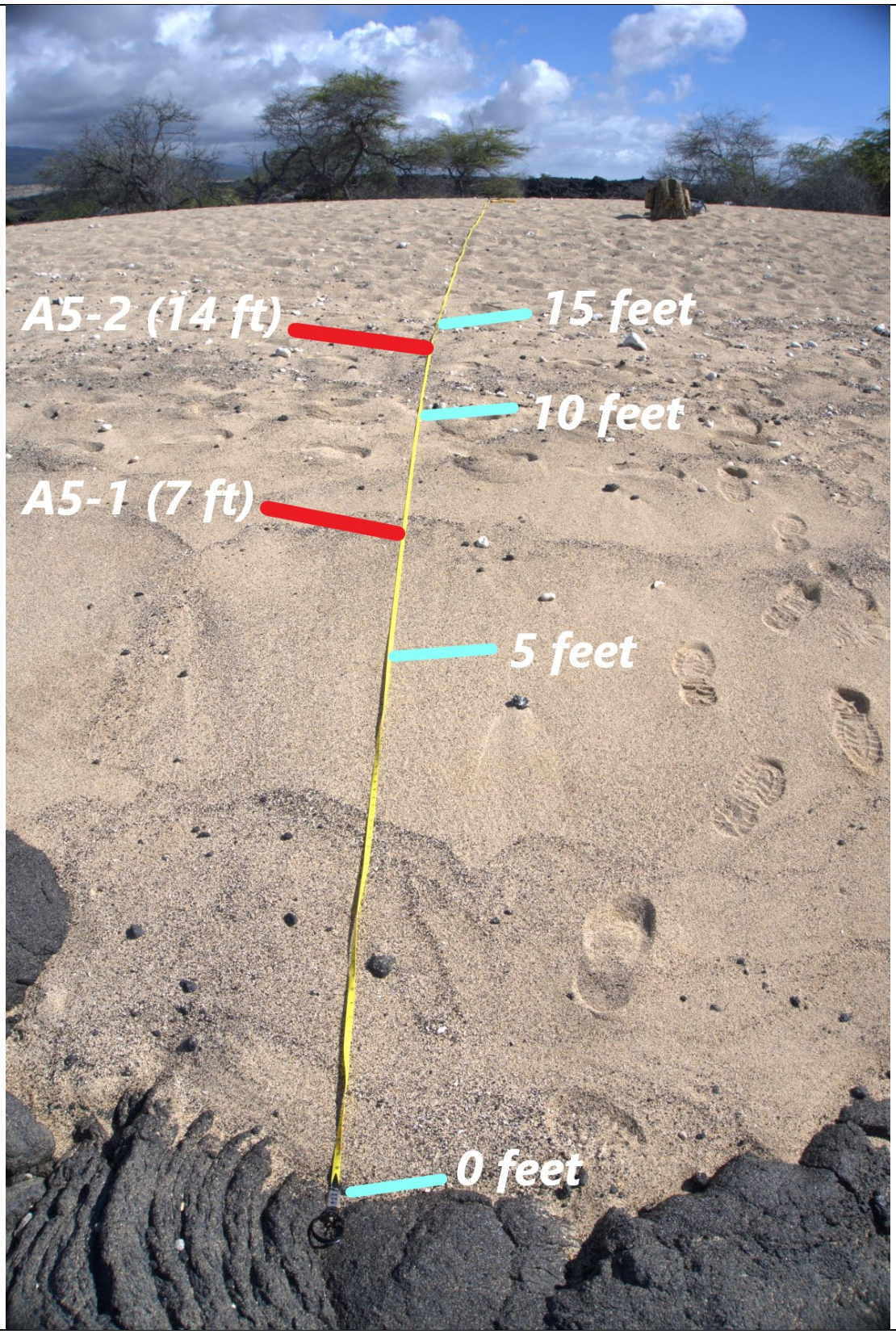

B.7.10: Mahai'ula Beach Transect A5 looking landward with annotated survey locations.

A5-1

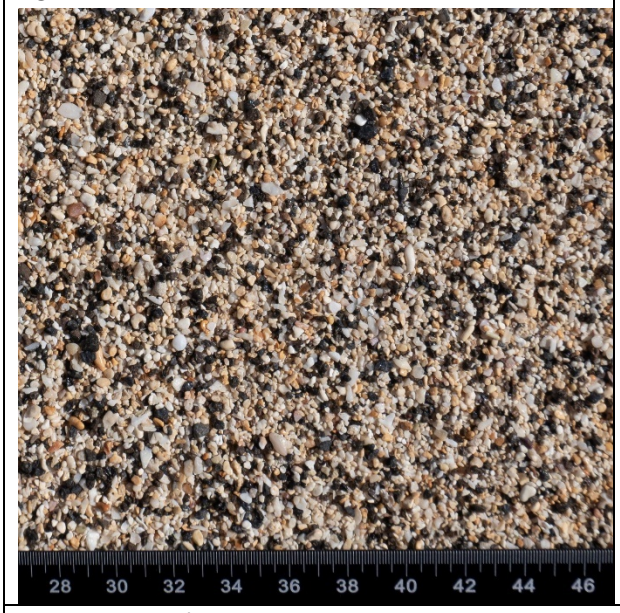

A5-2

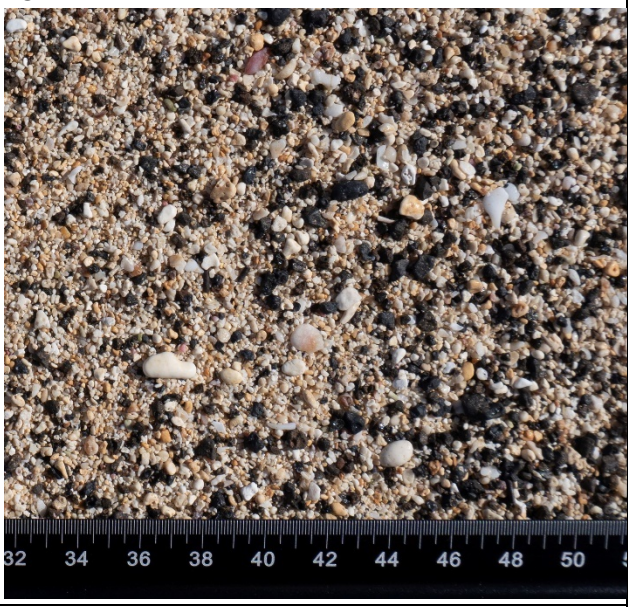

B.7.11: Mahai'ula Beach Transect A5 survey sites photographs with location labels. One inch is equal to 50 ticks (5 major scale units) on the laser-etched ruler.

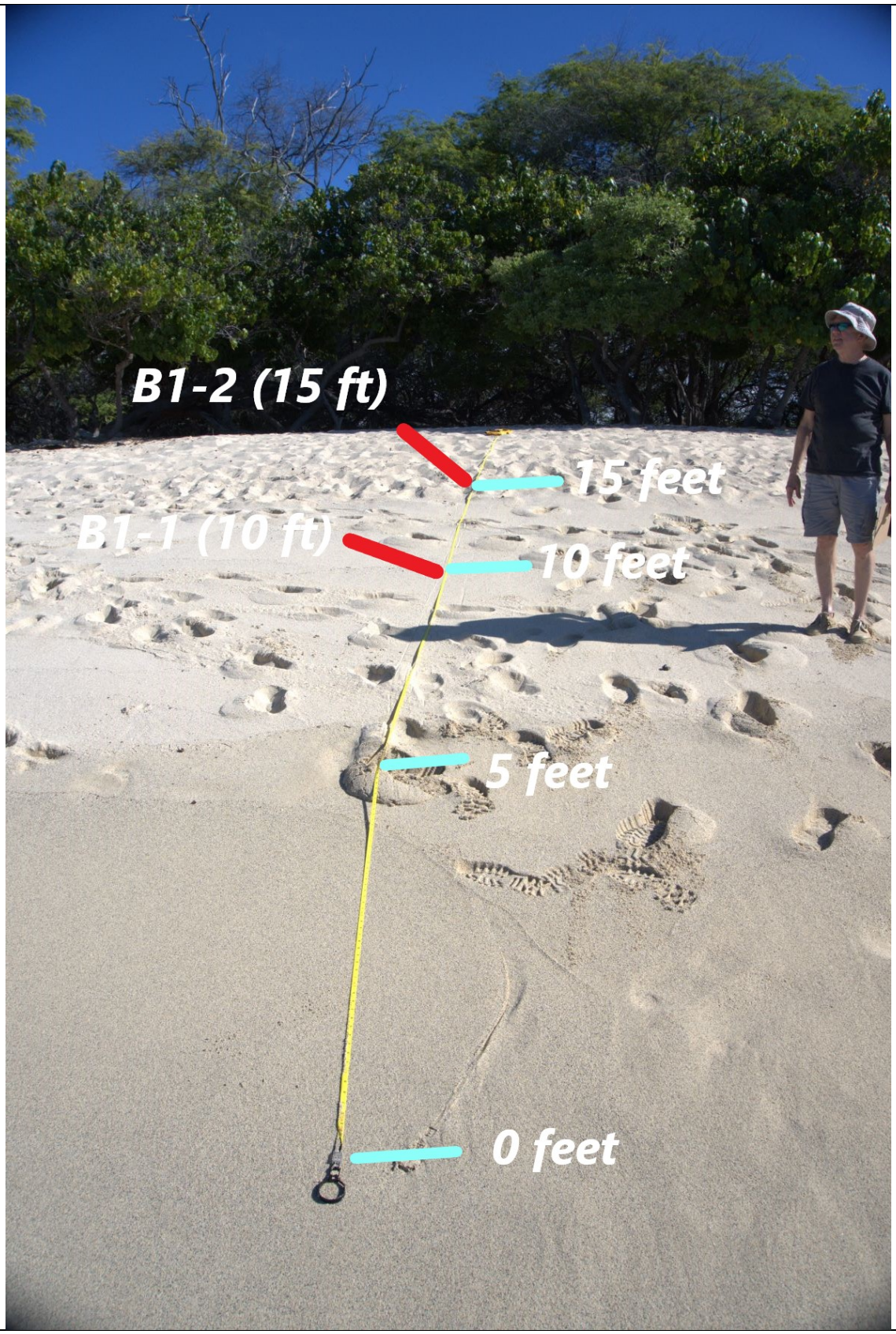

B.7.12: Mahai'ula Beach Transect B1 overview looking landward with annotated survey locations.

B1-1

B1-2

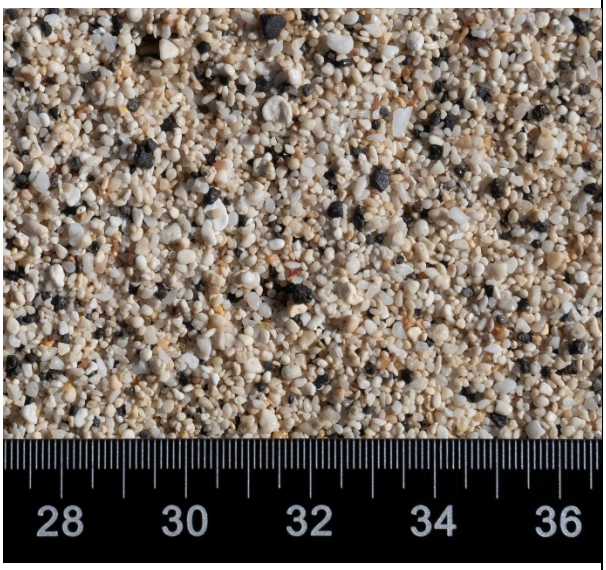

B.7.13: Mahai'ula Beach Transect B1 survey site photographs with location labels. One inch is equal to 50 ticks (5 major scale units) on the laser-etched ruler.

B.8.1: Old Kona Airport Beach overview photograph looking NW.

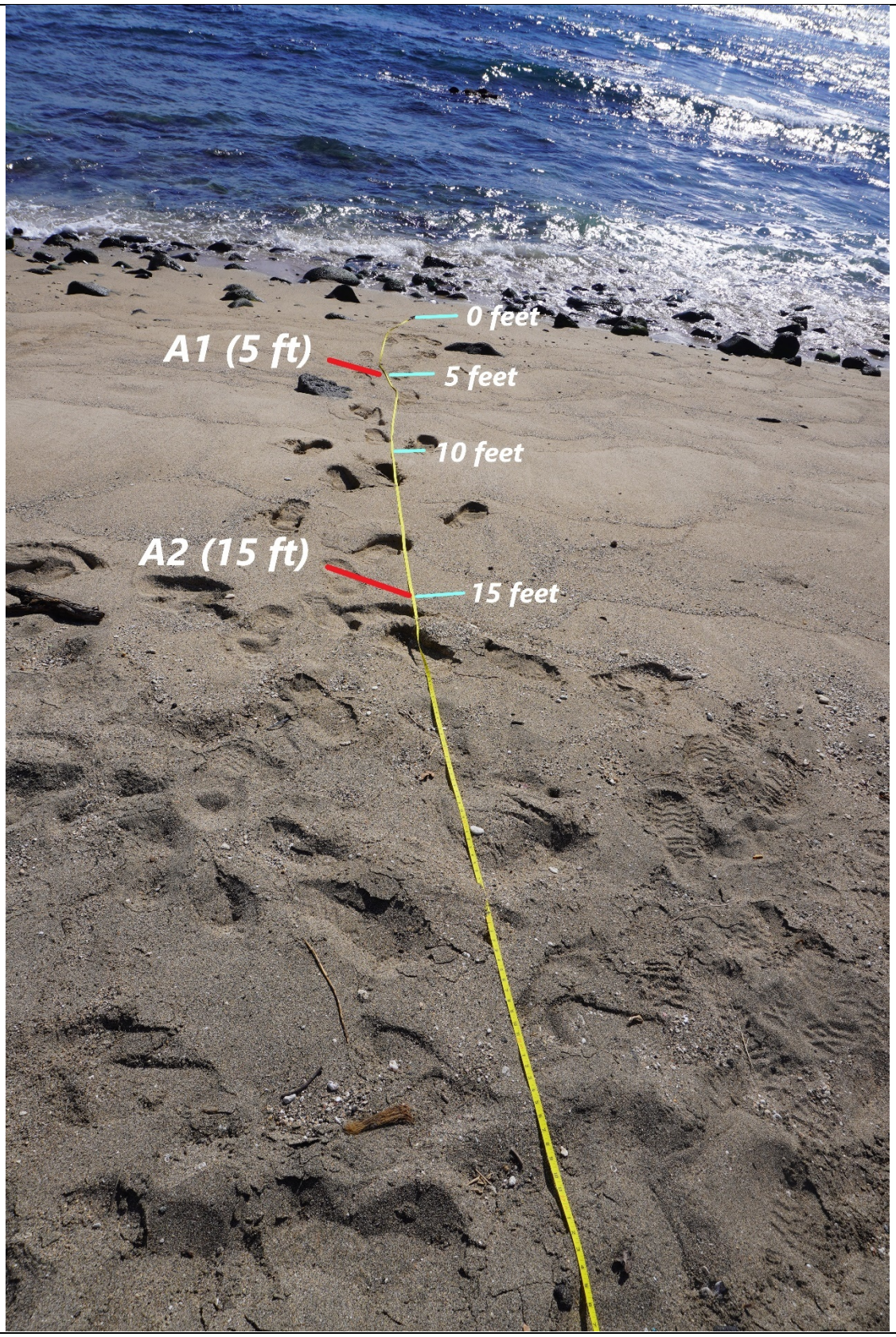

B.8.2: Old Kona Airport Beach Transect A looking seaward with annotated survey locations.

A-1

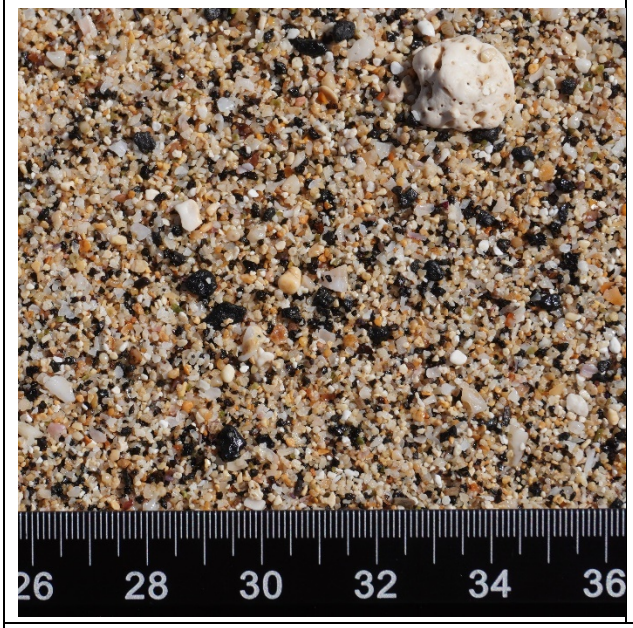

A-2

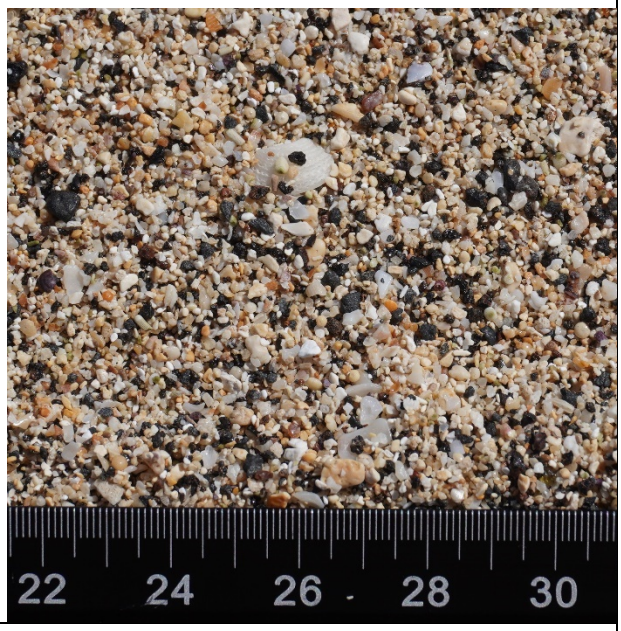

B.8.3: Old Kona Airport Beach Transect A survey sites and location labels. One inch is equal to 50 ticks (5 major scale units) on the laser-etched ruler.

B.9.1: Pahoehoe Beach Park overview photo looking S.

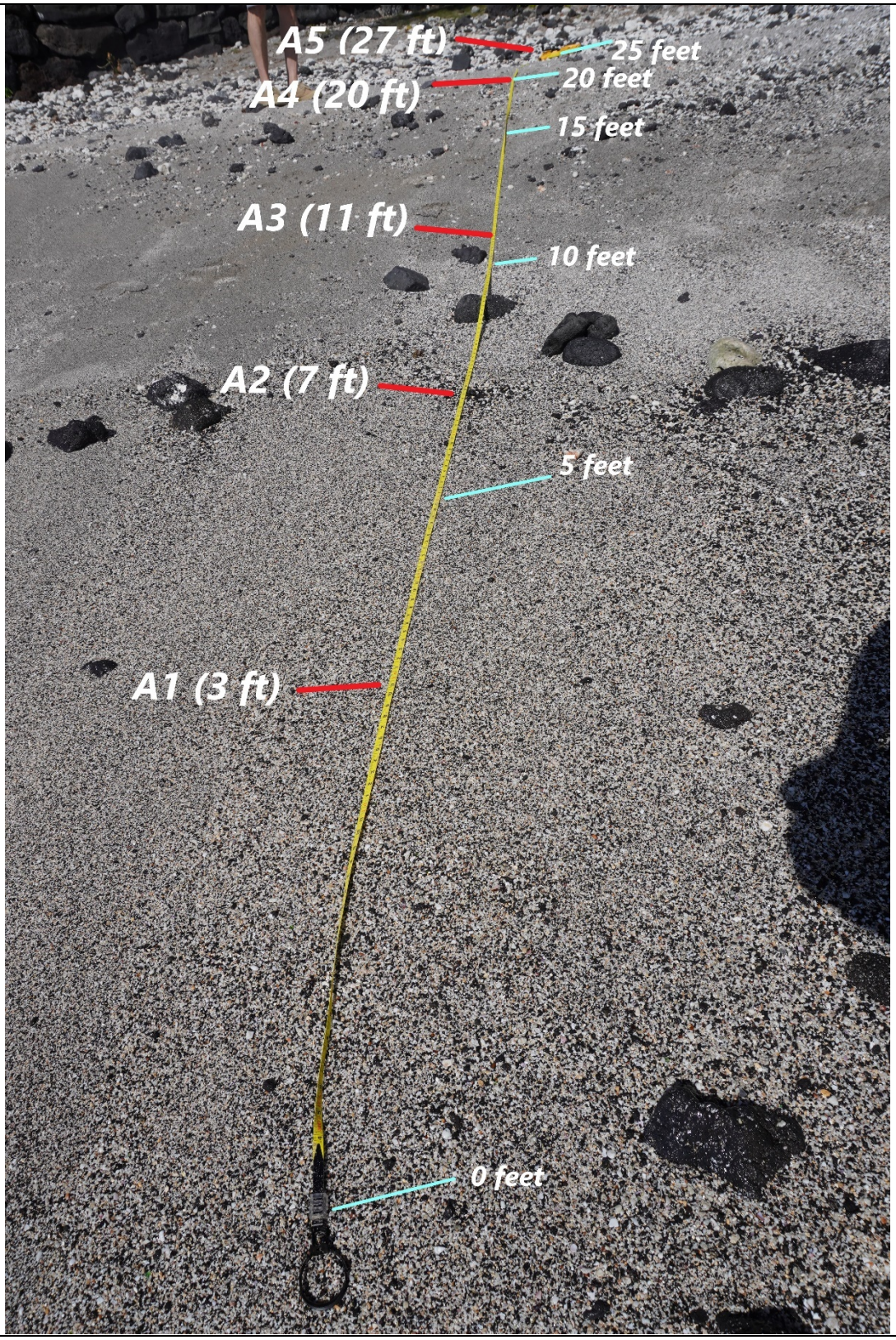

B.9.2: Pahoehoe Beach Park Transect A looking landward with annotated survey locations.


22
24
26
28
30


26
28
30
32

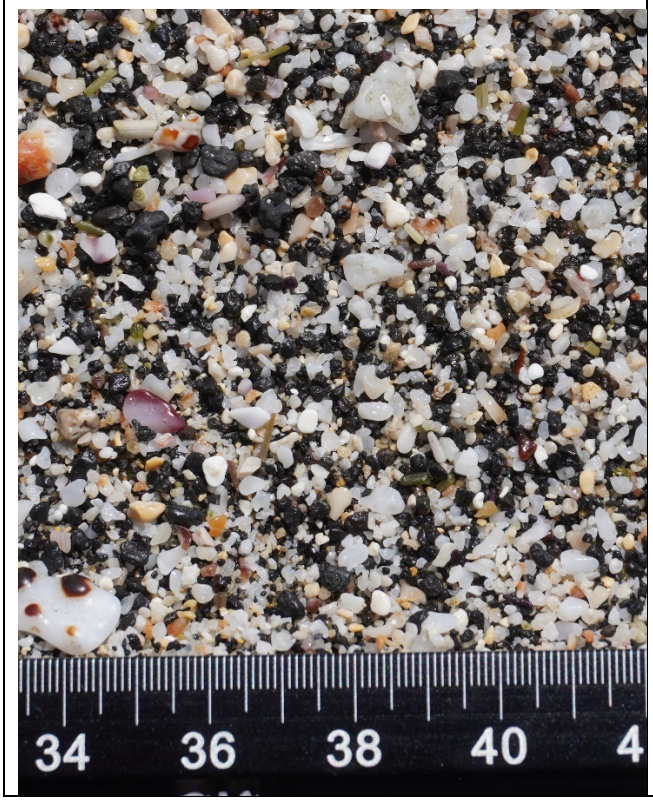
34
36
38
40


14
16
18
20

A-5

B.9.3: Pahoehoe Beach Park Transect A survey site photographs with location labels. One inch is equal to 50 ticks (5 major scale units) on the laser-etched ruler.

B.10.1: Magic Sands Beach overview looking S.

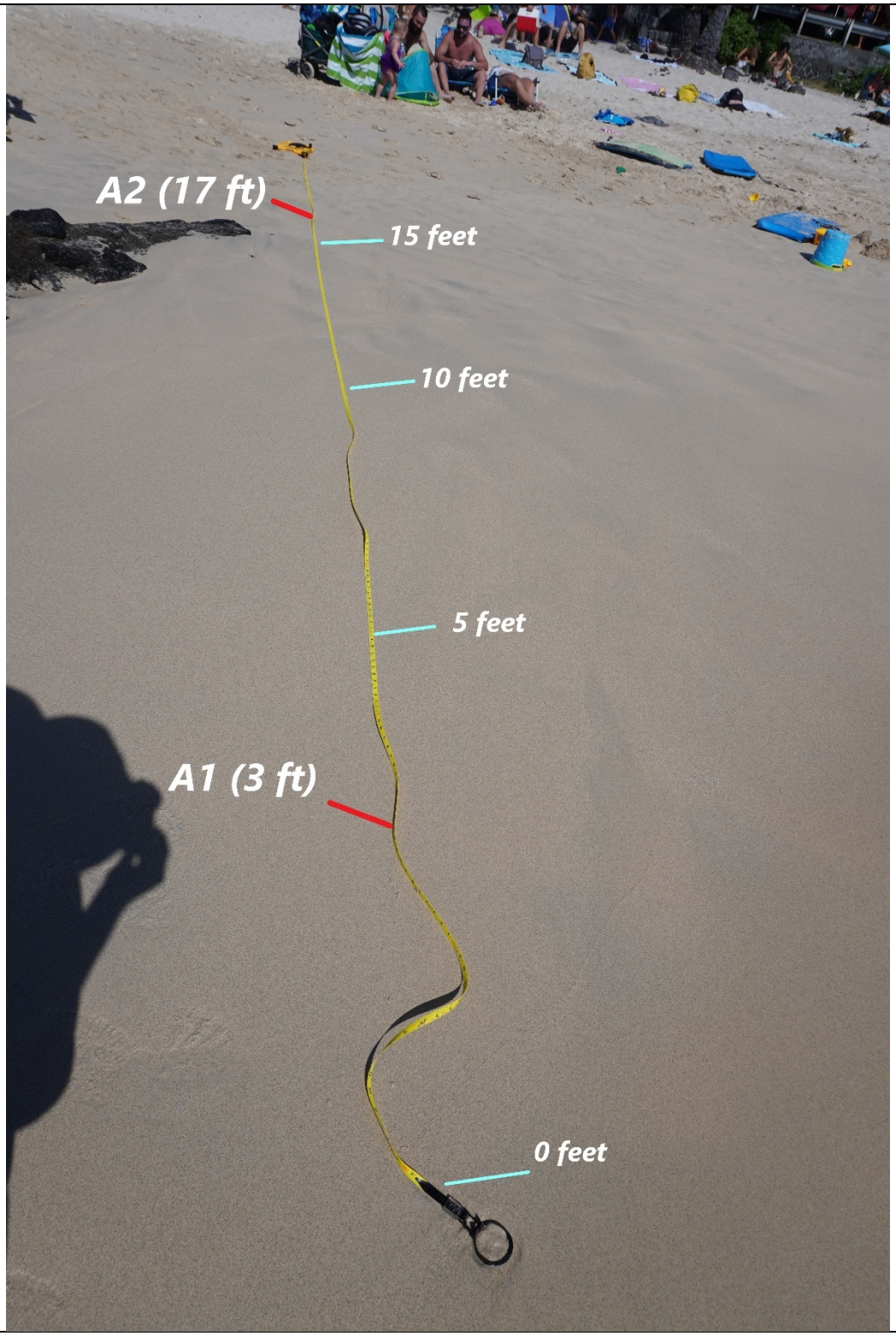

B.10.2: Magic Sands Beach Transect A overview looking landward with annotated survey locations.

A-1

A-2

B.10.3: Magic Sands Beach Transect A survey site photographs with location labels. One inch is equal to 50 ticks (5 major scale units) on the laser-etched ruler.

B.11.1: Kahalu'u Beach overview looking N.

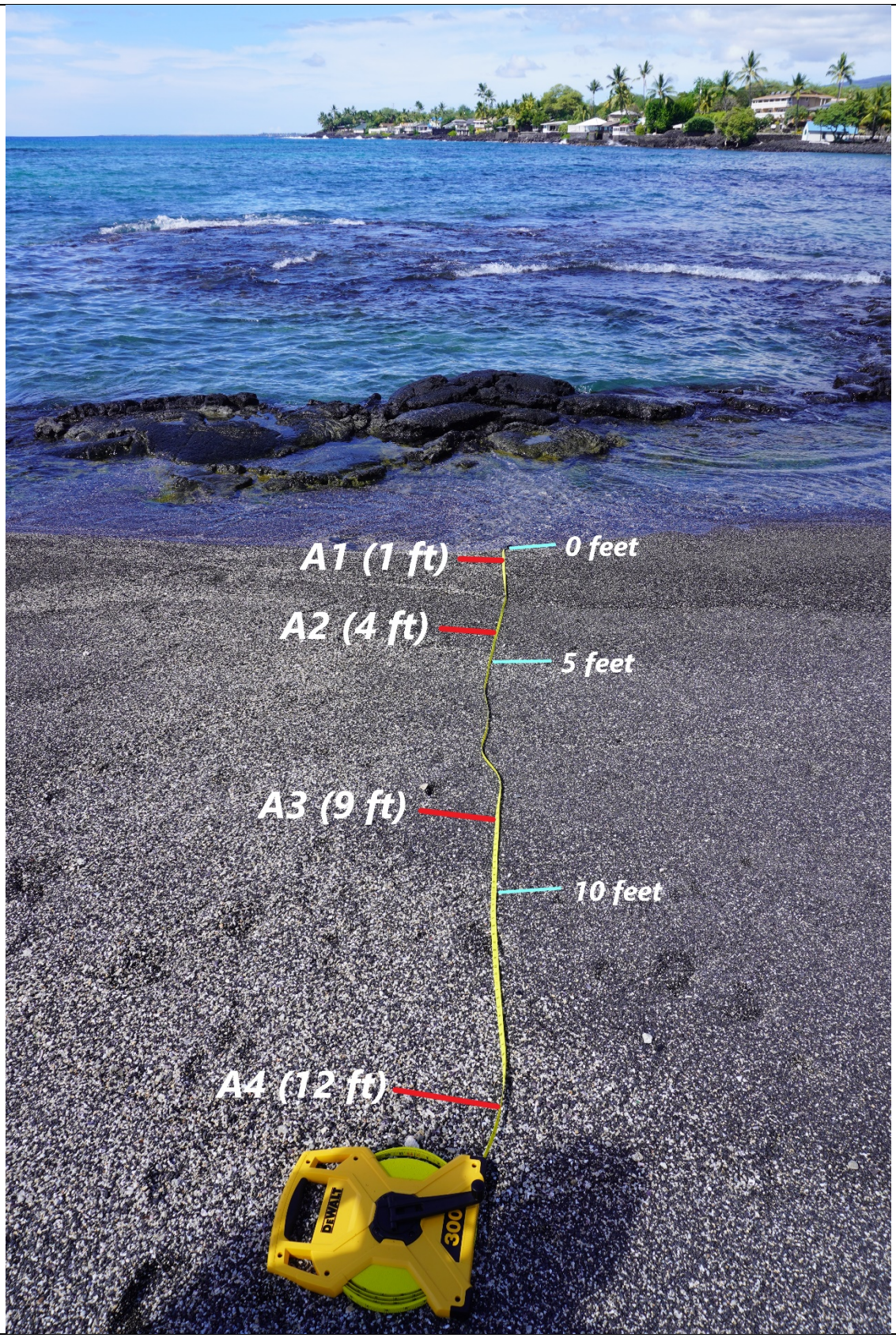

B.11.2: Kahalu'u Beach Transect A overview looking seaward with annotated survey locations.

A-1

A-2

A-3

A-4

B.11.3: Kahalu'u Beach Transect A survey site photographs with location labels. One inch is equal to 50 ticks (5 major scale units) on the laser-etched ruler.

B.12.1: Ho’okena Beach overview looking SE.

B.12.2: Ho’okena Beach Transect A overview looking seaward.

A-1

A-2

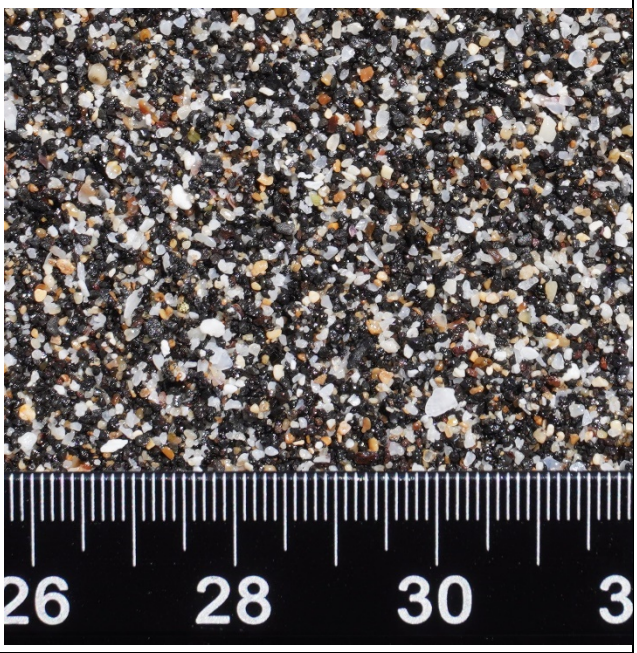

A-3

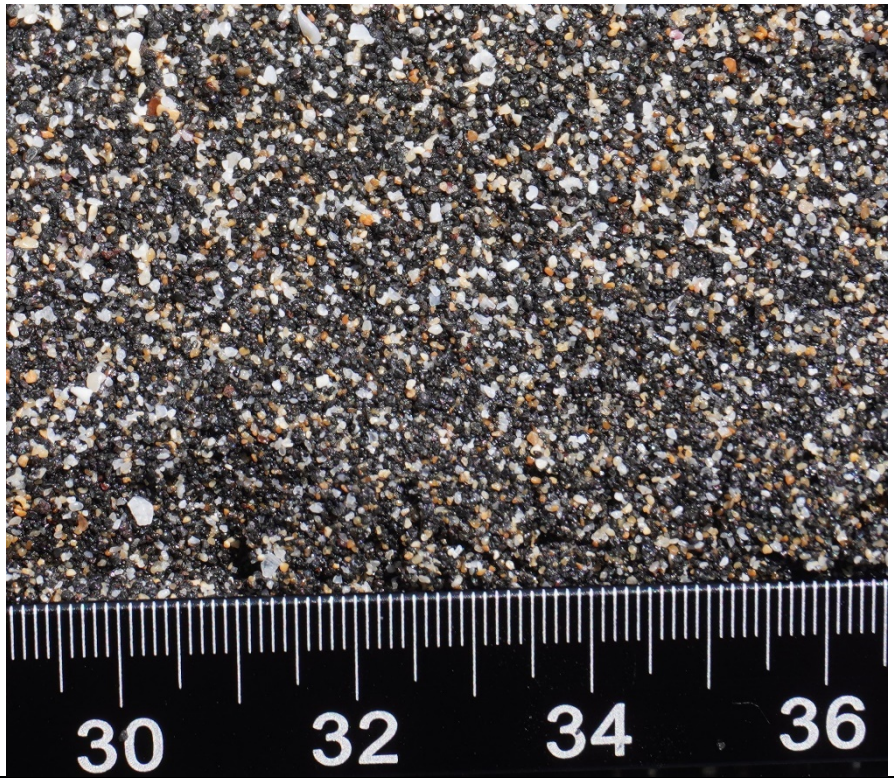

B.12.3: Ho'okena Beach Transect A survey site photographs with location labels. One inch is equal to 50 ticks (5 major scale units) on the laser-etched ruler.

B.13.1: Pebble Beach overview looking S.

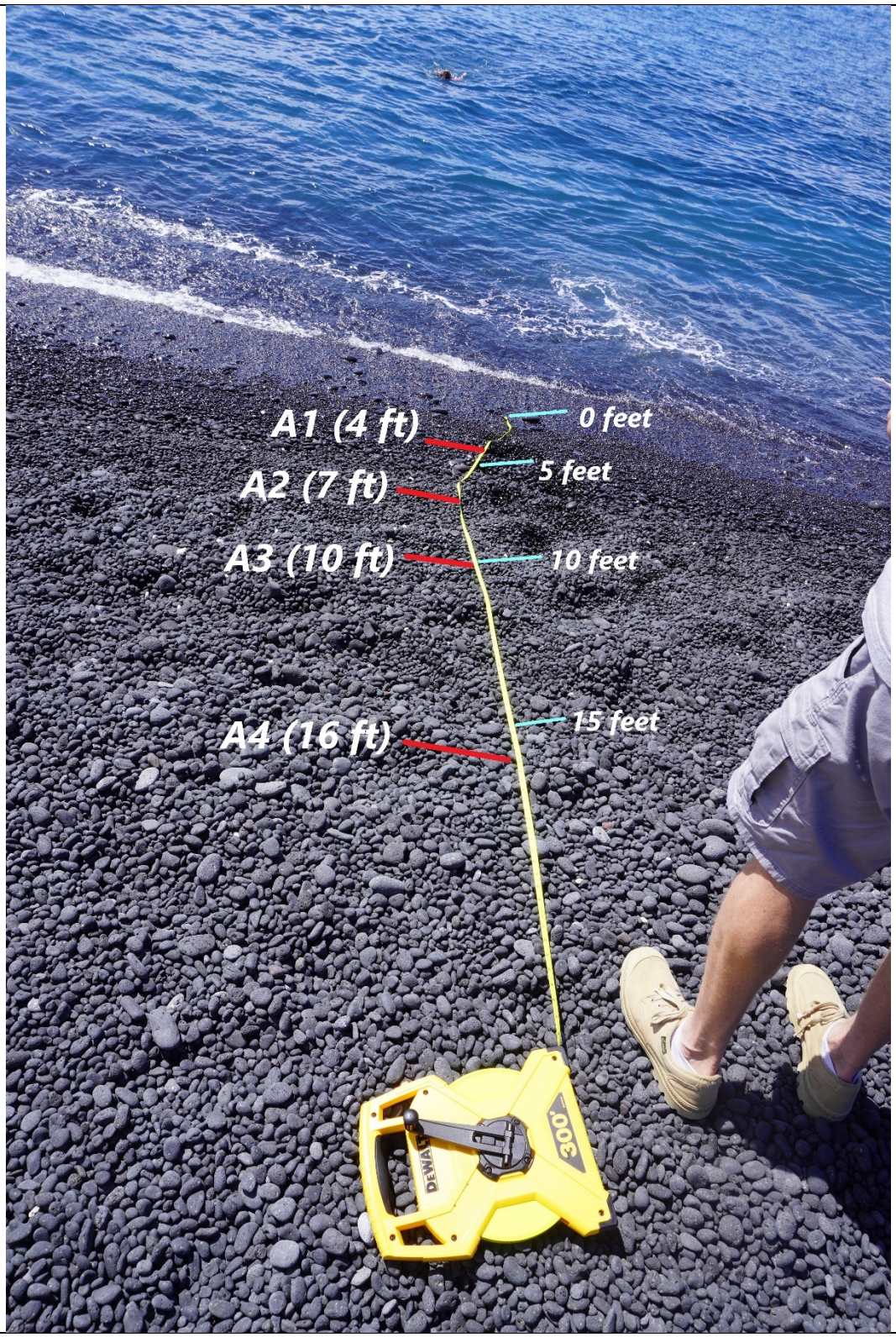

B.13.2: Pebble Beach Transect A overview looking seaward with annotated survey locations.

A-1

A-2

A-3

A-4

B.13.3: Pebble Beach Transect A survey site photographs with location labels. One inch is equal to 50 ticks (5 major scale units) on the laser-etched ruler.

B.14.1: Miloli'I Beach Overview looking NW.

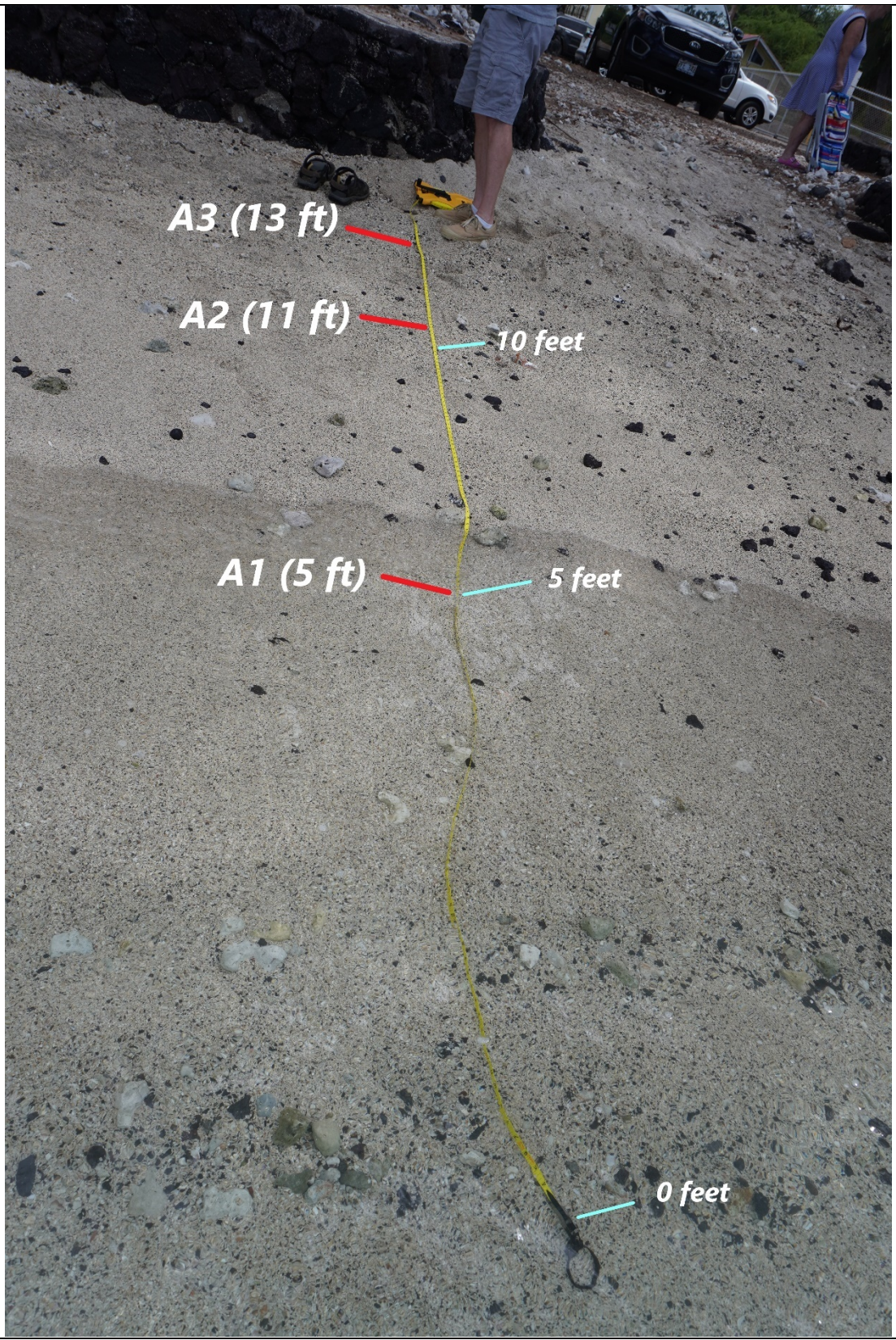

B.14.2: Miloli'I Beach Transect A looking landward with annotated survey locations.

A-1

A-2

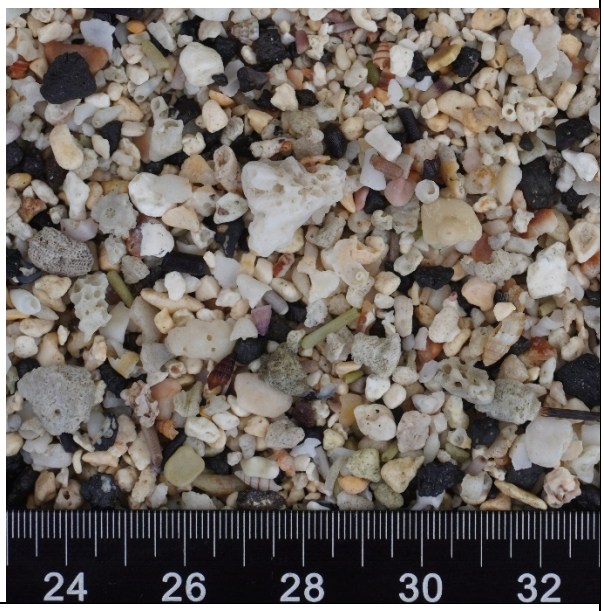

A-3

B.14.3: Miloli'I Beach Transect A survey site photographs with location labels. One inch is equal to 50 ticks (5 major scale units) on the laser-etched ruler.

B.15.1: Green Sand Beach overview looking S.

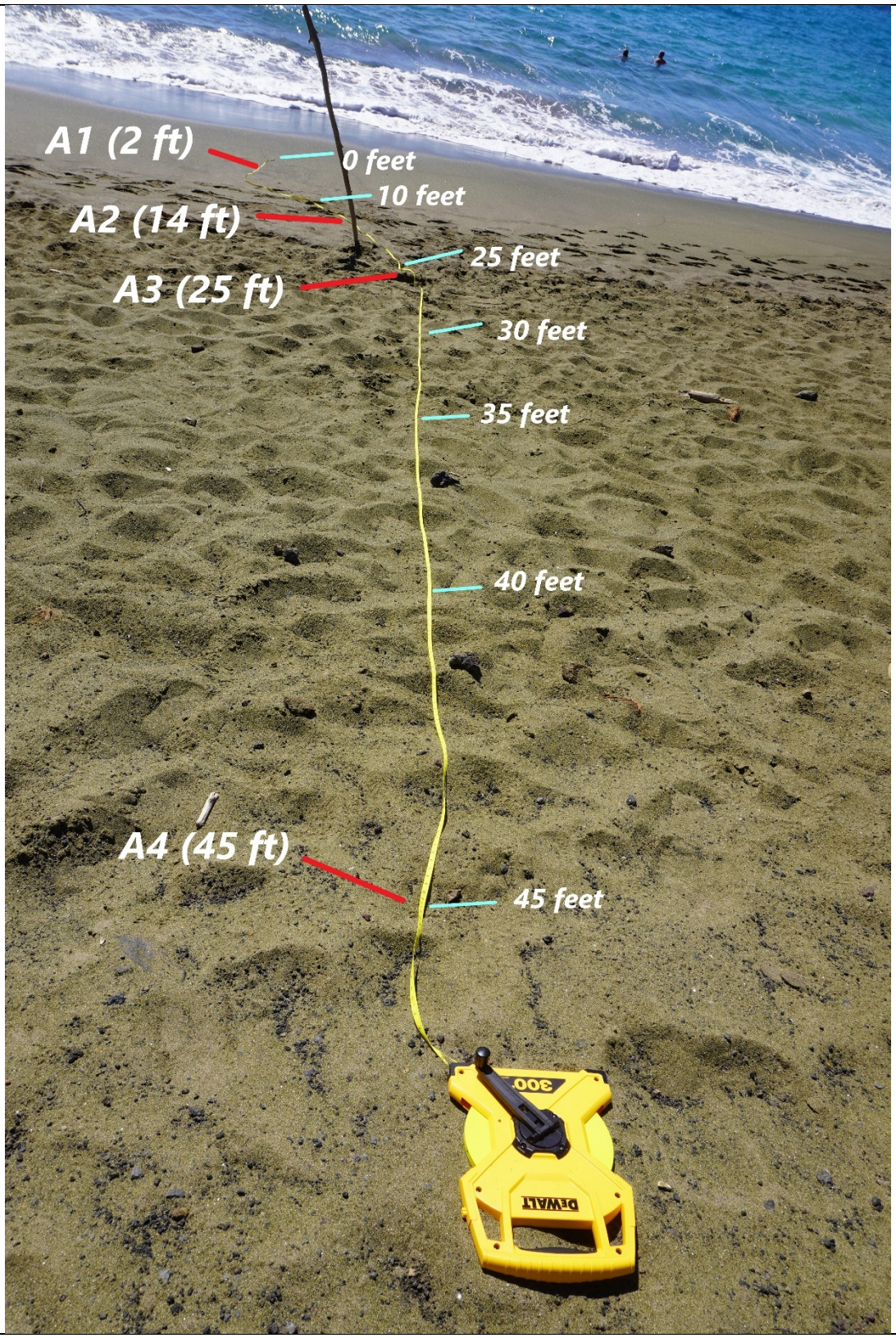

B.15.2: Green Sand Beach Transect A overview looking seaward with annotated survey locations.

A-1

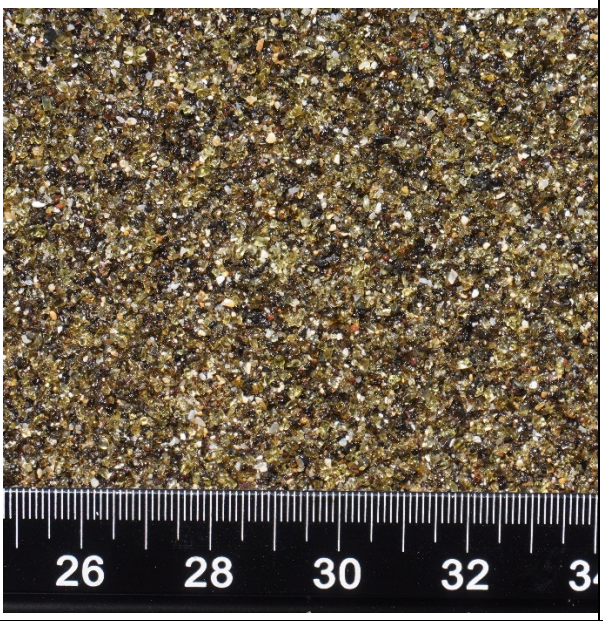

A-2

A-3

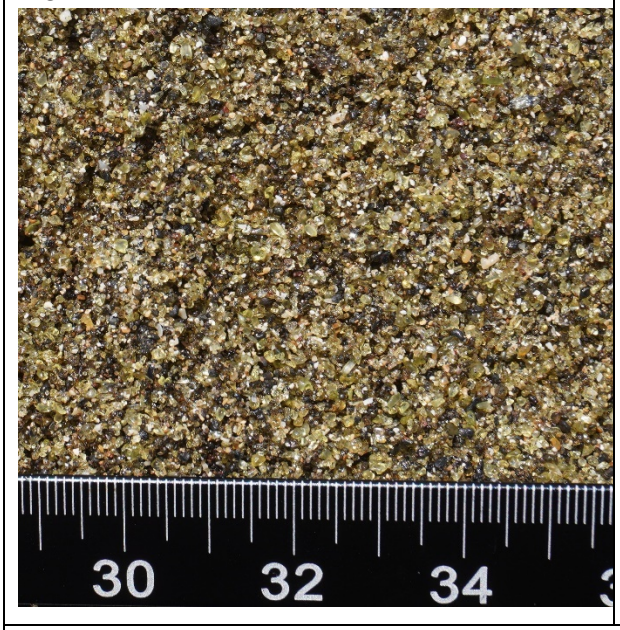

A-4

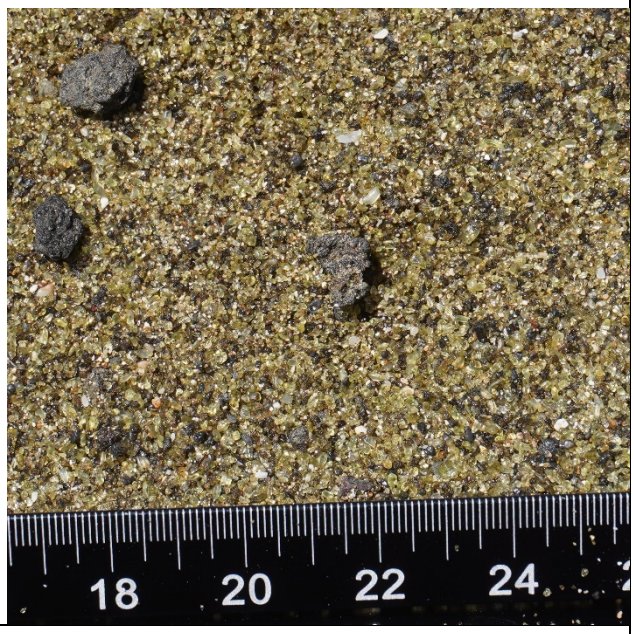

B.15.3: Green Sand Beach Transect A survey site photographs with location labels. One inch is equal to 50 ticks (5 major scale units) on the laser-etched ruler.

B.16.1: Punalu’u Beach overview looking SW from the NE corner.

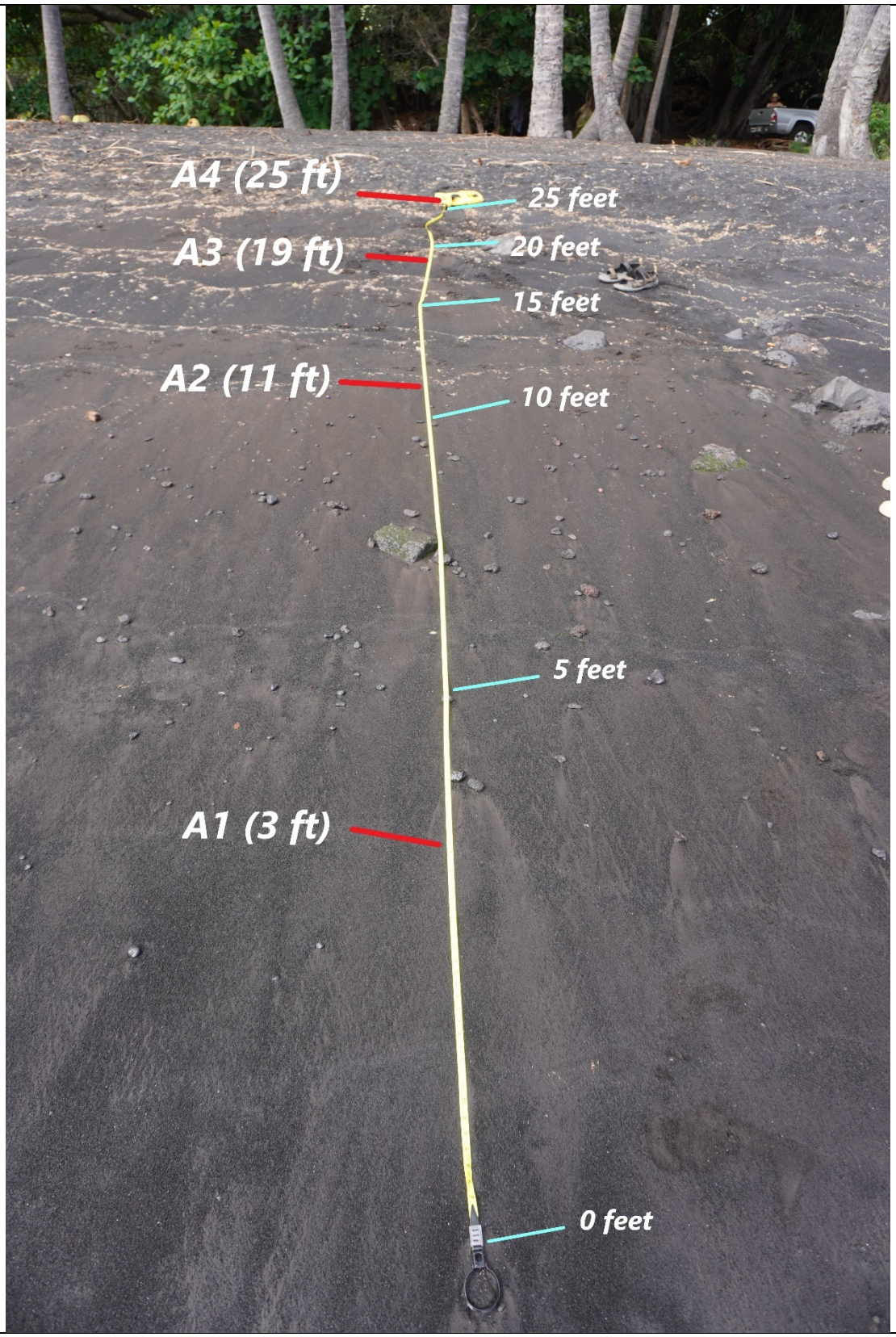

B.16.2: Punalu'u Beach Transect A overview looking landward with annotated survey locations.

A-1

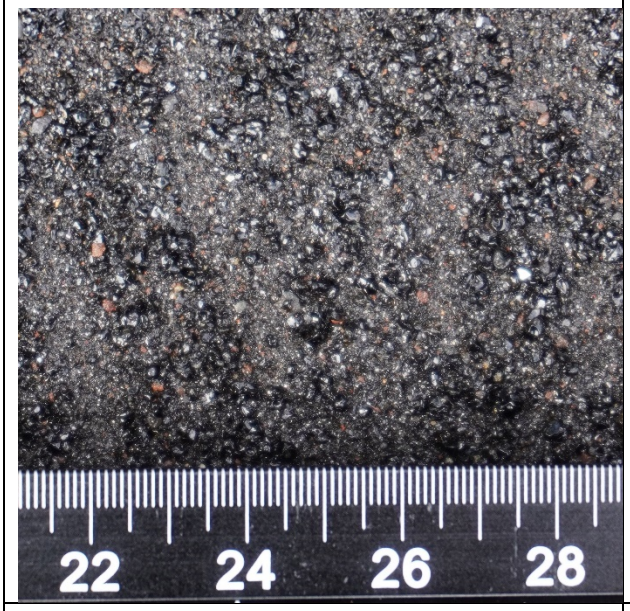

A-2

A-3

A-4

B.16.3: Punalu'u Beach Transect A survey site photographs with location labels. One inch is equal to 50 ticks (5 major scale units) on the laser-etched ruler.

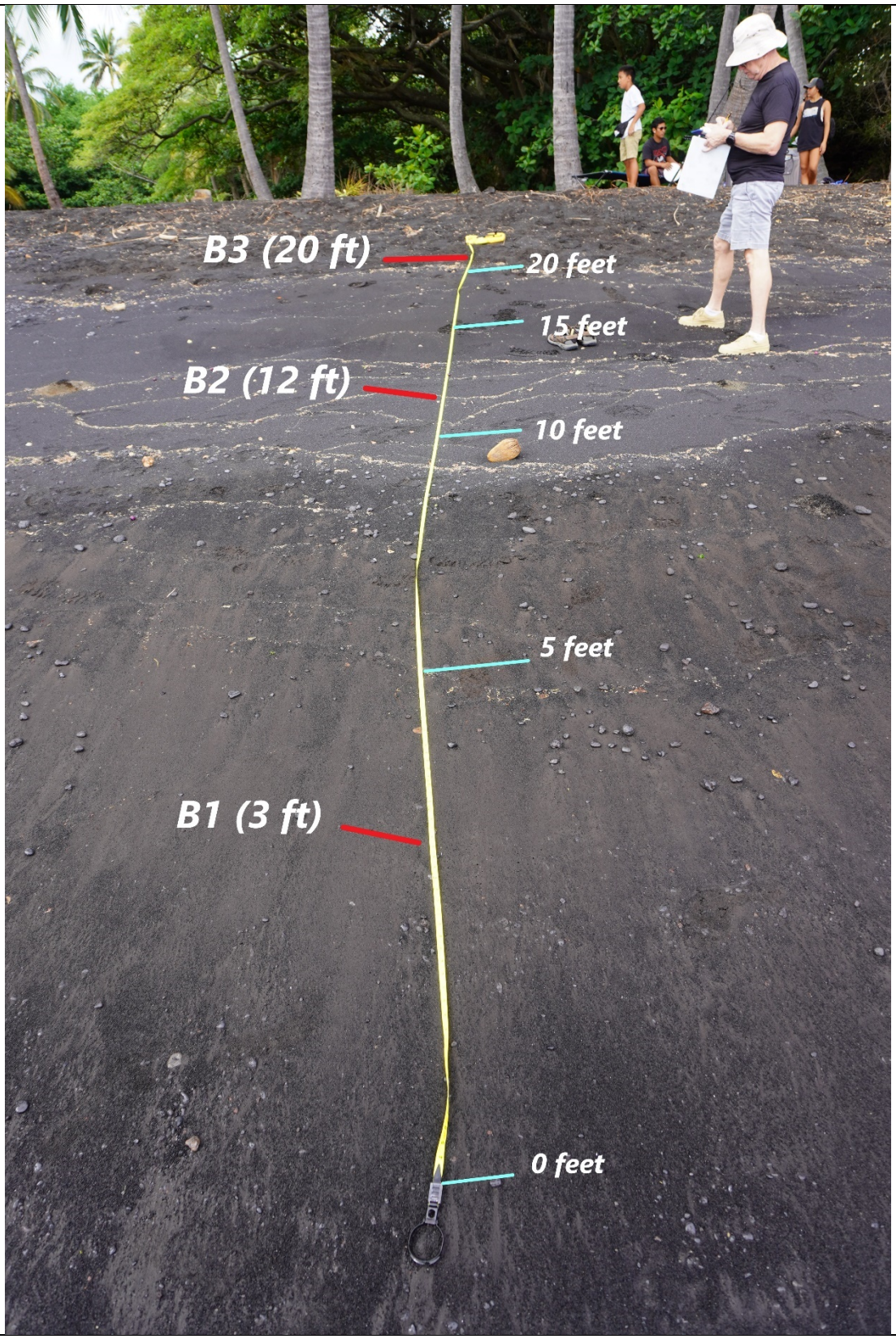

B.16.4: Punalu’u Beach Transect B overview looking landward with annotated survey locations.

B-1

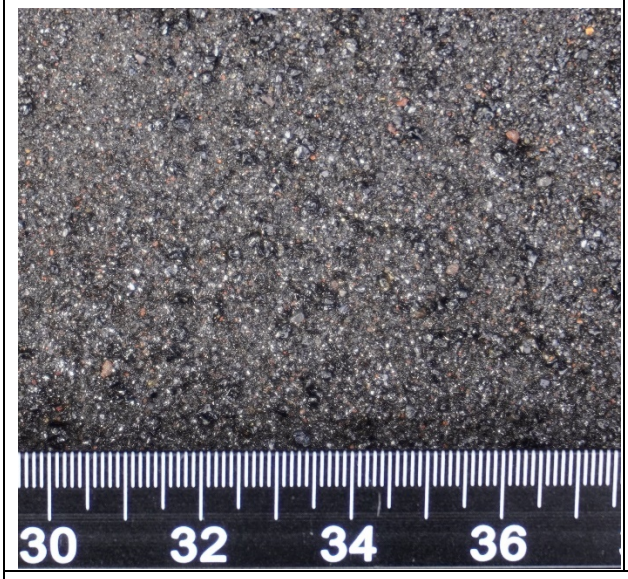

B-2

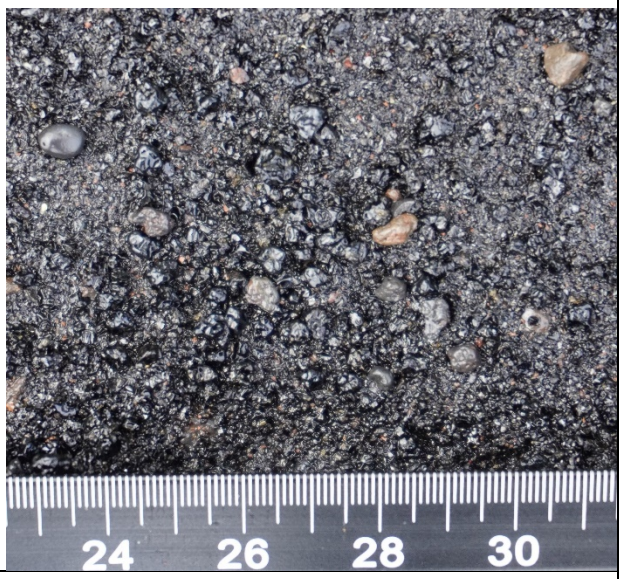

B-3

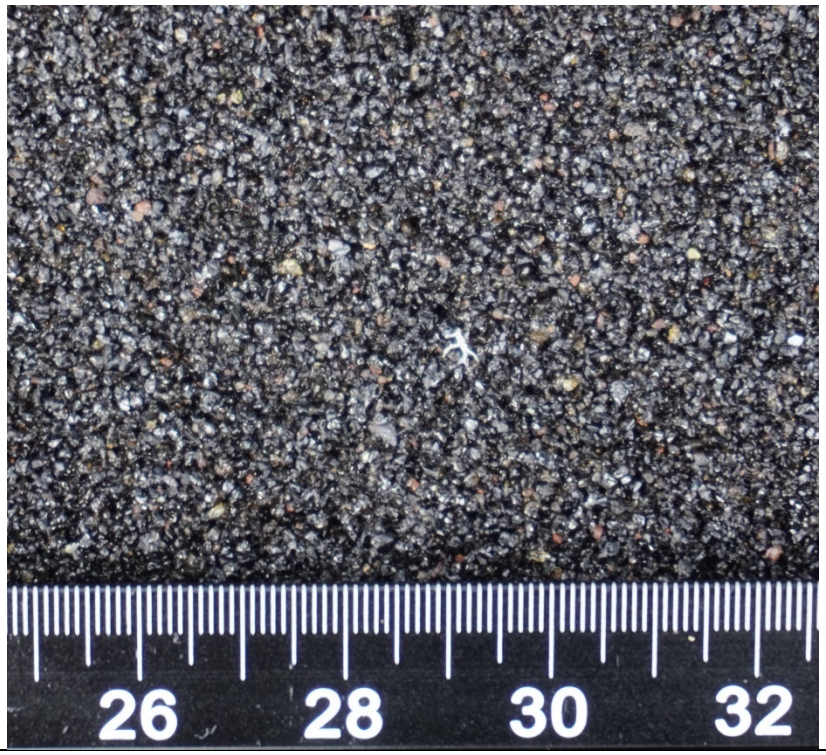

B.16.5: Punalu'u Beach Transect B survey site photographs with location labels. One inch is equal to 50 ticks (5 major scale units) on the laser-etched ruler.

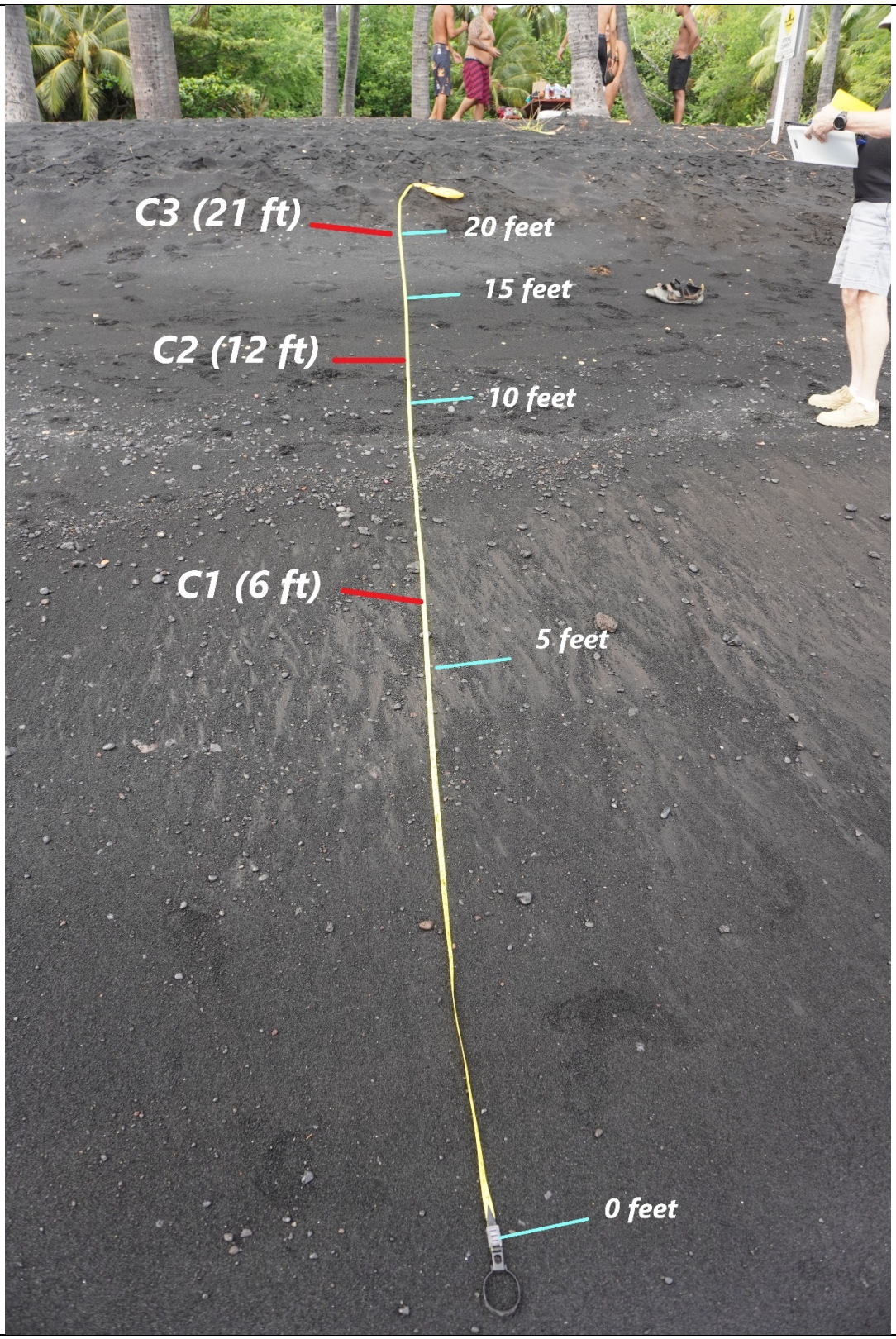

B.16.6: Punalu'u Beach Transect C overview looking landward with annotated survey locations.

C-1

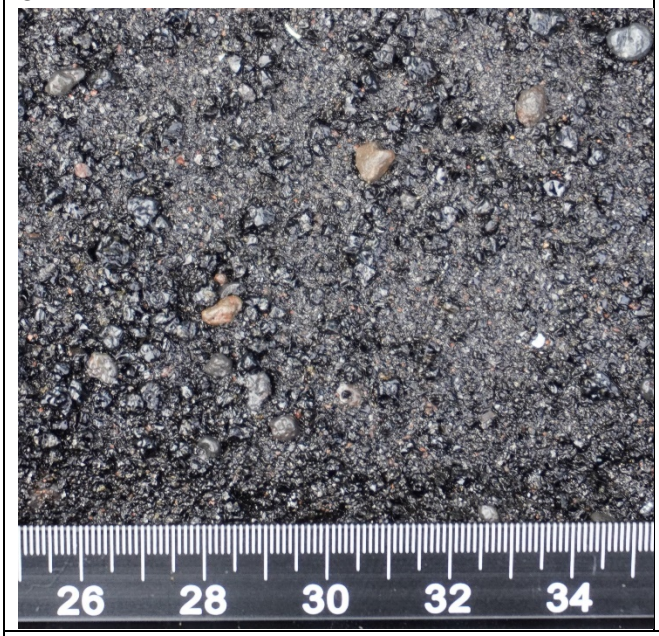

C-2

C-3

B.16.7: Punalu'u Beach Transect C survey site photographs with location labels. One inch is equal to 50 ticks (5 major scale units) on the laser-etched ruler.

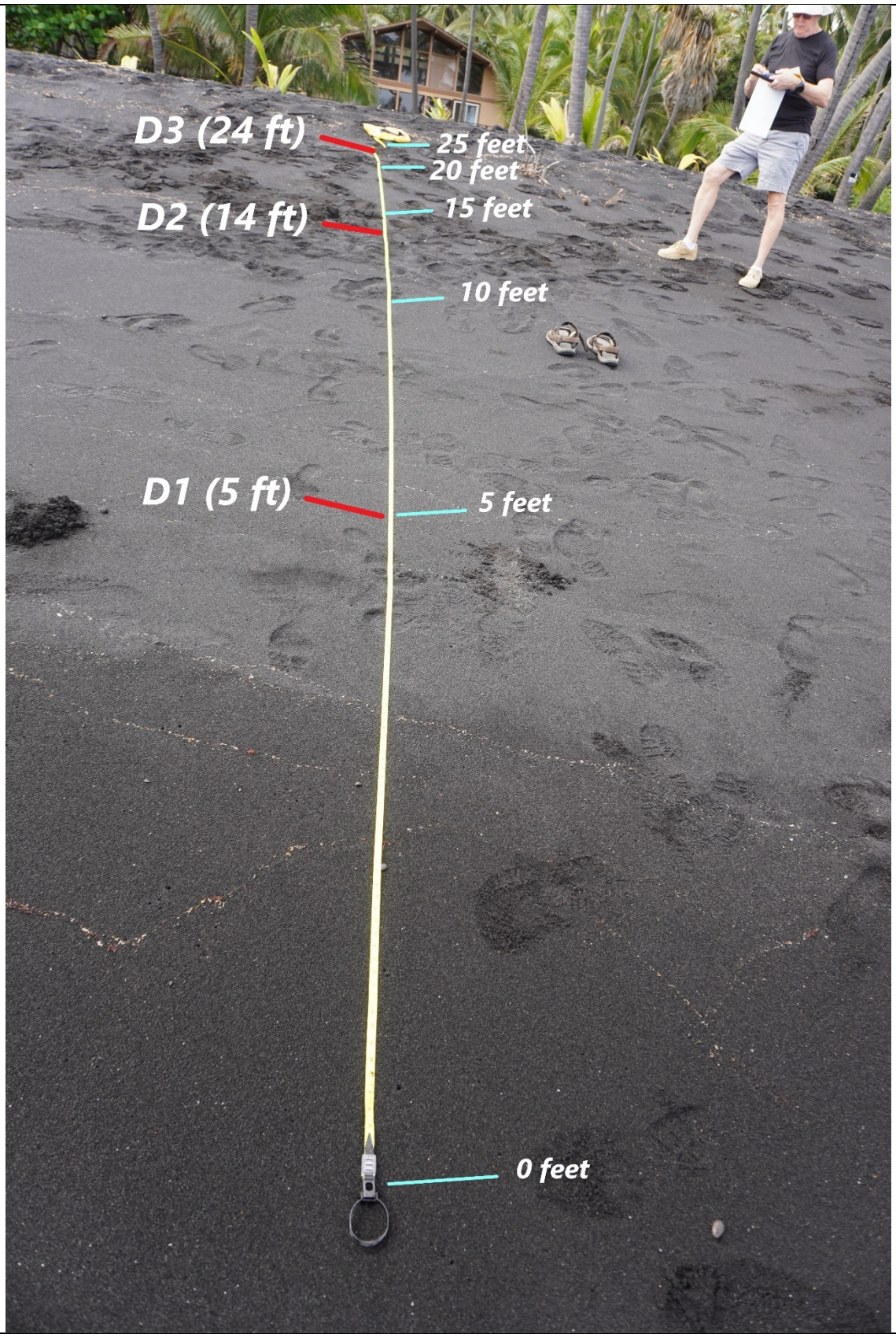

B.16.8: Punalu'u Beach Transect D overview looking landward with annotated survey locations.

D-1

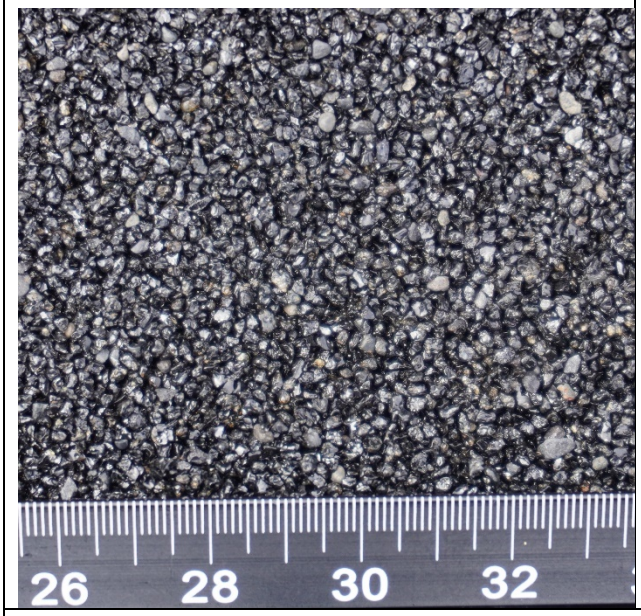

D-2

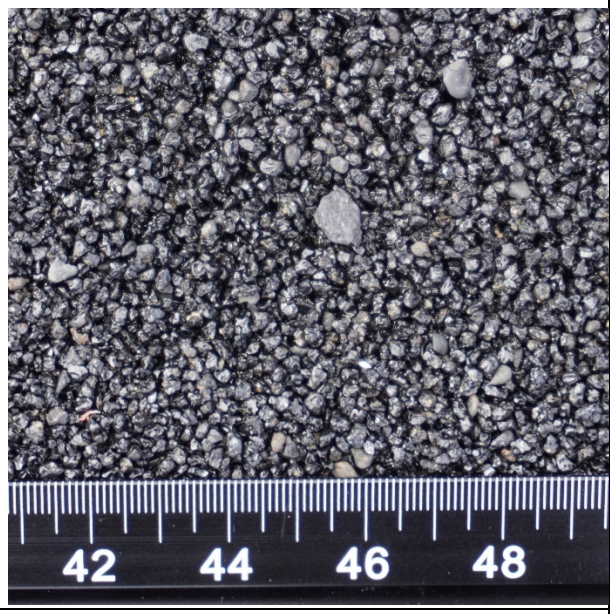

D-3

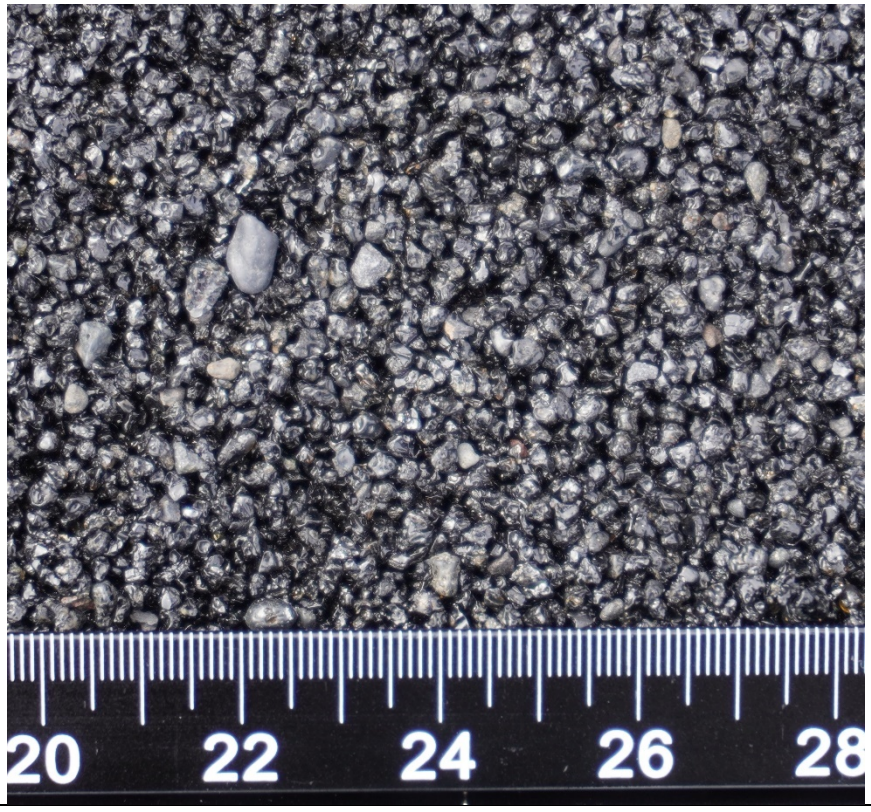

B.16.9: Punalu'u Beach Transect D survey site photographs with location labels. One inch is equal to 50 ticks (5 major scale units) on the laser-etched ruler.

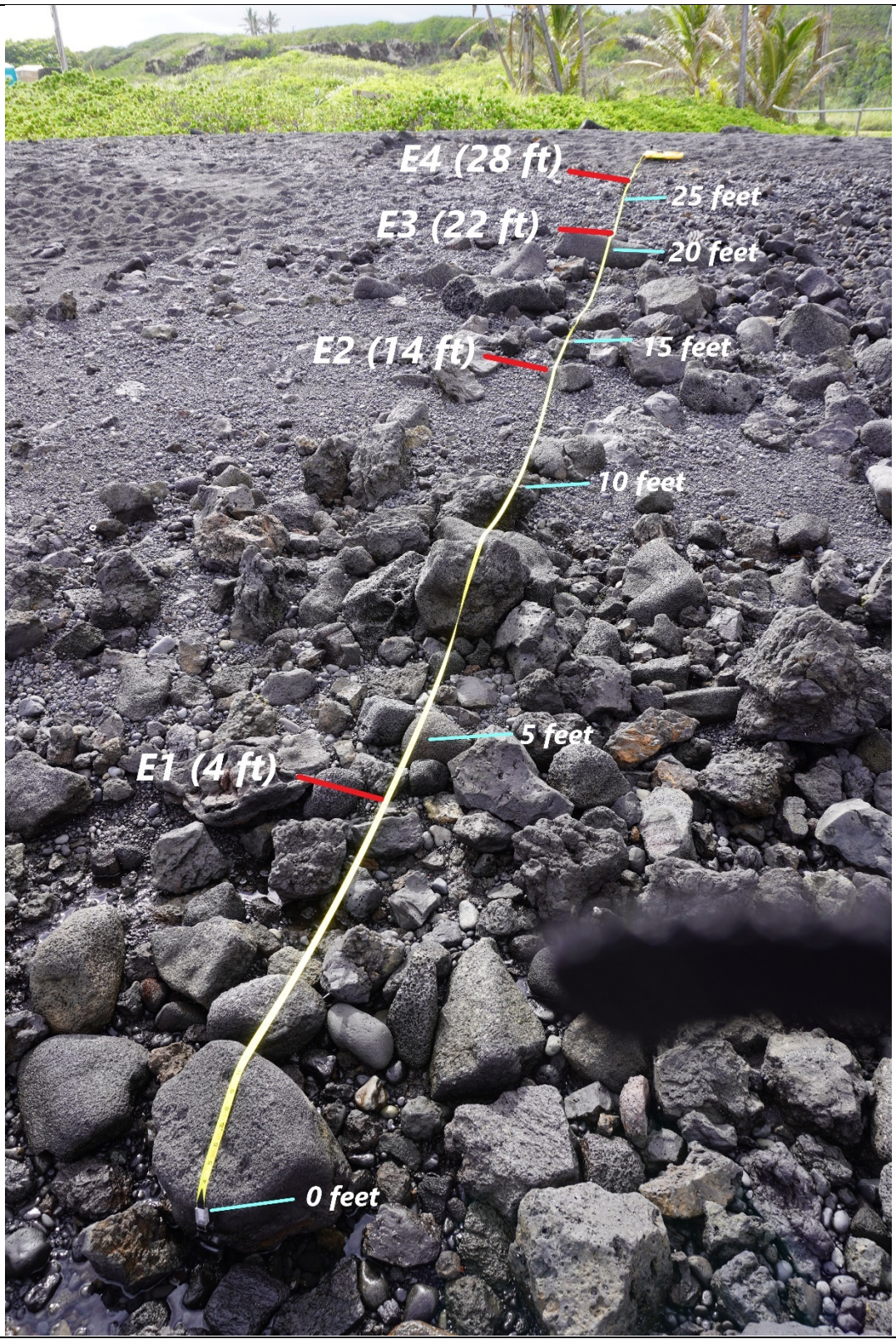

B.16.10: Punalu'u Beach Transect E overview looking landward with annotated survey locations.

E-1

E-2

E-3

E-4

B.16.11: Punalu'u Beach Transect E survey sites photographs with location labels. One inch is equal to 50 ticks (5 major scale units) on the laser-etched ruler.

B.17.1: Pohoiki Beach overview looking SW.

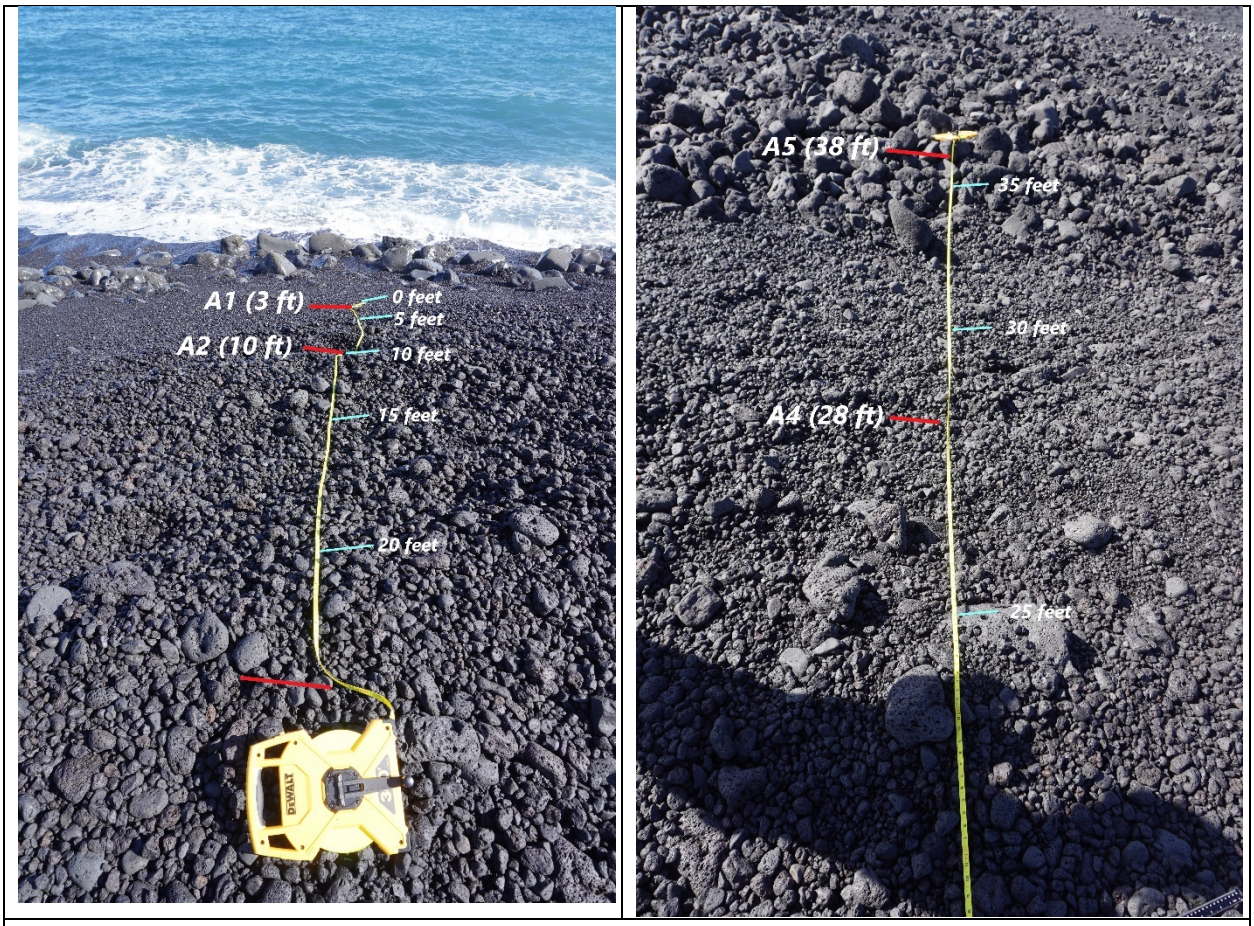

B.17.2: Pohoiki Beach Transect A overview looking seaward (left) and landward (right) with annotated survey locations.

A-1

A-2

A-3

A-4

A-5

B.17.3: Pohoiki Beach Transect A survey site photographs with location labels. One inch is equal to 50 ticks (5 major scale units) on the laser-etched ruler.

B.18.1: Honoli'I beach overview looking N.

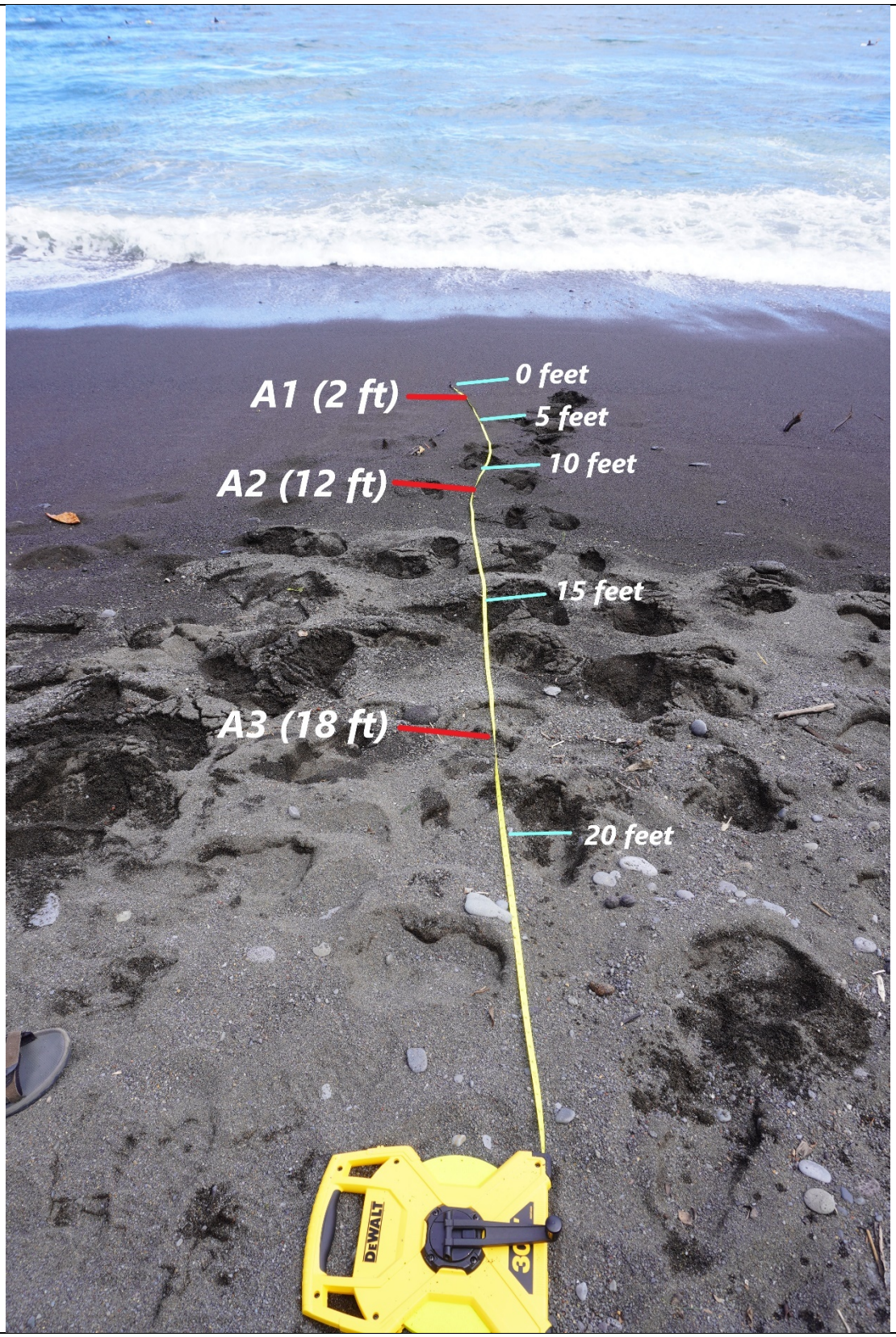

B.18.2: Honoli'I Beach Transect A overview looking seaward with annotated survey locations.

A-1

A-2

A-3

B.18.3: Honoli'I Beach Transect A survey site photographs with location labels. One inch is equal to 50 ticks (5 major scale units) on the laser-etched ruler.

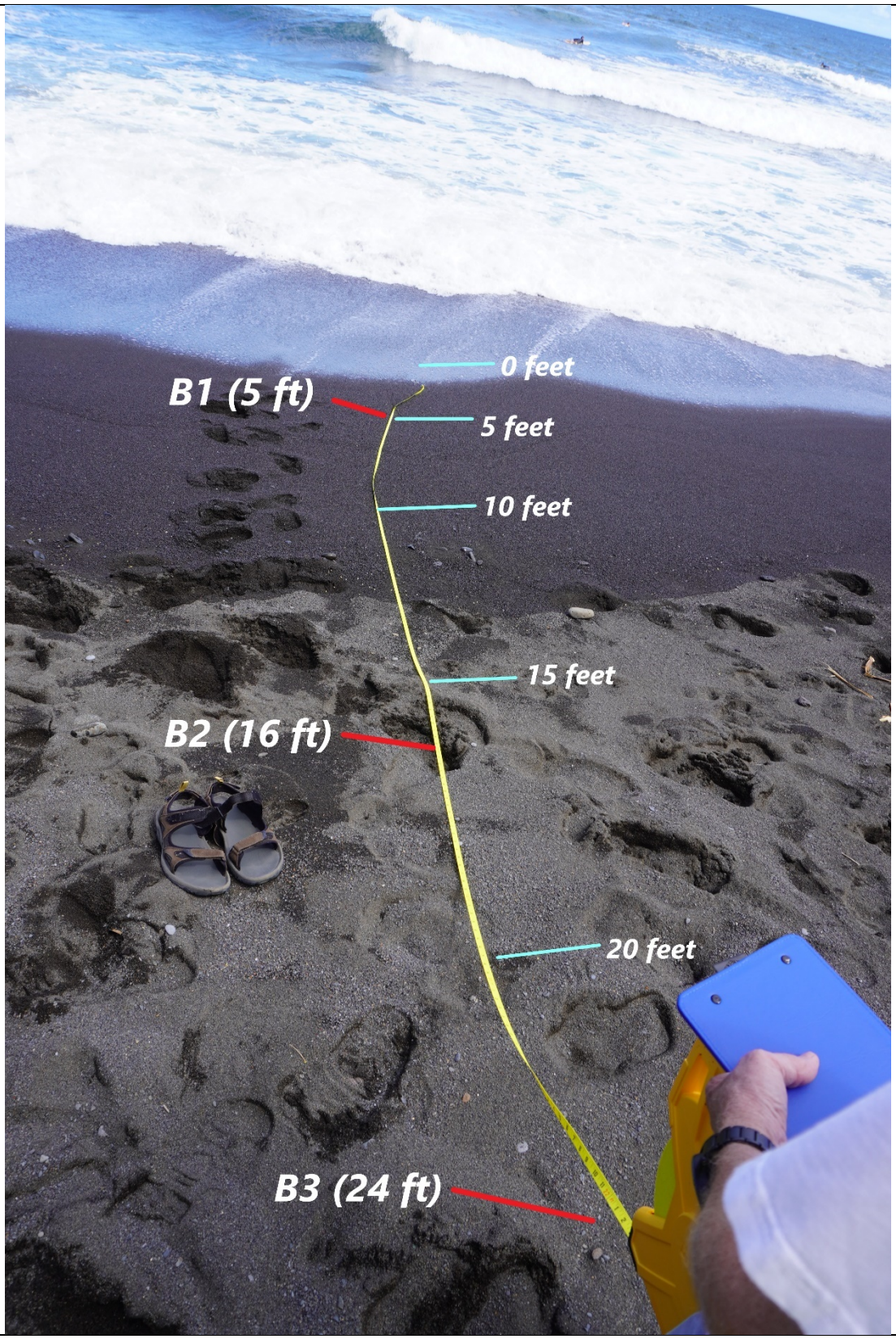

B.18.4: Honoli'I Beach Transect B overview looking seaward with annotated survey locations.

B-1

B-2

B-3

B.18.4: Honoli'I Beach Transect B survey site photographs with location labels. One inch is equal to 50 ticks (5 major scale units) on the laser-etched ruler.

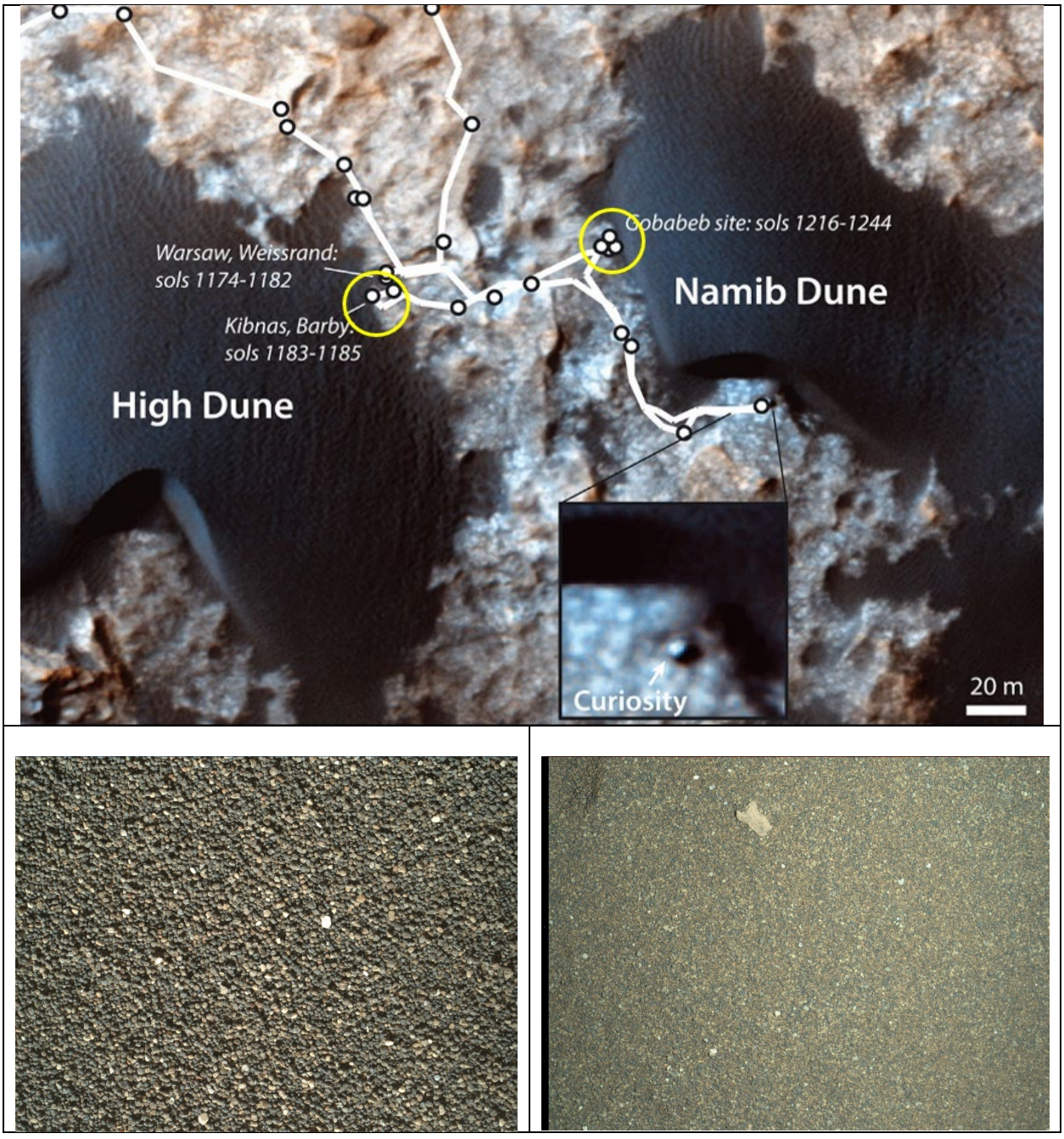
Gobabeb site: sols 1216-1244
Warsaw, Weissrand:
sols 1174-1182
Kibnas, Barby:
sols 1183-1185
Namib Dune
High Dune
Curiosity
20 m

B.19.1: Bagnold Dunes on Mars where the Curiosity Rover took pictures of sands at two dunes, namely the High Dune and the Namib Dune. Scale was provided in mm/pixels.

Appendix C – Distribution and cumulative curve graphs of standards (blue) and six samples taken from Hawaii (green). The graphs were derived using the weights sieved out and calculated through GRADISTAT.

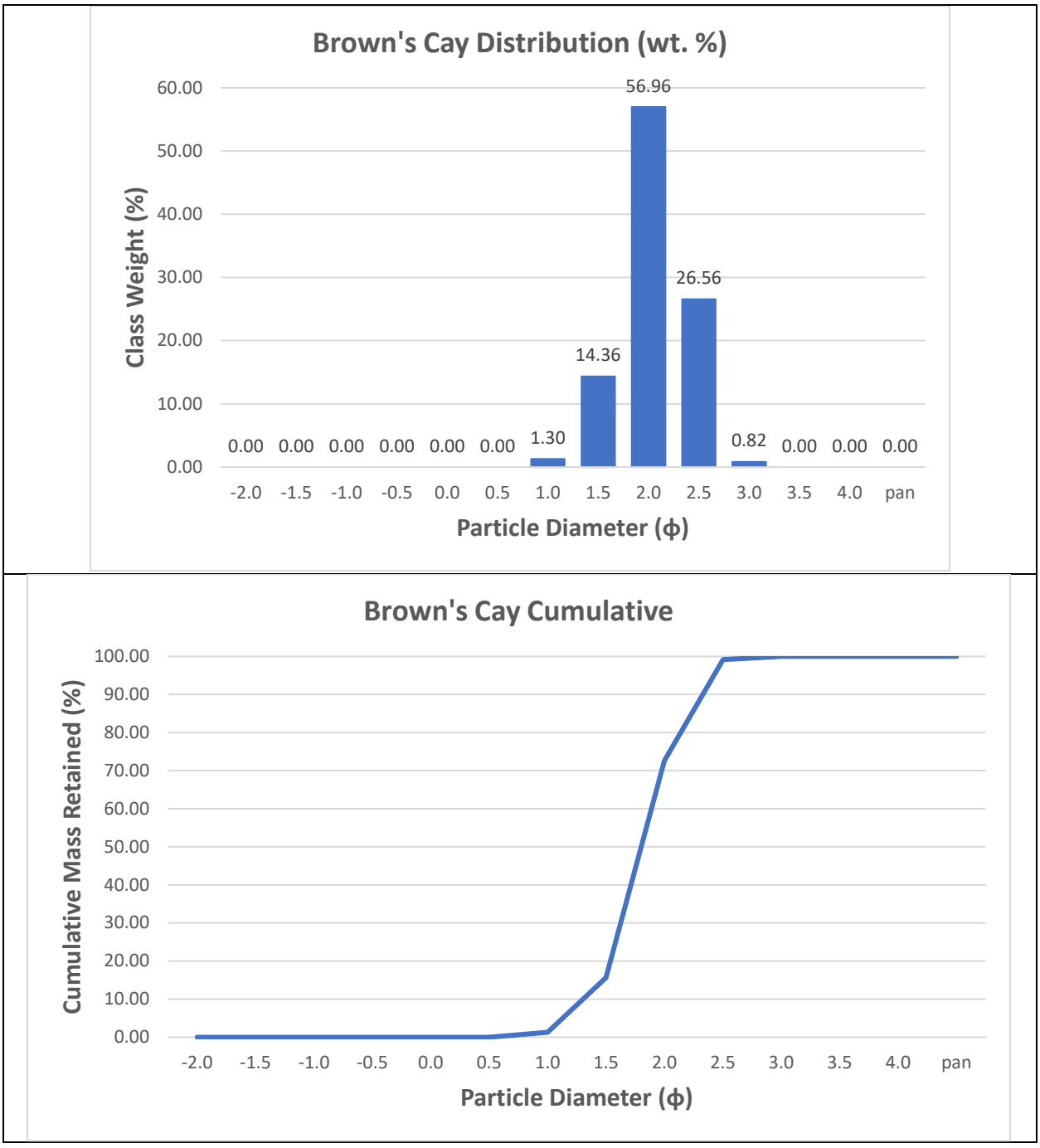

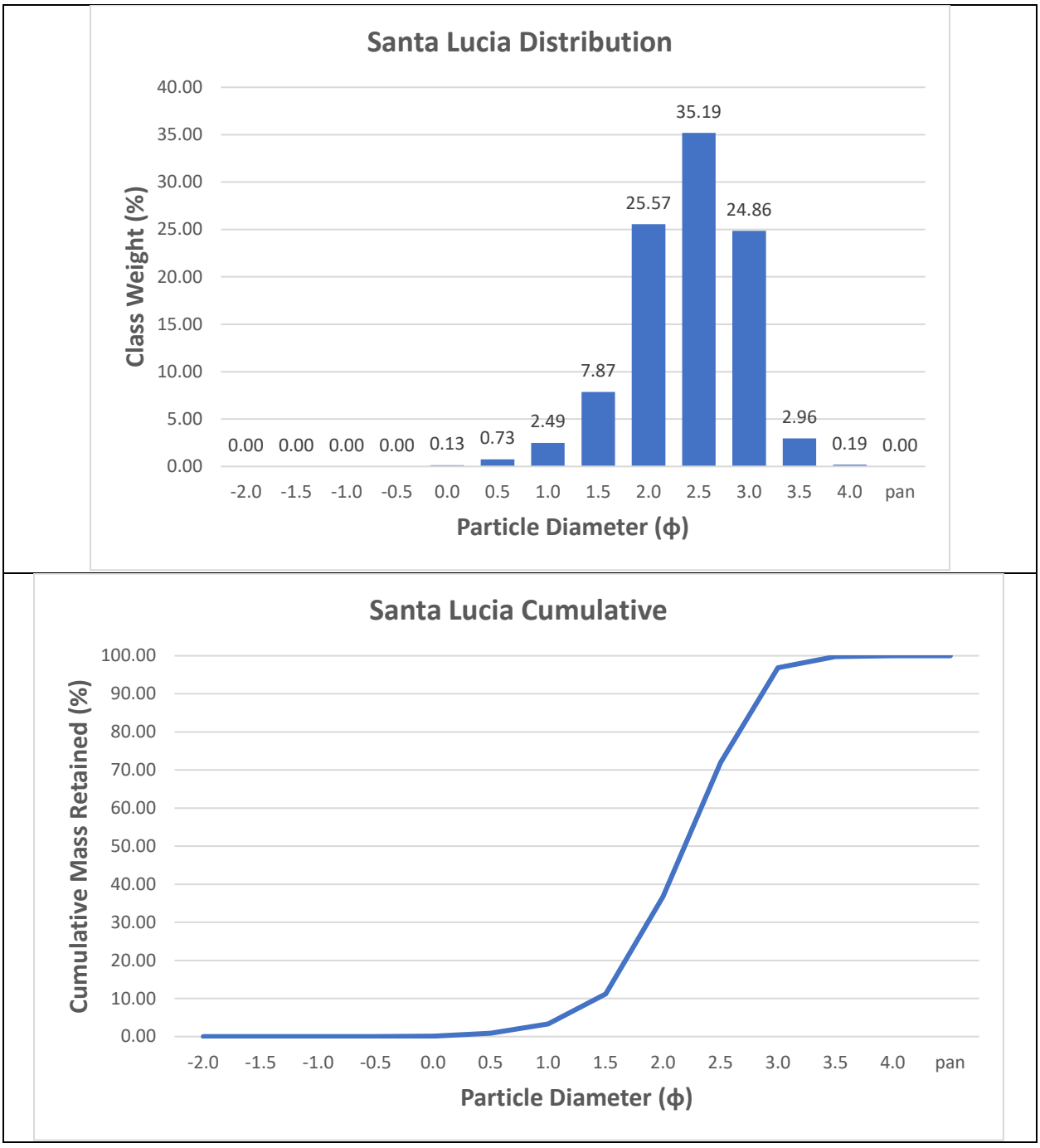
Santa Lucia Distribution
Class Weight (%)
40.00
35.00
30.00
25.00
20.00
15.00
10.00
5.00
0.00
0.00
0.00
0.00
0.00
0.13
0.73
2.49
7.87
25.57
35.19
24.86
2.96
0.19
0.00
-2.0
-1.5
-1.0
-0.5
0.0
0.5
1.0
1.5
2.0
2.5
3.0
3.5
4.0
pan
Particle Diameter (ϕ)
Santa Lucia Cumulative
Cumulative Mass Retained (%)
100.00
90.00
80.00
70.00
60.00
50.00
40.00
30.00
20.00
10.00
0.00
-2.0
-1.5
-1.0
-0.5
0.0
0.5
1.0
1.5
2.0
2.5
3.0
3.5
4.0
pan
Particle Diameter (ϕ)

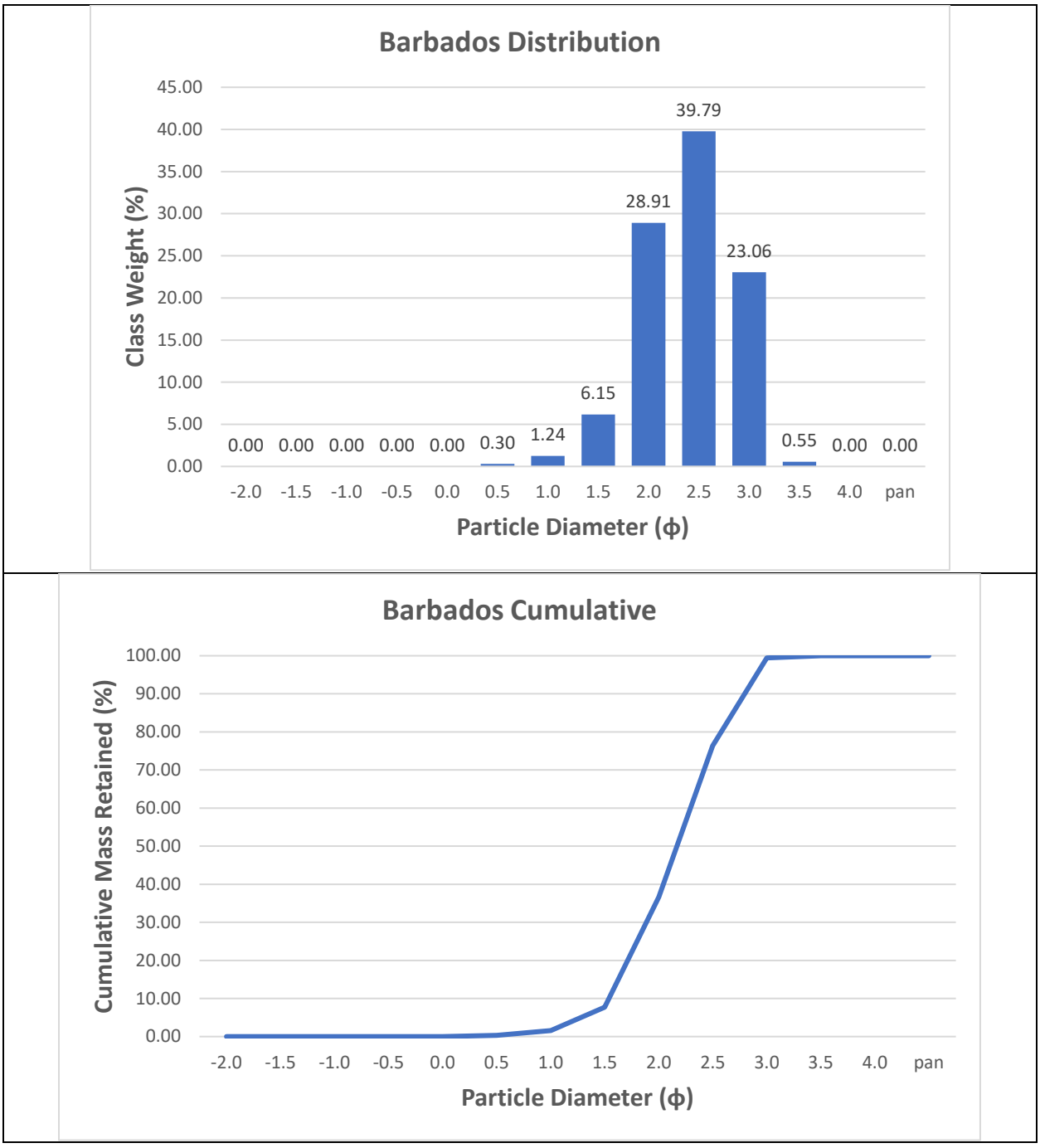
Barbados Distribution
Class Weight (%)
45.00
40.00
35.00
30.00
25.00
20.00
15.00
10.00
5.00
0.00
0.00 0.00 0.00 0.00 0.00 0.30 1.24 6.15 28.91 39.79 23.06 0.55 0.00 0.00
-2.0 -1.5 -1.0 -0.5 0.0 0.5 1.0 1.5 2.0 2.5 3.0 3.5 4.0 pan
Particle Diameter (ϕ)
Barbados Cumulative
Cumulative Mass Retained (%)
100.00
90.00
80.00
70.00
60.00
50.00
40.00
30.00
20.00
10.00
0.00
-2.0 -1.5 -1.0 -0.5 0.0 0.5 1.0 1.5 2.0 2.5 3.0 3.5 4.0 pan
Particle Diameter (ϕ)

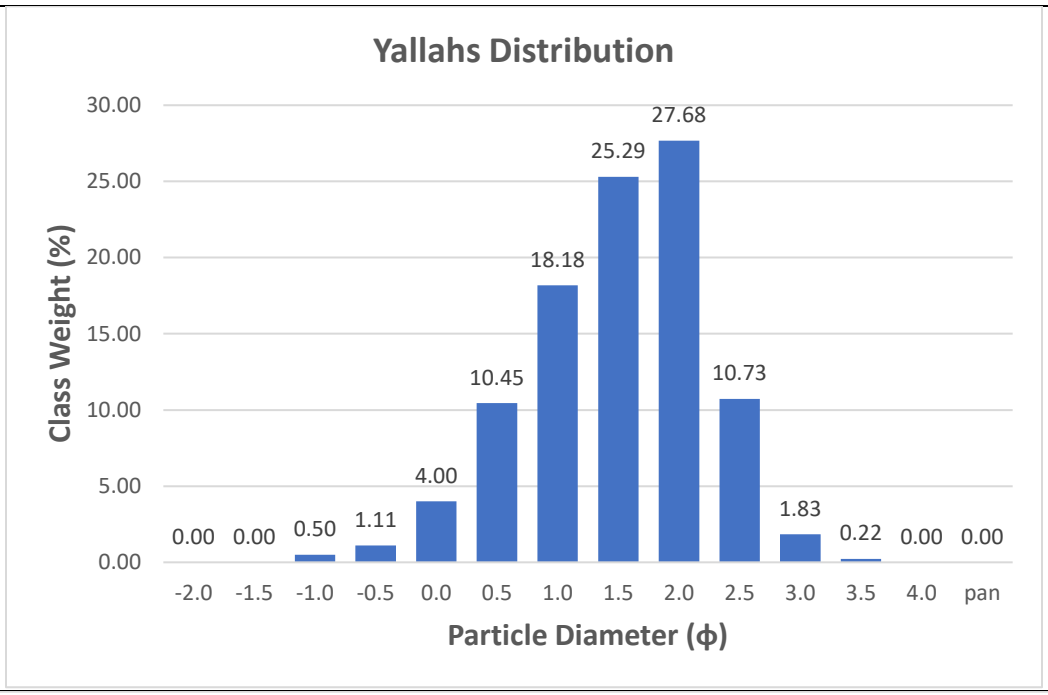
Yallahs Distribution
Class Weight (%)
30.00
25.00
20.00
15.00
10.00
5.00
0.00
0.00
0.00
0.50
1.11
4.00
10.45
18.18
25.29
27.68
10.73
1.83
0.22
0.00
0.00
-2.0
-1.5
-1.0
-0.5
0.0
0.5
1.0
1.5
2.0
2.5
3.0
3.5
4.0
pan
Particle Diameter (ϕ)

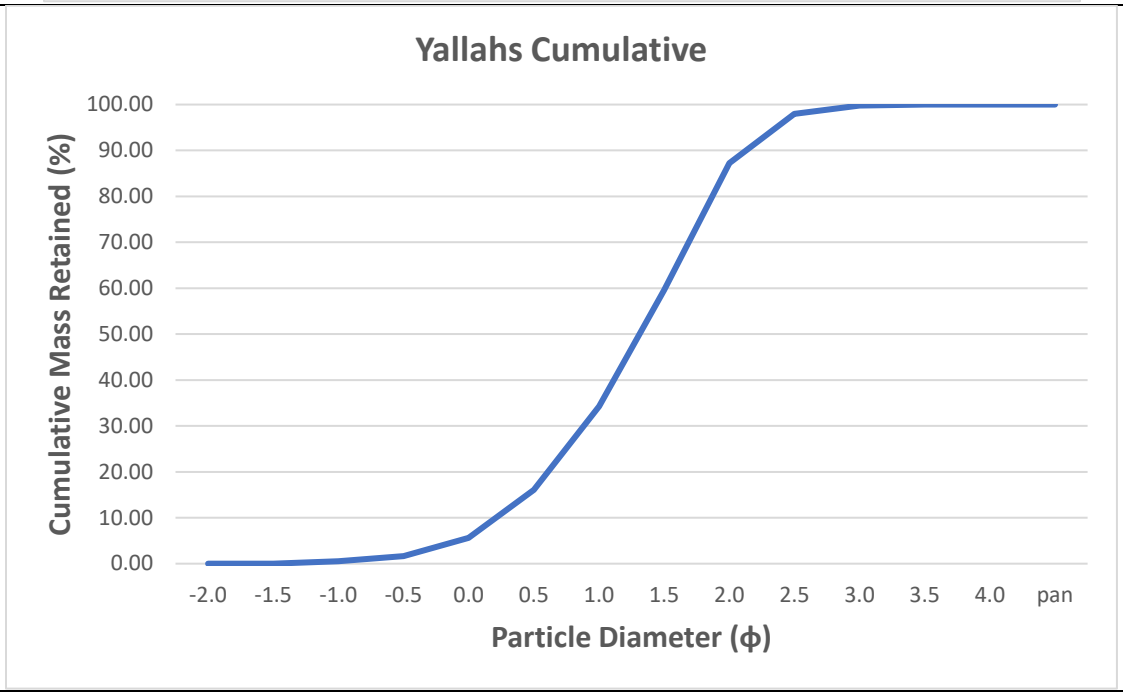
Yallahs Cumulative
Cumulative Mass Retained (%)
100.00
90.00
80.00
70.00
60.00
50.00
40.00
30.00
20.00
10.00
0.00
-2.0
-1.5
-1.0
-0.5
0.0
0.5
1.0
1.5
2.0
2.5
3.0
3.5
4.0
pan
Particle Diameter (ϕ)

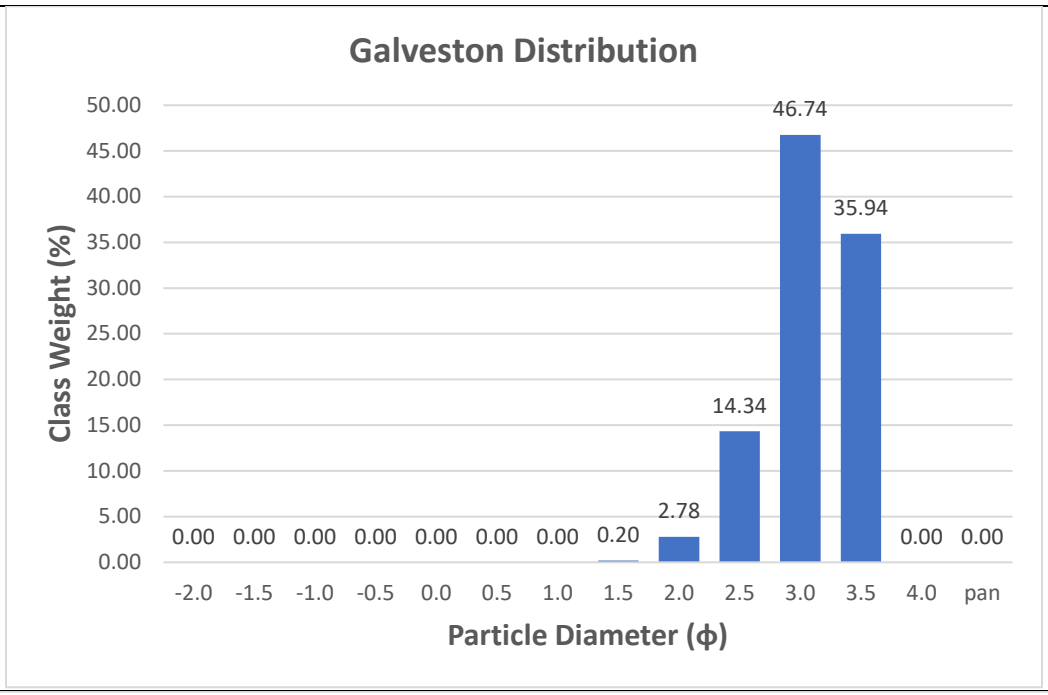
Galveston Distribution
Class Weight (%)
50.00
45.00
40.00
35.00
30.00
25.00
20.00
15.00
10.00
5.00
0.00
0.00 0.00 0.00 0.00 0.00 0.00 0.00 0.20 2.78 14.34 46.74 35.94 0.00 0.00
-2.0 -1.5 -1.0 -0.5 0.0 0.5 1.0 1.5 2.0 2.5 3.0 3.5 4.0 pan
Particle Diameter (ϕ)

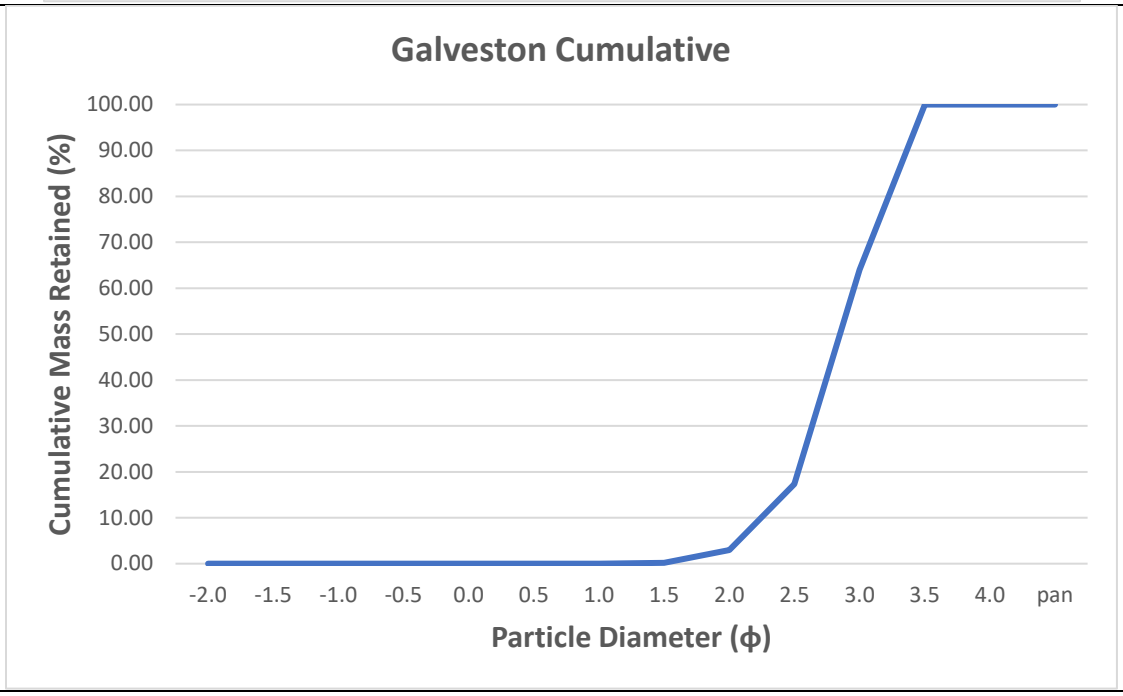
Galveston Cumulative
Cumulative Mass Retained (%)
100.00
90.00
80.00
70.00
60.00
50.00
40.00
30.00
20.00
10.00
0.00
-2.0 -1.5 -1.0 -0.5 0.0 0.5 1.0 1.5 2.0 2.5 3.0 3.5 4.0 pan
Particle Diameter (ϕ)

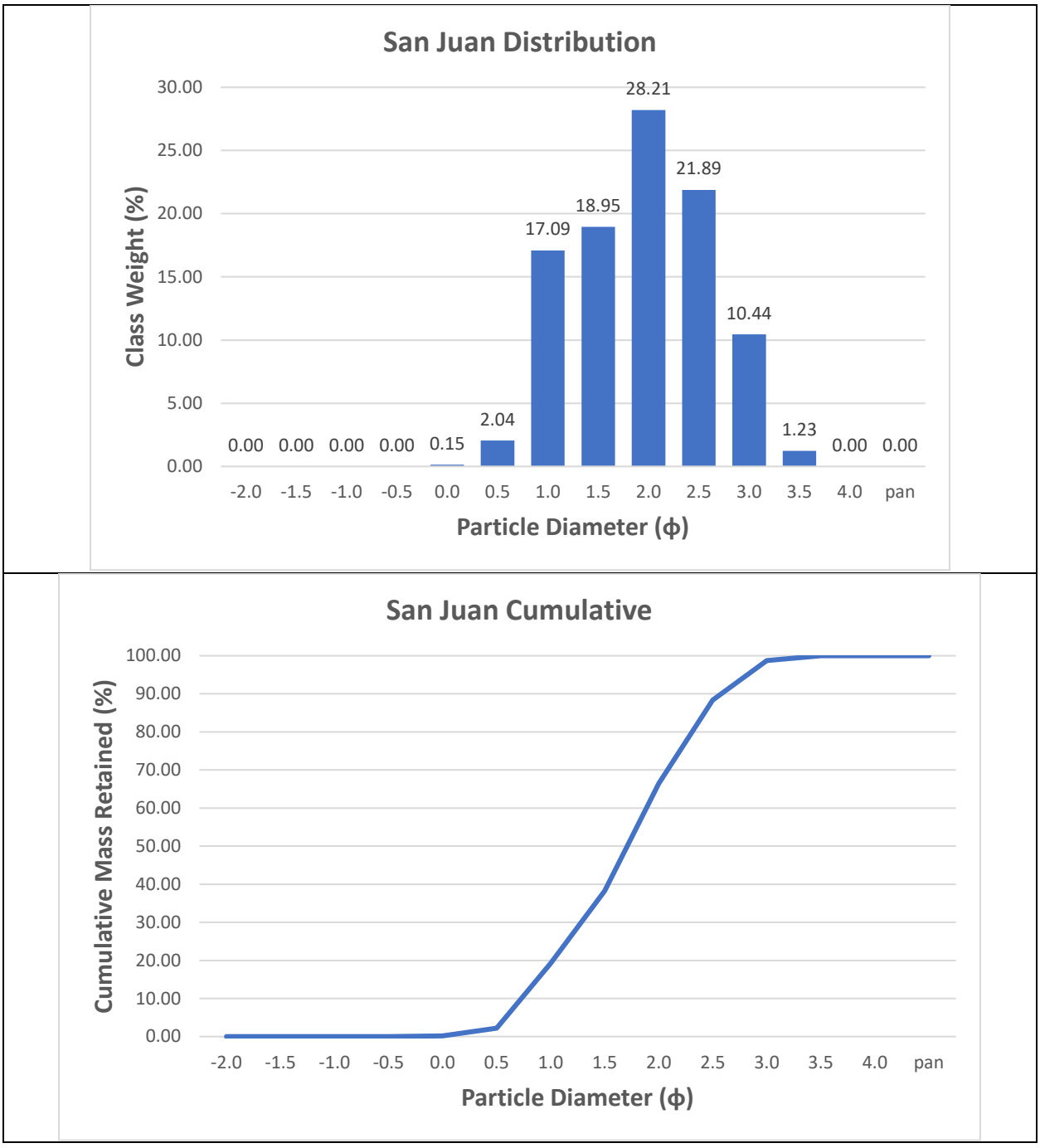
San Juan Distribution
Class Weight (%)
30.00
25.00
20.00
15.00
10.00
5.00
0.00
0.00 0.00 0.00 0.00 0.15 2.04 17.09 18.95 28.21 21.89 10.44 1.23 0.00 0.00
-2.0 -1.5 -1.0 -0.5 0.0 0.5 1.0 1.5 2.0 2.5 3.0 3.5 4.0 pan
Particle Diameter (ϕ)
San Juan Cumulative
Cumulative Mass Retained (%)
100.00
90.00
80.00
70.00
60.00
50.00
40.00
30.00
20.00
10.00
0.00
-2.0 -1.5 -1.0 -0.5 0.0 0.5 1.0 1.5 2.0 2.5 3.0 3.5 4.0 pan
Particle Diameter (ϕ)

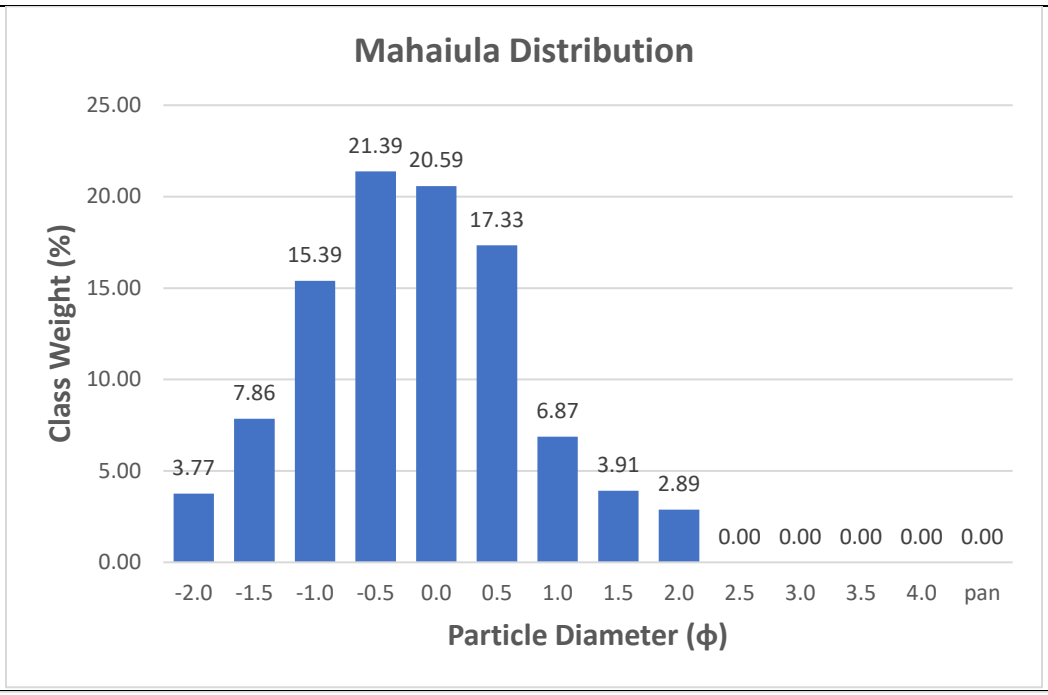
Mahaiula Distribution
Class Weight (%)
25.00
20.00
15.00
10.00
5.00
0.00
3.77
7.86
15.39
21.39
20.59
17.33
6.87
3.91
2.89
0.00
0.00
0.00
0.00
0.00
-2.0
-1.5
-1.0
-0.5
0.0
0.5
1.0
1.5
2.0
2.5
3.0
3.5
4.0
pan
Particle Diameter (ϕ)

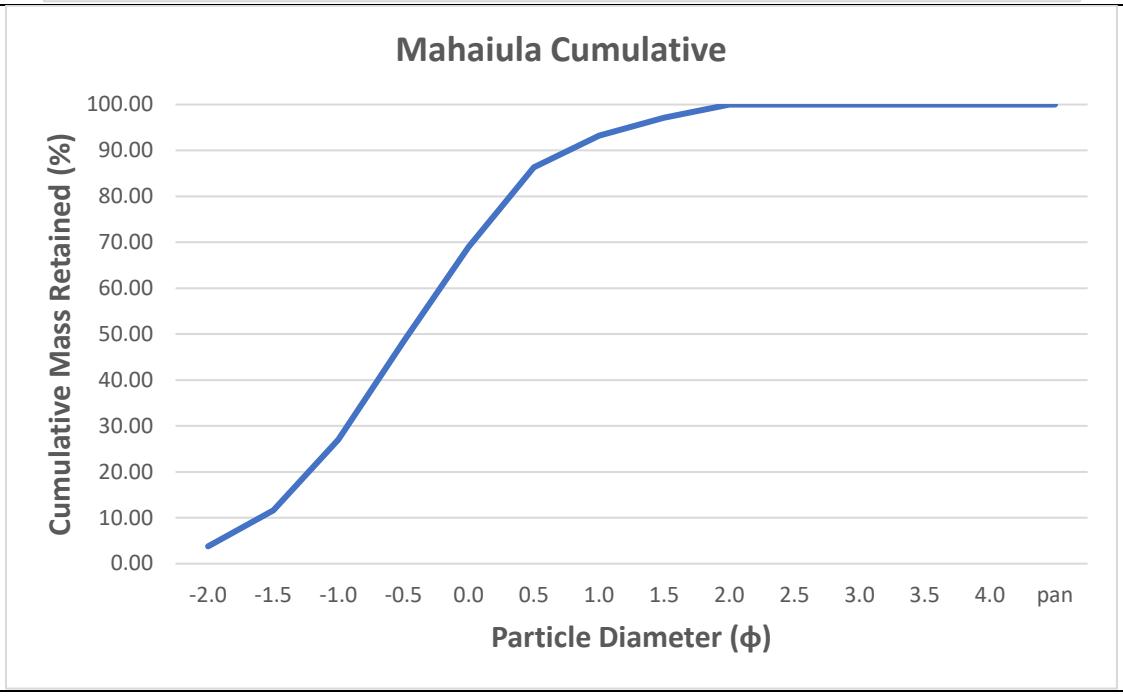
Mahaiula Cumulative
Cumulative Mass Retained (%)
100.00
90.00
80.00
70.00
60.00
50.00
40.00
30.00
20.00
10.00
0.00
-2.0
-1.5
-1.0
-0.5
0.0
0.5
1.0
1.5
2.0
2.5
3.0
3.5
4.0
pan
Particle Diameter (ϕ)

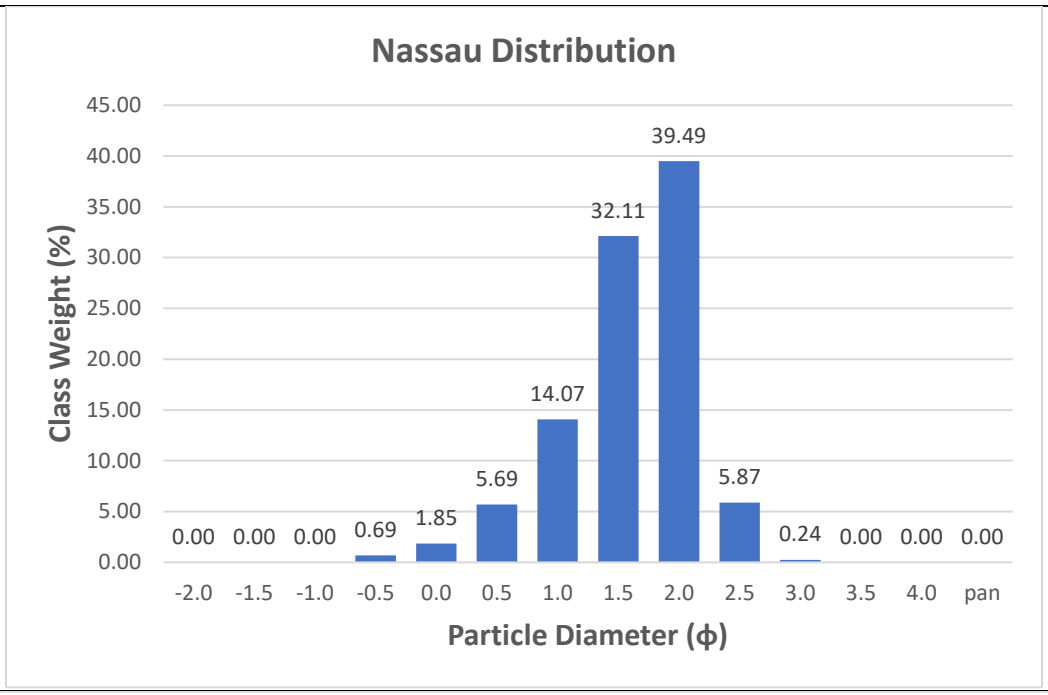
Nassau Distribution
Class Weight (%)
45.00
40.00
35.00
30.00
25.00
20.00
15.00
10.00
5.00
0.00
0.00
0.00
0.00
0.69
1.85
5.69
14.07
32.11
39.49
5.87
0.24
0.00
0.00
0.00
-2.0
-1.5
-1.0
-0.5
0.0
0.5
1.0
1.5
2.0
2.5
3.0
3.5
4.0
pan
Particle Diameter (ϕ)

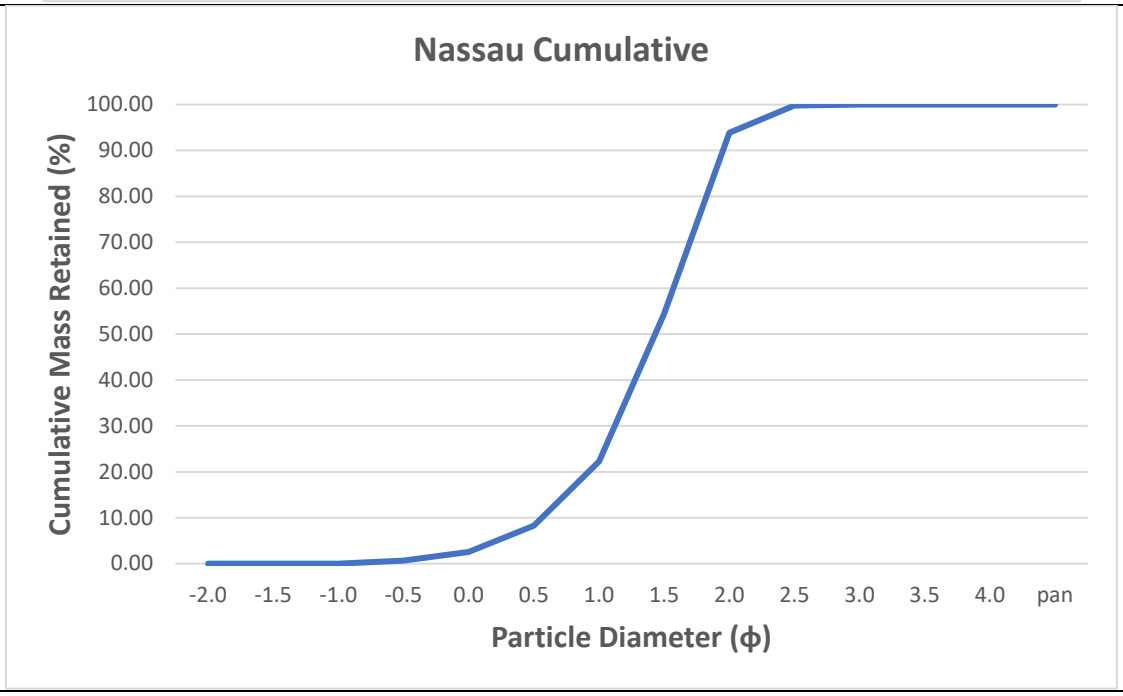
Nassau Cumulative
Cumulative Mass Retained (%)
100.00
90.00
80.00
70.00
60.00
50.00
40.00
30.00
20.00
10.00
0.00
-2.0
-1.5
-1.0
-0.5
0.0
0.5
1.0
1.5
2.0
2.5
3.0
3.5
4.0
pan
Particle Diameter (ϕ)

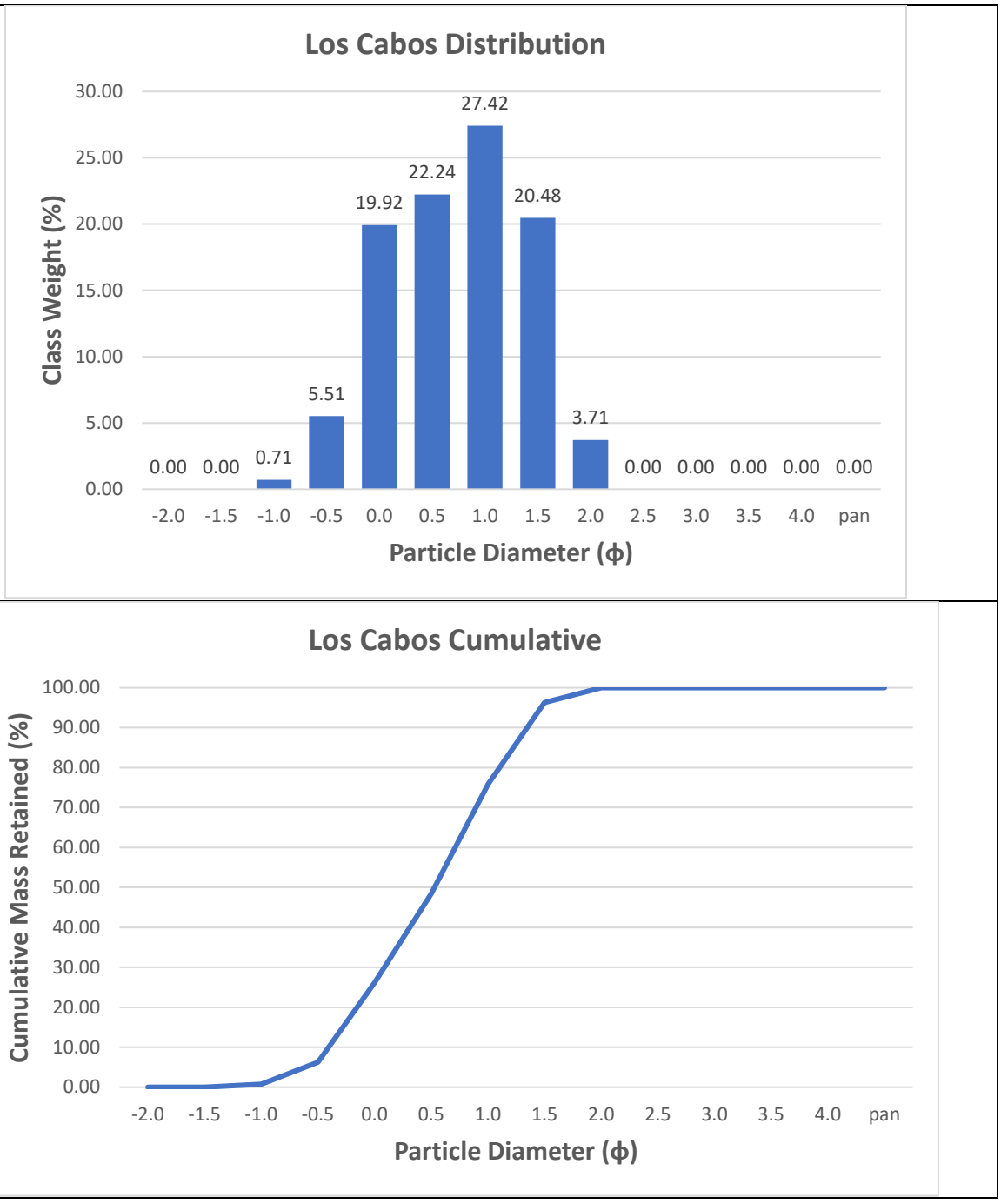
Los Cabos Distribution
Class Weight (%)
30.00
25.00
20.00
15.00
10.00
5.00
0.00
0.00
0.00
0.71
5.51
19.92
22.24
27.42
20.48
3.71
0.00
0.00
0.00
0.00
0.00
-2.0
-1.5
-1.0
-0.5
0.0
0.5
1.0
1.5
2.0
2.5
3.0
3.5
4.0
pan
Particle Diameter (ϕ)
Los Cabos Cumulative
Cumulative Mass Retained (%)
100.00
90.00
80.00
70.00
60.00
50.00
40.00
30.00
20.00
10.00
0.00
-2.0
-1.5
-1.0
-0.5
0.0
0.5
1.0
1.5
2.0
2.5
3.0
3.5
4.0
pan
Particle Diameter (ϕ)

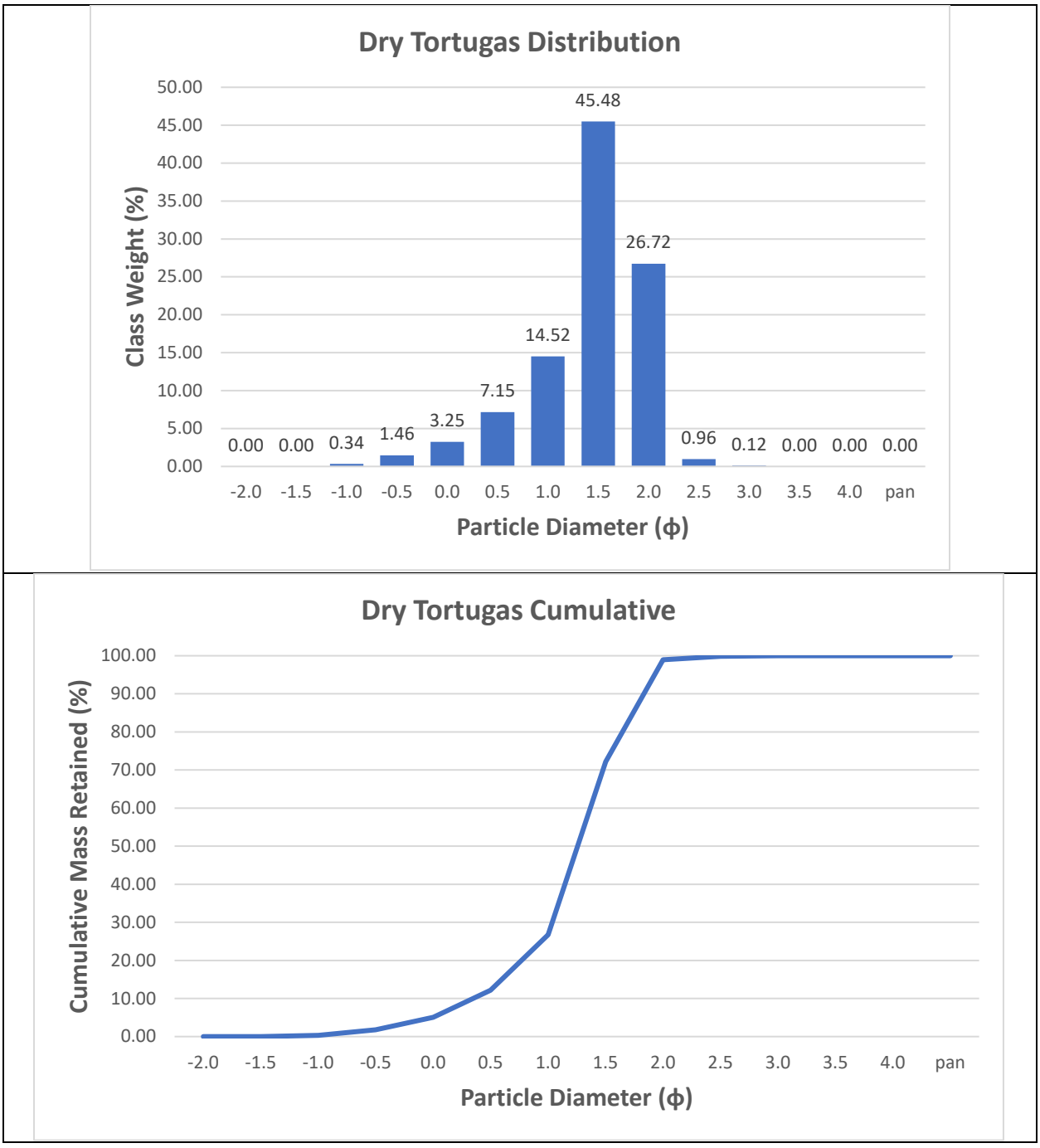
Dry Tortugas Distribution
Class Weight (%)
50.00
45.00
40.00
35.00
30.00
25.00
20.00
15.00
10.00
5.00
0.00
0.00
0.00
0.34
1.46
3.25
7.15
14.52
45.48
26.72
0.96
0.12
0.00
0.00
0.00
-2.0
-1.5
-1.0
-0.5
0.0
0.5
1.0
1.5
2.0
2.5
3.0
3.5
4.0
pan
Particle Diameter (ϕ)
Dry Tortugas Cumulative
Cumulative Mass Retained (%)
100.00
90.00
80.00
70.00
60.00
50.00
40.00
30.00
20.00
10.00
0.00
-2.0
-1.5
-1.0
-0.5
0.0
0.5
1.0
1.5
2.0
2.5
3.0
3.5
4.0
pan
Particle Diameter (ϕ)

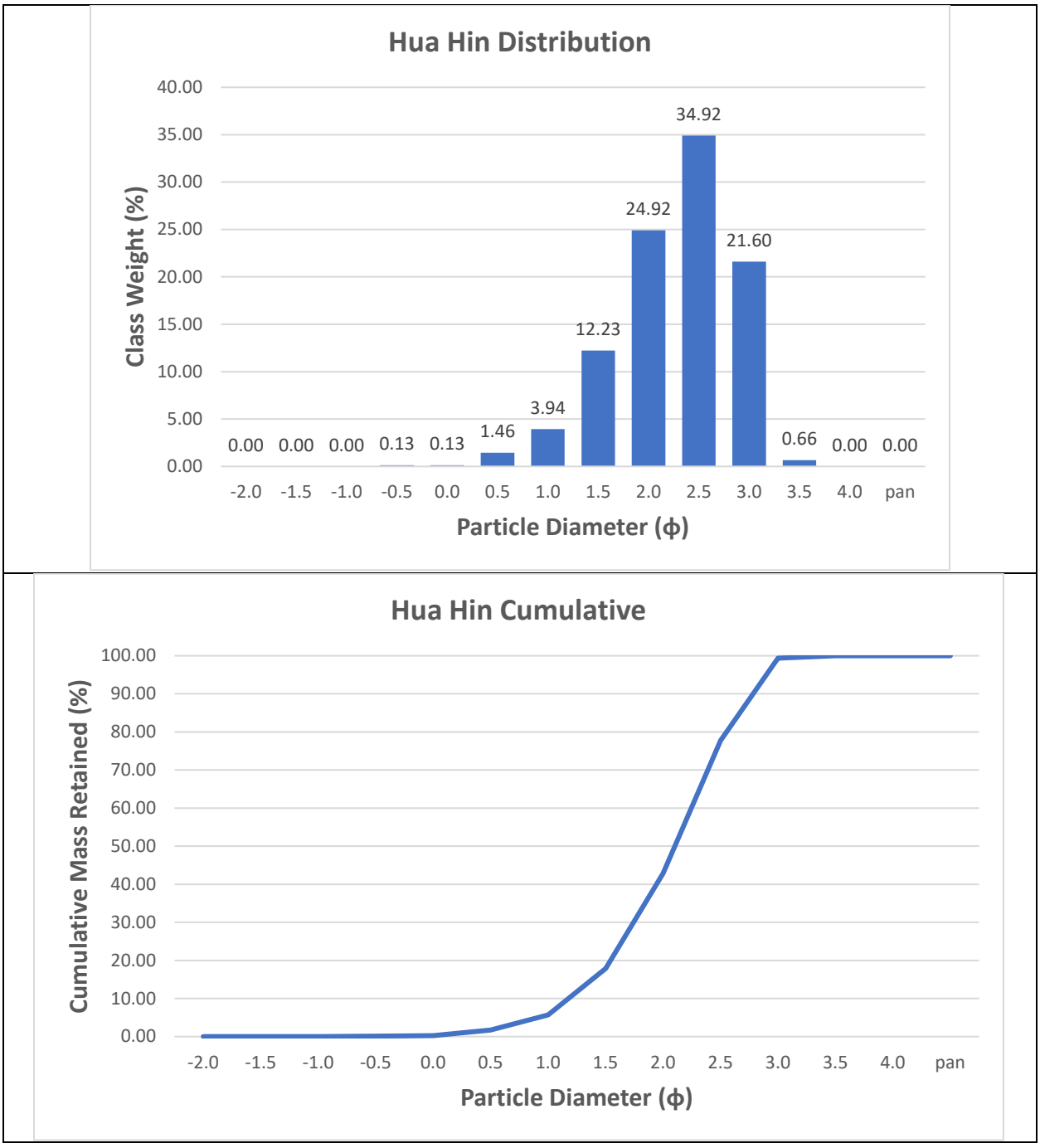
Hua Hin Distribution
Class Weight (%)
40.00
35.00
30.00
25.00
20.00
15.00
10.00
5.00
0.00
0.00 0.00 0.00 0.13 0.13 1.46 3.94 12.23 24.92 34.92 21.60 0.66 0.00 0.00
-2.0 -1.5 -1.0 -0.5 0.0 0.5 1.0 1.5 2.0 2.5 3.0 3.5 4.0 pan
Particle Diameter (ϕ)
Hua Hin Cumulative
Cumulative Mass Retained (%)
100.00
90.00
80.00
70.00
60.00
50.00
40.00
30.00
20.00
10.00
0.00
-2.0 -1.5 -1.0 -0.5 0.0 0.5 1.0 1.5 2.0 2.5 3.0 3.5 4.0 pan
Particle Diameter (ϕ)

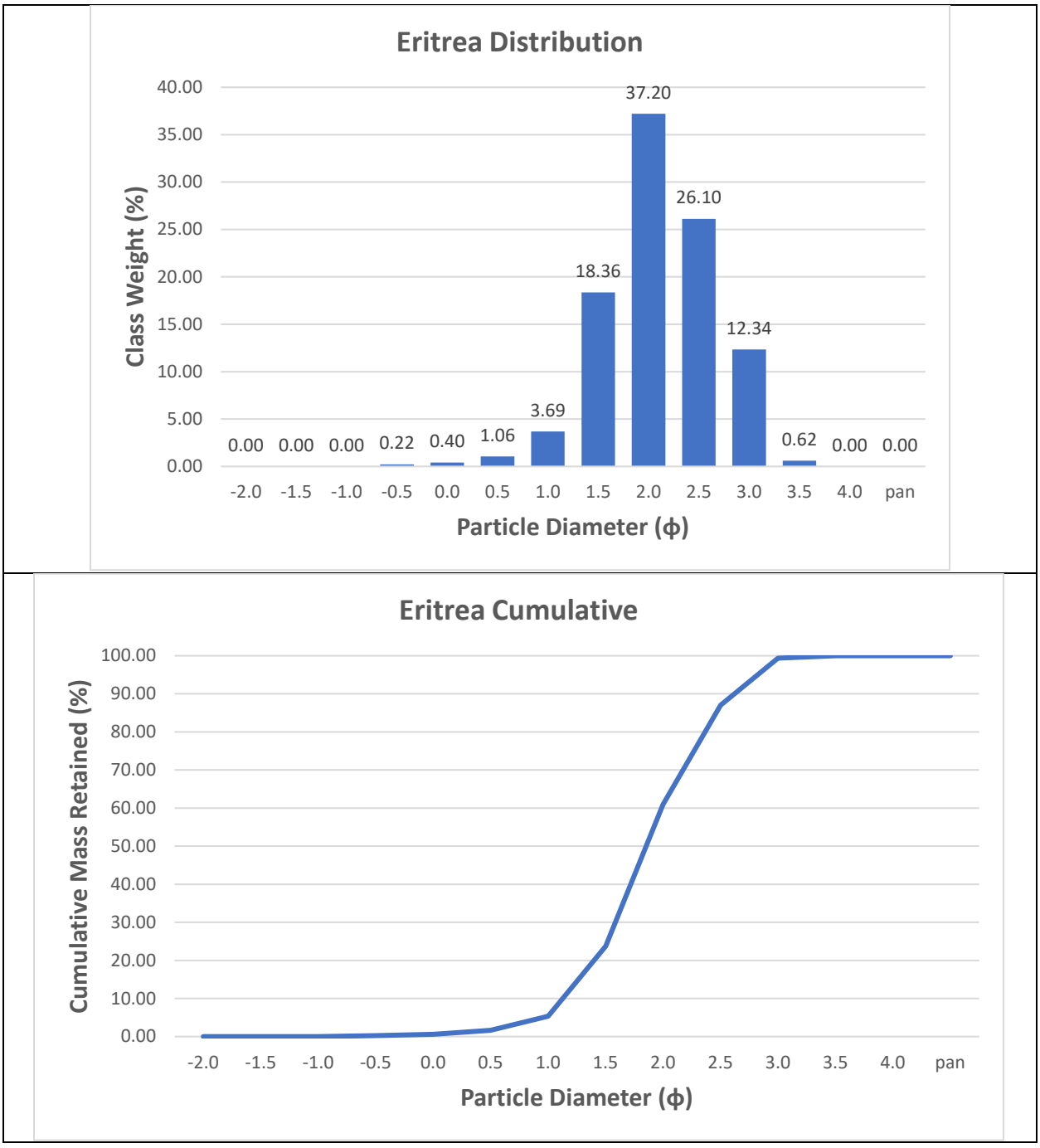
Eritrea Distribution
Class Weight (%)
40.00
35.00
30.00
25.00
20.00
15.00
10.00
5.00
0.00
0.00 0.00 0.00 0.22 0.40 1.06 3.69 18.36 37.20 26.10 12.34 0.62 0.00 0.00
-2.0 -1.5 -1.0 -0.5 0.0 0.5 1.0 1.5 2.0 2.5 3.0 3.5 4.0 pan
Particle Diameter (ϕ)
Eritrea Cumulative
Cumulative Mass Retained (%)
100.00
90.00
80.00
70.00
60.00
50.00
40.00
30.00
20.00
10.00
0.00
-2.0 -1.5 -1.0 -0.5 0.0 0.5 1.0 1.5 2.0 2.5 3.0 3.5 4.0 pan
Particle Diameter (ϕ)

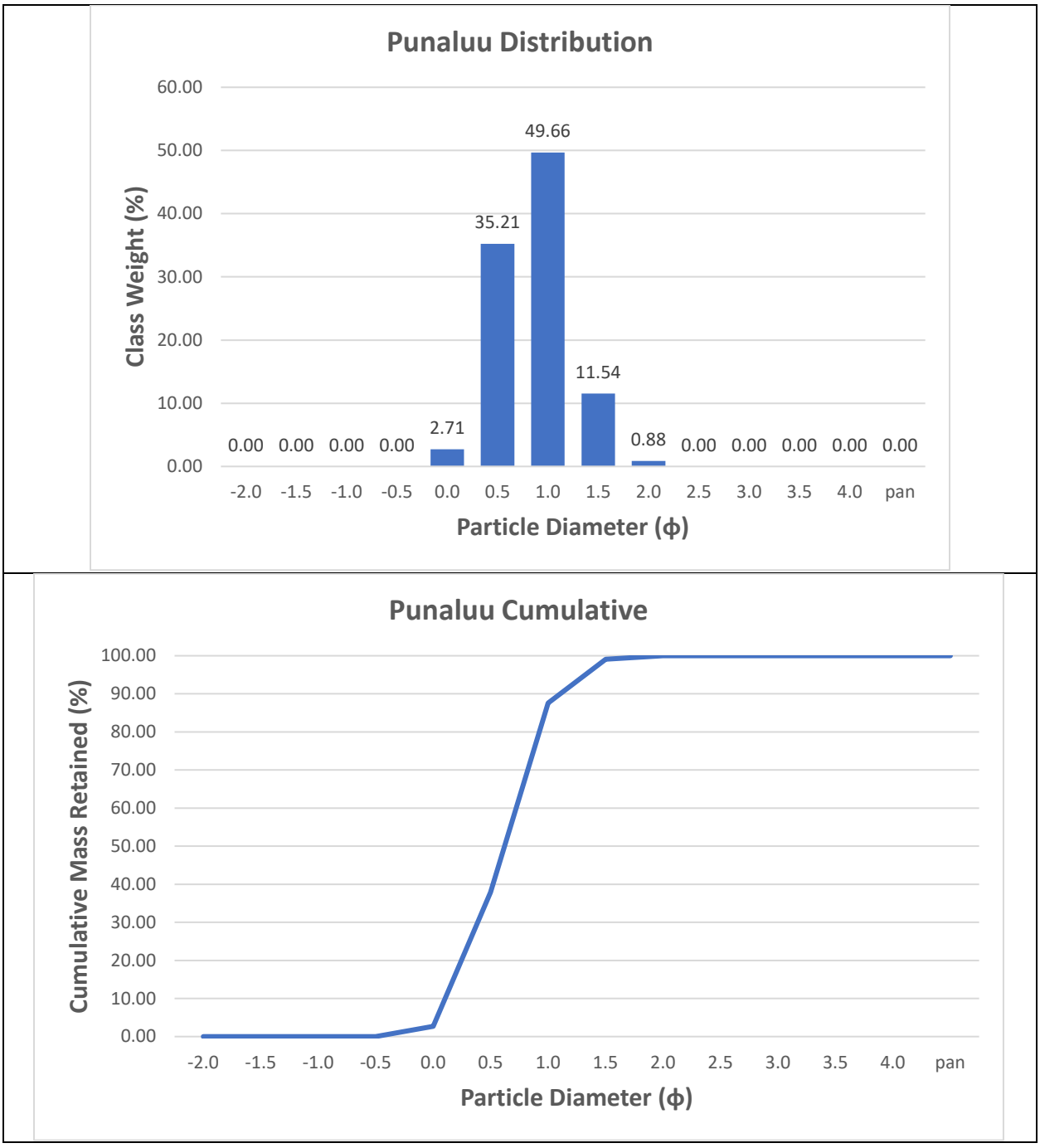
Punaluu Distribution
Class Weight (%)
60.00
50.00
40.00
30.00
20.00
10.00
0.00
0.00
0.00
0.00
0.00
2.71
35.21
49.66
11.54
0.88
0.00
0.00
0.00
0.00
0.00
-2.0
-1.5
-1.0
-0.5
0.0
0.5
1.0
1.5
2.0
2.5
3.0
3.5
4.0
pan
Particle Diameter (ϕ)
Punaluu Cumulative
Cumulative Mass Retained (%)
100.00
90.00
80.00
70.00
60.00
50.00
40.00
30.00
20.00
10.00
0.00
-2.0
-1.5
-1.0
-0.5
0.0
0.5
1.0
1.5
2.0
2.5
3.0
3.5
4.0
pan
Particle Diameter (ϕ)

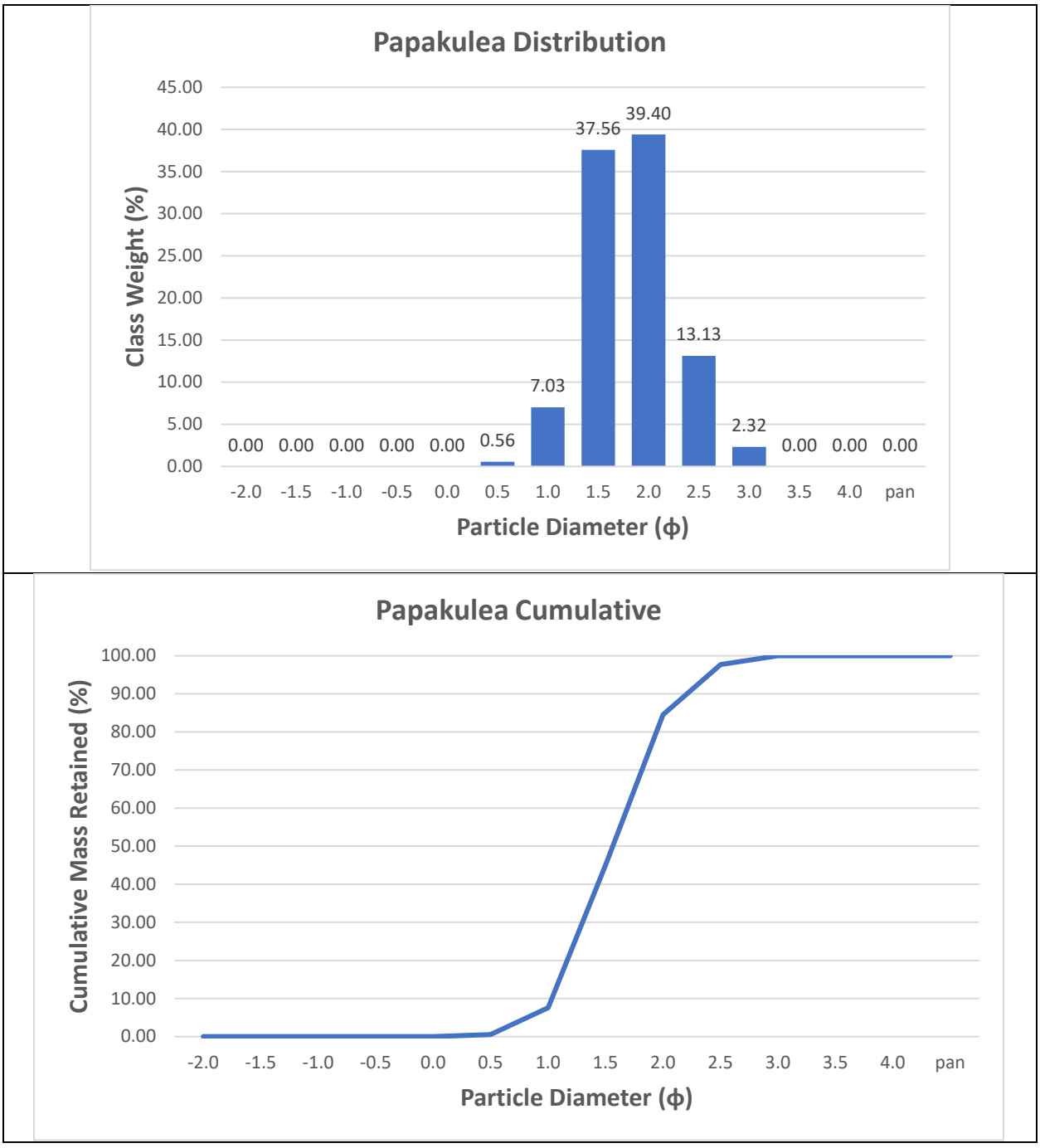
Papakulea Distribution
Class Weight (%)
45.00
40.00
35.00
30.00
25.00
20.00
15.00
10.00
5.00
0.00
0.00 0.00 0.00 0.00 0.00 0.56 7.03 37.56 39.40 13.13 2.32 0.00 0.00 0.00
-2.0 -1.5 -1.0 -0.5 0.0 0.5 1.0 1.5 2.0 2.5 3.0 3.5 4.0 pan
Particle Diameter (ϕ)
Papakulea Cumulative
Cumulative Mass Retained (%)
100.00
90.00
80.00
70.00
60.00
50.00
40.00
30.00
20.00
10.00
0.00
-2.0 -1.5 -1.0 -0.5 0.0 0.5 1.0 1.5 2.0 2.5 3.0 3.5 4.0 pan
Particle Diameter (ϕ)

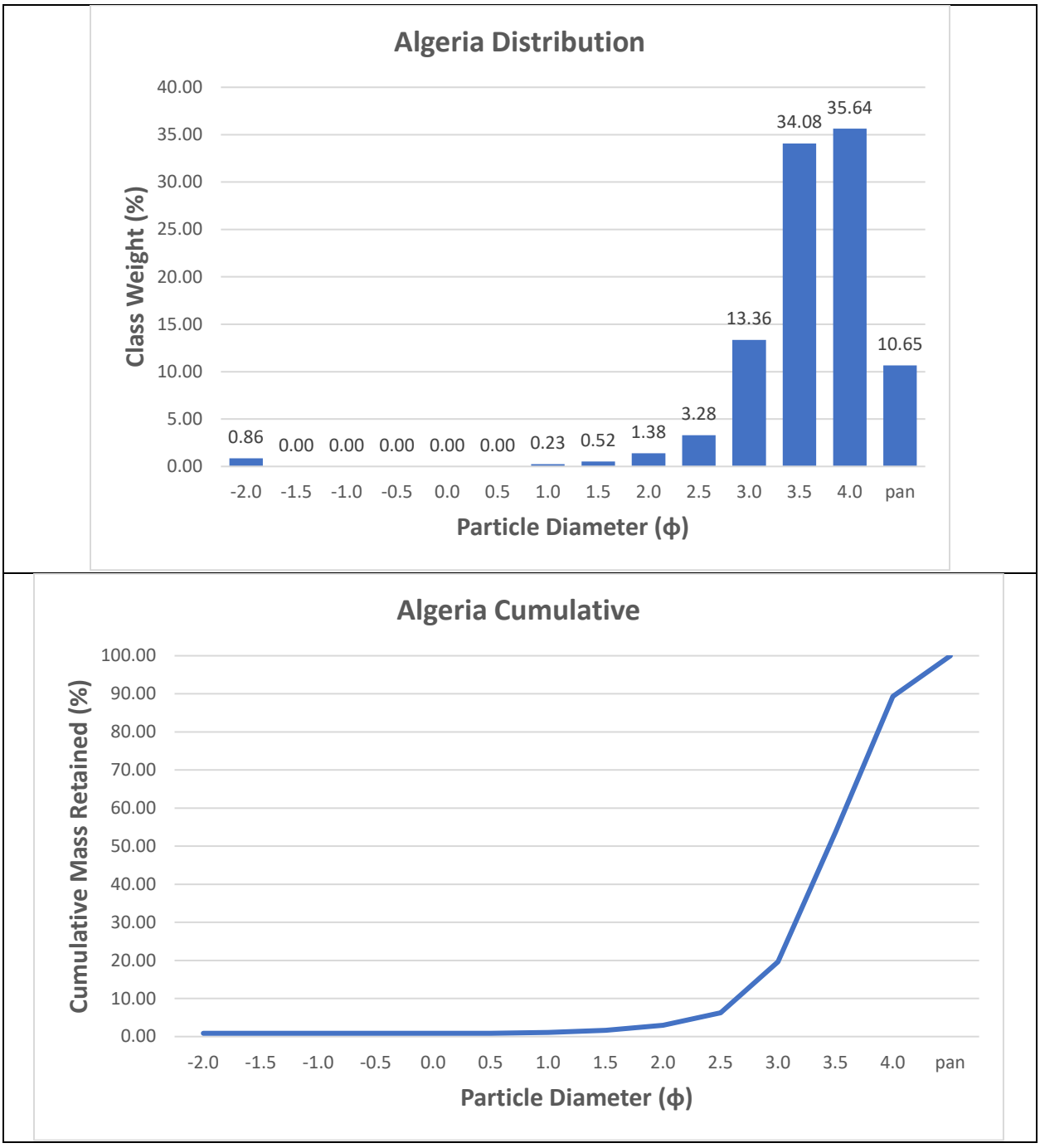
Algeria Distribution
Class Weight (%)
40.00
35.00
30.00
25.00
20.00
15.00
10.00
5.00
0.00
0.86
0.00
0.00
0.00
0.00
0.00
0.23
0.52
1.38
3.28
13.36
34.08
35.64
10.65
-2.0
-1.5
-1.0
-0.5
0.0
0.5
1.0
1.5
2.0
2.5
3.0
3.5
4.0
pan
Particle Diameter (ϕ)
Algeria Cumulative
Cumulative Mass Retained (%)
100.00
90.00
80.00
70.00
60.00
50.00
40.00
30.00
20.00
10.00
0.00
-2.0
-1.5
-1.0
-0.5
0.0
0.5
1.0
1.5
2.0
2.5
3.0
3.5
4.0
pan
Particle Diameter (ϕ)

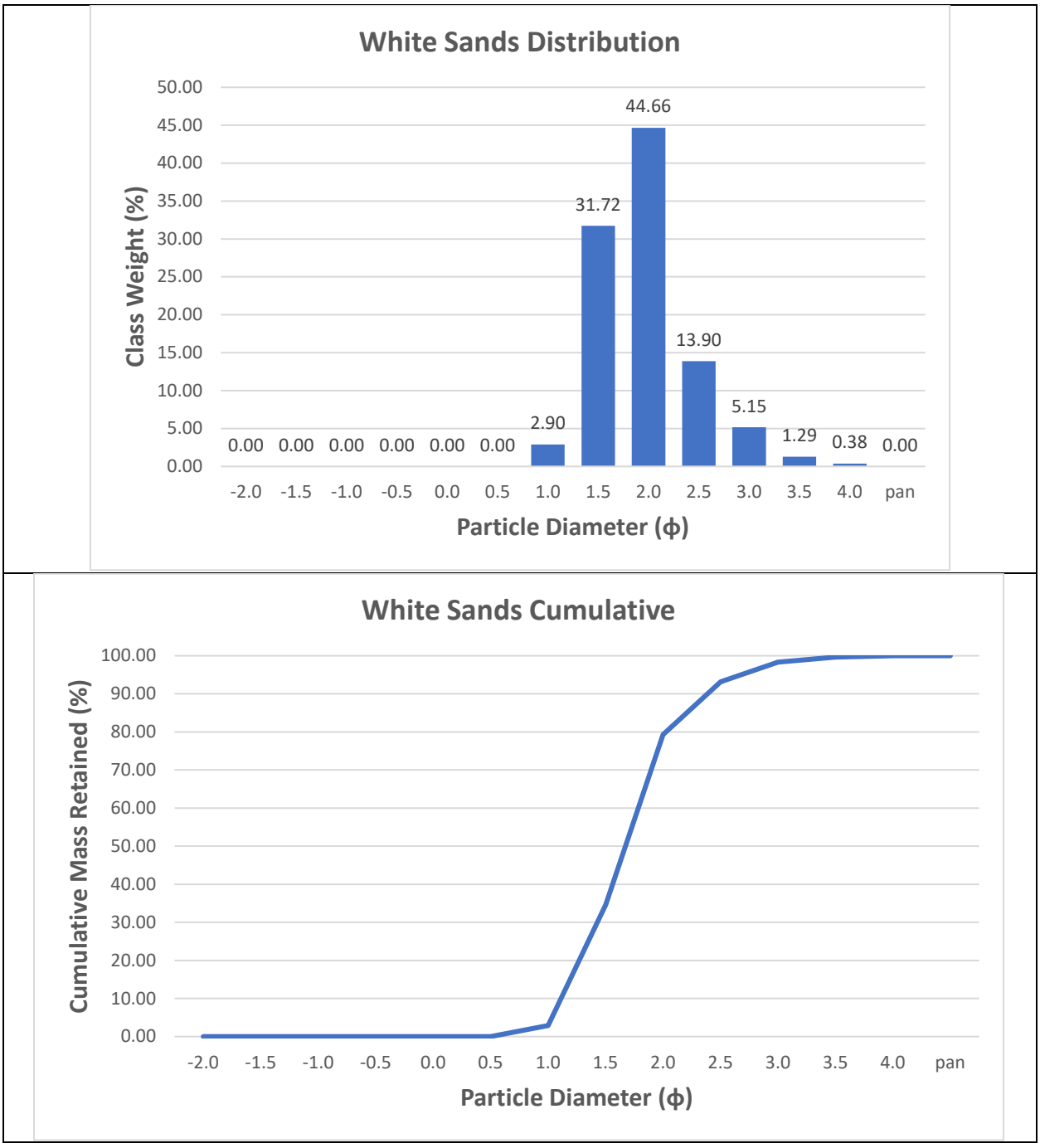
White Sands Distribution
Class Weight (%)
50.00
45.00
40.00
35.00
30.00
25.00
20.00
15.00
10.00
5.00
0.00
0.00 0.00 0.00 0.00 0.00 0.00 2.90 31.72 44.66 13.90 5.15 1.29 0.38 0.00
-2.0 -1.5 -1.0 -0.5 0.0 0.5 1.0 1.5 2.0 2.5 3.0 3.5 4.0 pan
Particle Diameter (ϕ)
White Sands Cumulative
Cumulative Mass Retained (%)
100.00
90.00
80.00
70.00
60.00
50.00
40.00
30.00
20.00
10.00
0.00
-2.0 -1.5 -1.0 -0.5 0.0 0.5 1.0 1.5 2.0 2.5 3.0 3.5 4.0 pan
Particle Diameter (ϕ)

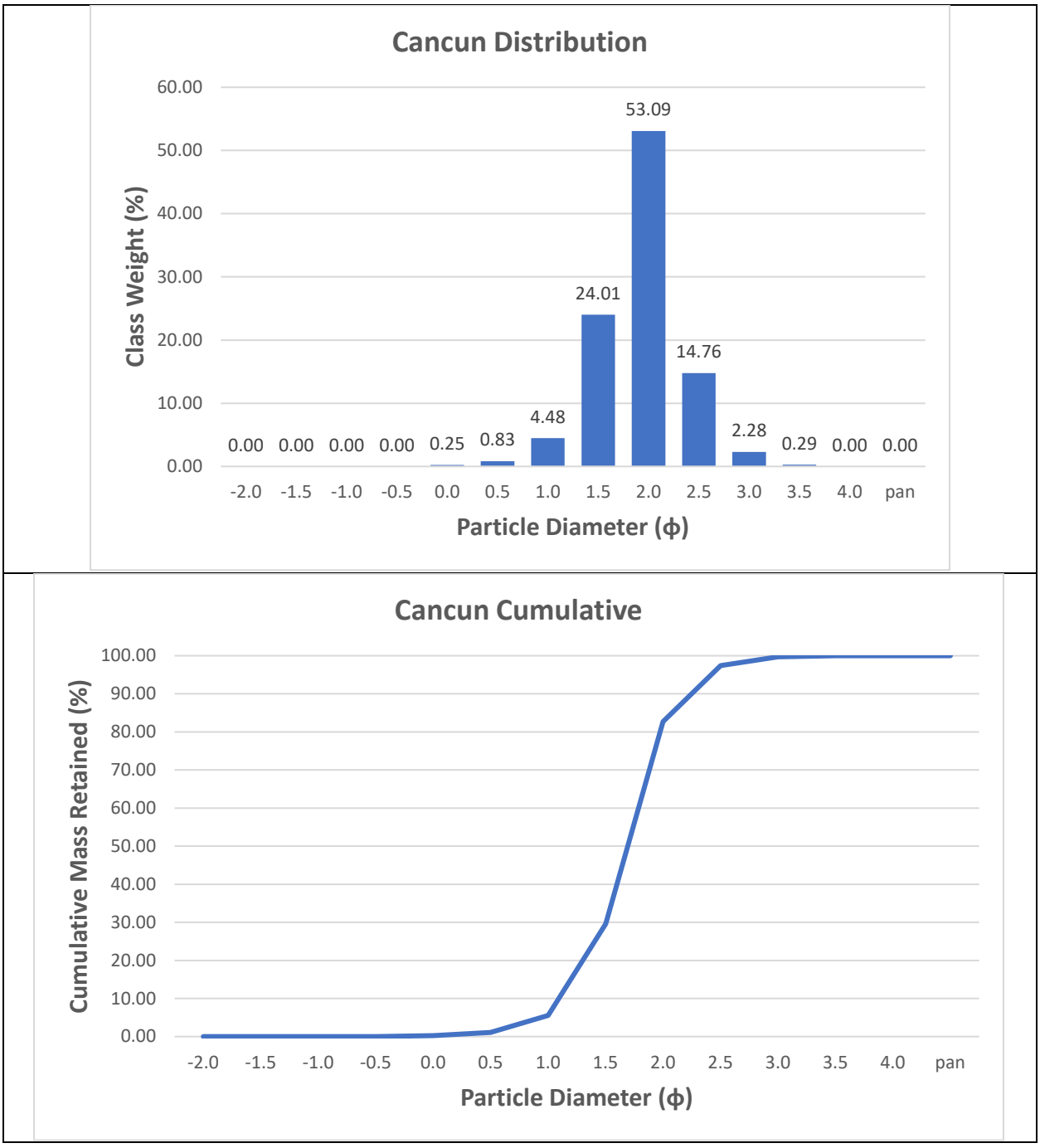
Cancun Distribution
Class Weight (%)
60.00
50.00
40.00
30.00
20.00
10.00
0.00
0.00
0.00
0.00
0.00
0.25
0.83
4.48
24.01
53.09
14.76
2.28
0.29
0.00
0.00
-2.0
-1.5
-1.0
-0.5
0.0
0.5
1.0
1.5
2.0
2.5
3.0
3.5
4.0
pan
Particle Diameter (ϕ)
Cancun Cumulative
Cumulative Mass Retained (%)
100.00
90.00
80.00
70.00
60.00
50.00
40.00
30.00
20.00
10.00
0.00
-2.0
-1.5
-1.0
-0.5
0.0
0.5
1.0
1.5
2.0
2.5
3.0
3.5
4.0
pan
Particle Diameter (ϕ)

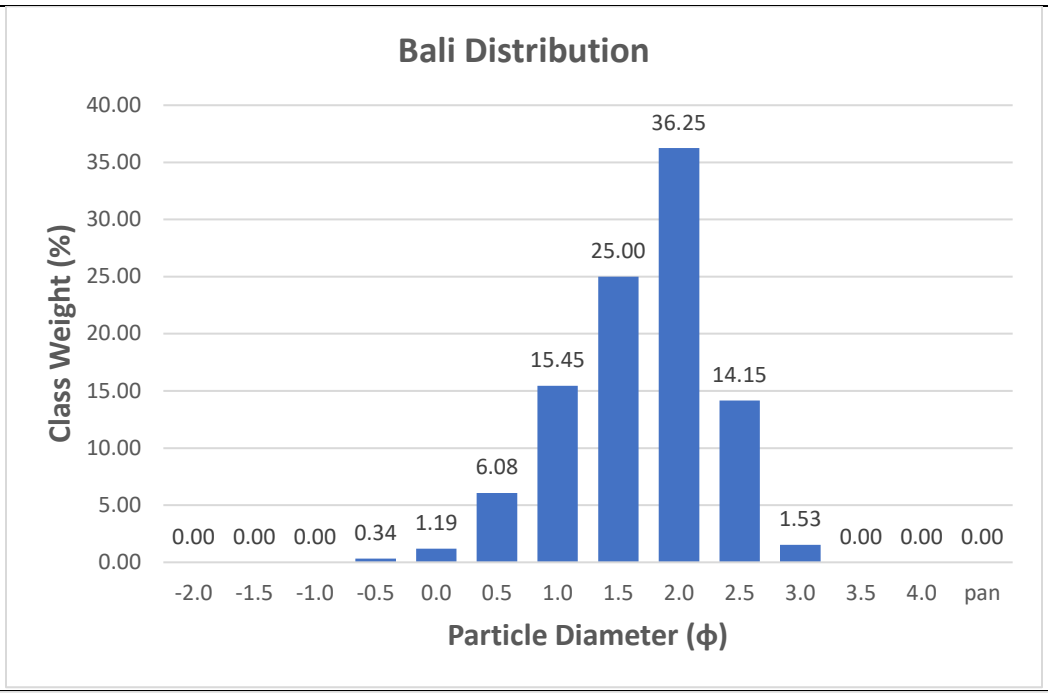
Bali Distribution
Class Weight (%)
40.00
35.00
30.00
25.00
20.00
15.00
10.00
5.00
0.00
0.00
0.00
0.00
0.34
1.19
6.08
15.45
25.00
36.25
14.15
1.53
0.00
0.00
0.00
-2.0
-1.5
-1.0
-0.5
0.0
0.5
1.0
1.5
2.0
2.5
3.0
3.5
4.0
pan
Particle Diameter (ϕ)

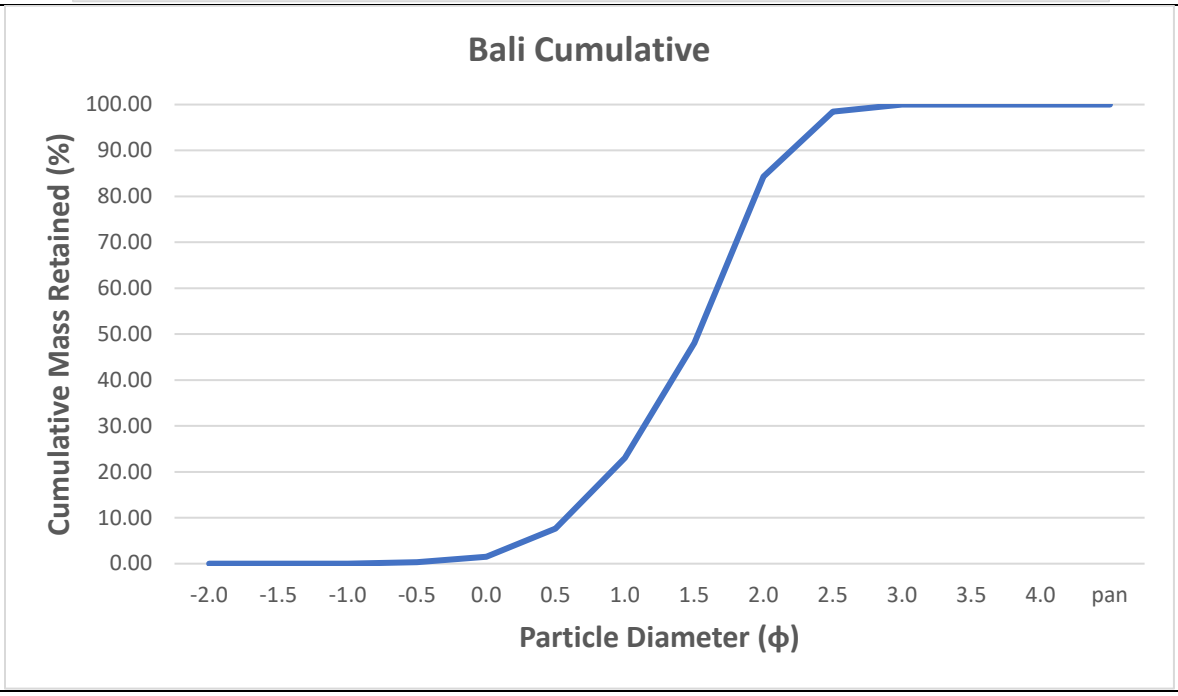
Bali Cumulative
Cumulative Mass Retained (%)
100.00
90.00
80.00
70.00
60.00
50.00
40.00
30.00
20.00
10.00
0.00
-2.0
-1.5
-1.0
-0.5
0.0
0.5
1.0
1.5
2.0
2.5
3.0
3.5
4.0
pan
Particle Diameter (ϕ)

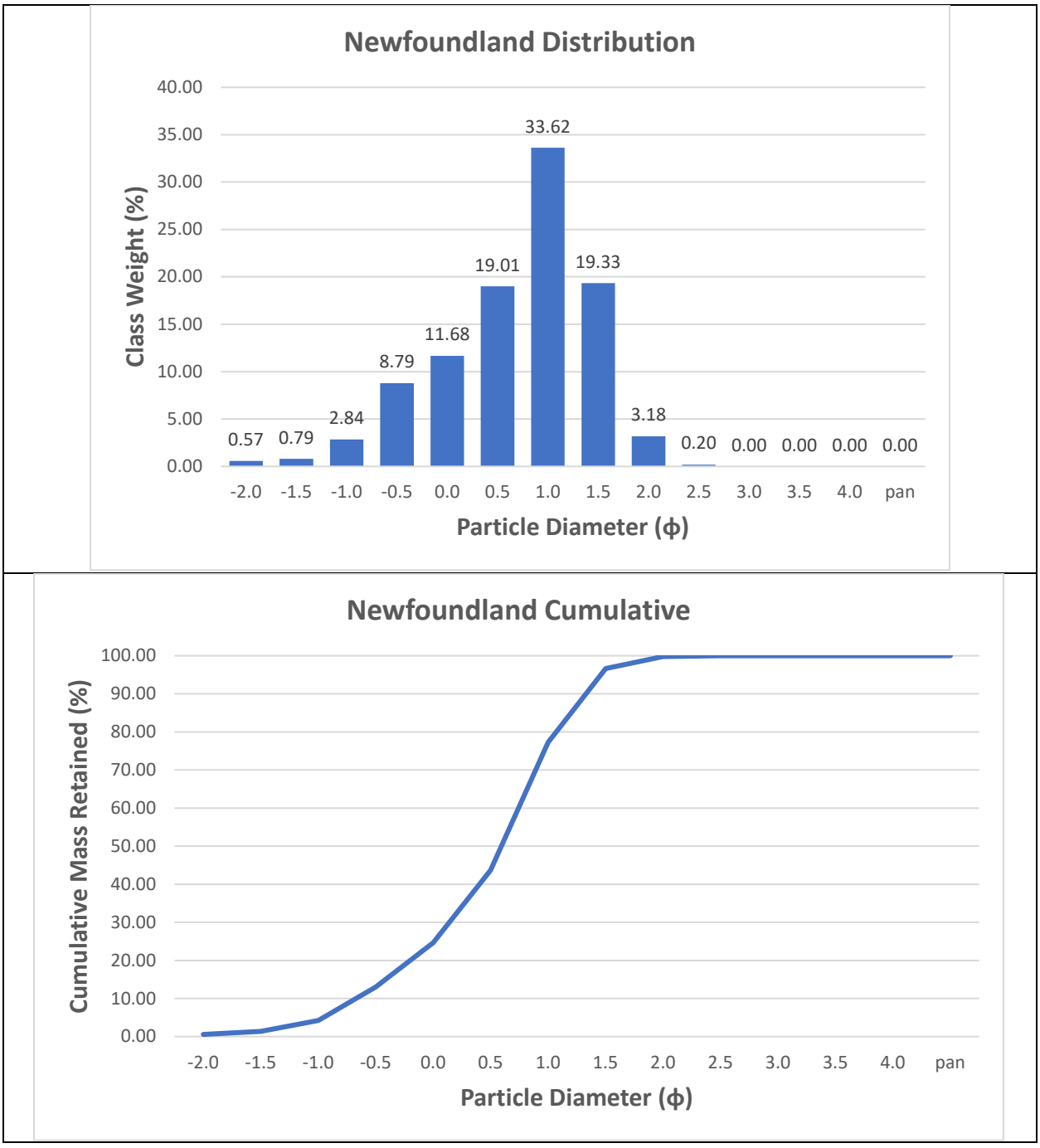
Newfoundland Distribution
Class Weight (%)
40.00
35.00
30.00
25.00
20.00
15.00
10.00
5.00
0.00
0.57
0.79
2.84
8.79
11.68
19.01
33.62
19.33
3.18
0.20
0.00
0.00
0.00
0.00
-2.0
-1.5
-1.0
-0.5
0.0
0.5
1.0
1.5
2.0
2.5
3.0
3.5
4.0
pan
Particle Diameter (ϕ)
Newfoundland Cumulative
Cumulative Mass Retained (%)
100.00
90.00
80.00
70.00
60.00
50.00
40.00
30.00
20.00
10.00
0.00
-2.0
-1.5
-1.0
-0.5
0.0
0.5
1.0
1.5
2.0
2.5
3.0
3.5
4.0
pan
Particle Diameter (ϕ)

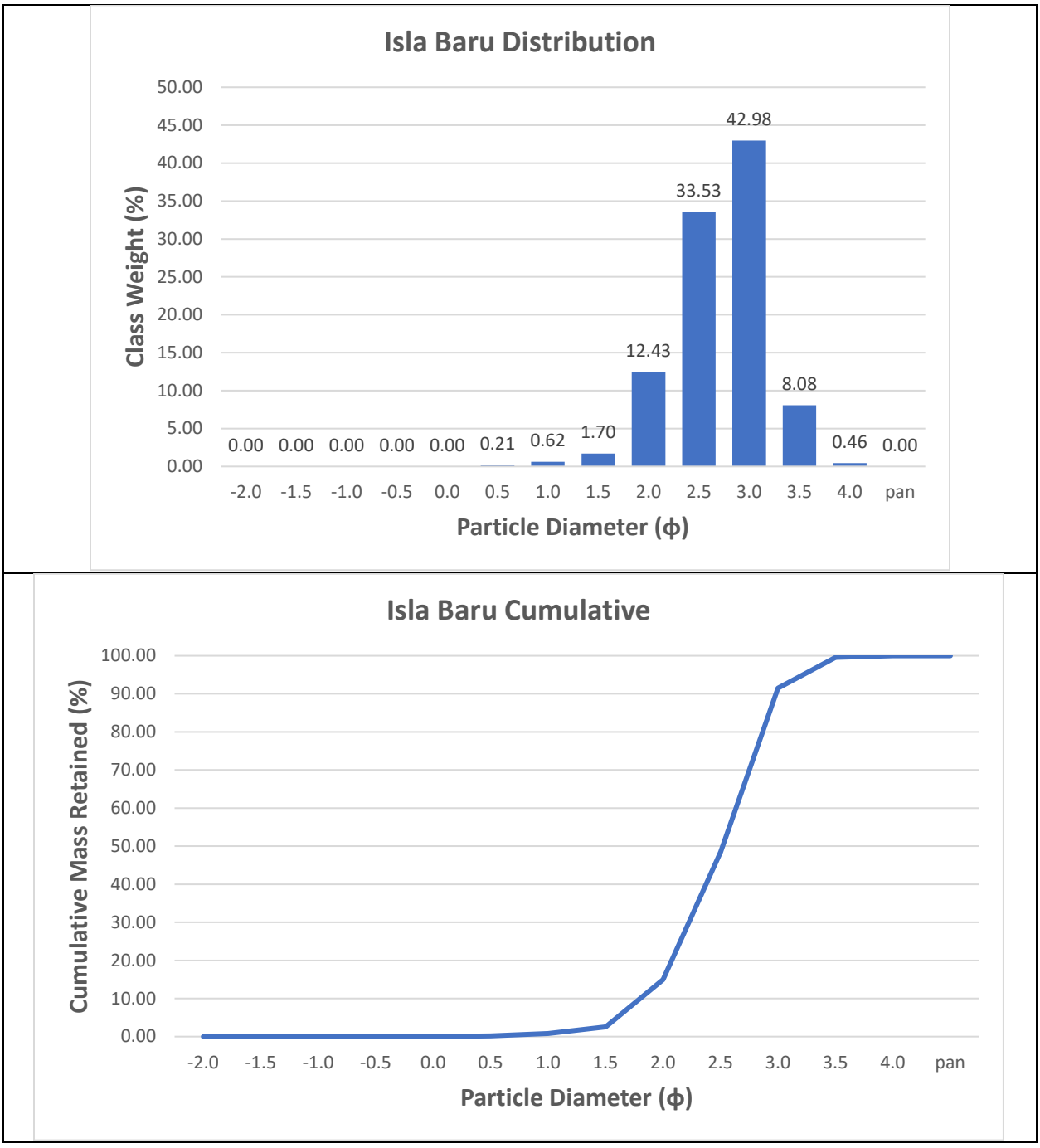
Isla Baru Distribution
Class Weight (%)
50.00
45.00
40.00
35.00
30.00
25.00
20.00
15.00
10.00
5.00
0.00
0.00 0.00 0.00 0.00 0.00 0.21 0.62 1.70 12.43 33.53 42.98 8.08 0.46 0.00
-2.0 -1.5 -1.0 -0.5 0.0 0.5 1.0 1.5 2.0 2.5 3.0 3.5 4.0 pan
Particle Diameter (ϕ)
Isla Baru Cumulative
Cumulative Mass Retained (%)
100.00
90.00
80.00
70.00
60.00
50.00
40.00
30.00
20.00
10.00
0.00
-2.0 -1.5 -1.0 -0.5 0.0 0.5 1.0 1.5 2.0 2.5 3.0 3.5 4.0 pan
Particle Diameter (ϕ)

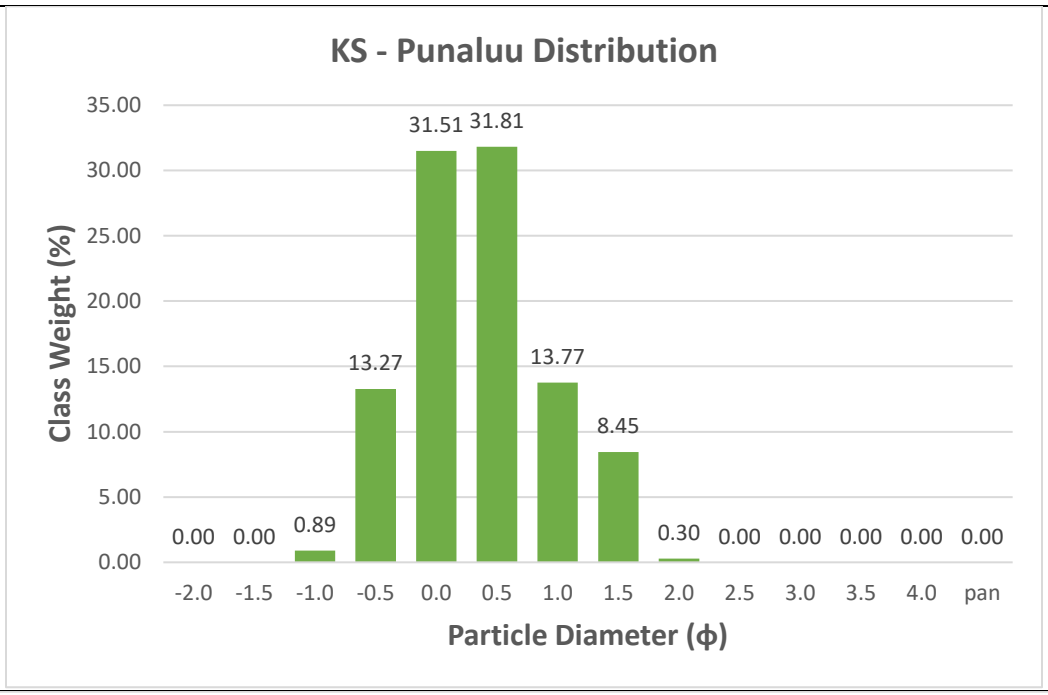
KS - Punaluu Distribution
Class Weight (%)
35.00
30.00
25.00
20.00
15.00
10.00
5.00
0.00
0.00
0.00
0.89
13.27
31.51
31.81
13.77
8.45
0.30
0.00
0.00
0.00
0.00
0.00
-2.0
-1.5
-1.0
-0.5
0.0
0.5
1.0
1.5
2.0
2.5
3.0
3.5
4.0
pan
Particle Diameter (ϕ)

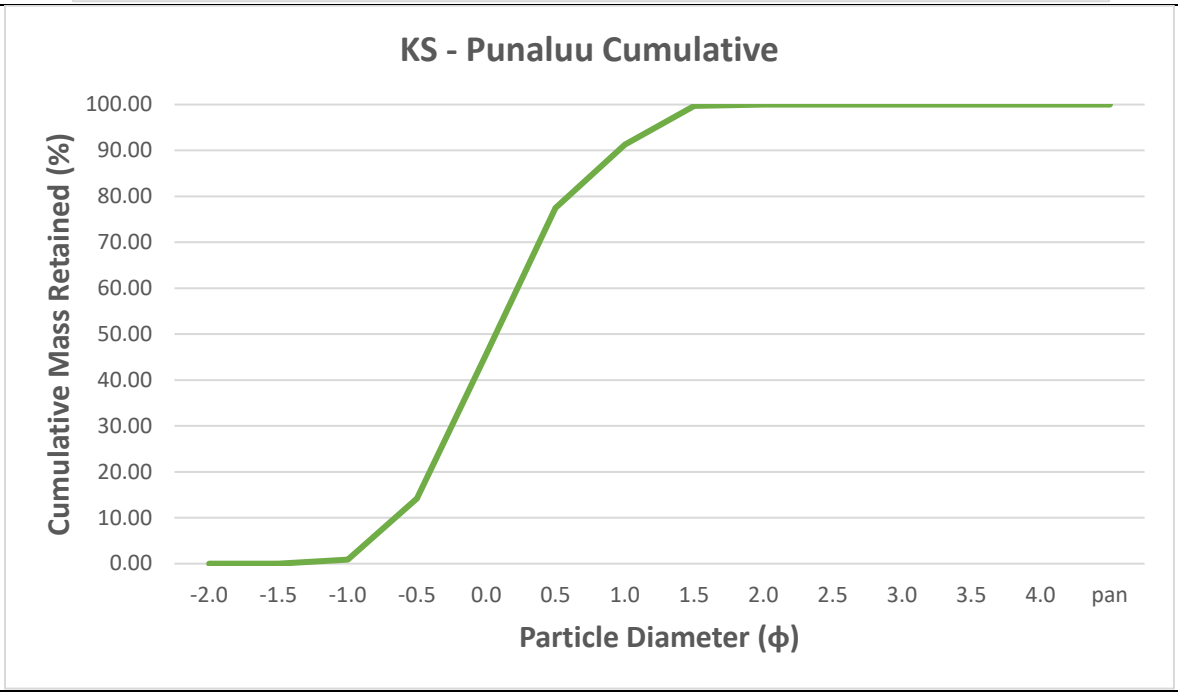
KS - Punaluu Cumulative
Cumulative Mass Retained (%)
100.00
90.00
80.00
70.00
60.00
50.00
40.00
30.00
20.00
10.00
0.00
-2.0
-1.5
-1.0
-0.5
0.0
0.5
1.0
1.5
2.0
2.5
3.0
3.5
4.0
pan
Particle Diameter (ϕ)

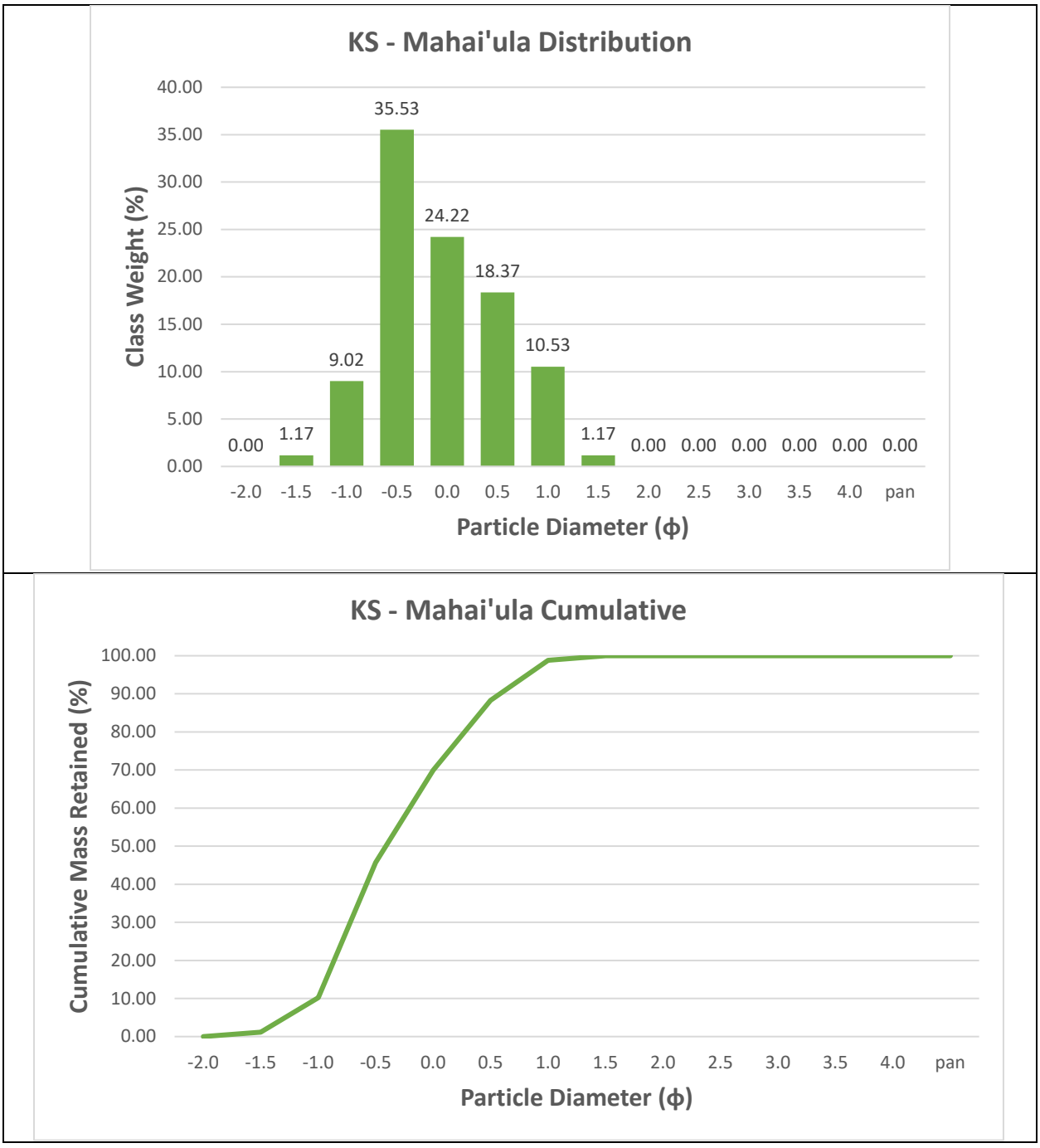
KS - Mahai'ula Distribution
Class Weight (%)
40.00
35.00
30.00
25.00
20.00
15.00
10.00
5.00
0.00
0.00
1.17
9.02
35.53
24.22
18.37
10.53
1.17
0.00
0.00
0.00
0.00
0.00
0.00
-2.0
-1.5
-1.0
-0.5
0.0
0.5
1.0
1.5
2.0
2.5
3.0
3.5
4.0
pan
Particle Diameter (ϕ)
KS - Mahai'ula Cumulative
Cumulative Mass Retained (%)
100.00
90.00
80.00
70.00
60.00
50.00
40.00
30.00
20.00
10.00
0.00
-2.0
-1.5
-1.0
-0.5
0.0
0.5
1.0
1.5
2.0
2.5
3.0
3.5
4.0
pan
Particle Diameter (ϕ)

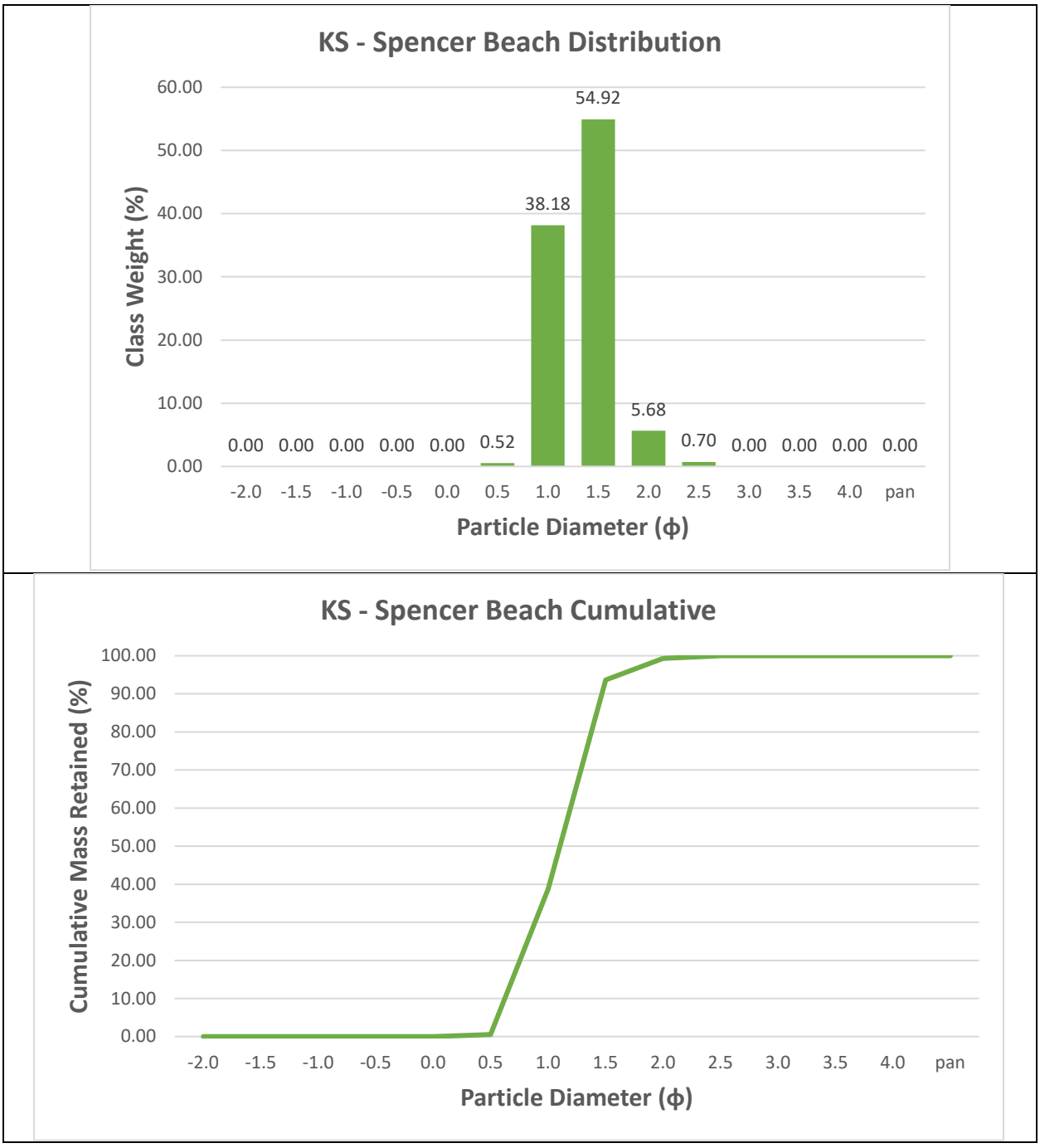
KS - Spencer Beach Distribution
Class Weight (%)
60.00
50.00
40.00
30.00
20.00
10.00
0.00
0.00 0.00 0.00 0.00 0.00 0.52 38.18 54.92 5.68 0.70 0.00 0.00 0.00 0.00
-2.0 -1.5 -1.0 -0.5 0.0 0.5 1.0 1.5 2.0 2.5 3.0 3.5 4.0 pan
Particle Diameter (ϕ)
KS - Spencer Beach Cumulative
Cumulative Mass Retained (%)
100.00
90.00
80.00
70.00
60.00
50.00
40.00
30.00
20.00
10.00
0.00
-2.0 -1.5 -1.0 -0.5 0.0 0.5 1.0 1.5 2.0 2.5 3.0 3.5 4.0 pan
Particle Diameter (ϕ)

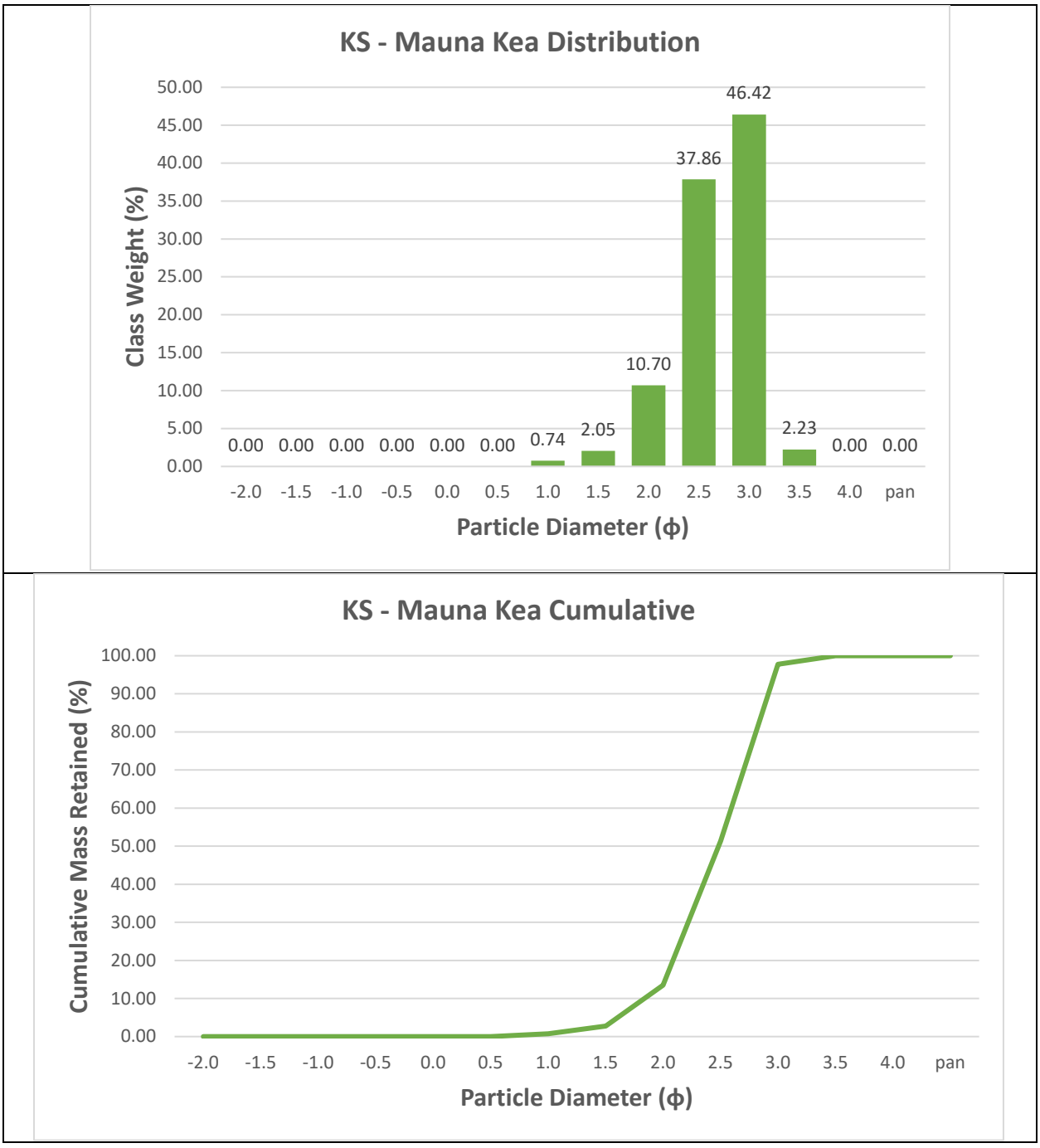
KS - Mauna Kea Distribution
Class Weight (%)
50.00
45.00
40.00
35.00
30.00
25.00
20.00
15.00
10.00
5.00
0.00
0.00 0.00 0.00 0.00 0.00 0.00 0.74 2.05 10.70 37.86 46.42 2.23 0.00 0.00
-2.0 -1.5 -1.0 -0.5 0.0 0.5 1.0 1.5 2.0 2.5 3.0 3.5 4.0 pan
Particle Diameter (ϕ)
KS - Mauna Kea Cumulative
Cumulative Mass Retained (%)
100.00
90.00
80.00
70.00
60.00
50.00
40.00
30.00
20.00
10.00
0.00
-2.0 -1.5 -1.0 -0.5 0.0 0.5 1.0 1.5 2.0 2.5 3.0 3.5 4.0 pan
Particle Diameter (ϕ)

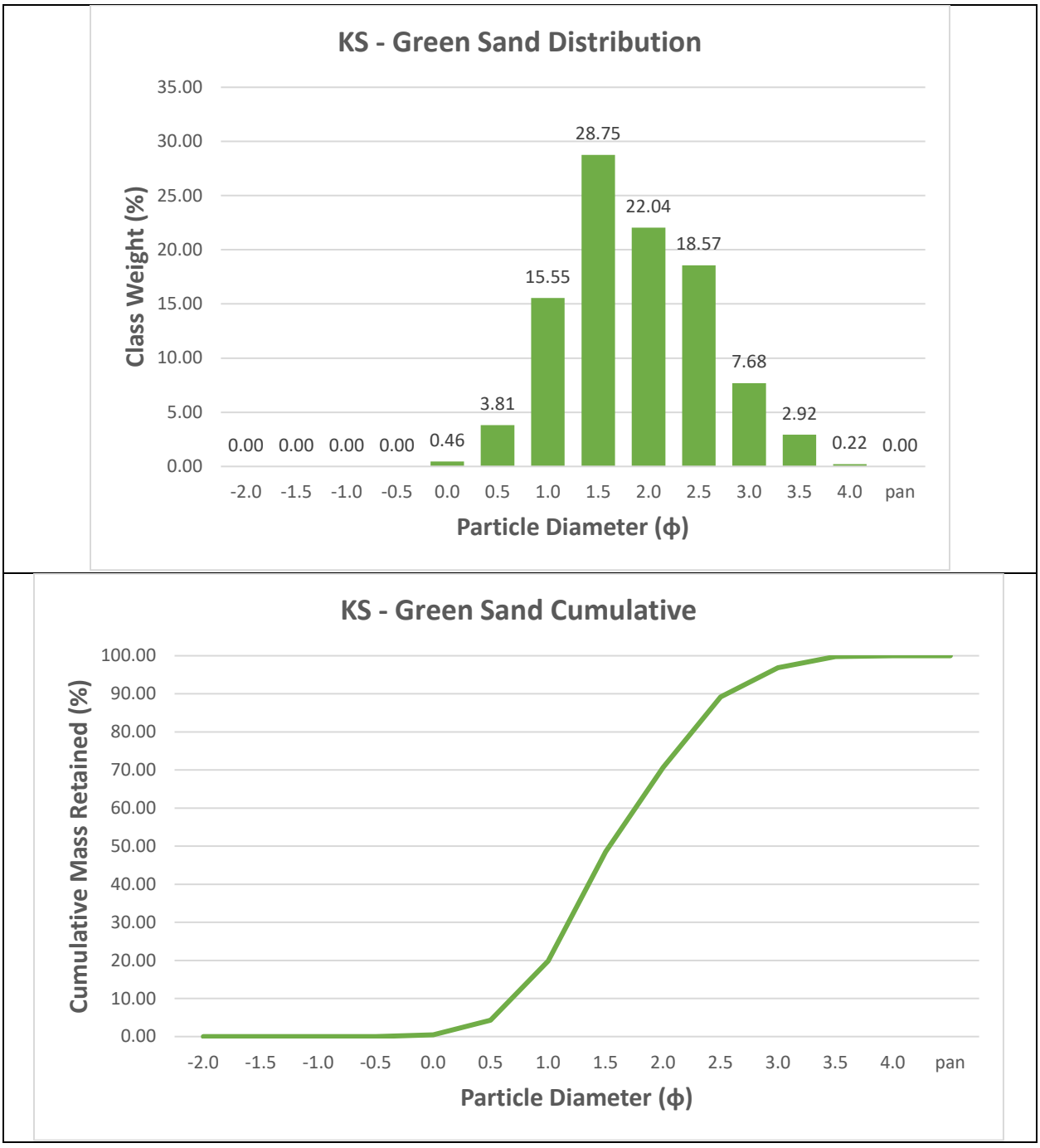
KS - Green Sand Distribution
Class Weight (%)
35.00
30.00
25.00
20.00
15.00
10.00
5.00
0.00
0.00 0.00 0.00 0.00 0.46 3.81 15.55 28.75 22.04 18.57 7.68 2.92 0.22 0.00
-2.0 -1.5 -1.0 -0.5 0.0 0.5 1.0 1.5 2.0 2.5 3.0 3.5 4.0 pan
Particle Diameter (ϕ)
KS - Green Sand Cumulative
Cumulative Mass Retained (%)
100.00
90.00
80.00
70.00
60.00
50.00
40.00
30.00
20.00
10.00
0.00
-2.0 -1.5 -1.0 -0.5 0.0 0.5 1.0 1.5 2.0 2.5 3.0 3.5 4.0 pan
Particle Diameter (ϕ)

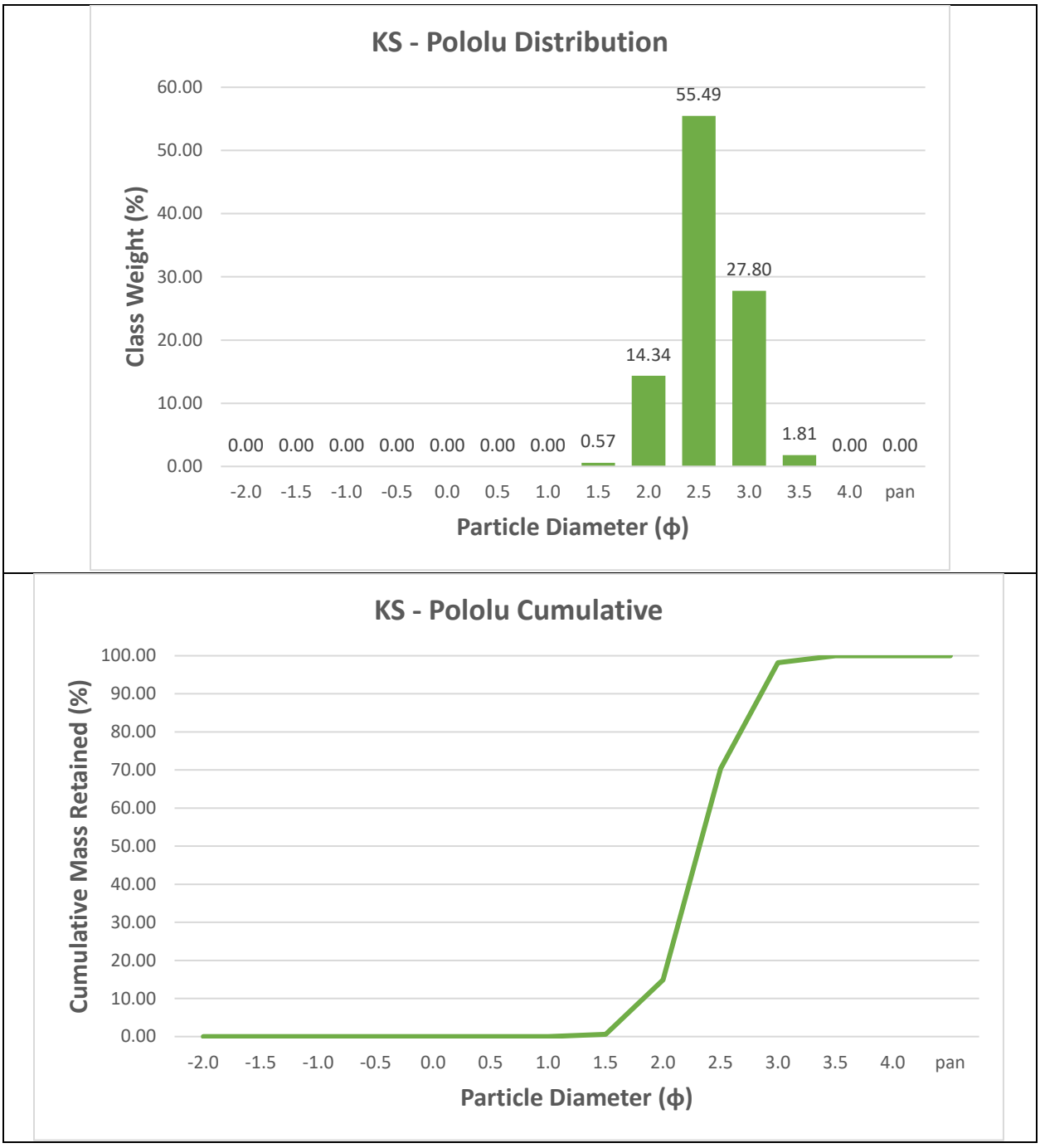
KS - Pololu Distribution
Class Weight (%)
60.00
50.00
40.00
30.00
20.00
10.00
0.00
0.00 0.00 0.00 0.00 0.00 0.00 0.00 0.57 14.34 55.49 27.80 1.81 0.00 0.00
-2.0 -1.5 -1.0 -0.5 0.0 0.5 1.0 1.5 2.0 2.5 3.0 3.5 4.0 pan
Particle Diameter (ϕ)
KS - Pololu Cumulative
Cumulative Mass Retained (%)
100.00
90.00
80.00
70.00
60.00
50.00
40.00
30.00
20.00
10.00
0.00
-2.0 -1.5 -1.0 -0.5 0.0 0.5 1.0 1.5 2.0 2.5 3.0 3.5 4.0 pan
Particle Diameter (ϕ)

Appendix D – The results from running each of the 116 survey points at all 18 beaches with associated labels, distance from water, slope, calculated percentile in mm and ϕ, statistical moments and descriptors, distribution and cumulative curve graphs, and elevation profiles.

Beach Name: Mahai'ula Beach

Date: 10/19/2020 **Time:** 1:52 PM

Location/ Transect	Survey #	Distance from Water (m)	Slope in Degrees	"x" used	Calculated mm percentile							
					5	10	16	25	50	75	84	90	95
A1	1	4.27	-5	8	5.3087	5.2759	5.2329	5.1642	4.9279	4.5509	4.3262	4.1028	3.7915
	2	9.75	-10	6.8	4.0626	4.0297	3.9867	3.9180	3.6817	3.3081	3.0887	2.8749	2.5889
A2	1	4.88	-7	6	4.1990	4.1584	4.1069	4.0235	3.7387	3.3039	3.0570	2.8207	2.5102
	2	6.10	-7	5.5	3.7154	3.6728	3.6194	3.5327	3.2428	2.8143	2.5750	2.3479	2.0489
A3	1	1.52	-9	8	5.8528	5.8163	5.7685	5.6919	5.4251	4.9990	4.7443	4.4899	4.1443
	2	4.93	-6	7	5.3981	5.3586	5.3081	5.2271	4.9471	4.5050	4.2437	3.9841	3.6325
	3	6.81	-7	6.8	3.9330	3.9024	3.8626	3.7990	3.5806	3.2379	3.0362	2.8394	2.5730
	4	8.33	-7	6.1	5.2491	5.2000	5.1384	5.0391	4.7042	4.1968	3.9062	3.6246	3.2461
	5	10.49	-12	6	4.3523	4.3108	4.2580	4.1732	3.8836	3.4312	3.1641	2.9034	2.5627
	6	12.19	-17	6	4.4720	4.4285	4.3737	4.2848	3.9822	3.5133	3.2424	2.9818	2.6369
	7	14.63	-6										
A4	1	1.52	-7	4	4.1747	4.1082	4.0249	3.8915	3.4499	2.8163	2.4770	2.1662	1.7807
	2	8.53	-12	4	4.0398	3.9762	3.8967	3.7689	3.3470	2.7431	2.4185	2.1240	1.7673
	3	10.36	-6	4	3.7641	3.7070	3.6356	3.5214	3.1401	2.5779	2.2725	1.9943	1.6466
A5	1	2.13	-6	6	4.8002	4.7531	4.6937	4.5965	4.2643	3.7503	3.4552	3.1715	2.7977
	2	4.27	-5	6	4.0626	4.0236	3.9738	3.8937	3.6197	3.1991	2.9590	2.7306	2.4273
B1	1	3.05	-9	5.5	3.3656	3.3283	3.2801	3.2036	2.9450	2.5548	2.3322	2.1209	1.8487
	2	4.57	-10	5.5	1.7476	1.7290	1.7056	1.6681	1.5414	1.3509	1.2427	1.1393	1.0039

Calculated ϕ percentiles with corrections								
5	10	16	25	50	75	84	90	95
-3.882	-3.839	-3.569	-3.316	-2.416	-1.902	-1.636	-1.527	-1.265
-3.260	-3.217	-2.983	-2.758	-1.974	-1.502	-1.259	-1.143	-0.903
-3.337	-3.290	-3.047	-2.812	-1.998	-1.500	-1.248	-1.122	-0.874
-3.052	-3.003	-2.774	-2.549	-1.782	-1.299	-1.056	-0.924	-0.681
-4.109	-4.064	-3.780	-3.512	-2.562	-2.020	-1.739	-1.625	-1.350
-3.921	-3.875	-3.600	-3.340	-2.422	-1.889	-1.614	-1.496	-1.225
-3.185	-3.143	-2.915	-2.696	-1.932	-1.475	-1.240	-1.129	-0.897
-3.856	-3.806	-3.530	-3.266	-2.346	-1.800	-1.522	-1.393	-1.118
-3.420	-3.373	-3.125	-2.886	-2.055	-1.547	-1.286	-1.153	-0.893
-3.483	-3.435	-3.183	-2.939	-2.093	-1.577	-1.314	-1.182	-0.920
-3.323	-3.262	-3.003	-2.744	-1.876	-1.300	-1.013	-0.836	-0.548
-3.247	-3.186	-2.934	-2.680	-1.830	-1.267	-0.986	-0.815	-0.541
-3.083	-3.024	-2.784	-2.543	-1.733	-1.189	-0.917	-0.747	-0.473
-3.648	-3.598	-3.335	-3.081	-2.197	-1.659	-1.385	-1.249	-0.977
-3.260	-3.214	-2.976	-2.746	-1.949	-1.460	-1.211	-1.087	-0.842
-2.822	-2.776	-2.562	-2.352	-1.636	-1.177	-0.946	-0.813	-0.583
-1.298	-1.264	-1.152	-1.034	-0.655	-0.377	-0.243	-0.141	-0.004

Moments						
Mean	Standard Deviation	*Descriptor*	Skewness	*Descriptor*	Kurtosis	*Descriptor*
-2.540	0.880	Moderately Sorted	-0.157	Coarse Skewed	0.759	Platykurtic
-2.072	0.788	Moderately Sorted	-0.131	Coarse Skewed	0.769	Platykurtic
-2.097	0.823	Moderately Sorted	-0.127	Coarse Skewed	0.770	Platykurtic
-1.871	0.789	Moderately Sorted	-0.113	Coarse Skewed	0.777	Platykurtic
-2.693	0.928	Moderately Sorted	-0.158	Coarse Skewed	0.758	Platykurtic
-2.545	0.905	Moderately Sorted	-0.149	Coarse Skewed	0.762	Platykurtic
-2.029	0.765	Moderately Sorted	-0.134	Coarse Skewed	0.768	Platykurtic
-2.466	0.917	Moderately Sorted	-0.141	Coarse Skewed	0.765	Platykurtic
-2.155	0.843	Moderately Sorted	-0.122	Coarse Skewed	0.774	Platykurtic
-2.196	0.856	Moderately Sorted	-0.125	Coarse Skewed	0.771	Platykurtic
-1.964	0.918	Moderately Sorted	-0.088	Symmetrical	0.787	Platykurtic
-1.917	0.897	Moderately Sorted	-0.090	Symmetrical	0.785	Platykurtic
-1.811	0.862	Moderately Sorted	-0.080	Symmetrical	0.790	Platykurtic
-2.305	0.892	Moderately Sorted	-0.127	Coarse Skewed	0.770	Platykurtic
-2.045	0.808	Moderately Sorted	-0.124	Coarse Skewed	0.771	Platykurtic
-1.715	0.743	Moderately Sorted	-0.103	Coarse Skewed	0.781	Platykurtic
-0.683	0.423	Well Sorted	-0.042	Symmetrical	0.809	Platykurtic

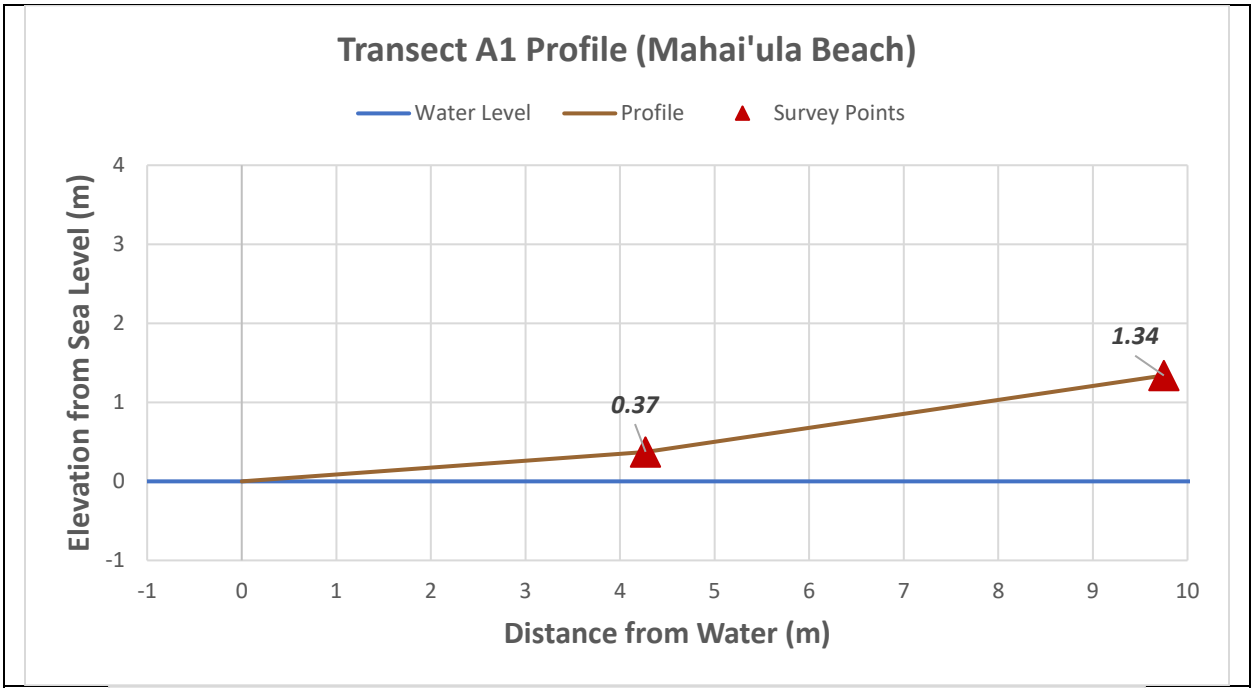
Transect A1 Profile (Mahai'ula Beach)
Water Level
Profile
Survey Points
Elevation from Sea Level (m)
4
3
2
1
0
-1
-1
0
1
2
3
4
5
6
7
8
9
10
0.37
1.34
Distance from Water (m)

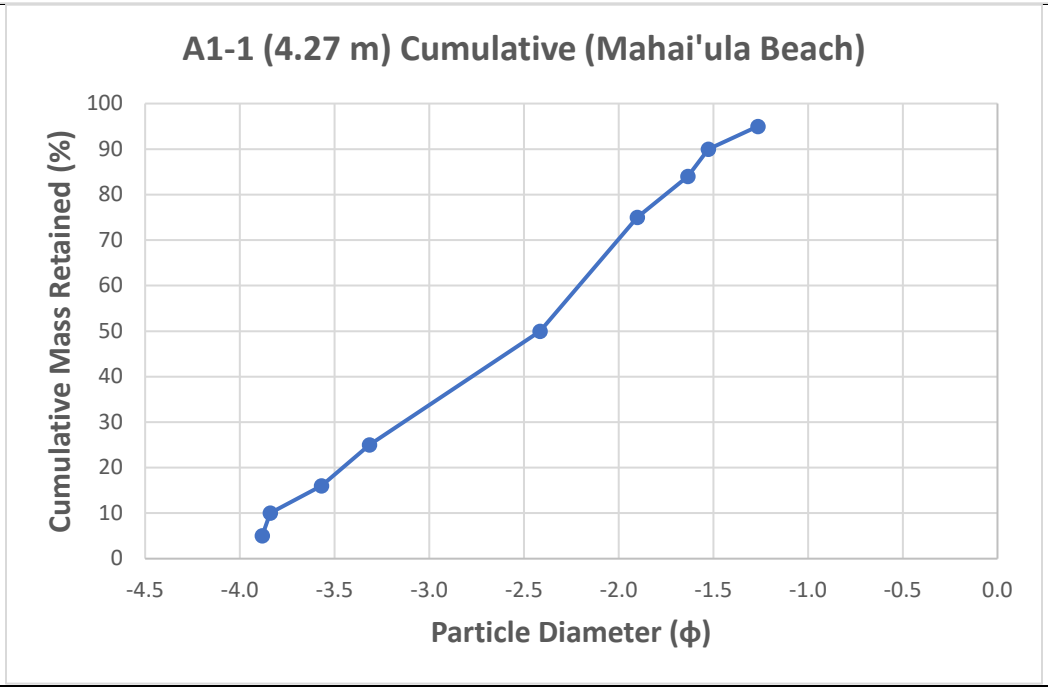
A1-1 (4.27 m) Cumulative (Mahai'ula Beach)
Cumulative Mass Retained (%)
100
90
80
70
60
50
40
30
20
10
0
-4.5
-4.0
-3.5
-3.0
-2.5
-2.0
-1.5
-1.0
-0.5
0.0
Particle Diameter (ϕ)

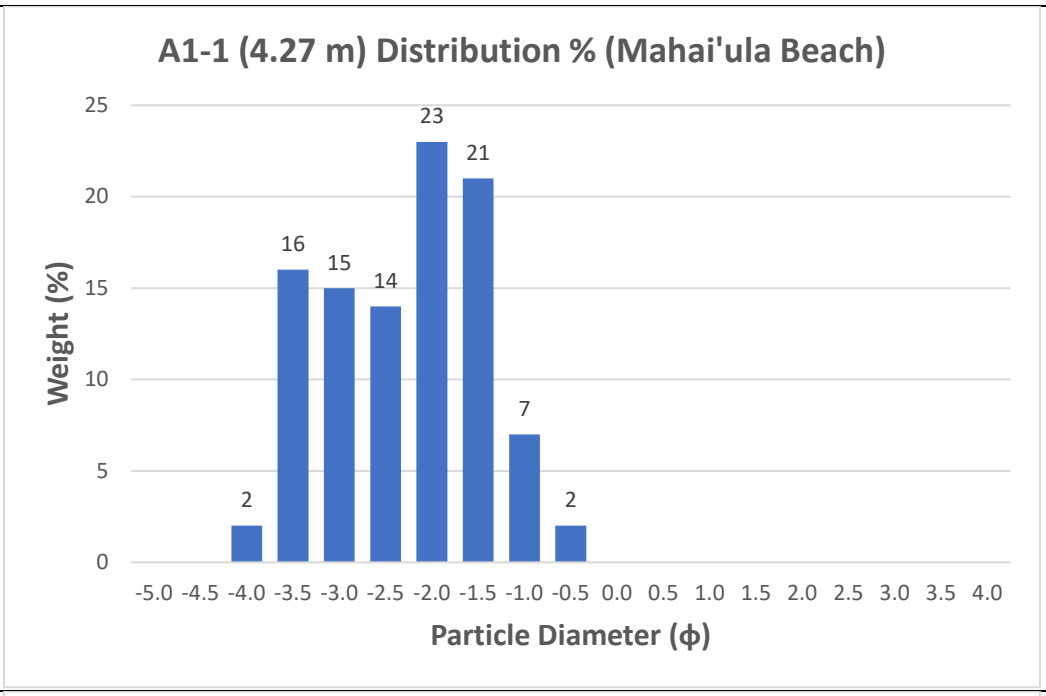
A1-1 (4.27 m) Distribution % (Mahai'ula Beach)
Weight (%)
25
20
15
10
5
0
2
16
15
14
23
21
7
2
-5.0 -4.5 -4.0 -3.5 -3.0 -2.5 -2.0 -1.5 -1.0 -0.5 0.0 0.5 1.0 1.5 2.0 2.5 3.0 3.5 4.0
Particle Diameter (ϕ)

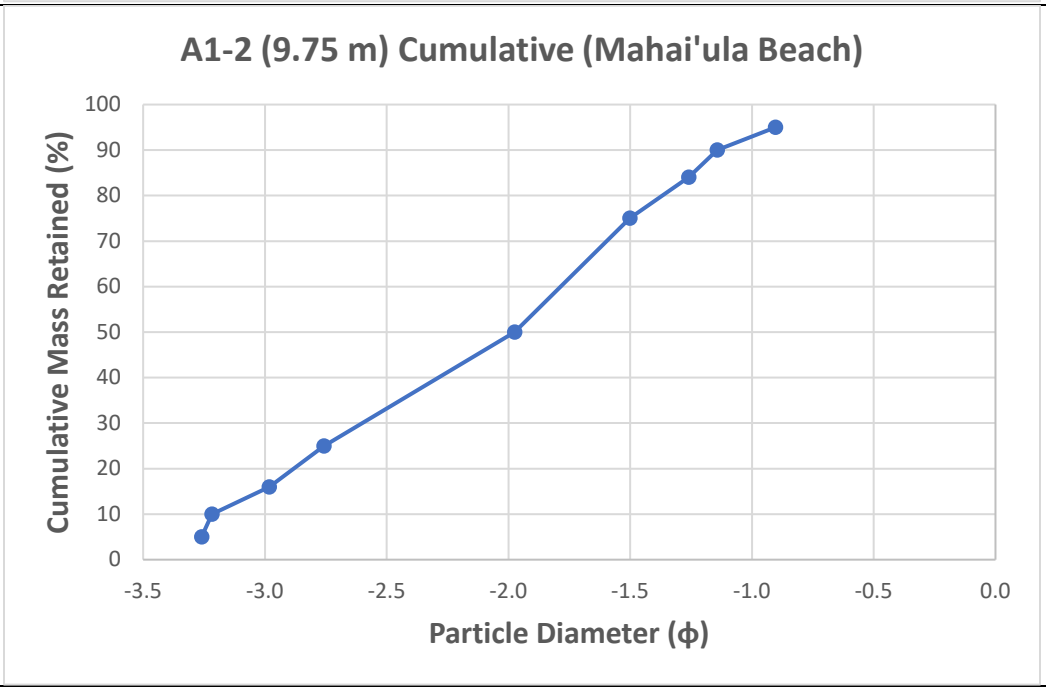
A1-2 (9.75 m) Cumulative (Mahai'ula Beach)
Cumulative Mass Retained (%)
100
90
80
70
60
50
40
30
20
10
0
-3.5
-3.0
-2.5
-2.0
-1.5
-1.0
-0.5
0.0
Particle Diameter (ϕ)

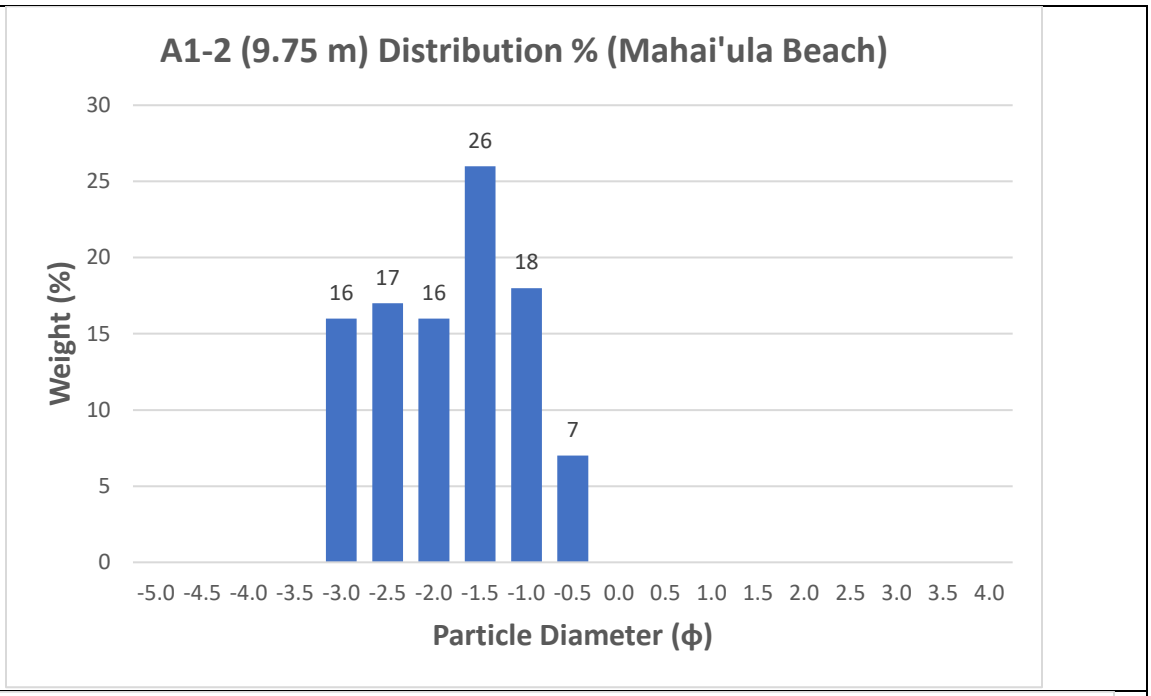
A1-2 (9.75 m) Distribution % (Mahai'ula Beach)
Weight (%)
30
25
20
15
10
5
0
16
17
16
26
18
7
-5.0 -4.5 -4.0 -3.5 -3.0 -2.5 -2.0 -1.5 -1.0 -0.5 0.0 0.5 1.0 1.5 2.0 2.5 3.0 3.5 4.0
Particle Diameter (ϕ)

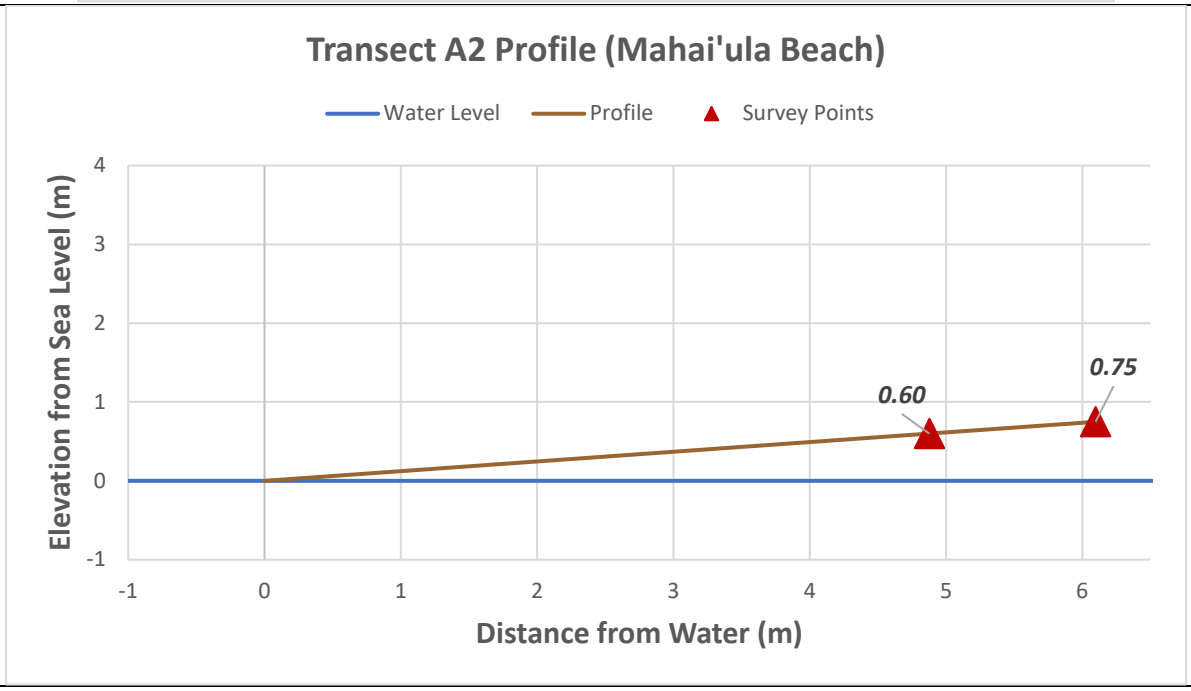
Transect A2 Profile (Mahai'ula Beach)
Water Level
Profile
Survey Points
Elevation from Sea Level (m)
4
3
2
1
0
-1
0.60
0.75
-1 0 1 2 3 4 5 6
Distance from Water (m)

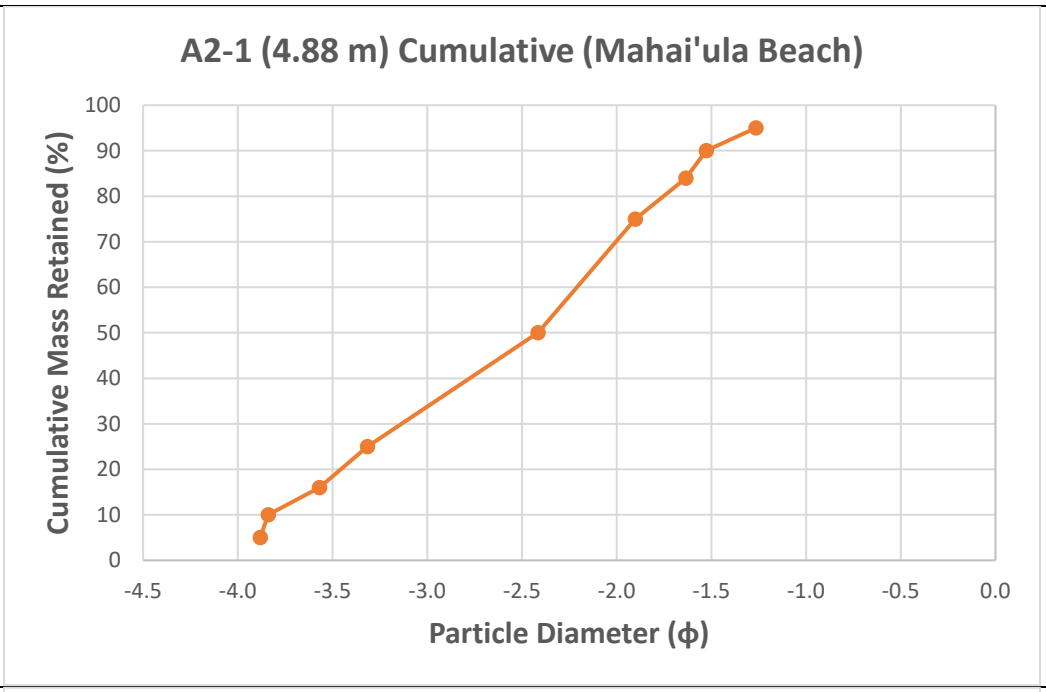
A2-1 (4.88 m) Cumulative (Mahai'ula Beach)
Cumulative Mass Retained (%)
100
90
80
70
60
50
40
30
20
10
0
-4.5
-4.0
-3.5
-3.0
-2.5
-2.0
-1.5
-1.0
-0.5
0.0
Particle Diameter (ϕ)

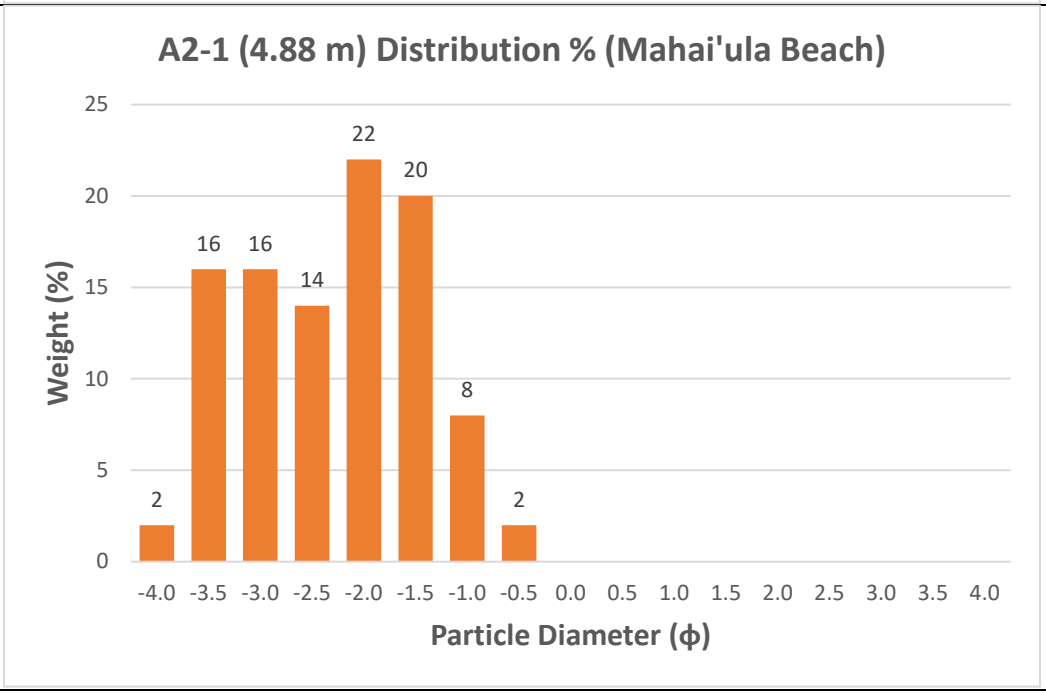
A2-1 (4.88 m) Distribution % (Mahai'ula Beach)
Weight (%)
25
20
15
10
5
0
2
16
16
14
22
20
8
2
-4.0
-3.5
-3.0
-2.5
-2.0
-1.5
-1.0
-0.5
0.0
0.5
1.0
1.5
2.0
2.5
3.0
3.5
4.0
Particle Diameter (ϕ)

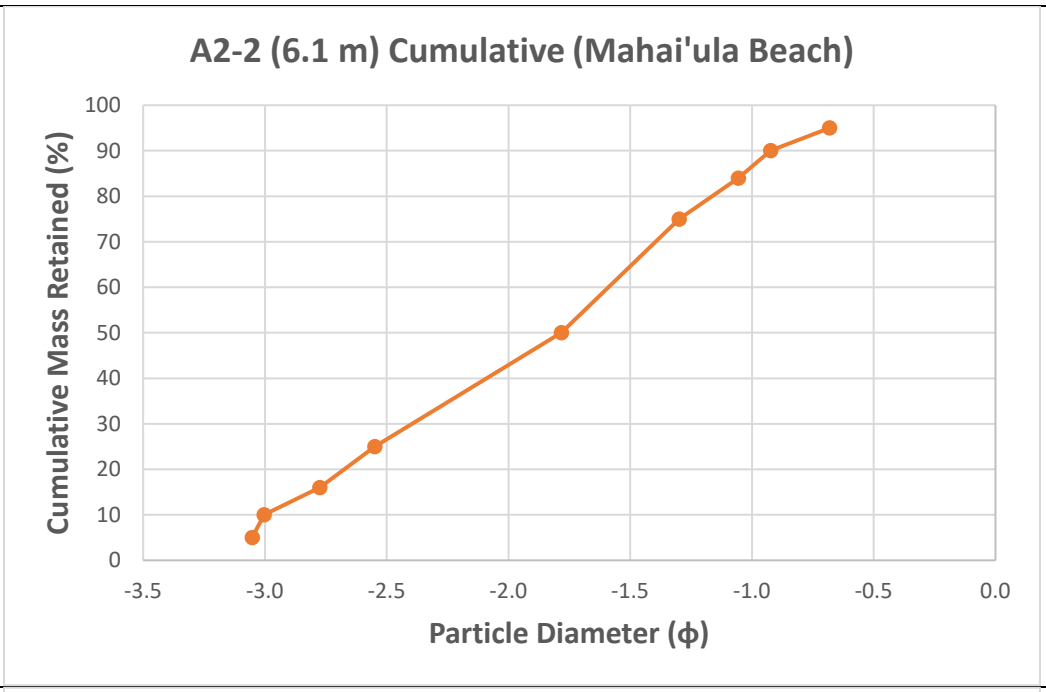
A2-2 (6.1 m) Cumulative (Mahai'ula Beach)
Cumulative Mass Retained (%)
100
90
80
70
60
50
40
30
20
10
0
-3.5
-3.0
-2.5
-2.0
-1.5
-1.0
-0.5
0.0
Particle Diameter (ϕ)

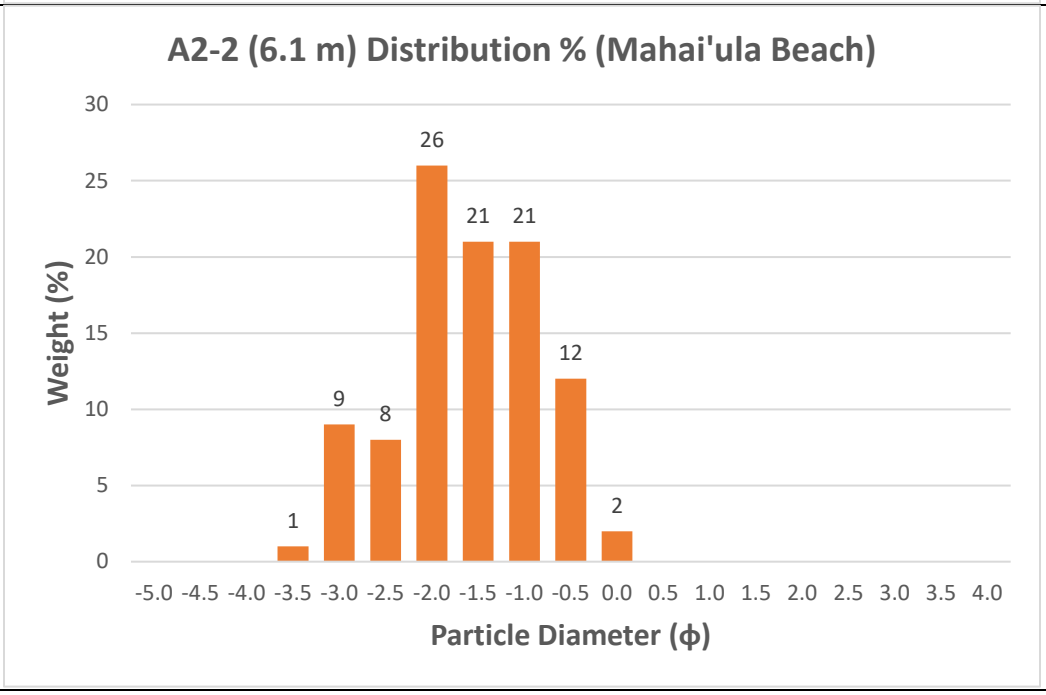
A2-2 (6.1 m) Distribution % (Mahai'ula Beach)
Weight (%)
30
25
20
15
10
5
0
1
9
8
26
21
21
12
2
-5.0 -4.5 -4.0 -3.5 -3.0 -2.5 -2.0 -1.5 -1.0 -0.5 0.0 0.5 1.0 1.5 2.0 2.5 3.0 3.5 4.0
Particle Diameter (ϕ)

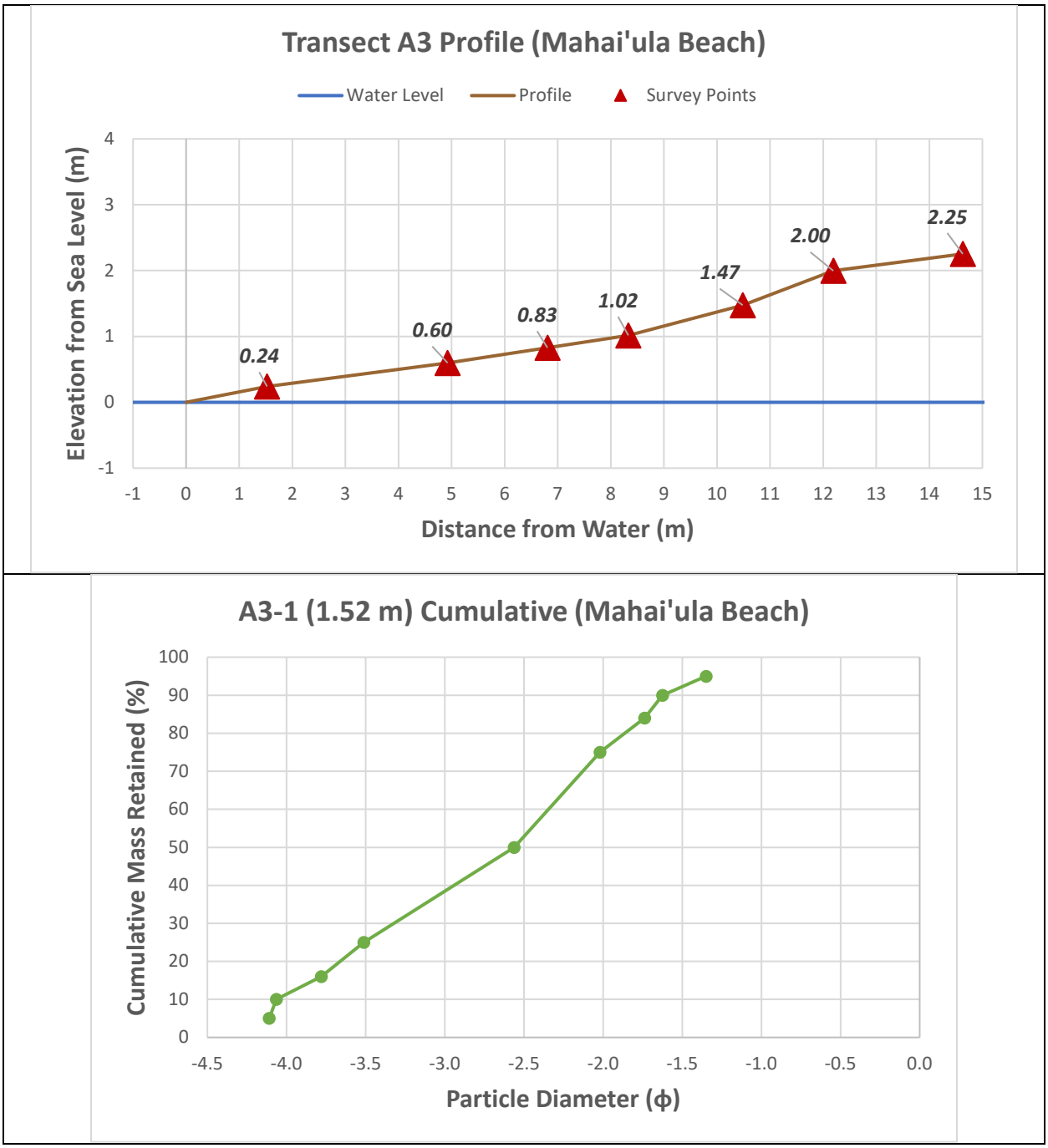
Transect A3 Profile (Mahai'ula Beach)
Water Level
Profile
Survey Points
Elevation from Sea Level (m)
Distance from Water (m)
0.24
0.60
0.83
1.02
1.47
2.00
2.25
A3-1 (1.52 m) Cumulative (Mahai'ula Beach)
Cumulative Mass Retained (%)
Particle Diameter (ϕ)

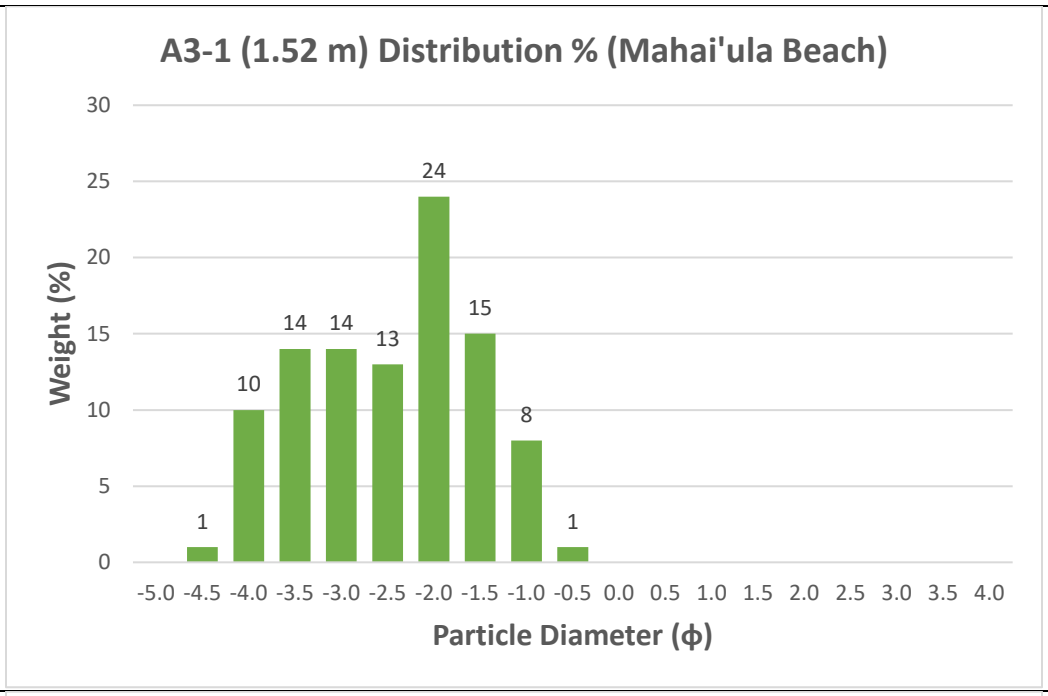
A3-1 (1.52 m) Distribution % (Mahai'ula Beach)
Weight (%)
30
25
20
15
10
5
0
1
10
14
14
13
24
15
8
1
-5.0 -4.5 -4.0 -3.5 -3.0 -2.5 -2.0 -1.5 -1.0 -0.5 0.0 0.5 1.0 1.5 2.0 2.5 3.0 3.5 4.0
Particle Diameter (ϕ)

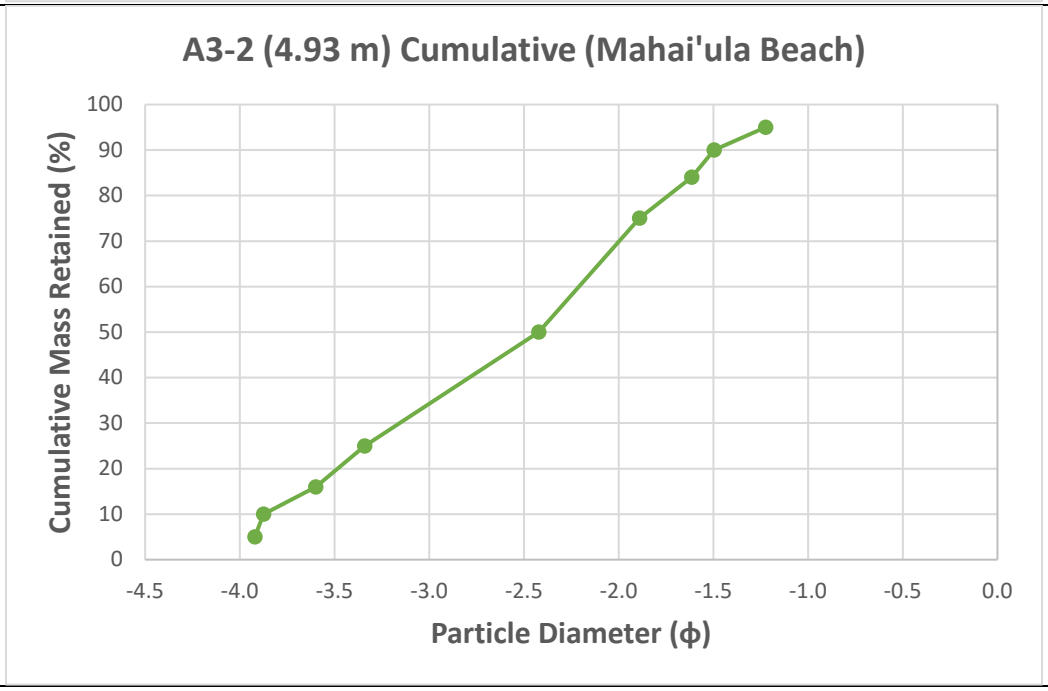
A3-2 (4.93 m) Cumulative (Mahai'ula Beach)
Cumulative Mass Retained (%)
100
90
80
70
60
50
40
30
20
10
0
-4.5 -4.0 -3.5 -3.0 -2.5 -2.0 -1.5 -1.0 -0.5 0.0
Particle Diameter (ϕ)

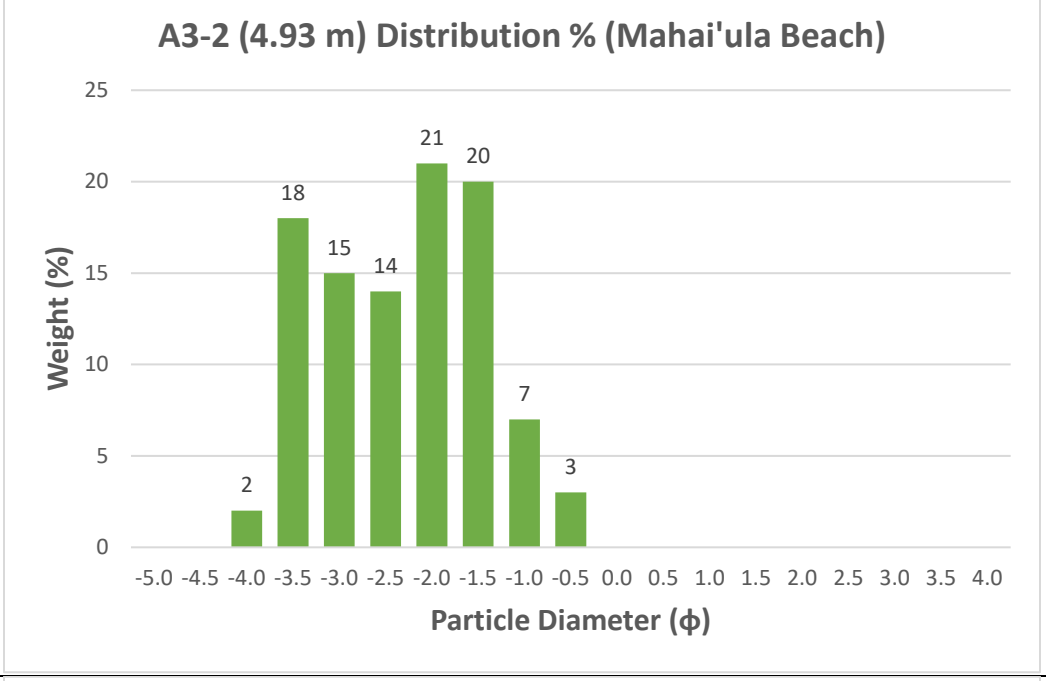
A3-2 (4.93 m) Distribution % (Mahai'ula Beach)
Weight (%)
25
20
15
10
5
0
2
18
15
14
21
20
7
3
-5.0 -4.5 -4.0 -3.5 -3.0 -2.5 -2.0 -1.5 -1.0 -0.5 0.0 0.5 1.0 1.5 2.0 2.5 3.0 3.5 4.0
Particle Diameter (ϕ)

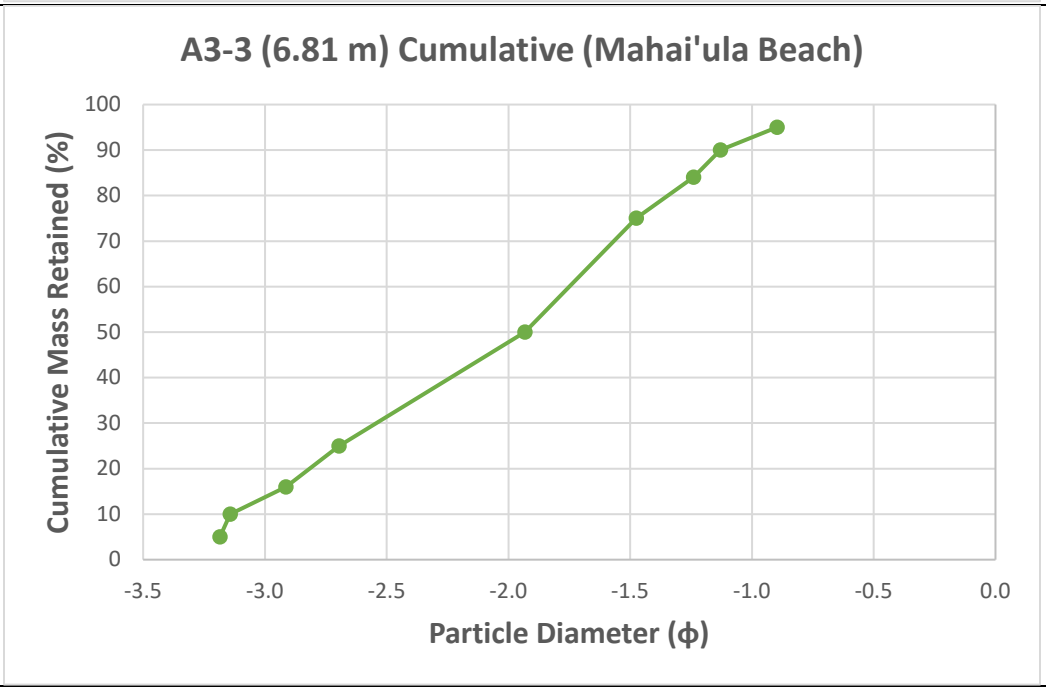
A3-3 (6.81 m) Cumulative (Mahai'ula Beach)
Cumulative Mass Retained (%)
100
90
80
70
60
50
40
30
20
10
0
-3.5 -3.0 -2.5 -2.0 -1.5 -1.0 -0.5 0.0
Particle Diameter (ϕ)

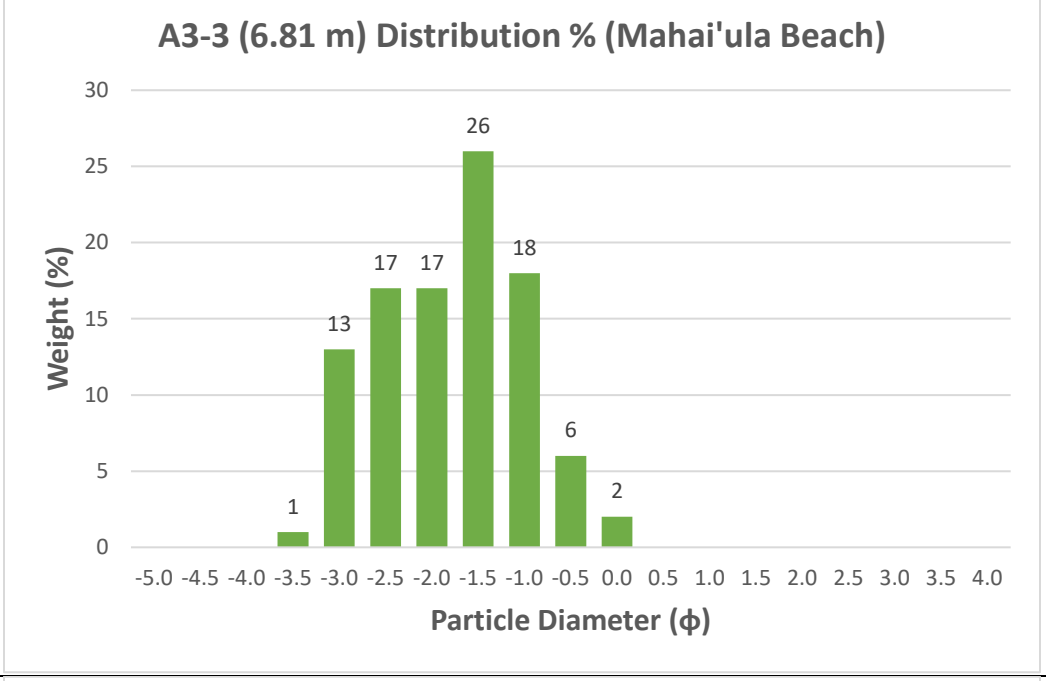
A3-3 (6.81 m) Distribution % (Mahai'ula Beach)
Weight (%)
30
25
20
15
10
5
0
1
13
17
17
26
18
6
2
-5.0 -4.5 -4.0 -3.5 -3.0 -2.5 -2.0 -1.5 -1.0 -0.5 0.0 0.5 1.0 1.5 2.0 2.5 3.0 3.5 4.0
Particle Diameter (ϕ)

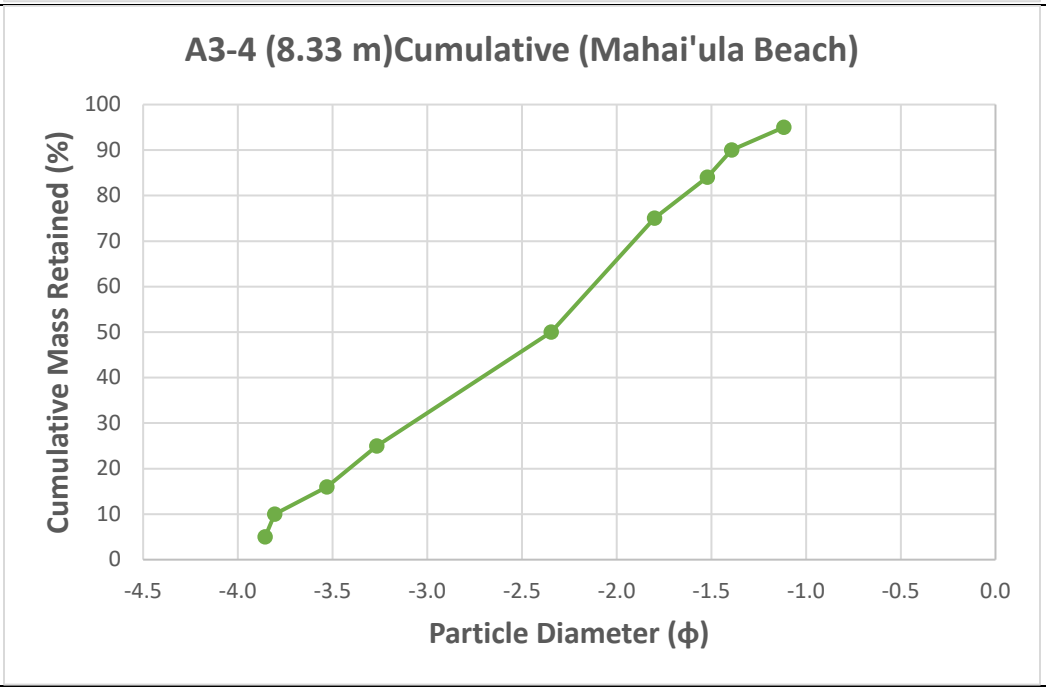
A3-4 (8.33 m)Cumulative (Mahai'ula Beach)
Cumulative Mass Retained (%)
100
90
80
70
60
50
40
30
20
10
0
-4.5 -4.0 -3.5 -3.0 -2.5 -2.0 -1.5 -1.0 -0.5 0.0
Particle Diameter (ϕ)

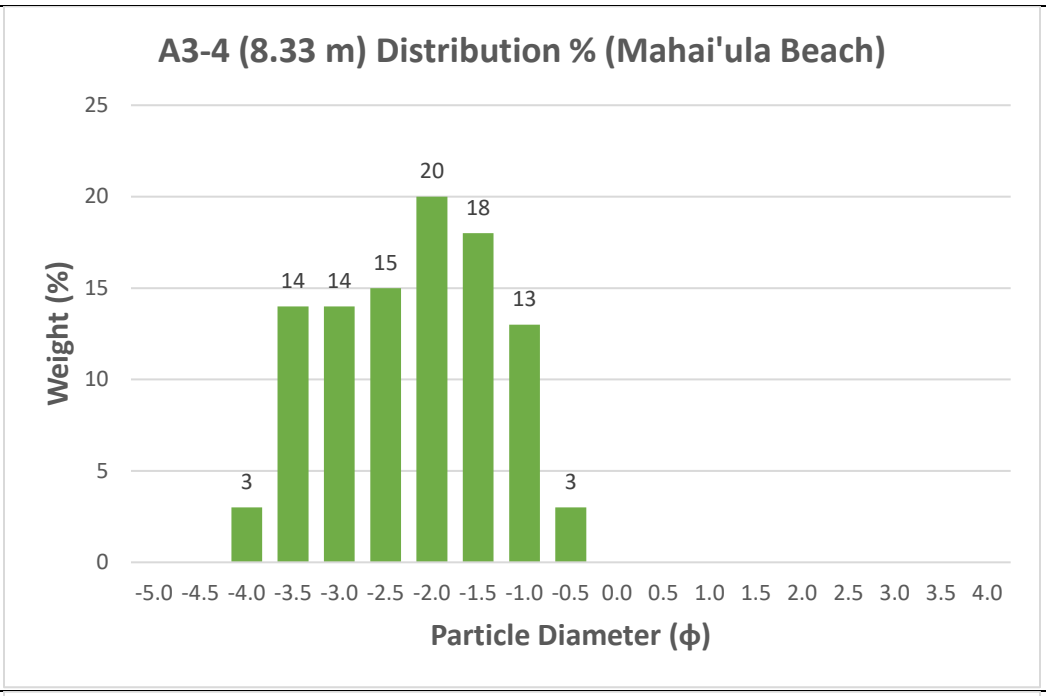
A3-4 (8.33 m) Distribution % (Mahai'ula Beach)
Weight (%)
25
20
15
10
5
0
3
14
14
15
20
18
13
3
-5.0 -4.5 -4.0 -3.5 -3.0 -2.5 -2.0 -1.5 -1.0 -0.5 0.0 0.5 1.0 1.5 2.0 2.5 3.0 3.5 4.0
Particle Diameter (ϕ)

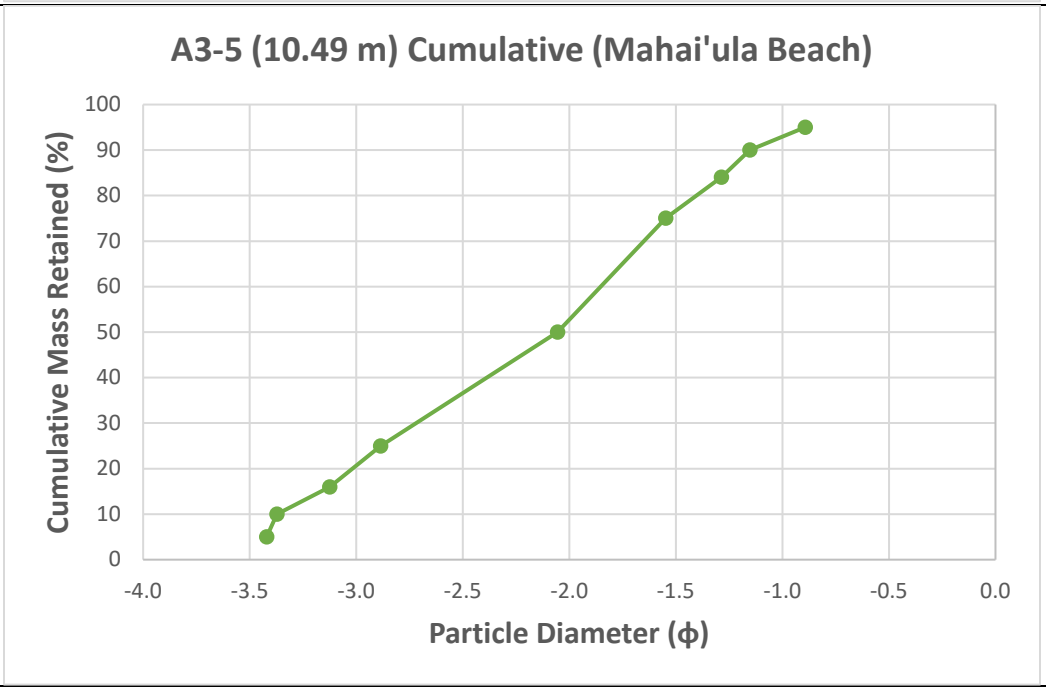
A3-5 (10.49 m) Cumulative (Mahai'ula Beach)
Cumulative Mass Retained (%)
100
90
80
70
60
50
40
30
20
10
0
-4.0 -3.5 -3.0 -2.5 -2.0 -1.5 -1.0 -0.5 0.0
Particle Diameter (ϕ)

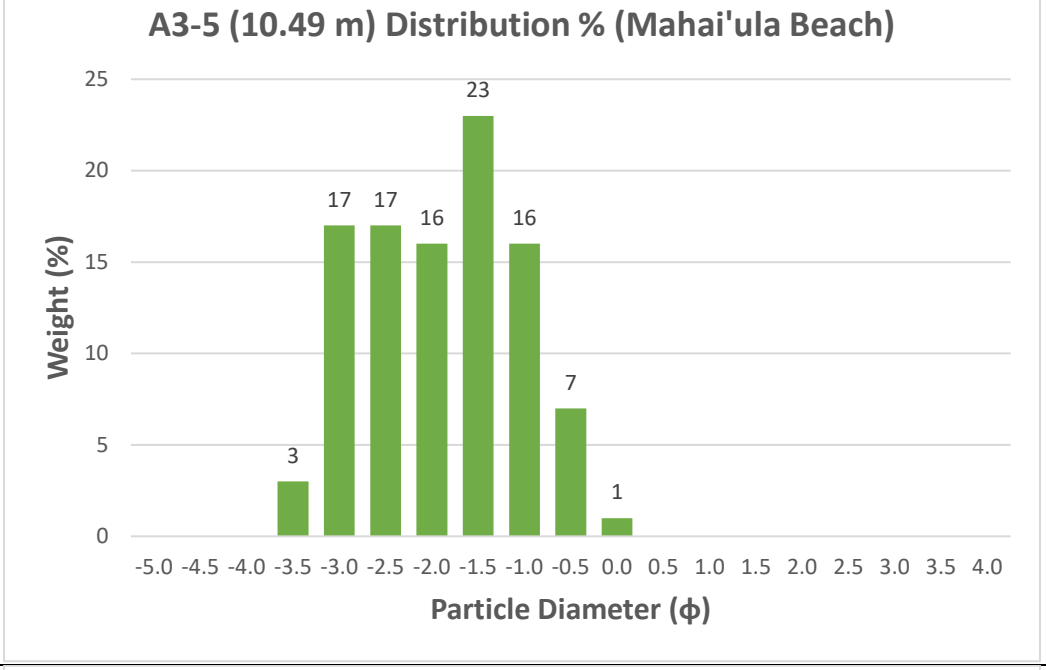
A3-5 (10.49 m) Distribution % (Mahai'ula Beach)
Weight (%)
25
20
15
10
5
0
3
17
17
16
23
16
7
1
-5.0 -4.5 -4.0 -3.5 -3.0 -2.5 -2.0 -1.5 -1.0 -0.5 0.0 0.5 1.0 1.5 2.0 2.5 3.0 3.5 4.0
Particle Diameter (ϕ)

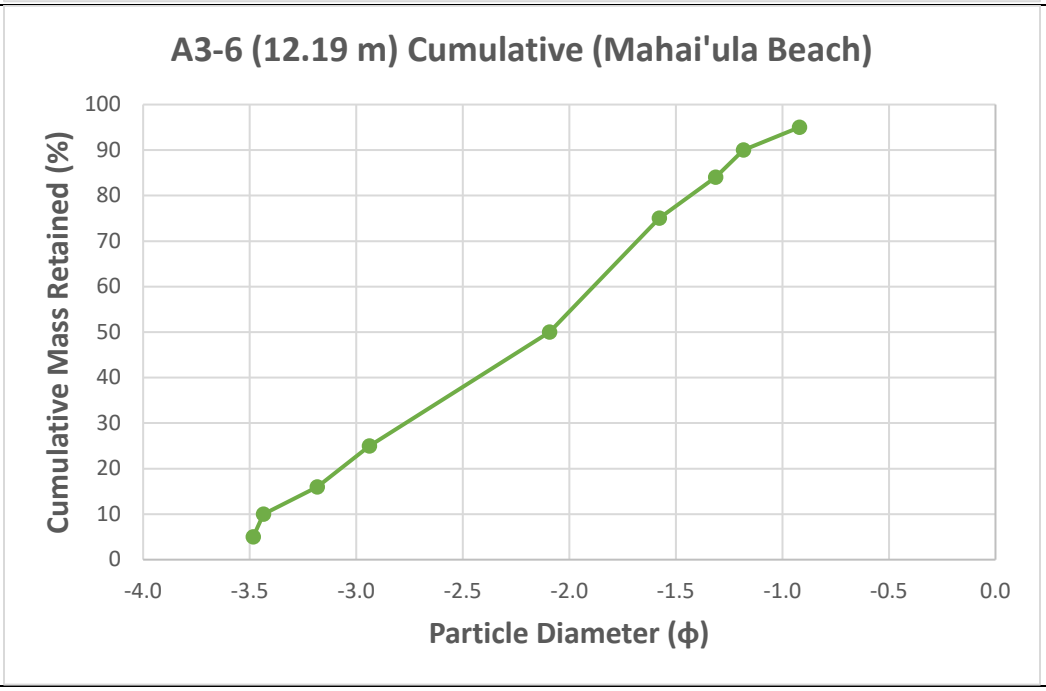
A3-6 (12.19 m) Cumulative (Mahai'ula Beach)
Cumulative Mass Retained (%)
100
90
80
70
60
50
40
30
20
10
0
-4.0 -3.5 -3.0 -2.5 -2.0 -1.5 -1.0 -0.5 0.0
Particle Diameter (ϕ)

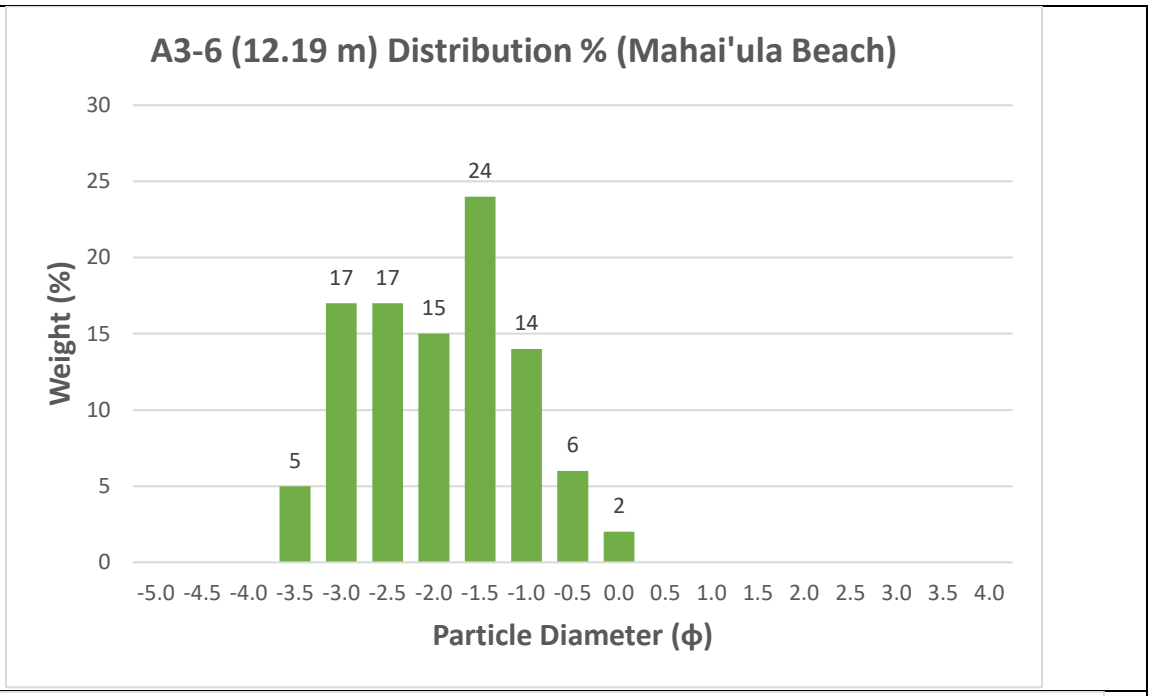
A3-6 (12.19 m) Distribution % (Mahai'ula Beach)
Weight (%)
30
25
20
15
10
5
0
5
17
17
15
24
14
6
2
-5.0 -4.5 -4.0 -3.5 -3.0 -2.5 -2.0 -1.5 -1.0 -0.5 0.0 0.5 1.0 1.5 2.0 2.5 3.0 3.5 4.0
Particle Diameter (ϕ)

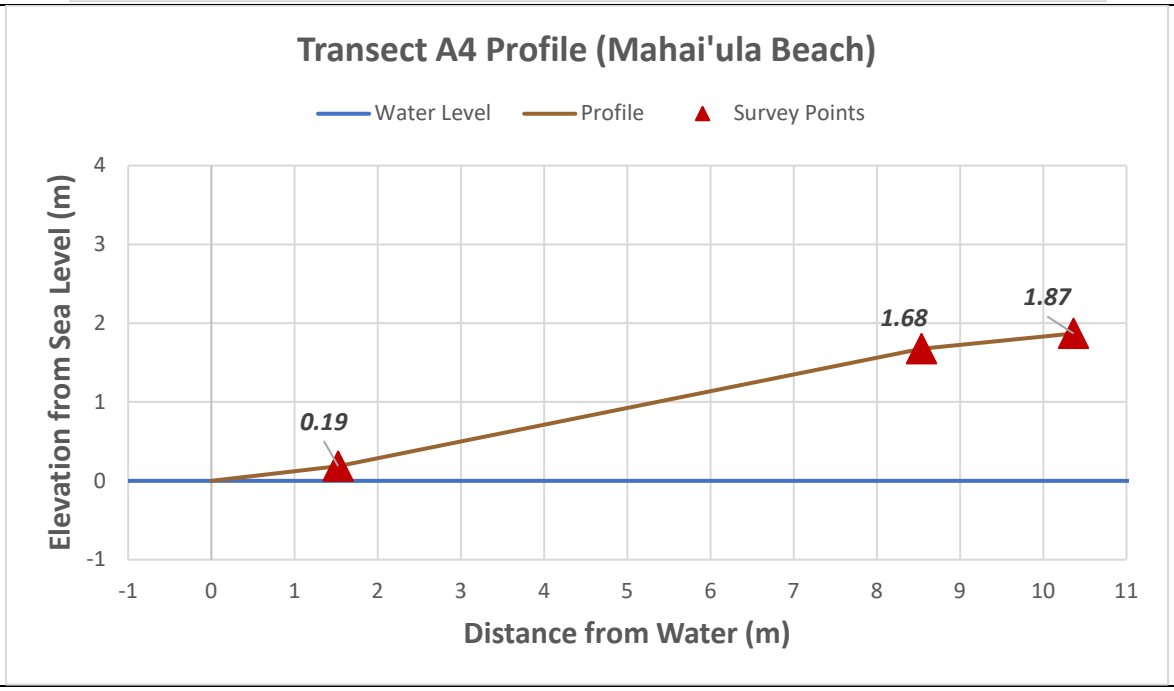
Transect A4 Profile (Mahai'ula Beach)
Water Level
Profile
Survey Points
Elevation from Sea Level (m)
4
3
2
1
0
-1
0.19
1.68
1.87
-1 0 1 2 3 4 5 6 7 8 9 10 11
Distance from Water (m)

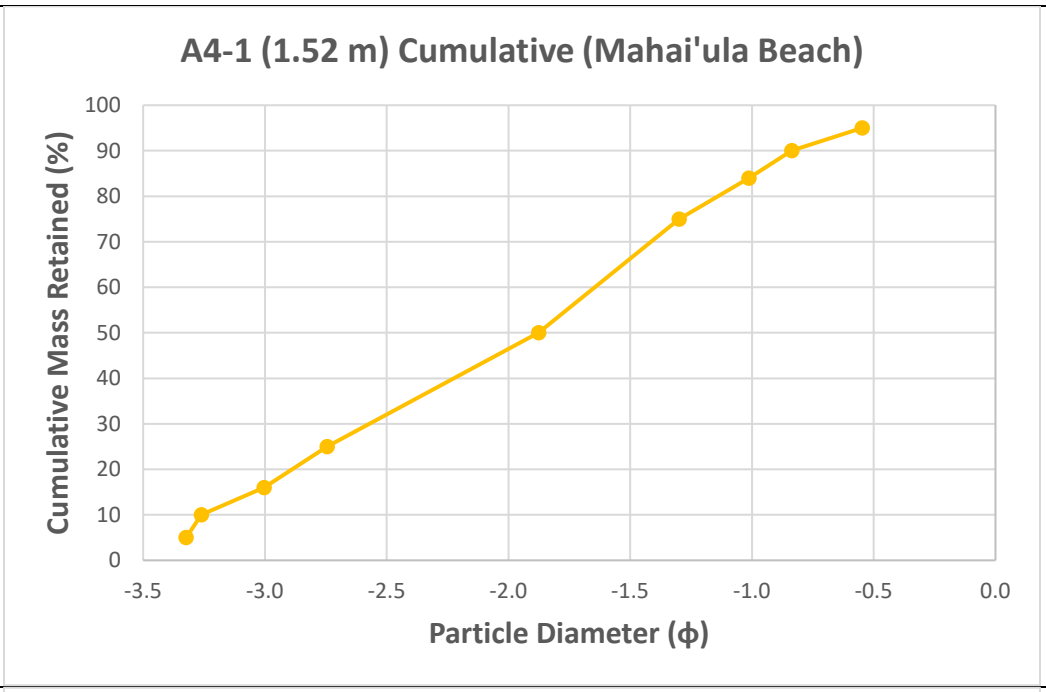
A4-1 (1.52 m) Cumulative (Mahai'ula Beach)
Cumulative Mass Retained (%)
100
90
80
70
60
50
40
30
20
10
0
-3.5
-3.0
-2.5
-2.0
-1.5
-1.0
-0.5
0.0
Particle Diameter (ϕ)

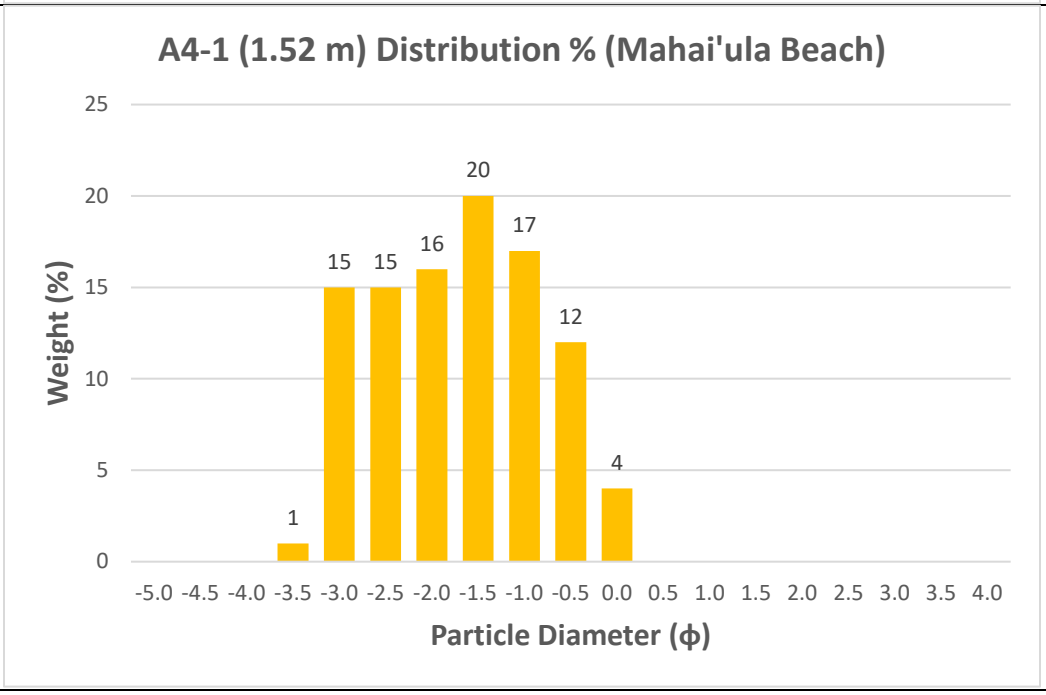
A4-1 (1.52 m) Distribution % (Mahai'ula Beach)
Weight (%)
25
20
15
10
5
0
1
15
15
16
20
17
12
4
-5.0 -4.5 -4.0 -3.5 -3.0 -2.5 -2.0 -1.5 -1.0 -0.5 0.0 0.5 1.0 1.5 2.0 2.5 3.0 3.5 4.0
Particle Diameter (ϕ)

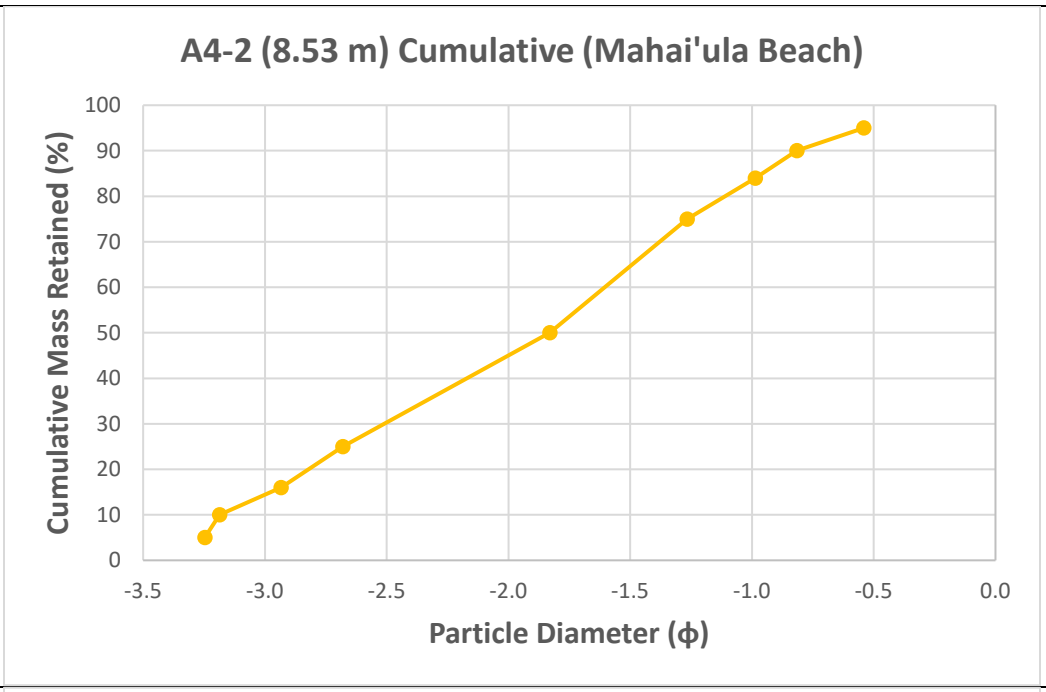
A4-2 (8.53 m) Cumulative (Mahai'ula Beach)
Cumulative Mass Retained (%)
100
90
80
70
60
50
40
30
20
10
0
-3.5
-3.0
-2.5
-2.0
-1.5
-1.0
-0.5
0.0
Particle Diameter (ϕ)

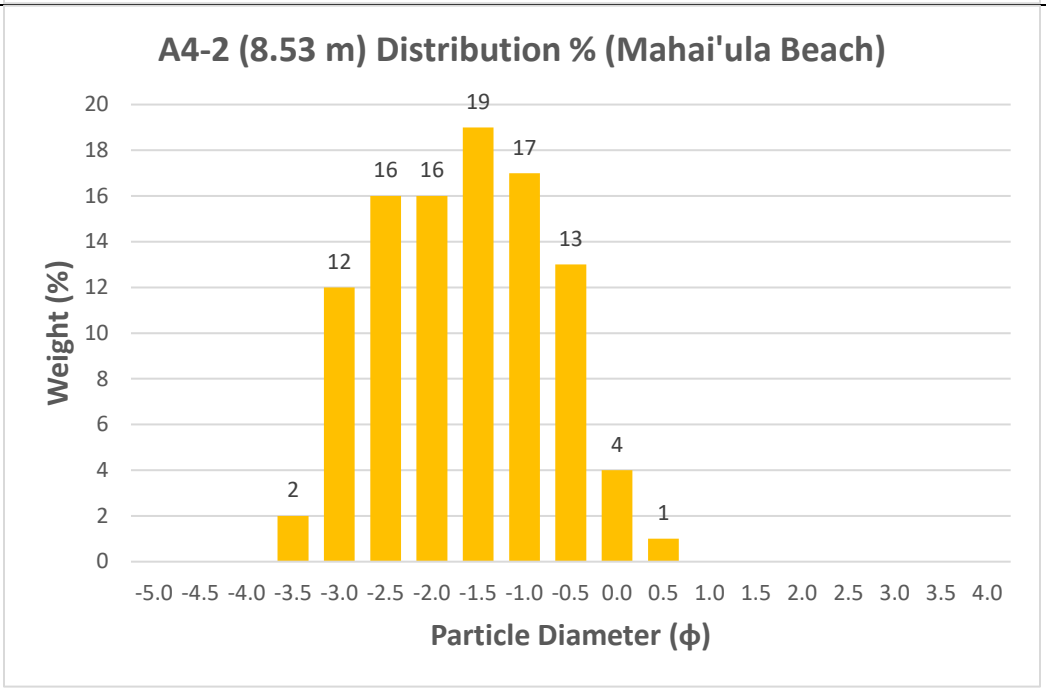
A4-2 (8.53 m) Distribution % (Mahai'ula Beach)
Weight (%)
20
18
16
14
12
10
8
6
4
2
0
2
12
16
16
19
17
13
4
1
-5.0 -4.5 -4.0 -3.5 -3.0 -2.5 -2.0 -1.5 -1.0 -0.5 0.0 0.5 1.0 1.5 2.0 2.5 3.0 3.5 4.0
Particle Diameter (ϕ)

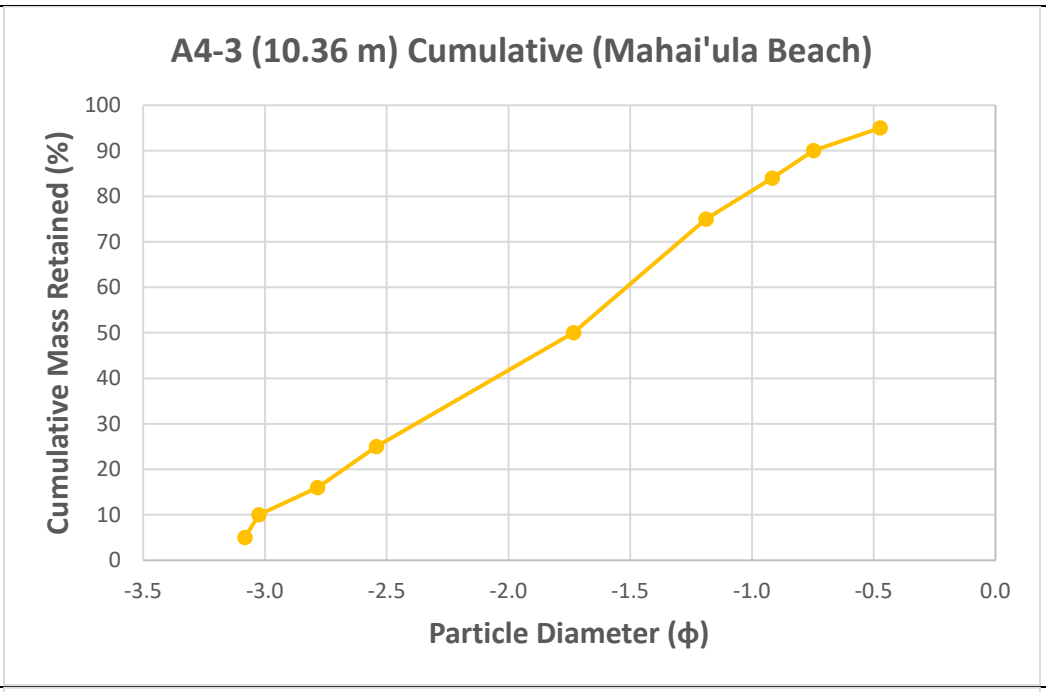
A4-3 (10.36 m) Cumulative (Mahai'ula Beach)
Cumulative Mass Retained (%)
100
90
80
70
60
50
40
30
20
10
0
-3.5
-3.0
-2.5
-2.0
-1.5
-1.0
-0.5
0.0
Particle Diameter (ϕ)

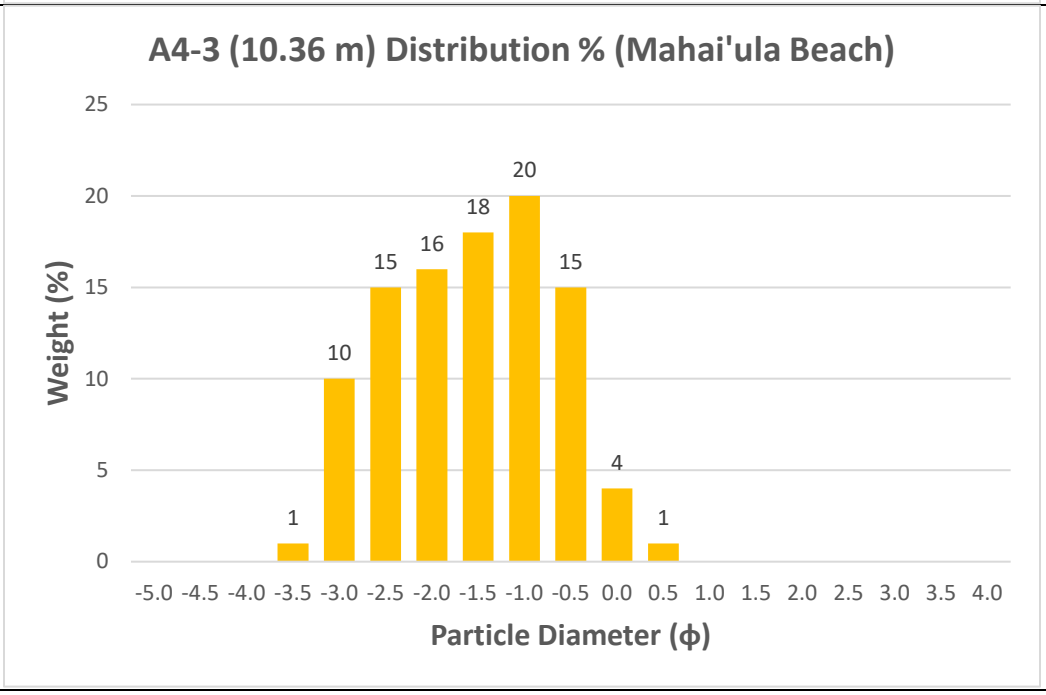
A4-3 (10.36 m) Distribution % (Mahai'ula Beach)
Weight (%)
25
20
15
10
5
0
1
10
15
16
18
20
15
4
1
-5.0 -4.5 -4.0 -3.5 -3.0 -2.5 -2.0 -1.5 -1.0 -0.5 0.0 0.5 1.0 1.5 2.0 2.5 3.0 3.5 4.0
Particle Diameter (ϕ)

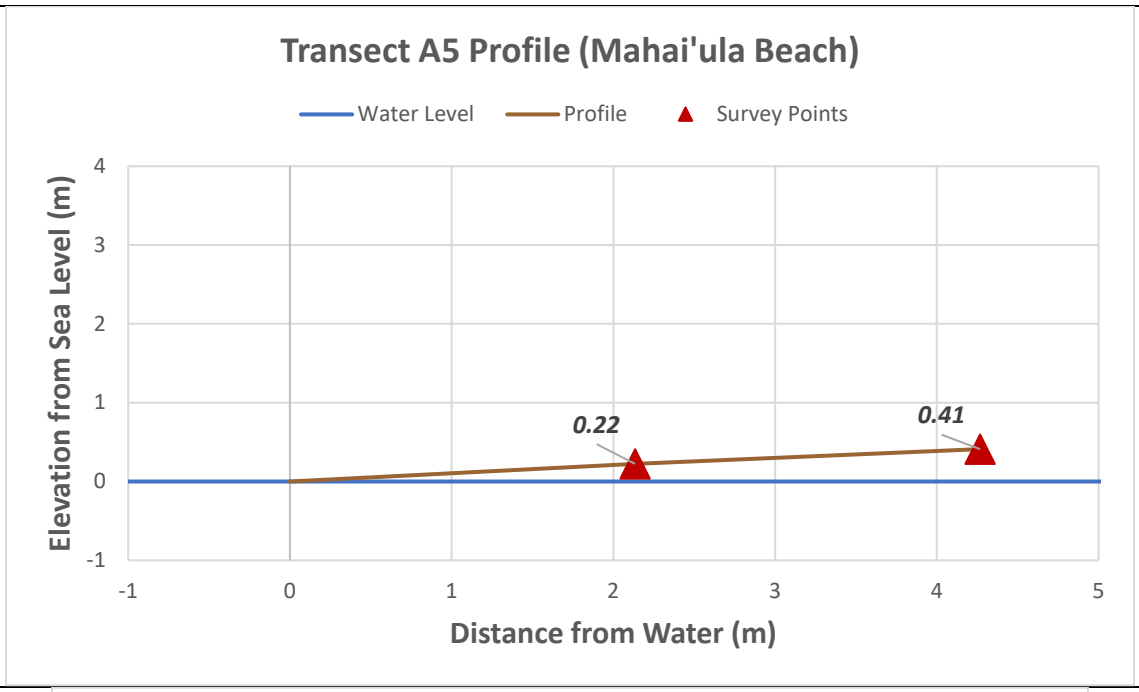
Transect A5 Profile (Mahai'ula Beach)
Water Level
Profile
Survey Points
Elevation from Sea Level (m)
4
3
2
1
0
-1
0.22
0.41
-1
0
1
2
3
4
5
Distance from Water (m)

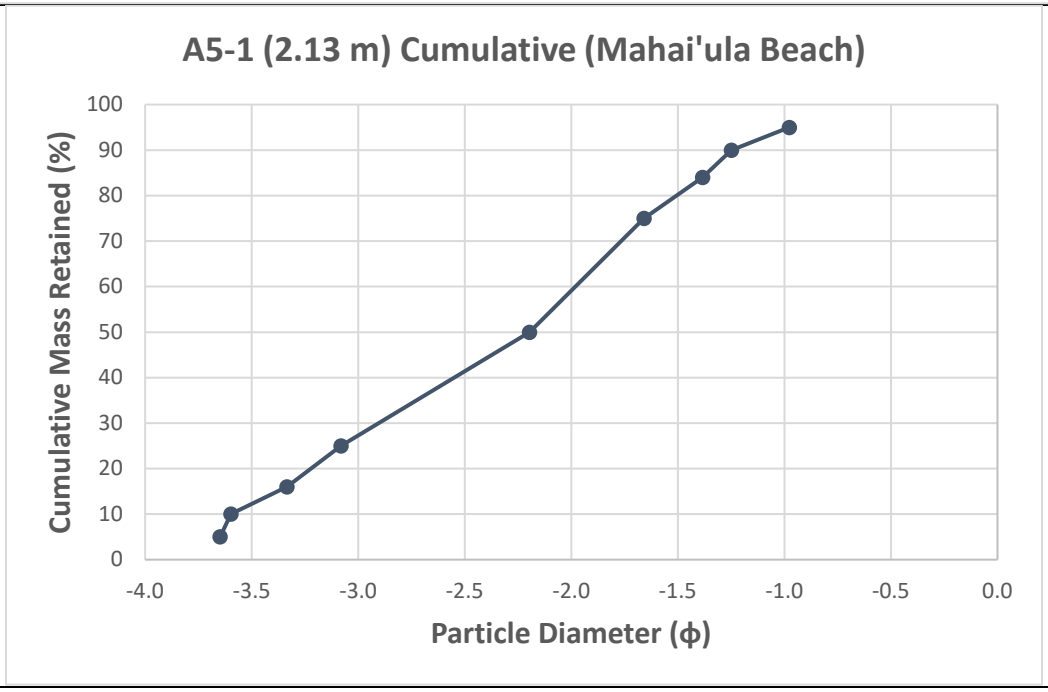
A5-1 (2.13 m) Cumulative (Mahai'ula Beach)
Cumulative Mass Retained (%)
100
90
80
70
60
50
40
30
20
10
0
-4.0
-3.5
-3.0
-2.5
-2.0
-1.5
-1.0
-0.5
0.0
Particle Diameter (ϕ)

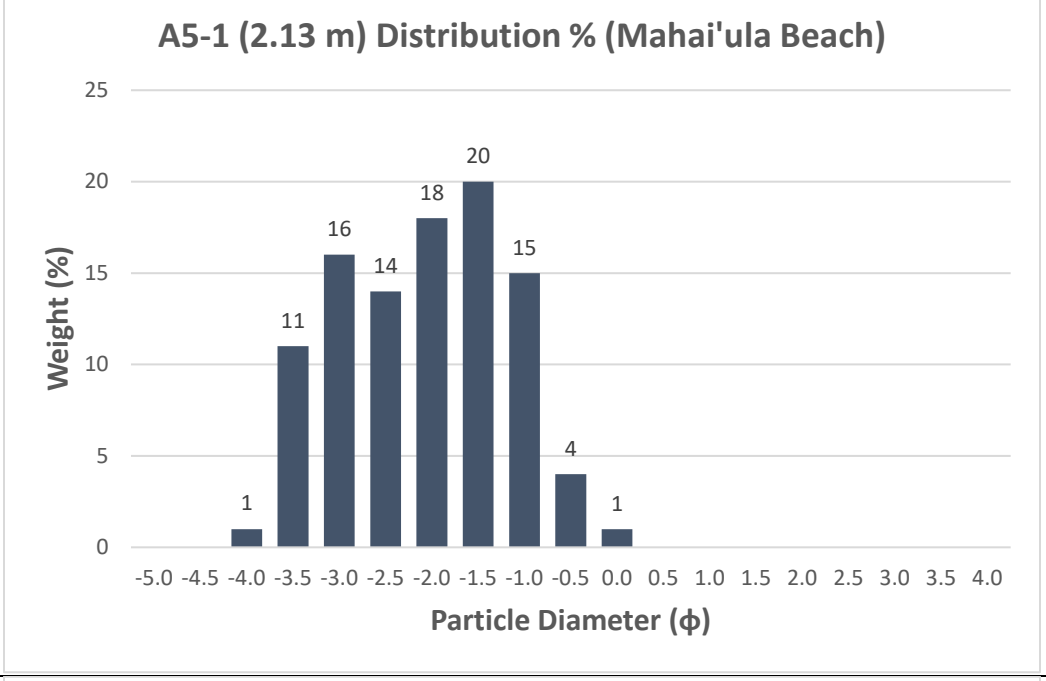
A5-1 (2.13 m) Distribution % (Mahai'ula Beach)
Weight (%)
25
20
15
10
5
0
1
11
16
14
18
20
15
4
1
-5.0 -4.5 -4.0 -3.5 -3.0 -2.5 -2.0 -1.5 -1.0 -0.5 0.0 0.5 1.0 1.5 2.0 2.5 3.0 3.5 4.0
Particle Diameter (ϕ)

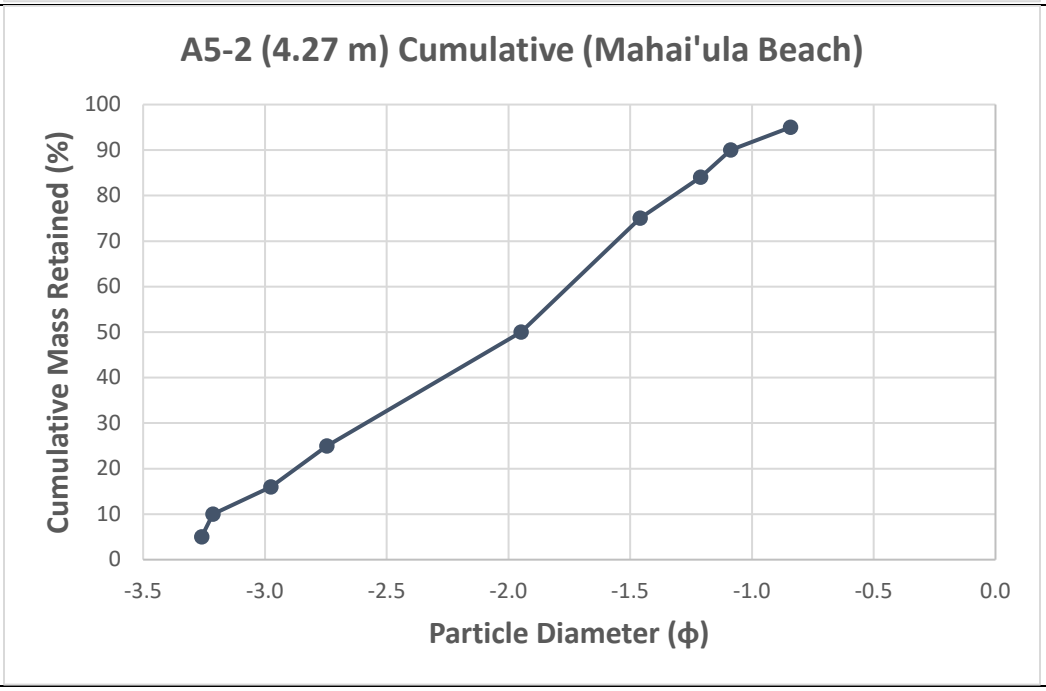
A5-2 (4.27 m) Cumulative (Mahai'ula Beach)
Cumulative Mass Retained (%)
100
90
80
70
60
50
40
30
20
10
0
-3.5 -3.0 -2.5 -2.0 -1.5 -1.0 -0.5 0.0
Particle Diameter (ϕ)

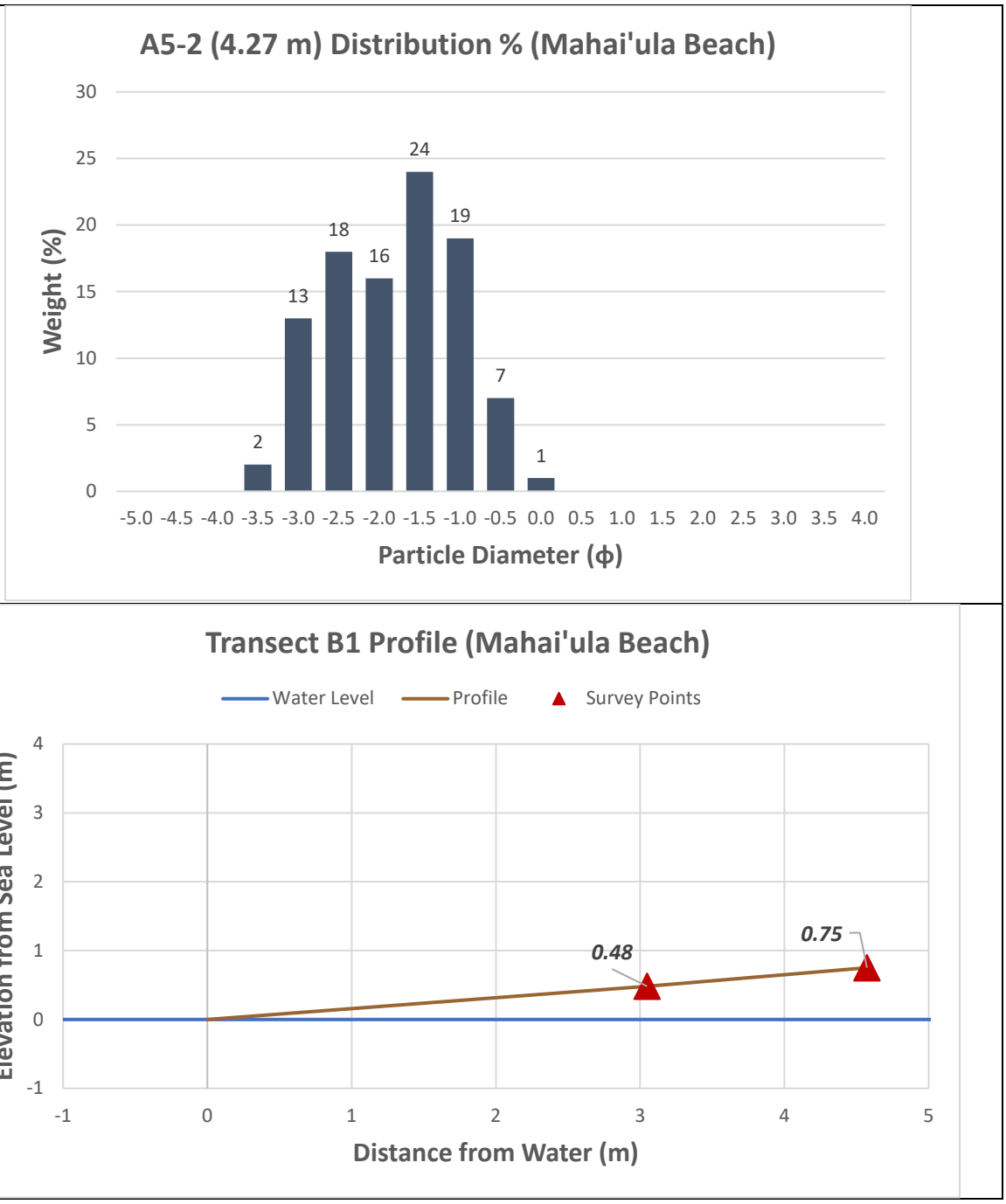
A5-2 (4.27 m) Distribution % (Mahai'ula Beach)
Weight (%)
30
25
20
15
10
5
0
2
13
18
16
24
19
7
1
-5.0 -4.5 -4.0 -3.5 -3.0 -2.5 -2.0 -1.5 -1.0 -0.5 0.0 0.5 1.0 1.5 2.0 2.5 3.0 3.5 4.0
Particle Diameter (ϕ)
Transect B1 Profile (Mahai'ula Beach)
Water Level
Profile
Survey Points
Elevation from Sea Level (m)
4
3
2
1
0
-1
0.48
0.75
-1 0 1 2 3 4 5
Distance from Water (m)

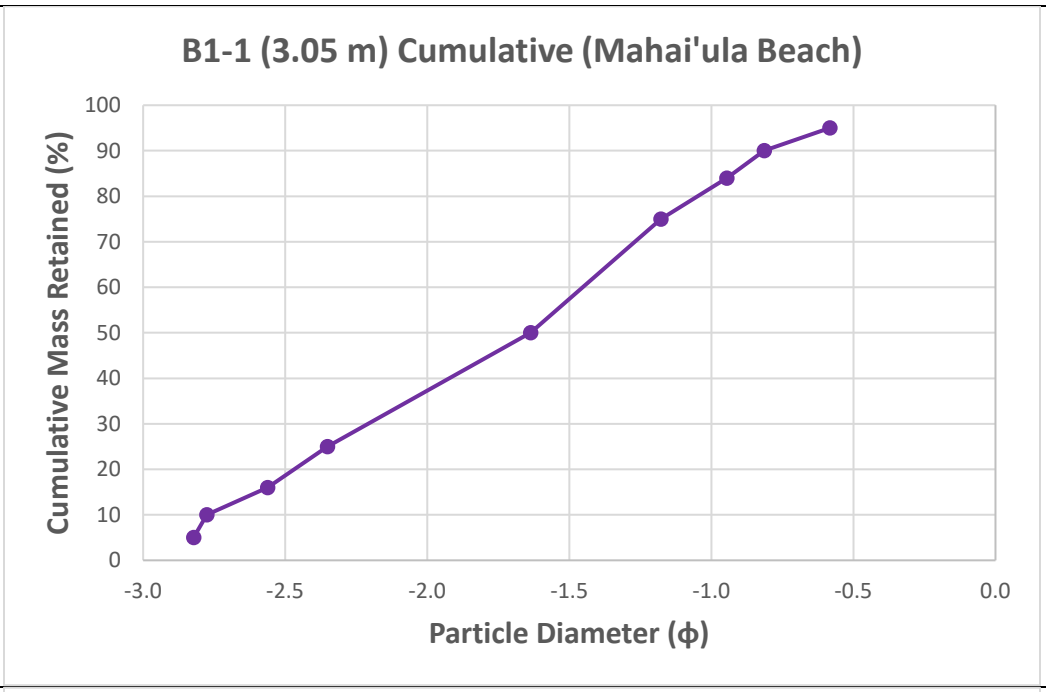
B1-1 (3.05 m) Cumulative (Mahai'ula Beach)
Cumulative Mass Retained (%)
100
90
80
70
60
50
40
30
20
10
0
-3.0
-2.5
-2.0
-1.5
-1.0
-0.5
0.0
Particle Diameter (ϕ)

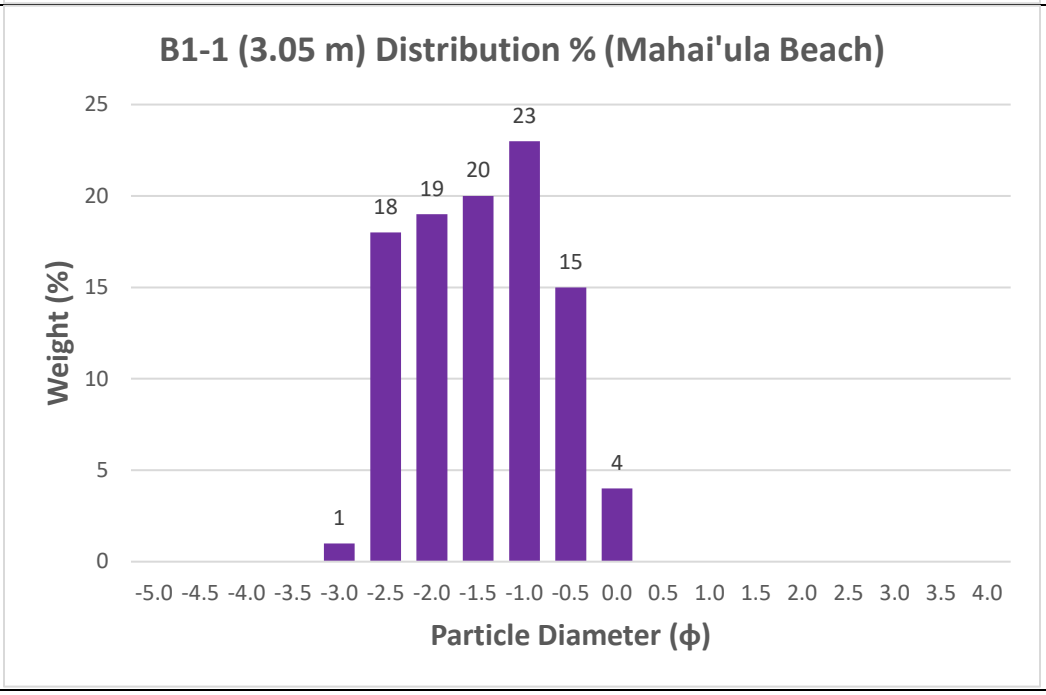
B1-1 (3.05 m) Distribution % (Mahai'ula Beach)
Weight (%)
25
20
15
10
5
0
1
18
19
20
23
15
4
-5.0 -4.5 -4.0 -3.5 -3.0 -2.5 -2.0 -1.5 -1.0 -0.5 0.0 0.5 1.0 1.5 2.0 2.5 3.0 3.5 4.0
Particle Diameter (ϕ)

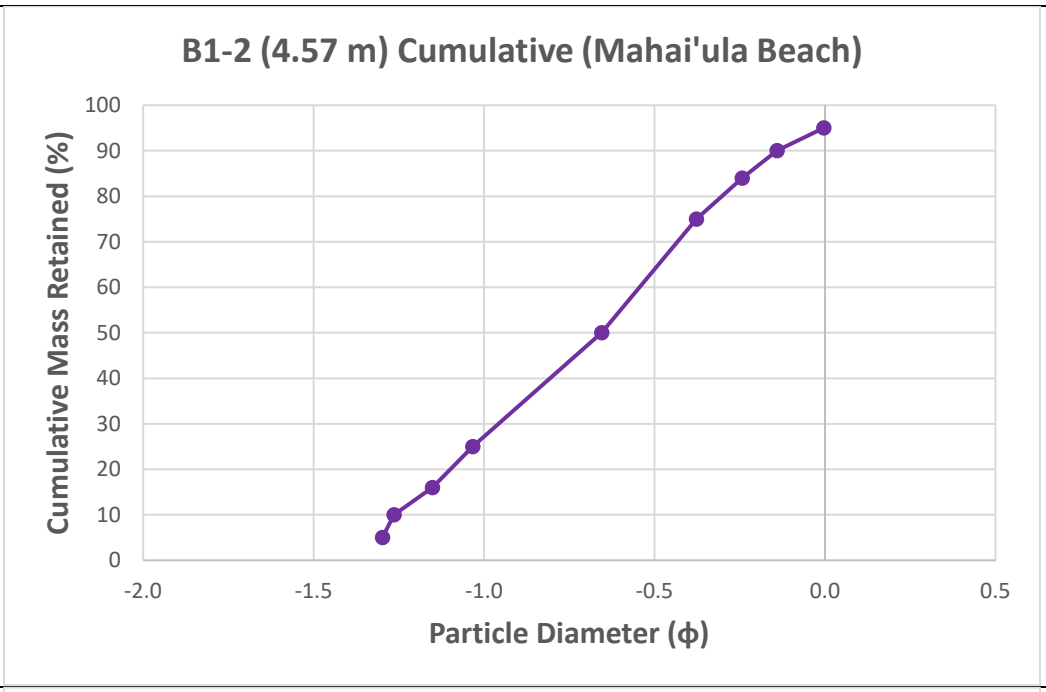
B1-2 (4.57 m) Cumulative (Mahai'ula Beach)
Cumulative Mass Retained (%)
100
90
80
70
60
50
40
30
20
10
0
-2.0
-1.5
-1.0
-0.5
0.0
0.5
Particle Diameter (ϕ)

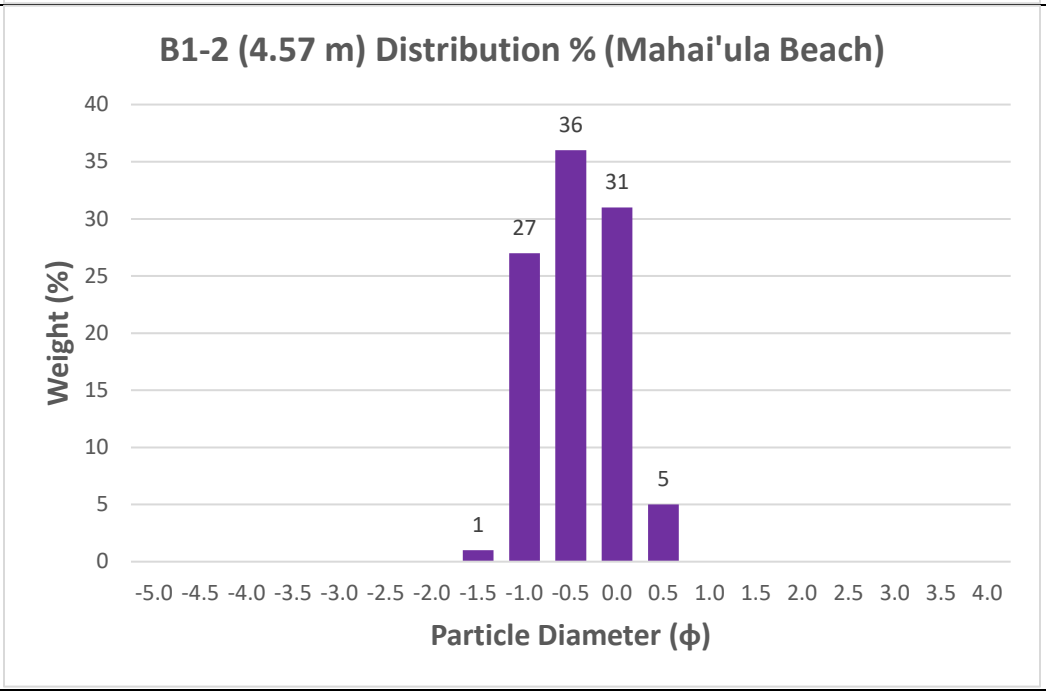
B1-2 (4.57 m) Distribution % (Mahai'ula Beach)
Weight (%)
40
35
30
25
20
15
10
5
0
1
27
36
31
5
-5.0 -4.5 -4.0 -3.5 -3.0 -2.5 -2.0 -1.5 -1.0 -0.5 0.0 0.5 1.0 1.5 2.0 2.5 3.0 3.5 4.0
Particle Diameter (ϕ)

Beach Name: Manini'owali Beach (Kua Bay)

Date: 10/20/2020 **Time:** 11:28 PM

Location/ Transect	Survey #	Distance from Water (m)	Slope in Degrees	"x" used	Calculated mm percentile								
					5	10	16	25	50	75	84	90	95
A	1	1.8288	-9	-0.8	1.657907	1.378817	1.138908	0.886633	0.480558	0.252728	0.192304	0.157859	0.120904
	2	3.3528	-7	-0.7	1.23582	1.017532	0.838675	0.656418	0.382118	0.226261	0.181958	0.154685	0.119418
	3	6.10	-11	-0.7	1.319606	1.05914	0.85893	0.668723	0.386667	0.226112	0.179572	0.150875	0.123609
B	1	1.52	-6	-0.7	1.399128	1.101468	0.880939	0.678784	0.382707	0.22948	0.186021	0.158902	0.114569
	2	4.57	-11	-0.6	1.314044	1.081797	0.887576	0.695777	0.401983	0.236572	0.190401	0.161955	0.124311
C	1	0.91	-8	-0.6	1.465371	1.188256	0.957604	0.736284	0.414406	0.247389	0.200053	0.170112	0.131134
	2	4.88	-10	-0.7	1.385421	1.119389	0.909279	0.701889	0.392952	0.228413	0.182631	0.154636	0.118119

Calculated ϕ percentiles with corrections

5	10	16	25	50	75	84	90	95
-1.176	-0.741	-0.281	0.243	1.110	1.726	1.841	1.997	2.006
-0.492	-0.040	0.379	0.850	1.457	1.865	1.903	2.019	2.017
-0.645	-0.133	0.328	0.813	1.439	1.866	1.917	2.046	1.985
-0.781	-0.223	0.273	0.783	1.455	1.847	1.878	1.990	2.057
-0.635	-0.181	0.257	0.733	1.381	1.809	1.852	1.970	1.979
-0.889	-0.398	0.093	0.618	1.334	1.753	1.797	1.917	1.929
-0.758	-0.260	0.205	0.715	1.415	1.853	1.899	2.020	2.028

Moments

Mean	Standard Deviation	*Descriptor*	Skewness	*Descriptor*	Kurtosis	*Descriptor*
0.890	1.012	Poorly Sorted	-0.374	Very Coarse Skewed	0.879	Platykurtic
1.247	0.761	Moderately Sorted	-0.484	Very Coarse Skewed	1.013	Platykurtic
1.228	0.796	Moderately Sorted	-0.492	Very Coarse Skewed	1.023	Platykurtic
1.202	0.831	Moderately Sorted	-0.524	Very Coarse Skewed	1.092	Platykurtic
1.163	0.795	Moderately Sorted	-0.475	Very Coarse Skewed	0.995	Platykurtic
1.075	0.853	Moderately Sorted	-0.518	Very Coarse Skewed	1.017	Platykurtic
1.173	0.845	Moderately Sorted	-0.494	Very Coarse Skewed	1.003	Platykurtic

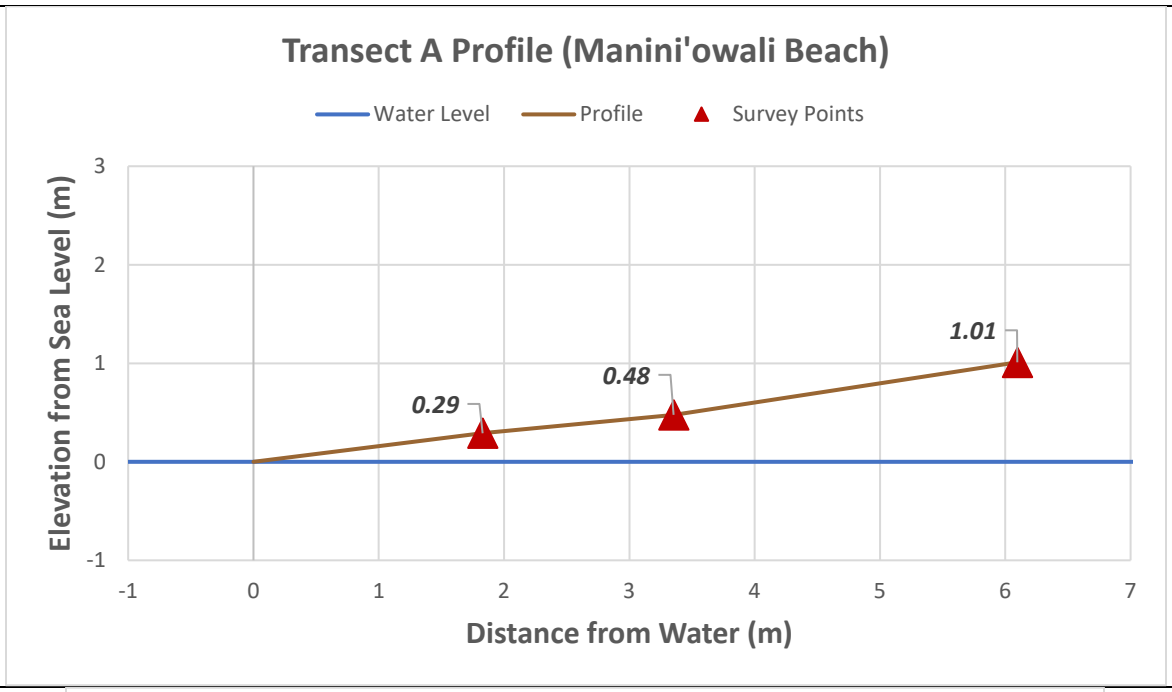
Transect A Profile (Manini'owali Beach)
Water Level
Profile
Survey Points
Elevation from Sea Level (m)
3
2
1
0
-1
-1
0
1
2
3
4
5
6
7
0.29
0.48
1.01
Distance from Water (m)

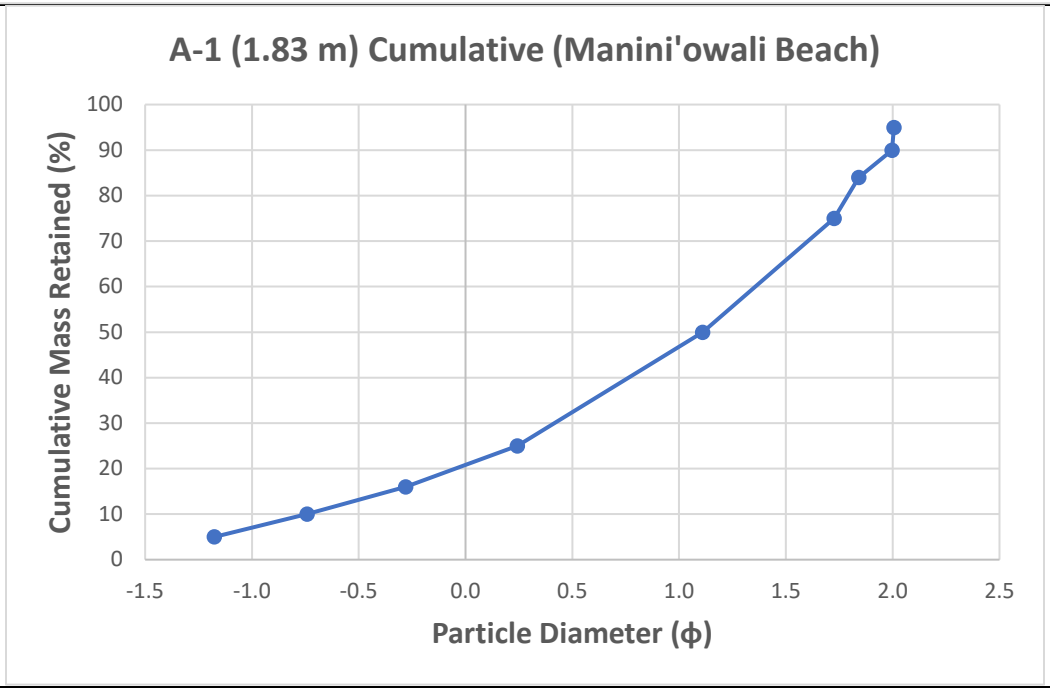
A-1 (1.83 m) Cumulative (Manini'owali Beach)
Cumulative Mass Retained (%)
100
90
80
70
60
50
40
30
20
10
0
-1.5
-1.0
-0.5
0.0
0.5
1.0
1.5
2.0
2.5
Particle Diameter (ϕ)

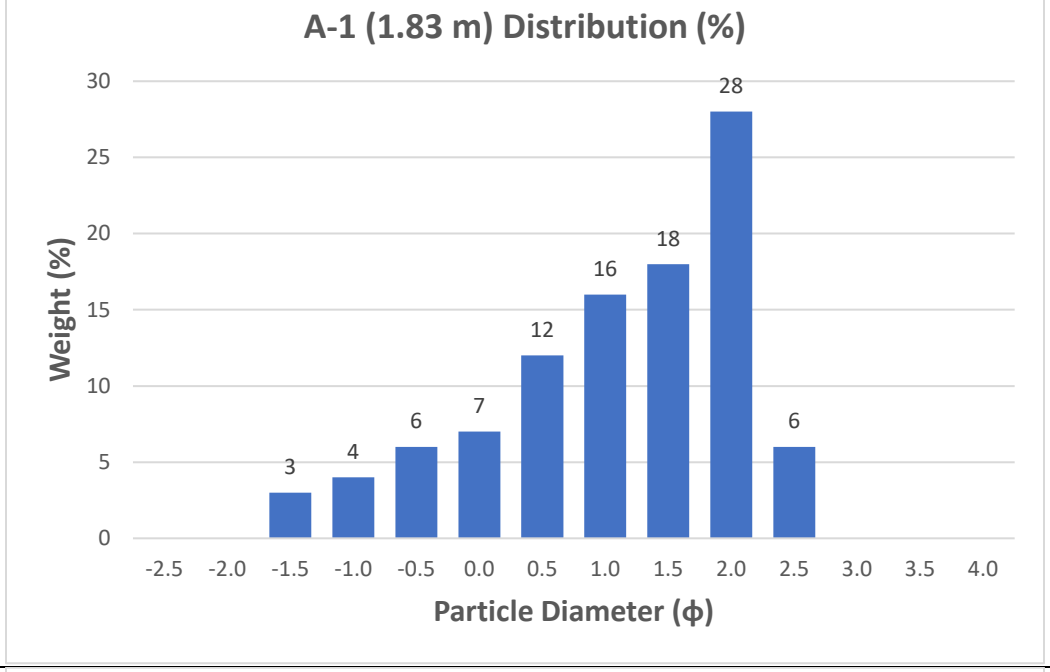
A-1 (1.83 m) Distribution (%)
Weight (%)
30
25
20
15
10
5
0
3
4
6
7
12
16
18
28
6
-2.5
-2.0
-1.5
-1.0
-0.5
0.0
0.5
1.0
1.5
2.0
2.5
3.0
3.5
4.0
Particle Diameter (ϕ)

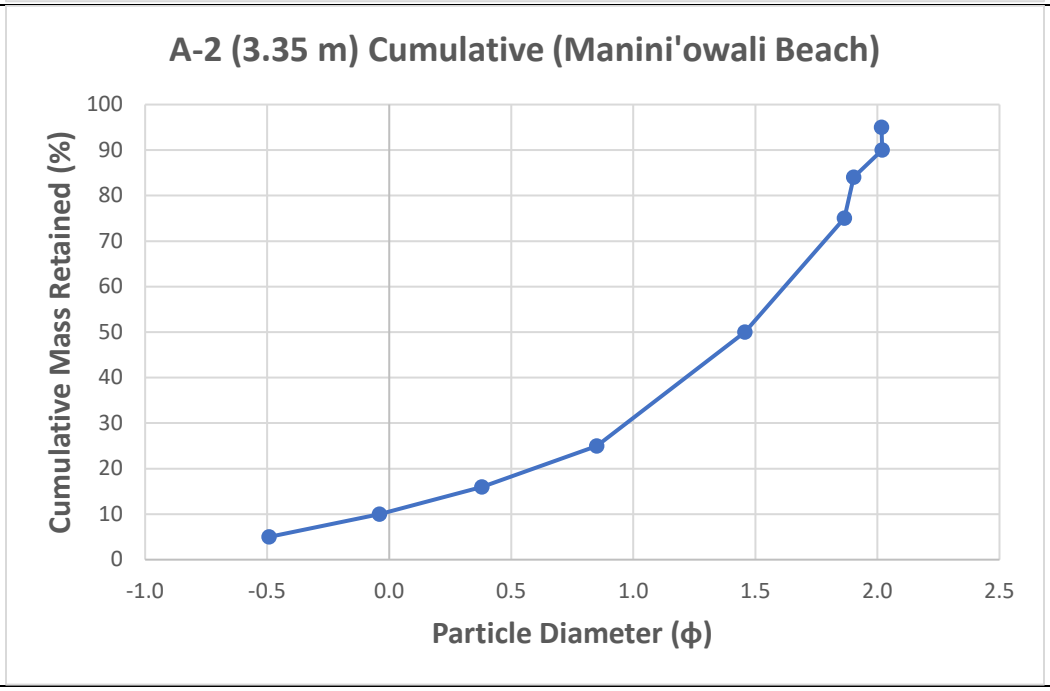
A-2 (3.35 m) Cumulative (Manini'owali Beach)
Cumulative Mass Retained (%)
100
90
80
70
60
50
40
30
20
10
0
-1.0
-0.5
0.0
0.5
1.0
1.5
2.0
2.5
Particle Diameter (ϕ)

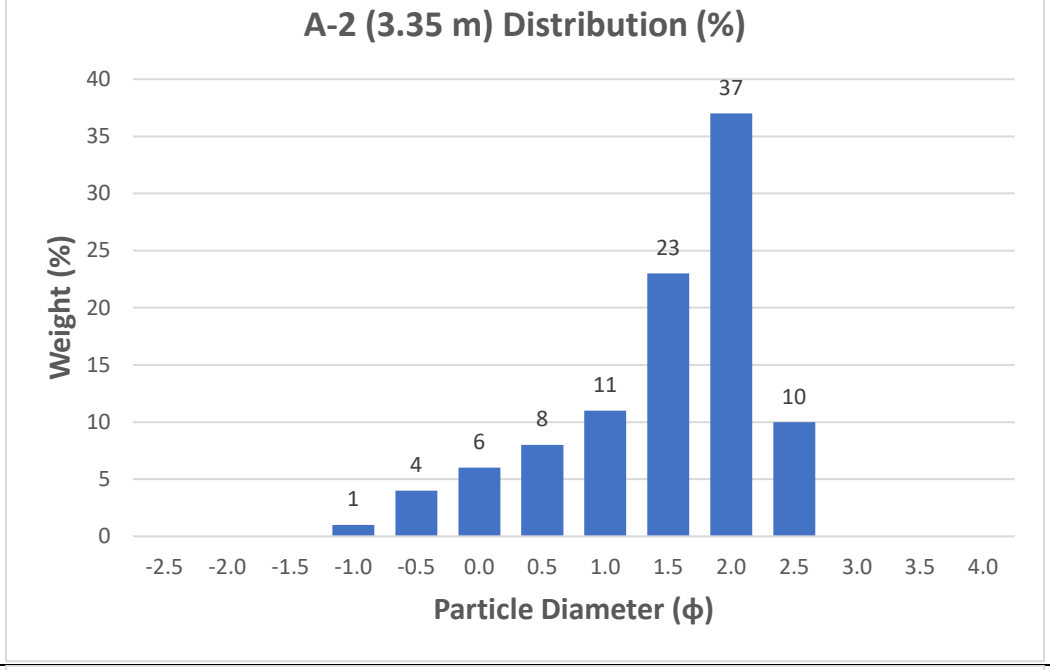
A-2 (3.35 m) Distribution (%)
Weight (%)
40
35
30
25
20
15
10
5
0
1
4
6
8
11
23
37
10
-2.5
-2.0
-1.5
-1.0
-0.5
0.0
0.5
1.0
1.5
2.0
2.5
3.0
3.5
4.0
Particle Diameter (ϕ)

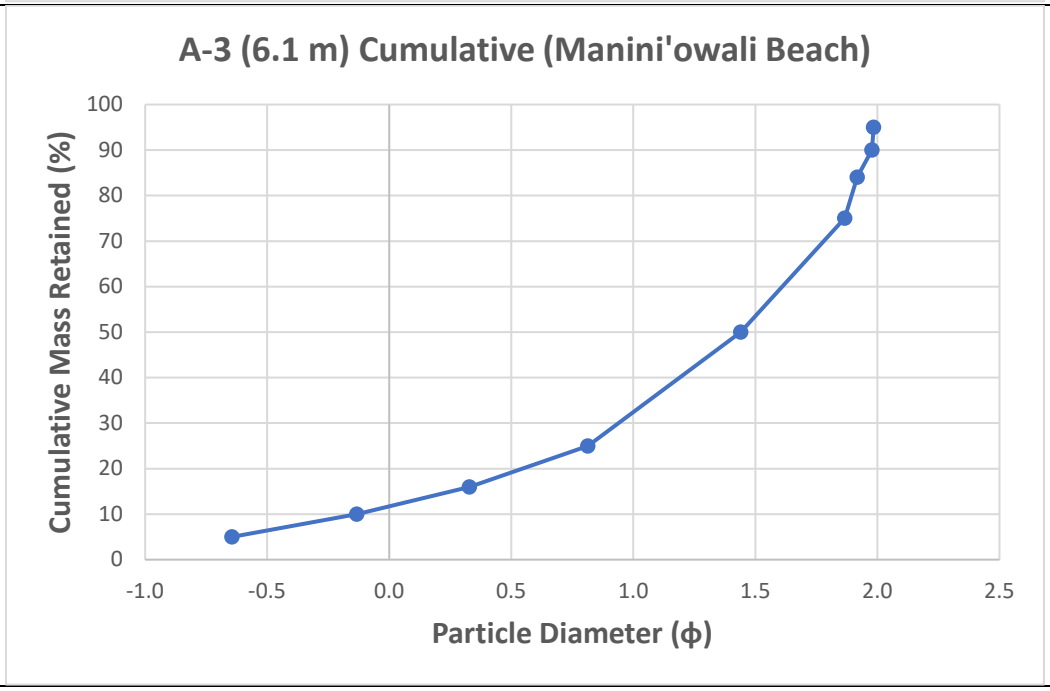
A-3 (6.1 m) Cumulative (Manini'owali Beach)
Cumulative Mass Retained (%)
100
90
80
70
60
50
40
30
20
10
0
-1.0
-0.5
0.0
0.5
1.0
1.5
2.0
2.5
Particle Diameter (ϕ)

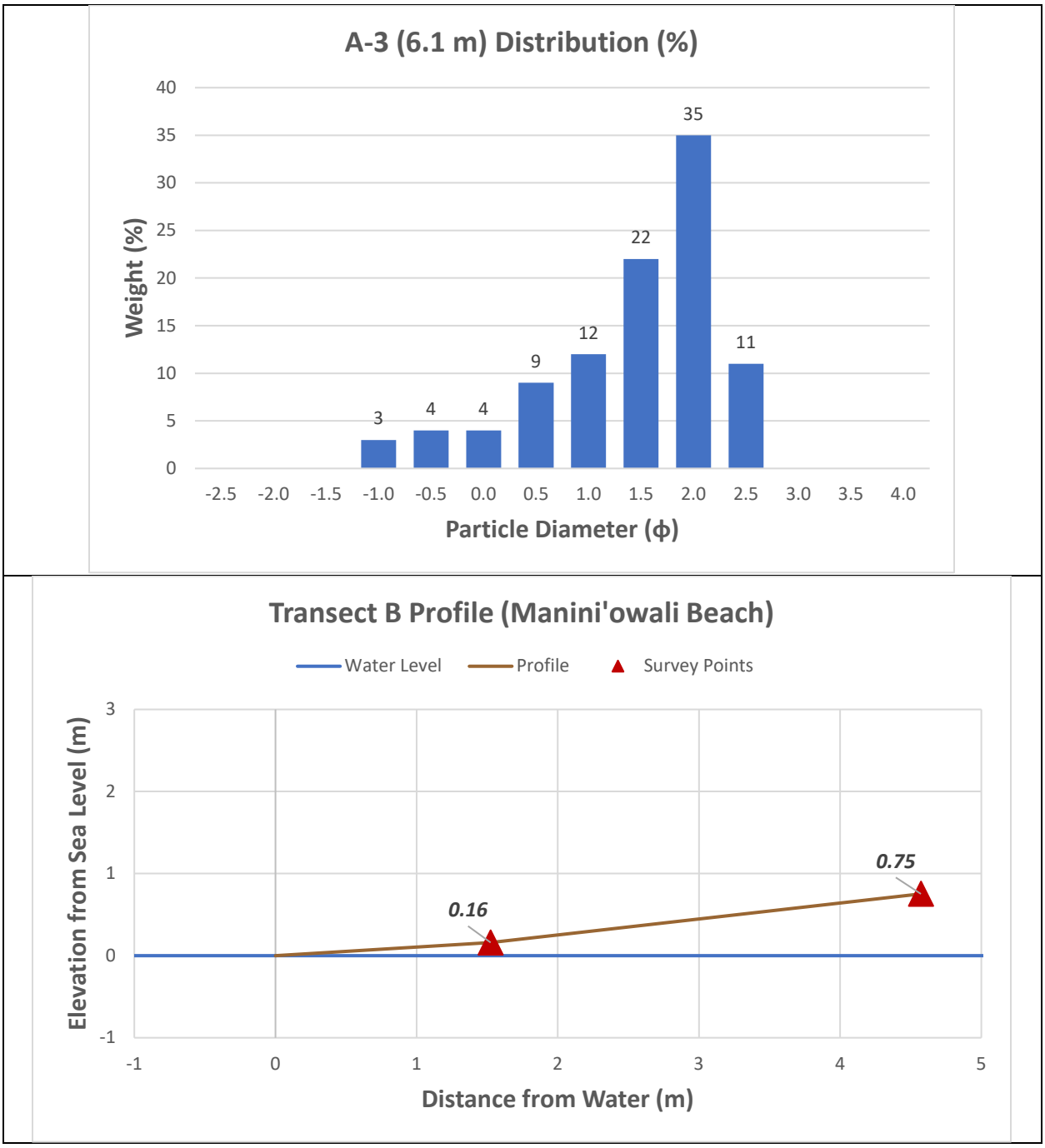
A-3 (6.1 m) Distribution (%)
Weight (%)
40
35
30
25
20
15
10
5
0
3
4
4
9
12
22
35
11
-2.5
-2.0
-1.5
-1.0
-0.5
0.0
0.5
1.0
1.5
2.0
2.5
3.0
3.5
4.0
Particle Diameter (ϕ)
Transect B Profile (Manini'owali Beach)
Water Level
Profile
Survey Points
Elevation from Sea Level (m)
3
2
1
0
-1
0.16
0.75
-1
0
1
2
3
4
5
Distance from Water (m)

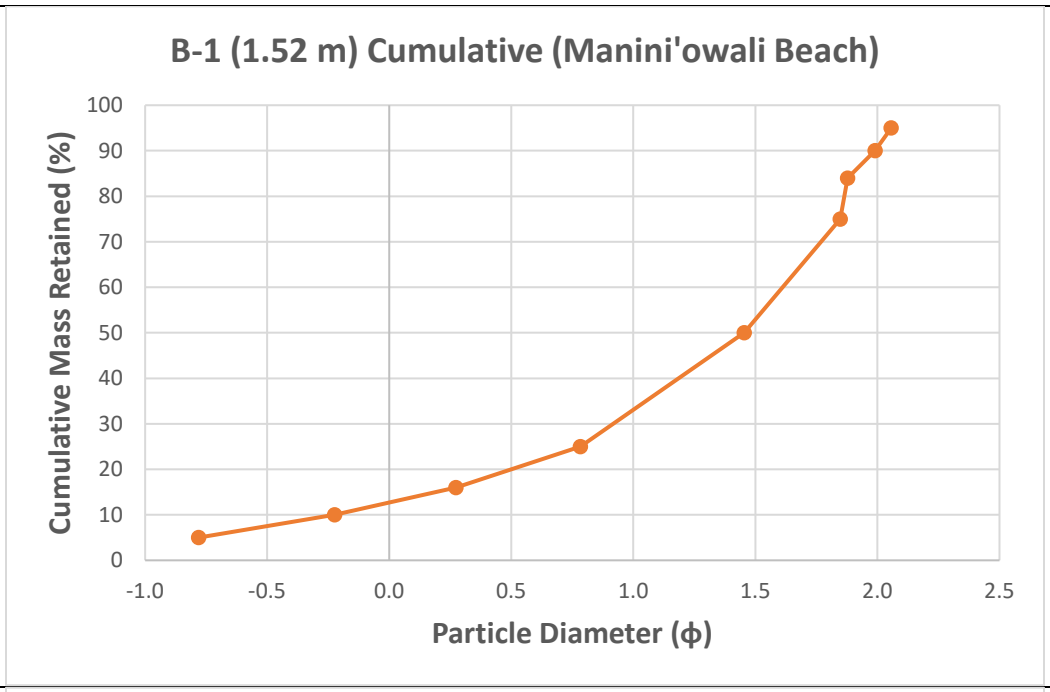
B-1 (1.52 m) Cumulative (Manini'owali Beach)
Cumulative Mass Retained (%)
100
90
80
70
60
50
40
30
20
10
0
-1.0
-0.5
0.0
0.5
1.0
1.5
2.0
2.5
Particle Diameter (ϕ)

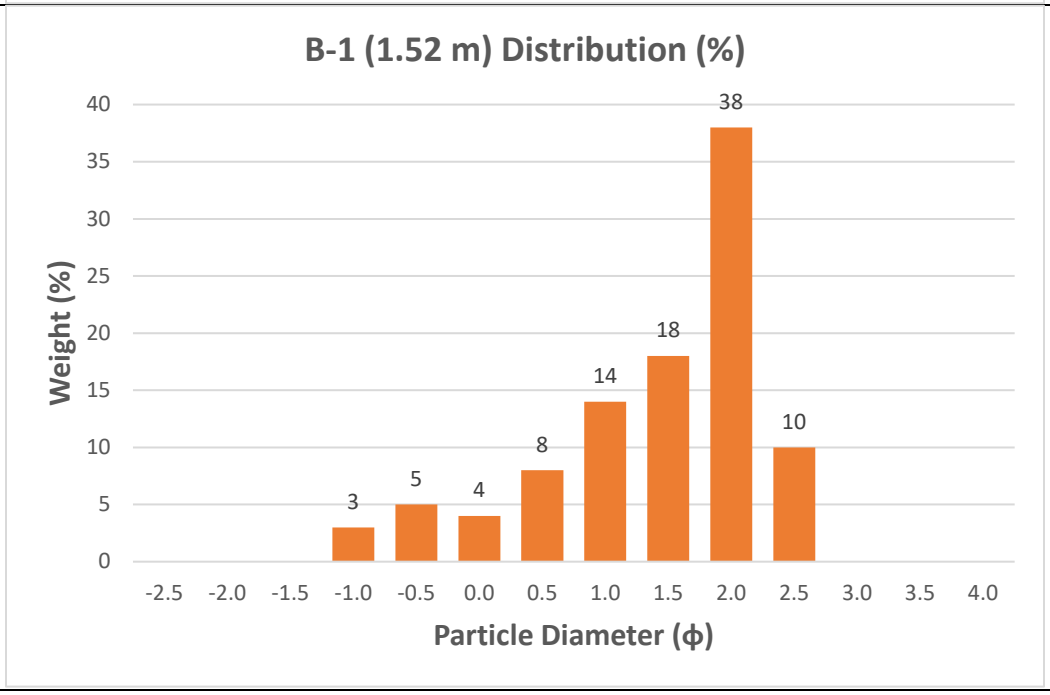
B-1 (1.52 m) Distribution (%)
Weight (%)
40
35
30
25
20
15
10
5
0
3
5
4
8
14
18
38
10
-2.5
-2.0
-1.5
-1.0
-0.5
0.0
0.5
1.0
1.5
2.0
2.5
3.0
3.5
4.0
Particle Diameter (ϕ)

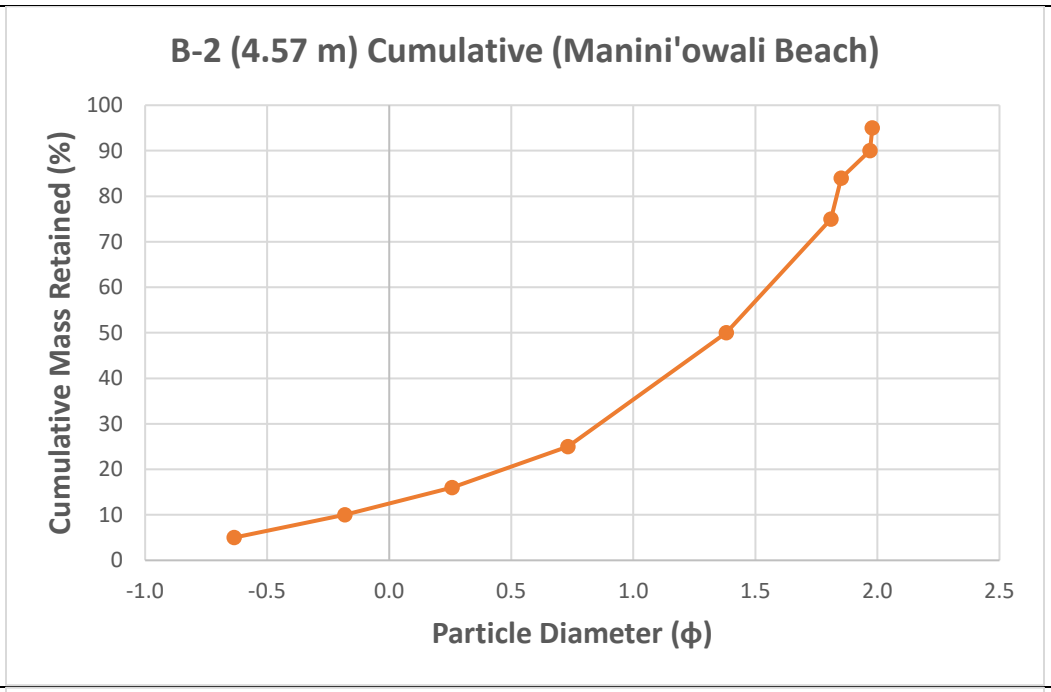
B-2 (4.57 m) Cumulative (Manini'owali Beach)
Cumulative Mass Retained (%)
100
90
80
70
60
50
40
30
20
10
0
-1.0
-0.5
0.0
0.5
1.0
1.5
2.0
2.5
Particle Diameter (ϕ)

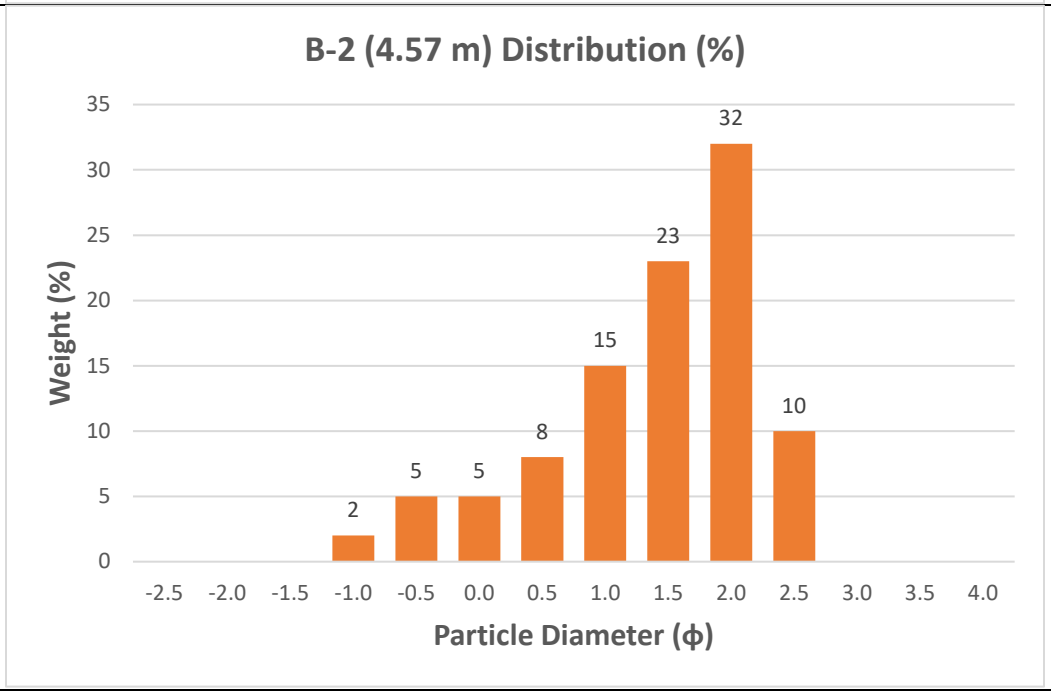
B-2 (4.57 m) Distribution (%)
Weight (%)
35
30
25
20
15
10
5
0
2
5
5
8
15
23
32
10
-2.5
-2.0
-1.5
-1.0
-0.5
0.0
0.5
1.0
1.5
2.0
2.5
3.0
3.5
4.0
Particle Diameter (ϕ)

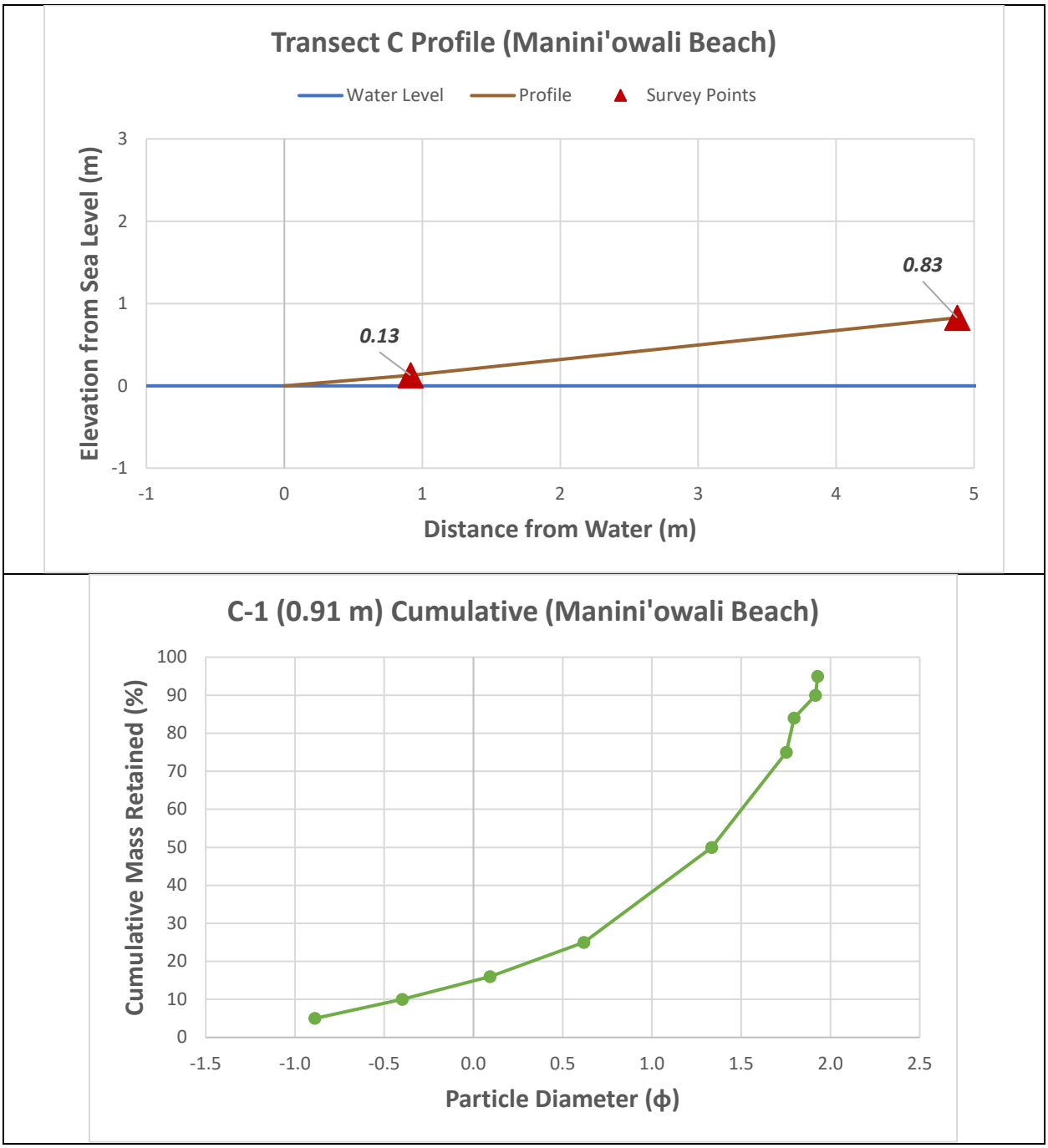
Transect C Profile (Manini'owali Beach)
Water Level
Profile
Survey Points
Elevation from Sea Level (m)
3
2
1
0
-1
-1
0
1
2
3
4
5
0.13
0.83
Distance from Water (m)
C-1 (0.91 m) Cumulative (Manini'owali Beach)
Cumulative Mass Retained (%)
100
90
80
70
60
50
40
30
20
10
0
-1.5
-1.0
-0.5
0.0
0.5
1.0
1.5
2.0
2.5
Particle Diameter (ϕ)

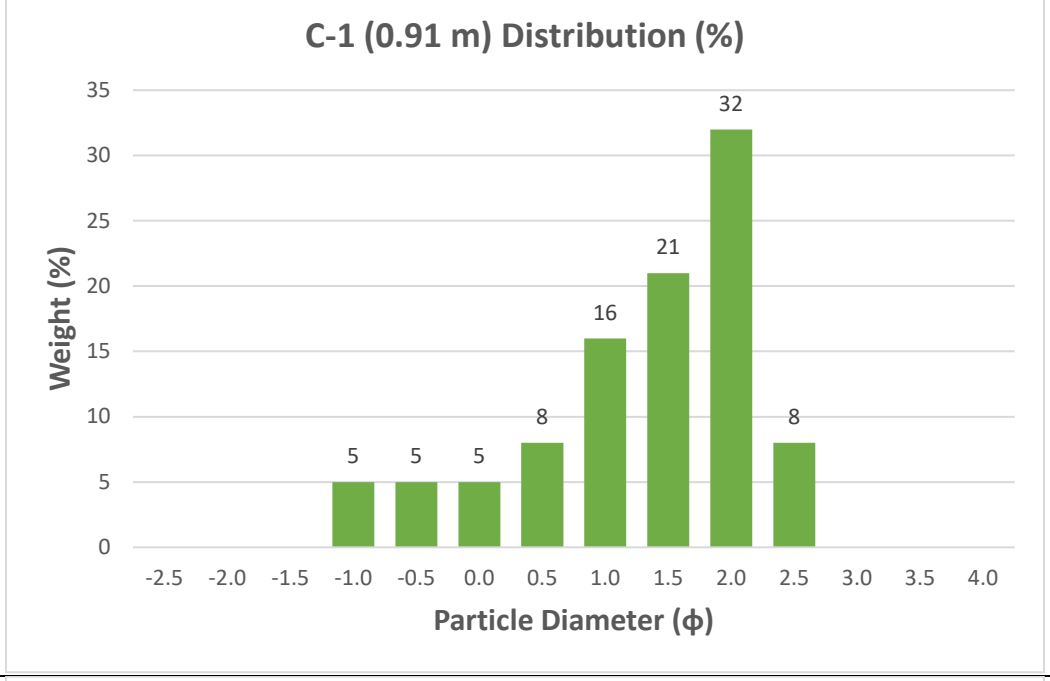
C-1 (0.91 m) Distribution (%)
Weight (%)
35
30
25
20
15
10
5
0
5
5
5
8
16
21
32
8
-2.5
-2.0
-1.5
-1.0
-0.5
0.0
0.5
1.0
1.5
2.0
2.5
3.0
3.5
4.0
Particle Diameter (ϕ)

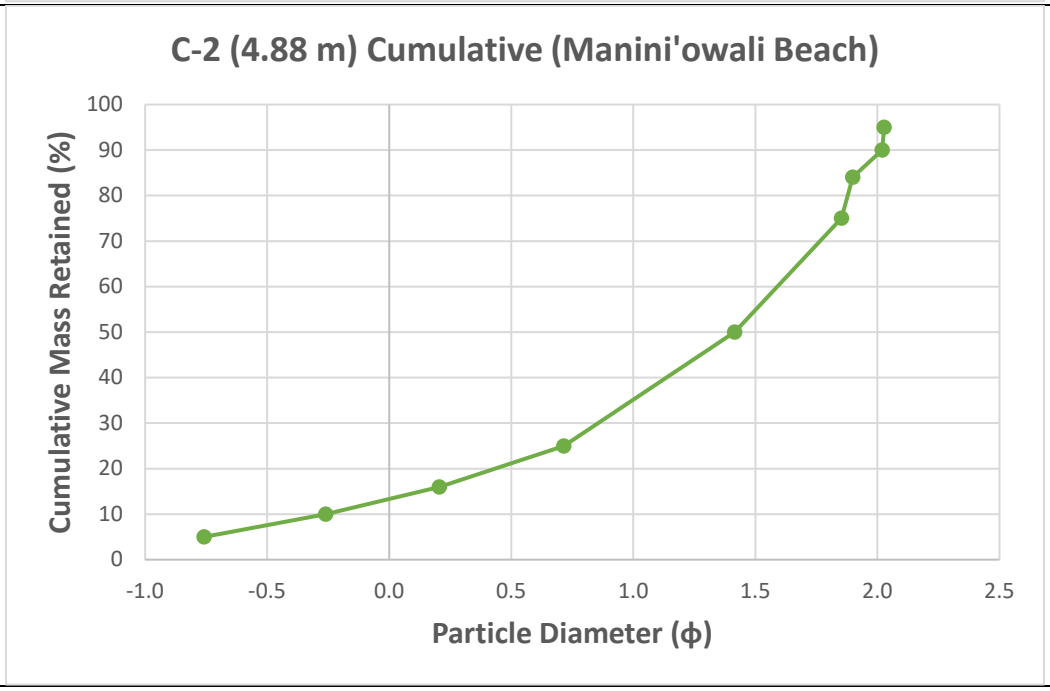
C-2 (4.88 m) Cumulative (Manini'owali Beach)
Cumulative Mass Retained (%)
100
90
80
70
60
50
40
30
20
10
0
-1.0
-0.5
0.0
0.5
1.0
1.5
2.0
2.5
Particle Diameter (ϕ)

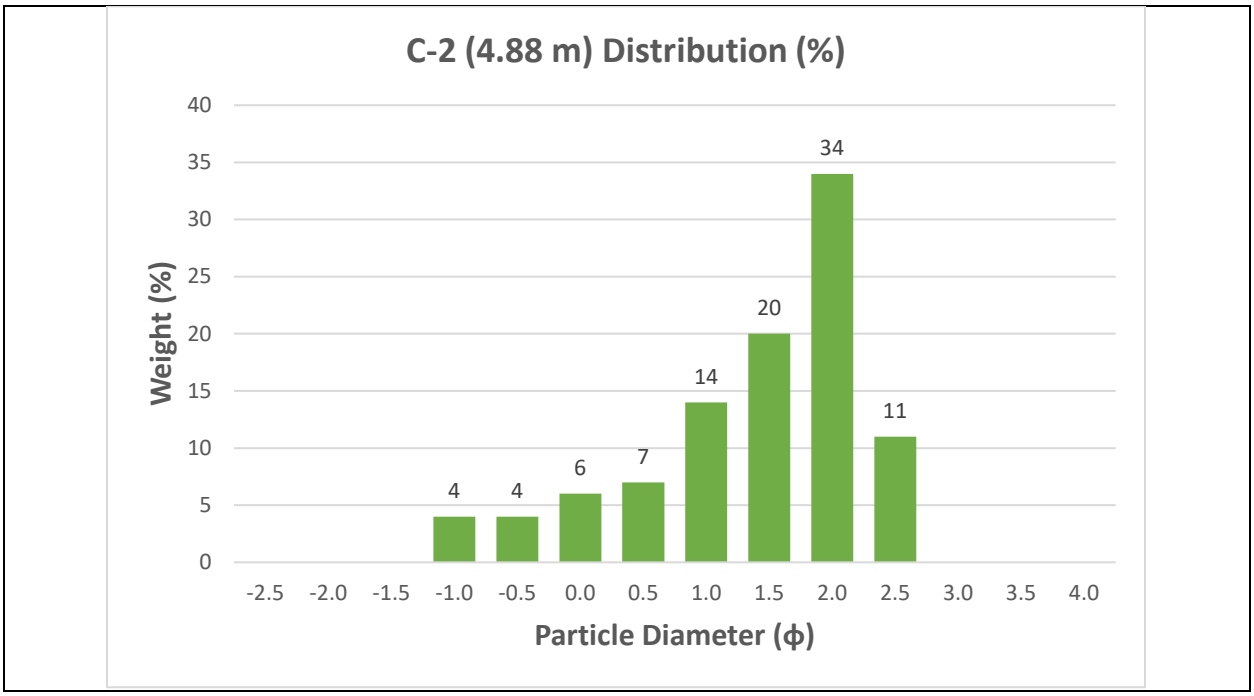
C-2 (4.88 m) Distribution (%)
Weight (%)
40
35
30
25
20
15
10
5
0
4
4
6
7
14
20
34
11
-2.5
-2.0
-1.5
-1.0
-0.5
0.0
0.5
1.0
1.5
2.0
2.5
3.0
3.5
4.0
Particle Diameter (ϕ)

Beach Name:	Waialea Beach	
Date: 10/20/2020	**Time:** Afternoon	-1

					Calculated mm percentile								
Location/ Transect	Survey #	Distance from Water (m)	Slope in Degrees	"x" used	5	10	16	25	50	75	84	90	95
A	1	0.3048	-5	-1.5	1.190402	0.912482	0.721039	0.553254	0.31248	0.187382	0.147588	0.131712	0.065856
	2	0.9144	-5	4	4.36479	4.311523	4.24457	4.136797	3.775535	3.23203	2.916152	2.608302	2.20548
	3	6.40	-5	-0.7	1.346692	1.035083	0.817198	0.627561	0.370892	0.232802	0.193784	0.168656	0.113052
B1	1	1.22	-7	-1.4	0.733954	0.561448	0.449943	0.355597	0.229069	0.160215	0.12124	0.102416	0.051208
	2	3.96	-5	-1.4	0.810646	0.630368	0.513975	0.412621	0.268577	0.184457	0.149253	0.132935	0.073179
B2	1	0.91	-7	-1.4	0.809797	0.603726	0.480697	0.37821	0.240171	0.165361	0.124096	0.11085	0.055425

Calculated ϕ percentiles with corrections								
5	10	16	25	50	75	84	90	95
-0.405	0.211	0.705	1.196	1.762	2.102	2.137	2.193	2.582
-3.427	-3.373	-3.118	-2.868	-2.013	-1.472	-1.195	-1.037	-0.751
-0.692	-0.080	0.435	0.941	1.502	1.829	1.832	1.926	2.069
0.719	1.332	1.723	2.088	2.232	2.298	2.356	2.466	2.821
0.488	1.065	1.436	1.788	1.991	2.122	2.124	2.183	2.482
0.491	1.165	1.580	1.964	2.161	2.259	2.330	2.380	2.746

Moments						
Mean	Standard Deviation	*Descriptor*	Skewness	*Descriptor*	Kurtosis	*Descriptor*
1.535	0.810	Moderately Sorted	-0.464	Very Coarse Skewed	1.351	Leptokurtic
-2.109	0.886	Moderately Sorted	-0.103	Coarse Skewed	0.786	Platykurtic
1.257	0.768	Moderately Sorted	-0.559	Very Coarse Skewed	1.274	Leptokurtic
2.104	0.477	Well Sorted	-0.525	Very Coarse Skewed	4.100	Extremely Leptokurtic
1.850	0.474	Well Sorted	-0.561	Very Coarse Skewed	2.449	Very Leptokurtic
2.024	0.529	Well Sorted	-0.515	Very Coarse Skewed	3.134	Extremely Leptokurtic

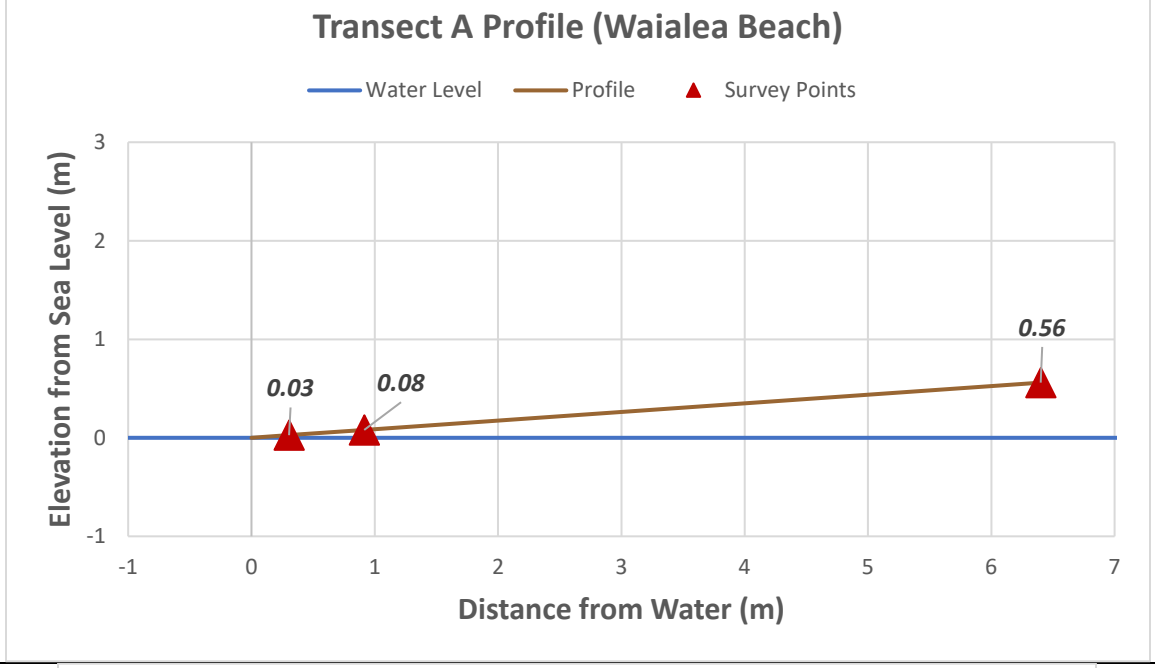
Transect A Profile (Waialea Beach)
Water Level
Profile
Survey Points
Elevation from Sea Level (m)
3
2
1
0
-1
-1
0
1
2
3
4
5
6
7
0.03
0.08
0.56
Distance from Water (m)

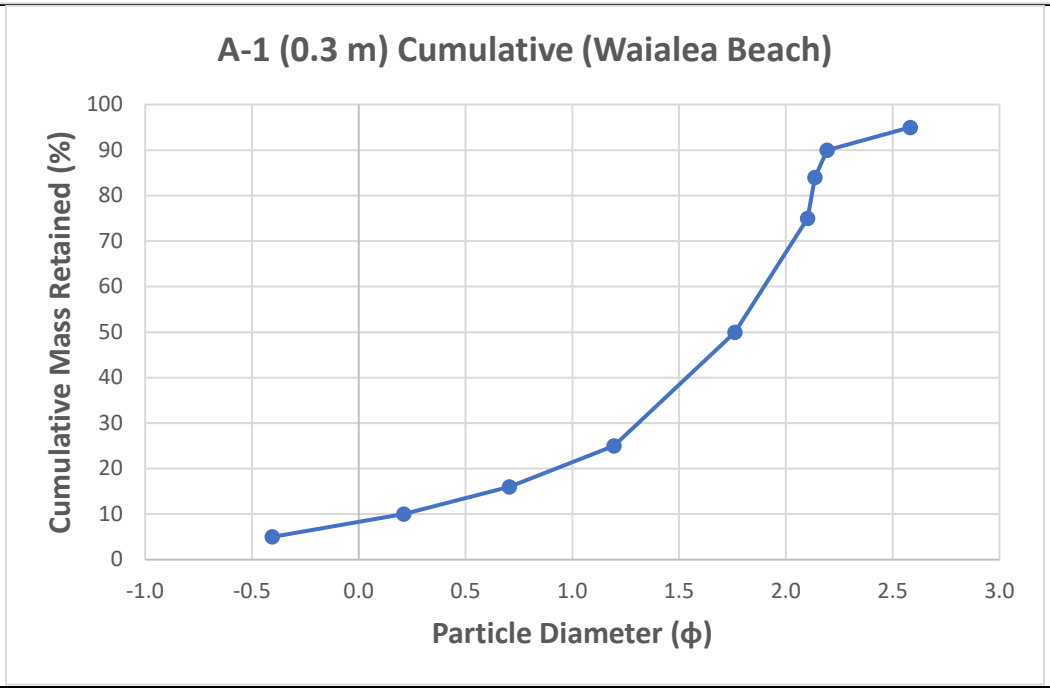
A-1 (0.3 m) Cumulative (Waialea Beach)
Cumulative Mass Retained (%)
100
90
80
70
60
50
40
30
20
10
0
-1.0
-0.5
0.0
0.5
1.0
1.5
2.0
2.5
3.0
Particle Diameter (ϕ)

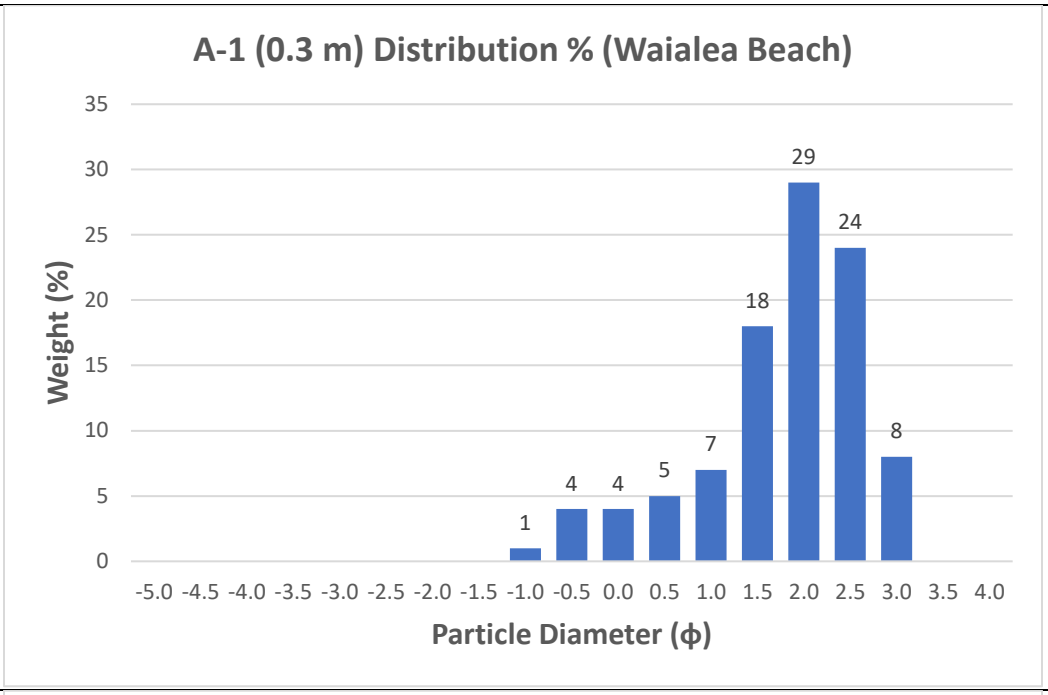
A-1 (0.3 m) Distribution % (Waialea Beach)
Weight (%)
35
30
25
20
15
10
5
0
1
4
4
5
7
18
29
24
8
-5.0 -4.5 -4.0 -3.5 -3.0 -2.5 -2.0 -1.5 -1.0 -0.5 0.0 0.5 1.0 1.5 2.0 2.5 3.0 3.5 4.0
Particle Diameter (ϕ)

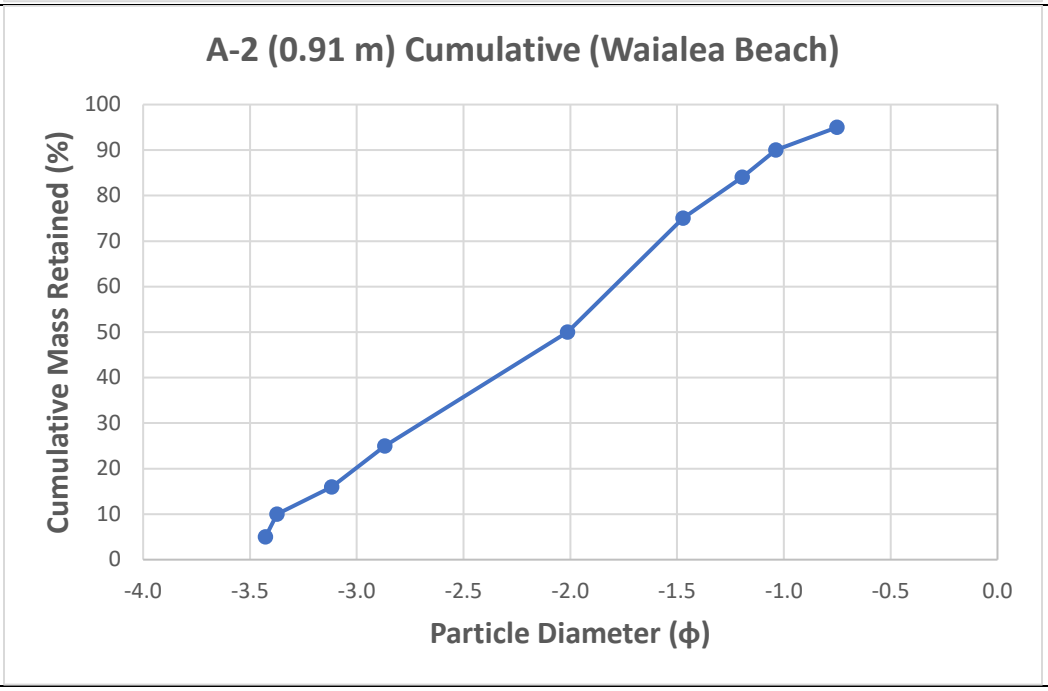
A-2 (0.91 m) Cumulative (Waialea Beach)
Cumulative Mass Retained (%)
100
90
80
70
60
50
40
30
20
10
0
-4.0 -3.5 -3.0 -2.5 -2.0 -1.5 -1.0 -0.5 0.0
Particle Diameter (ϕ)

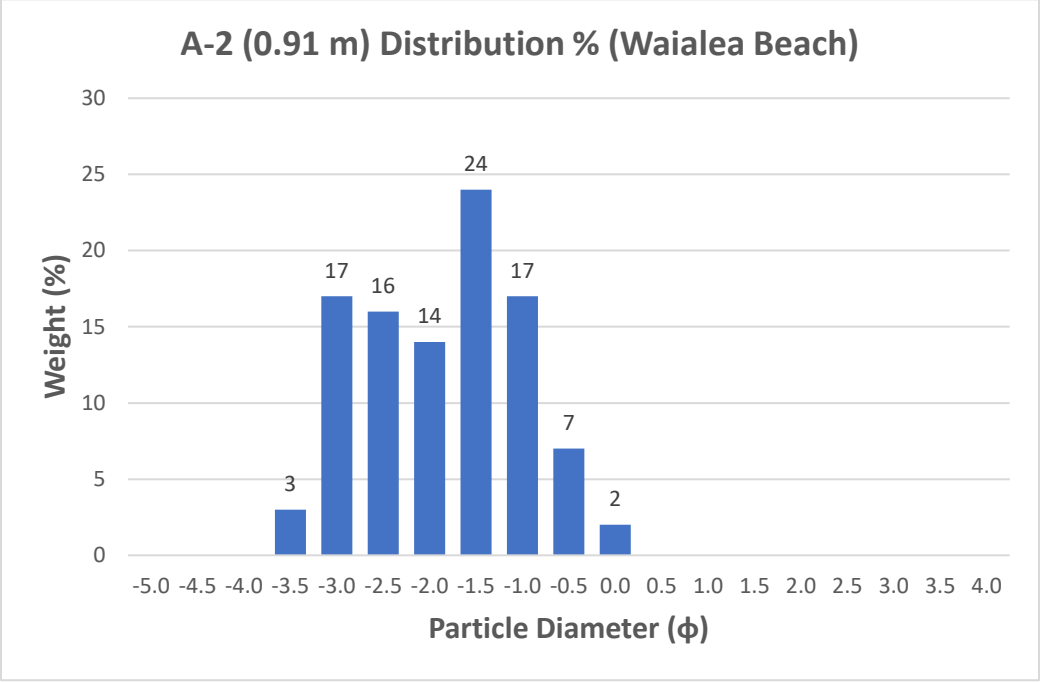
A-2 (0.91 m) Distribution % (Waialea Beach)
Weight (%)
30
25
20
15
10
5
0
3
17
16
14
24
17
7
2
-5.0 -4.5 -4.0 -3.5 -3.0 -2.5 -2.0 -1.5 -1.0 -0.5 0.0 0.5 1.0 1.5 2.0 2.5 3.0 3.5 4.0
Particle Diameter (ϕ)

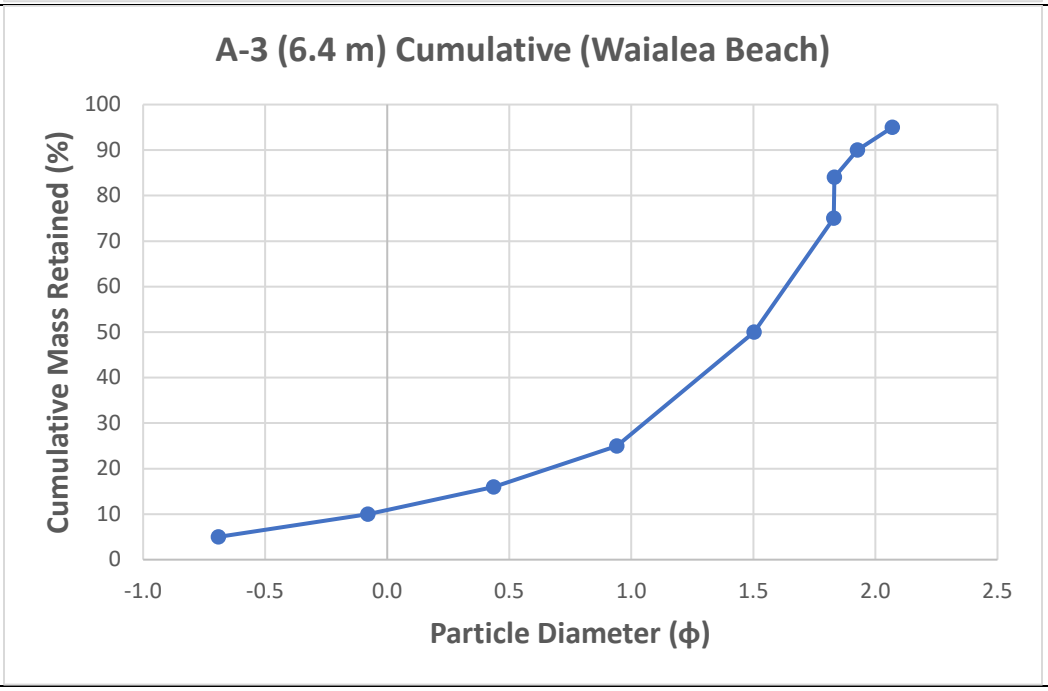
A-3 (6.4 m) Cumulative (Waialea Beach)
Cumulative Mass Retained (%)
100
90
80
70
60
50
40
30
20
10
0
-1.0 -0.5 0.0 0.5 1.0 1.5 2.0 2.5
Particle Diameter (ϕ)

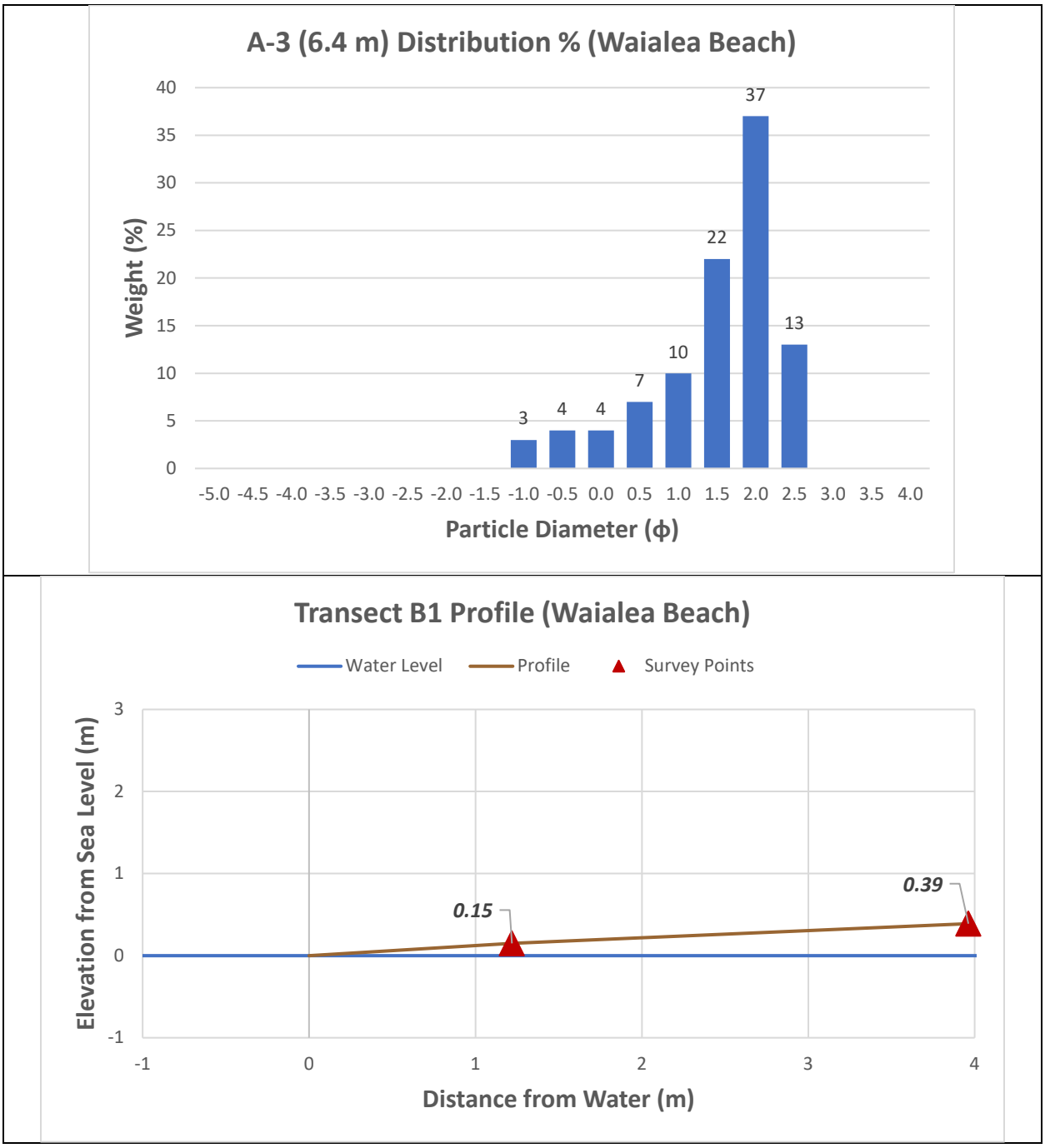
A-3 (6.4 m) Distribution % (Waialea Beach)
Weight (%)
40
35
30
25
20
15
10
5
0
3
4
4
7
10
22
37
13
-5.0 -4.5 -4.0 -3.5 -3.0 -2.5 -2.0 -1.5 -1.0 -0.5 0.0 0.5 1.0 1.5 2.0 2.5 3.0 3.5 4.0
Particle Diameter (ϕ)
Transect B1 Profile (Waialea Beach)
Water Level
Profile
Survey Points
Elevation from Sea Level (m)
3
2
1
0
-1
0.15
0.39
-1
0
1
2
3
4
Distance from Water (m)

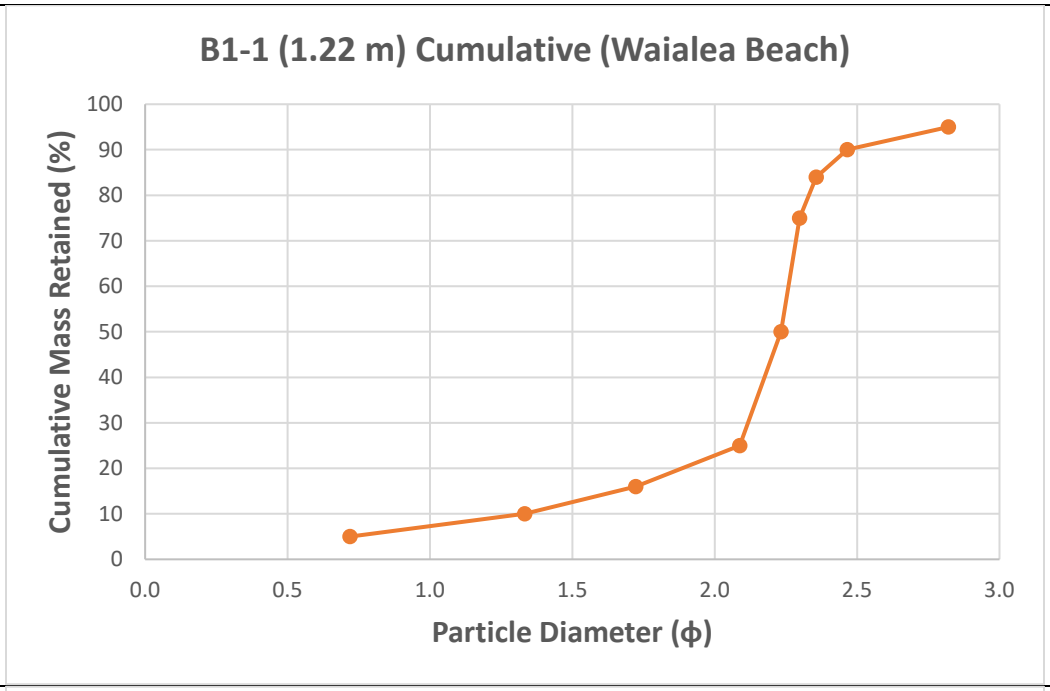
B1-1 (1.22 m) Cumulative (Waialea Beach)
Cumulative Mass Retained (%)
100
90
80
70
60
50
40
30
20
10
0
0.0
0.5
1.0
1.5
2.0
2.5
3.0
Particle Diameter (ϕ)

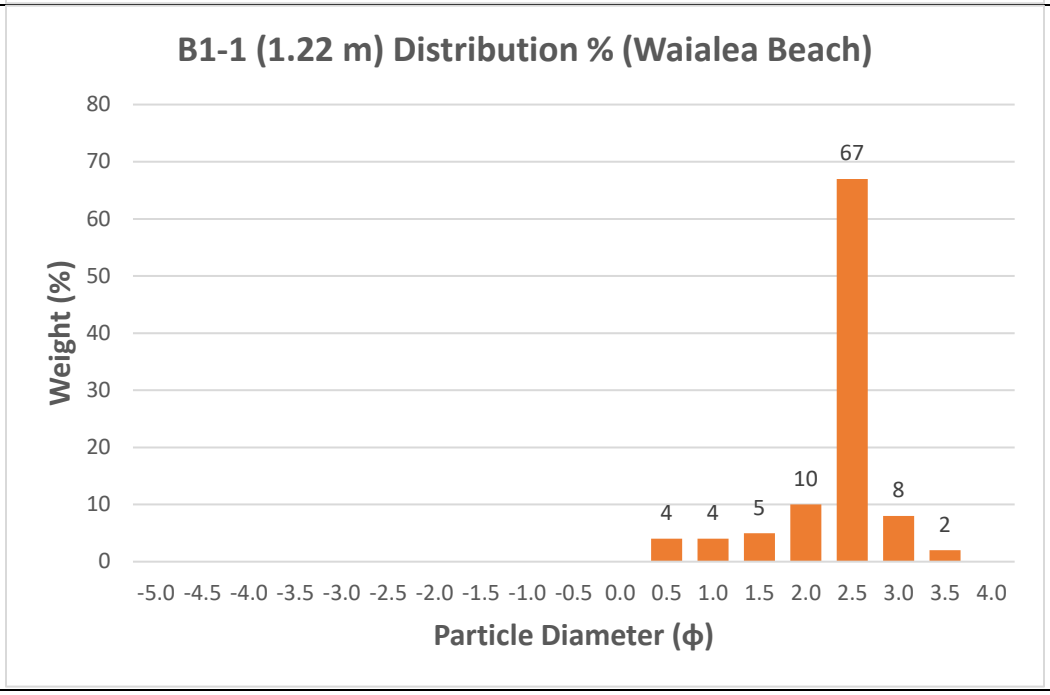
B1-1 (1.22 m) Distribution % (Waialea Beach)
Weight (%)
80
70
60
50
40
30
20
10
0
67
10
8
4
4
5
2
-5.0 -4.5 -4.0 -3.5 -3.0 -2.5 -2.0 -1.5 -1.0 -0.5 0.0 0.5 1.0 1.5 2.0 2.5 3.0 3.5 4.0
Particle Diameter (ϕ)

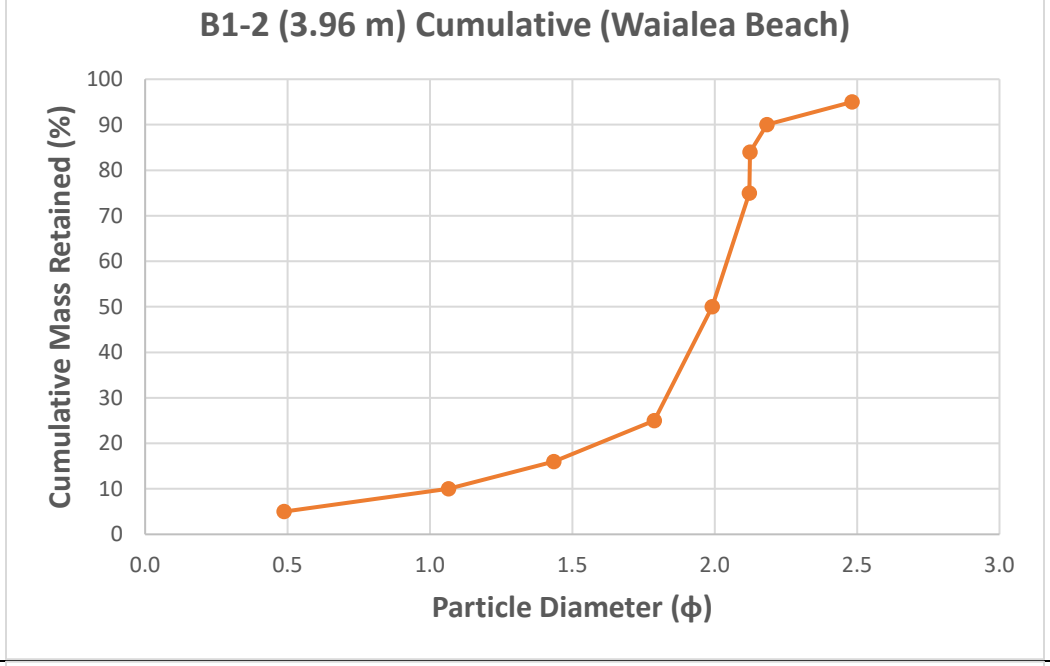
B1-2 (3.96 m) Cumulative (Waialea Beach)
Cumulative Mass Retained (%)
100
90
80
70
60
50
40
30
20
10
0
0.0
0.5
1.0
1.5
2.0
2.5
3.0
Particle Diameter (ϕ)

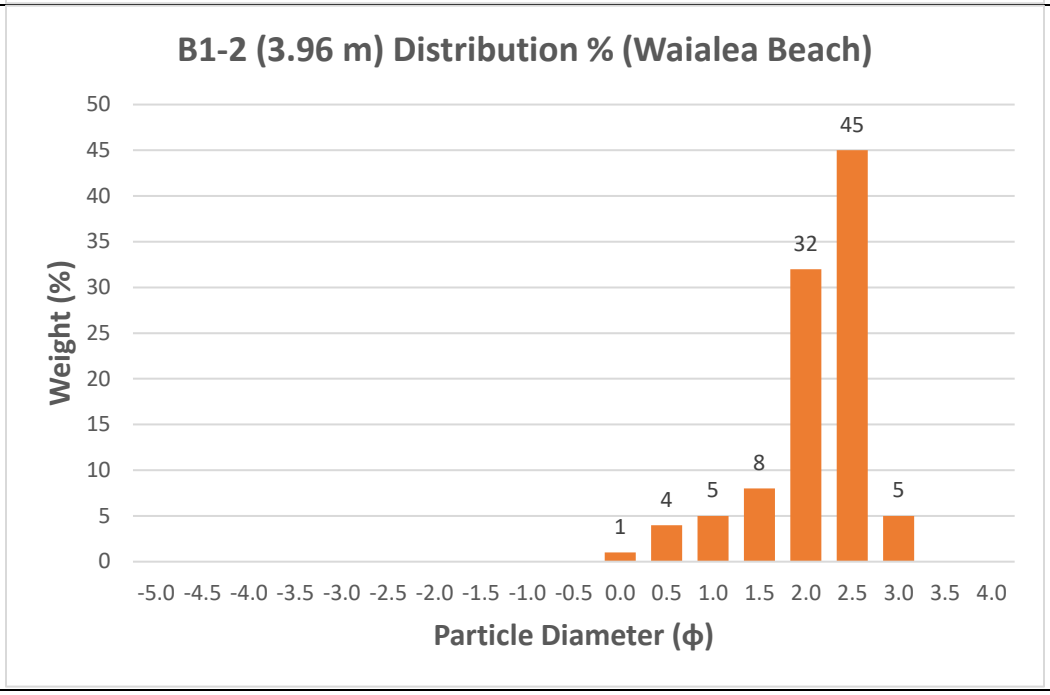
B1-2 (3.96 m) Distribution % (Waialea Beach)
Weight (%)
50
45
40
35
30
25
20
15
10
5
0
1
4
5
8
32
45
5
-5.0 -4.5 -4.0 -3.5 -3.0 -2.5 -2.0 -1.5 -1.0 -0.5 0.0 0.5 1.0 1.5 2.0 2.5 3.0 3.5 4.0
Particle Diameter (ϕ)

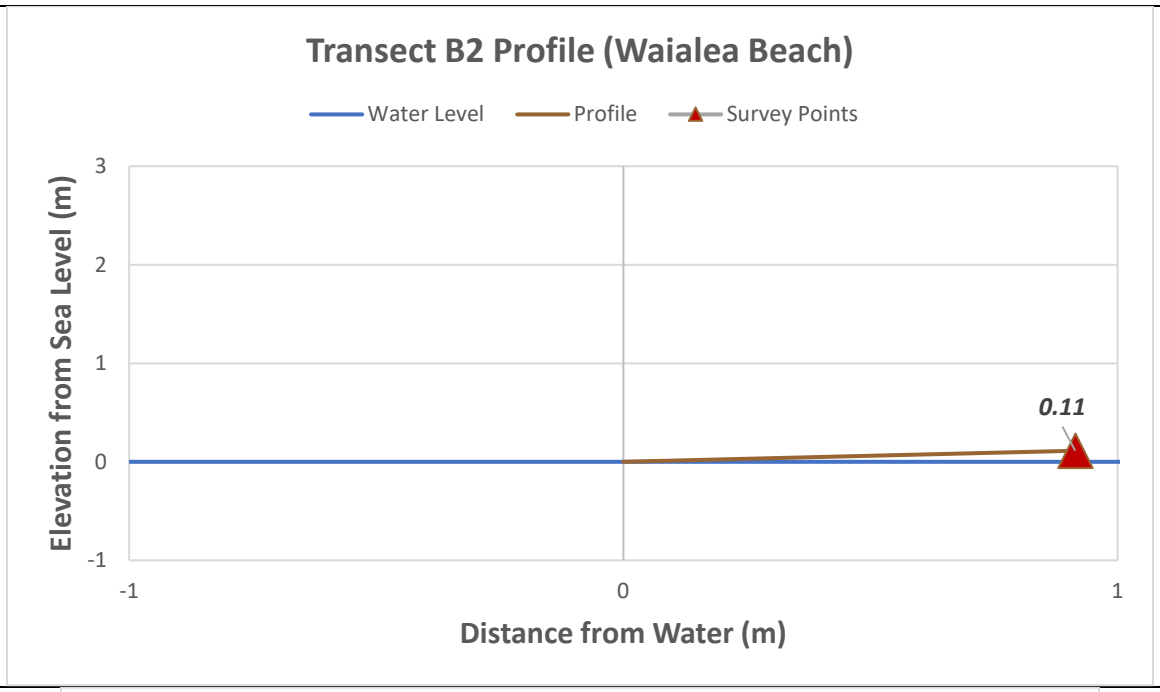
Transect B2 Profile (Waialea Beach)
Water Level
Profile
Survey Points
Elevation from Sea Level (m)
3
2
1
0
-1
-1
0
1
0.11
Distance from Water (m)

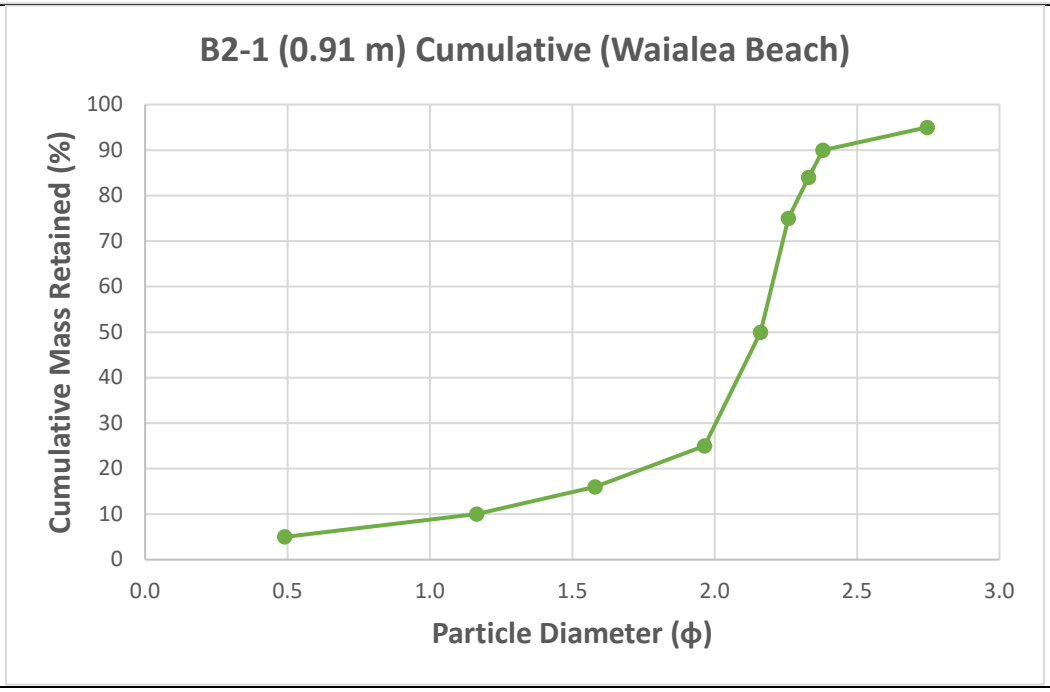
B2-1 (0.91 m) Cumulative (Waialea Beach)
Cumulative Mass Retained (%)
100
90
80
70
60
50
40
30
20
10
0
0.0
0.5
1.0
1.5
2.0
2.5
3.0
Particle Diameter (ϕ)

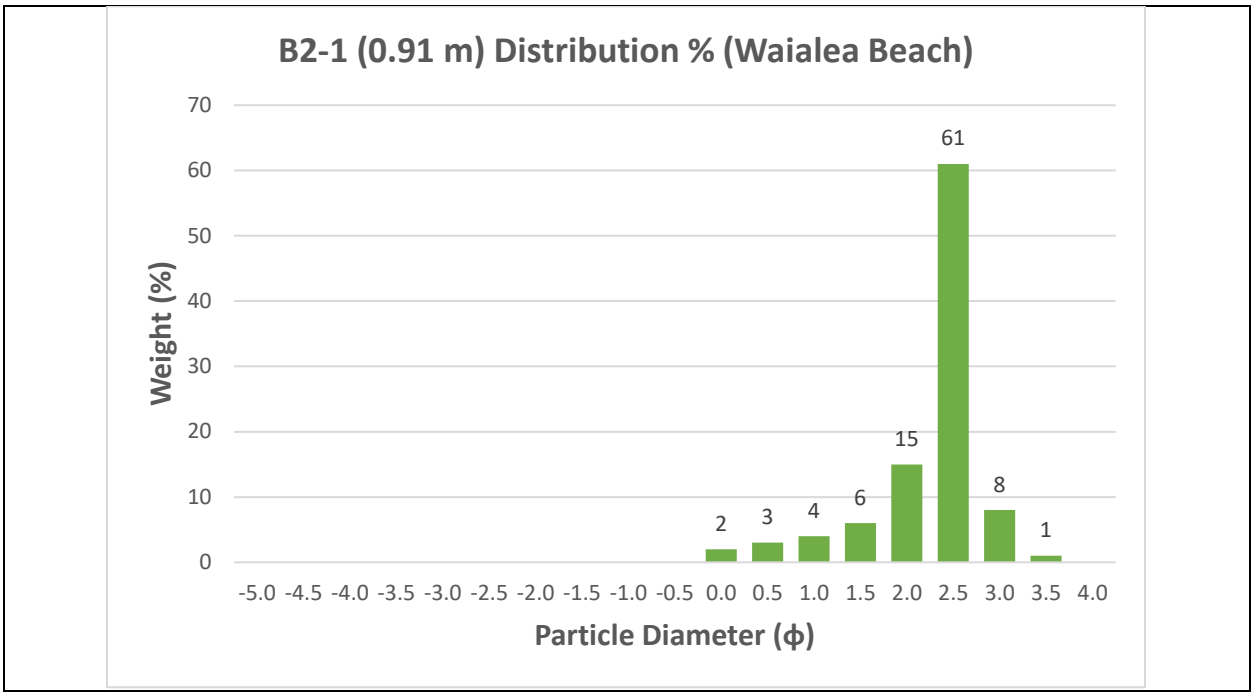
B2-1 (0.91 m) Distribution % (Waialea Beach)
Weight (%)
70
60
50
40
30
20
10
0
61
15
8
6
4
3
2
1
-5.0 -4.5 -4.0 -3.5 -3.0 -2.5 -2.0 -1.5 -1.0 -0.5 0.0 0.5 1.0 1.5 2.0 2.5 3.0 3.5 4.0
Particle Diameter (ϕ)

Beach Name:	Mauna Kea Beach

Date: 10/20/2020 **Time:** Afternoon -1

Location/ Transect	Survey #	Distance from Water (m)	Slope in Degrees	"x" used	Calculated mm percentile								
					5	10	16	25	50	75	84	90	95
A	1	4.572	-4	-0.7	1.133296	0.857964	0.677006	0.520874	0.306291	0.197105	0.146515	0.127385	0.085028

Calculated ϕ percentiles with corrections

5	10	16	25	50	75	84	90	95
-0.291	0.354	0.841	1.317	1.792	2.038	2.145	2.230	2.340

Moments

Mean	Standard Deviation	*Descriptor*	Skewness	*Descriptor*	Kurtosis	*Descriptor*
1.593	0.724	Moderately Well Sorted	-0.522	Very Coarse Skewed	1.495	Leptokurtic

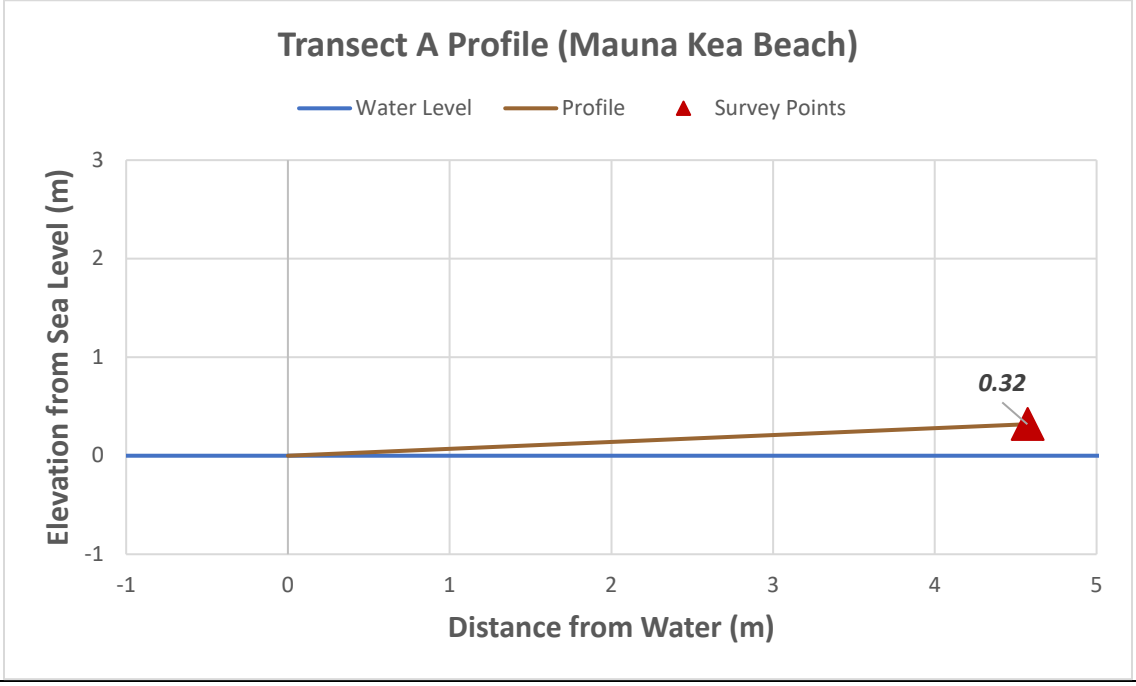

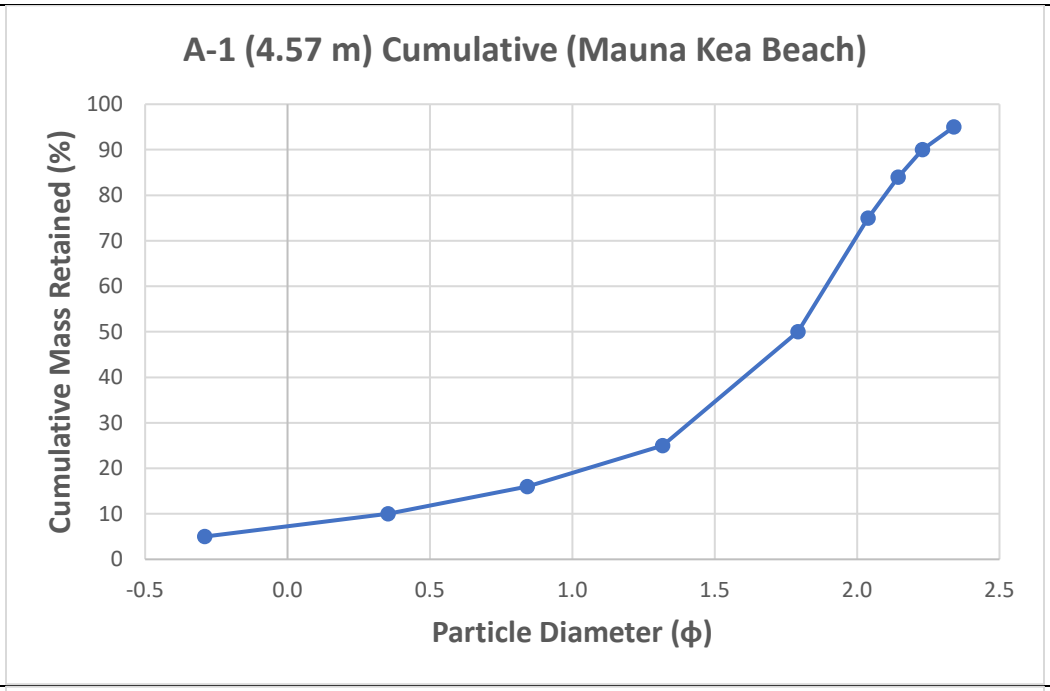
A-1 (4.57 m) Cumulative (Mauna Kea Beach)
Cumulative Mass Retained (%)
100
90
80
70
60
50
40
30
20
10
0
-0.5
0.0
0.5
1.0
1.5
2.0
2.5
Particle Diameter (ϕ)

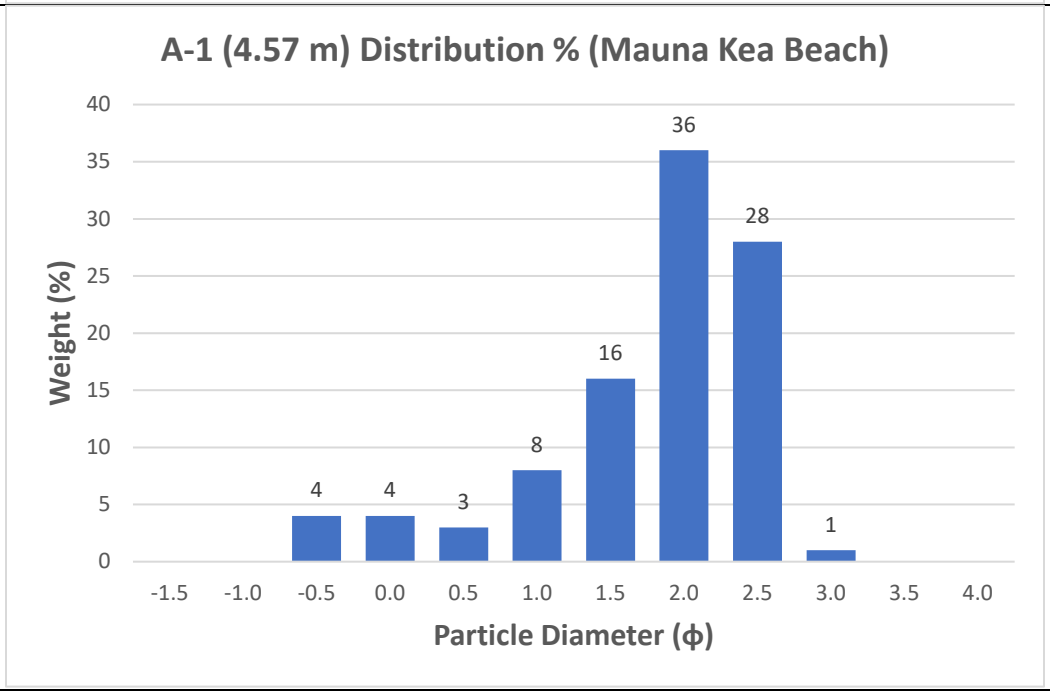
A-1 (4.57 m) Distribution % (Mauna Kea Beach)
Weight (%)
40
35
30
25
20
15
10
5
0
4
4
3
8
16
36
28
1
-1.5
-1.0
-0.5
0.0
0.5
1.0
1.5
2.0
2.5
3.0
3.5
4.0
Particle Diameter (ϕ)

Beach Name: Hapuna Beach

Date: 10/20/2020 **Time:** Afternoon

Location/ Transect	Survey #	Distance from Water (m)	Slope in Degrees	"x" used	Calculated mm percentile								
					5	10	16	25	50	75	84	90	95
A	1	1.2192	-4	-1.9	0.585785	0.441089	0.357296	0.287562	0.185033	0.125576	0.095158	0.071973	0.035987
	2	5.4864	-5	-1.9	0.614958	0.463733	0.374558	0.300312	0.200204	0.137075	0.099066	0.074416	0.037208
	3	8.53	-4	-1.9	0.645596	0.482052	0.388664	0.3091	0.203337	0.142983	0.101518	0.075949	0.037975

Calculated ϕ percentiles with corrections

5	10	16	25	50	75	84	90	95
1.244	1.889	2.220	2.517	2.556	2.604	2.627	2.847	3.156
1.131	1.774	2.118	2.430	2.436	2.494	2.582	2.811	3.124
1.018	1.684	2.038	2.371	2.413	2.441	2.554	2.789	3.105

Moments

Mean	Standard Deviation	*Descriptor*	Skewness	*Descriptor*	Kurtosis	*Descriptor*
2.467	0.391	Very Well Sorted	-0.512	Very Coarse Skewed	9.013	Extremely Leptokurtic
2.379	0.418	Well Sorted	-0.342	Very Coarse Skewed	12.646	Extremely Leptokurtic
2.335	0.445	Well Sorted	-0.394	Very Coarse Skewed	12.238	Extremely Leptokurtic

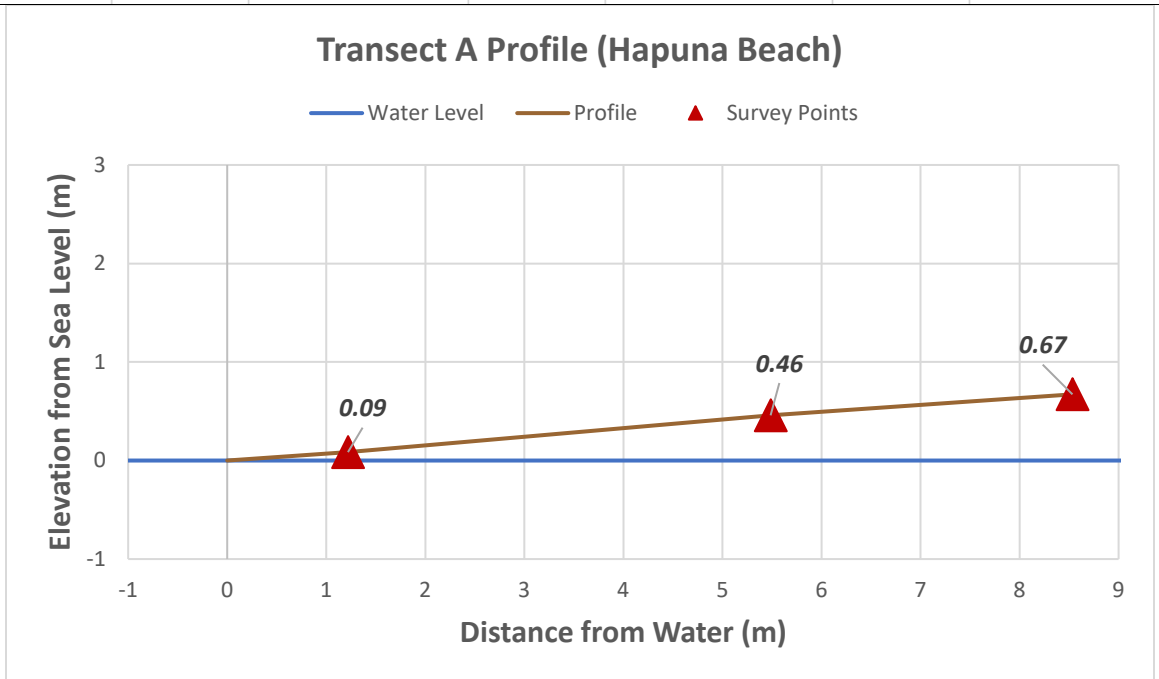

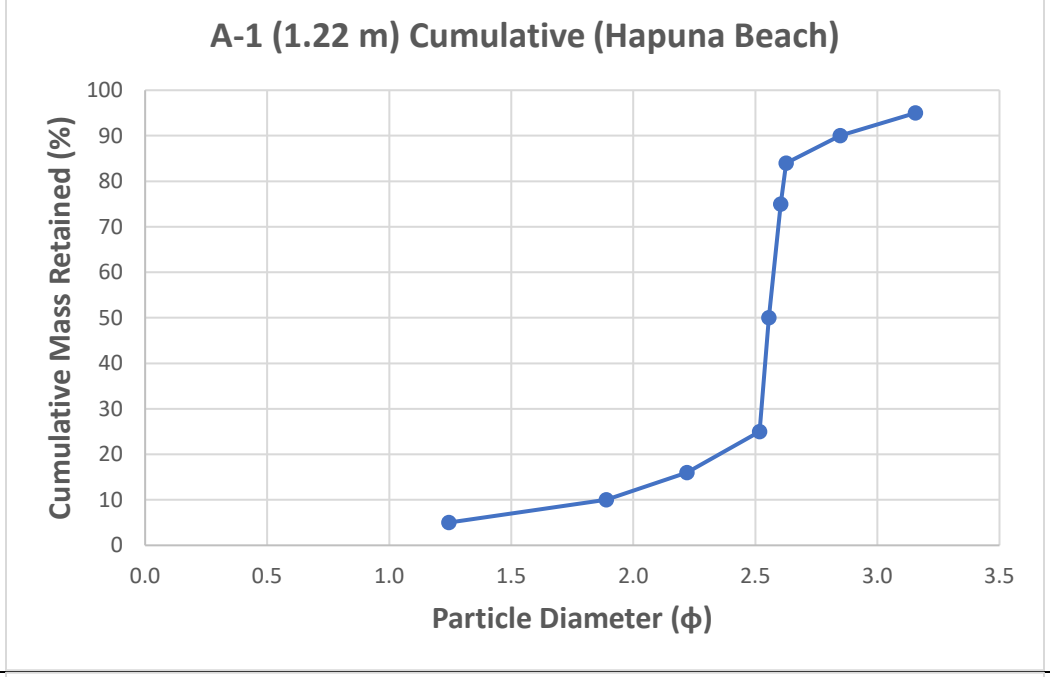
A-1 (1.22 m) Cumulative (Hapuna Beach)
Cumulative Mass Retained (%)
100
90
80
70
60
50
40
30
20
10
0
0.0
0.5
1.0
1.5
2.0
2.5
3.0
3.5
Particle Diameter (ϕ)

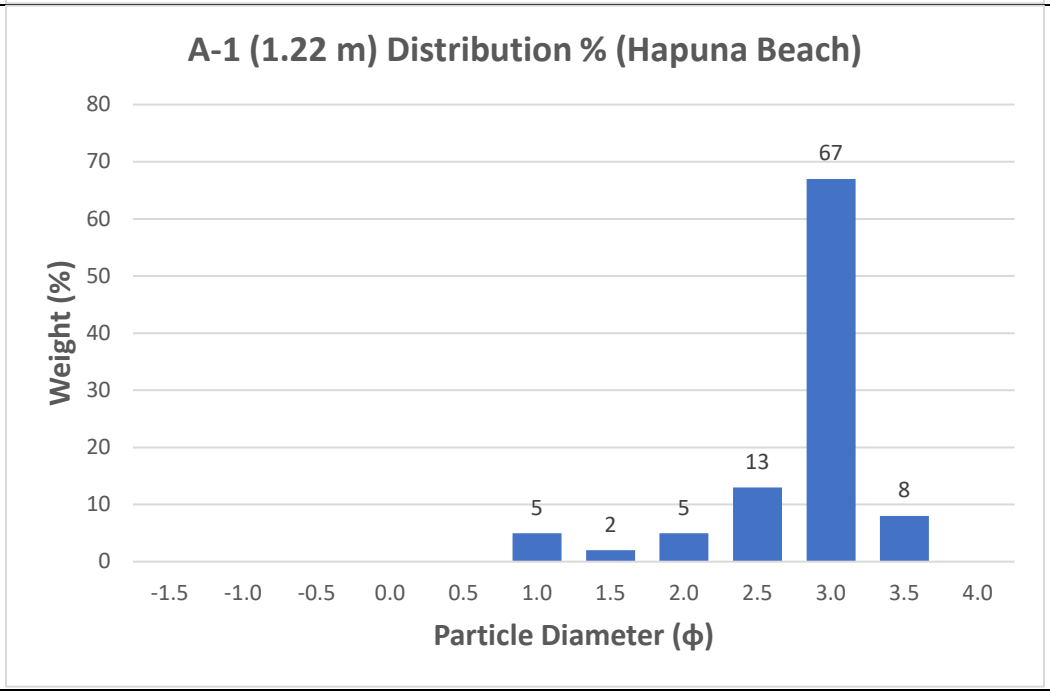
A-1 (1.22 m) Distribution % (Hapuna Beach)
Weight (%)
80
70
60
50
40
30
20
10
0
67
13
8
5
2
5
-1.5
-1.0
-0.5
0.0
0.5
1.0
1.5
2.0
2.5
3.0
3.5
4.0
Particle Diameter (ϕ)

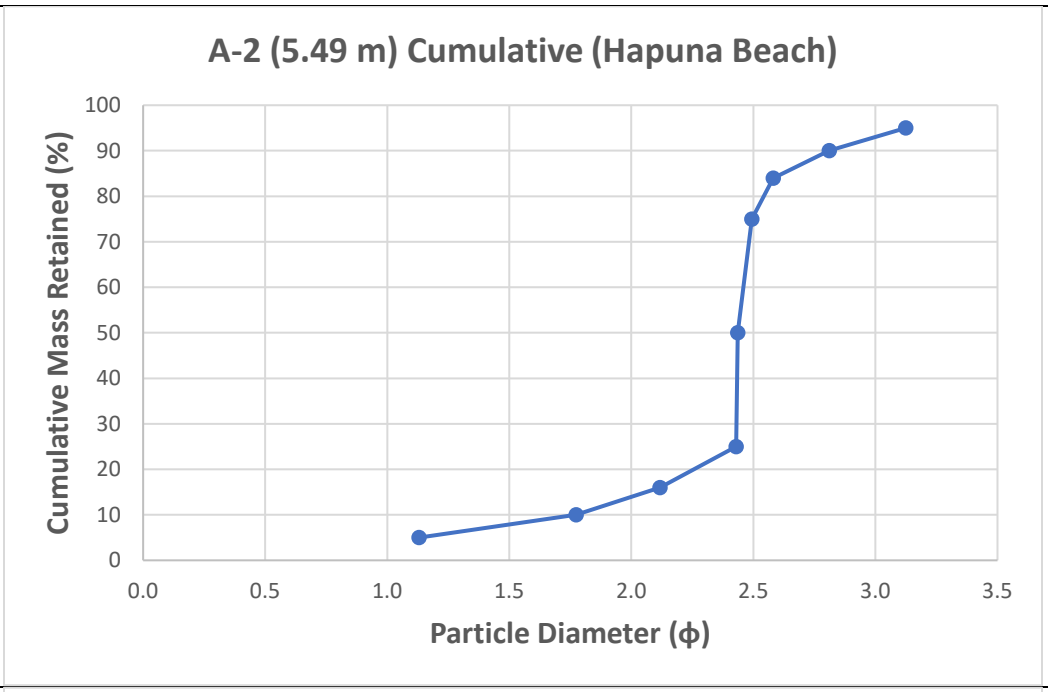
A-2 (5.49 m) Cumulative (Hapuna Beach)
Cumulative Mass Retained (%)
100
90
80
70
60
50
40
30
20
10
0
0.0
0.5
1.0
1.5
2.0
2.5
3.0
3.5
Particle Diameter (ϕ)

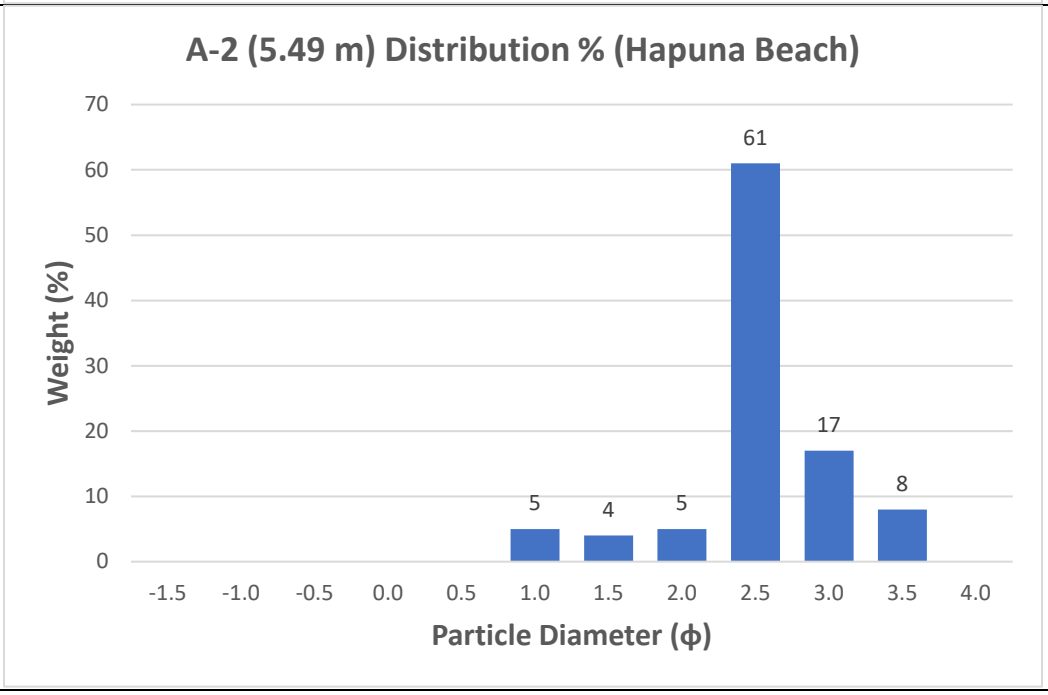
A-2 (5.49 m) Distribution % (Hapuna Beach)
Weight (%)
70
60
50
40
30
20
10
0
61
17
8
5
4
5
-1.5
-1.0
-0.5
0.0
0.5
1.0
1.5
2.0
2.5
3.0
3.5
4.0
Particle Diameter (ϕ)

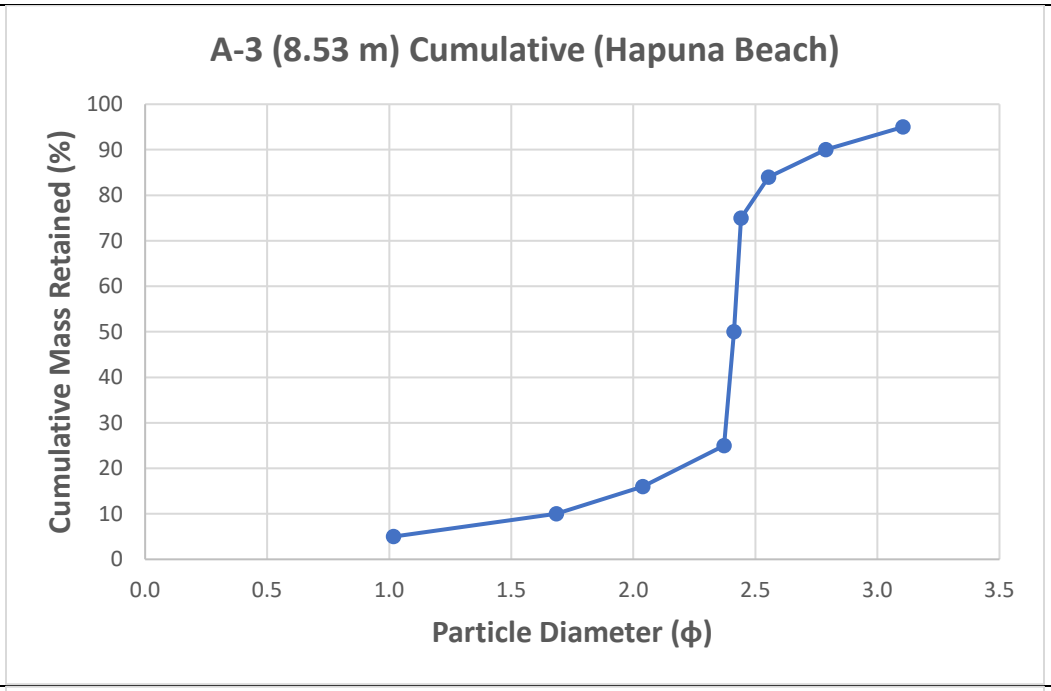
A-3 (8.53 m) Cumulative (Hapuna Beach)
Cumulative Mass Retained (%)
100
90
80
70
60
50
40
30
20
10
0
0.0
0.5
1.0
1.5
2.0
2.5
3.0
3.5
Particle Diameter (ϕ)

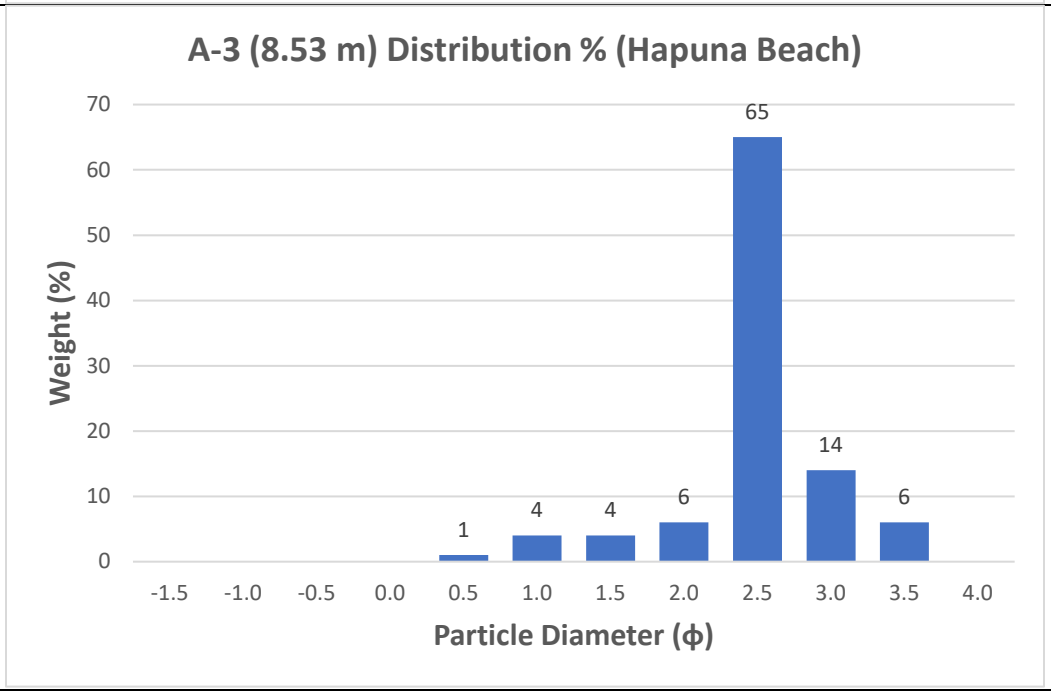
A-3 (8.53 m) Distribution % (Hapuna Beach)
Weight (%)
70
60
50
40
30
20
10
0
65
14
6
6
4
4
1
-1.5
-1.0
-0.5
0.0
0.5
1.0
1.5
2.0
2.5
3.0
3.5
4.0
Particle Diameter (ϕ)

Beach Name:	Spencer Beach
Date: 10/20/2020	**Time:** Afternoon

					Calculated mm percentile								
Location/ Transect	Survey #	Distance from Water (m)	Slope in Degrees	"x" used	5	10	16	25	50	75	84	90	95
A	1	0.6096	-3	-1.9	0.873419	0.659161	0.528251	0.414193	0.255679	0.17091	0.129034	0.108419	0.05421
	2	4.572	-3	-1.9	0.784759	0.590497	0.472607	0.370357	0.230047	0.157515	0.118631	0.093676	0.046838
	3	8.84	-2	-1.9	0.683794	0.530146	0.434998	0.349578	0.224688	0.153575	0.114321	0.09668	0.04834

Calculated ϕ percentiles with corrections								
5	10	16	25	50	75	84	90	95
0.315	0.962	1.376	1.780	2.066	2.217	2.287	2.404	2.767
0.564	1.216	1.617	2.006	2.226	2.320	2.380	2.562	2.906
0.884	1.465	1.795	2.123	2.262	2.352	2.422	2.528	2.876

Moments						
Mean	Standard Deviation	*Descriptor*	Skewness	*Descriptor*	Kurtosis	*Descriptor*
1.910	0.599	Moderately Well Sorted	-0.472	Very Coarse Skewed	2.299	Very Leptokurtic
2.074	0.546	Moderately Well Sorted	-0.508	Very Coarse Skewed	3.061	Extremely Leptokurtic
2.160	0.458	Well Sorted	-0.436	Very Coarse Skewed	3.569	Extremely Leptokurtic

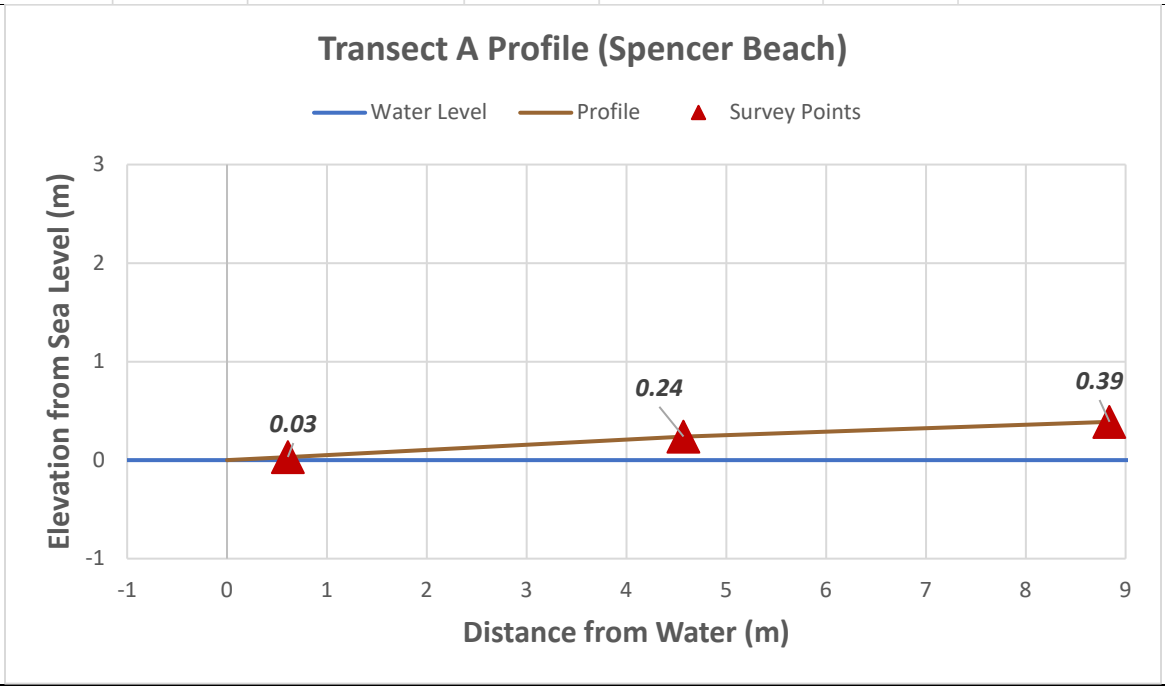

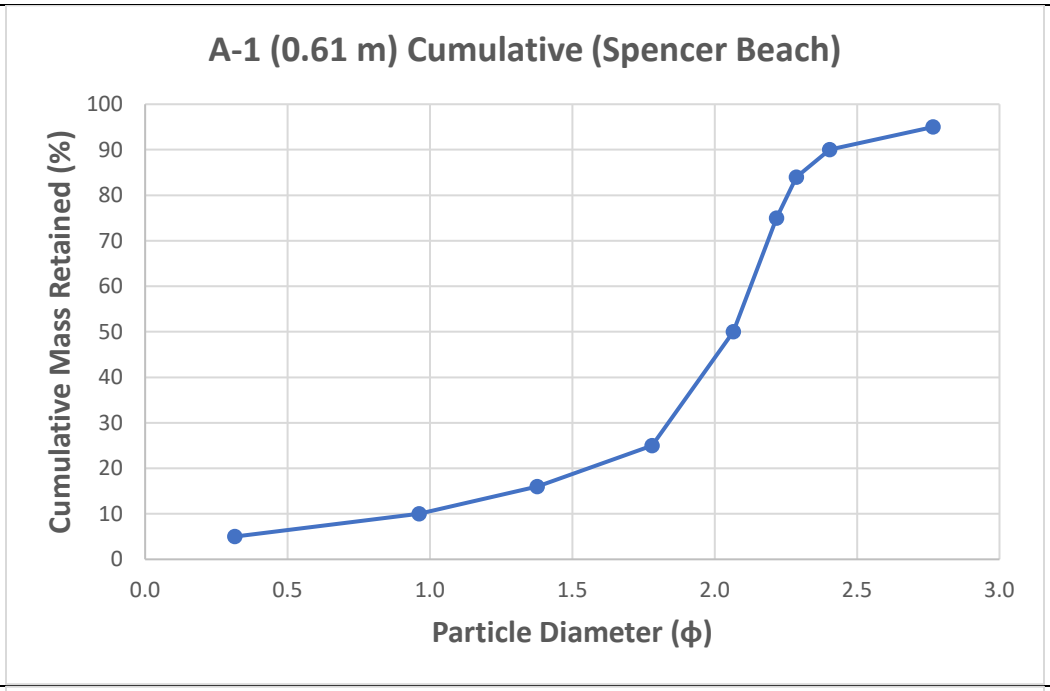
A-1 (0.61 m) Cumulative (Spencer Beach)
Cumulative Mass Retained (%)
100
90
80
70
60
50
40
30
20
10
0
0.0
0.5
1.0
1.5
2.0
2.5
3.0
Particle Diameter (ϕ)

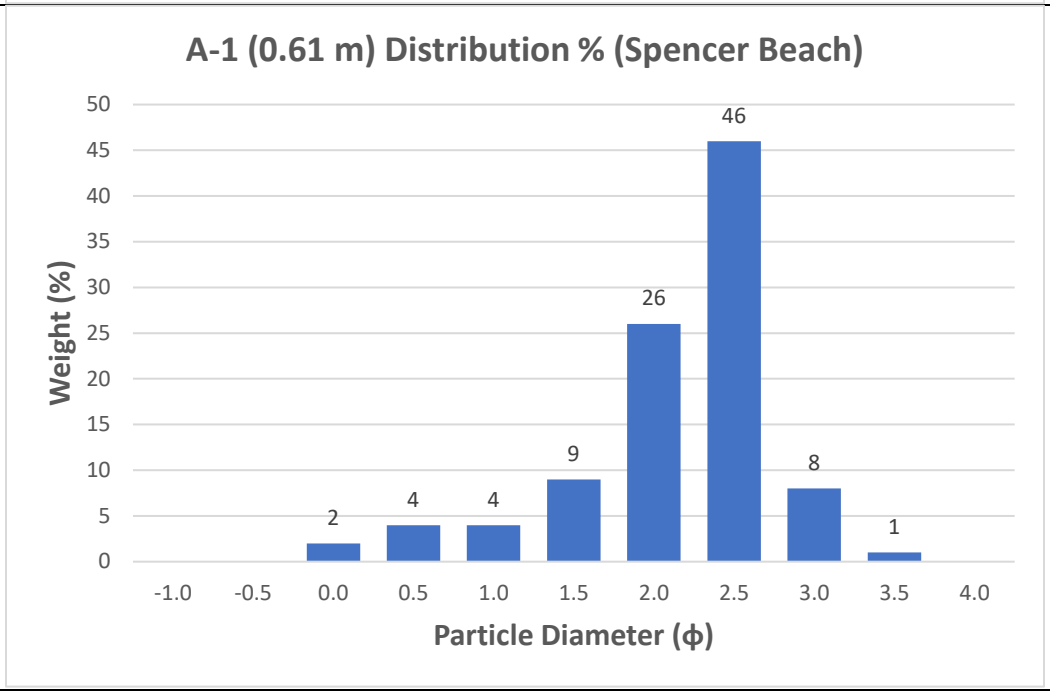
A-1 (0.61 m) Distribution % (Spencer Beach)
Weight (%)
50
45
40
35
30
25
20
15
10
5
0
2
4
4
9
26
46
8
1
-1.0
-0.5
0.0
0.5
1.0
1.5
2.0
2.5
3.0
3.5
4.0
Particle Diameter (ϕ)

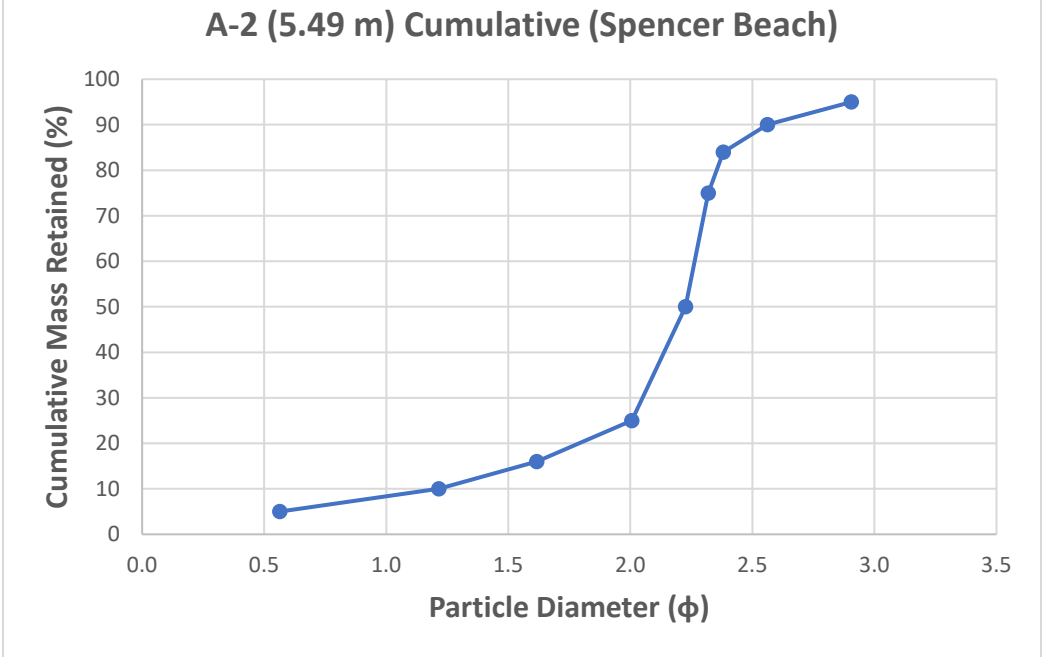
A-2 (5.49 m) Cumulative (Spencer Beach)
Cumulative Mass Retained (%)
100
90
80
70
60
50
40
30
20
10
0
0.0
0.5
1.0
1.5
2.0
2.5
3.0
3.5
Particle Diameter (ϕ)

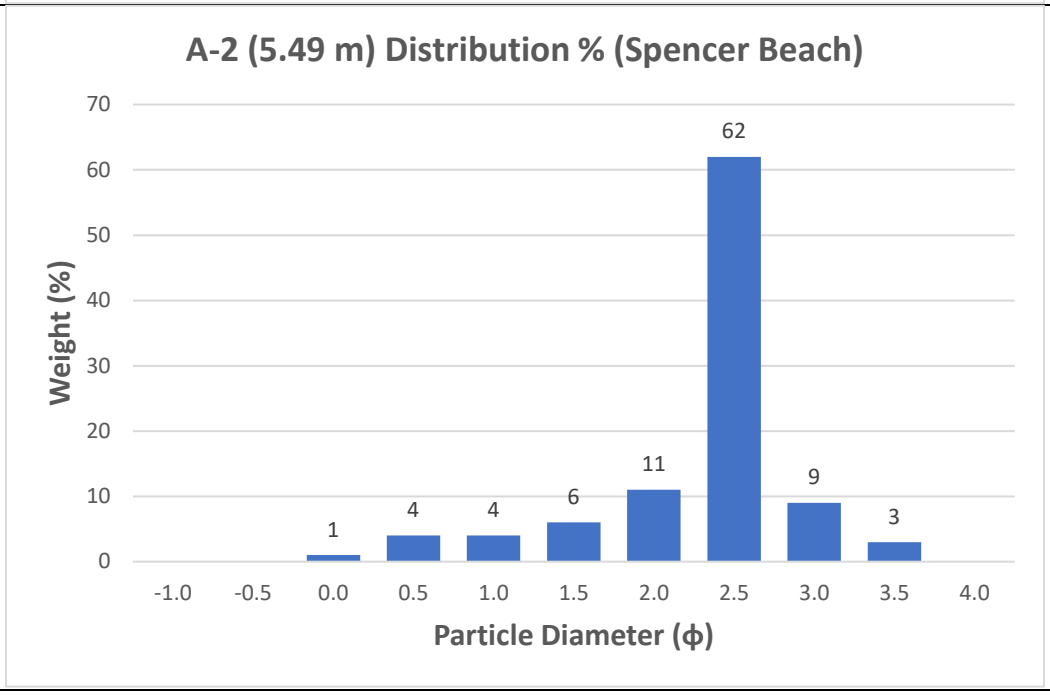
A-2 (5.49 m) Distribution % (Spencer Beach)
Weight (%)
70
60
50
40
30
20
10
0
1
4
4
6
11
62
9
3
-1.0
-0.5
0.0
0.5
1.0
1.5
2.0
2.5
3.0
3.5
4.0
Particle Diameter (ϕ)

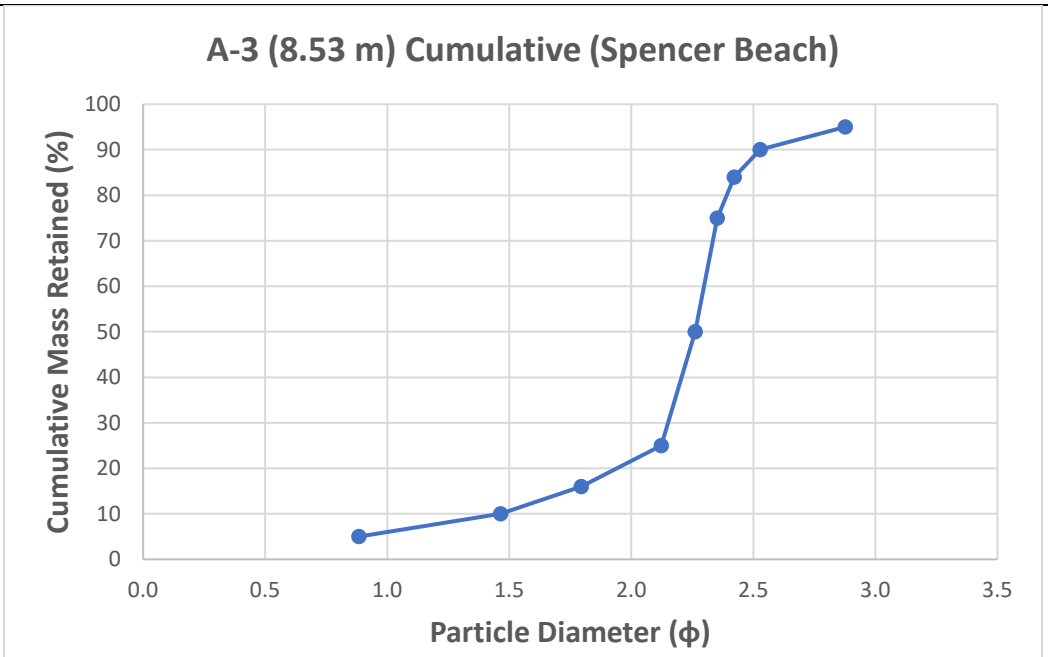
A-3 (8.53 m) Cumulative (Spencer Beach)
Cumulative Mass Retained (%)
100
90
80
70
60
50
40
30
20
10
0
0.0
0.5
1.0
1.5
2.0
2.5
3.0
3.5
Particle Diameter (ϕ)

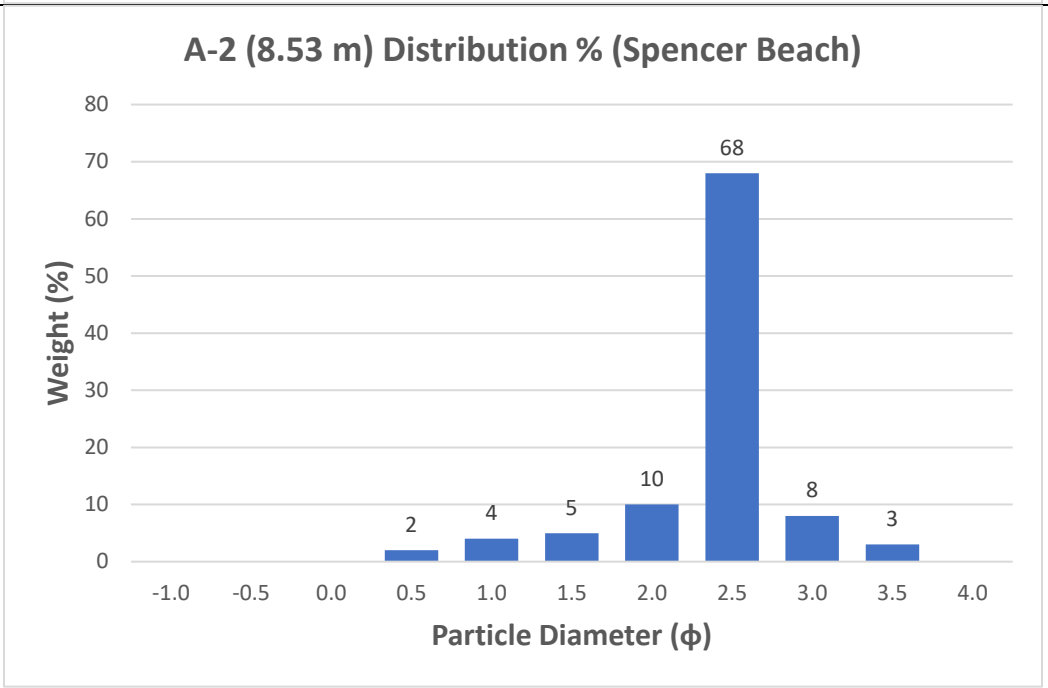
A-2 (8.53 m) Distribution % (Spencer Beach)
Weight (%)
80
70
60
50
40
30
20
10
0
2
4
5
10
68
8
3
-1.0
-0.5
0.0
0.5
1.0
1.5
2.0
2.5
3.0
3.5
4.0
Particle Diameter (ϕ)

Beach Name:	Punalu'u Beach
Date: 10/21/2020	**Time:** 2:30 PM

Location/ Transect	Survey #	Distance from Water (m)	Slope in Degrees	"x" used	Calculated mm percentile								
					5	10	16	25	50	75	84	90	95
A	1	0.9144	-6	0.8	1.278802	1.192804	1.094356	0.956094	0.632769	0.385311	0.300755	0.240944	0.181665
	2	3.3528	-7	0.7	1.1593	1.061142	0.952325	0.807146	0.500402	0.295076	0.231085	0.187502	0.147685
	3	5.79	-10	0.8	1.460198	1.34706	1.223755	1.057261	0.687528	0.416106	0.325816	0.260896	0.197241
	4	7.62	-10	1.4	1.386184	1.325015	1.252231	1.14645	0.868898	0.58272	0.469888	0.383376	0.29107
B	1	0.91	-6	0.7	1.254554	1.147612	1.027858	0.867458	0.534989	0.311023	0.240834	0.193572	0.149661
	2	3.66	-7	1	1.351239	1.276887	1.190213	1.064495	0.743272	0.458314	0.352847	0.278685	0.207913
	3	6.10	-12	0.9	1.254413	1.166265	1.068426	0.935855	0.632798	0.392242	0.31094	0.252533	0.193821
C	1	1.83	-7	0.9	1.920173	1.790864	1.643406	1.438631	0.956721	0.552397	0.413399	0.319331	0.233696
	2	3.66	-8	1.1	1.478898	1.402541	1.314221	1.186304	0.858586	0.569796	0.454193	0.363474	0.270663
	3	6.40	-16	1.6	1.650196	1.596864	1.53245	1.435022	1.153329	0.830465	0.685882	0.564911	0.430319
D	1	1.52	-9	0.9	1.159973	1.093019	1.01841	0.917126	0.675026	0.45136	0.363612	0.294461	0.222324
	2	4.27	-12	1	1.408773	1.334567	1.249773	1.130349	0.8317	0.55304	0.443728	0.356066	0.265346
	3	7.32	-14	1	1.354374	1.283577	1.202132	1.087857	0.814531	0.555195	0.444717	0.357059	0.266066
E	1	1.22	-3	9	13.17232	13.09321	12.99337	12.83062	12.26907	11.38396	10.86042	10.34066	9.620797
	2	4.27	-11	9	18.28803	18.17108	18.02349	17.784	16.95753	15.65704	14.88651	14.1234	13.07181
	3	6.71	-11	5	7.101214	7.023525	6.9256	6.767727	6.235198	5.437821	4.995288	4.582684	4.05471
	4	8.53	-6	5	2.662624	2.632457	2.594555	2.533725	2.328881	2.020436	1.845993	1.680561	1.467191

Calculated ϕ percentiles with corrections								
5	10	16	25	50	75	84	90	95
-0.572	-0.407	-0.194	0.091	0.693	1.197	1.342	1.540	1.619
-0.344	-0.137	0.105	0.433	1.049	1.532	1.636	1.811	1.816
-0.880	-0.688	-0.436	-0.112	0.568	1.101	1.252	1.454	1.541
-0.759	-0.650	-0.485	-0.276	0.213	0.678	0.843	1.037	1.172
-0.527	-0.318	-0.059	0.287	0.948	1.466	1.590	1.777	1.803
-0.700	-0.564	-0.376	-0.126	0.449	0.979	1.163	1.382	1.491
-0.527	-0.355	-0.143	0.134	0.693	1.175	1.304	1.489	1.558
-1.517	-1.345	-1.071	-0.735	0.067	0.745	0.986	1.235	1.380
-0.910	-0.781	-0.589	-0.345	0.231	0.706	0.881	1.095	1.241
-1.165	-1.080	-0.921	-0.730	-0.216	0.233	0.421	0.618	0.800
-0.345	-0.205	-0.039	0.175	0.595	0.998	1.130	1.323	1.427
-0.797	-0.666	-0.481	-0.247	0.279	0.743	0.907	1.117	1.259
-0.705	-0.576	-0.397	-0.170	0.311	0.739	0.905	1.114	1.257
-5.996	-5.937	-5.531	-5.154	-3.798	-3.053	-2.663	-2.528	-2.149
-6.759	-6.694	-6.237	-5.814	-4.288	-3.453	-3.015	-2.865	-2.440
-4.559	-4.500	-4.174	-3.862	-2.772	-2.125	-1.796	-1.647	-1.329
-2.278	-2.234	-2.056	-1.878	-1.281	-0.883	-0.685	-0.562	-0.364

Moments						
Mean	Standard Deviation	*Descriptor*	Skewness	*Descriptor*	Kurtosis	*Descriptor*
0.613	0.716	Moderately Sorted	-0.155	Coarse Skewed	0.812	Platykurtic
0.930	0.710	Moderately Sorted	-0.261	Coarse Skewed	0.805	Platykurtic
0.461	0.789	Moderately Sorted	-0.192	Coarse Skewed	0.818	Platykurtic
0.190	0.625	Moderately Well Sorted	-0.029	Symmetrical	0.830	Platykurtic
0.826	0.765	Moderately Sorted	-0.243	Coarse Skewed	0.810	Platykurtic
0.412	0.717	Moderately Sorted	-0.061	Symmetrical	0.812	Platykurtic
0.618	0.678	Moderately Well Sorted	-0.163	Coarse Skewed	0.821	Platykurtic
-0.006	0.953	Moderately Sorted	-0.100	Coarse Skewed	0.803	Platykurtic
0.174	0.694	Moderately Well Sorted	-0.088	Symmetrical	0.839	Platykurtic
-0.239	0.633	Moderately Well Sorted	-0.008	Symmetrical	0.837	Platykurtic
0.562	0.561	Moderately Well Sorted	-0.073	Symmetrical	0.882	Platykurtic
0.235	0.659	Moderately Well Sorted	-0.071	Symmetrical	0.851	Platykurtic
0.273	0.623	Moderately Well Sorted	-0.062	Symmetrical	0.885	Platykurtic
-3.997	1.300	Poorly Sorted	-0.176	Coarse Skewed	0.750	Platykurtic
-4.513	1.460	Poorly Sorted	-0.177	Coarse Skewed	0.750	Platykurtic
-2.914	1.084	Poorly Sorted	-0.142	Coarse Skewed	0.762	Platykurtic
-1.340	0.633	Moderately Well Sorted	-0.086	Symmetrical	0.788	Platykurtic

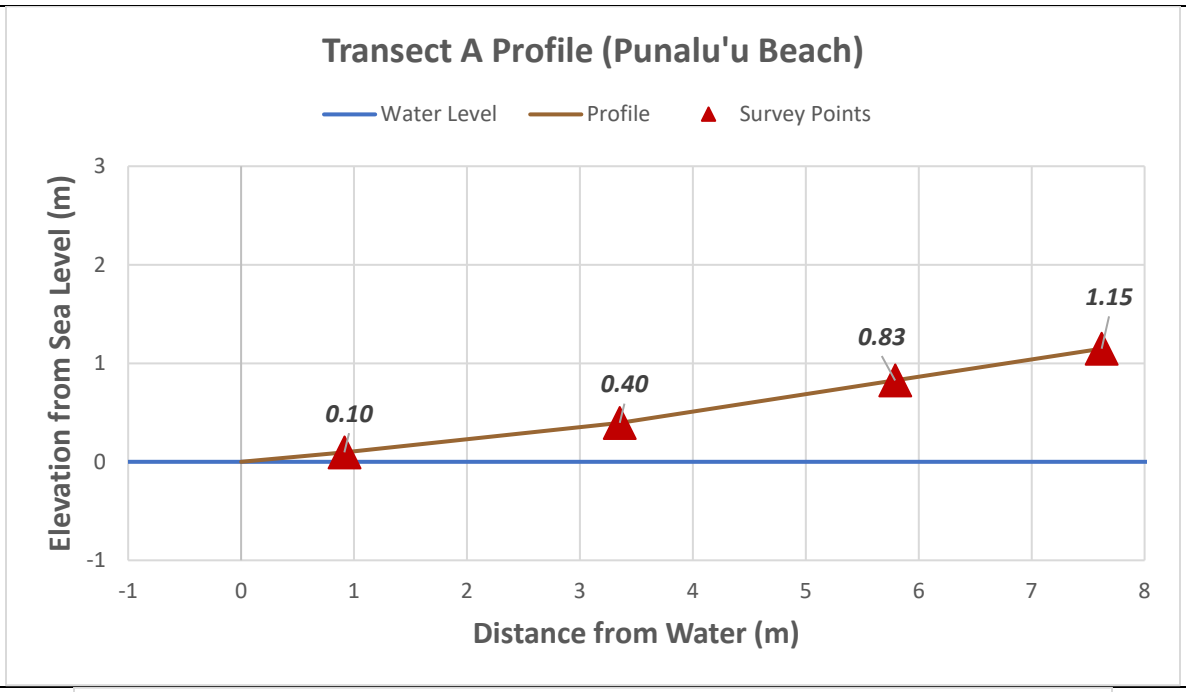
Transect A Profile (Punalu'u Beach)
Water Level
Profile
Survey Points
Elevation from Sea Level (m)
3
2
1
0
-1
-1
0
1
2
3
4
5
6
7
8
0.10
0.40
0.83
1.15
Distance from Water (m)

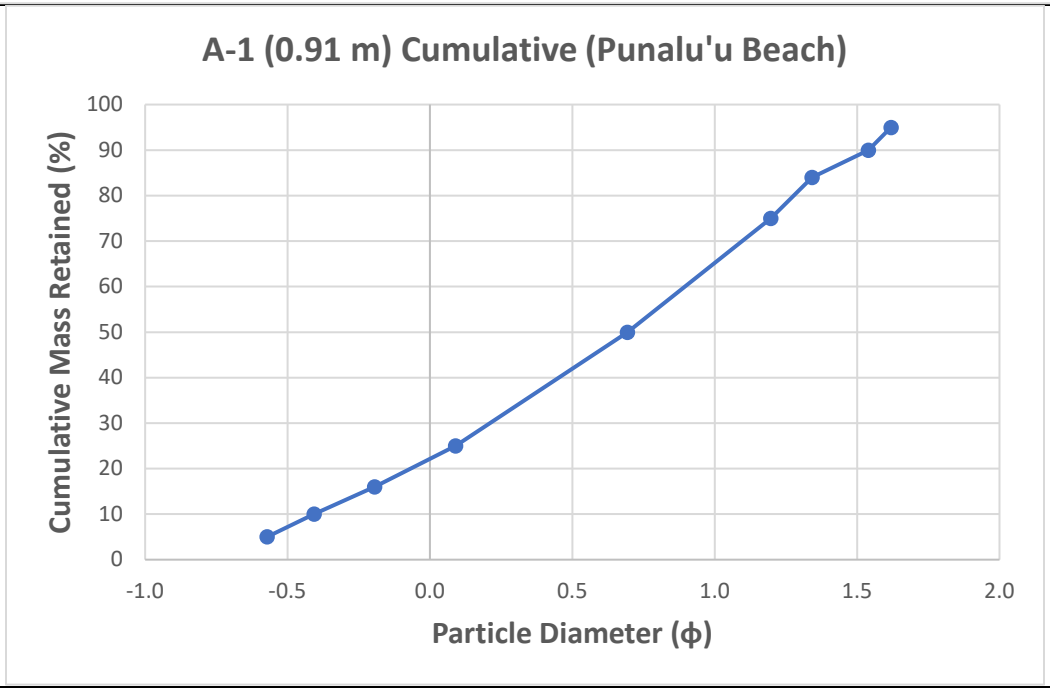
A-1 (0.91 m) Cumulative (Punalu'u Beach)
Cumulative Mass Retained (%)
100
90
80
70
60
50
40
30
20
10
0
-1.0
-0.5
0.0
0.5
1.0
1.5
2.0
Particle Diameter (ϕ)

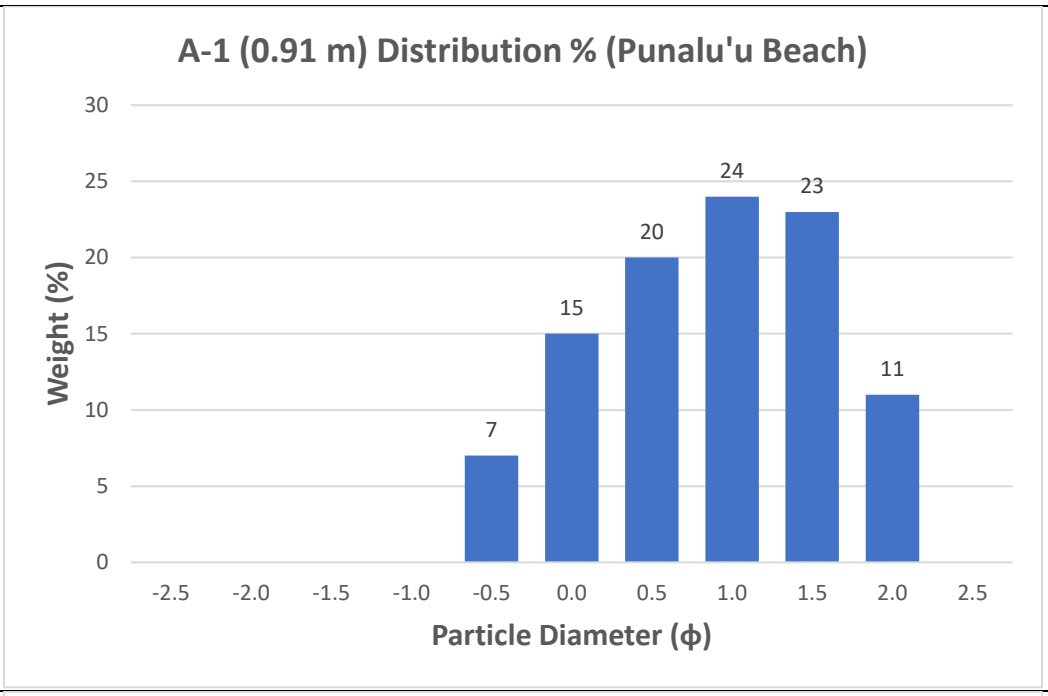
A-1 (0.91 m) Distribution % (Punalu'u Beach)
Weight (%)
30
25
20
15
10
5
0
7
15
20
24
23
11
-2.5
-2.0
-1.5
-1.0
-0.5
0.0
0.5
1.0
1.5
2.0
2.5
Particle Diameter (ϕ)

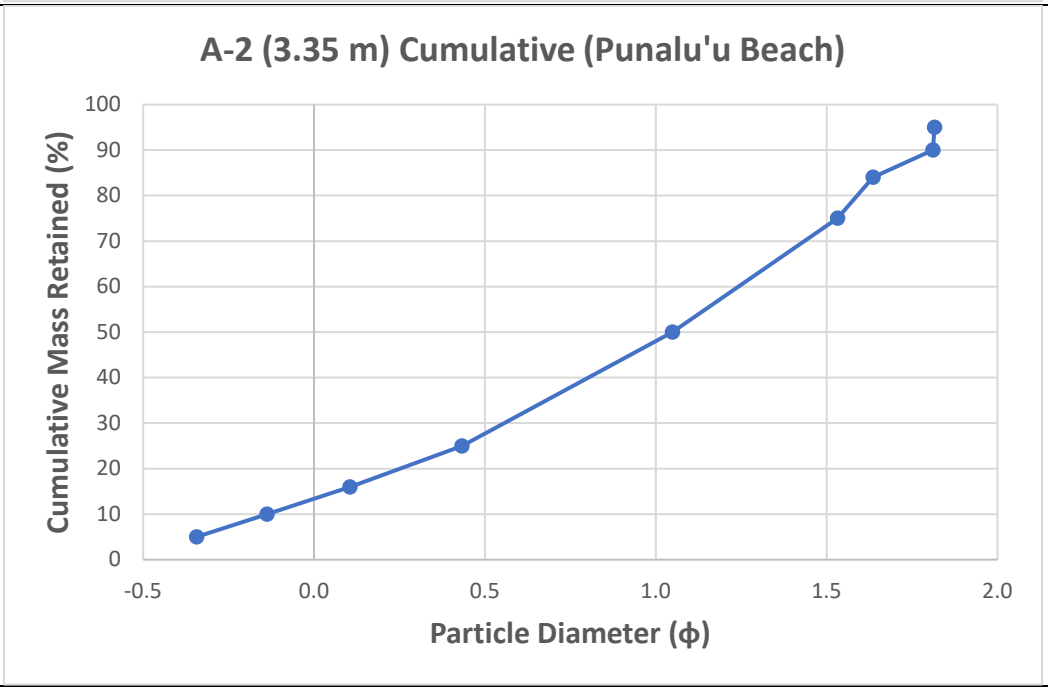
A-2 (3.35 m) Cumulative (Punalu'u Beach)
Cumulative Mass Retained (%)
100
90
80
70
60
50
40
30
20
10
0
-0.5
0.0
0.5
1.0
1.5
2.0
Particle Diameter (ϕ)

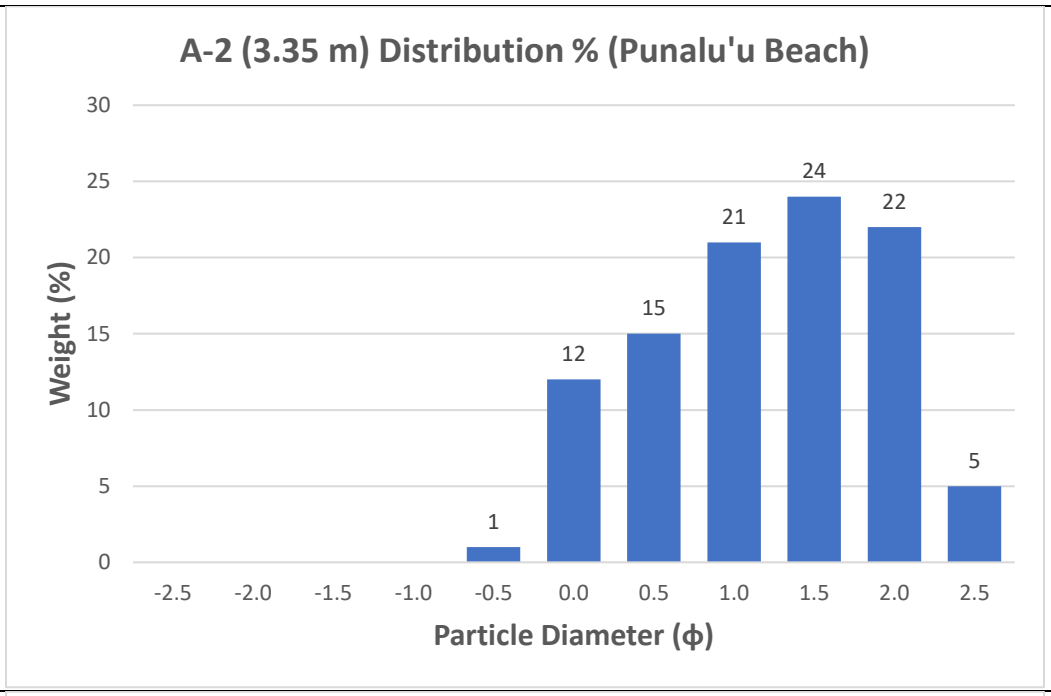
A-2 (3.35 m) Distribution % (Punalu'u Beach)
Weight (%)
30
25
20
15
10
5
0
1
12
15
21
24
22
5
-2.5
-2.0
-1.5
-1.0
-0.5
0.0
0.5
1.0
1.5
2.0
2.5
Particle Diameter (ϕ)

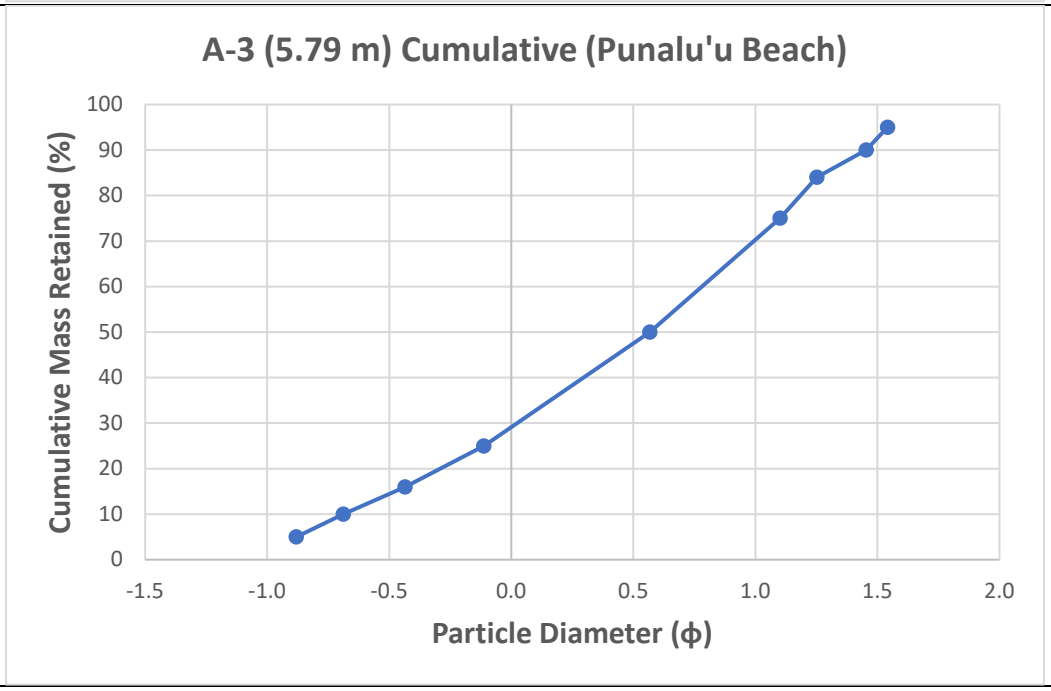
A-3 (5.79 m) Cumulative (Punalu'u Beach)
Cumulative Mass Retained (%)
100
90
80
70
60
50
40
30
20
10
0
-1.5
-1.0
-0.5
0.0
0.5
1.0
1.5
2.0
Particle Diameter (ϕ)

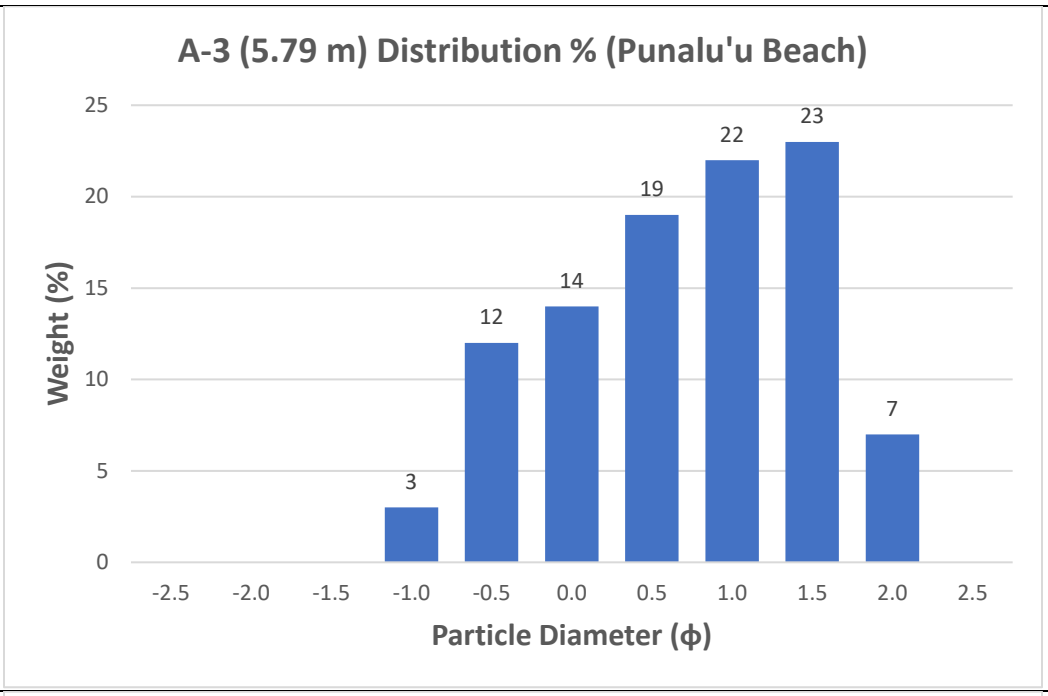
A-3 (5.79 m) Distribution % (Punalu'u Beach)
Weight (%)
25
20
15
10
5
0
3
12
14
19
22
23
7
-2.5
-2.0
-1.5
-1.0
-0.5
0.0
0.5
1.0
1.5
2.0
2.5
Particle Diameter (ϕ)

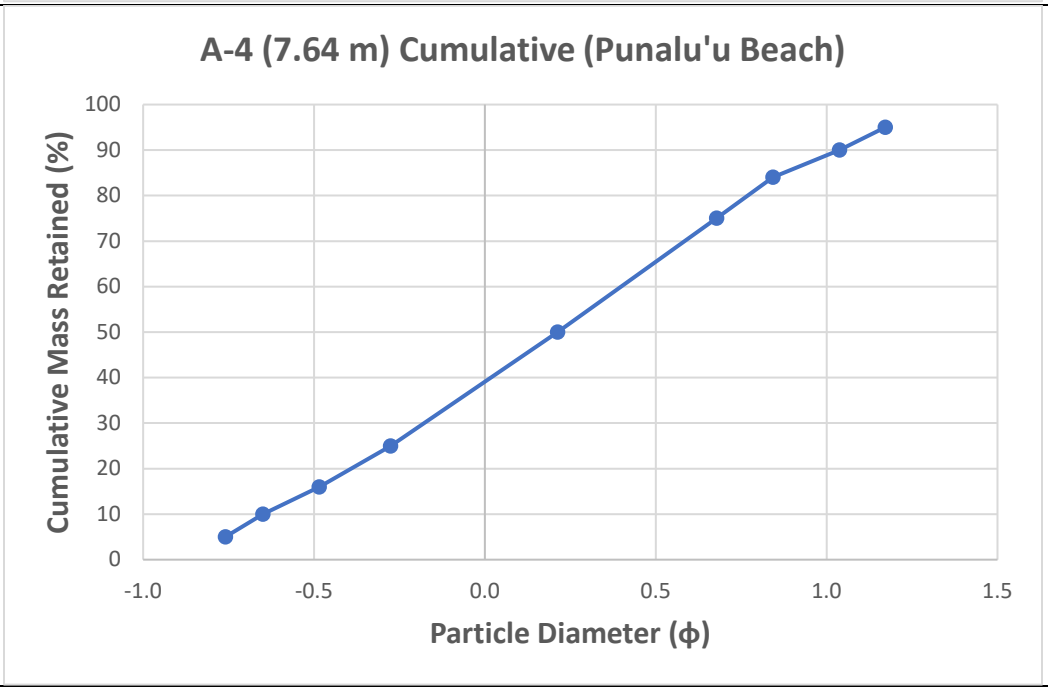
A-4 (7.64 m) Cumulative (Punalu'u Beach)
Cumulative Mass Retained (%)
100
90
80
70
60
50
40
30
20
10
0
-1.0
-0.5
0.0
0.5
1.0
1.5
Particle Diameter (ϕ)

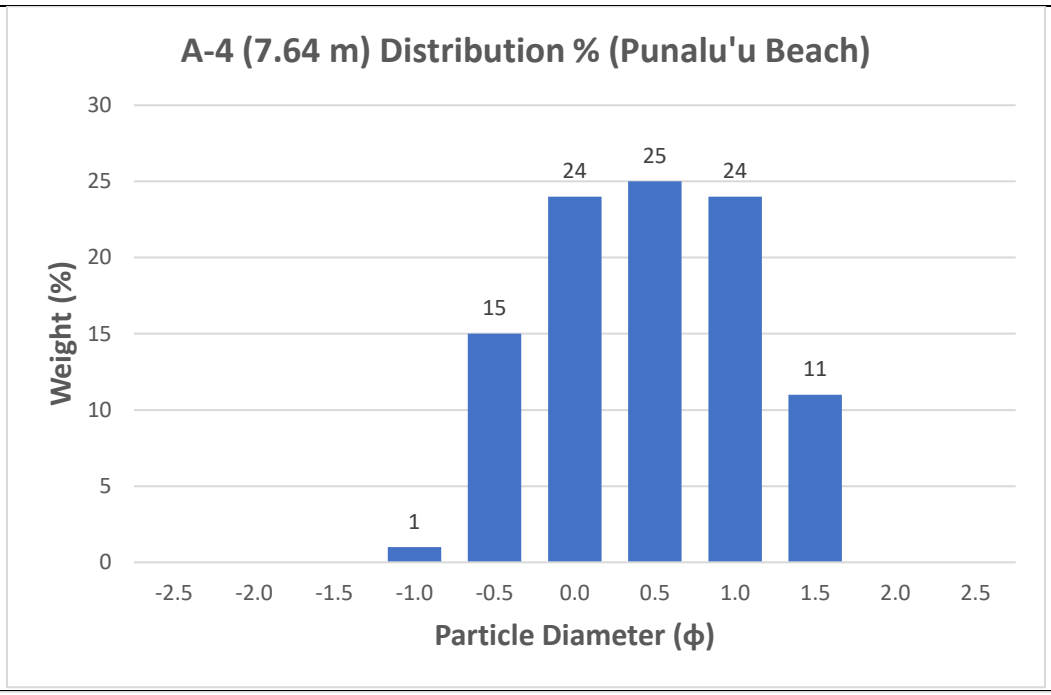
A-4 (7.64 m) Distribution % (Punalu'u Beach)
Weight (%)
30
25
20
15
10
5
0
1
15
24
25
24
11
-2.5
-2.0
-1.5
-1.0
-0.5
0.0
0.5
1.0
1.5
2.0
2.5
Particle Diameter (ϕ)

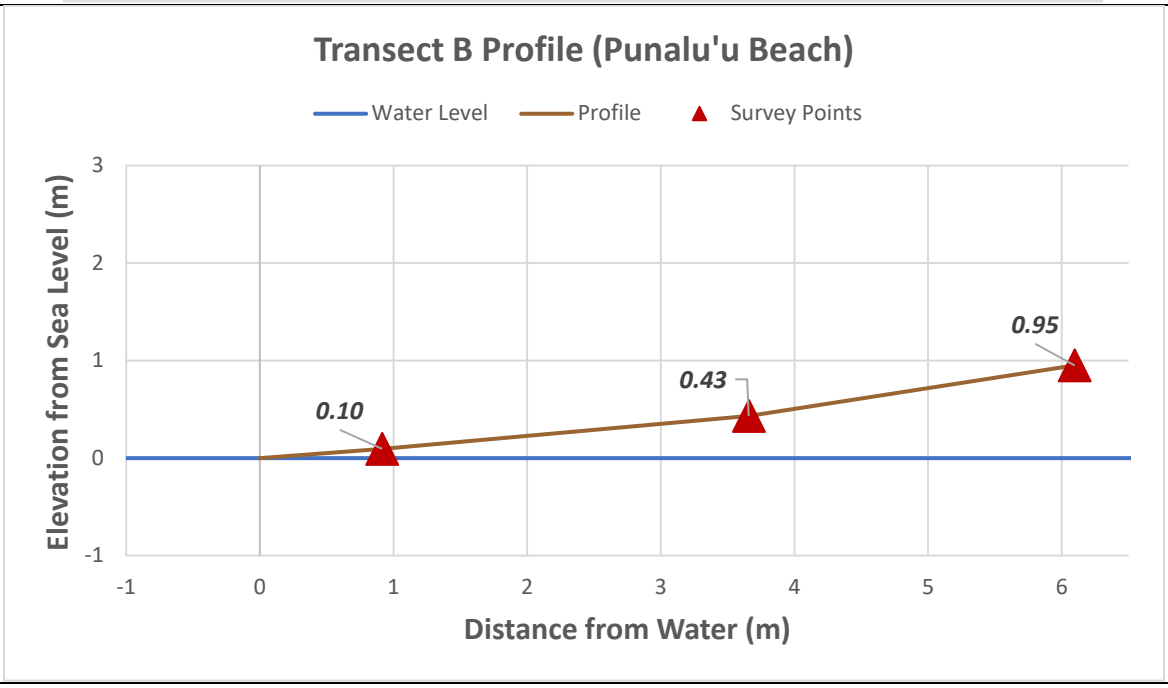
Transect B Profile (Punalu'u Beach)
Water Level
Profile
Survey Points
Elevation from Sea Level (m)
3
2
1
0
-1
0.10
0.43
0.95
-1
0
1
2
3
4
5
6
Distance from Water (m)

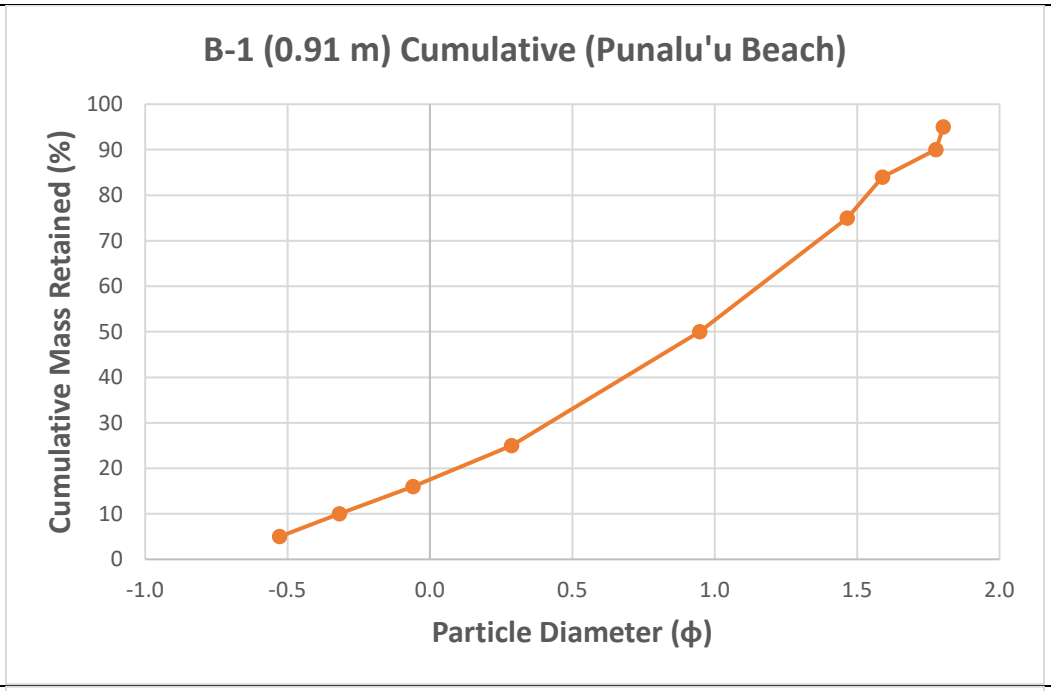
B-1 (0.91 m) Cumulative (Punalu'u Beach)
Cumulative Mass Retained (%)
100
90
80
70
60
50
40
30
20
10
0
-1.0
-0.5
0.0
0.5
1.0
1.5
2.0
Particle Diameter (ϕ)

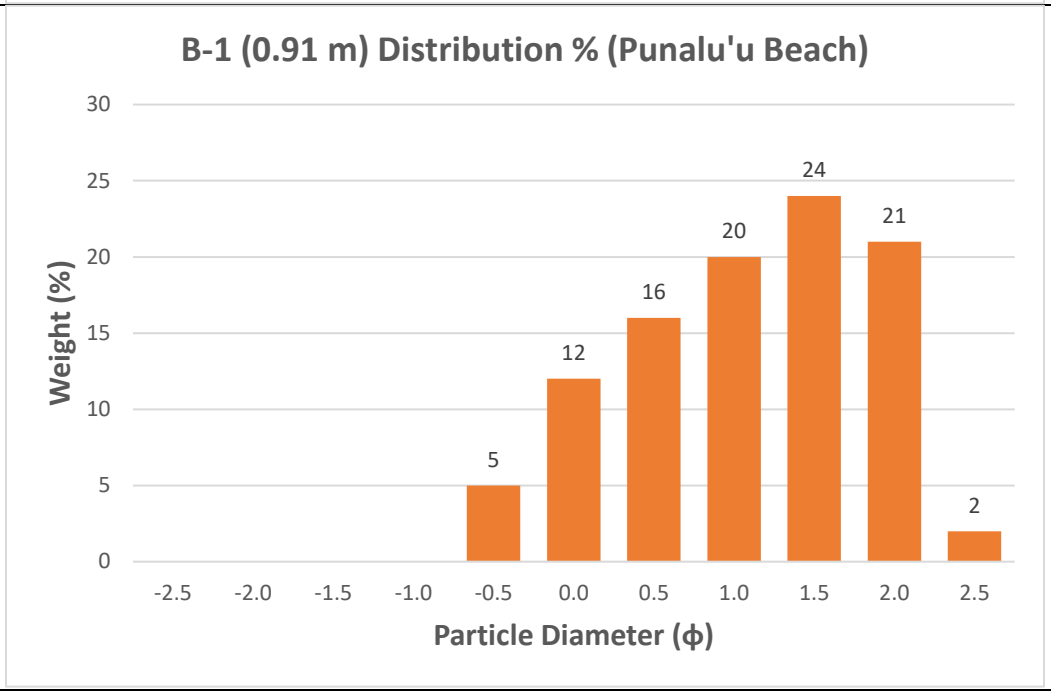
B-1 (0.91 m) Distribution % (Punalu'u Beach)
Weight (%)
30
25
20
15
10
5
0
5
12
16
20
24
21
2
-2.5
-2.0
-1.5
-1.0
-0.5
0.0
0.5
1.0
1.5
2.0
2.5
Particle Diameter (ϕ)

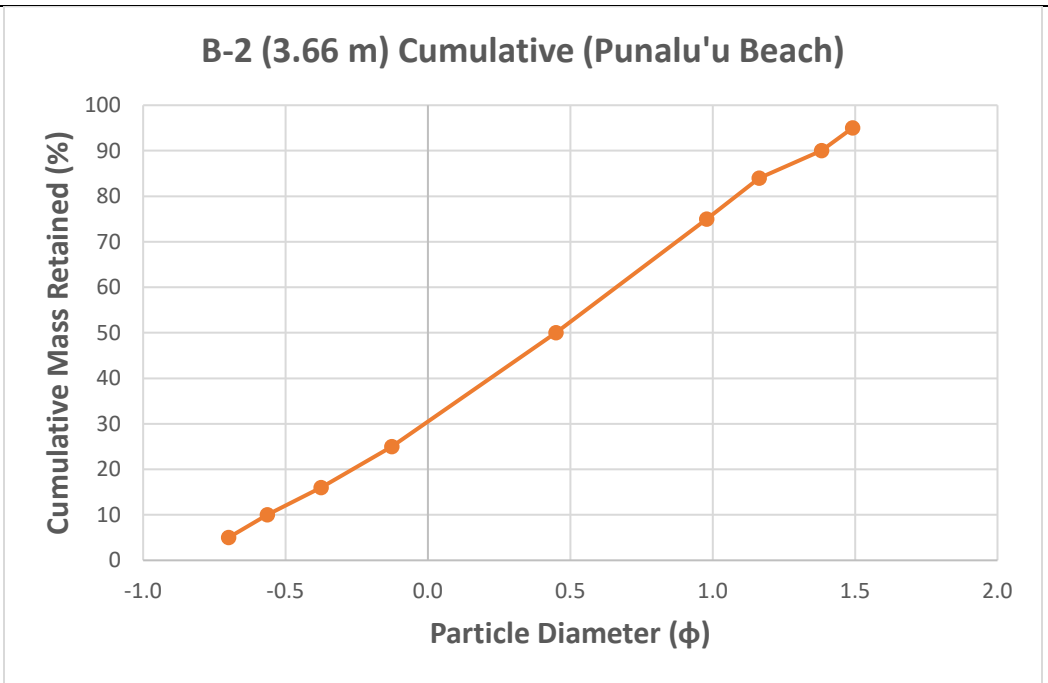
B-2 (3.66 m) Cumulative (Punalu'u Beach)
Cumulative Mass Retained (%)
100
90
80
70
60
50
40
30
20
10
0
-1.0
-0.5
0.0
0.5
1.0
1.5
2.0
Particle Diameter (ϕ)

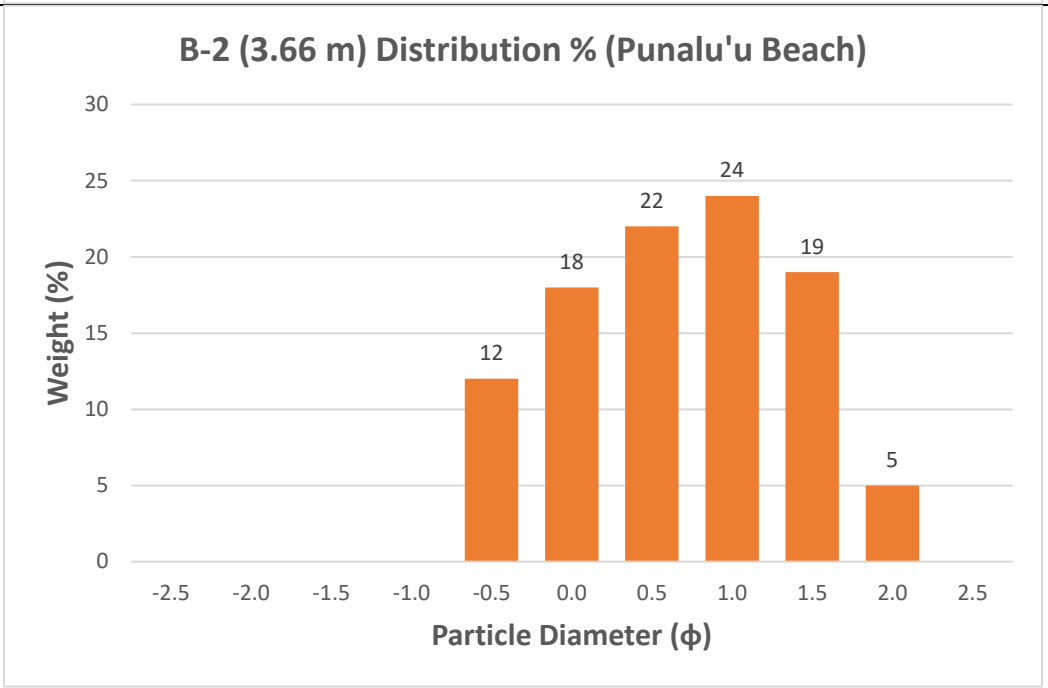
B-2 (3.66 m) Distribution % (Punalu'u Beach)
Weight (%)
30
25
20
15
10
5
0
12
18
22
24
19
5
-2.5
-2.0
-1.5
-1.0
-0.5
0.0
0.5
1.0
1.5
2.0
2.5
Particle Diameter (ϕ)

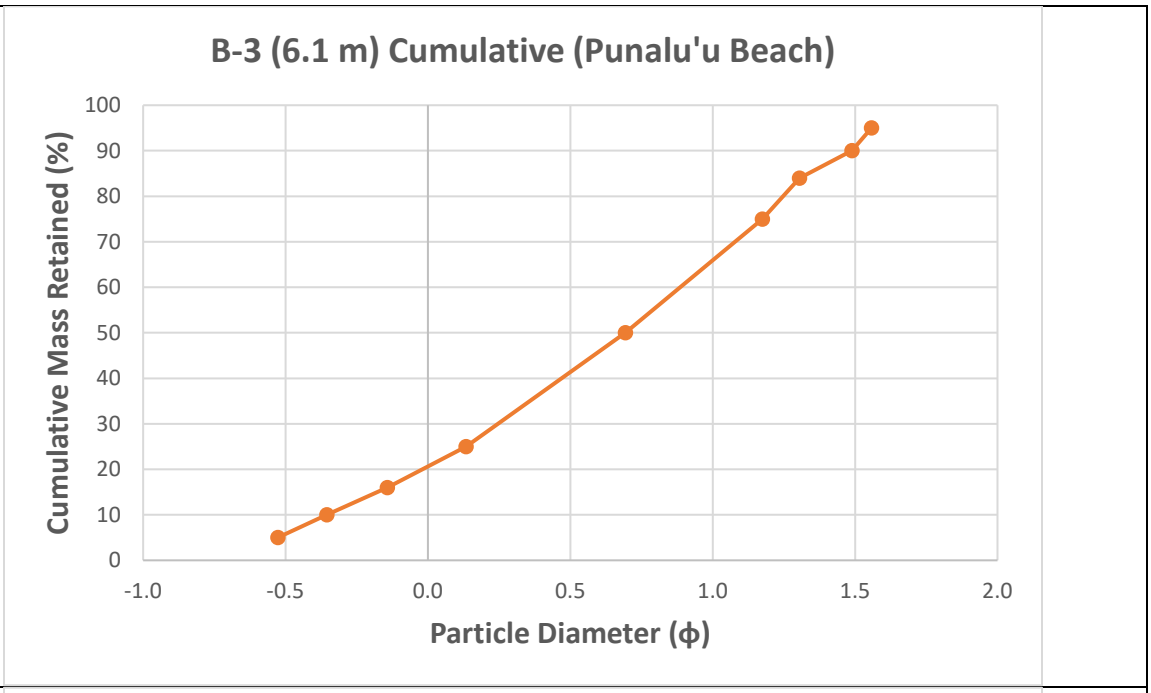
B-3 (6.1 m) Cumulative (Punalu'u Beach)
Cumulative Mass Retained (%)
100
90
80
70
60
50
40
30
20
10
0
-1.0
-0.5
0.0
0.5
1.0
1.5
2.0
Particle Diameter (ϕ)

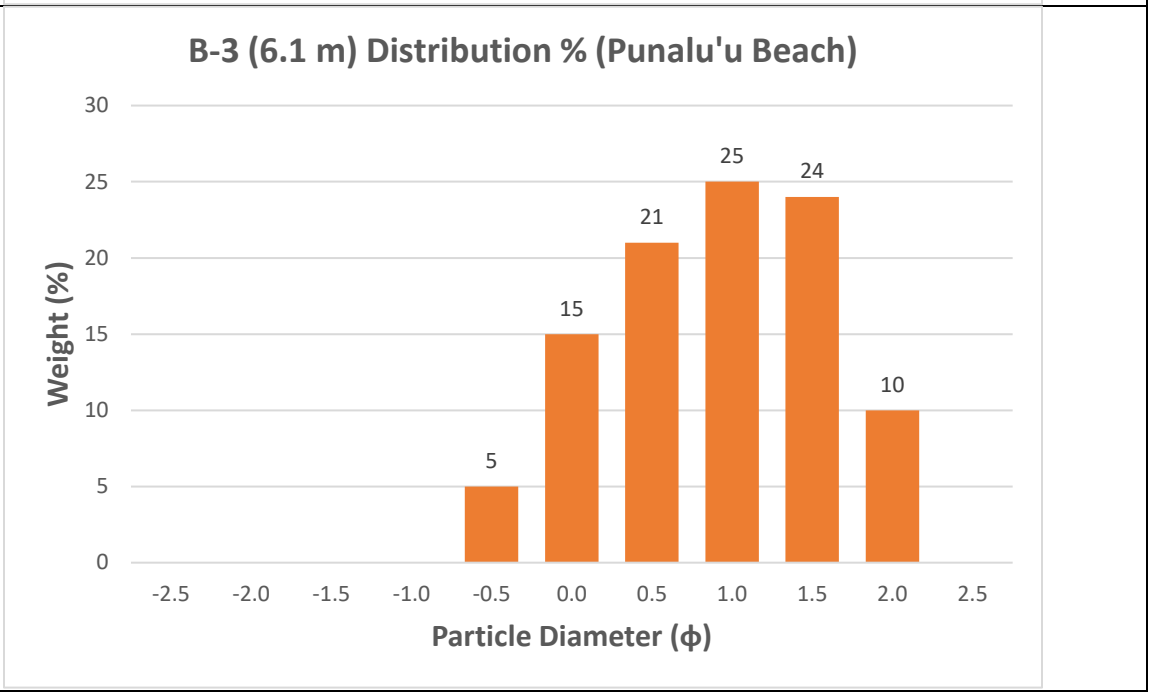
B-3 (6.1 m) Distribution % (Punalu'u Beach)
Weight (%)
30
25
20
15
10
5
0
5
15
21
25
24
10
-2.5
-2.0
-1.5
-1.0
-0.5
0.0
0.5
1.0
1.5
2.0
2.5
Particle Diameter (ϕ)

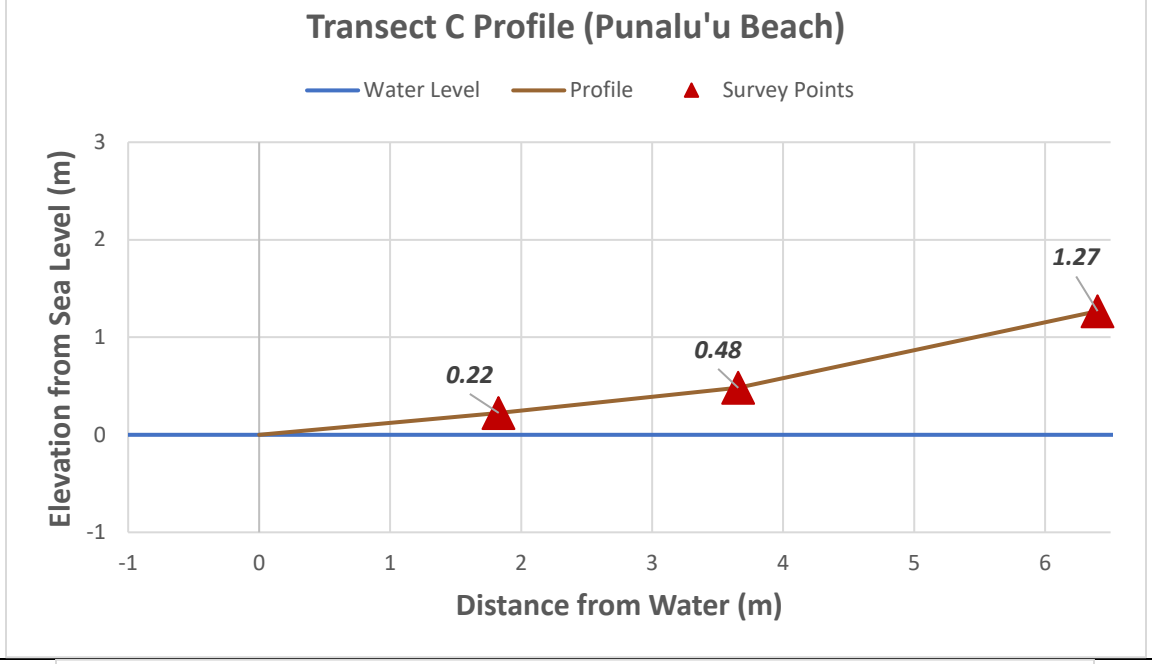
Transect C Profile (Punalu'u Beach)
Water Level
Profile
Survey Points
Elevation from Sea Level (m)
3
2
1
0
-1
-1
0
1
2
3
4
5
6
0.22
0.48
1.27
Distance from Water (m)

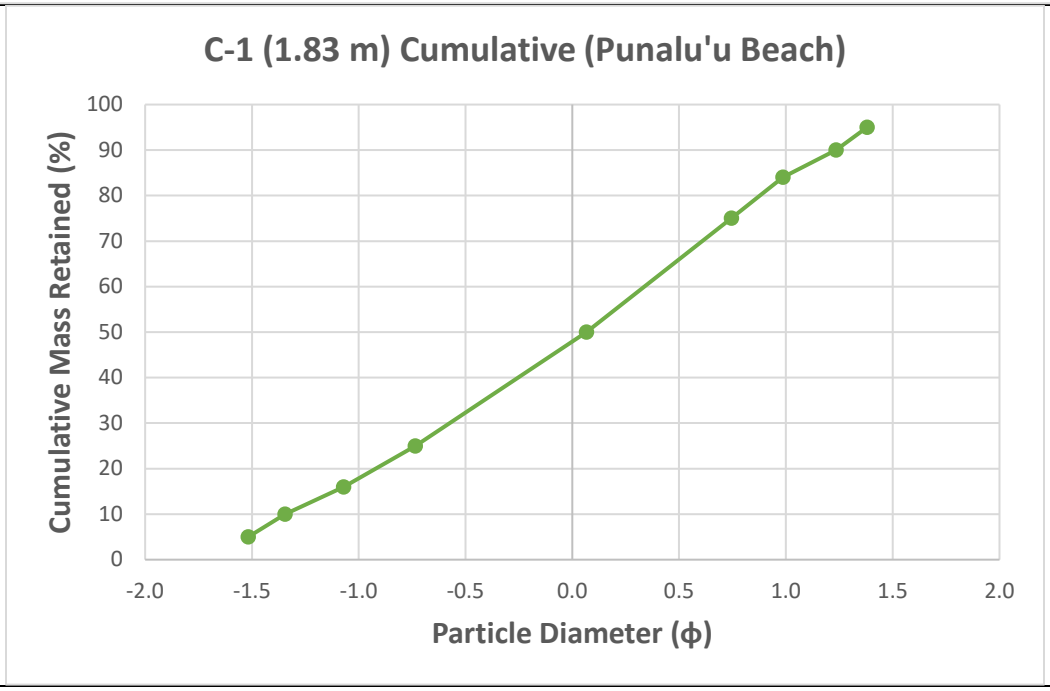
C-1 (1.83 m) Cumulative (Punalu'u Beach)
Cumulative Mass Retained (%)
100
90
80
70
60
50
40
30
20
10
0
-2.0
-1.5
-1.0
-0.5
0.0
0.5
1.0
1.5
2.0
Particle Diameter (ϕ)

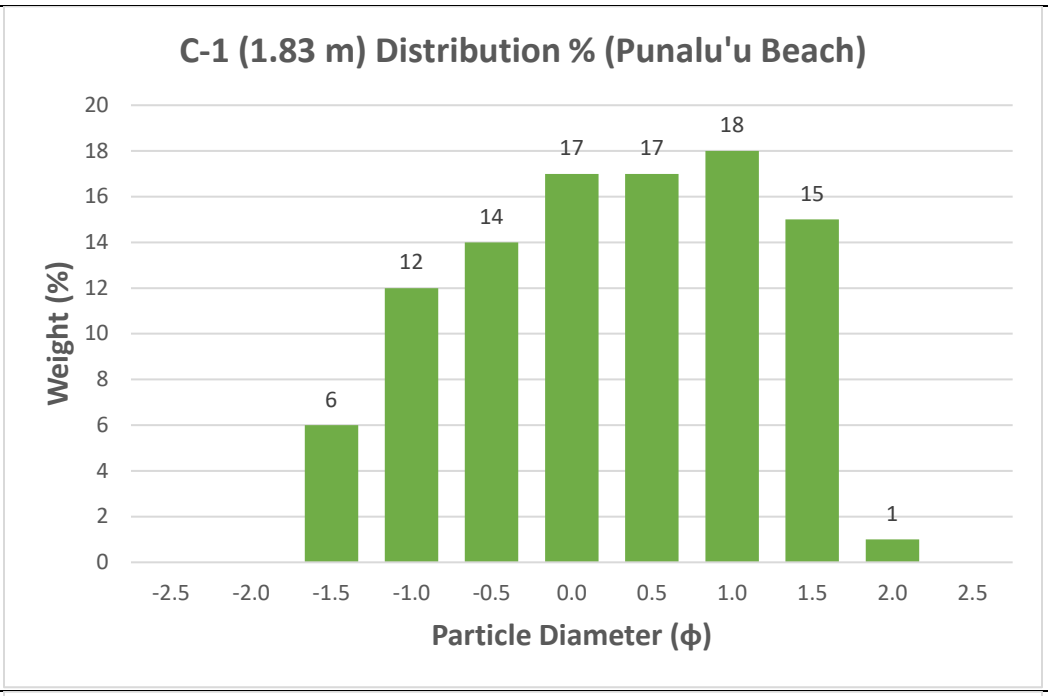
C-1 (1.83 m) Distribution % (Punalu'u Beach)
Weight (%)
20
18
16
14
12
10
8
6
4
2
0
6
12
14
17
17
18
15
1
-2.5
-2.0
-1.5
-1.0
-0.5
0.0
0.5
1.0
1.5
2.0
2.5
Particle Diameter (ϕ)

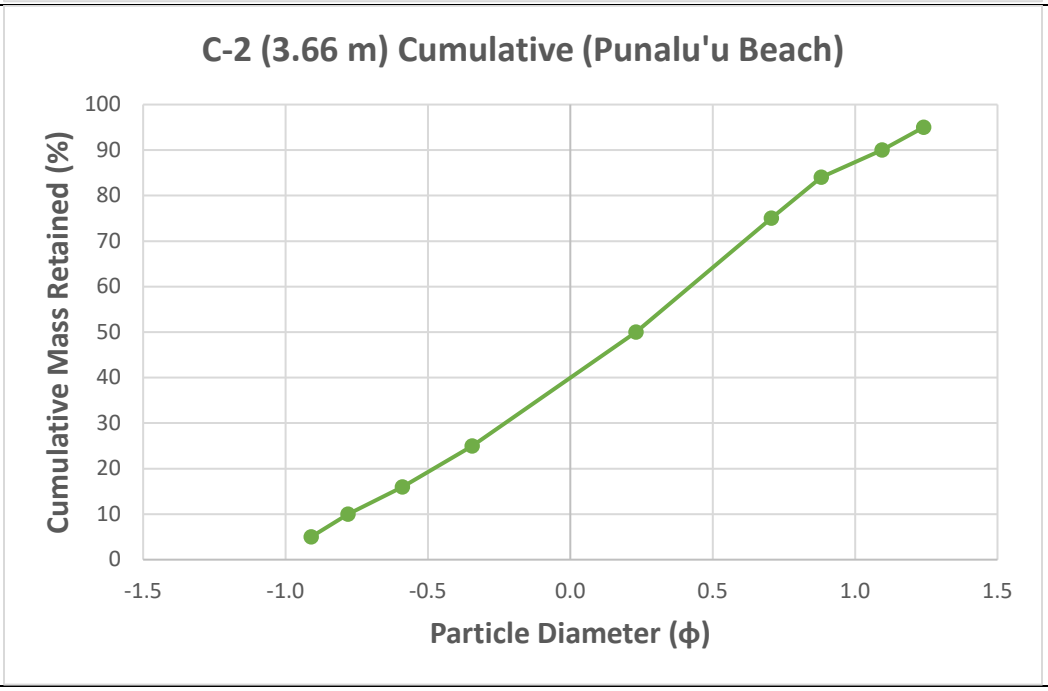
C-2 (3.66 m) Cumulative (Punalu'u Beach)
Cumulative Mass Retained (%)
100
90
80
70
60
50
40
30
20
10
0
-1.5
-1.0
-0.5
0.0
0.5
1.0
1.5
Particle Diameter (ϕ)

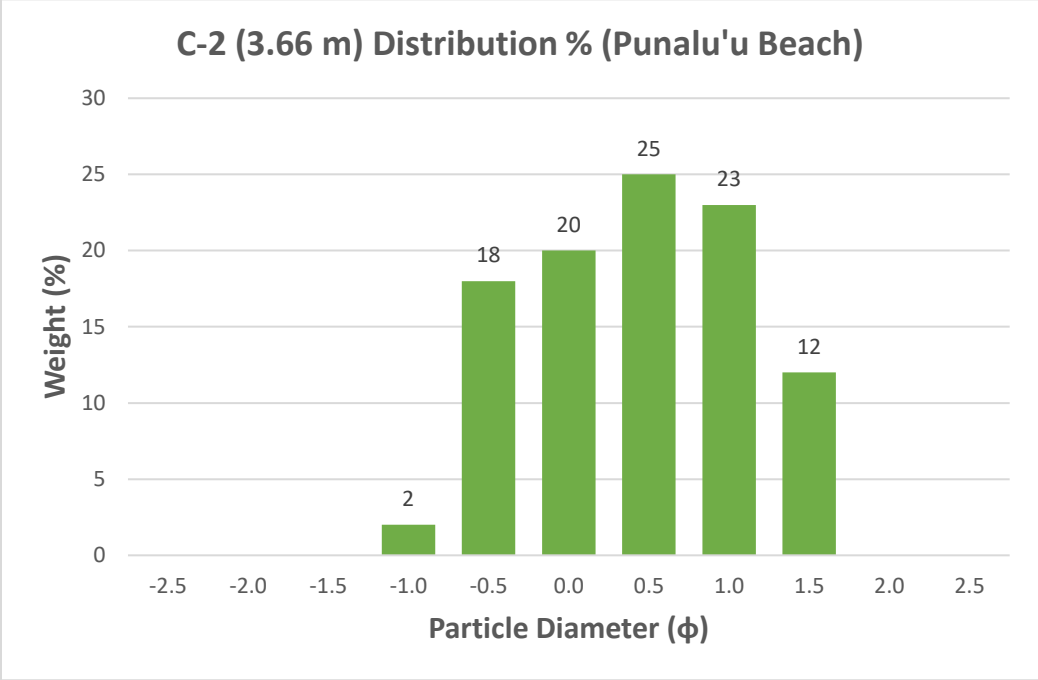
C-2 (3.66 m) Distribution % (Punalu'u Beach)
Weight (%)
30
25
20
15
10
5
0
2
18
20
25
23
12
-2.5
-2.0
-1.5
-1.0
-0.5
0.0
0.5
1.0
1.5
2.0
2.5
Particle Diameter (ϕ)

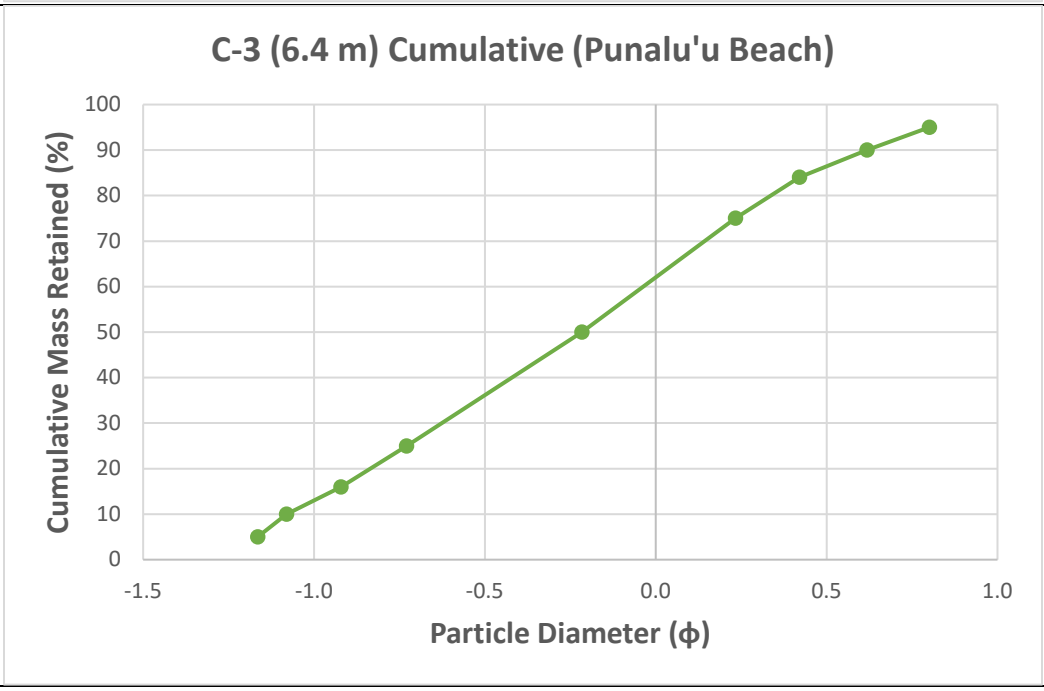
C-3 (6.4 m) Cumulative (Punalu'u Beach)
Cumulative Mass Retained (%)
100
90
80
70
60
50
40
30
20
10
0
-1.5
-1.0
-0.5
0.0
0.5
1.0
Particle Diameter (ϕ)

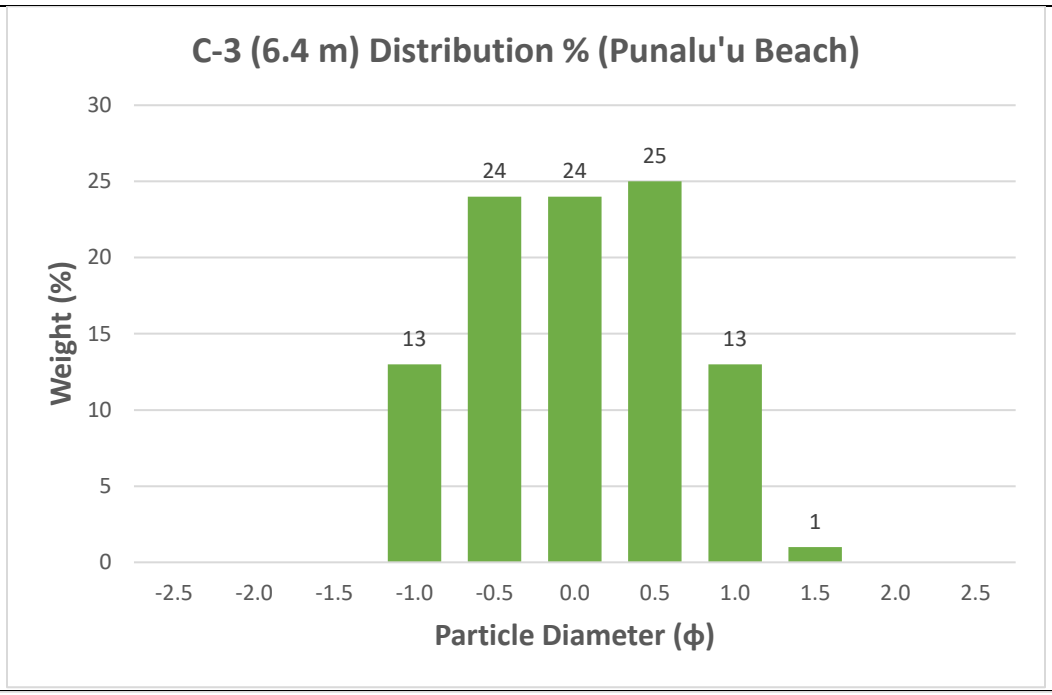
C-3 (6.4 m) Distribution % (Punalu'u Beach)
Weight (%)
30
25
20
15
10
5
0
13
24
24
25
13
1
-2.5
-2.0
-1.5
-1.0
-0.5
0.0
0.5
1.0
1.5
2.0
2.5
Particle Diameter (ϕ)

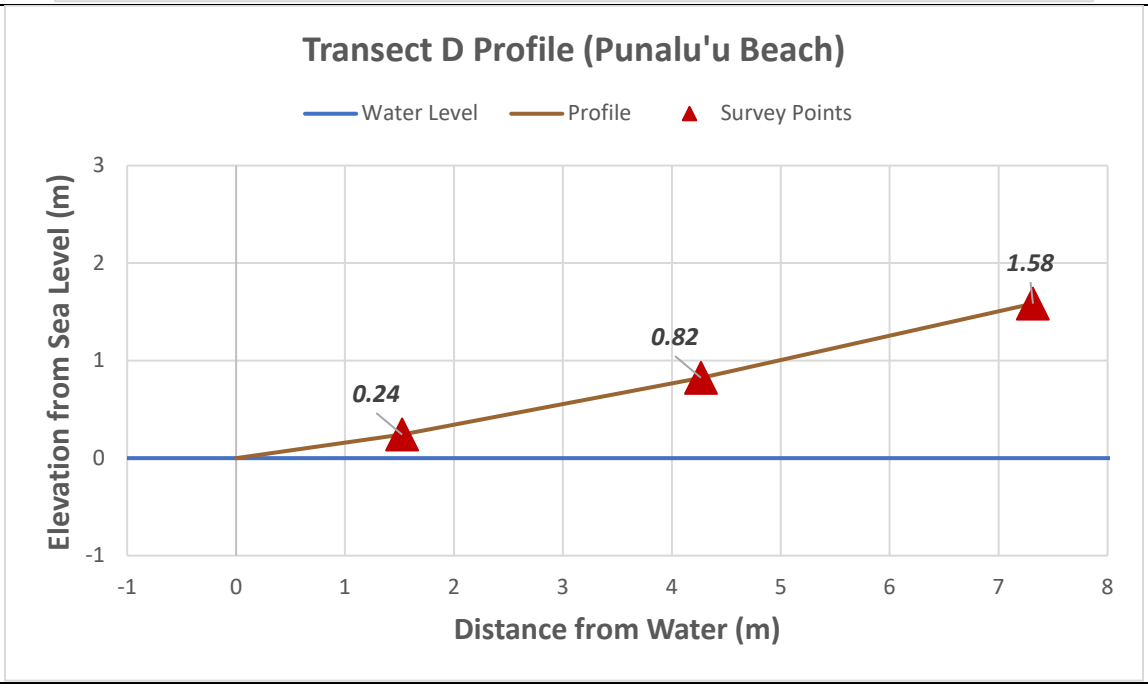
Transect D Profile (Punalu'u Beach)
Water Level
Profile
Survey Points
Elevation from Sea Level (m)
3
2
1
0
-1
0.24
0.82
1.58
-1
0
1
2
3
4
5
6
7
8
Distance from Water (m)

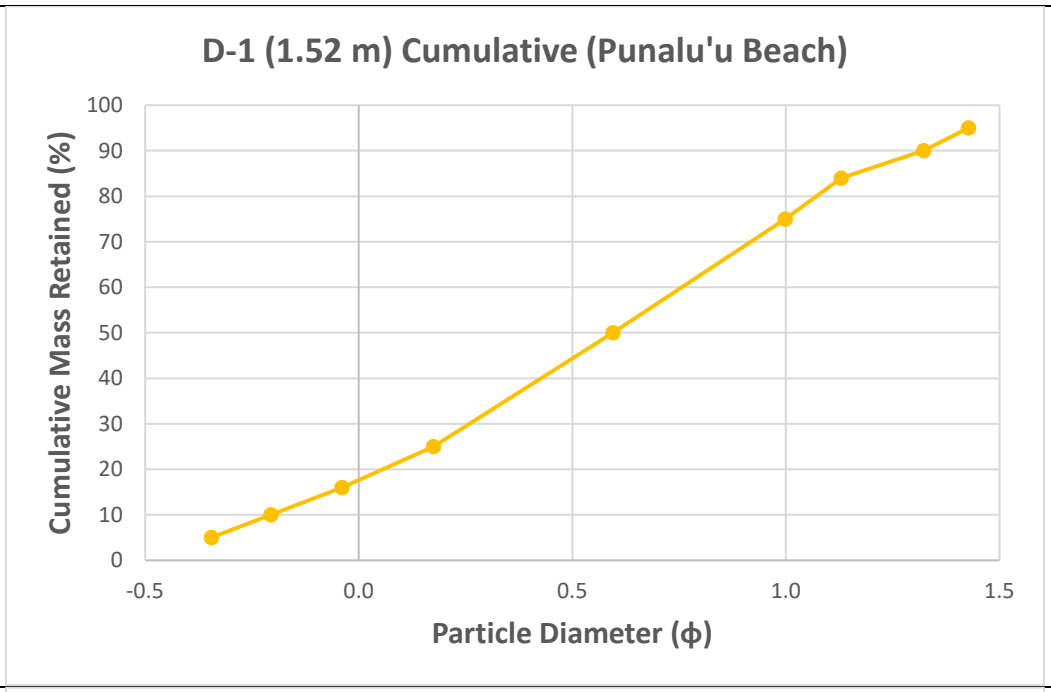
D-1 (1.52 m) Cumulative (Punalu'u Beach)
Cumulative Mass Retained (%)
100
90
80
70
60
50
40
30
20
10
0
-0.5
0.0
0.5
1.0
1.5
Particle Diameter (ϕ)

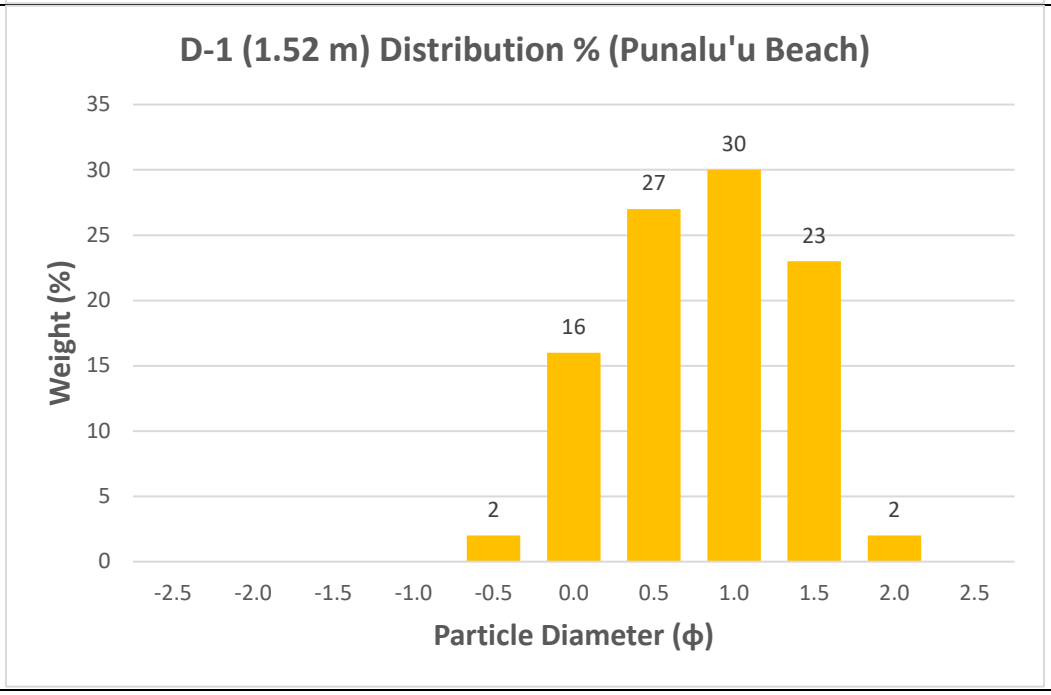
D-1 (1.52 m) Distribution % (Punalu'u Beach)
Weight (%)
35
30
25
20
15
10
5
0
2
16
27
30
23
2
-2.5
-2.0
-1.5
-1.0
-0.5
0.0
0.5
1.0
1.5
2.0
2.5
Particle Diameter (ϕ)

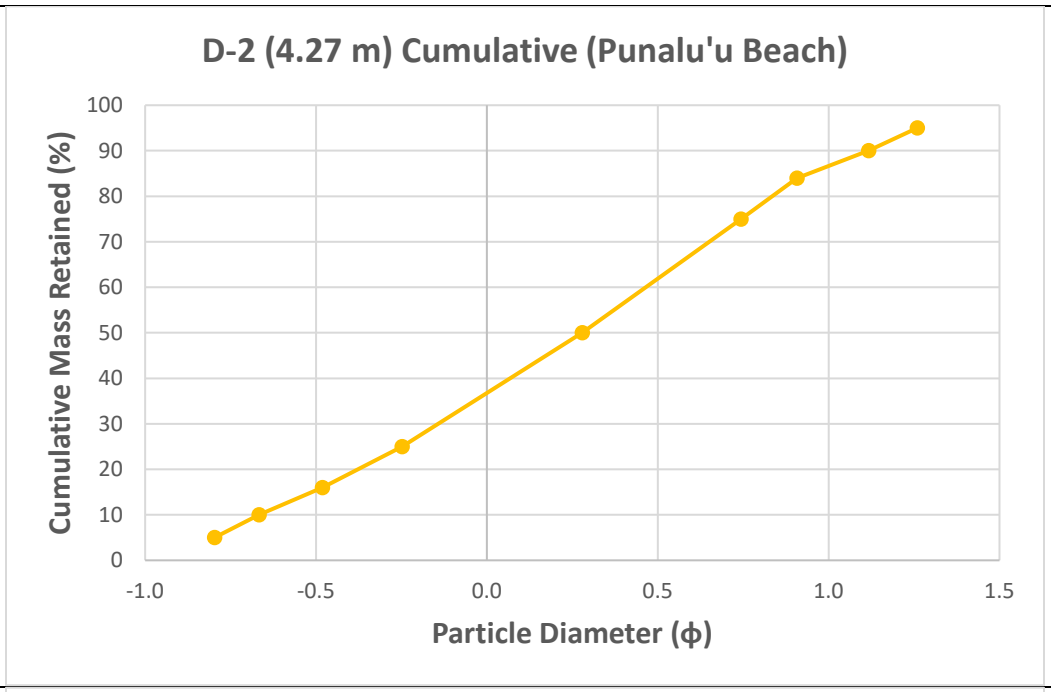
D-2 (4.27 m) Cumulative (Punalu'u Beach)
Cumulative Mass Retained (%)
100
90
80
70
60
50
40
30
20
10
0
-1.0
-0.5
0.0
0.5
1.0
1.5
Particle Diameter (ϕ)

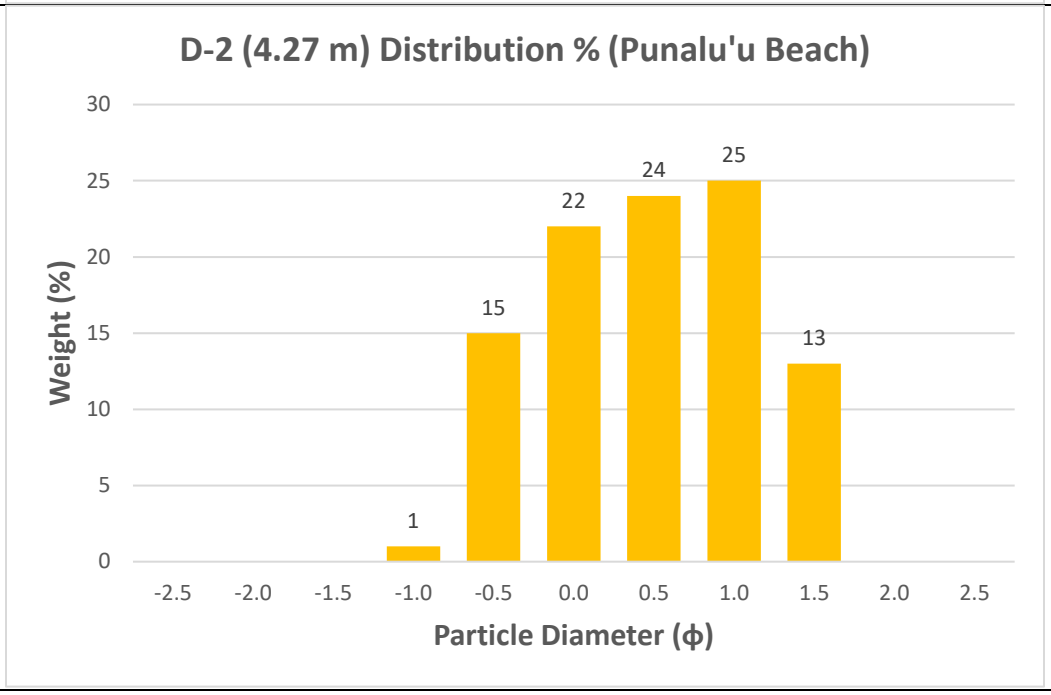
D-2 (4.27 m) Distribution % (Punalu'u Beach)
Weight (%)
30
25
20
15
10
5
0
1
15
22
24
25
13
-2.5
-2.0
-1.5
-1.0
-0.5
0.0
0.5
1.0
1.5
2.0
2.5
Particle Diameter (ϕ)

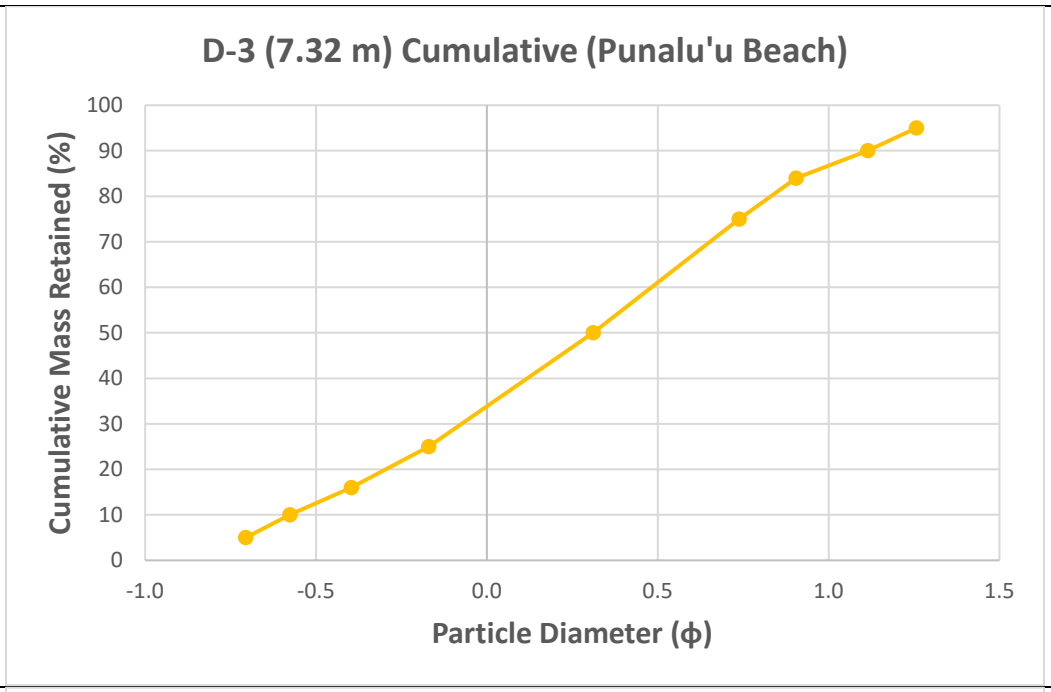
D-3 (7.32 m) Cumulative (Punalu'u Beach)
Cumulative Mass Retained (%)
100
90
80
70
60
50
40
30
20
10
0
-1.0
-0.5
0.0
0.5
1.0
1.5
Particle Diameter (ϕ)

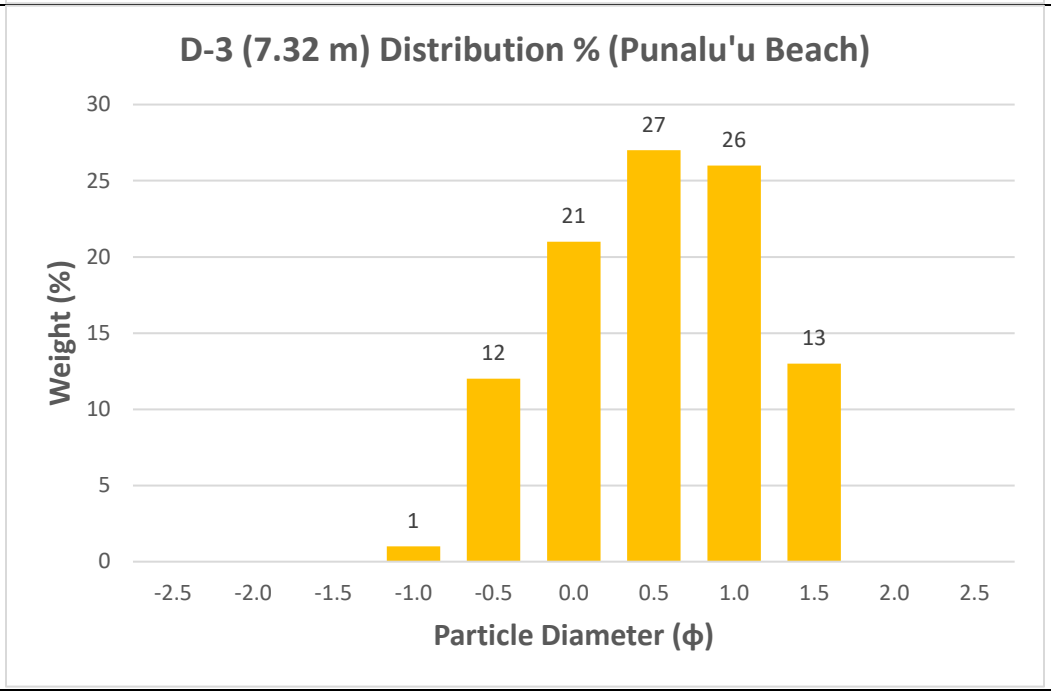
D-3 (7.32 m) Distribution % (Punalu'u Beach)
Weight (%)
30
25
20
15
10
5
0
1
12
21
27
26
13
-2.5
-2.0
-1.5
-1.0
-0.5
0.0
0.5
1.0
1.5
2.0
2.5
Particle Diameter (ϕ)

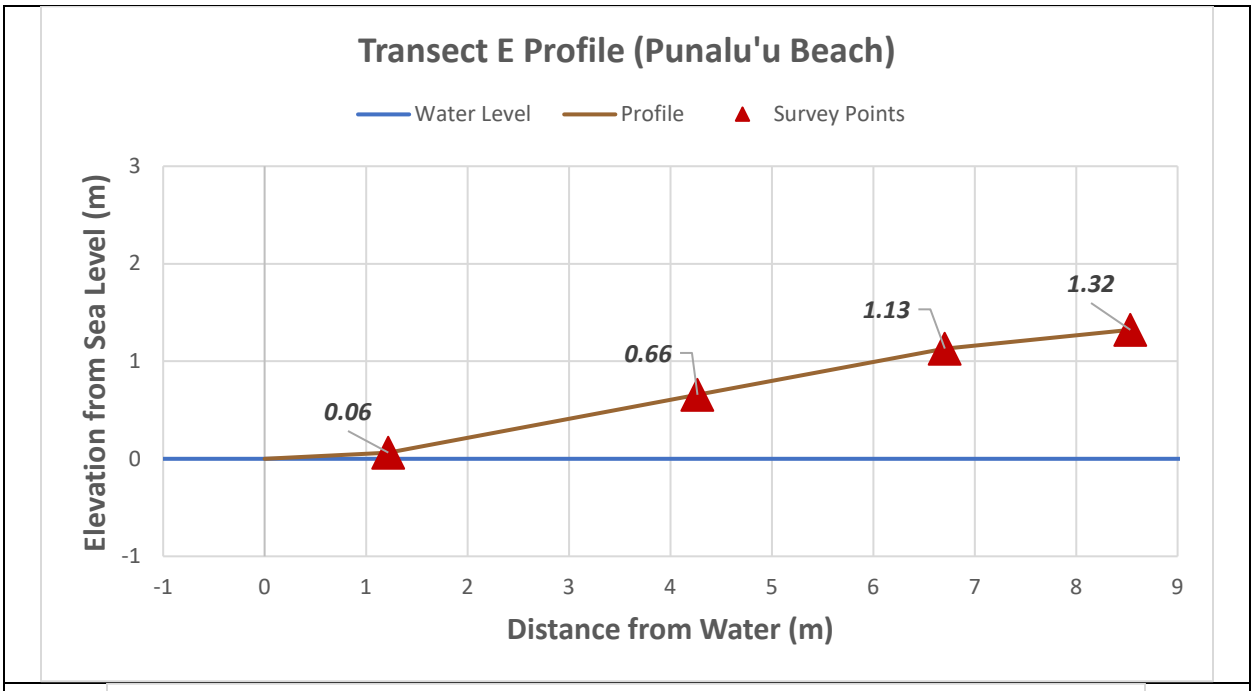
Transect E Profile (Punalu'u Beach)
Water Level
Profile
Survey Points
Elevation from Sea Level (m)
3
2
1
0
-1
0.06
0.66
1.13
1.32
-1
0
1
2
3
4
5
6
7
8
9
Distance from Water (m)

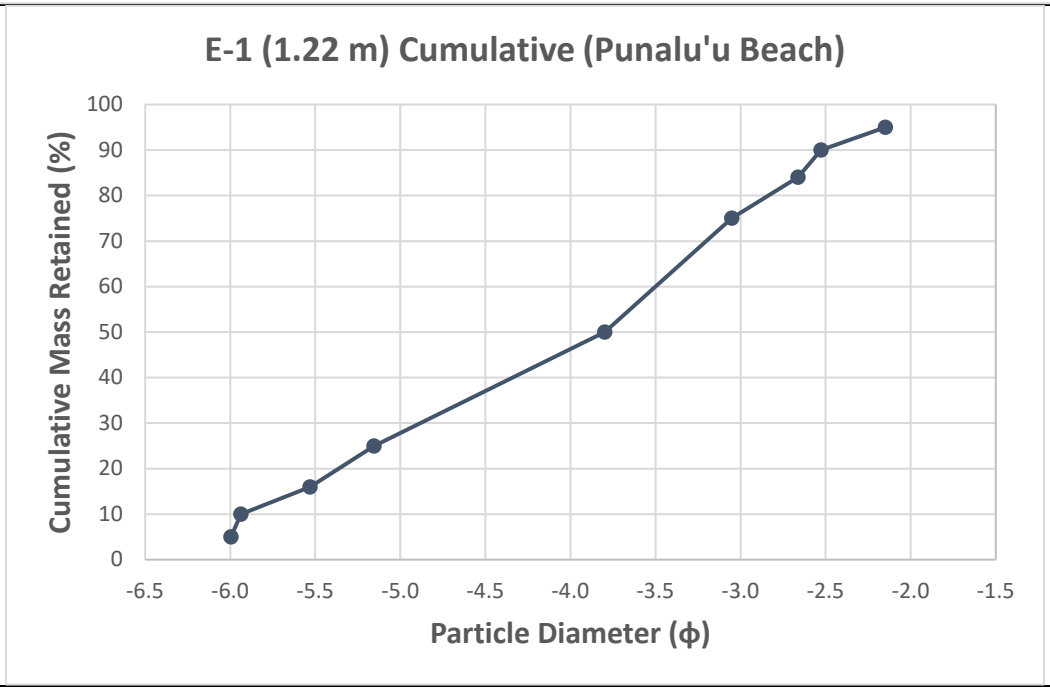
E-1 (1.22 m) Cumulative (Punalu'u Beach)
Cumulative Mass Retained (%)
100
90
80
70
60
50
40
30
20
10
0
-6.5
-6.0
-5.5
-5.0
-4.5
-4.0
-3.5
-3.0
-2.5
-2.0
-1.5
Particle Diameter (ϕ)

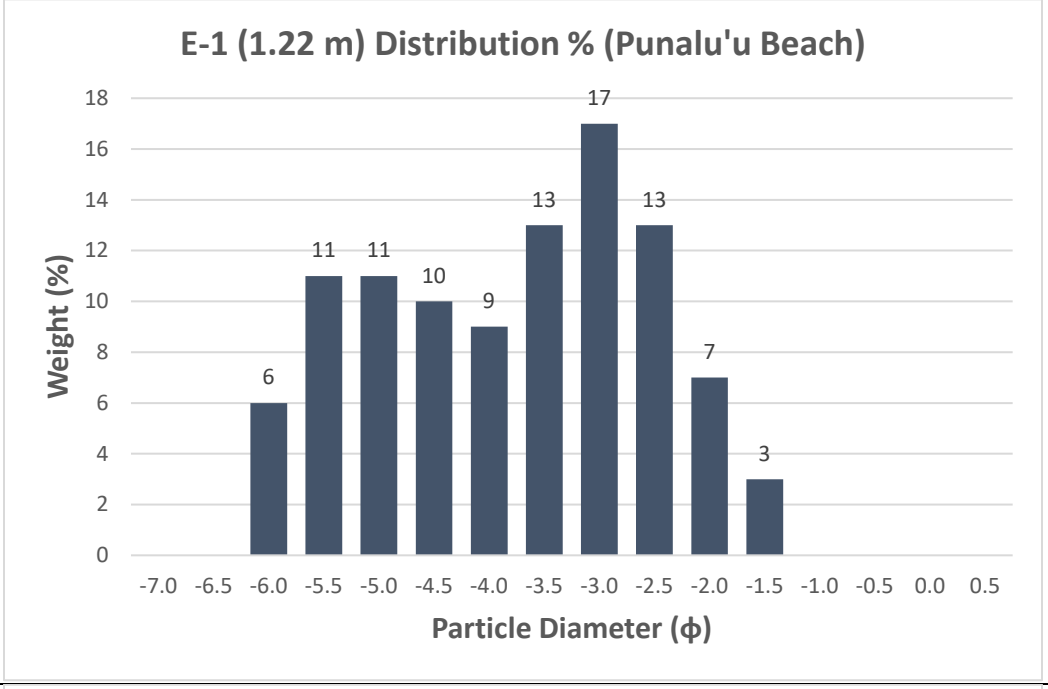
E-1 (1.22 m) Distribution % (Punalu'u Beach)
Weight (%)
18
16
14
12
10
8
6
4
2
0
6
11
11
10
9
13
17
13
7
3
-7.0 -6.5 -6.0 -5.5 -5.0 -4.5 -4.0 -3.5 -3.0 -2.5 -2.0 -1.5 -1.0 -0.5 0.0 0.5
Particle Diameter (ϕ)

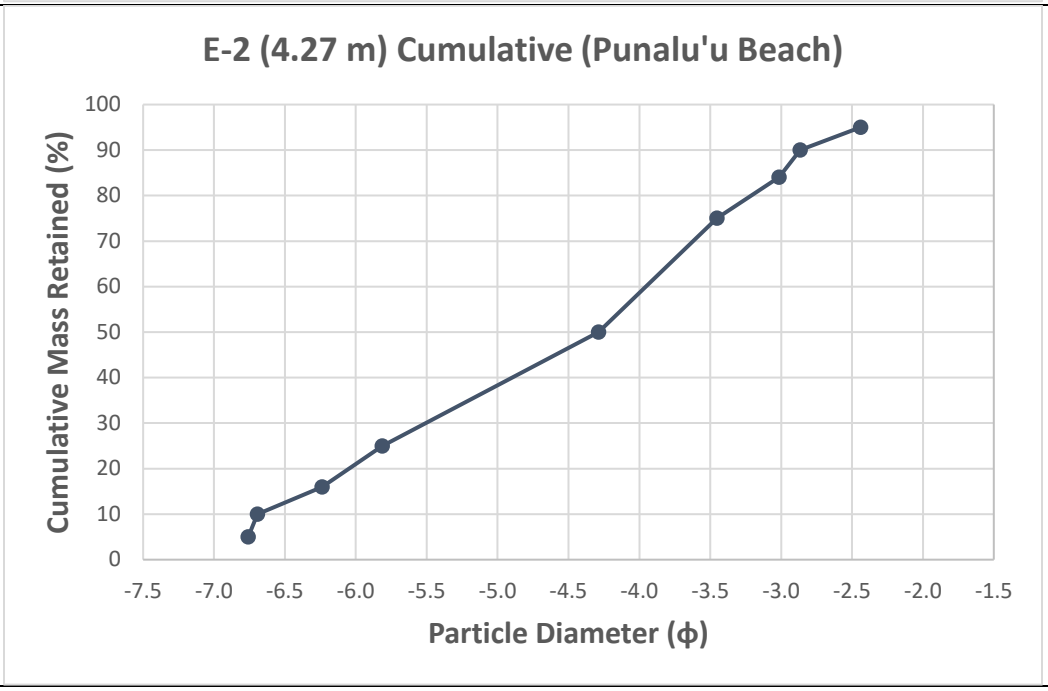
E-2 (4.27 m) Cumulative (Punalu'u Beach)
Cumulative Mass Retained (%)
100
90
80
70
60
50
40
30
20
10
0
-7.5 -7.0 -6.5 -6.0 -5.5 -5.0 -4.5 -4.0 -3.5 -3.0 -2.5 -2.0 -1.5
Particle Diameter (ϕ)

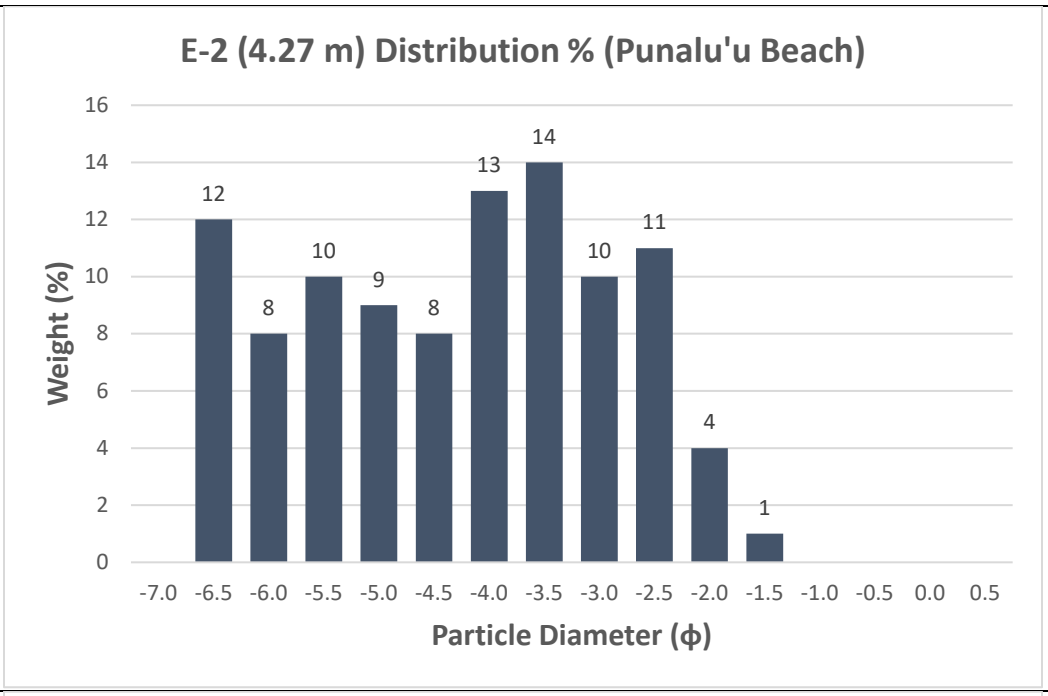
E-2 (4.27 m) Distribution % (Punalu'u Beach)
Weight (%)
16
14
12
10
8
6
4
2
0
12
8
10
9
8
13
14
10
11
4
1
-7.0 -6.5 -6.0 -5.5 -5.0 -4.5 -4.0 -3.5 -3.0 -2.5 -2.0 -1.5 -1.0 -0.5 0.0 0.5
Particle Diameter (ϕ)

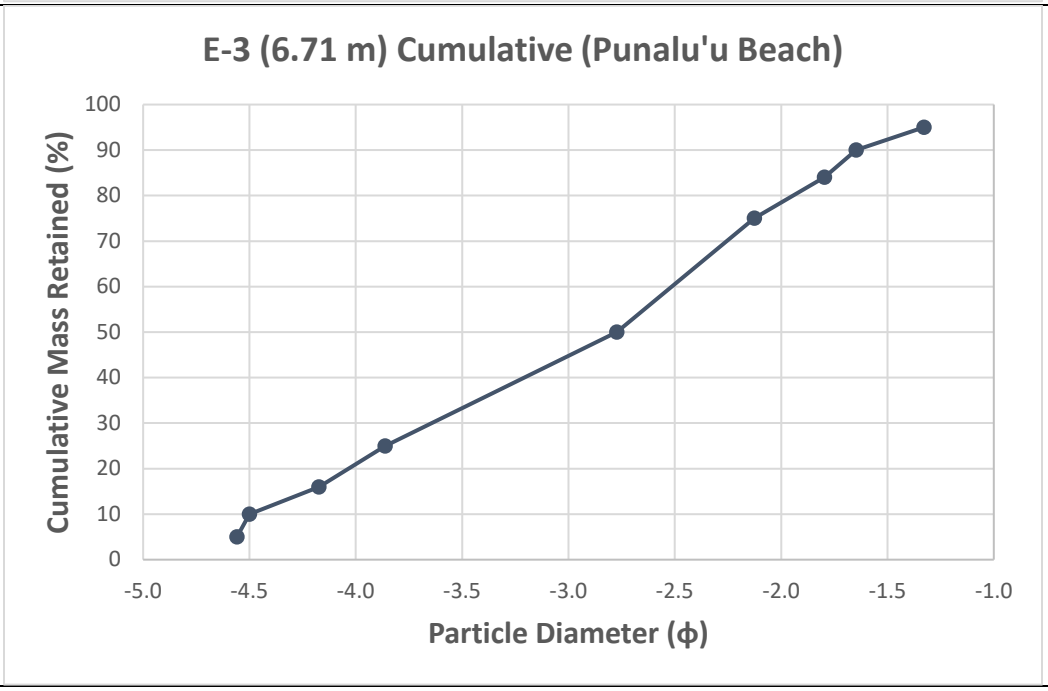
E-3 (6.71 m) Cumulative (Punalu'u Beach)
Cumulative Mass Retained (%)
100
90
80
70
60
50
40
30
20
10
0
-5.0 -4.5 -4.0 -3.5 -3.0 -2.5 -2.0 -1.5 -1.0
Particle Diameter (ϕ)

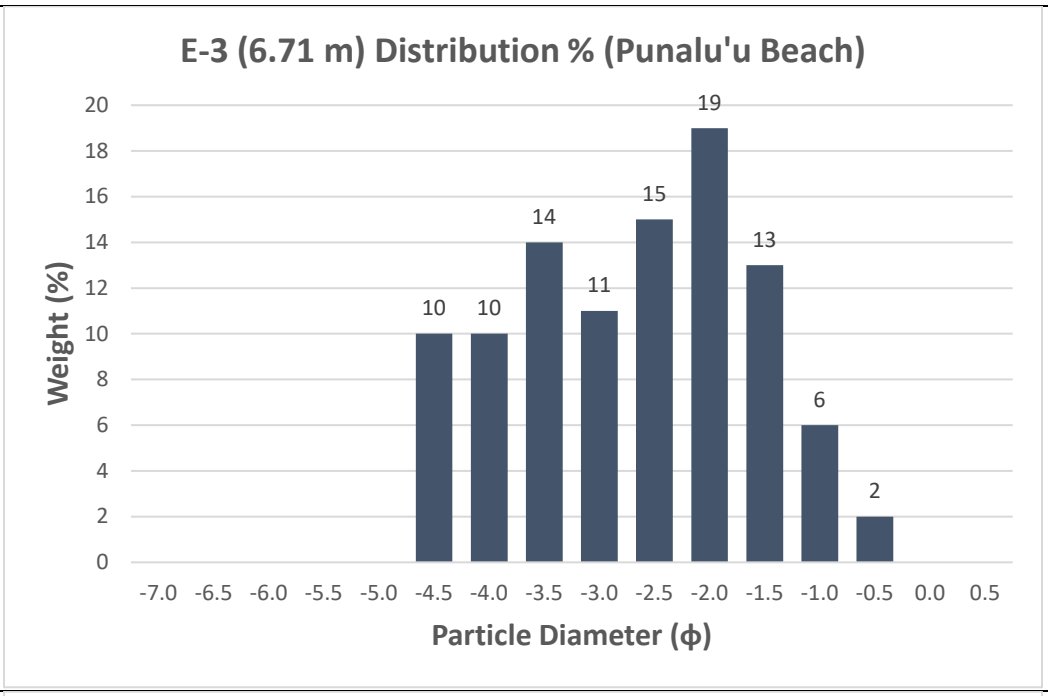
E-3 (6.71 m) Distribution % (Punalu'u Beach)
Weight (%)
20
18
16
14
12
10
8
6
4
2
0
10
10
14
11
15
19
13
6
2
-7.0 -6.5 -6.0 -5.5 -5.0 -4.5 -4.0 -3.5 -3.0 -2.5 -2.0 -1.5 -1.0 -0.5 0.0 0.5
Particle Diameter (ϕ)

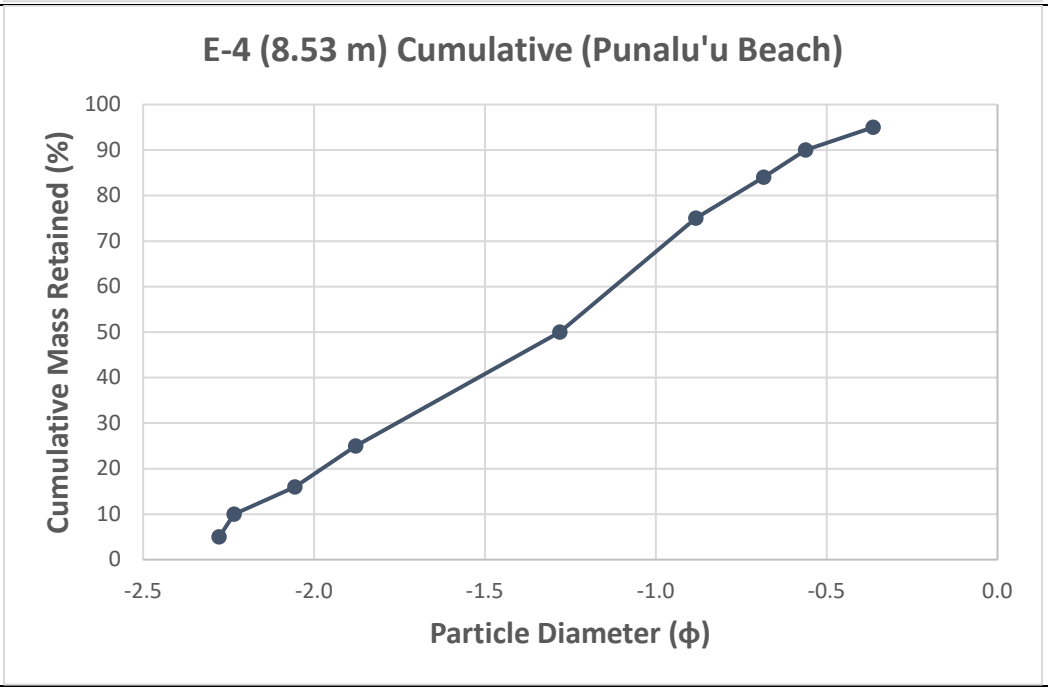
E-4 (8.53 m) Cumulative (Punalu'u Beach)
Cumulative Mass Retained (%)
100
90
80
70
60
50
40
30
20
10
0
-2.5 -2.0 -1.5 -1.0 -0.5 0.0
Particle Diameter (ϕ)

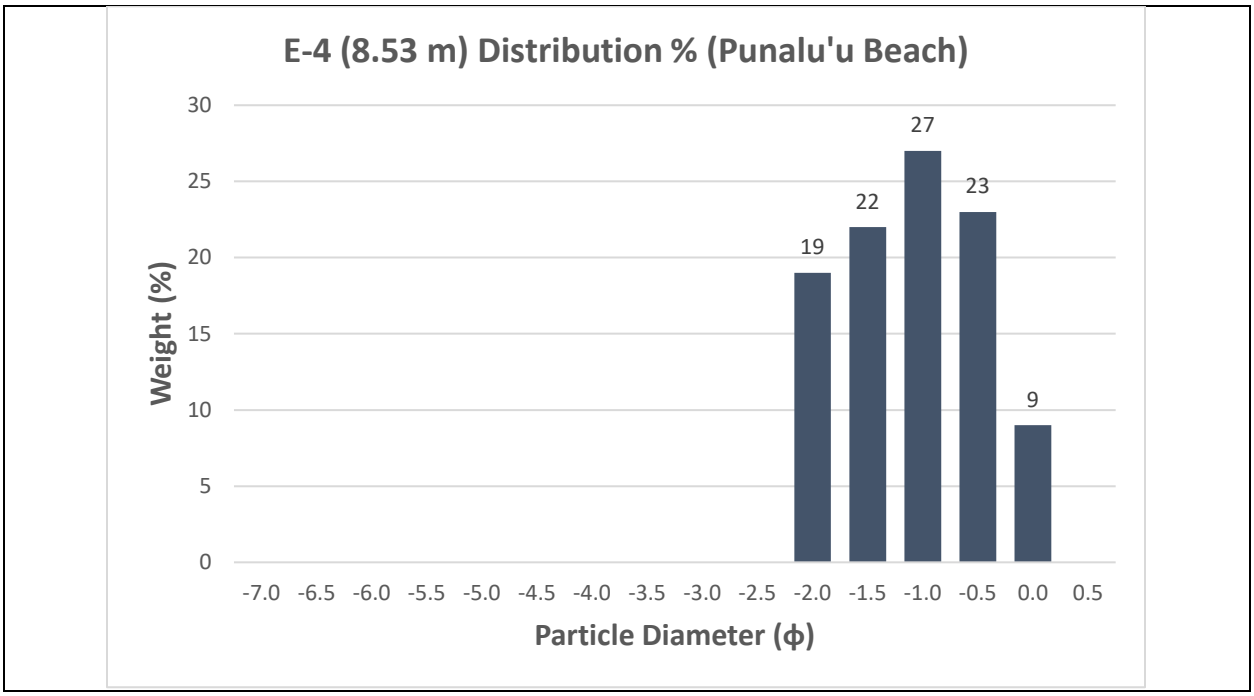
E-4 (8.53 m) Distribution % (Punalu'u Beach)
Weight (%)
30
25
20
15
10
5
0
19
22
27
23
9
-7.0 -6.5 -6.0 -5.5 -5.0 -4.5 -4.0 -3.5 -3.0 -2.5 -2.0 -1.5 -1.0 -0.5 0.0 0.5
Particle Diameter (ϕ)

Beach Name: Honoli'I Beach

Date: 10/22/2020 **Time:** 12:30 PM

Location/ Transect	Survey #	Distance from Water (m)	Slope in Degrees	"x" used	Calculated mm percentile								
					5	10	16	25	50	75	84	90	95
A	1	0.6096	-10	1.5	1.912241	1.842643	1.758467	1.630737	1.268425	0.889552	0.729599	0.599486	0.459356
	2	3.6576	-11	1.7	1.470945	1.435064	1.391379	1.323949	1.116317	0.853439	0.726204	0.616183	0.489475
	3	5.49	-13	1.7	1.597303	1.549715	1.491951	1.403974	1.150768	0.863168	0.729647	0.616454	0.487986
B	1	1.52	-10	1.6	1.731976	1.680539	1.618719	1.525769	1.259835	0.946616	0.803049	0.681364	0.538146
	2	4.88	-11	1.8	1.978647	1.933778	1.878733	1.79293	1.524446	1.168283	0.995949	0.849534	0.679332
	3	7.32	-11	1.8	1.684616	1.645078	1.596207	1.519619	1.282359	0.978015	0.827301	0.701089	0.555521

Calculated ϕ percentiles with corrections								
5	10	16	25	50	75	84	90	95
-1.508	-1.411	-1.217	-0.988	-0.360	0.147	0.352	0.554	0.738
-0.897	-0.834	-0.712	-0.567	-0.167	0.199	0.357	0.524	0.678
-1.089	-1.011	-0.863	-0.685	-0.213	0.185	0.352	0.523	0.681
-1.277	-1.198	-1.039	-0.853	-0.350	0.069	0.245	0.415	0.588
-1.587	-1.522	-1.360	-1.179	-0.639	-0.195	0.005	0.176	0.367
-1.213	-1.149	-1.009	-0.845	-0.377	0.028	0.212	0.384	0.558

Moments						
Mean	Standard Deviation	*Descriptor*	Skewness	*Descriptor*	Kurtosis	*Descriptor*
-0.409	0.733	Moderately Sorted	-0.057	Symmetrical	0.811	Platykurtic
-0.174	0.506	Moderately Well Sorted	0.026	Symmetrical	0.843	Platykurtic
-0.241	0.572	Moderately Well Sorted	-0.030	Symmetrical	0.834	Platykurtic
-0.381	0.604	Moderately Well Sorted	-0.034	Symmetrical	0.829	Platykurtic
-0.665	0.637	Moderately Well Sorted	-0.014	Symmetrical	0.814	Platykurtic
-0.391	0.573	Moderately Well Sorted	0.010	Symmetrical	0.831	Platykurtic

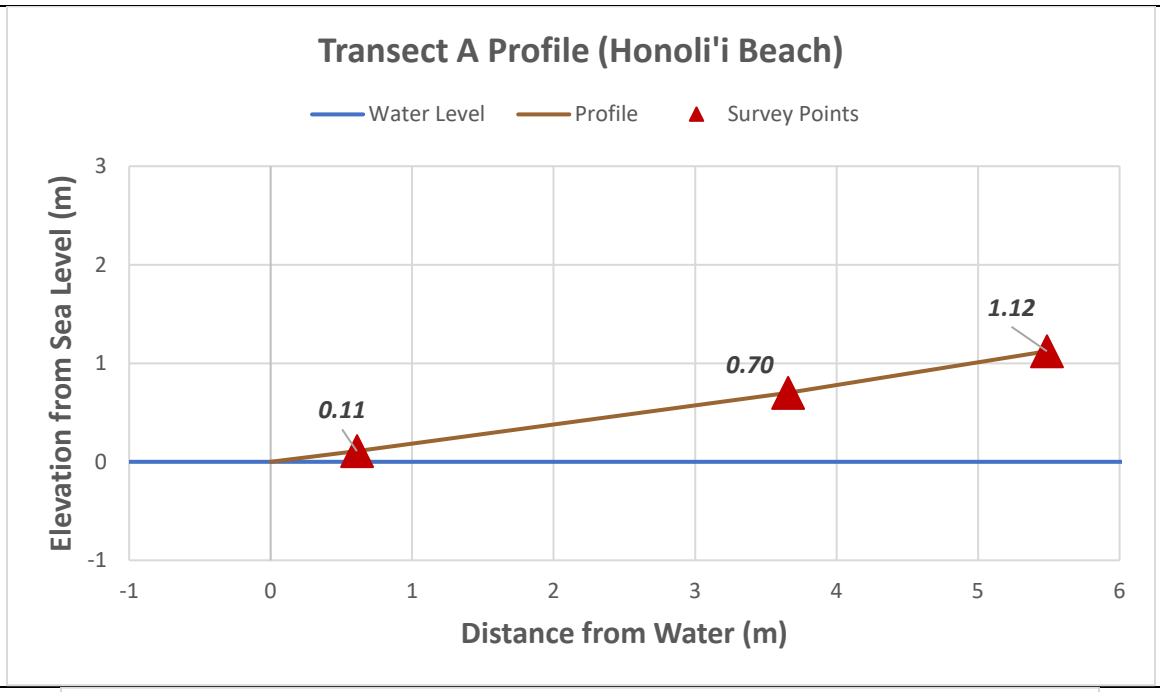
Transect A Profile (Honoli'i Beach)
Water Level
Profile
Survey Points
Elevation from Sea Level (m)
3
2
1
0
-1
-1
0
1
2
3
4
5
6
0.11
0.70
1.12
Distance from Water (m)

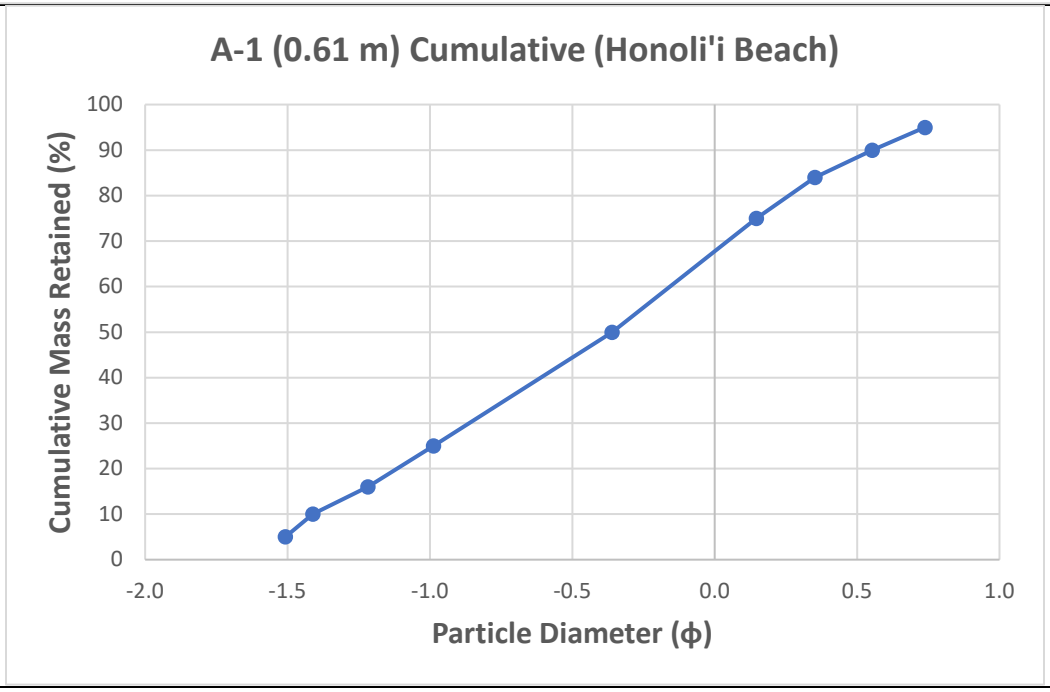
A-1 (0.61 m) Cumulative (Honoli'i Beach)
Cumulative Mass Retained (%)
100
90
80
70
60
50
40
30
20
10
0
-2.0
-1.5
-1.0
-0.5
0.0
0.5
1.0
Particle Diameter (ϕ)

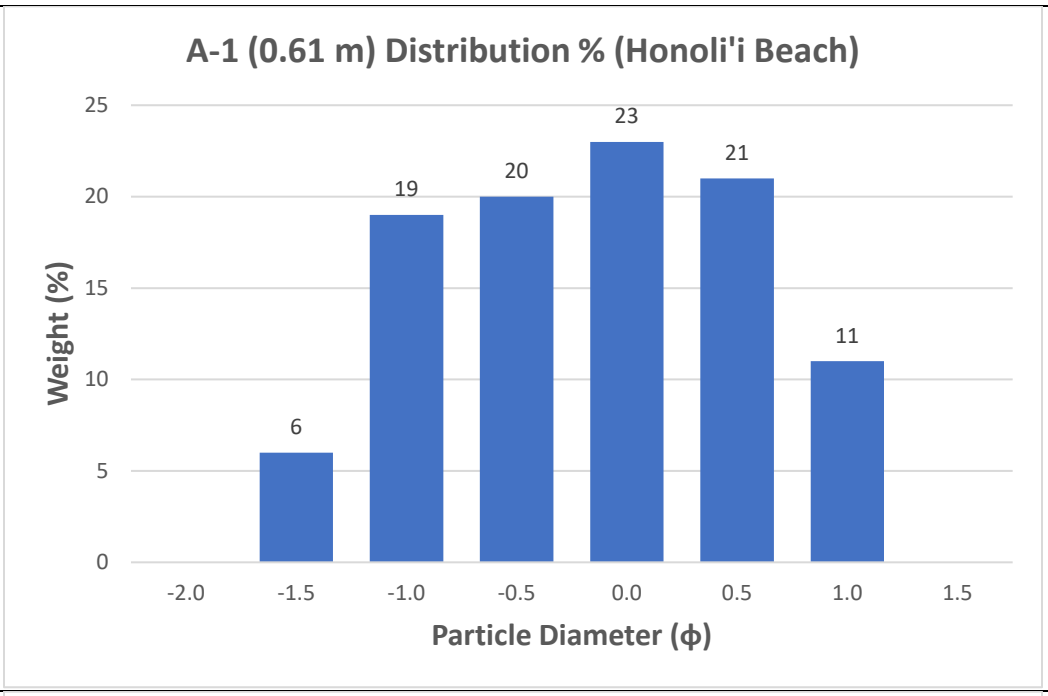
A-1 (0.61 m) Distribution % (Honoli'i Beach)
Weight (%)
25
20
15
10
5
0
6
19
20
23
21
11
-2.0
-1.5
-1.0
-0.5
0.0
0.5
1.0
1.5
Particle Diameter (ϕ)

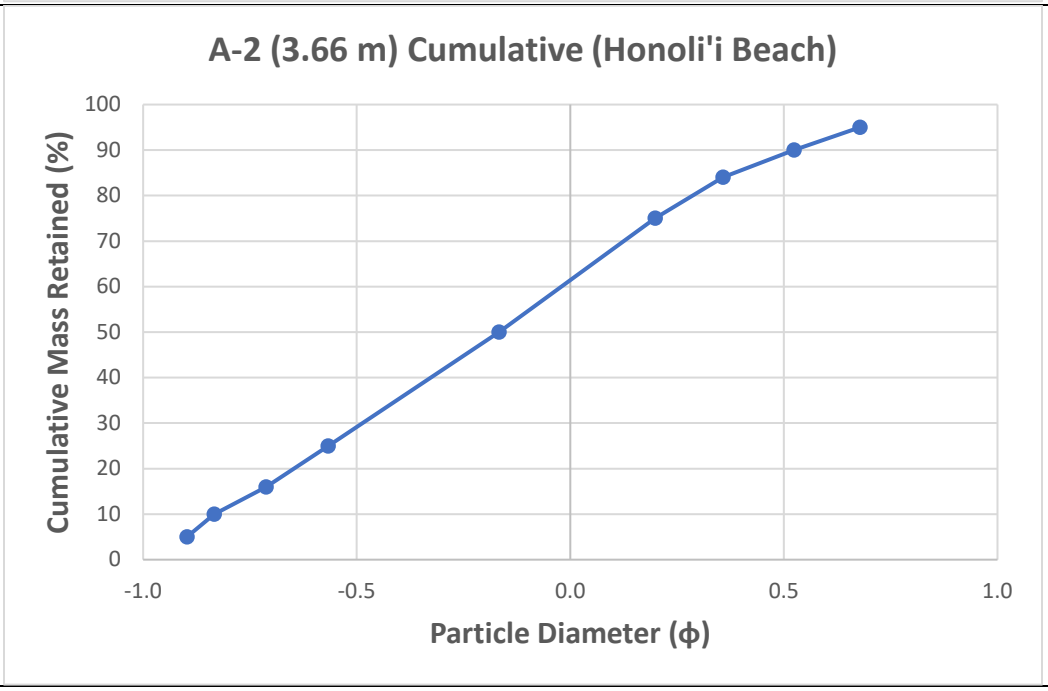
A-2 (3.66 m) Cumulative (Honoli'i Beach)
Cumulative Mass Retained (%)
100
90
80
70
60
50
40
30
20
10
0
-1.0
-0.5
0.0
0.5
1.0
Particle Diameter (ϕ)

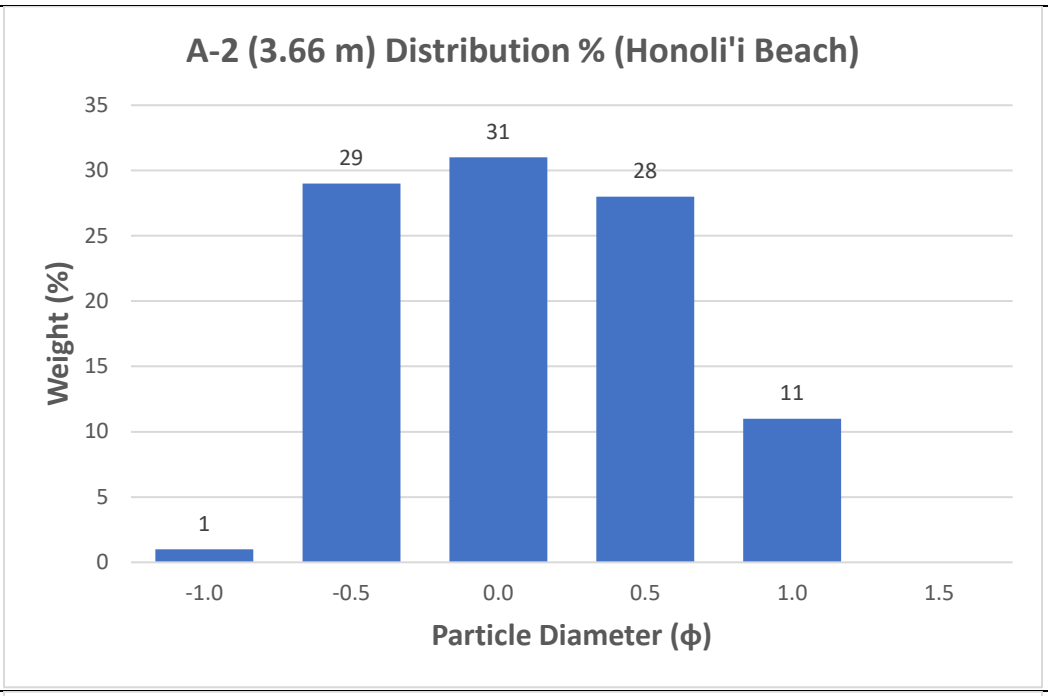
A-2 (3.66 m) Distribution % (Honoli'i Beach)
Weight (%)
35
30
25
20
15
10
5
0
1
29
31
28
11
-1.0
-0.5
0.0
0.5
1.0
1.5
Particle Diameter (ϕ)

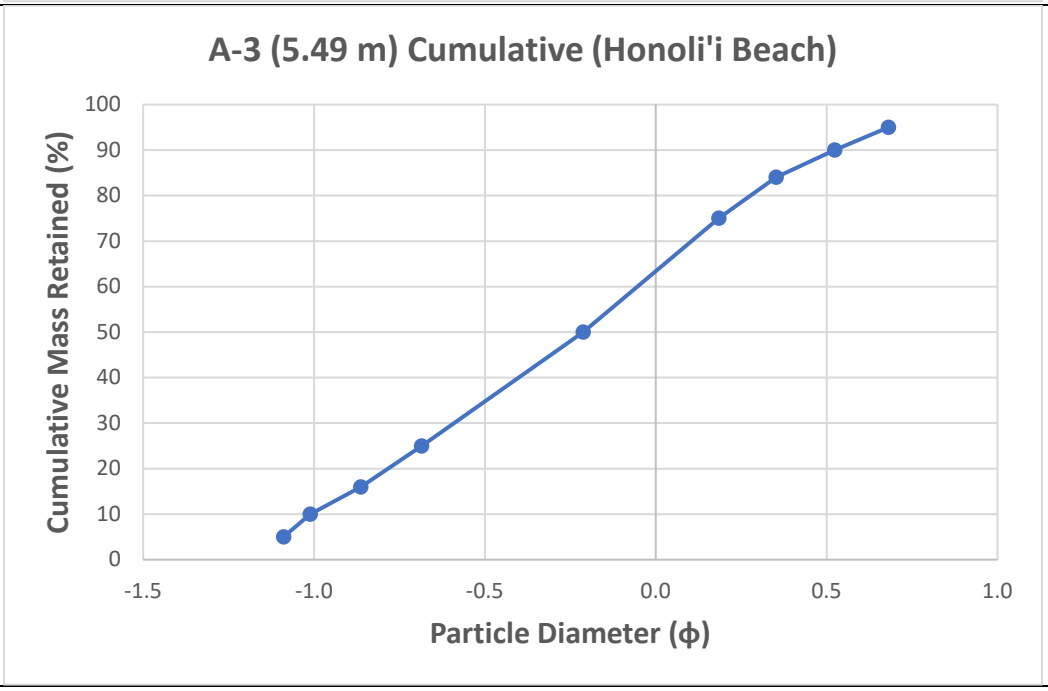
A-3 (5.49 m) Cumulative (Honoli'i Beach)
Cumulative Mass Retained (%)
100
90
80
70
60
50
40
30
20
10
0
-1.5
-1.0
-0.5
0.0
0.5
1.0
Particle Diameter (ϕ)

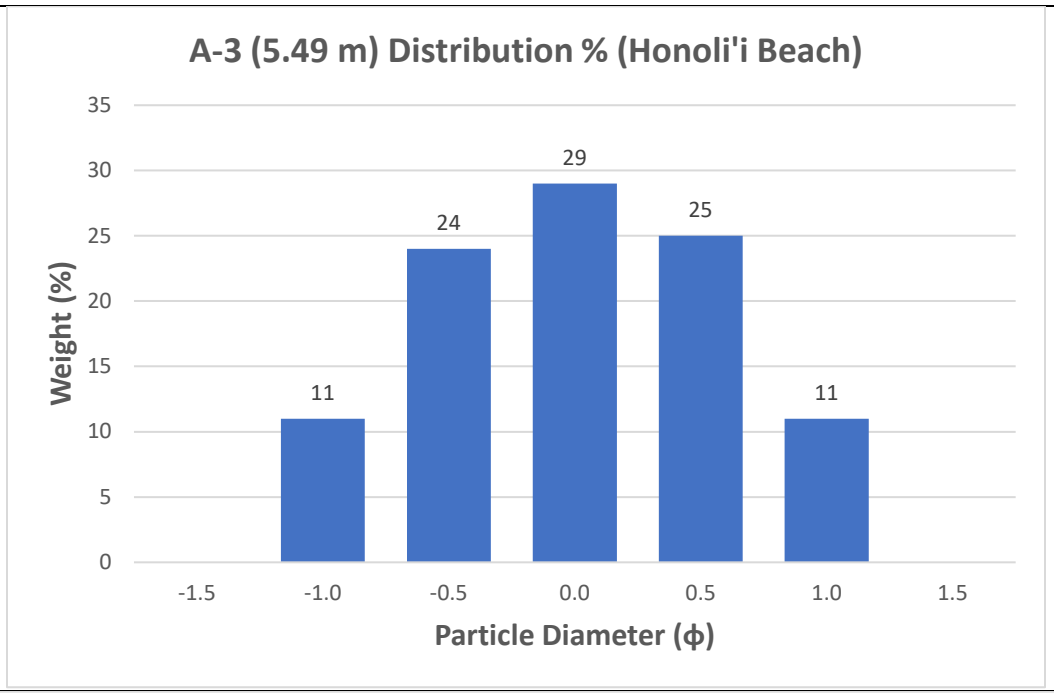
A-3 (5.49 m) Distribution % (Honoli'i Beach)
Weight (%)
35
30
25
20
15
10
5
0
11
24
29
25
11
-1.5
-1.0
-0.5
0.0
0.5
1.0
1.5
Particle Diameter (ϕ)

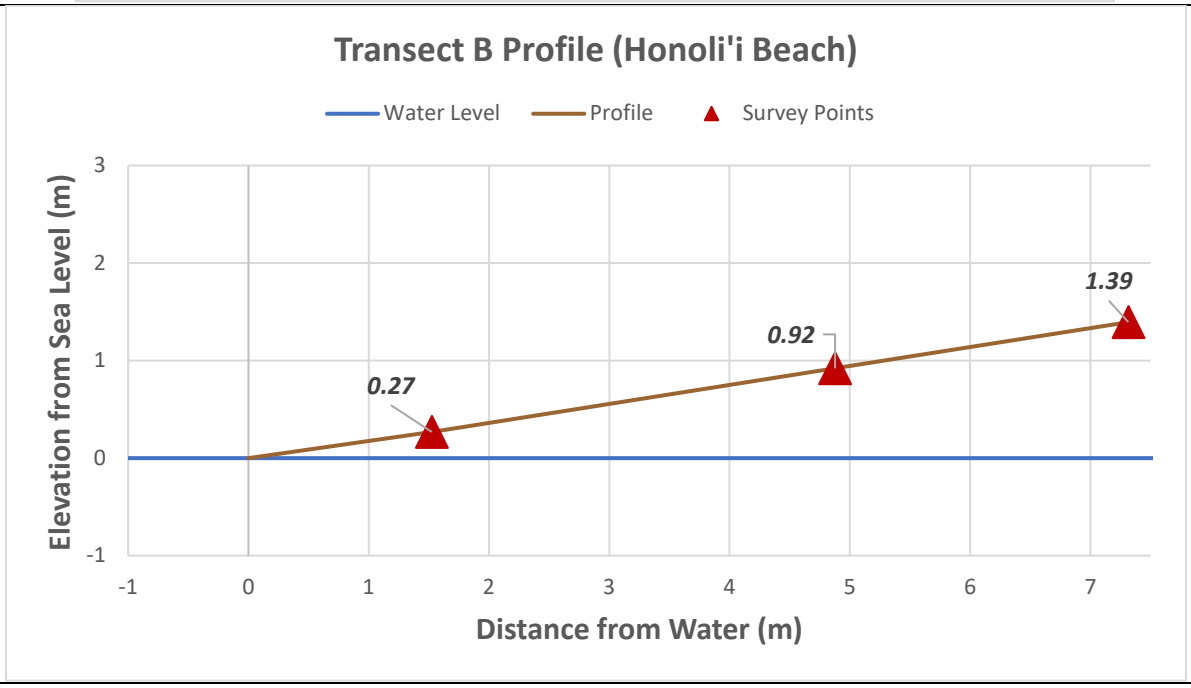
Transect B Profile (Honoli'i Beach)
Water Level
Profile
Survey Points
Elevation from Sea Level (m)
3
2
1
0
-1
0.27
0.92
1.39
-1
0
1
2
3
4
5
6
7
Distance from Water (m)

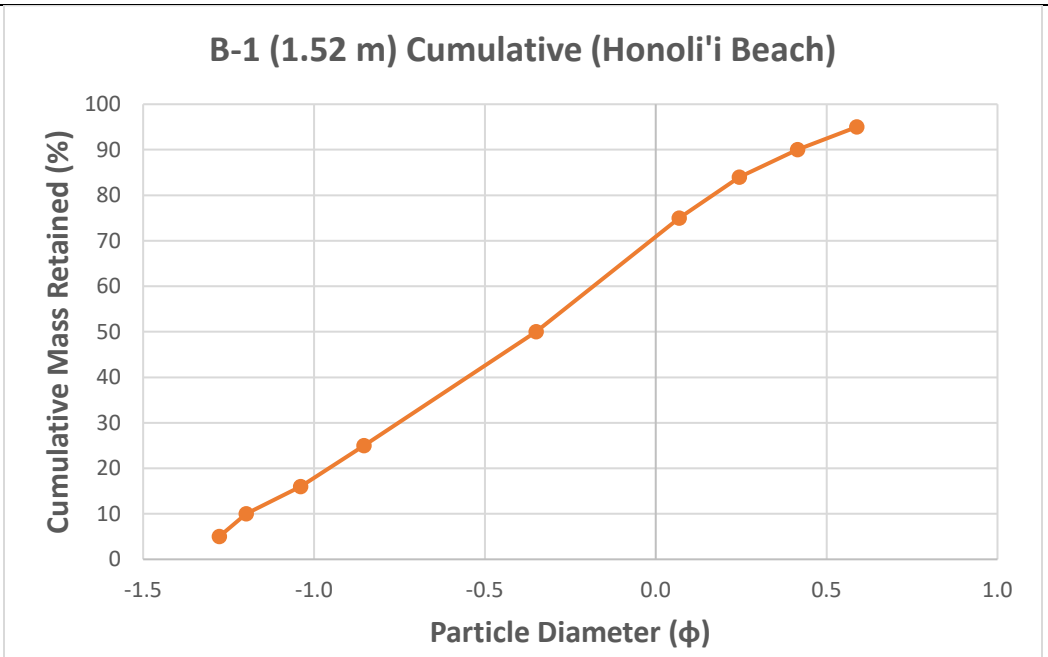
B-1 (1.52 m) Cumulative (Honoli'i Beach)
Cumulative Mass Retained (%)
100
90
80
70
60
50
40
30
20
10
0
-1.5
-1.0
-0.5
0.0
0.5
1.0
Particle Diameter (ϕ)

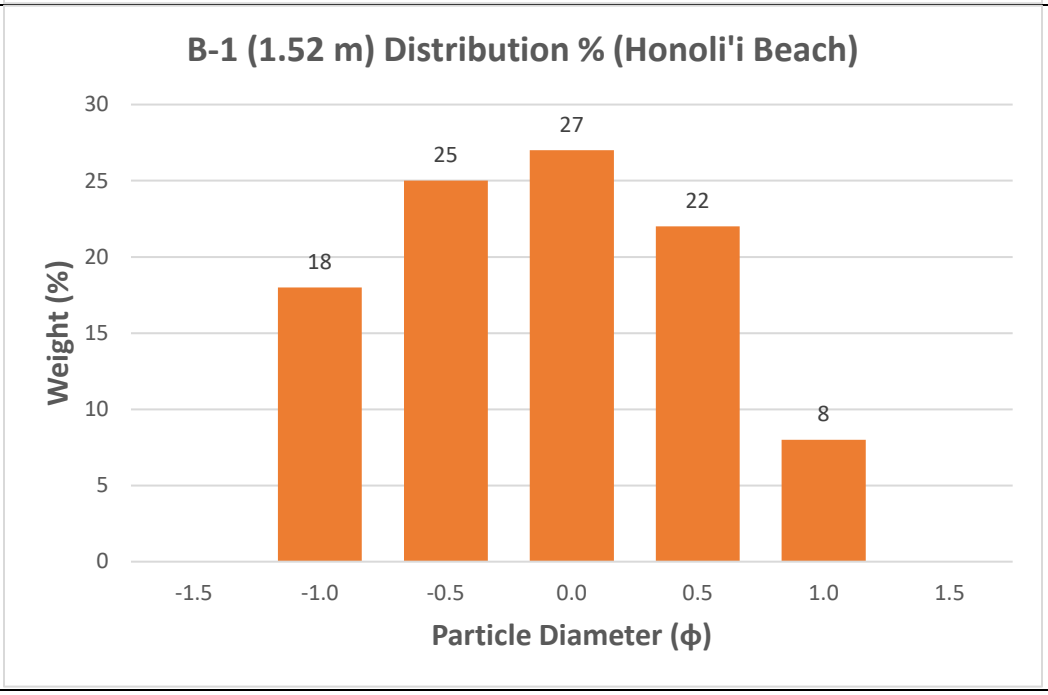
B-1 (1.52 m) Distribution % (Honoli'i Beach)
Weight (%)
30
25
20
15
10
5
0
18
25
27
22
8
-1.5
-1.0
-0.5
0.0
0.5
1.0
1.5
Particle Diameter (ϕ)

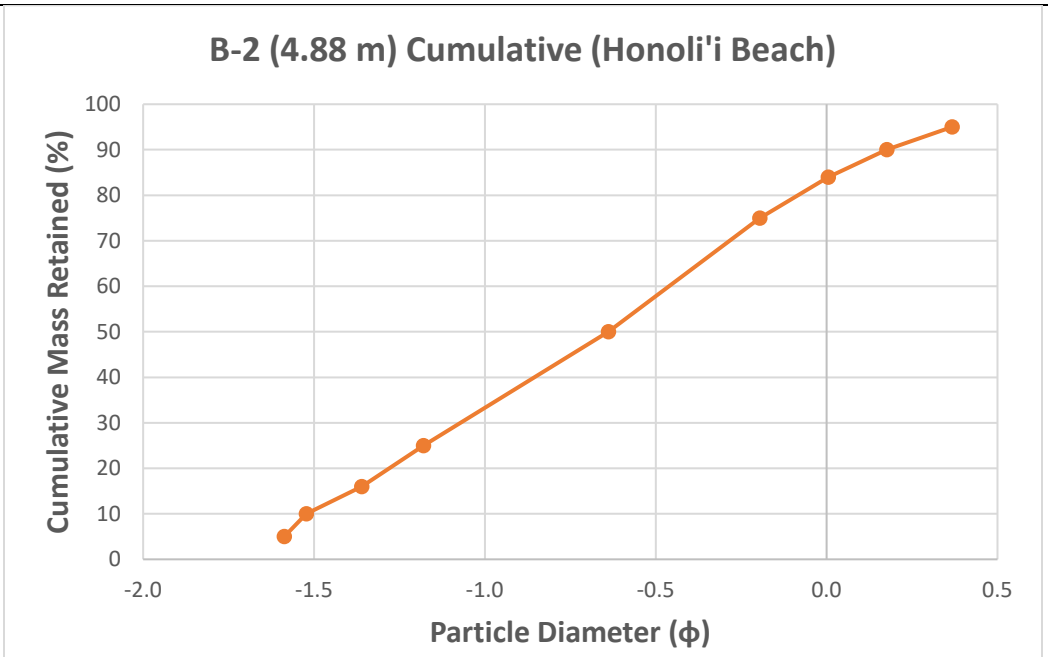
B-2 (4.88 m) Cumulative (Honoli'i Beach)
Cumulative Mass Retained (%)
100
90
80
70
60
50
40
30
20
10
0
-2.0
-1.5
-1.0
-0.5
0.0
0.5
Particle Diameter (ϕ)

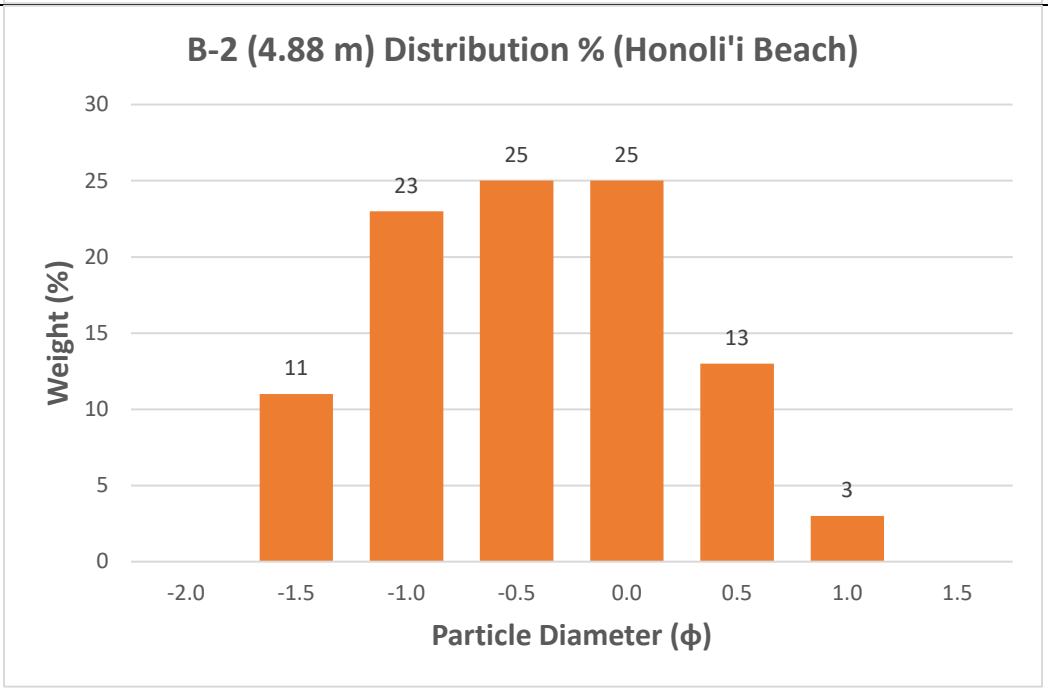
B-2 (4.88 m) Distribution % (Honoli'i Beach)
Weight (%)
30
25
20
15
10
5
0
11
23
25
25
13
3
-2.0
-1.5
-1.0
-0.5
0.0
0.5
1.0
1.5
Particle Diameter (ϕ)

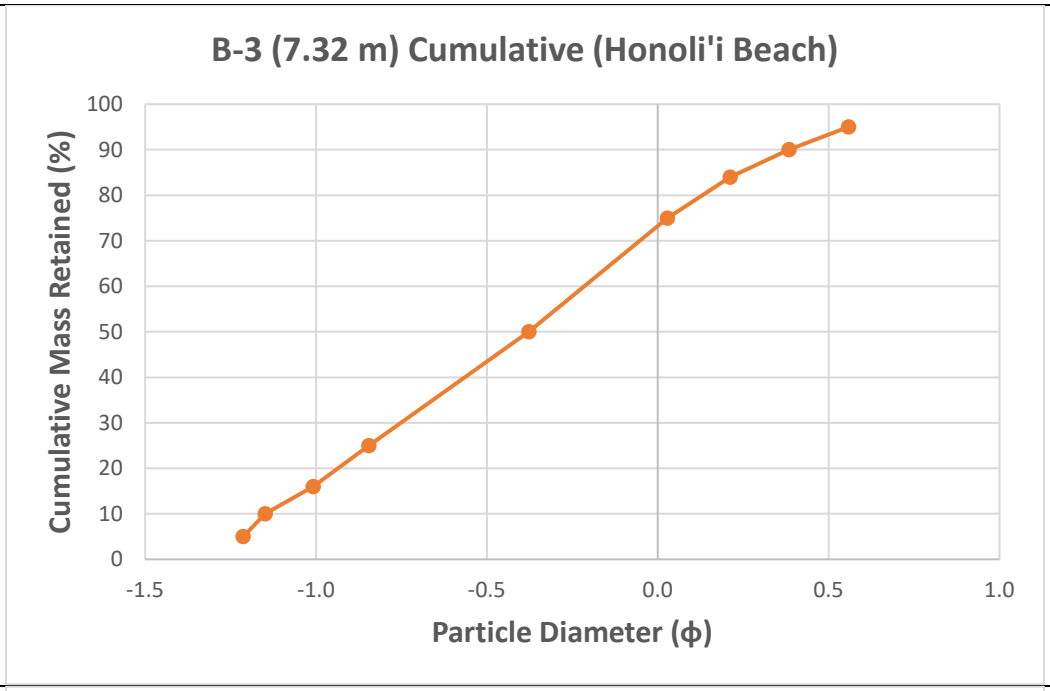
B-3 (7.32 m) Cumulative (Honoli'i Beach)
Cumulative Mass Retained (%)
100
90
80
70
60
50
40
30
20
10
0
-1.5
-1.0
-0.5
0.0
0.5
1.0
Particle Diameter (ϕ)

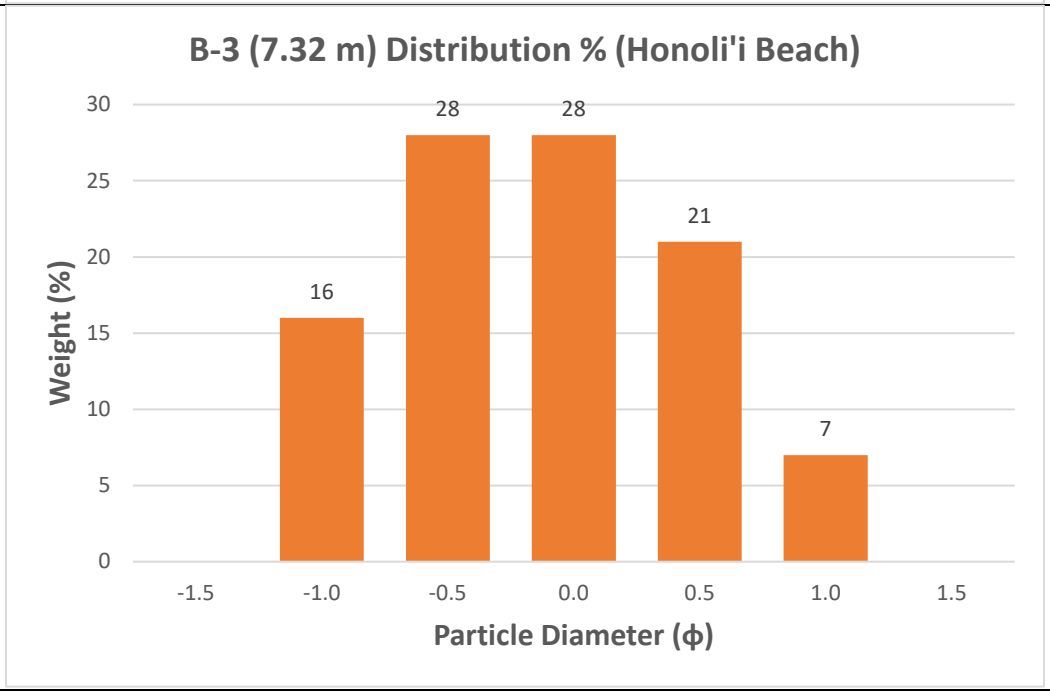
B-3 (7.32 m) Distribution % (Honoli'i Beach)
Weight (%)
30
25
20
15
10
5
0
16
28
28
21
7
-1.5
-1.0
-0.5
0.0
0.5
1.0
1.5
Particle Diameter (ϕ)

Beach Name:	Pohoiki Beach

Date: 10/22/2020 **Time:** 3:00 PM

					Calculated mm percentile								
Location/ Transect	Survey #	Distance from Water (m)	Slope in Degrees	"x" used	5	10	16	25	50	75	84	90	95
A	1	0.9144	-23	7	4.386532	4.355761	4.316823	4.254058	4.038941	3.699546	3.496136	3.292672	3.010314
	2	3.048	-25	7	8.586378	8.524906	8.447501	8.322324	7.891059	7.215712	6.81834	6.426307	5.886912
	3	6.71	-4	7	6.536851	6.49176	6.433281	6.339485	6.012969	5.488517	5.169223	4.849549	4.411758
	4	8.53	-11	7	6.045666	6.004151	5.950463	5.864381	5.566282	5.091983	4.805836	4.520483	4.125938
	5	11.58	-15	7	9.593686	9.524749	9.436331	9.294047	8.801502	8.024156	7.565183	7.108566	6.487263

Calculated ϕ percentiles with corrections								
5	10	16	25	50	75	84	90	95
-3.439	-3.397	-3.154	-2.924	-2.115	-1.642	-1.398	-1.289	-1.046
-5.001	-4.947	-4.602	-4.280	-3.129	-2.480	-2.144	-2.013	-1.683
-4.366	-4.318	-4.015	-3.730	-2.717	-2.137	-1.834	-1.708	-1.409
-4.185	-4.138	-3.847	-3.573	-2.601	-2.043	-1.753	-1.632	-1.345
-5.258	-5.203	-4.841	-4.503	-3.295	-2.614	-2.260	-2.122	-1.775

Moments						
Mean	Standard Deviation	*Descriptor*	Skewness	*Descriptor*	Kurtosis	*Descriptor*
-2.222	0.802	Moderately Sorted	-0.145	Coarse Skewed	0.765	Platykurtic
-3.292	1.117	Poorly Sorted	-0.163	Coarse Skewed	0.756	Platykurtic
-2.856	0.993	Moderately Sorted	-0.153	Coarse Skewed	0.761	Platykurtic
-2.733	0.954	Moderately Sorted	-0.153	Coarse Skewed	0.761	Platykurtic
-3.465	1.173	Poorly Sorted	-0.163	Coarse Skewed	0.756	Platykurtic

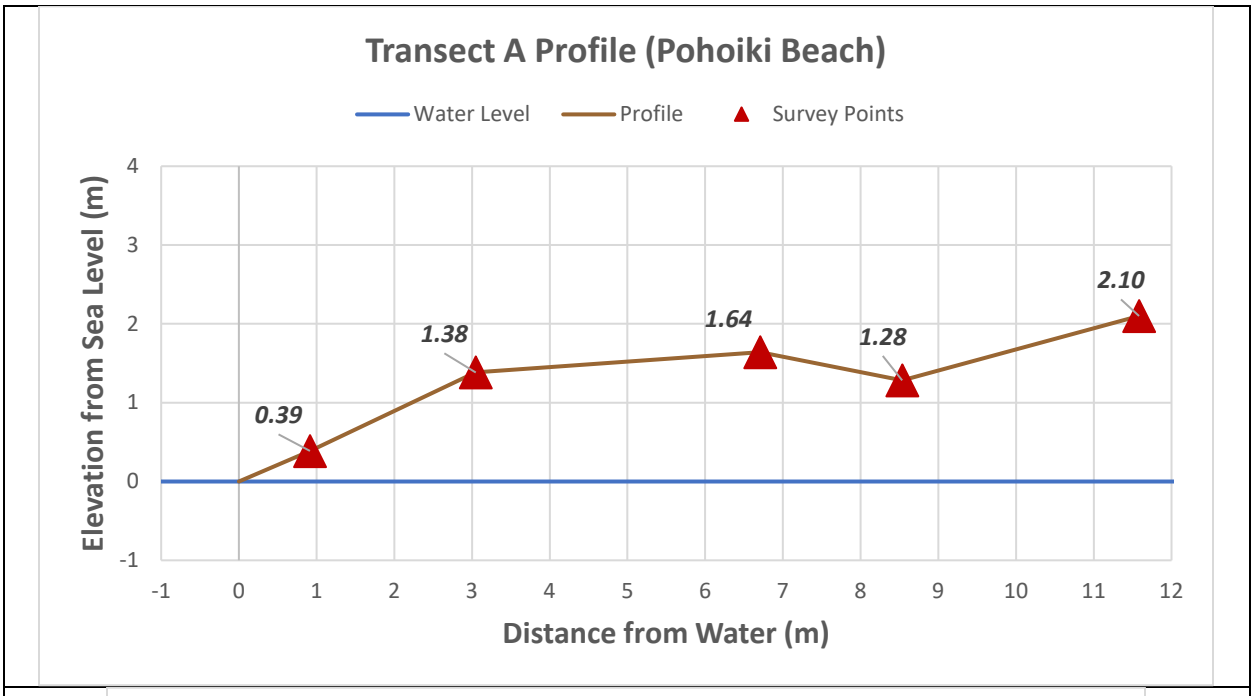
Transect A Profile (Pohoiki Beach)
Water Level
Profile
Survey Points
Elevation from Sea Level (m)
Distance from Water (m)
0.39
1.38
1.64
1.28
2.10

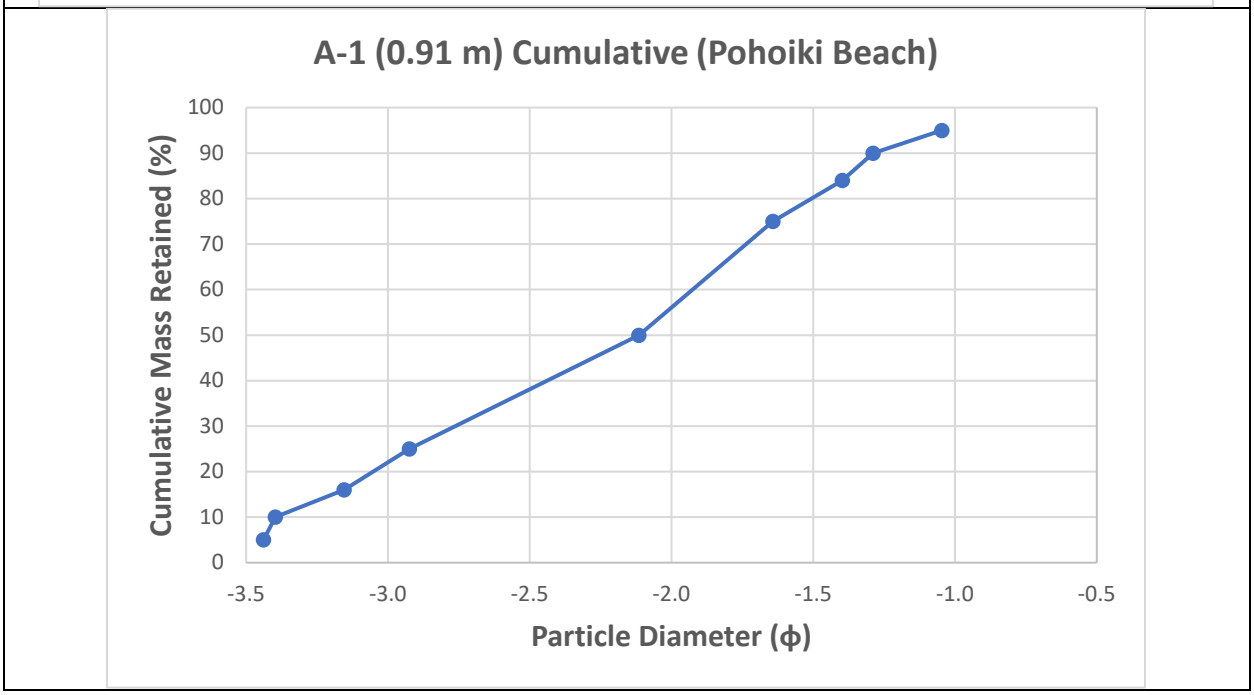
A-1 (0.91 m) Cumulative (Pohoiki Beach)
Cumulative Mass Retained (%)
Particle Diameter (ϕ)

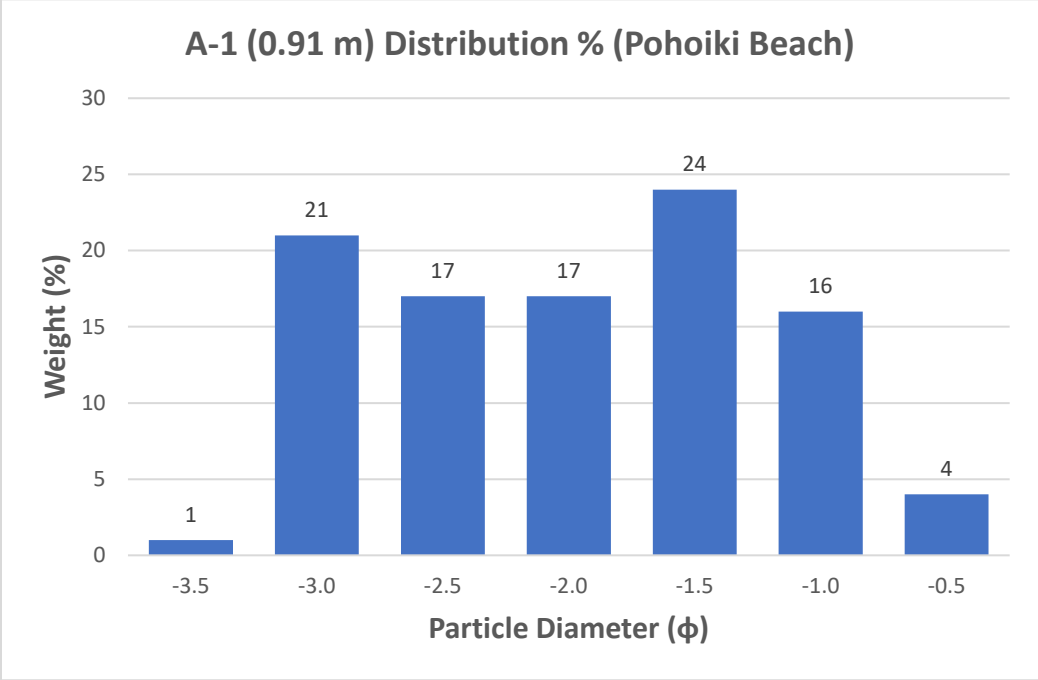
A-1 (0.91 m) Distribution % (Pohoiki Beach)
Weight (%)
30
25
20
15
10
5
0
1
21
17
17
24
16
4
-3.5
-3.0
-2.5
-2.0
-1.5
-1.0
-0.5
Particle Diameter (ϕ)

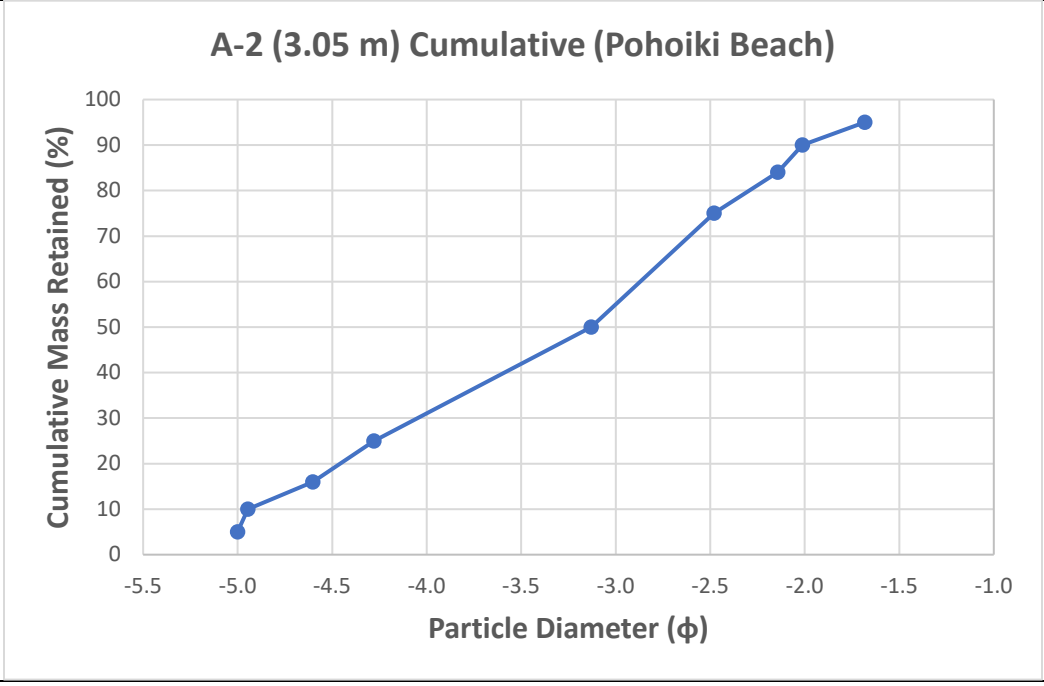
A-2 (3.05 m) Cumulative (Pohoiki Beach)
Cumulative Mass Retained (%)
100
90
80
70
60
50
40
30
20
10
0
-5.5
-5.0
-4.5
-4.0
-3.5
-3.0
-2.5
-2.0
-1.5
-1.0
Particle Diameter (ϕ)

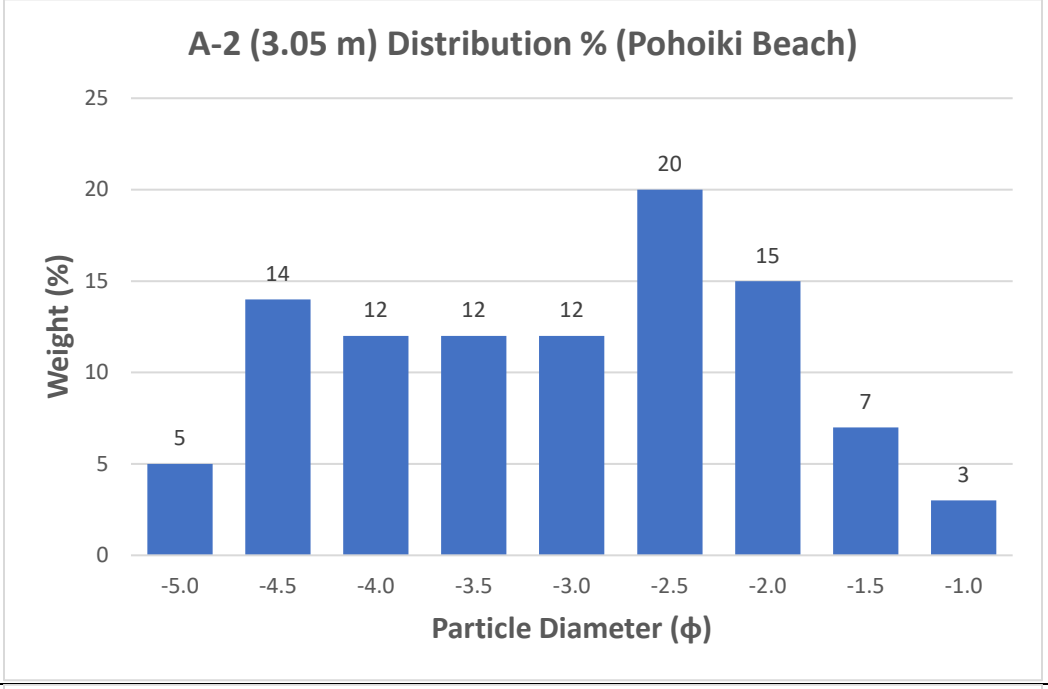
A-2 (3.05 m) Distribution % (Pohoiki Beach)
Weight (%)
25
20
15
10
5
0
5
14
12
12
12
20
15
7
3
-5.0
-4.5
-4.0
-3.5
-3.0
-2.5
-2.0
-1.5
-1.0
Particle Diameter (ϕ)

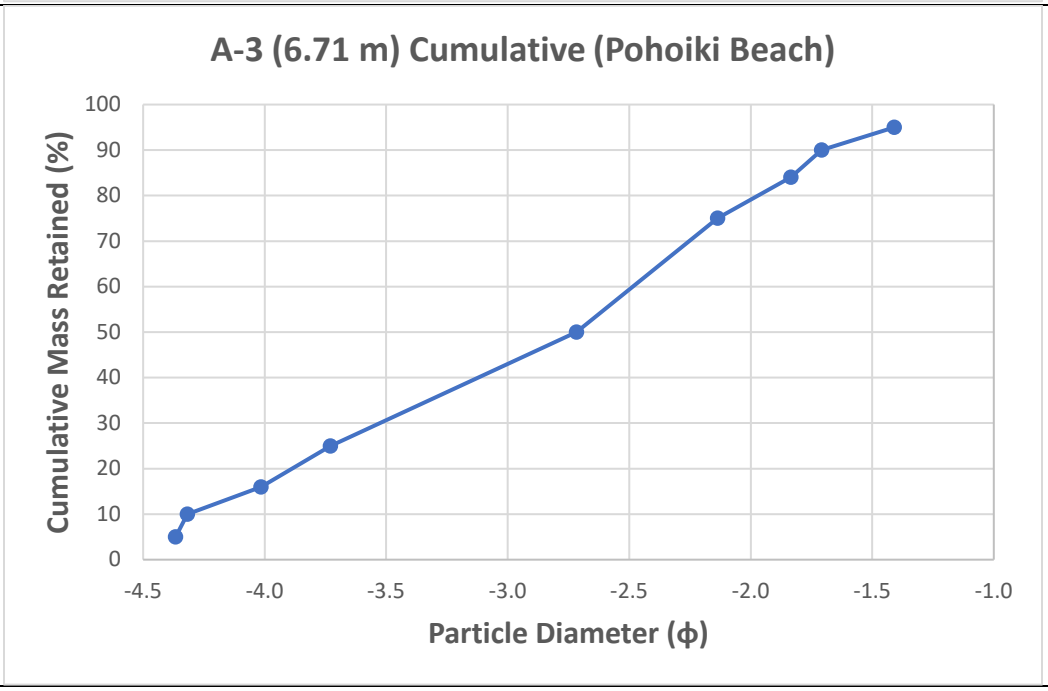
A-3 (6.71 m) Cumulative (Pohoiki Beach)
Cumulative Mass Retained (%)
100
90
80
70
60
50
40
30
20
10
0
-4.5
-4.0
-3.5
-3.0
-2.5
-2.0
-1.5
-1.0
Particle Diameter (ϕ)

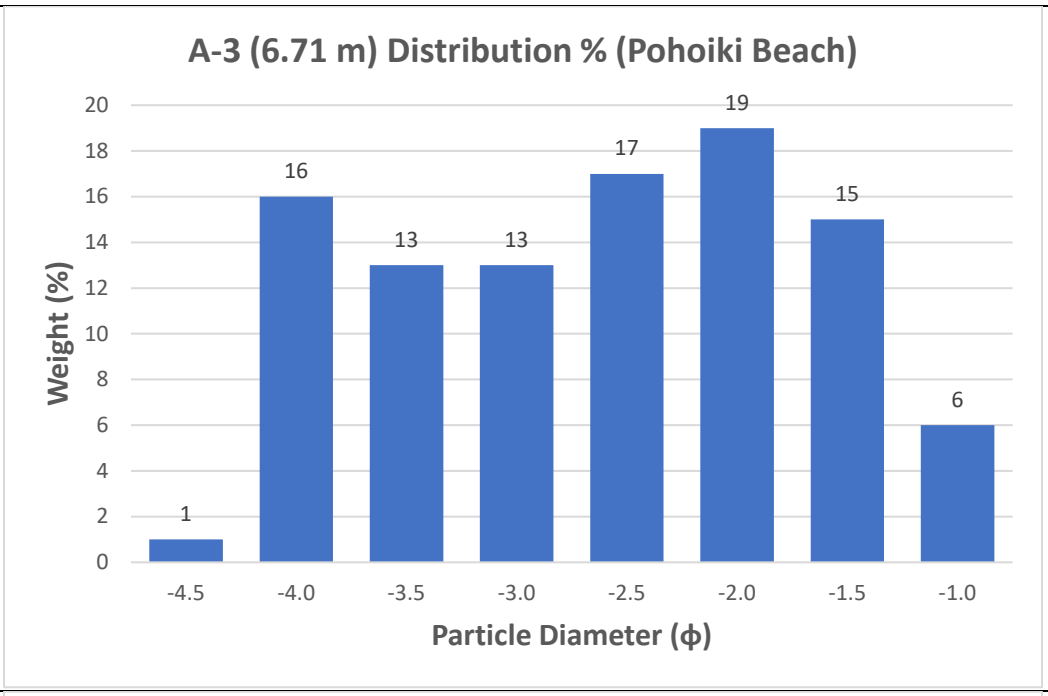
A-3 (6.71 m) Distribution % (Pohoiki Beach)
Weight (%)
20
18
16
14
12
10
8
6
4
2
0
1
16
13
13
17
19
15
6
-4.5
-4.0
-3.5
-3.0
-2.5
-2.0
-1.5
-1.0
Particle Diameter (ϕ)

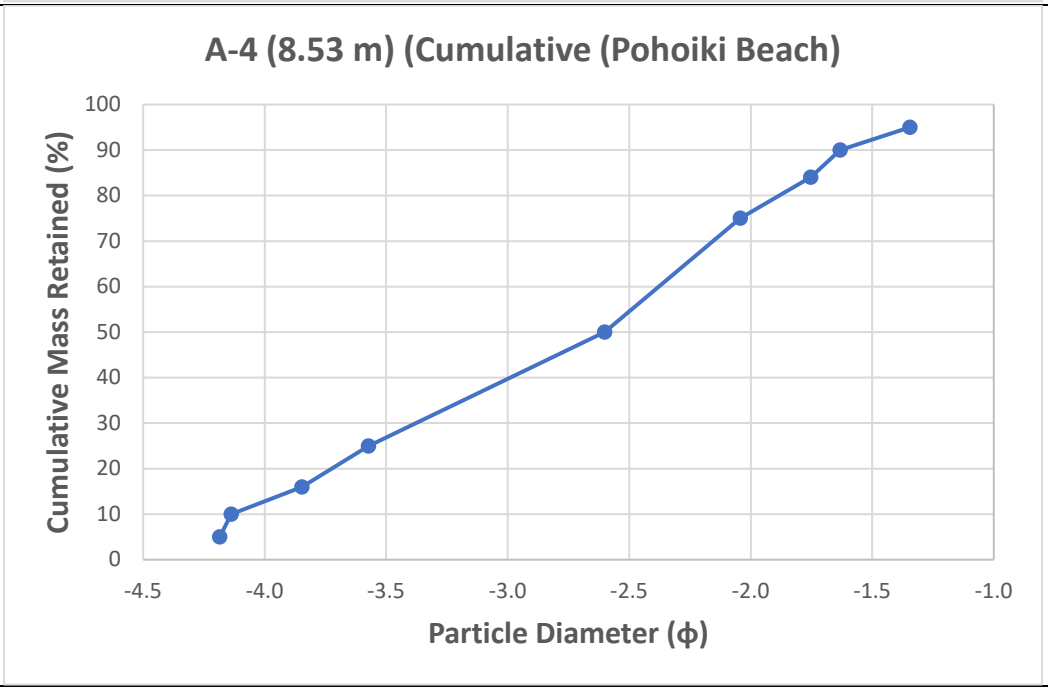
A-4 (8.53 m) (Cumulative (Pohoiki Beach)
Cumulative Mass Retained (%)
100
90
80
70
60
50
40
30
20
10
0
-4.5
-4.0
-3.5
-3.0
-2.5
-2.0
-1.5
-1.0
Particle Diameter (ϕ)

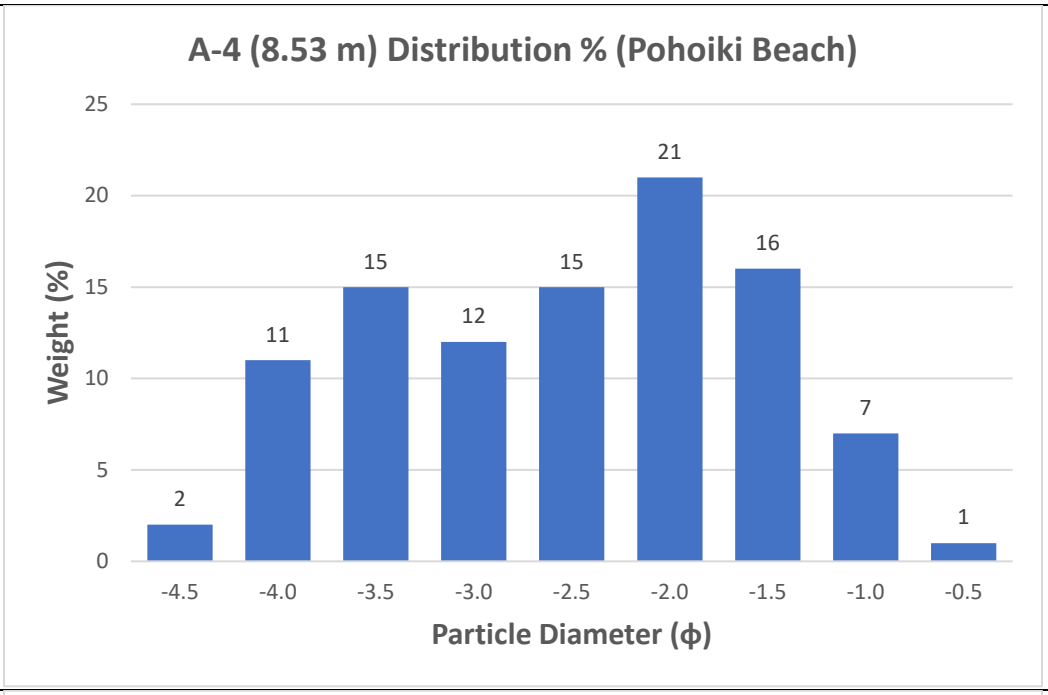
A-4 (8.53 m) Distribution % (Pohoiki Beach)
Weight (%)
25
20
15
10
5
0
2
11
15
12
15
21
16
7
1
-4.5
-4.0
-3.5
-3.0
-2.5
-2.0
-1.5
-1.0
-0.5
Particle Diameter (ϕ)

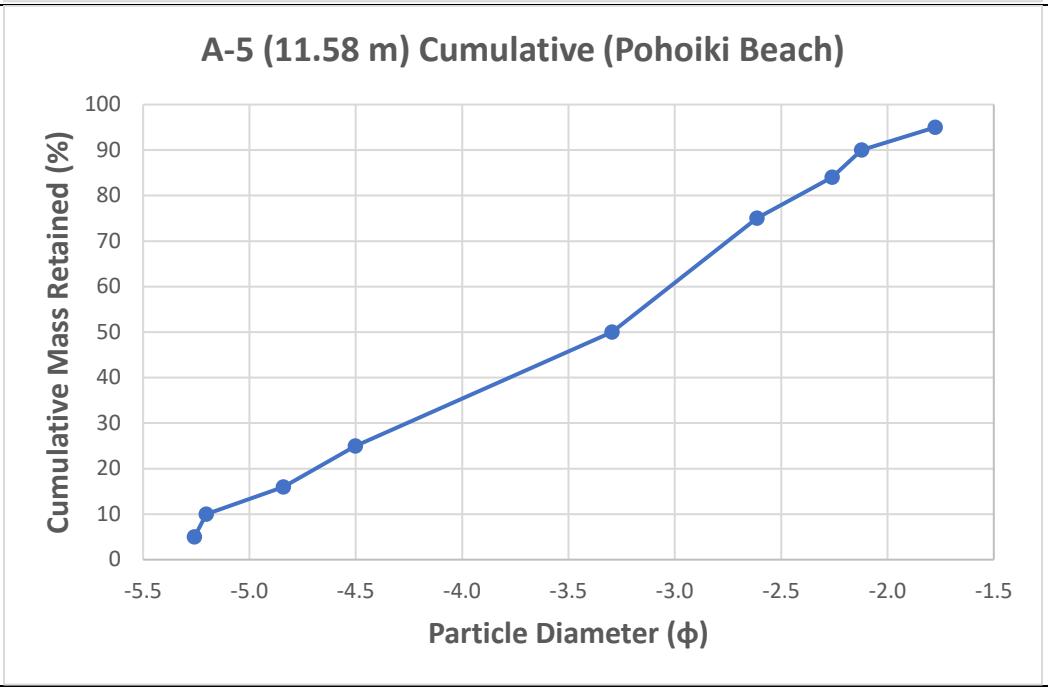
A-5 (11.58 m) Cumulative (Pohoiki Beach)
Cumulative Mass Retained (%)
100
90
80
70
60
50
40
30
20
10
0
-5.5
-5.0
-4.5
-4.0
-3.5
-3.0
-2.5
-2.0
-1.5
Particle Diameter (ϕ)

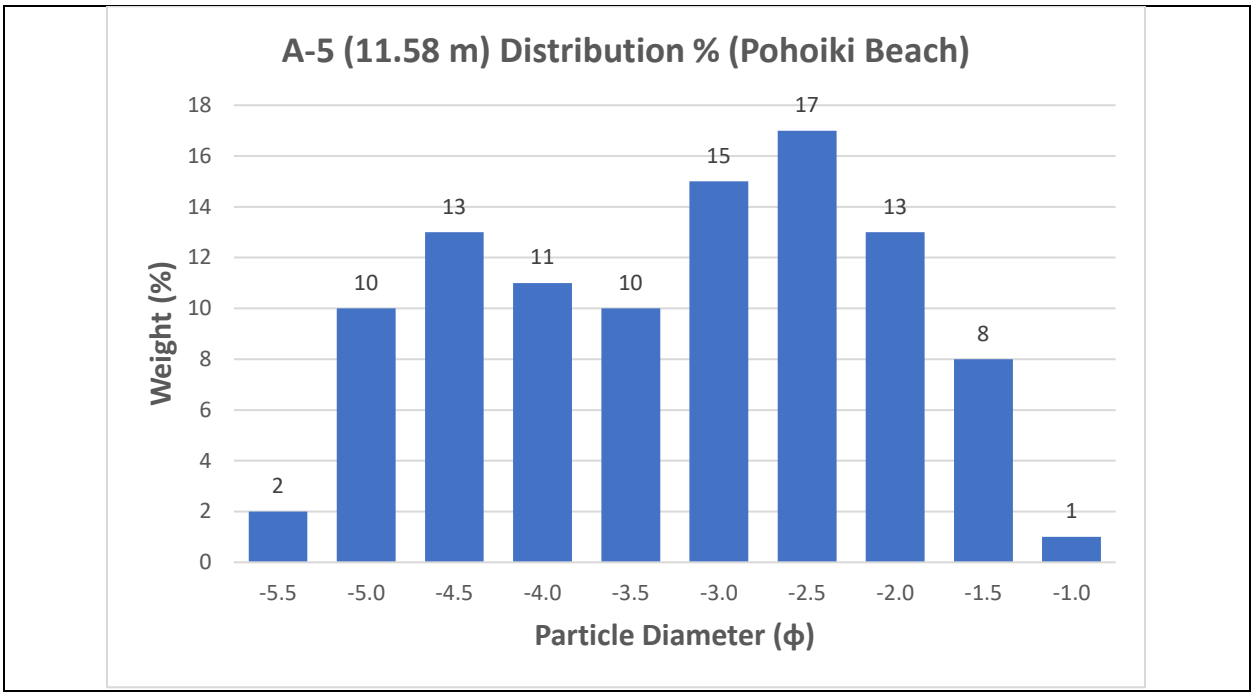
A-5 (11.58 m) Distribution % (Pohoiki Beach)
Weight (%)
18
16
14
12
10
8
6
4
2
0
2
10
13
11
10
15
17
13
8
1
-5.5
-5.0
-4.5
-4.0
-3.5
-3.0
-2.5
-2.0
-1.5
-1.0
Particle Diameter (ϕ)

Beach Name: Green Sand Beach

Date: 10/23/2020 **Time:** 9:50 AM

Location/ Transect	Survey #	Distance from Water (m)	Slope in Degrees	"x" used	Calculated mm percentile								
					5	10	16	25	50	75	84	90	95
A	1	0.6096	-8	-1	0.988992	0.793278	0.64241	0.498712	0.28948	0.179367	0.141353	0.121006	0.065503
	2	4.2672	-10	-1.1	1.091048	0.804372	0.624754	0.474369	0.278253	0.177519	0.140685	0.129479	0.064739
	3	7.62	-10	-1	0.996443	0.741876	0.578367	0.436555	0.247739	0.152699	0.117309	0.102065	0.063552
	4	13.72	-25	-0.9	1.21391	0.915227	0.715424	0.540873	0.305794	0.189761	0.148644	0.129821	0.078843

Calculated ϕ percentiles with corrections

5	10	16	25	50	75	84	90	95
0.026	0.535	0.954	1.405	1.878	2.157	2.185	2.285	2.587
-0.203	0.503	1.015	1.506	1.938	2.170	2.190	2.212	2.599
0.008	0.689	1.181	1.674	2.114	2.359	2.393	2.469	2.616
-0.451	0.204	0.722	1.241	1.795	2.086	2.129	2.209	2.411

Moments

Mean	Standard Deviation	*Descriptor*	Skewness	*Descriptor*	Kurtosis	*Descriptor*
1.672	0.696	Moderately Well Sorted	-0.474	Very Coarse Skewed	1.397	Leptokurtic
1.714	0.718	Moderately Well Sorted	-0.550	Very Coarse Skewed	1.730	Very Leptokurtic
1.896	0.698	Moderately Well Sorted	-0.577	Very Coarse Skewed	1.561	Very Leptokurtic
1.549	0.785	Moderately Sorted	-0.547	Very Coarse Skewed	1.389	Leptokurtic

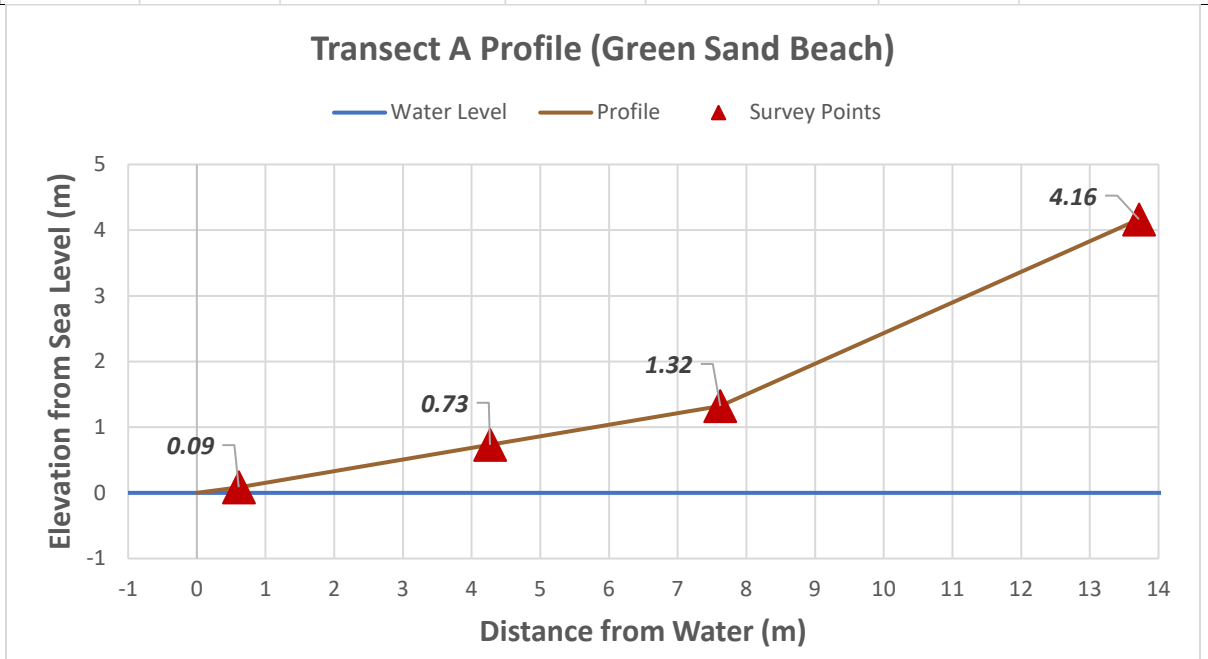

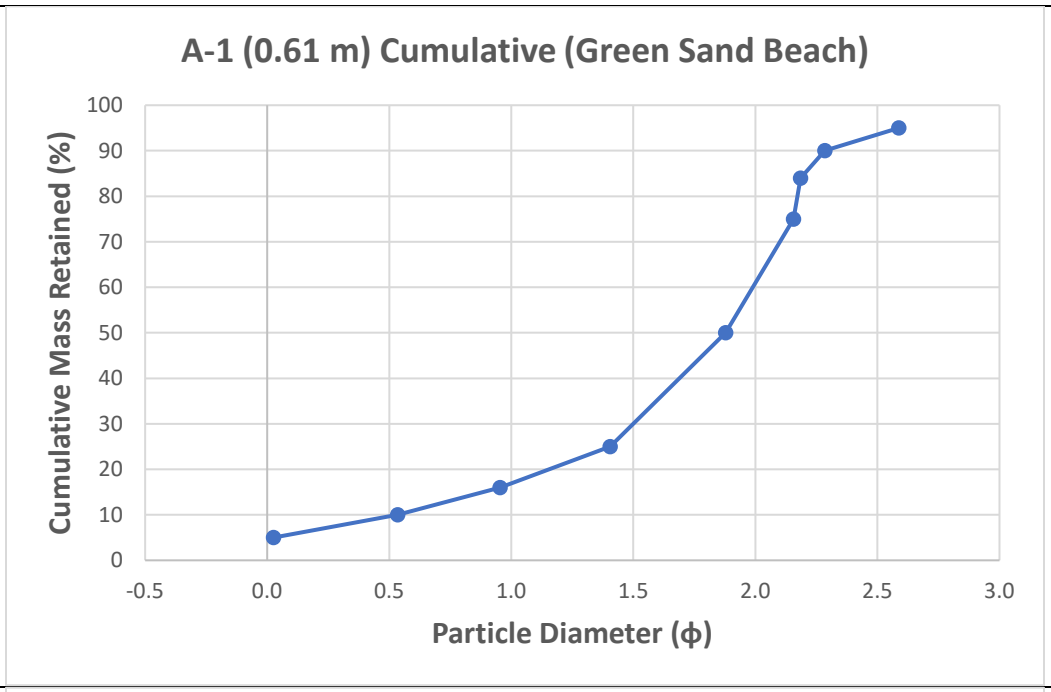
A-1 (0.61 m) Cumulative (Green Sand Beach)
Cumulative Mass Retained (%)
100
90
80
70
60
50
40
30
20
10
0
-0.5
0.0
0.5
1.0
1.5
2.0
2.5
3.0
Particle Diameter (ϕ)

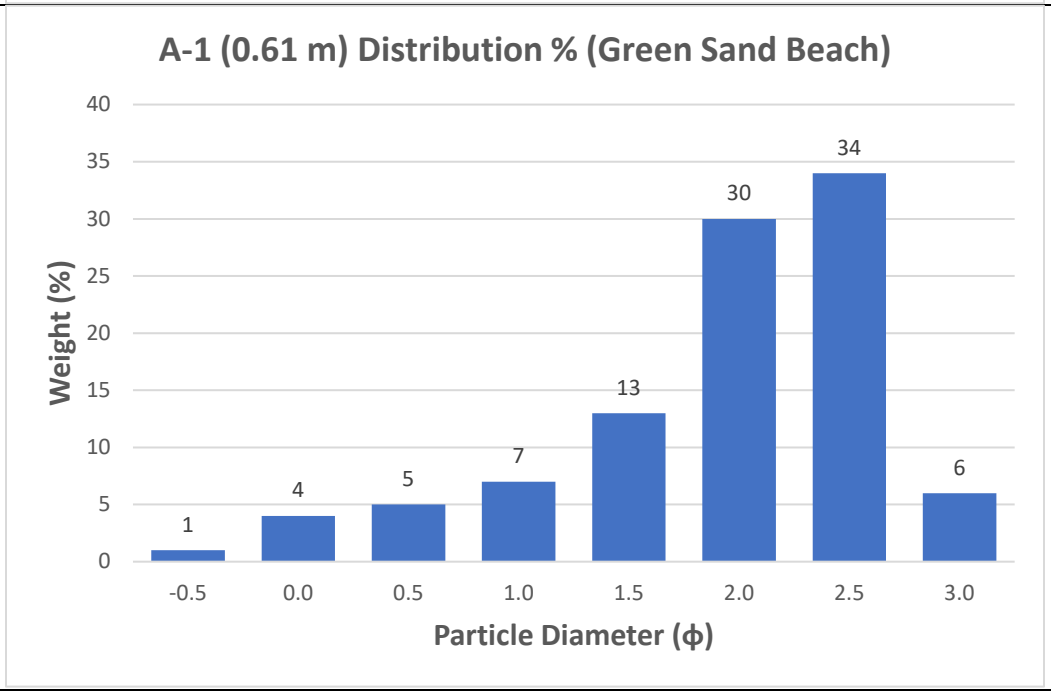
A-1 (0.61 m) Distribution % (Green Sand Beach)
Weight (%)
40
35
30
25
20
15
10
5
0
1
4
5
7
13
30
34
6
-0.5
0.0
0.5
1.0
1.5
2.0
2.5
3.0
Particle Diameter (ϕ)

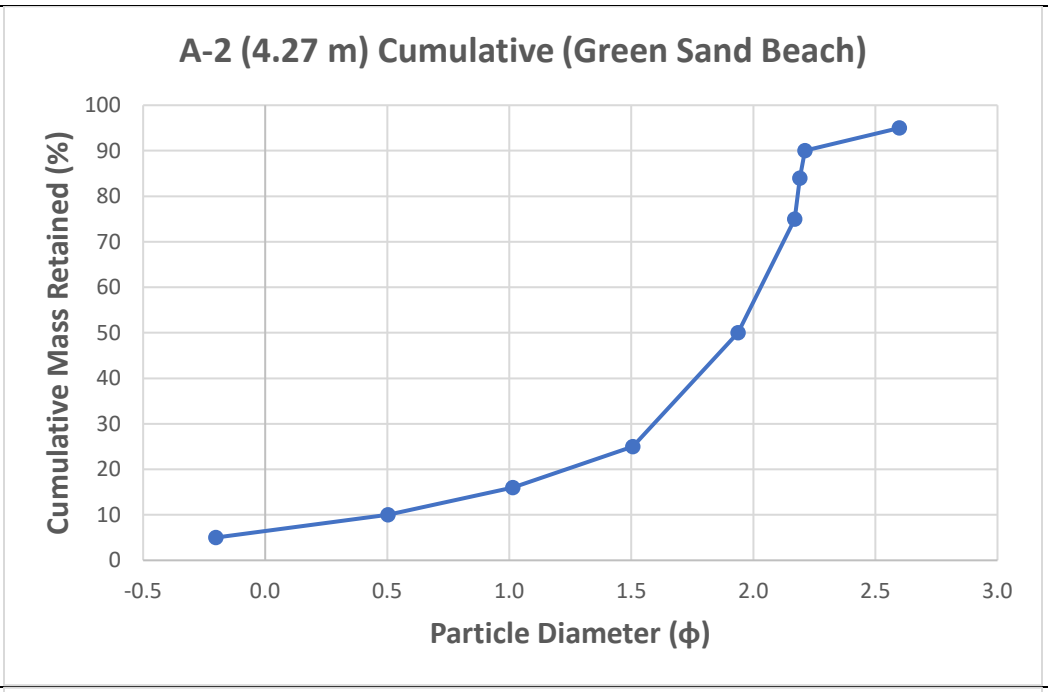
A-2 (4.27 m) Cumulative (Green Sand Beach)
Cumulative Mass Retained (%)
100
90
80
70
60
50
40
30
20
10
0
-0.5
0.0
0.5
1.0
1.5
2.0
2.5
3.0
Particle Diameter (ϕ)

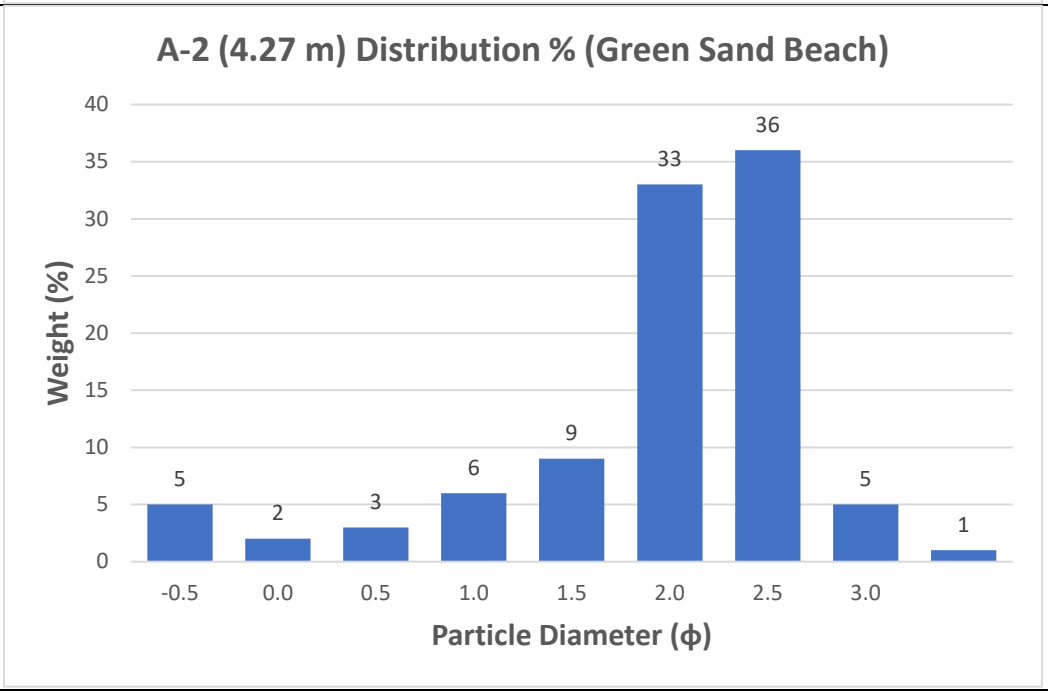
A-2 (4.27 m) Distribution % (Green Sand Beach)
Weight (%)
40
35
30
25
20
15
10
5
0
5
2
3
6
9
33
36
5
1
-0.5
0.0
0.5
1.0
1.5
2.0
2.5
3.0
Particle Diameter (ϕ)

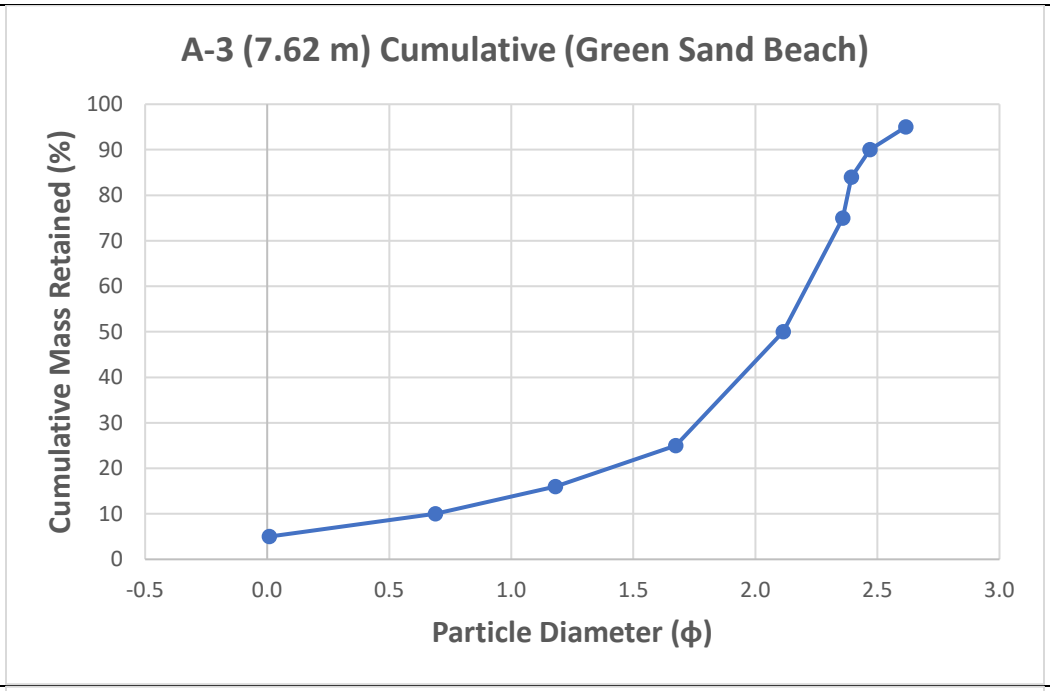
A-3 (7.62 m) Cumulative (Green Sand Beach)
Cumulative Mass Retained (%)
100
90
80
70
60
50
40
30
20
10
0
-0.5
0.0
0.5
1.0
1.5
2.0
2.5
3.0
Particle Diameter (ϕ)

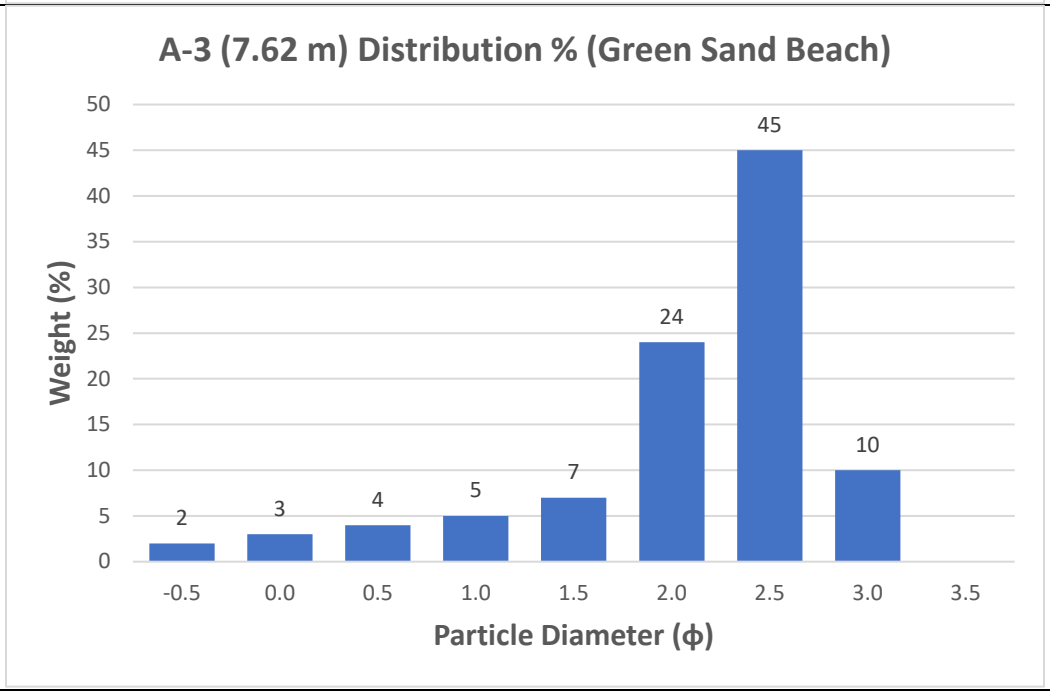
A-3 (7.62 m) Distribution % (Green Sand Beach)
Weight (%)
50
45
40
35
30
25
20
15
10
5
0
2
3
4
5
7
24
45
10
-0.5
0.0
0.5
1.0
1.5
2.0
2.5
3.0
3.5
Particle Diameter (ϕ)

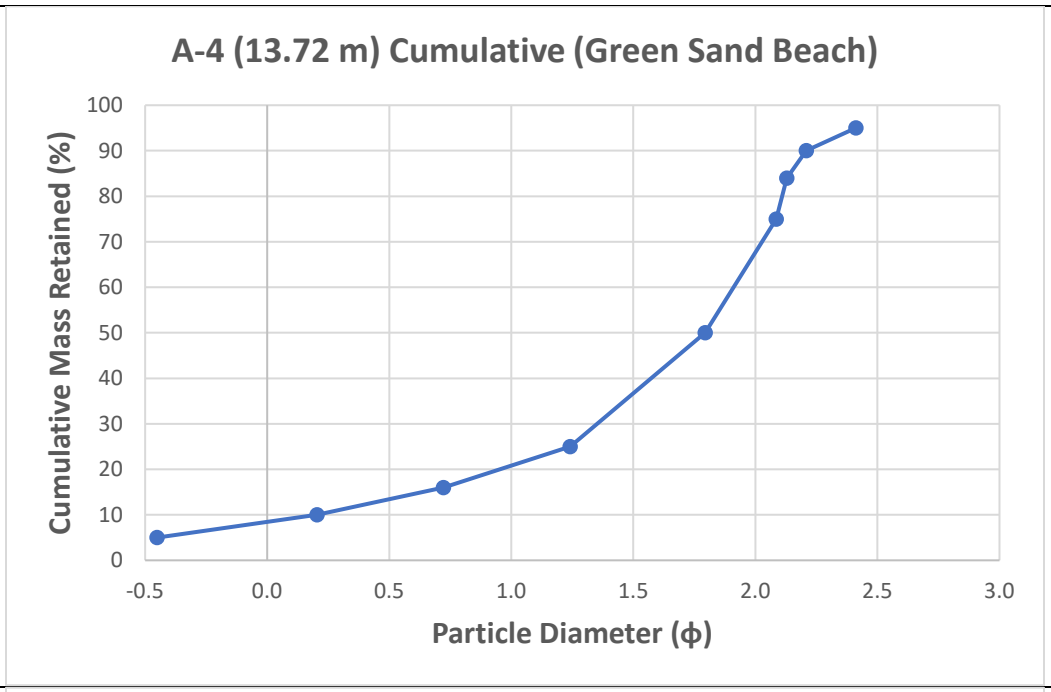
A-4 (13.72 m) Cumulative (Green Sand Beach)
Cumulative Mass Retained (%)
100
90
80
70
60
50
40
30
20
10
0
-0.5
0.0
0.5
1.0
1.5
2.0
2.5
3.0
Particle Diameter (ϕ)

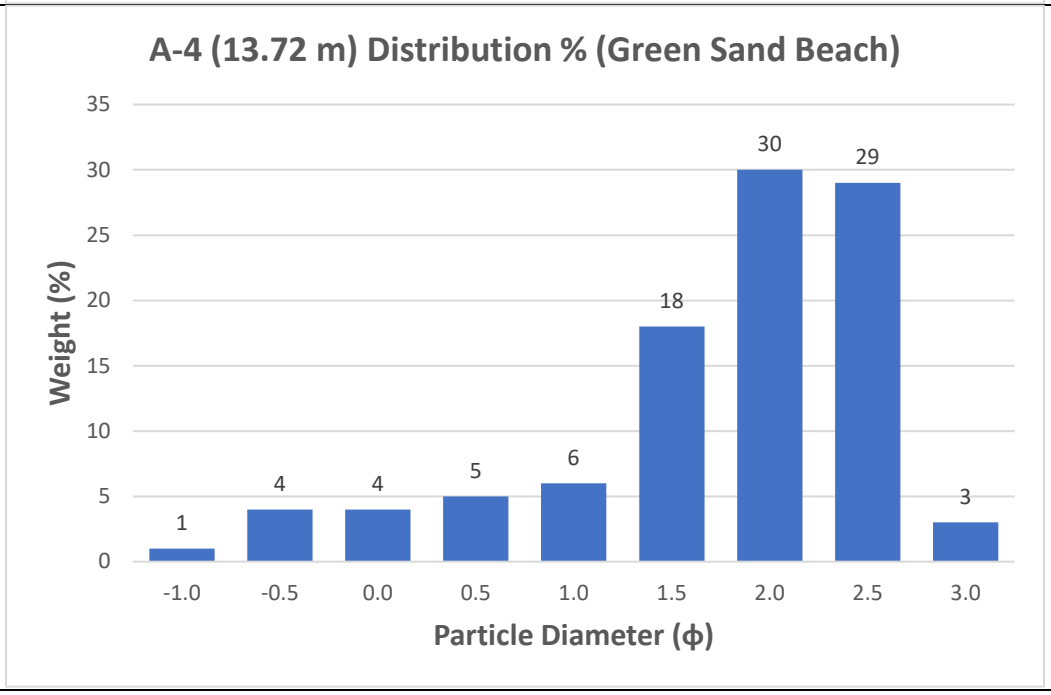
A-4 (13.72 m) Distribution % (Green Sand Beach)
Weight (%)
35
30
25
20
15
10
5
0
1
4
4
5
6
18
30
29
3
-1.0
-0.5
0.0
0.5
1.0
1.5
2.0
2.5
3.0
Particle Diameter (ϕ)

Beach Name: Miloli'i Beach

Date: 10/23/2020 **Time:** 11:50 AM

Location/ Transect	Survey #	Distance from Water (m)	Slope in Degrees	"x" used	Calculated mm percentile								
					5	10	16	25	50	75	84	90	95
A	1	1.524	-6	5.2	1.481814	1.467166	1.448739	1.418871	1.317012	1.160935	1.071743	0.986655	0.875694
	2	3.3528	-9	5.2	1.832115	1.813699	1.790589	1.753362	1.627818	1.437012	1.32825	1.223982	1.08644
	3	3.96	-12	5.3	1.710474	1.694166	1.673607	1.640329	1.526327	1.351752	1.252373	1.157642	1.032834

Calculated ϕ percentiles with corrections

5	10	16	25	50	75	84	90	95
-0.915	-0.885	-0.800	-0.707	-0.417	-0.187	-0.077	0.015	0.126
-1.408	-1.374	-1.256	-1.134	-0.738	-0.455	-0.317	-0.219	-0.079
-1.248	-1.217	-1.111	-1.000	-0.641	-0.378	-0.251	-0.158	-0.031

Moments

Mean	Standard Deviation	*Descriptor*	Skewness	*Descriptor*	Kurtosis	*Descriptor*
-0.431	0.338	Well Sorted	-0.008	Symmetrical	0.821	Platykurtic
-0.771	0.436	Well Sorted	-0.056	Symmetrical	0.802	Platykurtic
-0.668	0.399	Well Sorted	-0.046	Symmetrical	0.803	Platykurtic

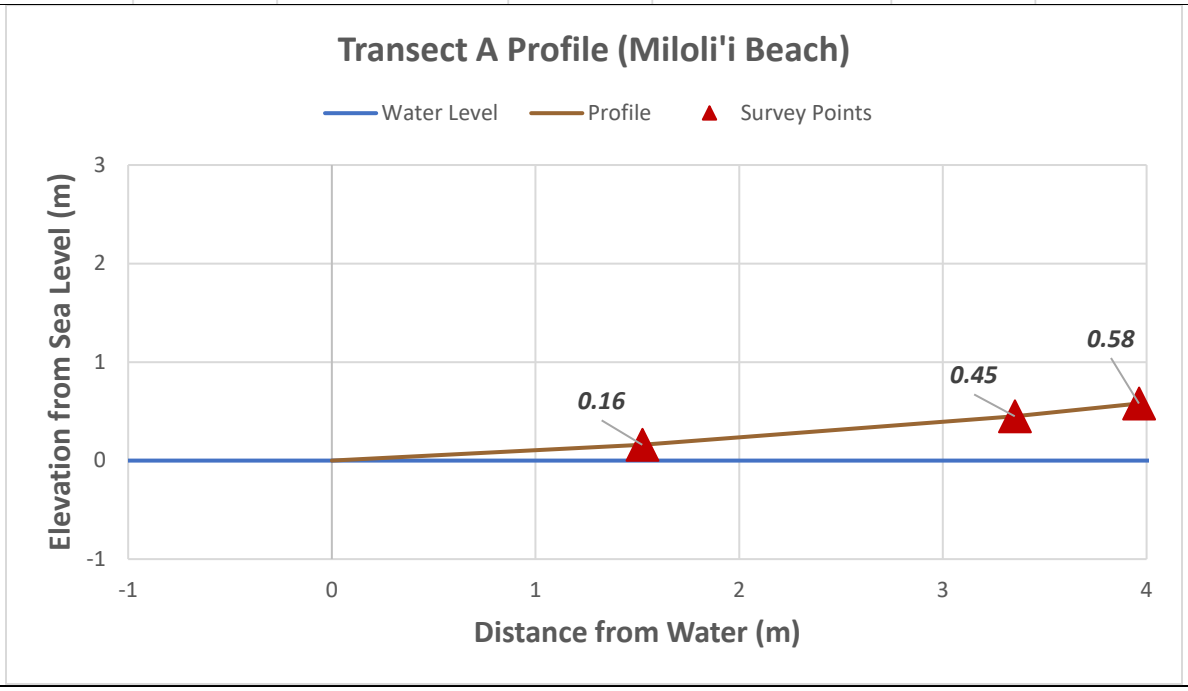

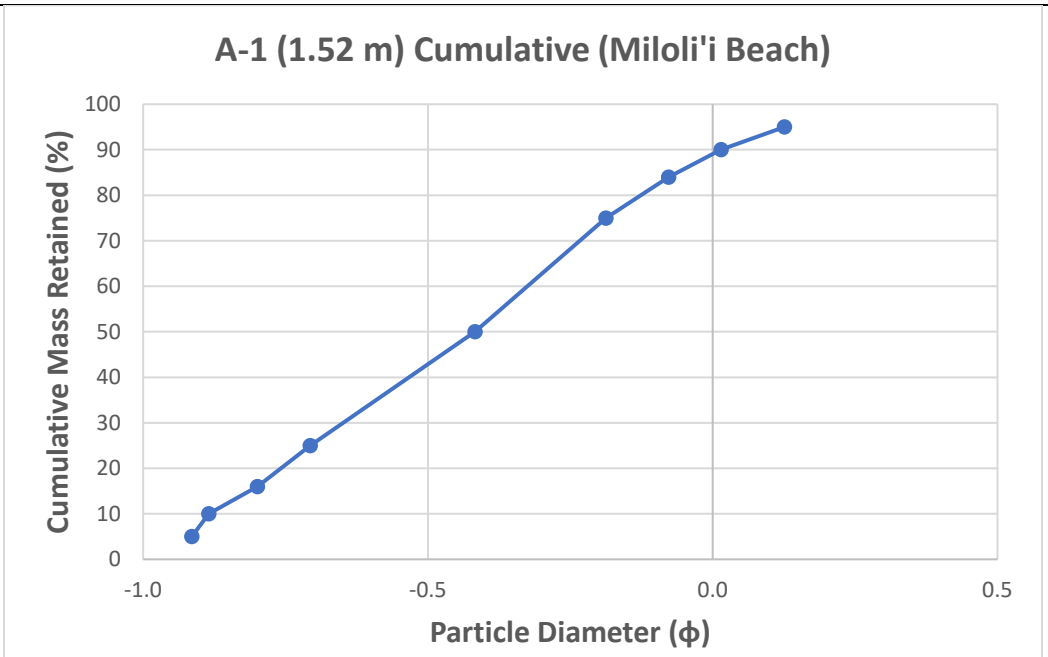
A-1 (1.52 m) Cumulative (Miloli'i Beach)
Cumulative Mass Retained (%)
100
90
80
70
60
50
40
30
20
10
0
-1.0
-0.5
0.0
0.5
Particle Diameter (ϕ)

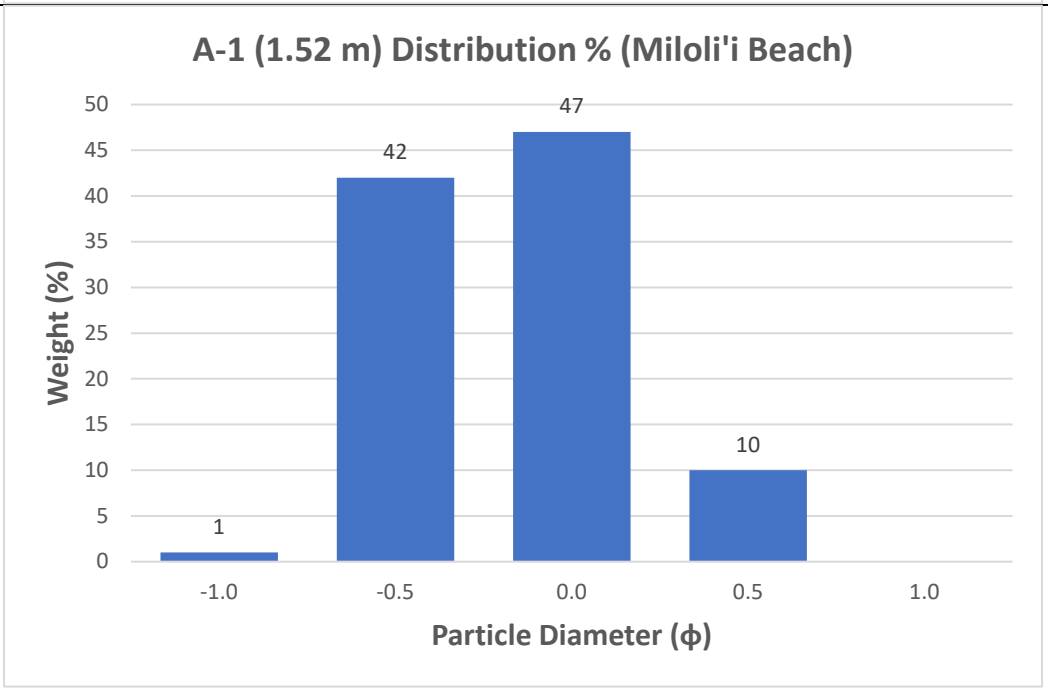
A-1 (1.52 m) Distribution % (Miloli'i Beach)
Weight (%)
50
45
40
35
30
25
20
15
10
5
0
1
42
47
10
-1.0
-0.5
0.0
0.5
1.0
Particle Diameter (ϕ)

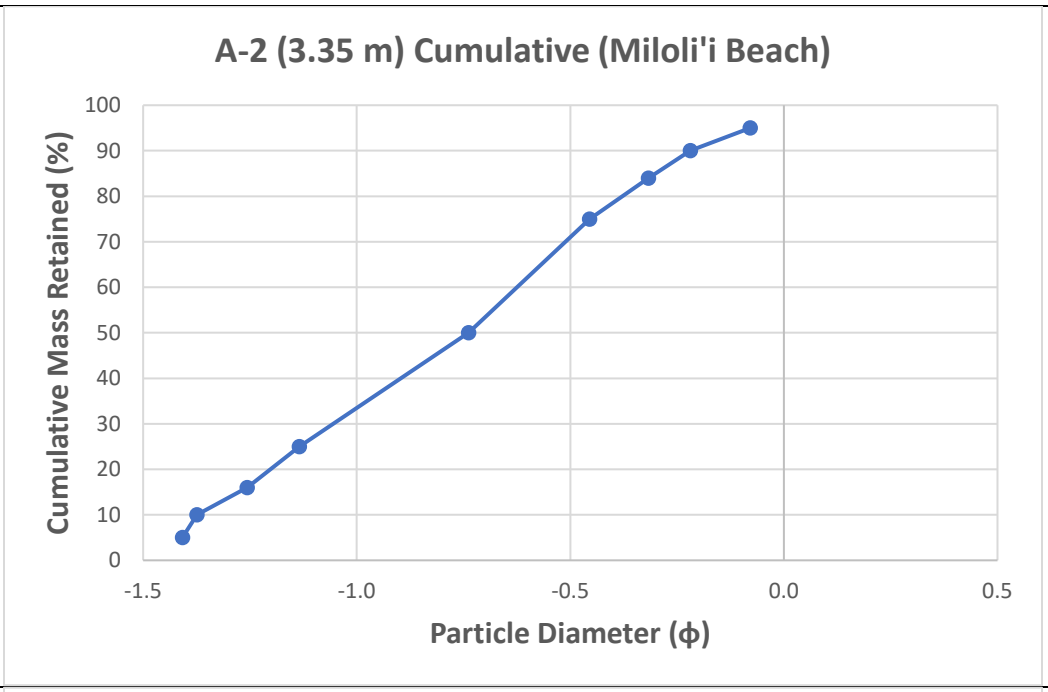
A-2 (3.35 m) Cumulative (Miloli'i Beach)
Cumulative Mass Retained (%)
100
90
80
70
60
50
40
30
20
10
0
-1.5
-1.0
-0.5
0.0
0.5
Particle Diameter (ϕ)

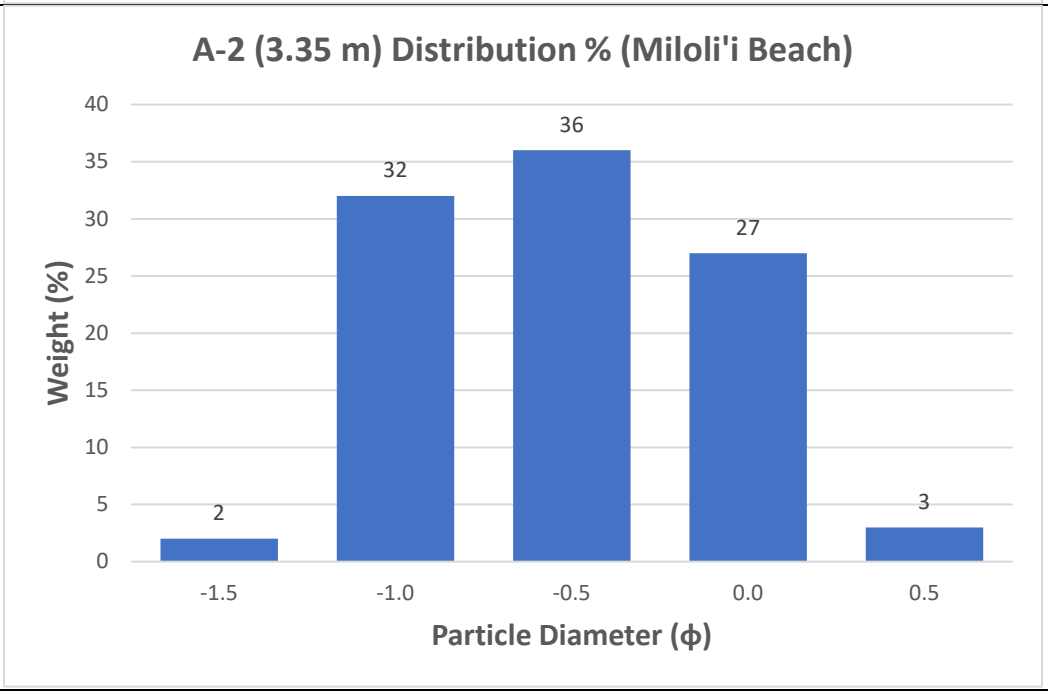
A-2 (3.35 m) Distribution % (Miloli'i Beach)
Weight (%)
40
35
30
25
20
15
10
5
0
2
32
36
27
3
-1.5
-1.0
-0.5
0.0
0.5
Particle Diameter (ϕ)

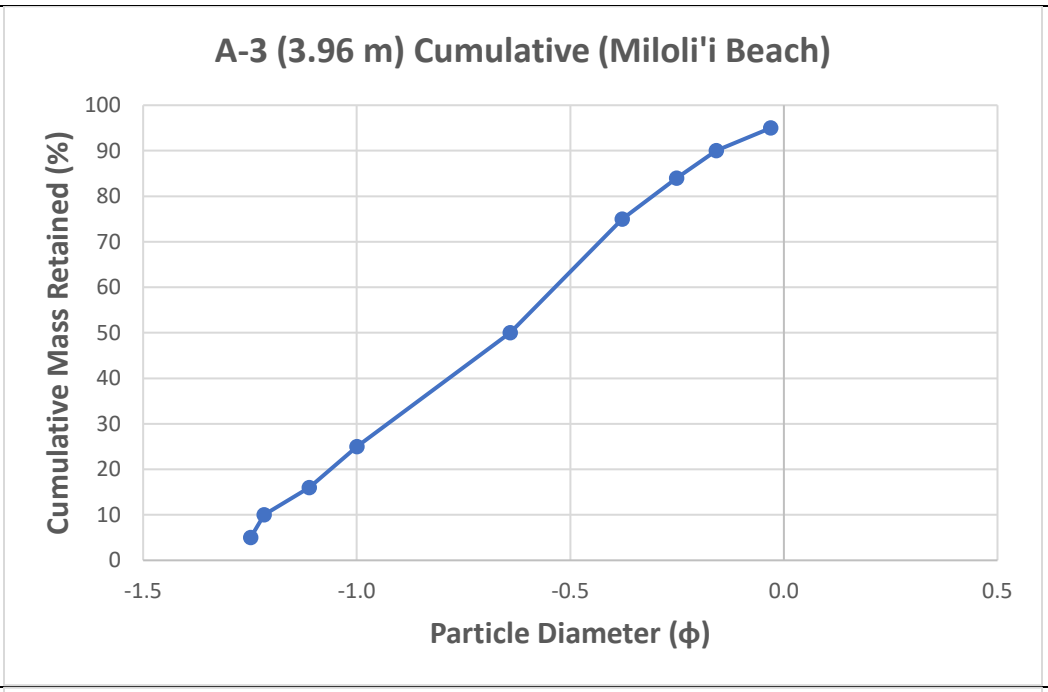
A-3 (3.96 m) Cumulative (Miloli'i Beach)
Cumulative Mass Retained (%)
100
90
80
70
60
50
40
30
20
10
0
-1.5
-1.0
-0.5
0.0
0.5
Particle Diameter (ϕ)

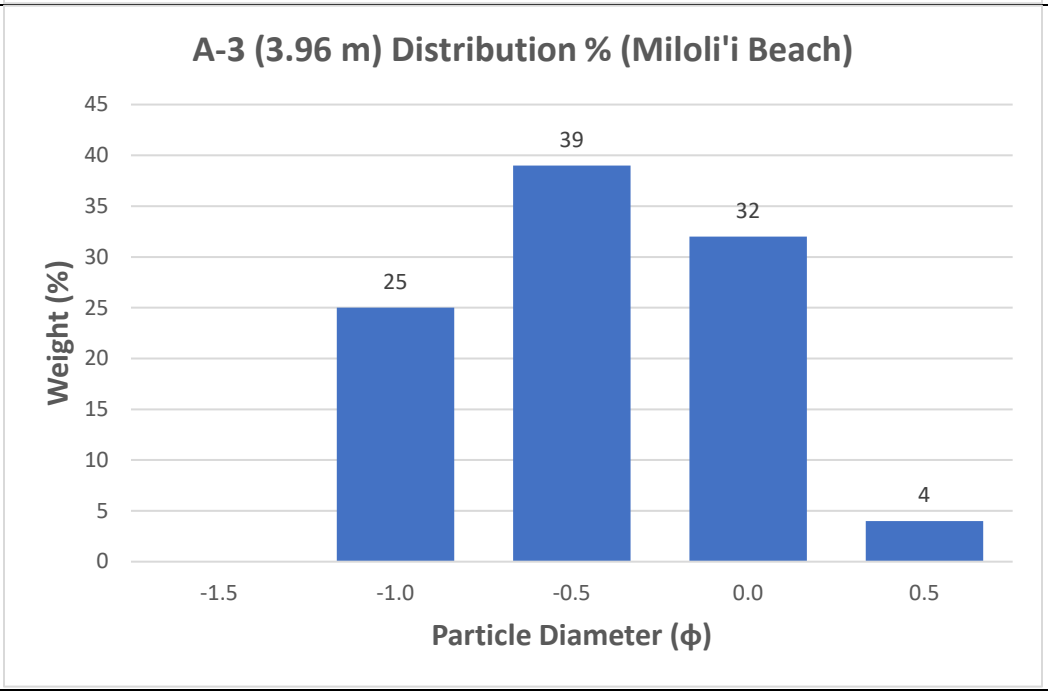
A-3 (3.96 m) Distribution % (Miloli'i Beach)
Weight (%)
45
40
35
30
25
20
15
10
5
0
25
39
32
4
-1.5
-1.0
-0.5
0.0
0.5
Particle Diameter (ϕ)

Beach Name:	Pebble Beach

Date: 10/23/2020 **Time:** 12:40 PM

Location/ Transect	Survey #	Distance from Water (m)	Slope in Degrees	"x" used	Calculated mm percentile								
					5	10	16	25	50	75	84	90	95
A	1	1.2192	-17	4	3.824414	3.783148	3.730866	3.646011	3.356024	2.914326	2.662419	2.420516	2.106553
	2	2.1336	-16	4	4.186698	4.139624	4.080348	3.984953	3.664233	3.177843	2.895299	2.621275	2.266428
	3	3.05	-15	4	4.368185	4.318488	4.255918	4.155214	3.816446	3.307108	3.015018	2.731626	2.356067
	4	4.88	-6	4	6.554729	6.482639	6.391561	6.244165	5.740454	4.962454	4.51891	4.09699	3.543527

Calculated ϕ percentiles with corrections								
5	10	16	25	50	75	84	90	95
-3.120	-3.071	-2.840	-2.613	-1.834	-1.343	-1.093	-0.956	-0.707
-3.330	-3.279	-3.033	-2.792	-1.967	-1.451	-1.187	-1.043	-0.777
-3.429	-3.377	-3.124	-2.877	-2.029	-1.501	-1.232	-1.087	-0.814
-4.373	-4.315	-4.001	-3.700	-2.647	-2.011	-1.684	-1.526	-1.201

Moments						
Mean	Standard Deviation	*Descriptor*	Skewness	*Descriptor*	Kurtosis	*Descriptor*
-1.922	0.802	Moderately Sorted	-0.109	Coarse Skewed	0.778	Platykurtic
-2.062	0.848	Moderately Sorted	-0.111	Coarse Skewed	0.780	Platykurtic
-2.128	0.869	Moderately Sorted	-0.114	Coarse Skewed	0.779	Platykurtic
-2.777	1.060	Poorly Sorted	-0.128	Coarse Skewed	0.770	Platykurtic

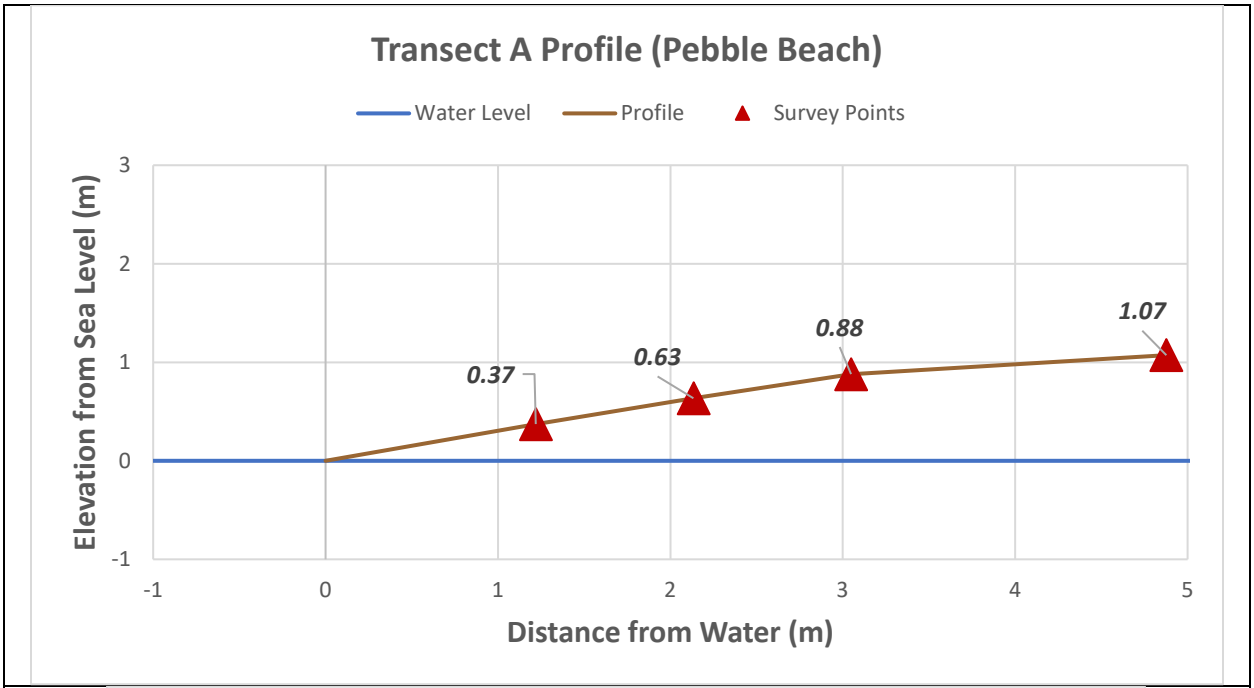
Transect A Profile (Pebble Beach)
Water Level
Profile
Survey Points
Elevation from Sea Level (m)
Distance from Water (m)
0.37
0.63
0.88
1.07

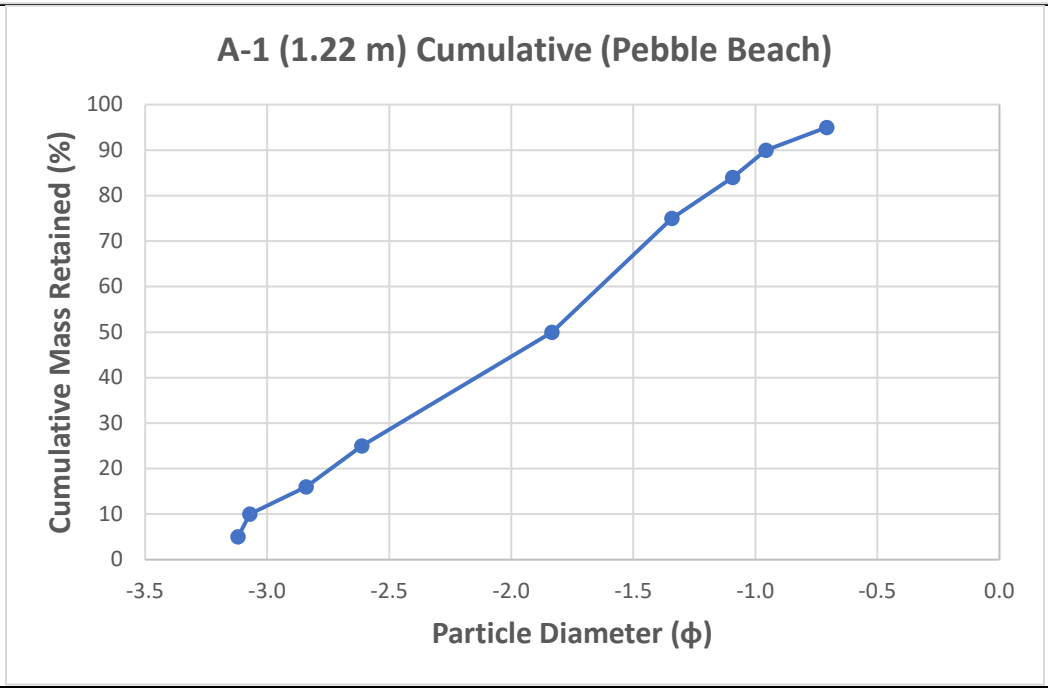
A-1 (1.22 m) Cumulative (Pebble Beach)
Cumulative Mass Retained (%)
Particle Diameter (ϕ)

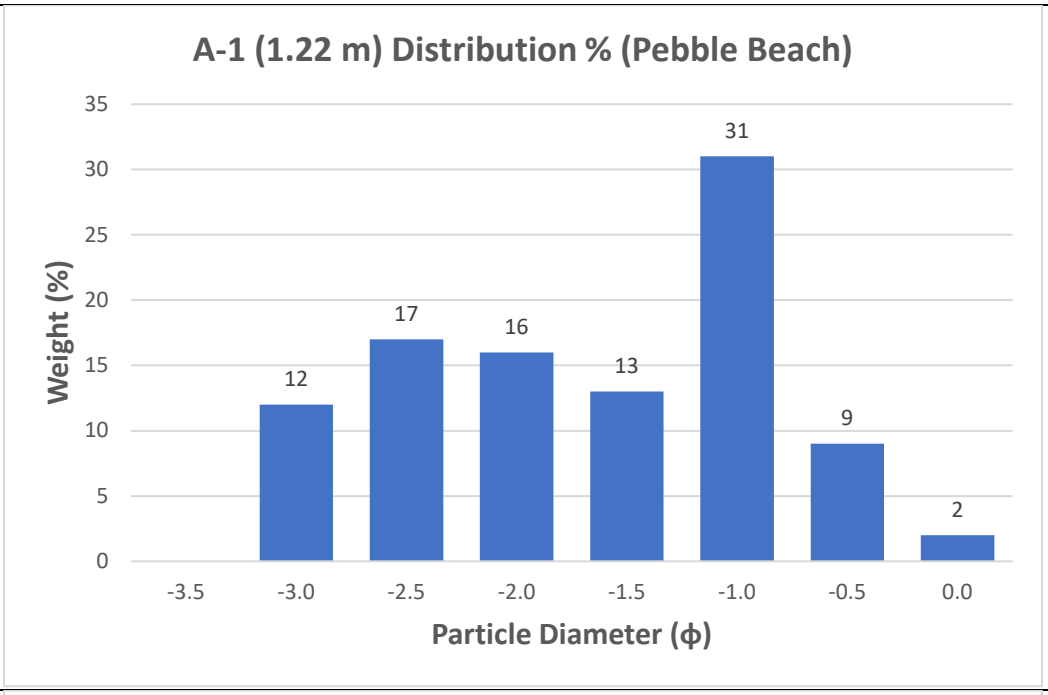
A-1 (1.22 m) Distribution % (Pebble Beach)
Weight (%)
35
30
25
20
15
10
5
0
12
17
16
13
31
9
2
-3.5
-3.0
-2.5
-2.0
-1.5
-1.0
-0.5
0.0
Particle Diameter (ϕ)

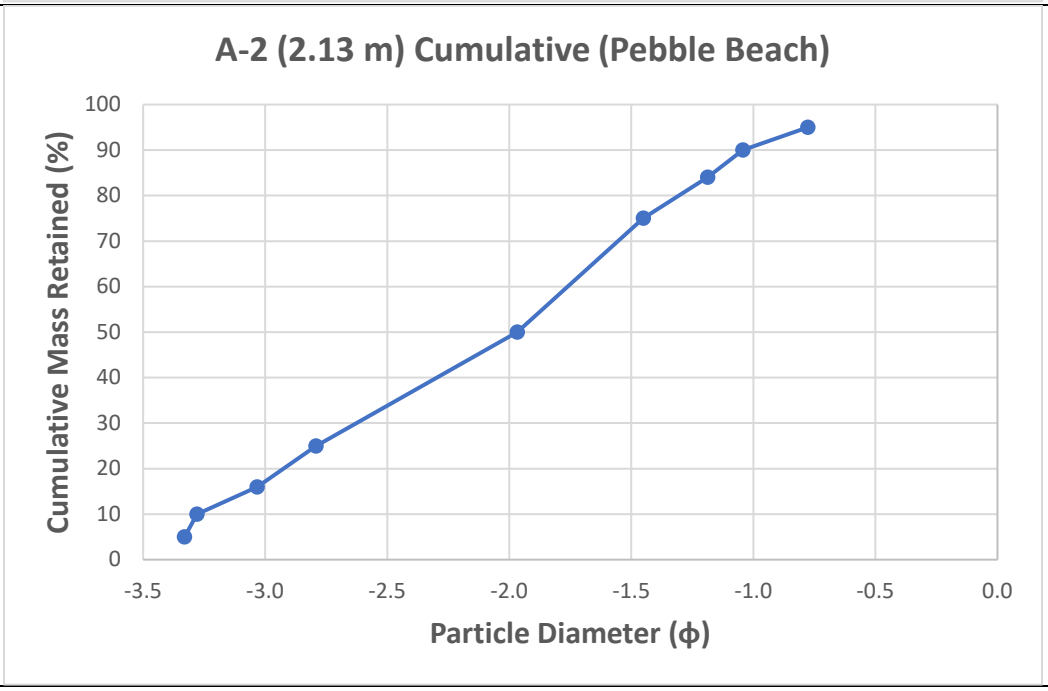
A-2 (2.13 m) Cumulative (Pebble Beach)
Cumulative Mass Retained (%)
100
90
80
70
60
50
40
30
20
10
0
-3.5
-3.0
-2.5
-2.0
-1.5
-1.0
-0.5
0.0
Particle Diameter (ϕ)

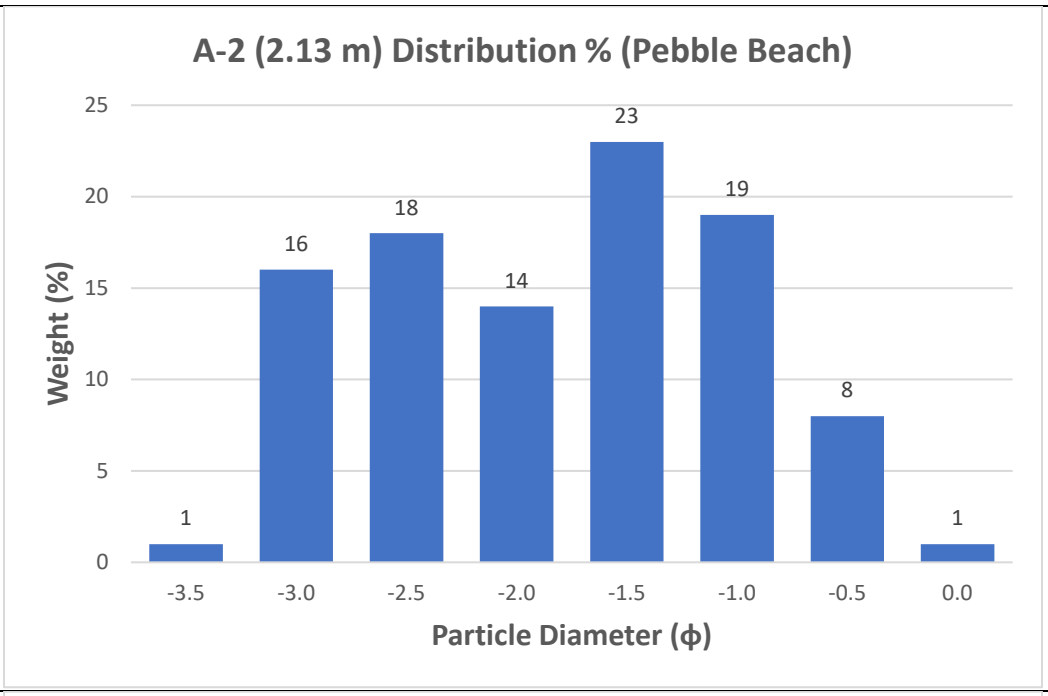
A-2 (2.13 m) Distribution % (Pebble Beach)
Weight (%)
25
20
15
10
5
0
1
16
18
14
23
19
8
1
-3.5
-3.0
-2.5
-2.0
-1.5
-1.0
-0.5
0.0
Particle Diameter (ϕ)

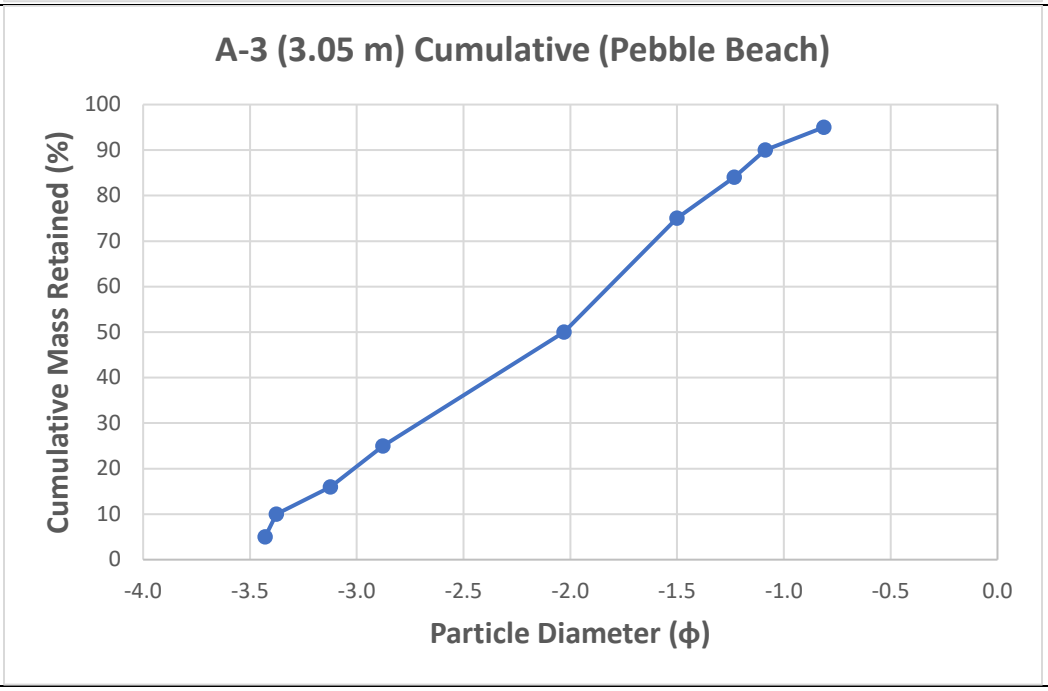
A-3 (3.05 m) Cumulative (Pebble Beach)
Cumulative Mass Retained (%)
100
90
80
70
60
50
40
30
20
10
0
-4.0
-3.5
-3.0
-2.5
-2.0
-1.5
-1.0
-0.5
0.0
Particle Diameter (ϕ)

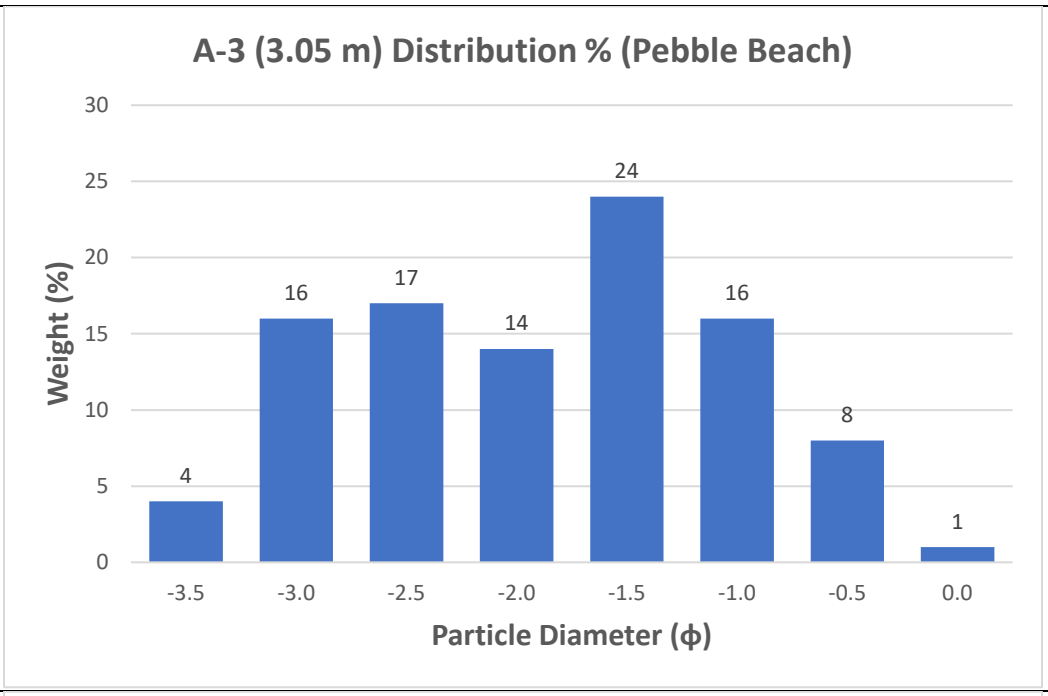
A-3 (3.05 m) Distribution % (Pebble Beach)
Weight (%)
30
25
20
15
10
5
0
4
16
17
14
24
16
8
1
-3.5
-3.0
-2.5
-2.0
-1.5
-1.0
-0.5
0.0
Particle Diameter (ϕ)

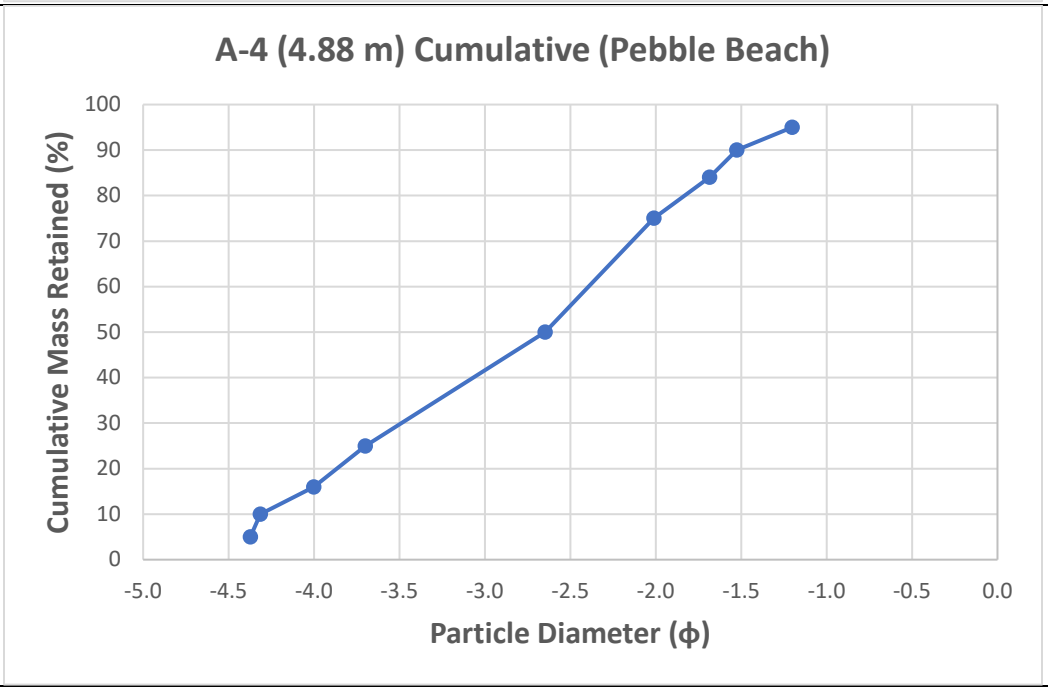
A-4 (4.88 m) Cumulative (Pebble Beach)
Cumulative Mass Retained (%)
100
90
80
70
60
50
40
30
20
10
0
-5.0
-4.5
-4.0
-3.5
-3.0
-2.5
-2.0
-1.5
-1.0
-0.5
0.0
Particle Diameter (ϕ)

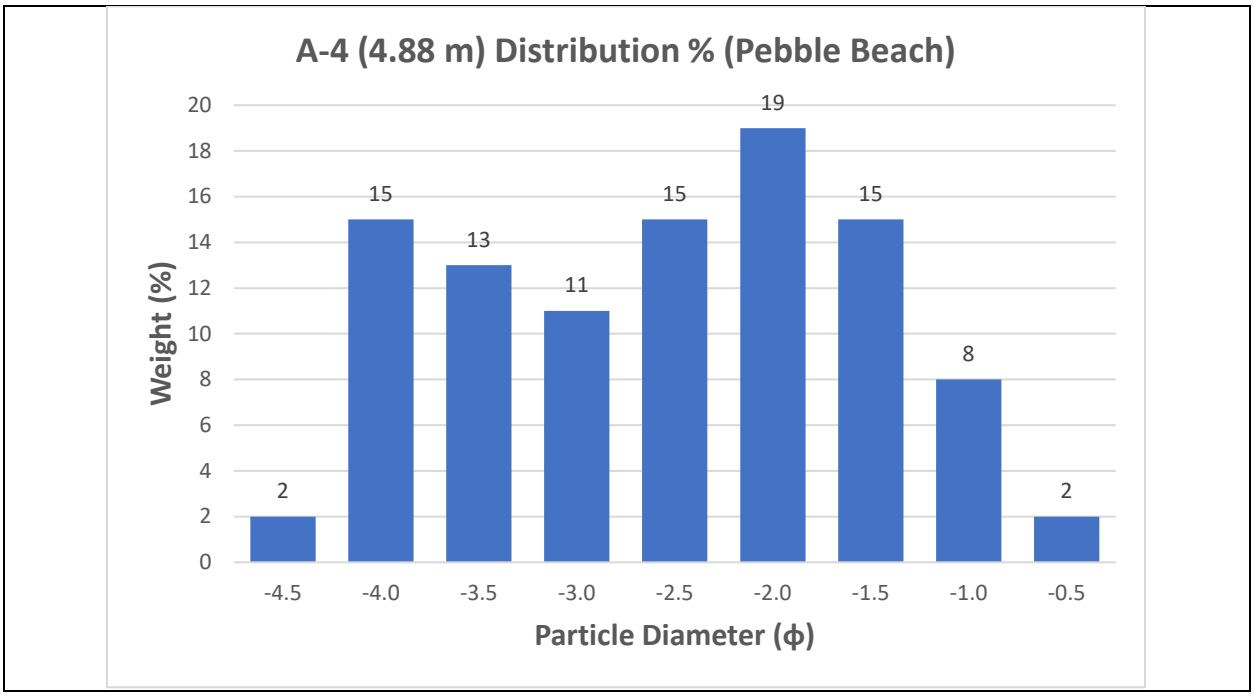
A-4 (4.88 m) Distribution % (Pebble Beach)
Weight (%)
20
18
16
14
12
10
8
6
4
2
0
2
15
13
11
15
19
15
8
2
-4.5
-4.0
-3.5
-3.0
-2.5
-2.0
-1.5
-1.0
-0.5
Particle Diameter (ϕ)

Beach Name: Ho'okena Beach

Date: 10/23/2020 **Time:** 1:15 PM

Location/ Transect	Survey #	Distance from Water (m)	Slope in Degrees	"x" used	Calculated mm percentile								
					5	10	16	25	50	75	84	90	95
A	1	1.2192	-9	0.5	1.710965	1.556693	1.390921	1.175761	0.741023	0.442845	0.345169	0.276297	0.208773
	2	2.7432	-11	0.5	1.768156	1.618784	1.455006	1.243115	0.813489	0.492336	0.378802	0.296786	0.216194
	3	4.57	-24	0.5	1.590118	1.455284	1.311968	1.126432	0.722159	0.428538	0.332414	0.26449	0.198178

Calculated ϕ percentiles with corrections								
5	10	16	25	50	75	84	90	95
-1.249	-1.022	-0.712	-0.327	0.454	1.022	1.188	1.392	1.487
-1.325	-1.112	-0.809	-0.440	0.313	0.889	1.084	1.314	1.454
-1.079	-0.866	-0.586	-0.240	0.493	1.064	1.230	1.439	1.537

Moments						
Mean	Standard Deviation	*Descriptor*	Skewness	*Descriptor*	Kurtosis	*Descriptor*
0.310	0.889	Moderately Sorted	-0.236	Coarse Skewed	0.831	Platykurtic
0.196	0.894	Moderately Sorted	-0.182	Coarse Skewed	0.857	Platykurtic
0.379	0.850	Moderately Sorted	-0.195	Coarse Skewed	0.822	Platykurtic

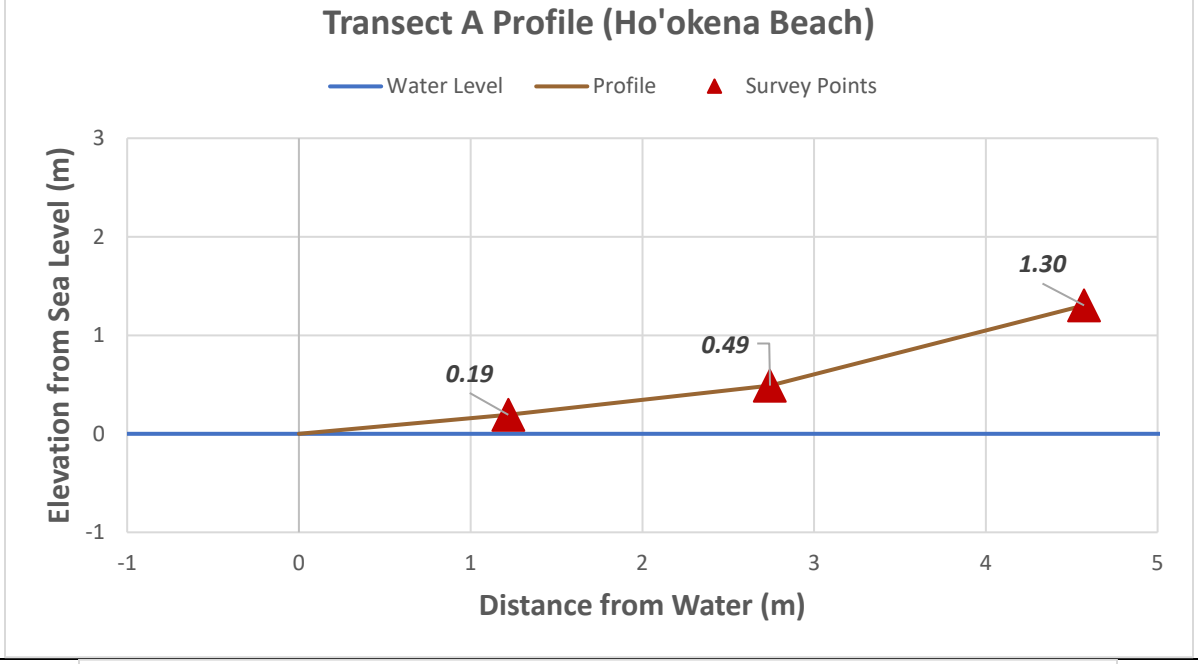
Transect A Profile (Ho'okena Beach)
Water Level
Profile
Survey Points
Elevation from Sea Level (m)
3
2
1
0
-1
-1
0
1
2
3
4
5
0.19
0.49
1.30
Distance from Water (m)

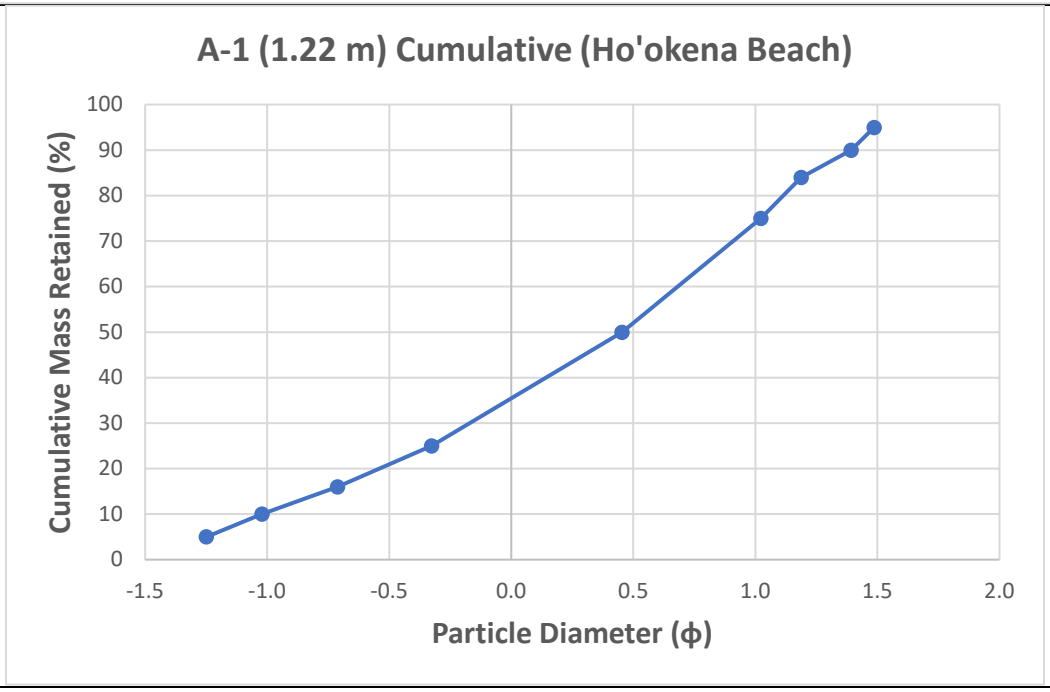
A-1 (1.22 m) Cumulative (Ho'okena Beach)
Cumulative Mass Retained (%)
100
90
80
70
60
50
40
30
20
10
0
-1.5
-1.0
-0.5
0.0
0.5
1.0
1.5
2.0
Particle Diameter (ϕ)

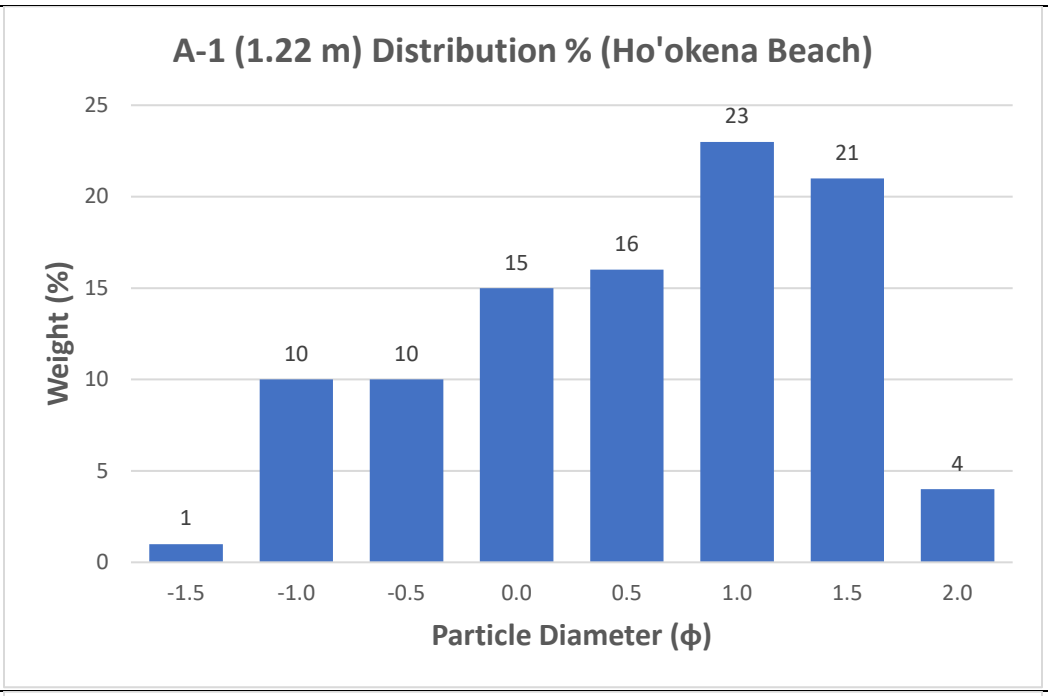
A-1 (1.22 m) Distribution % (Ho'okena Beach)
Weight (%)
25
20
15
10
5
0
1
10
10
15
16
23
21
4
-1.5
-1.0
-0.5
0.0
0.5
1.0
1.5
2.0
Particle Diameter (ϕ)

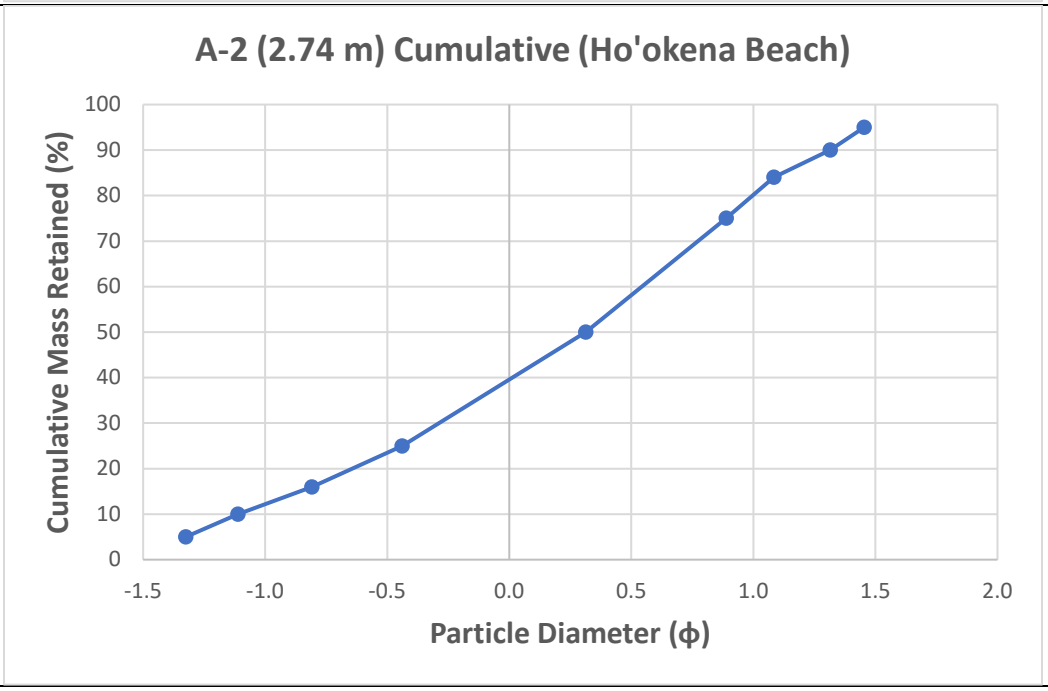
A-2 (2.74 m) Cumulative (Ho'okena Beach)
Cumulative Mass Retained (%)
100
90
80
70
60
50
40
30
20
10
0
-1.5
-1.0
-0.5
0.0
0.5
1.0
1.5
2.0
Particle Diameter (ϕ)

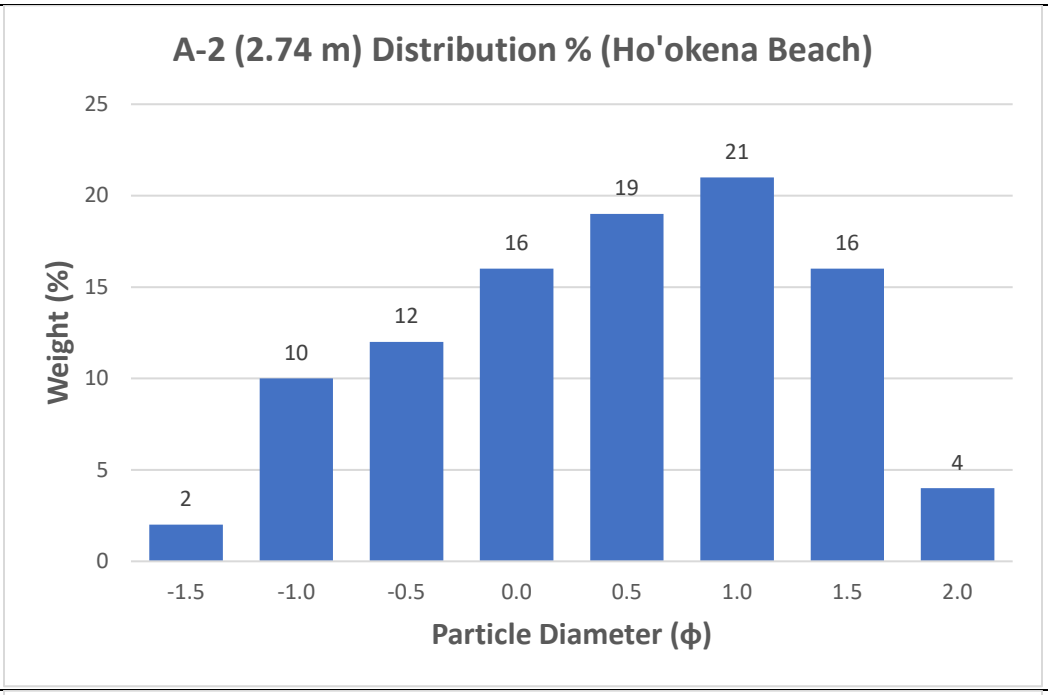
A-2 (2.74 m) Distribution % (Ho'okena Beach)
Weight (%)
25
20
15
10
5
0
2
10
12
16
19
21
16
4
-1.5
-1.0
-0.5
0.0
0.5
1.0
1.5
2.0
Particle Diameter (ϕ)

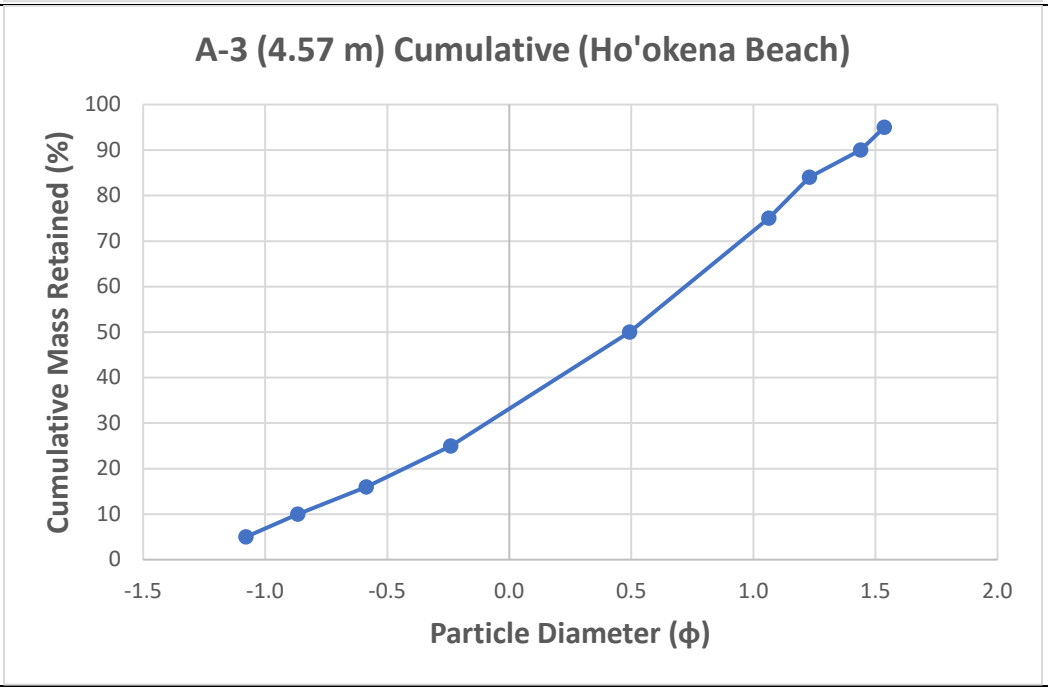
A-3 (4.57 m) Cumulative (Ho'okena Beach)
Cumulative Mass Retained (%)
100
90
80
70
60
50
40
30
20
10
0
-1.5
-1.0
-0.5
0.0
0.5
1.0
1.5
2.0
Particle Diameter (ϕ)

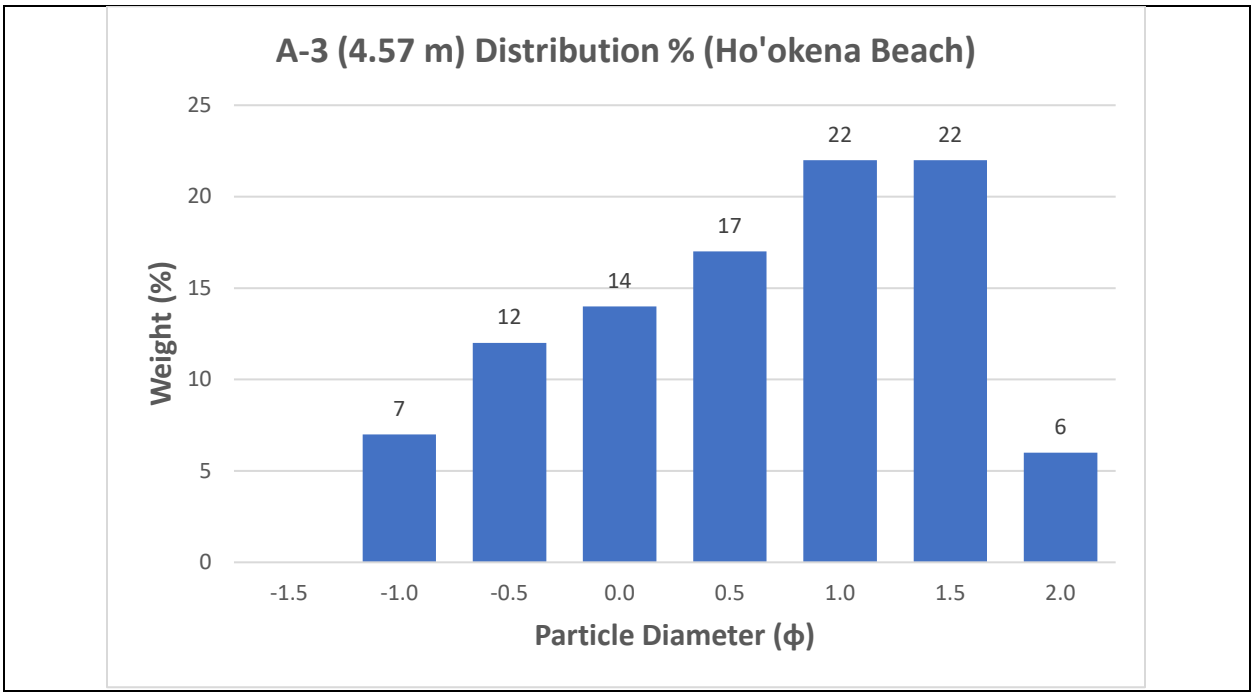
A-3 (4.57 m) Distribution % (Ho'okena Beach)
Weight (%)
25
20
15
10
5
0
7
12
14
17
22
22
6
-1.5
-1.0
-0.5
0.0
0.5
1.0
1.5
2.0
Particle Diameter (ϕ)

Beach Name: Kahalu'u Beach

Date: 10/23/2020 **Time:** 2:00 PM

Location/ Transect	Survey #	Distance from Water (m)	Slope in Degrees	"x" used	Calculated mm percentile								
					5	10	16	25	50	75	84	90	95
A	1	0.3048	-8	-0.5	1.69163	1.534435	1.367156	1.146257	0.64925	0.312085	0.222482	0.171644	0.133928
	2	1.2192	-4	-0.6	1.819172	1.621833	1.422091	1.175327	0.677009	0.33752	0.244239	0.18942	0.148358
	3	2.74	-5	-0.6	1.584272	1.414896	1.243661	1.030516	0.582847	0.287729	0.209559	0.164104	0.124416
	4	3.66	-4	-0.4	1.540455	1.416988	1.280888	1.097938	0.673626	0.336108	0.237737	0.180172	0.138037

Calculated ϕ percentiles with corrections

5	10	16	25	50	75	84	90	95
-1.223	-0.988	-0.675	-0.276	0.654	1.462	1.678	1.907	1.909
-1.392	-1.116	-0.759	-0.326	0.591	1.363	1.574	1.800	1.811
-1.070	-0.801	-0.470	-0.061	0.818	1.564	1.745	1.955	1.978
-1.005	-0.805	-0.534	-0.189	0.598	1.369	1.604	1.854	1.880

Moments

Mean	Standard Deviation	*Descriptor*	Skewness	*Descriptor*	Kurtosis	*Descriptor*
0.553	1.063	Poorly Sorted	-0.164	Coarse Skewed	0.739	Platykurtic
0.468	1.069	Poorly Sorted	-0.198	Coarse Skewed	0.777	Platykurtic
0.697	1.016	Poorly Sorted	-0.201	Coarse Skewed	0.769	Platykurtic
0.556	0.972	Moderately Sorted	-0.085	Symmetrical	0.759	Platykurtic

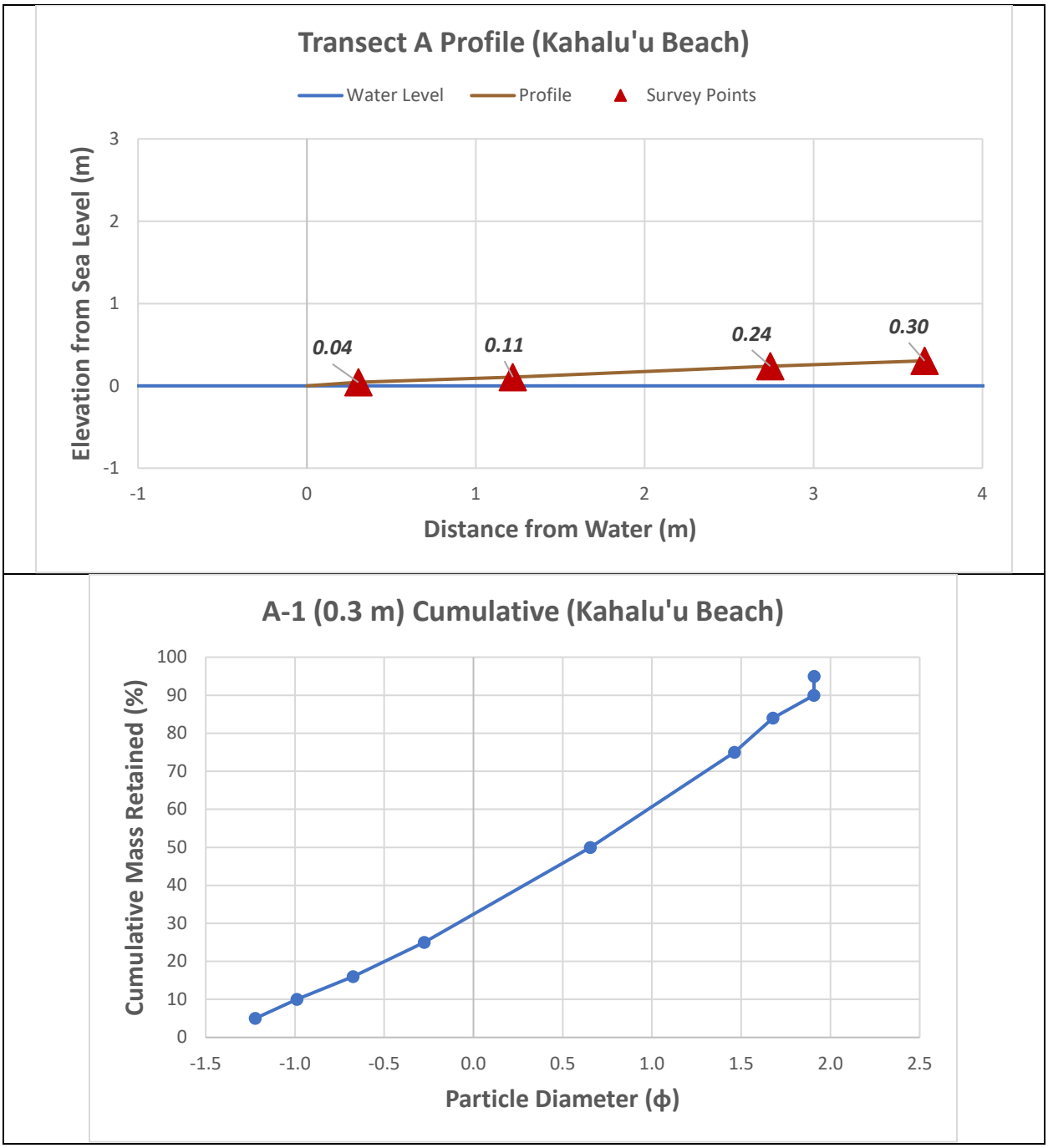
Transect A Profile (Kahalu'u Beach)
Water Level
Profile
Survey Points
Elevation from Sea Level (m)
3
2
1
0
-1
-1
0
1
2
3
4
0.04
0.11
0.24
0.30
Distance from Water (m)

A-1 (0.3 m) Cumulative (Kahalu'u Beach)
Cumulative Mass Retained (%)
100
90
80
70
60
50
40
30
20
10
0
-1.5
-1.0
-0.5
0.0
0.5
1.0
1.5
2.0
2.5
Particle Diameter (ϕ)

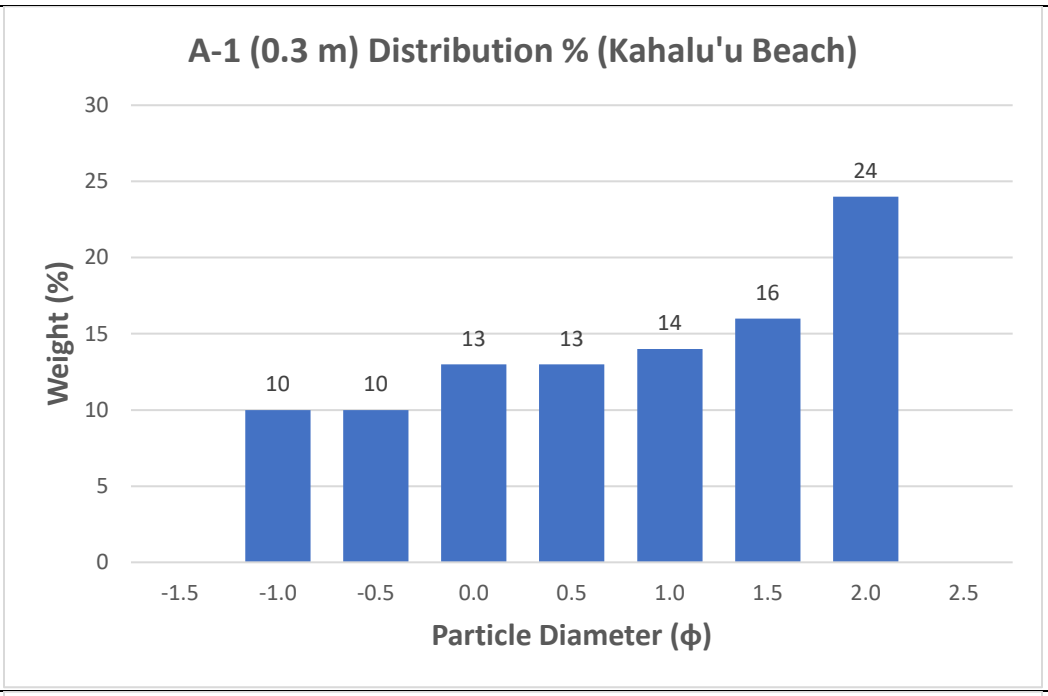
A-1 (0.3 m) Distribution % (Kahalu'u Beach)
Weight (%)
30
25
20
15
10
5
0
10
10
13
13
14
16
24
-1.5
-1.0
-0.5
0.0
0.5
1.0
1.5
2.0
2.5
Particle Diameter (ϕ)

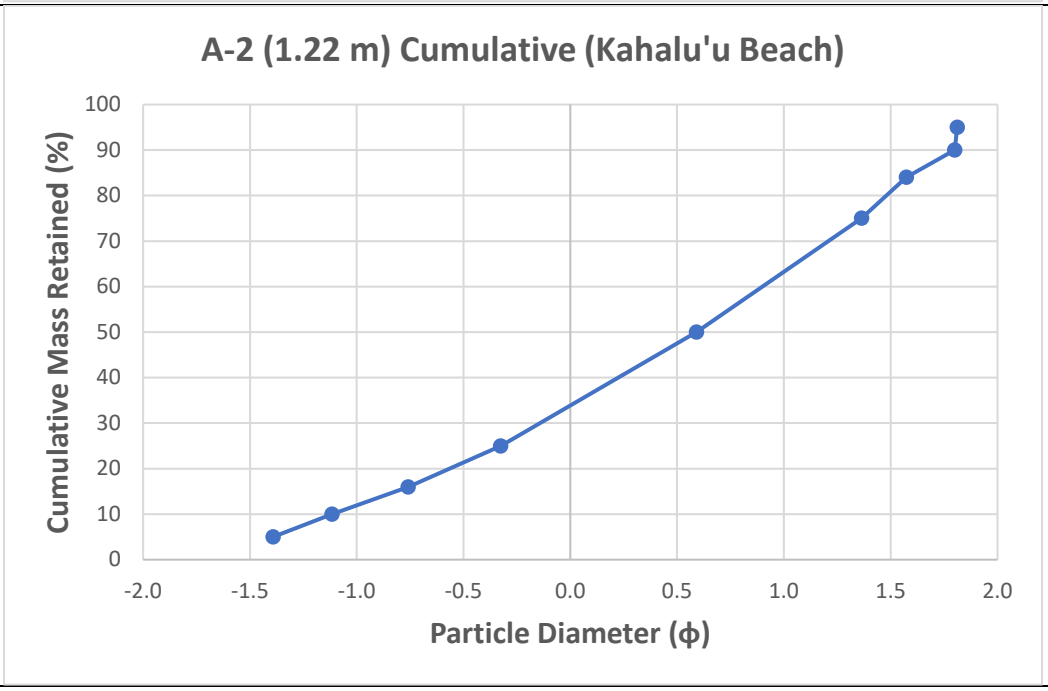
A-2 (1.22 m) Cumulative (Kahalu'u Beach)
Cumulative Mass Retained (%)
100
90
80
70
60
50
40
30
20
10
0
-2.0
-1.5
-1.0
-0.5
0.0
0.5
1.0
1.5
2.0
Particle Diameter (ϕ)

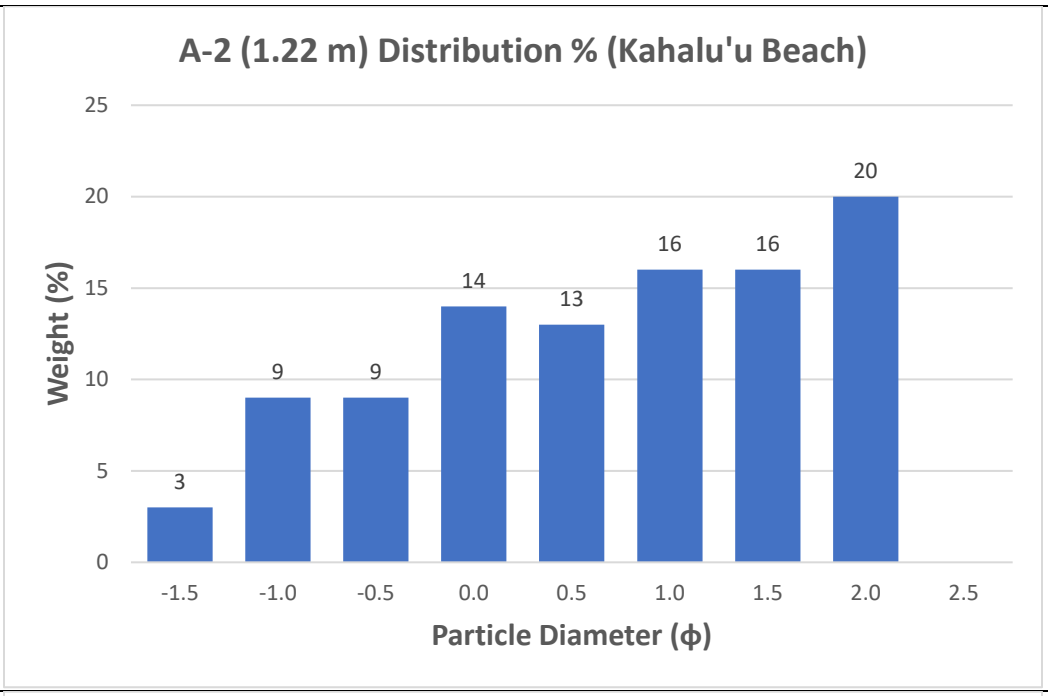
A-2 (1.22 m) Distribution % (Kahalu'u Beach)
Weight (%)
25
20
15
10
5
0
3
9
9
14
13
16
16
20
-1.5
-1.0
-0.5
0.0
0.5
1.0
1.5
2.0
2.5
Particle Diameter (ϕ)

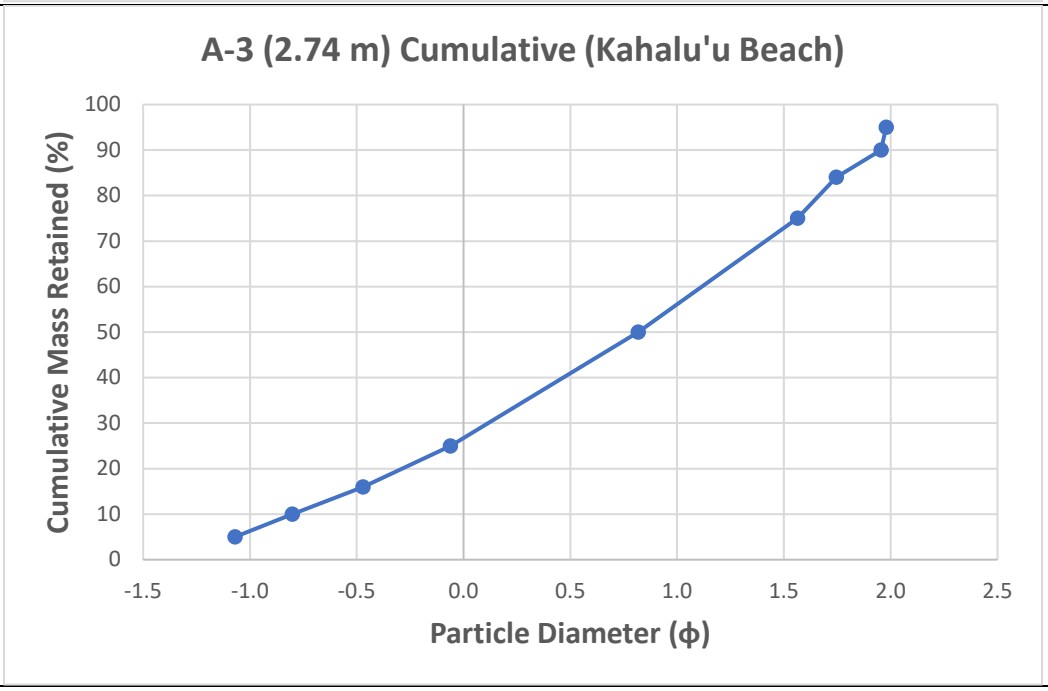
A-3 (2.74 m) Cumulative (Kahalu'u Beach)
Cumulative Mass Retained (%)
100
90
80
70
60
50
40
30
20
10
0
-1.5
-1.0
-0.5
0.0
0.5
1.0
1.5
2.0
2.5
Particle Diameter (ϕ)

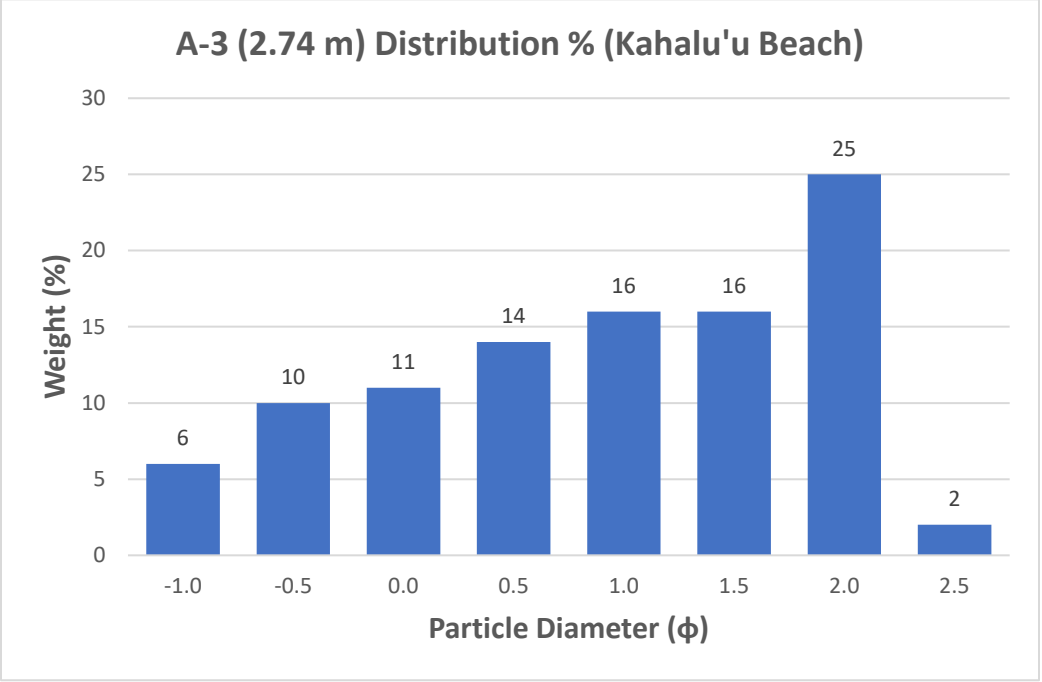
A-3 (2.74 m) Distribution % (Kahalu'u Beach)
Weight (%)
30
25
20
15
10
5
0
6
10
11
14
16
16
25
2
-1.0
-0.5
0.0
0.5
1.0
1.5
2.0
2.5
Particle Diameter (ϕ)

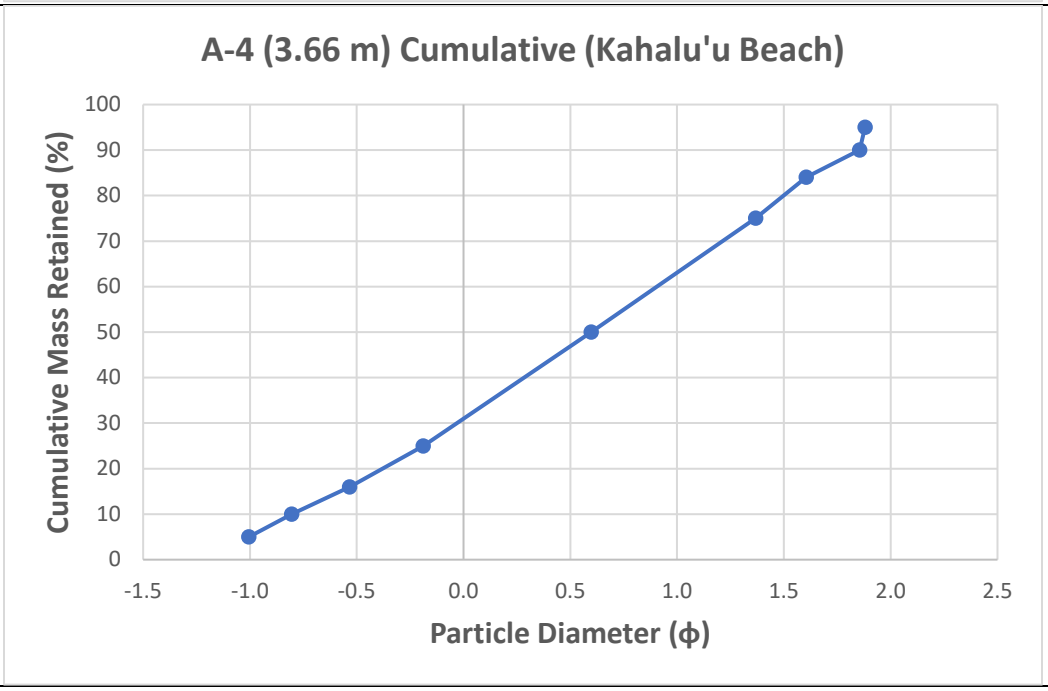
A-4 (3.66 m) Cumulative (Kahalu'u Beach)
Cumulative Mass Retained (%)
100
90
80
70
60
50
40
30
20
10
0
-1.5
-1.0
-0.5
0.0
0.5
1.0
1.5
2.0
2.5
Particle Diameter (ϕ)

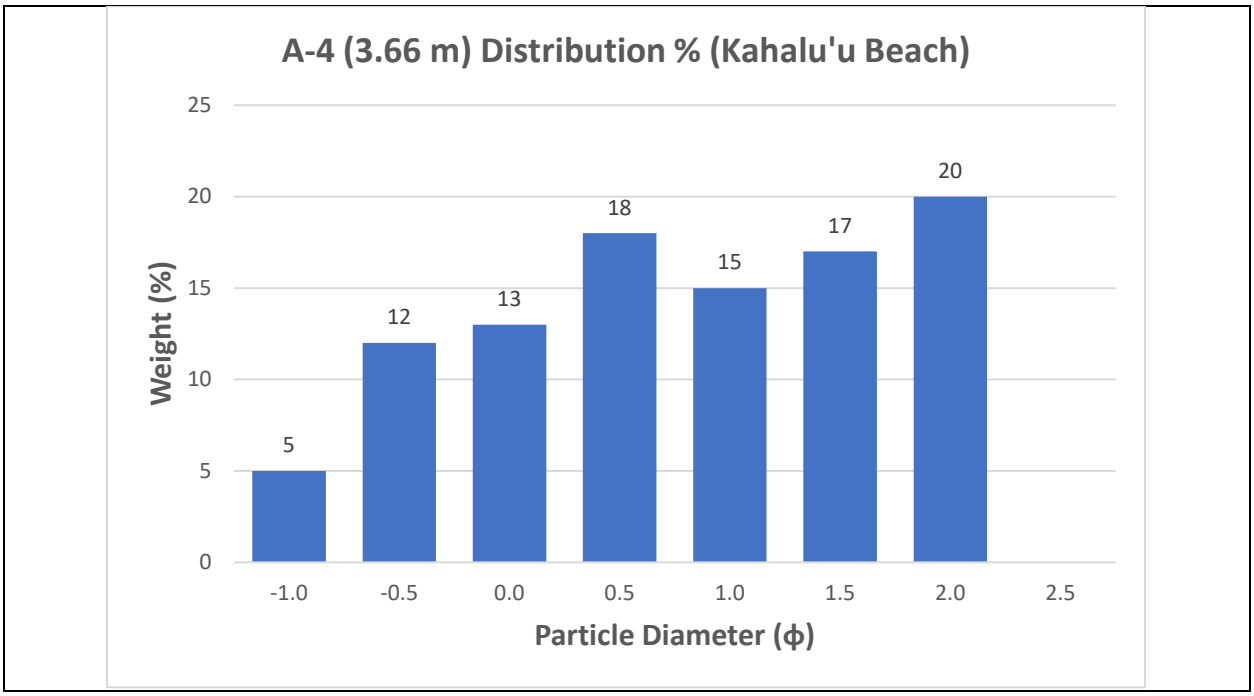
A-4 (3.66 m) Distribution % (Kahalu'u Beach)
Weight (%)
25
20
15
10
5
0
5
12
13
18
15
17
20
-1.0
-0.5
0.0
0.5
1.0
1.5
2.0
2.5
Particle Diameter (ϕ)

Beach Name: Magic Sands Beach

Date: 10/23/2020 **Time:** 2:15 PM

Location/ Transect	Survey #	Distance from Water (m)	Slope in Degrees	"x" used	Calculated mm percentile								
					5	10	16	25	50	75	84	90	95
A	1	0.9144	-3	-0.7	1.351131	1.048347	0.827571	0.623778	0.360933	0.223762	0.185574	0.161387	0.108375
	2	5.1816	-1	-0.7	1.473765	1.127894	0.878531	0.654298	0.367537	0.225141	0.186623	0.16202	0.109841

Calculated ϕ percentiles with corrections

5	10	16	25	50	75	84	90	95
-0.700	-0.109	0.408	0.953	1.544	1.879	1.881	1.974	2.109
-0.902	-0.278	0.279	0.857	1.516	1.871	1.874	1.969	2.097

Moments

Mean	Standard Deviation	*Descriptor*	Skewness	*Descriptor*	Kurtosis	*Descriptor*
1.278	0.794	Moderately Sorted	-0.570	Very Coarse Skewed	1.244	Leptokurtic
1.223	0.853	Moderately Sorted	-0.582	Very Coarse Skewed	1.211	Leptokurtic

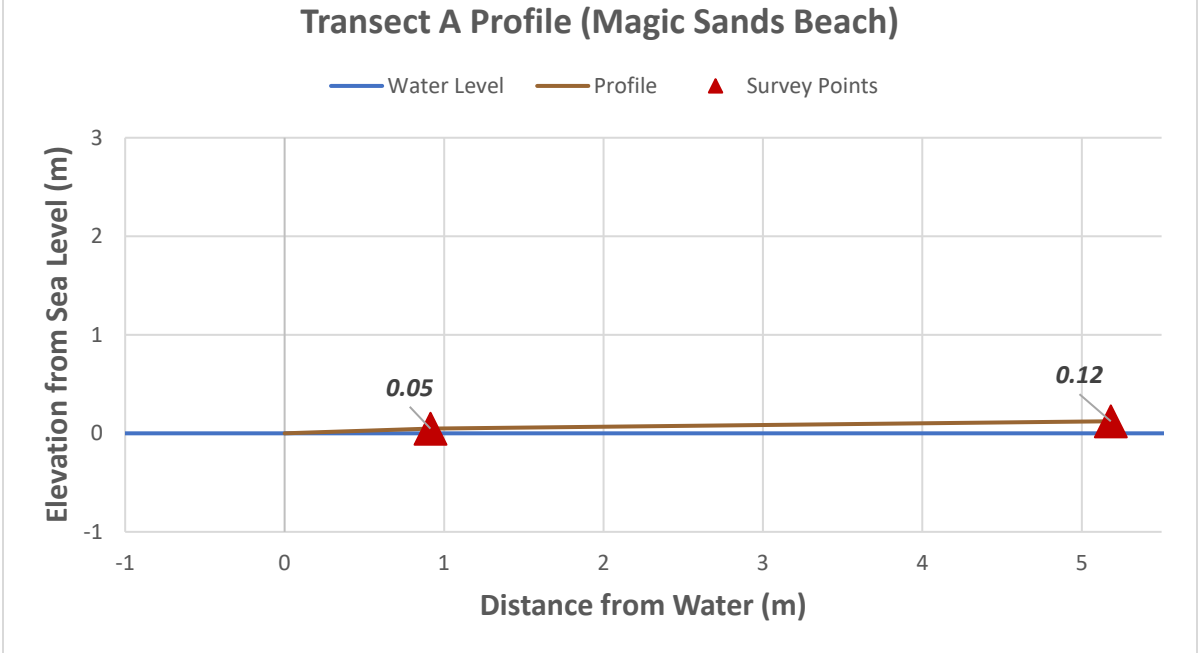

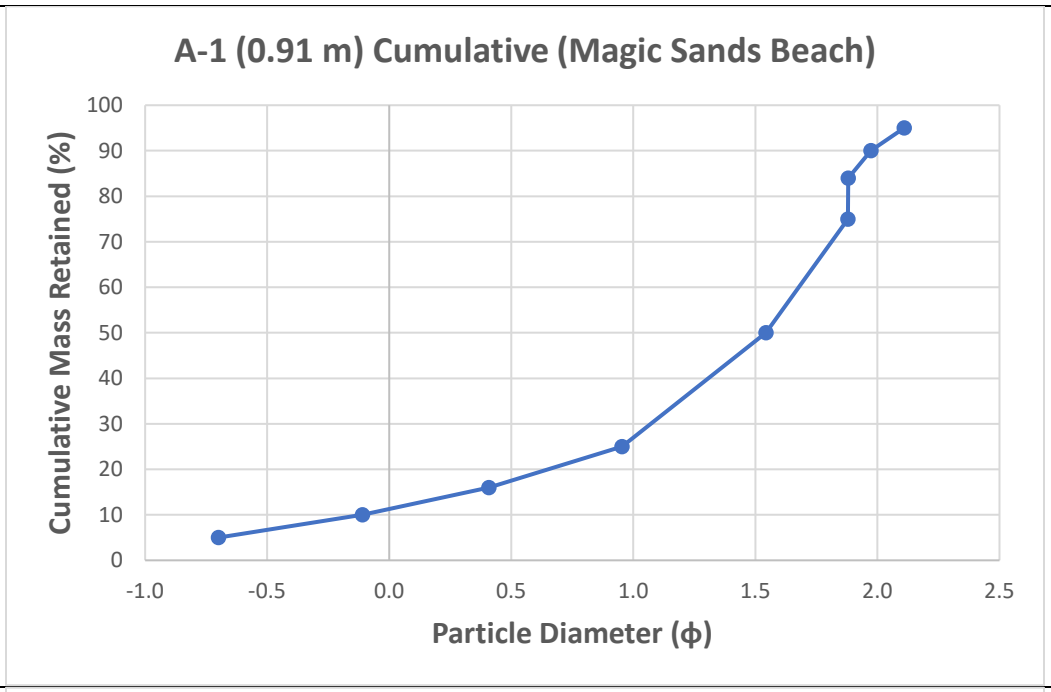
A-1 (0.91 m) Cumulative (Magic Sands Beach)
Cumulative Mass Retained (%)
100
90
80
70
60
50
40
30
20
10
0
-1.0
-0.5
0.0
0.5
1.0
1.5
2.0
2.5
Particle Diameter (ϕ)

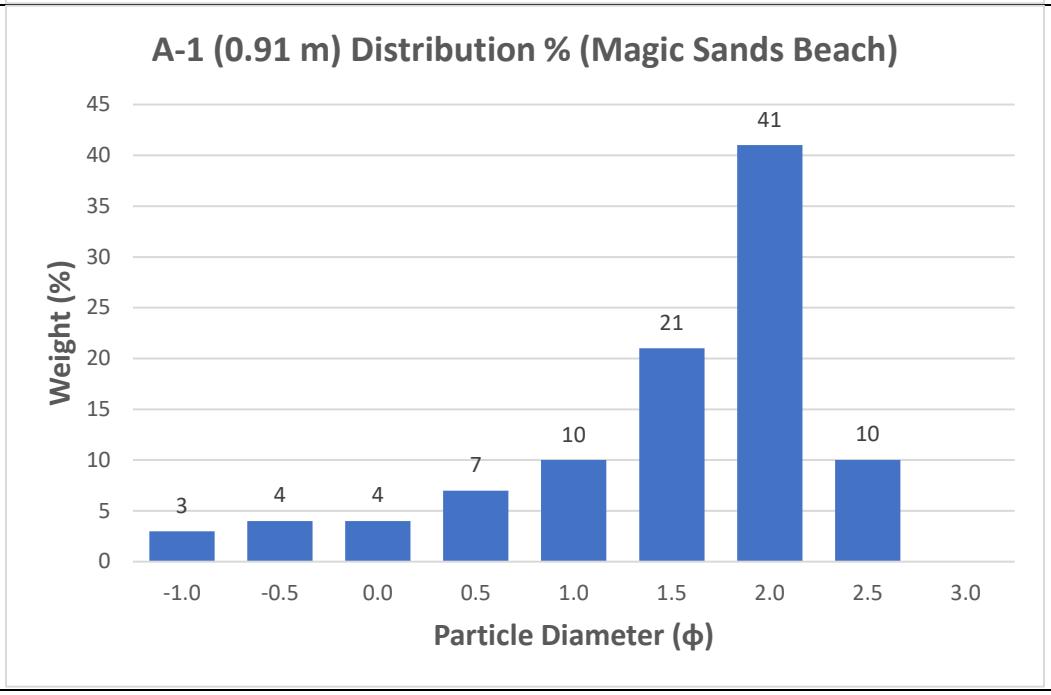
A-1 (0.91 m) Distribution % (Magic Sands Beach)
Weight (%)
45
40
35
30
25
20
15
10
5
0
3
4
4
7
10
21
41
10
-1.0
-0.5
0.0
0.5
1.0
1.5
2.0
2.5
3.0
Particle Diameter (ϕ)

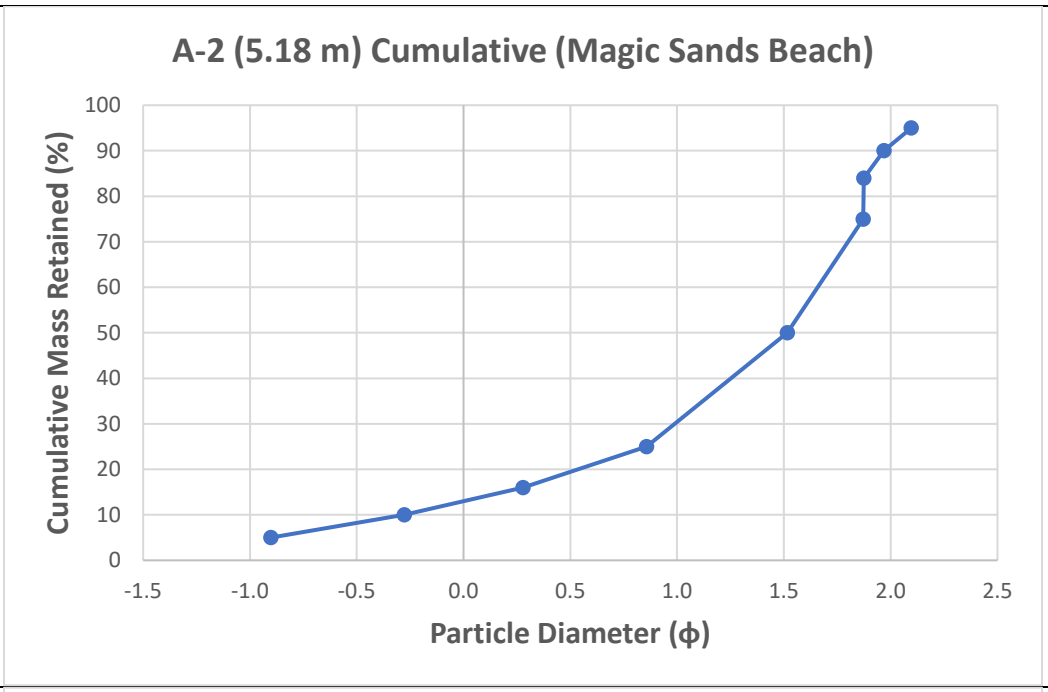
A-2 (5.18 m) Cumulative (Magic Sands Beach)
Cumulative Mass Retained (%)
100
90
80
70
60
50
40
30
20
10
0
-1.5
-1.0
-0.5
0.0
0.5
1.0
1.5
2.0
2.5
Particle Diameter (ϕ)

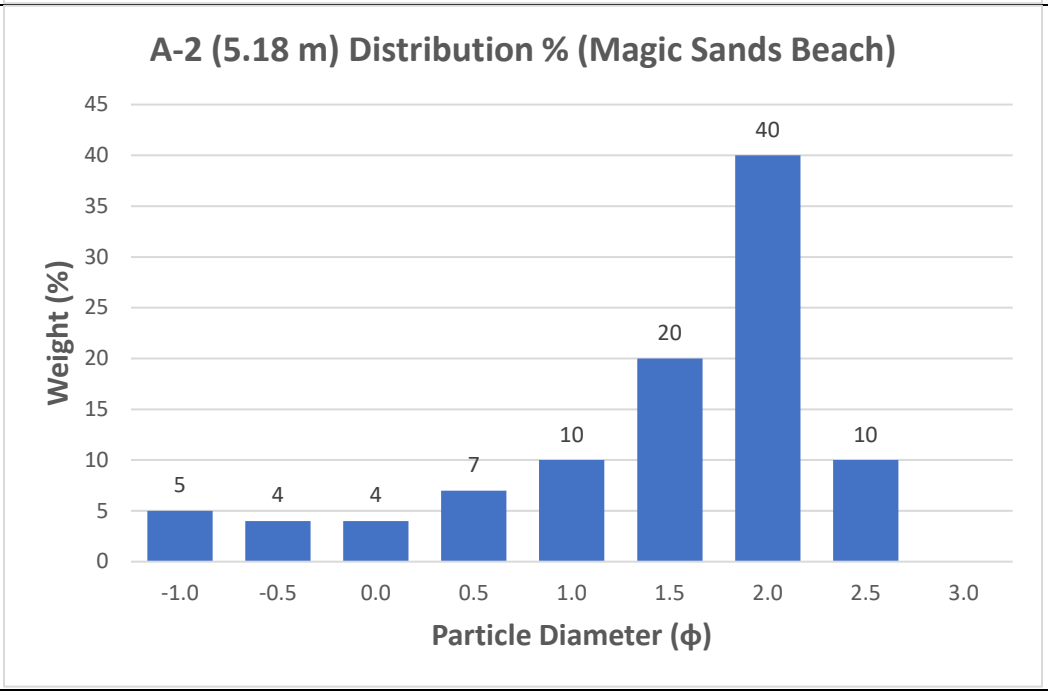
A-2 (5.18 m) Distribution % (Magic Sands Beach)
Weight (%)
45
40
35
30
25
20
15
10
5
0
5
4
4
7
10
20
40
10
-1.0
-0.5
0.0
0.5
1.0
1.5
2.0
2.5
3.0
Particle Diameter (ϕ)

Beach Name:	Pahoehoe Beach Park
Date: 10/23/2020	**Time:** 2:30 PM

Location/ Transect	Survey #	Distance from Water (m)	Slope in Degrees	"x" used	Calculated mm percentile								
					5	10	16	25	50	75	84	90	95
A	1	0.9144	-7	3	2.146537	2.112179	2.069489	2.00147	1.781304	1.477409	1.312072	1.156883	0.966852
	2	2.1336	-5	3.2	1.54563	1.524996	1.499038	1.457521	1.318701	1.113664	1.000096	0.894096	0.757971
	3	3.35	-12	2.9	2.094934	2.056773	2.009423	1.935333	1.69789	1.362542	1.18914	1.037268	0.855289
	4	6.10	0	2.9	1.641984	1.61042	1.571067	1.508753	1.306622	1.027651	0.887261	0.76562	0.622075
	5	8.23	-5	4	6.552286	6.477815	6.384135	6.233464	5.725308	4.953131	4.512382	4.091145	3.540548

Calculated ϕ percentiles with corrections								
5	10	16	25	50	75	84	90	95
-1.776	-1.726	-1.569	-1.401	-0.875	-0.490	-0.303	-0.158	0.032
-1.013	-0.974	-0.873	-0.761	-0.419	-0.135	0.000	0.121	0.263
-1.720	-1.665	-1.505	-1.334	-0.802	-0.388	-0.193	-0.040	0.148
-1.153	-1.100	-0.974	-0.831	-0.405	-0.034	0.134	0.289	0.451
-4.372	-4.313	-3.998	-3.696	-2.643	-2.008	-1.683	-1.524	-1.200

Moments						
Mean	Standard Deviation	*Descriptor*	Skewness	*Descriptor*	Kurtosis	*Descriptor*
-0.916	0.590	Moderately Well Sorted	-0.047	Symmetrical	0.813	Platykurtic
-0.431	0.412	Well Sorted	0.015	Symmetrical	0.835	Platykurtic
-0.834	0.611	Moderately Well Sorted	-0.027	Symmetrical	0.810	Platykurtic
-0.415	0.520	Moderately Well Sorted	0.020	Symmetrical	0.825	Platykurtic
-2.775	1.059	Poorly Sorted	-0.130	Coarse Skewed	0.770	Platykurtic

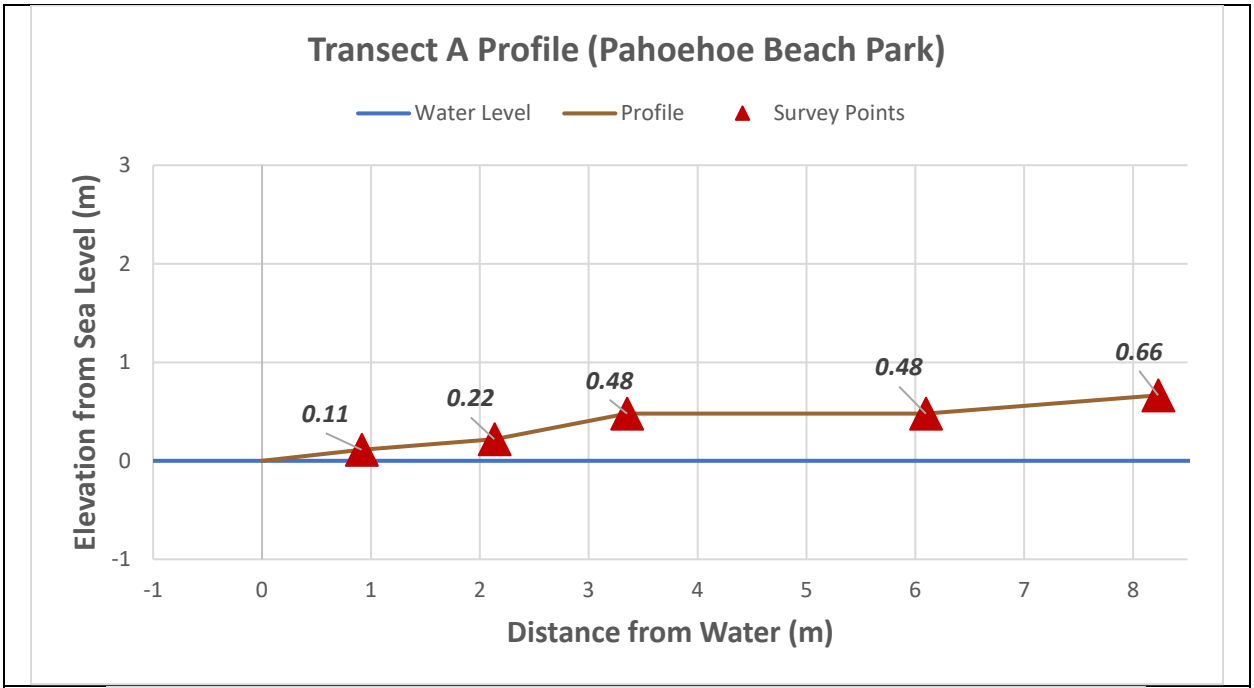
Transect A Profile (Pahoehoe Beach Park)
Water Level
Profile
Survey Points
Elevation from Sea Level (m)
3
2
1
0
-1
-1
0
1
2
3
4
5
6
7
8
Distance from Water (m)
0.11
0.22
0.48
0.48
0.66

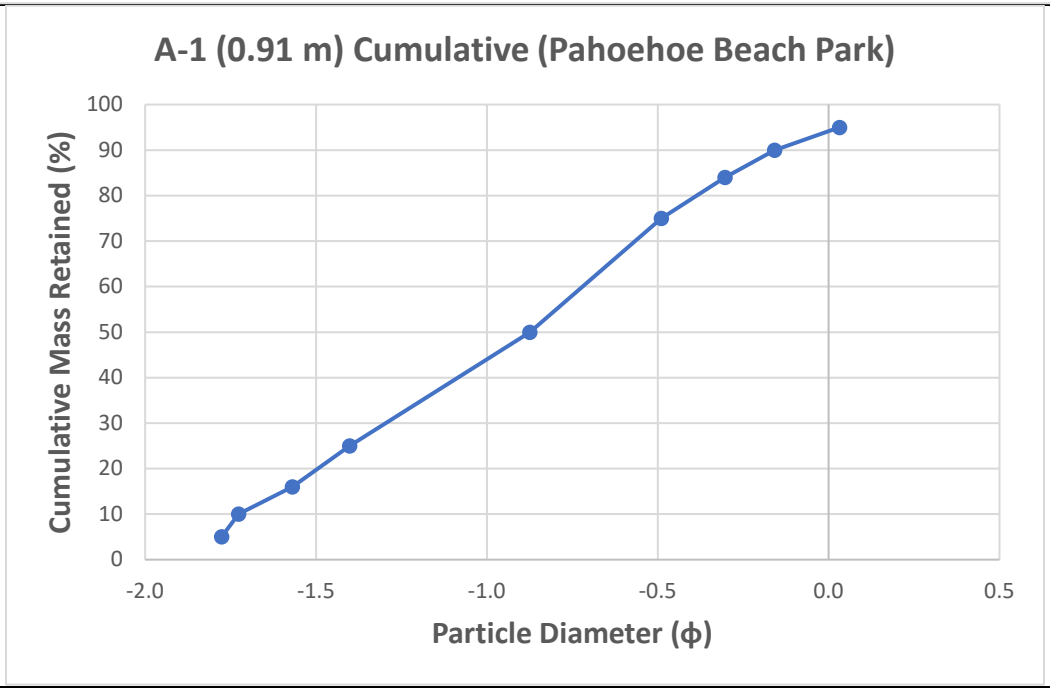
A-1 (0.91 m) Cumulative (Pahoehoe Beach Park)
Cumulative Mass Retained (%)
100
90
80
70
60
50
40
30
20
10
0
-2.0
-1.5
-1.0
-0.5
0.0
0.5
Particle Diameter (ϕ)

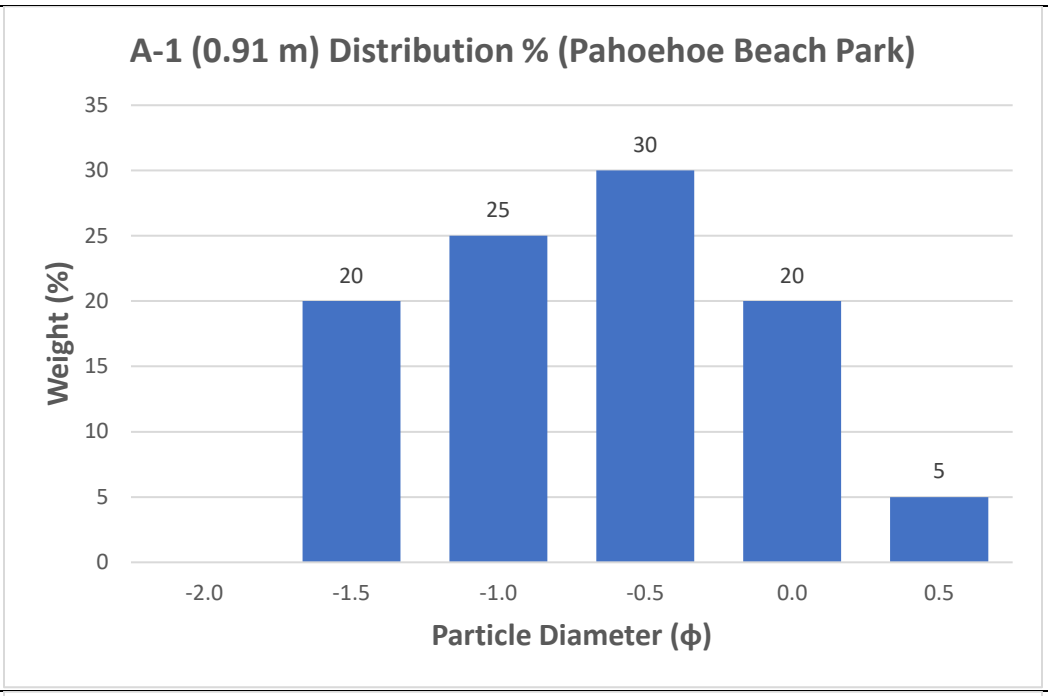
A-1 (0.91 m) Distribution % (Pahoehoe Beach Park)
Weight (%)
35
30
25
20
15
10
5
0
20
25
30
20
5
-2.0
-1.5
-1.0
-0.5
0.0
0.5
Particle Diameter (ϕ)

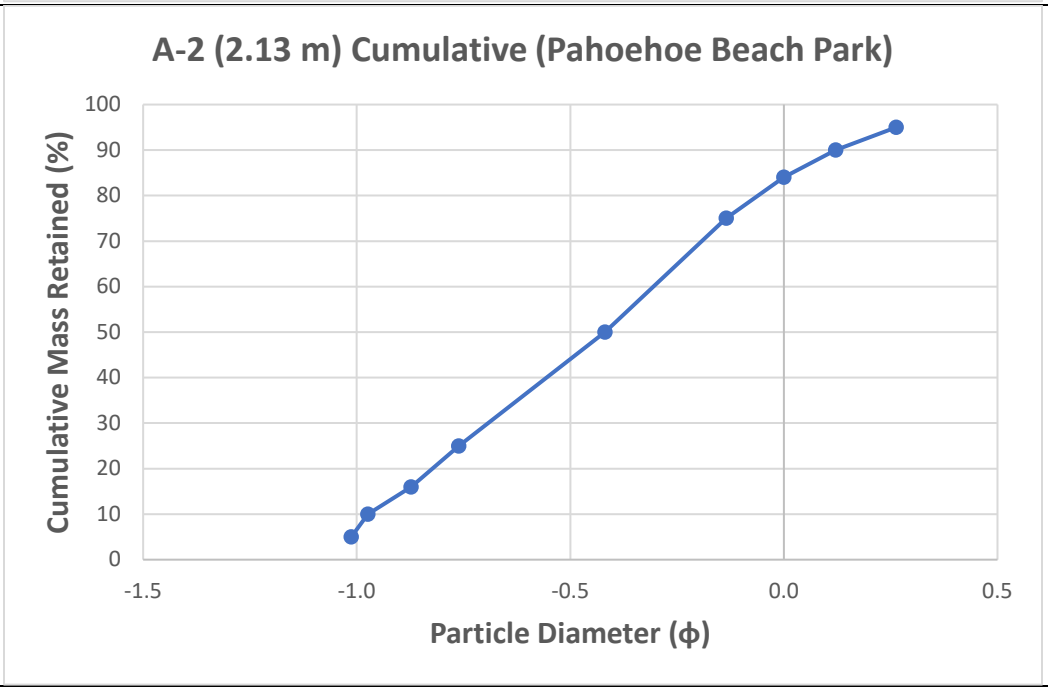
A-2 (2.13 m) Cumulative (Pahoehoe Beach Park)
Cumulative Mass Retained (%)
100
90
80
70
60
50
40
30
20
10
0
-1.5
-1.0
-0.5
0.0
0.5
Particle Diameter (ϕ)

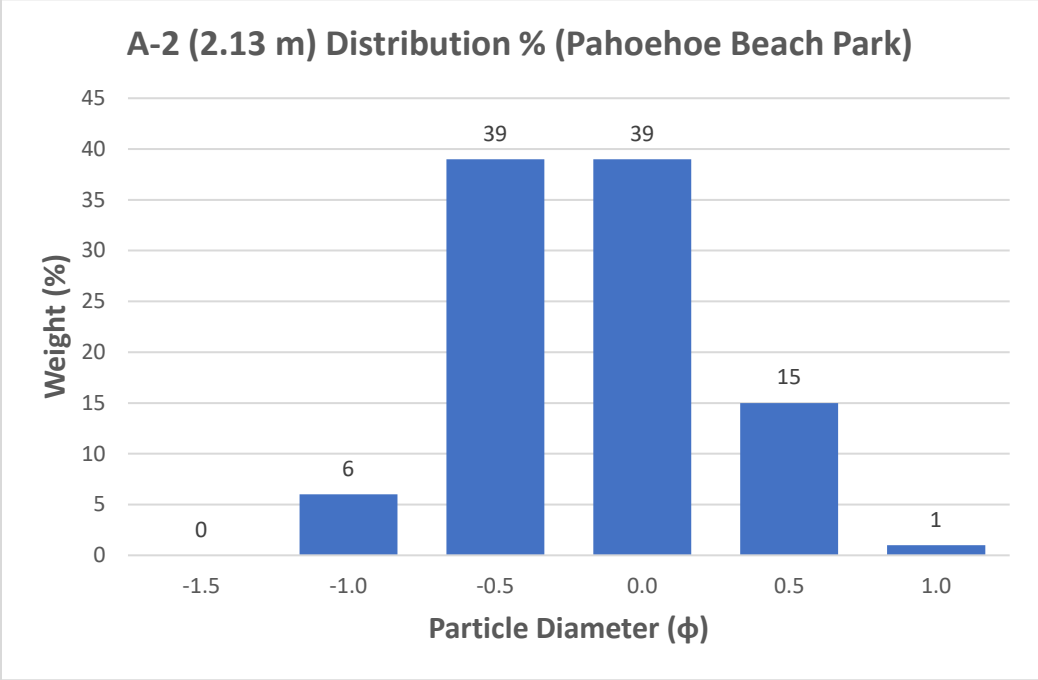
A-2 (2.13 m) Distribution % (Pahoehoe Beach Park)
Weight (%)
45
40
35
30
25
20
15
10
5
0
0
6
39
39
15
1
-1.5
-1.0
-0.5
0.0
0.5
1.0
Particle Diameter (ϕ)

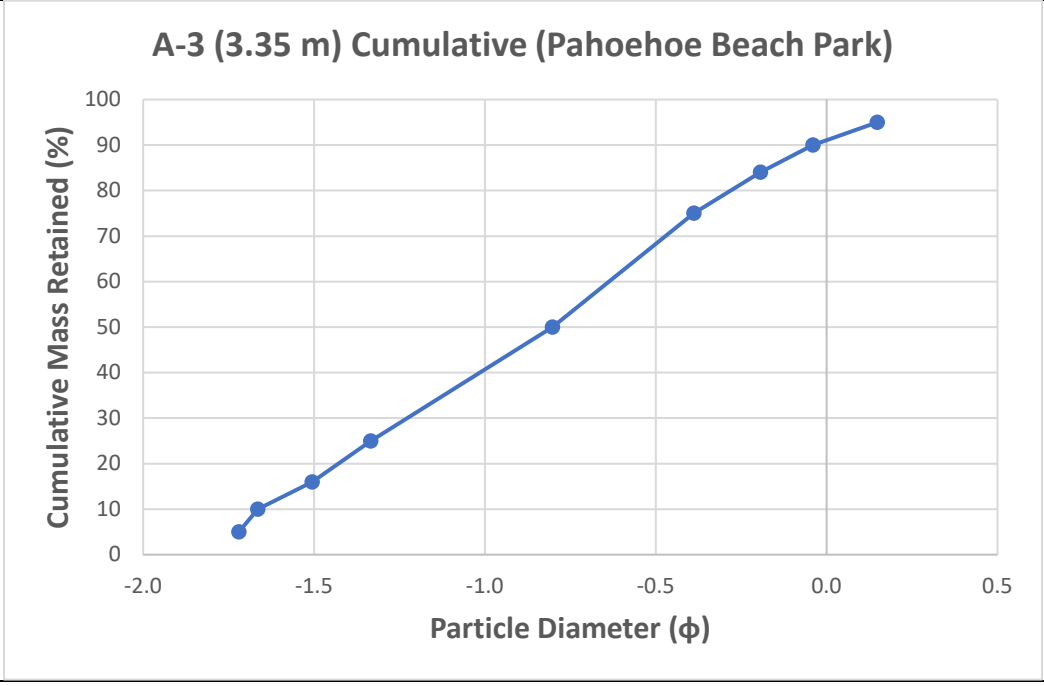
A-3 (3.35 m) Cumulative (Pahoehoe Beach Park)
Cumulative Mass Retained (%)
100
90
80
70
60
50
40
30
20
10
0
-2.0
-1.5
-1.0
-0.5
0.0
0.5
Particle Diameter (ϕ)

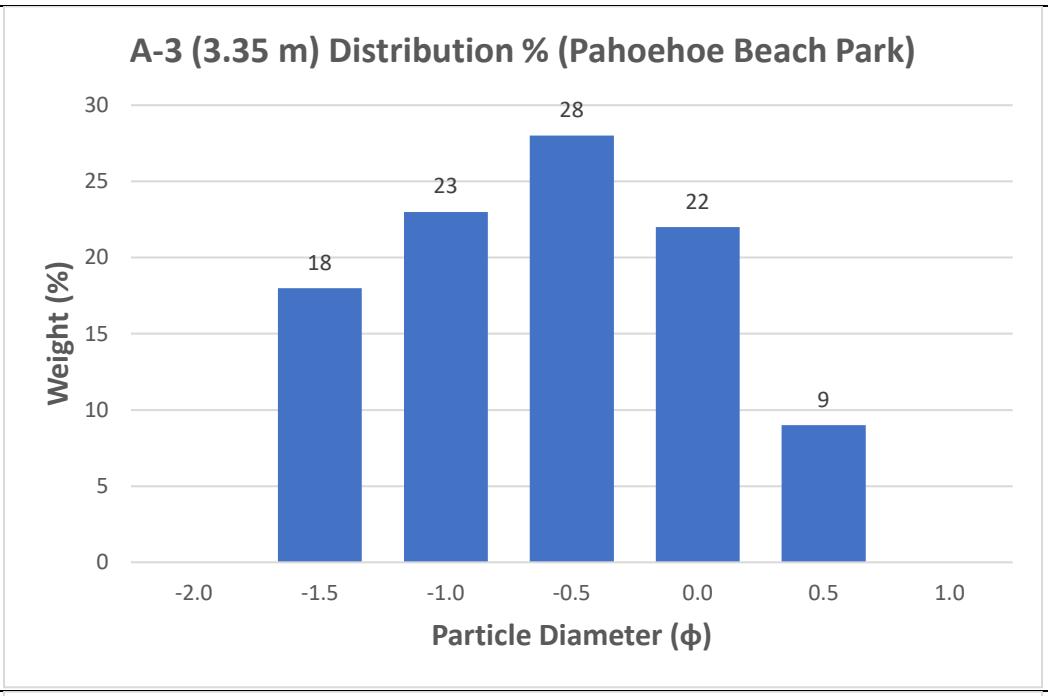
A-3 (3.35 m) Distribution % (Pahoehoe Beach Park)
Weight (%)
30
25
20
15
10
5
0
18
23
28
22
9
-2.0
-1.5
-1.0
-0.5
0.0
0.5
1.0
Particle Diameter (ϕ)

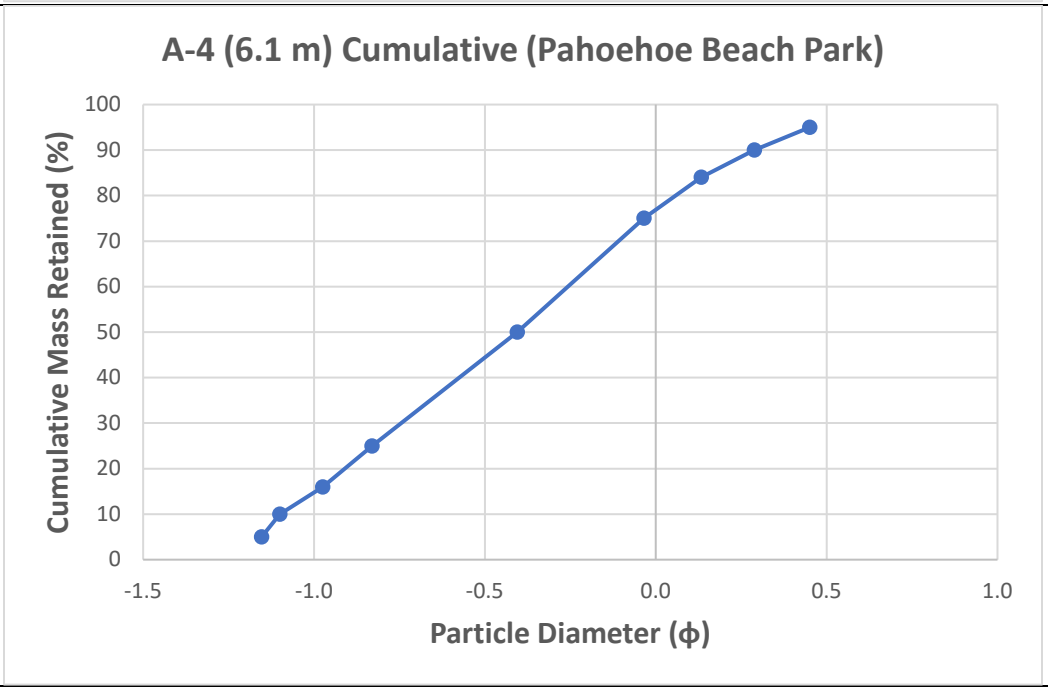
A-4 (6.1 m) Cumulative (Pahoehoe Beach Park)
Cumulative Mass Retained (%)
100
90
80
70
60
50
40
30
20
10
0
-1.5
-1.0
-0.5
0.0
0.5
1.0
Particle Diameter (ϕ)

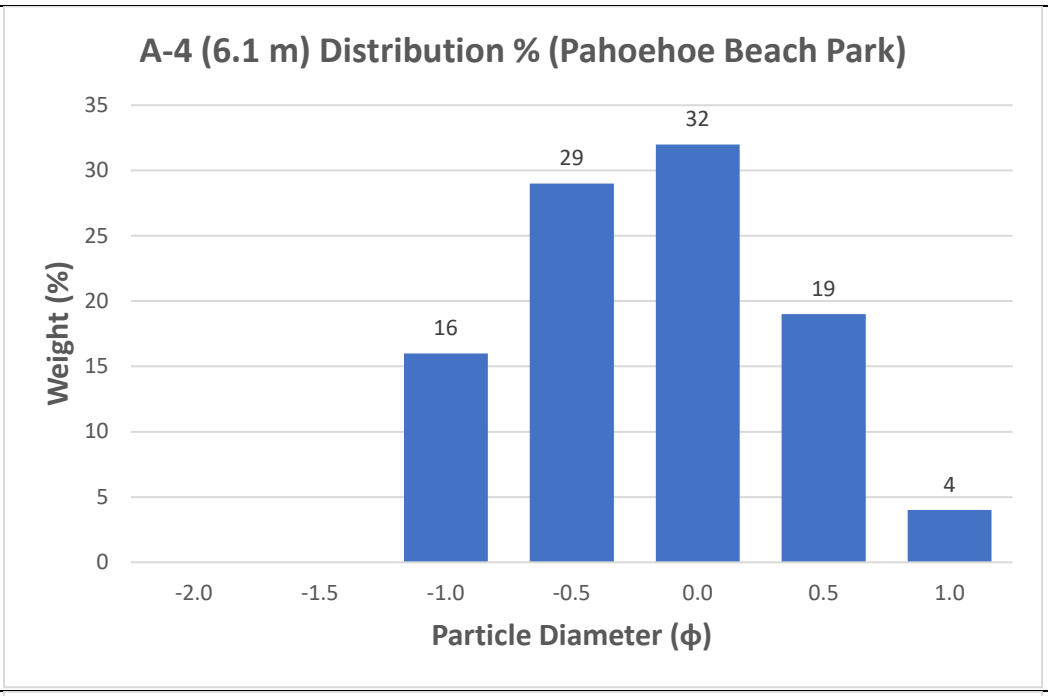
A-4 (6.1 m) Distribution % (Pahoehoe Beach Park)
Weight (%)
35
30
25
20
15
10
5
0
16
29
32
19
4
-2.0
-1.5
-1.0
-0.5
0.0
0.5
1.0
Particle Diameter (ϕ)

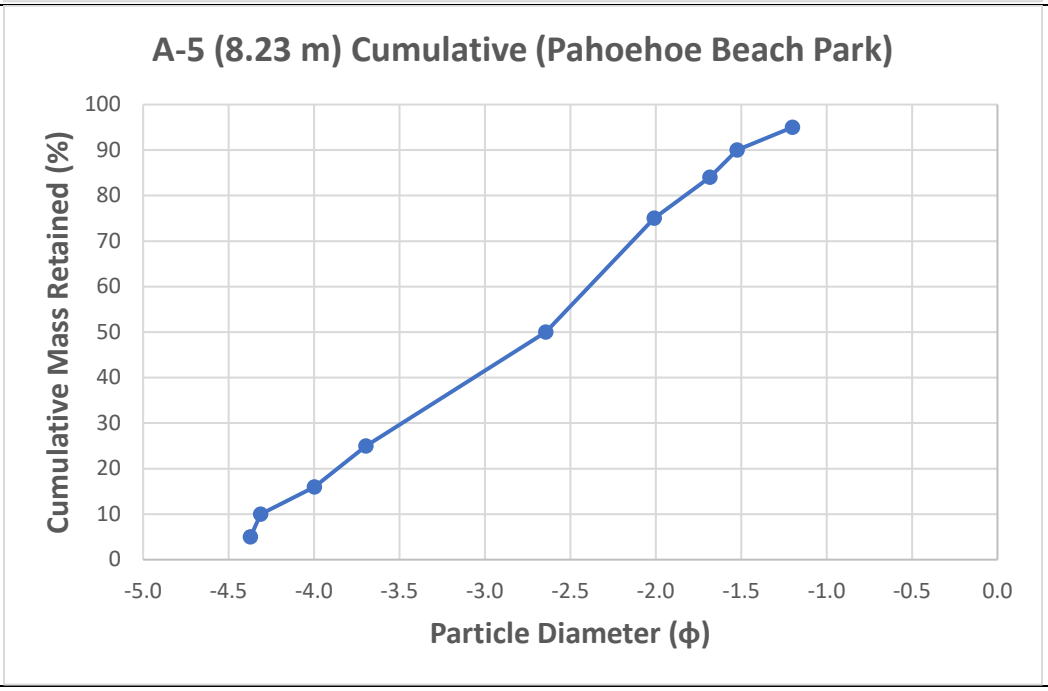
A-5 (8.23 m) Cumulative (Pahoehoe Beach Park)
Cumulative Mass Retained (%)
100
90
80
70
60
50
40
30
20
10
0
-5.0
-4.5
-4.0
-3.5
-3.0
-2.5
-2.0
-1.5
-1.0
-0.5
0.0
Particle Diameter (ϕ)

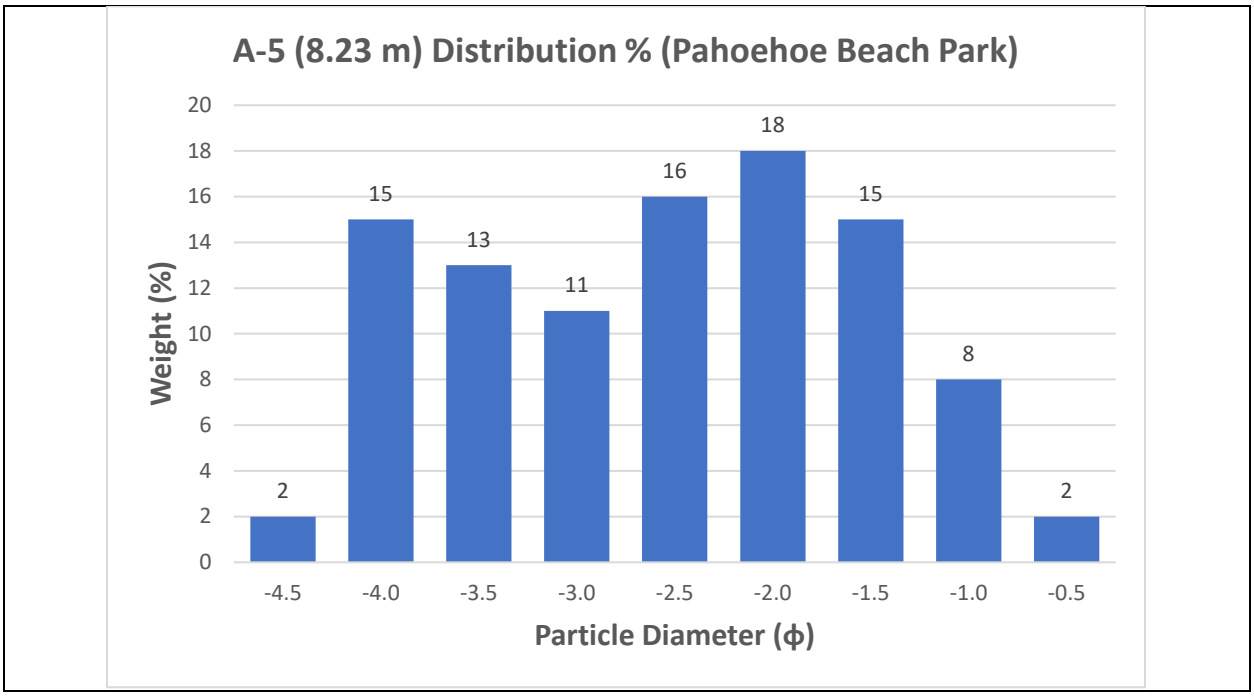
A-5 (8.23 m) Distribution % (Pahoehoe Beach Park)
Weight (%)
20
18
16
14
12
10
8
6
4
2
0
2
15
13
11
16
18
15
8
2
-4.5
-4.0
-3.5
-3.0
-2.5
-2.0
-1.5
-1.0
-0.5
Particle Diameter (ϕ)

Beach Name: Old Kona Airport

Date: 10/23/2020 **Time:** 3:00 PM

Location/ Transect	Survey #	Distance from Water (m)	Slope in Degrees	"x" used	Calculated mm percentile								
					5	10	16	25	50	75	84	90	95
A	1	1.524	-10	4	1.949775	1.921322	1.885673	1.828877	1.640186	1.359804	1.20843	1.07385	0.907957
	2	4.572	-11	4	1.880082	1.851522	1.815874	1.759185	1.573467	1.312183	1.174815	1.048589	0.886844

Calculated ϕ percentiles with corrections

5	10	16	25	50	75	84	90	95
-1.553	-1.507	-1.368	-1.219	-0.750	-0.386	-0.211	-0.077	0.092
-1.468	-1.422	-1.287	-1.141	-0.687	-0.341	-0.180	-0.051	0.114

Moments

Mean	Standard Deviation	*Descriptor*	Skewness	*Descriptor*	Kurtosis	*Descriptor*
-0.776	0.538	Moderately Well Sorted	-0.023	Symmetrical	0.809	Platykurtic
-0.718	0.516	Moderately Well Sorted	-0.036	Symmetrical	0.811	Platykurtic

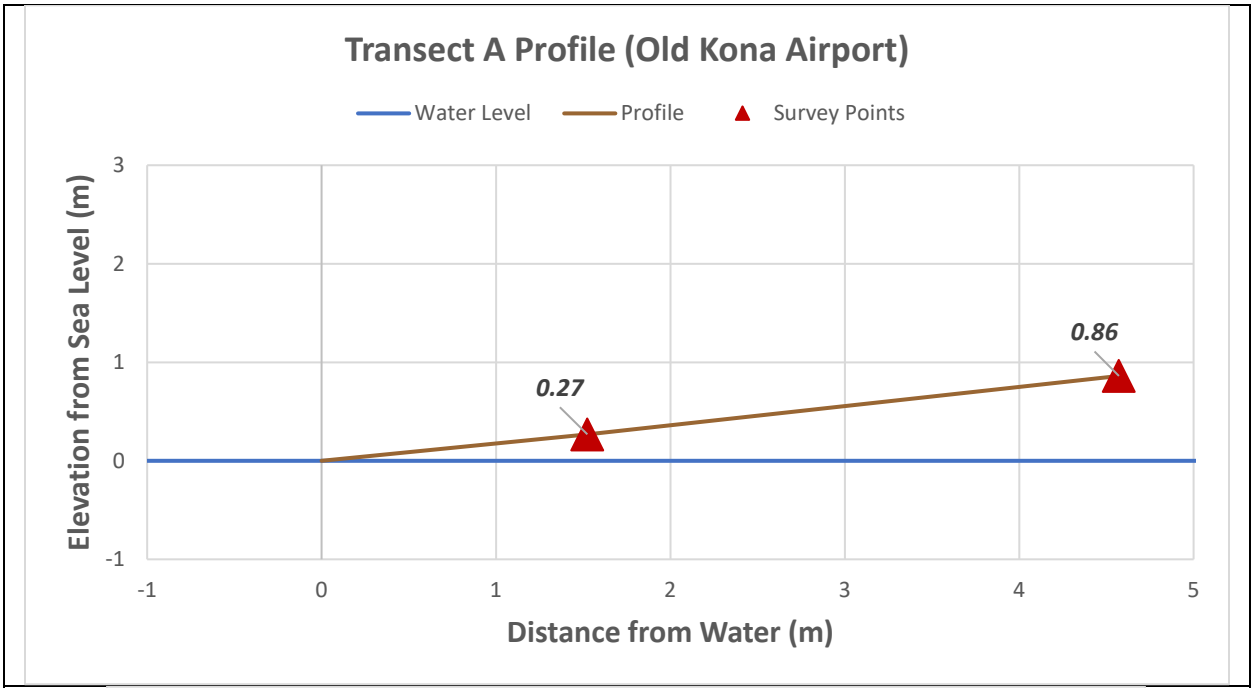
Transect A Profile (Old Kona Airport)
Water Level
Profile
Survey Points
Elevation from Sea Level (m)
3
2
1
0
-1
-1
0
1
2
3
4
5
0.27
0.86
Distance from Water (m)

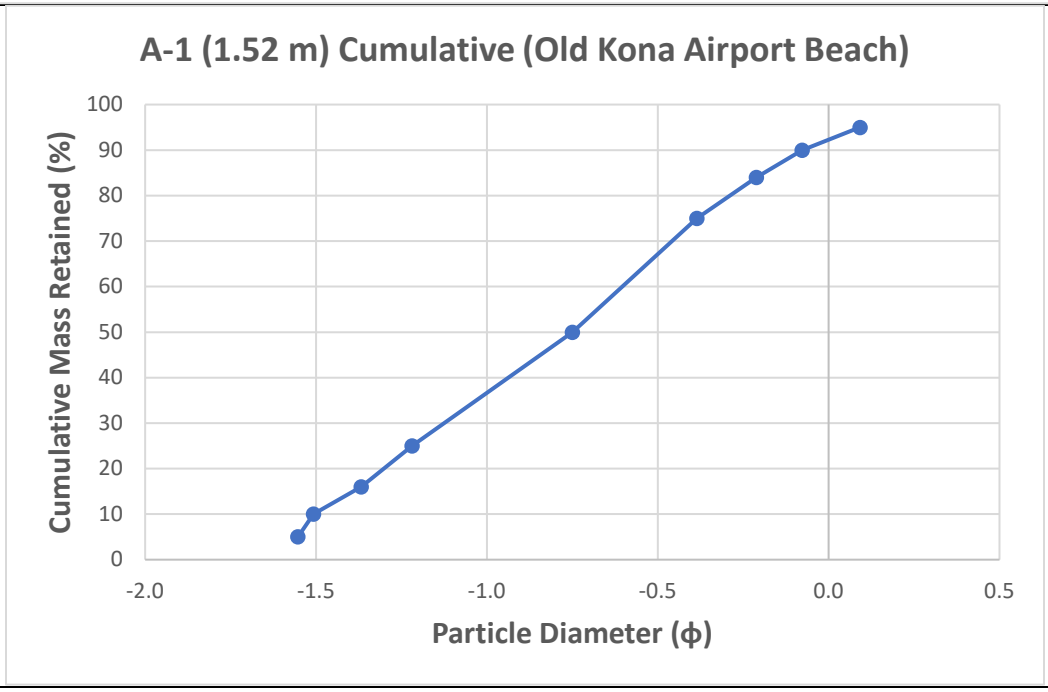
A-1 (1.52 m) Cumulative (Old Kona Airport Beach)
Cumulative Mass Retained (%)
100
90
80
70
60
50
40
30
20
10
0
-2.0
-1.5
-1.0
-0.5
0.0
0.5
Particle Diameter (ϕ)

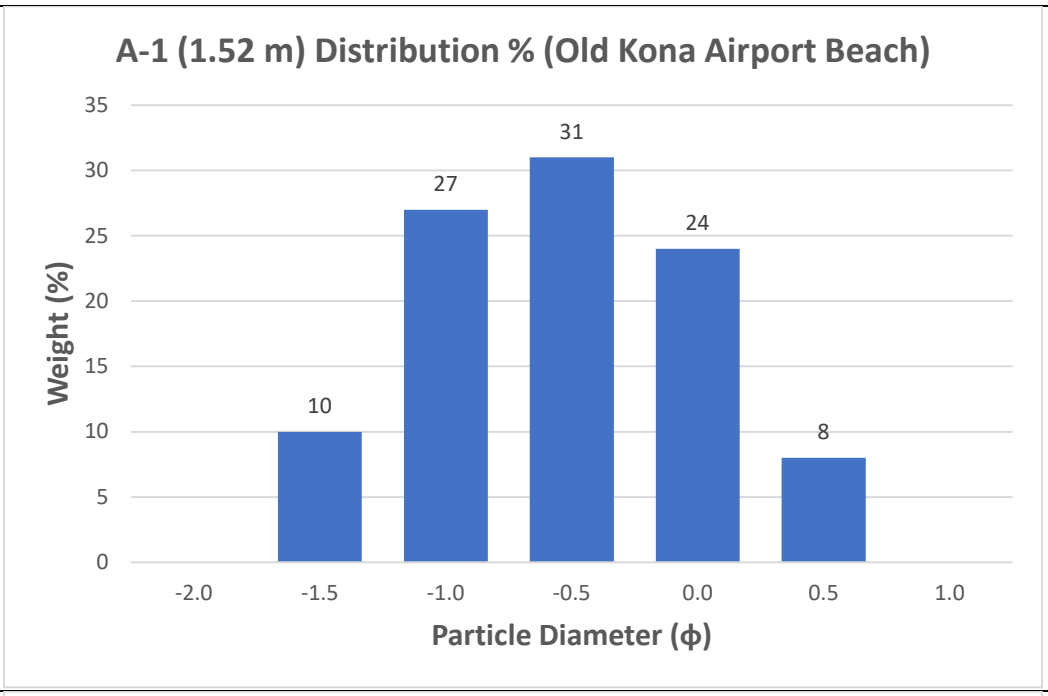
A-1 (1.52 m) Distribution % (Old Kona Airport Beach)
Weight (%)
35
30
25
20
15
10
5
0
10
27
31
24
8
-2.0
-1.5
-1.0
-0.5
0.0
0.5
1.0
Particle Diameter (ϕ)

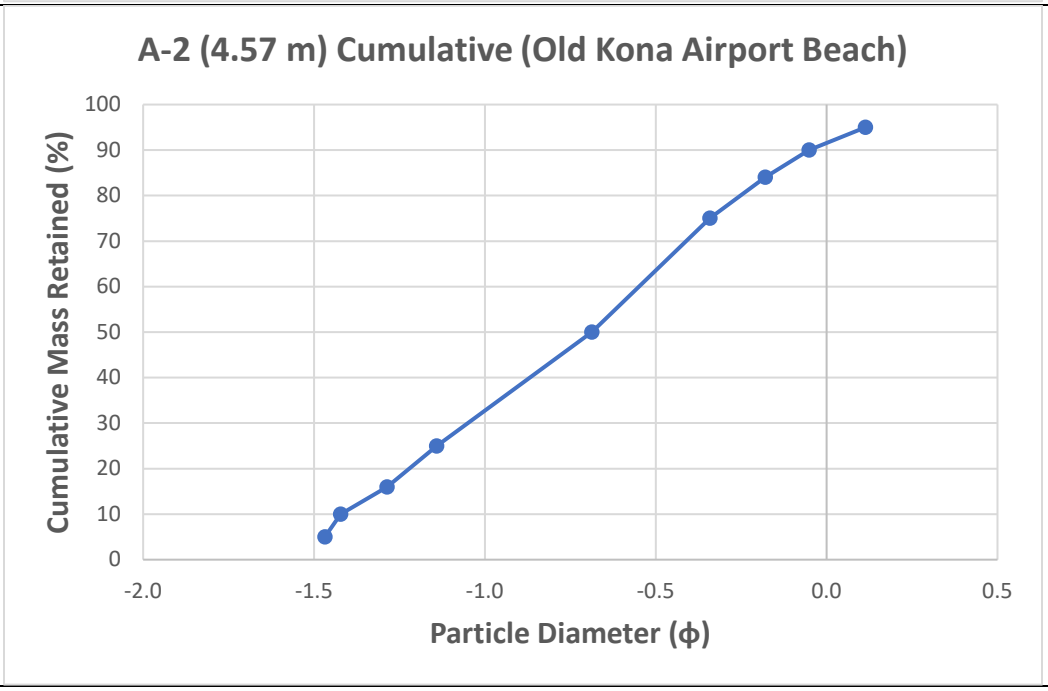
A-2 (4.57 m) Cumulative (Old Kona Airport Beach)
Cumulative Mass Retained (%)
100
90
80
70
60
50
40
30
20
10
0
-2.0
-1.5
-1.0
-0.5
0.0
0.5
Particle Diameter (ϕ)

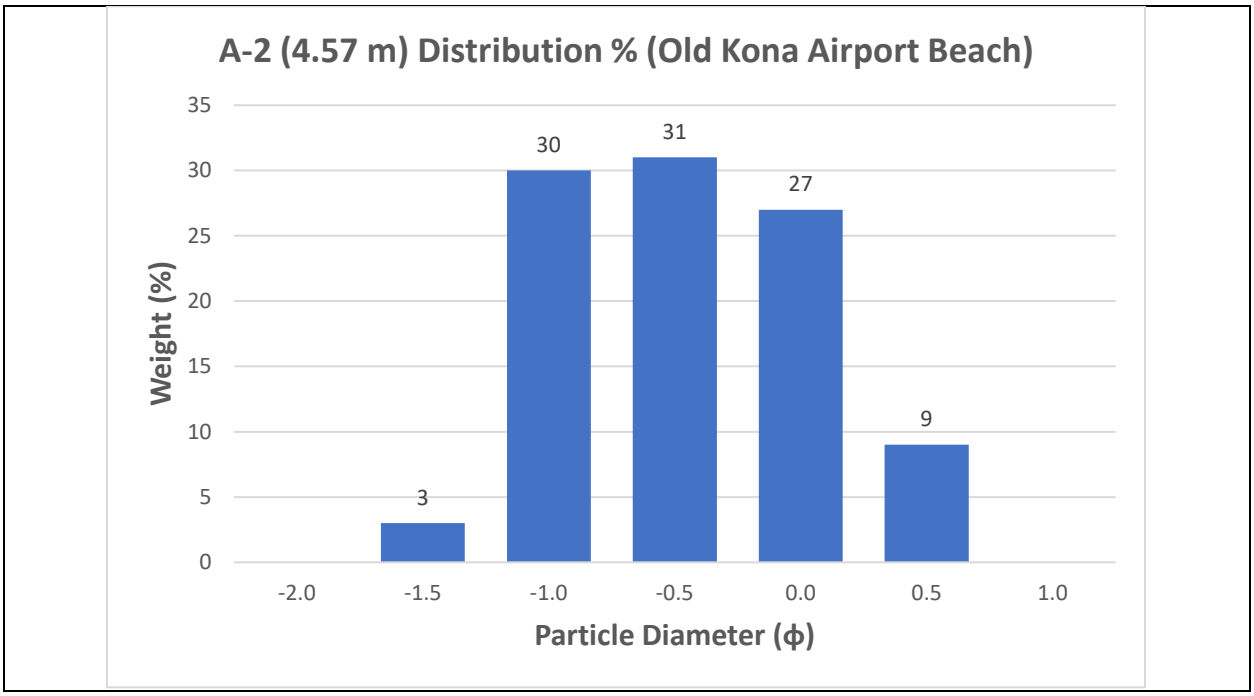
A-2 (4.57 m) Distribution % (Old Kona Airport Beach)
Weight (%)
35
30
25
20
15
10
5
0
3
30
31
27
9
-2.0
-1.5
-1.0
-0.5
0.0
0.5
1.0
Particle Diameter (ϕ)

Beach Name:	Pololu Beach
Date: 10/24/2020	**Time:** 1:30 PM

Location/ Transect	Survey #	Distance from Water (m)	Slope in Degrees	"x" used	Calculated mm percentile							
					5	10	16	25	50	75	84	90	95
A	1	0.3048	-5	-1.4	0.536823	0.404487	0.325039	0.258393	0.159546	0.102234	0.07578	0.069056	0.034528
	2	4.572	-4	-1.5	0.566646	0.421147	0.336888	0.268164	0.170929	0.116599	0.084671	0.06542	0.03271
	3	7.32	-3	-1.5	0.527146	0.396738	0.320417	0.256974	0.162126	0.107099	0.079736	0.068585	0.034293
	4	9.75	-19	9	63.72174	63.33963	62.84772	62.05439	59.28628	54.84164	52.17118	49.51189	45.85223
B	1	0.61	-2	-1.5	0.321661	0.244381	0.199066	0.161084	0.087021	0.051902	0.035099	0.029812	0.011906
	2	2.13	-2	-1.4	0.284315	0.225255	0.185492	0.150161	0.079065	0.04428	0.029123	0.024827	0.012413
	3	10.36	-3	-1.5	0.598486	0.466023	0.380791	0.306256	0.202459	0.13802	0.102076	0.076298	0.038149
C	1	0.61	-4	-1.5	0.569055	0.425919	0.342852	0.273956	0.174618	0.118369	0.09039	0.068994	0.034497
	2	5.79	-5	-1.5	0.491589	0.364086	0.294999	0.239382	0.14637	0.098321	0.070605	0.060378	0.030189
	3	9.75	-5	-1.5	0.595573	0.450398	0.365735	0.293507	0.193126	0.134265	0.099031	0.081636	0.040818
	4	11.89	-9	9	14.14692	14.07154	13.97218	13.81313	13.2593	12.3659	11.82322	11.27271	10.50641
	5	14.33	-16	9	20.45189	20.34109	20.20096	19.97309	19.1824	17.90849	17.13002	16.34092	15.22621
	6	17.68	-13	9	26.51907	26.3705	26.18263	25.87838	24.82333	23.13343	22.11365	21.09048	19.66575
	7	21.34	-9	9	32.03101	31.85209	31.6219	31.25171	29.96974	27.93171	26.71439	25.49398	23.8055

Calculated ϕ percentiles with corrections								
5	10	16	25	50	75	84	90	95
1.447	2.089	2.424	2.733	2.780	2.862	2.881	2.892	3.195
1.321	1.996	2.347	2.658	2.676	2.697	2.757	2.951	3.247
1.489	2.134	2.455	2.744	2.756	2.804	2.824	2.899	3.202
-9.662	-9.576	-8.931	-8.338	-6.184	-5.026	-4.416	-4.222	-3.631
2.638	3.252	3.481	3.688	3.699	3.713	3.740	3.801	4.206
2.925	3.441	3.634	3.830	3.844	3.913	3.949	3.999	4.166
1.194	1.762	2.082	2.390	2.420	2.486	2.548	2.784	3.101
1.311	1.970	2.309	2.615	2.644	2.678	2.684	2.893	3.196
1.651	2.332	2.633	2.888	2.911	2.911	2.960	3.037	3.323
1.205	1.841	2.169	2.476	2.491	2.520	2.582	2.711	3.036
-6.162	-6.104	-5.688	-5.303	-3.915	-3.157	-2.758	-2.621	-2.233
-7.019	-6.954	-6.483	-6.048	-4.475	-3.621	-3.172	-3.023	-2.585
-7.623	-7.553	-7.042	-6.571	-4.865	-3.943	-3.457	-3.299	-2.828
-8.062	-7.989	-7.449	-6.952	-5.151	-4.179	-3.668	-3.504	-3.009

Moments						
Mean	Standard Deviation	*Descriptor*	Skewness	*Descriptor*	Kurtosis	*Descriptor*
2.695	0.379	Well Sorted	-0.543	Very Coarse Skewed	5.553	Extremely Leptokurtic
2.593	0.394	Well Sorted	-0.506	Very Coarse Skewed	20.241	Extremely Leptokurtic
2.678	0.352	Well Sorted	-0.556	Very Coarse Skewed	11.784	Extremely Leptokurtic
-6.510	2.042	Very Poorly Sorted	-0.185	Coarse Skewed	0.746	Platykurtic
3.640	0.302	Very Well Sorted	-0.516	Very Coarse Skewed	25.253	Extremely Leptokurtic
3.809	0.267	Very Well Sorted	-0.407	Very Coarse Skewed	6.132	Extremely Leptokurtic
2.350	0.405	Well Sorted	-0.366	Very Coarse Skewed	8.177	Extremely Leptokurtic
2.545	0.379	Well Sorted	-0.599	Very Coarse Skewed	12.217	Extremely Leptokurtic
2.835	0.335	Very Well Sorted	-0.604	Very Fine Skewed	28.941	Extremely Leptokurtic
2.414	0.381	Well Sorted	-0.481	Very Coarse Skewed	16.938	Extremely Leptokurtic
-4.120	1.328	Poorly Sorted	-0.177	Coarse Skewed	0.750	Platykurtic
-4.710	1.499	Poorly Sorted	-0.180	Coarse Skewed	0.749	Platykurtic
-5.122	1.623	Poorly Sorted	-0.182	Coarse Skewed	0.748	Platykurtic
-5.423	1.711	Poorly Sorted	-0.184	Coarse Skewed	0.747	Platykurtic

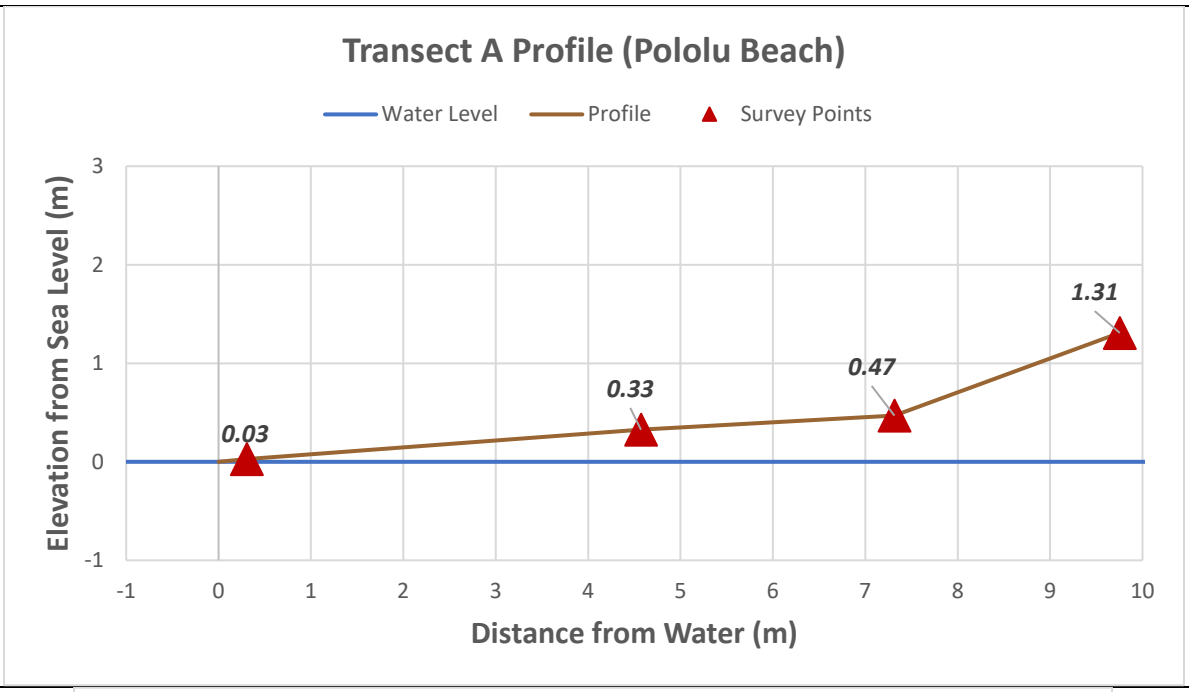
Transect A Profile (Pololu Beach)
Water Level
Profile
Survey Points
Elevation from Sea Level (m)
Distance from Water (m)
0.03
0.33
0.47
1.31

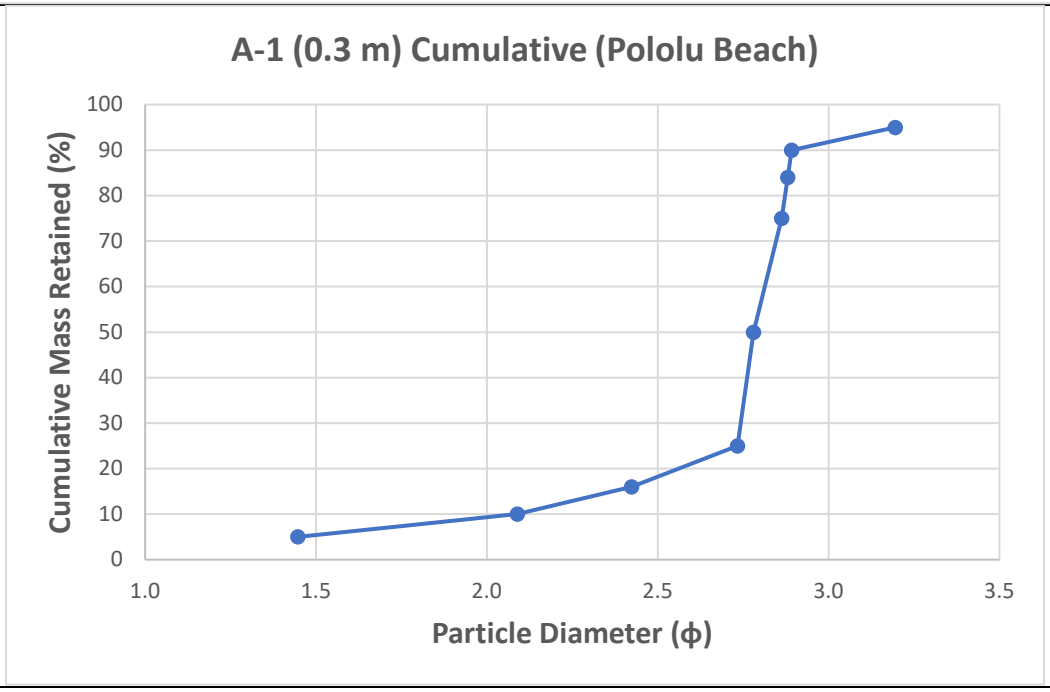
A-1 (0.3 m) Cumulative (Pololu Beach)
Cumulative Mass Retained (%)
Particle Diameter (ϕ)

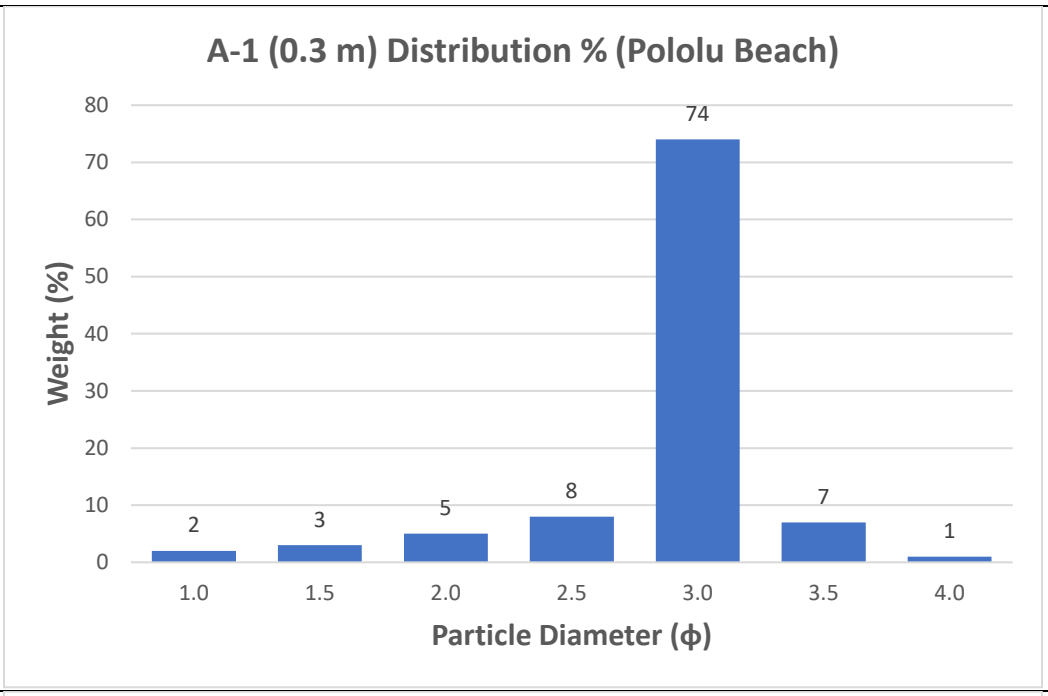
A-1 (0.3 m) Distribution % (Pololu Beach)
Weight (%)
80
70
60
50
40
30
20
10
0
2
3
5
8
74
7
1
1.0
1.5
2.0
2.5
3.0
3.5
4.0
Particle Diameter (ϕ)

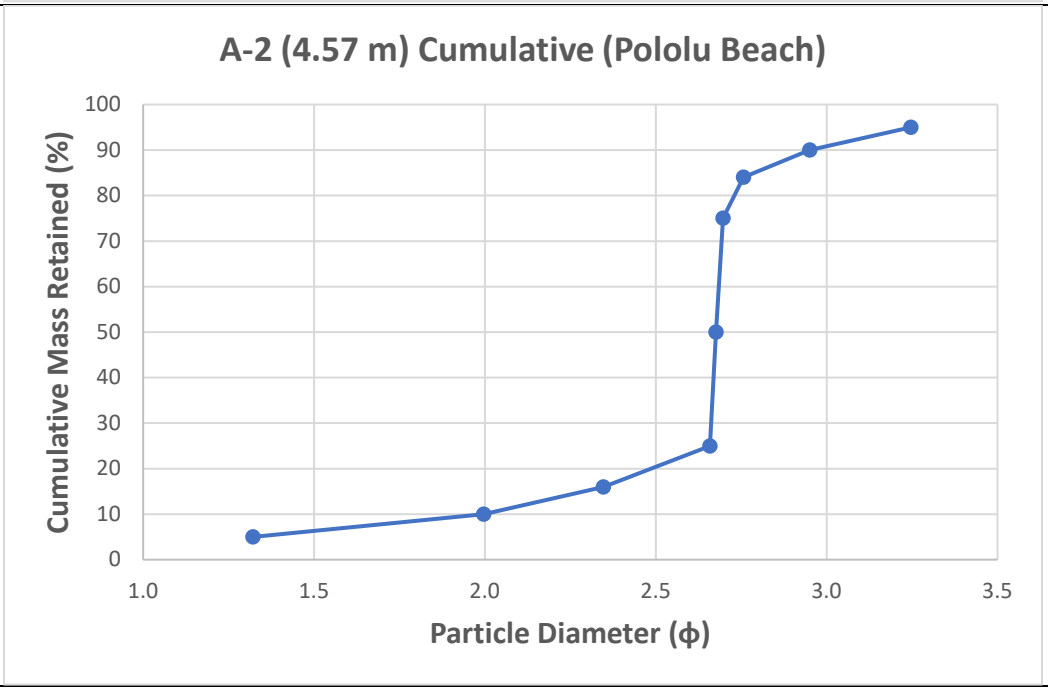
A-2 (4.57 m) Cumulative (Pololu Beach)
Cumulative Mass Retained (%)
100
90
80
70
60
50
40
30
20
10
0
1.0
1.5
2.0
2.5
3.0
3.5
Particle Diameter (ϕ)

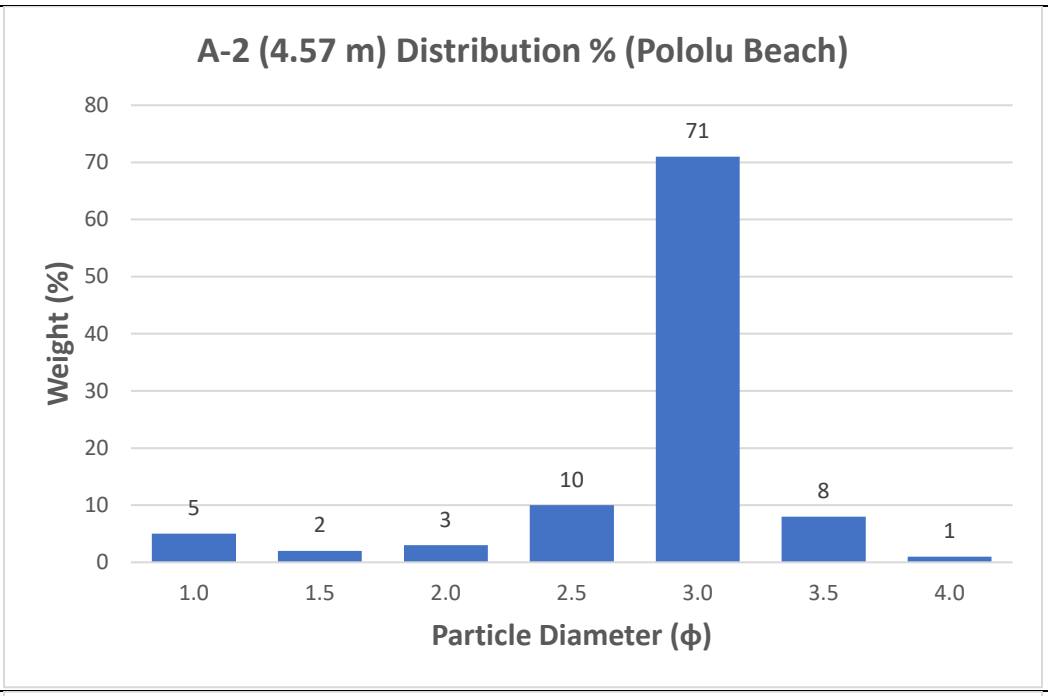
A-2 (4.57 m) Distribution % (Pololu Beach)
Weight (%)
80
70
60
50
40
30
20
10
0
5
2
3
10
71
8
1
1.0
1.5
2.0
2.5
3.0
3.5
4.0
Particle Diameter (ϕ)

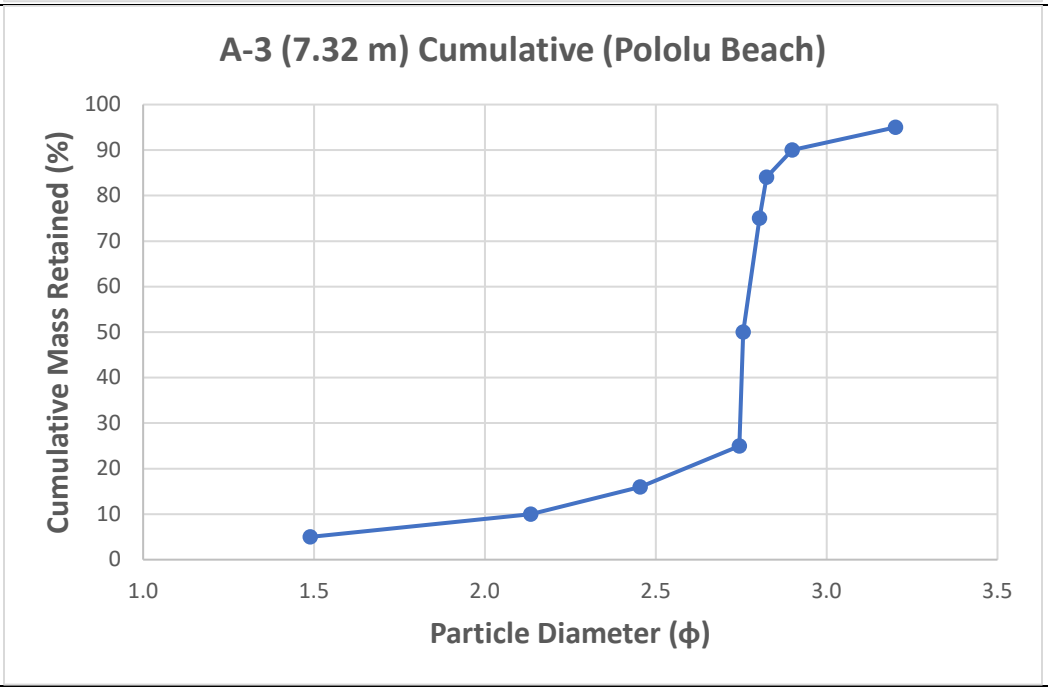
A-3 (7.32 m) Cumulative (Pololu Beach)
Cumulative Mass Retained (%)
100
90
80
70
60
50
40
30
20
10
0
1.0
1.5
2.0
2.5
3.0
3.5
Particle Diameter (ϕ)

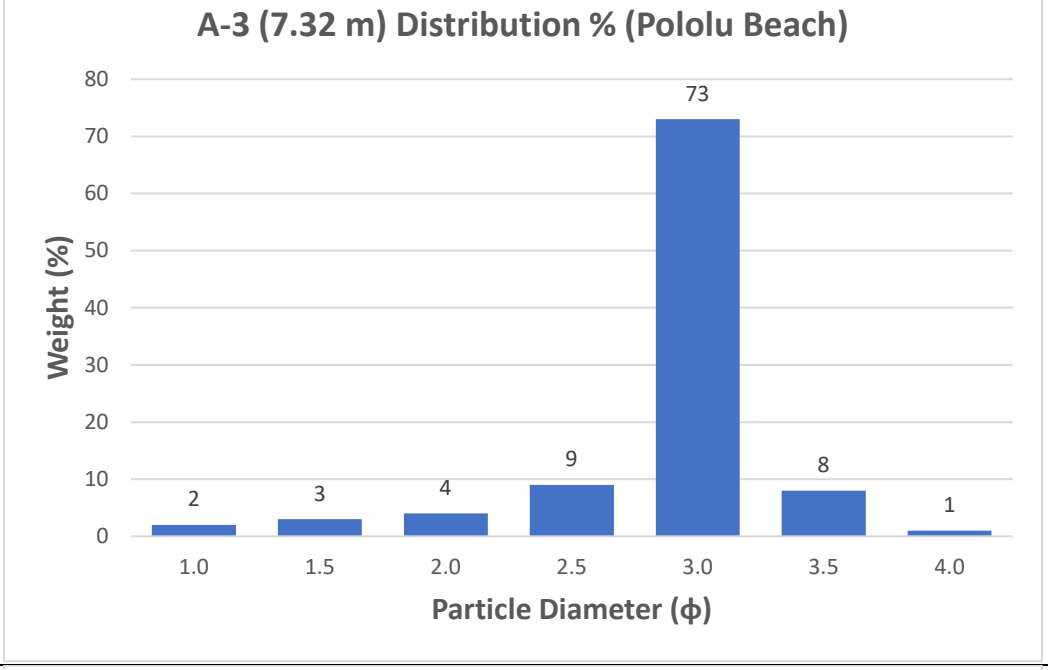
A-3 (7.32 m) Distribution % (Pololu Beach)
Weight (%)
80
70
60
50
40
30
20
10
0
2
3
4
9
73
8
1
1.0
1.5
2.0
2.5
3.0
3.5
4.0
Particle Diameter (ϕ)

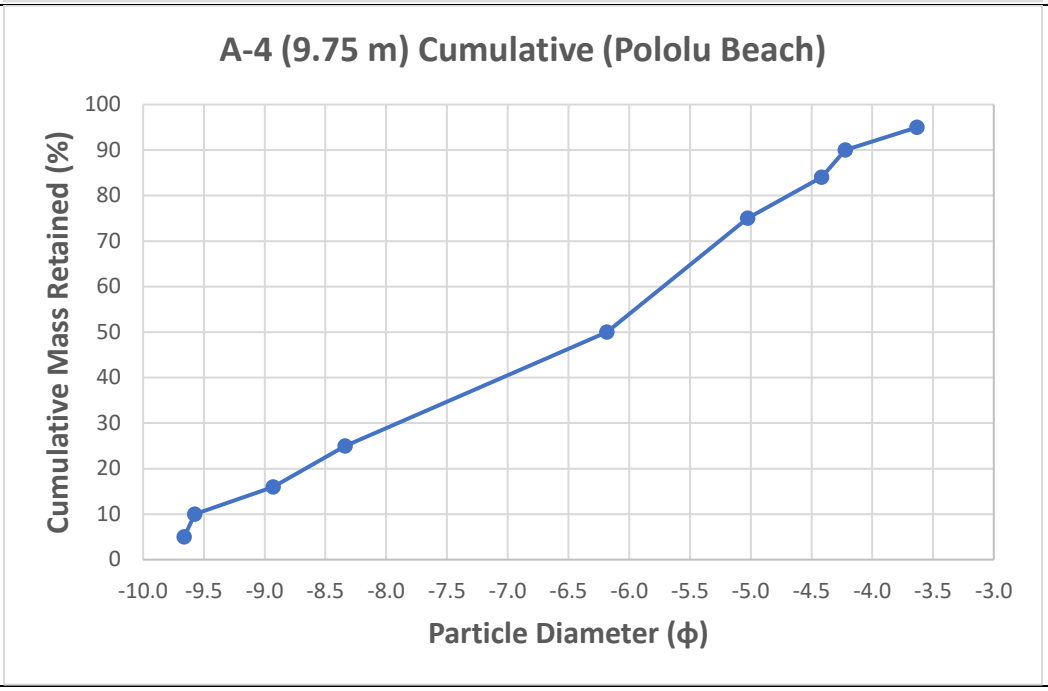
A-4 (9.75 m) Cumulative (Pololu Beach)
Cumulative Mass Retained (%)
100
90
80
70
60
50
40
30
20
10
0
-10.0
-9.5
-9.0
-8.5
-8.0
-7.5
-7.0
-6.5
-6.0
-5.5
-5.0
-4.5
-4.0
-3.5
-3.0
Particle Diameter (ϕ)

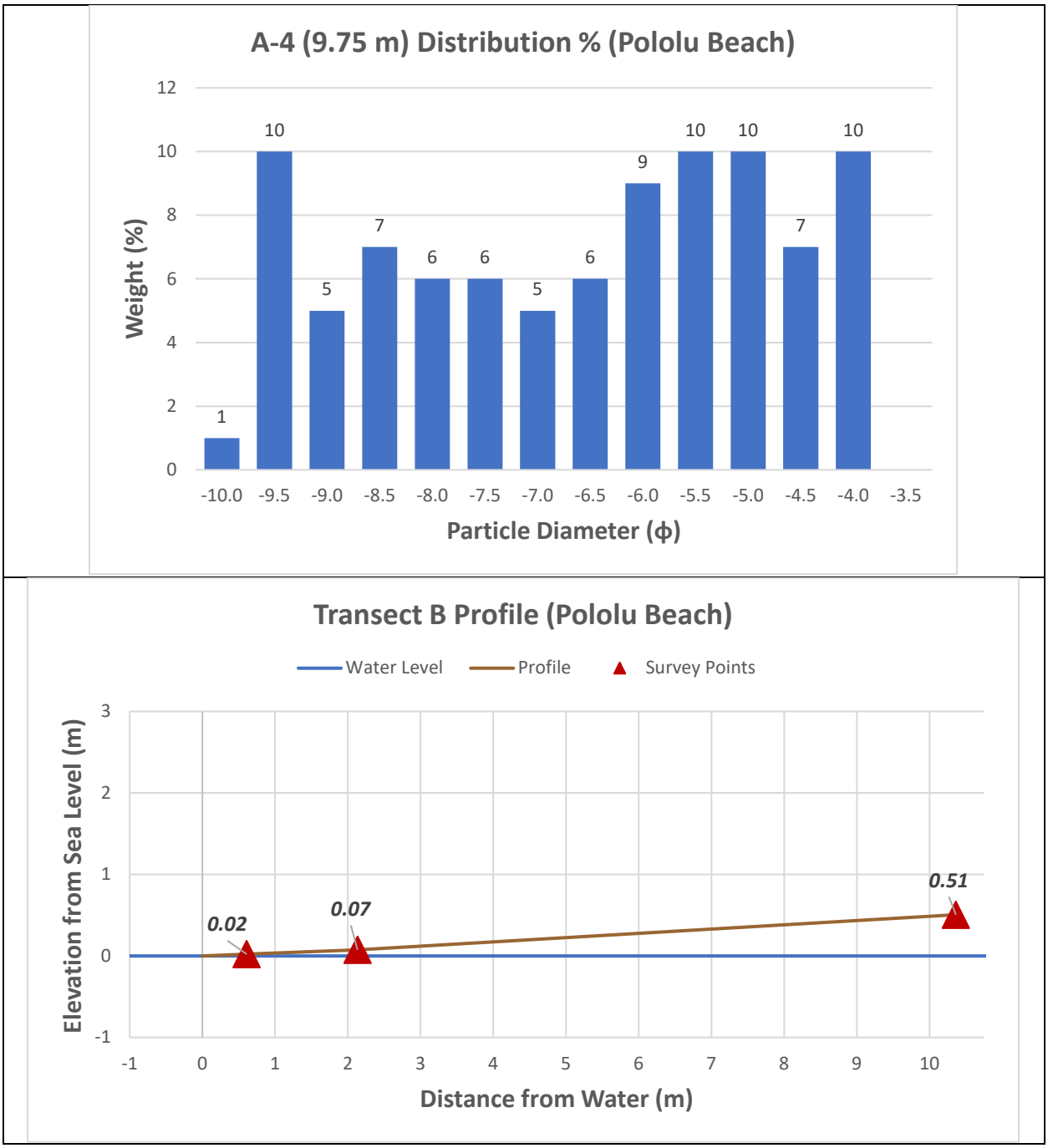
A-4 (9.75 m) Distribution % (Pololu Beach)
Weight (%)
Particle Diameter (ϕ)
12
10
8
6
4
2
0
1
10
5
7
6
6
5
6
9
10
10
10
7
-10.0
-9.5
-9.0
-8.5
-8.0
-7.5
-7.0
-6.5
-6.0
-5.5
-5.0
-4.5
-4.0
-3.5
Transect B Profile (Pololu Beach)
Water Level
Profile
Survey Points
Elevation from Sea Level (m)
Distance from Water (m)
3
2
1
0
-1
0.02
0.07
0.51
-1
0
1
2
3
4
5
6
7
8
9
10

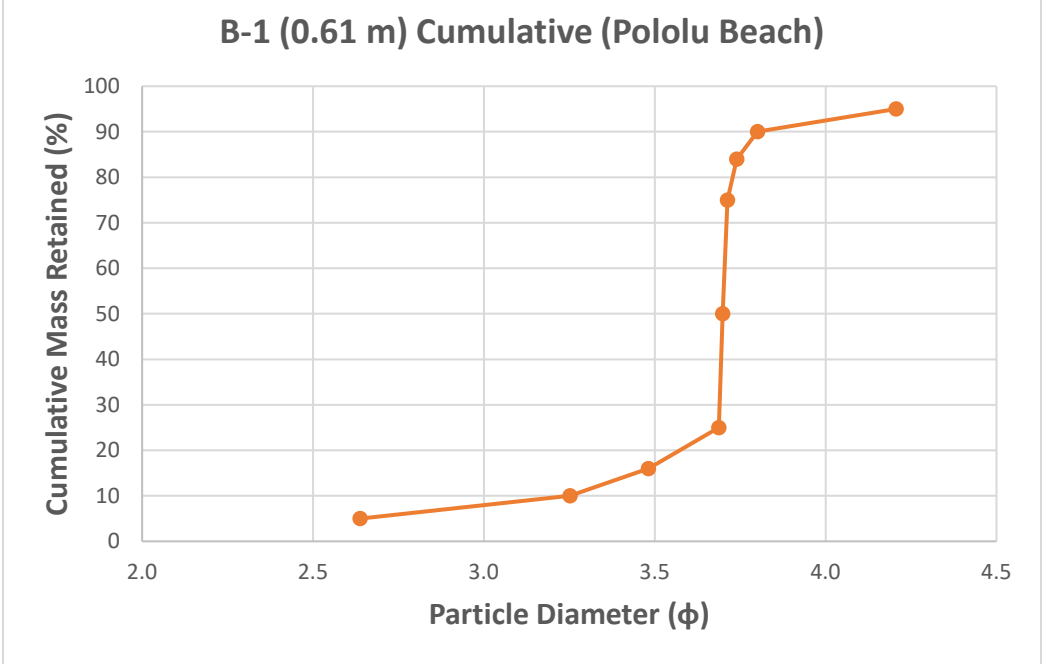
B-1 (0.61 m) Cumulative (Pololu Beach)
Cumulative Mass Retained (%)
100
90
80
70
60
50
40
30
20
10
0
2.0
2.5
3.0
3.5
4.0
4.5
Particle Diameter (ϕ)

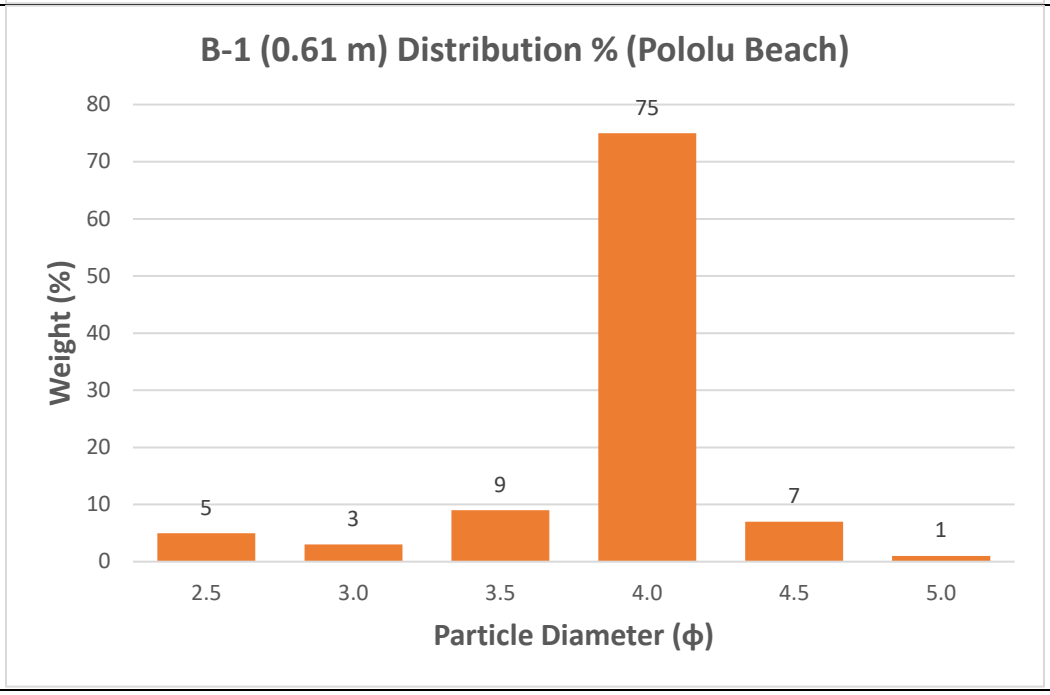
B-1 (0.61 m) Distribution % (Pololu Beach)
Weight (%)
80
70
60
50
40
30
20
10
0
5
3
9
75
7
1
2.5
3.0
3.5
4.0
4.5
5.0
Particle Diameter (ϕ)

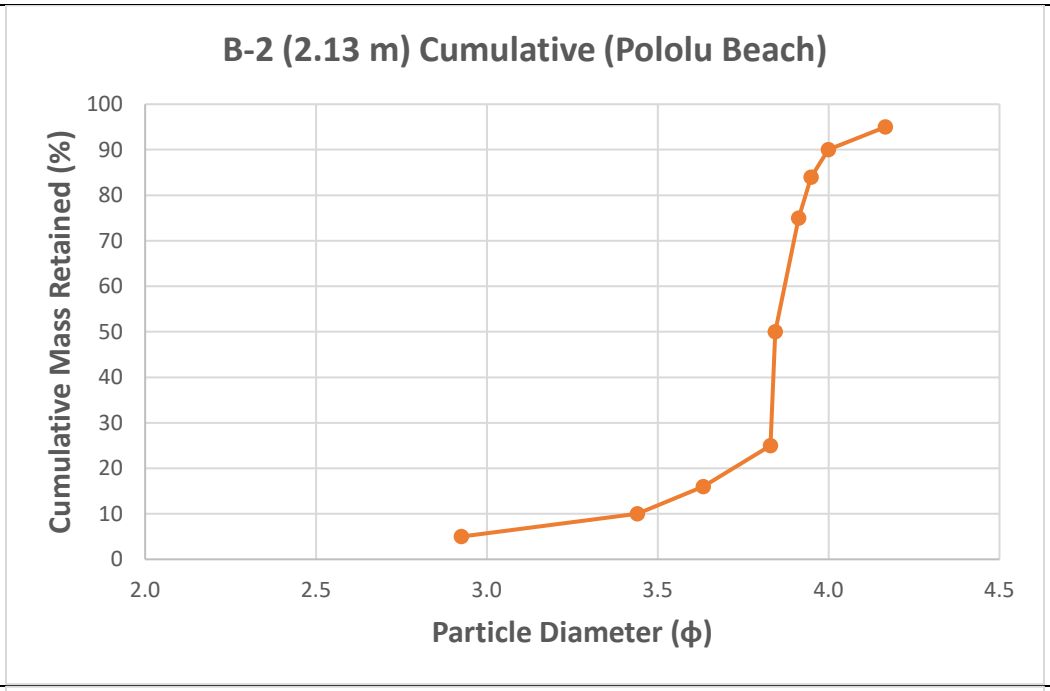
B-2 (2.13 m) Cumulative (Pololu Beach)
Cumulative Mass Retained (%)
100
90
80
70
60
50
40
30
20
10
0
2.0
2.5
3.0
3.5
4.0
4.5
Particle Diameter (ϕ)

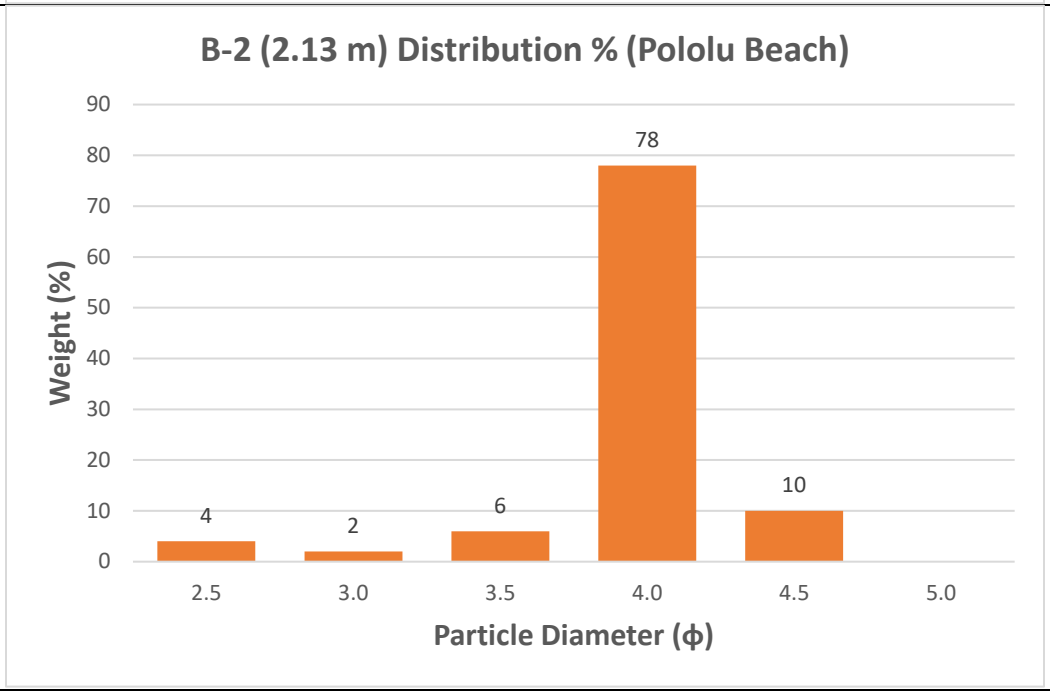
B-2 (2.13 m) Distribution % (Pololu Beach)
Weight (%)
90
80
70
60
50
40
30
20
10
0
4
2
6
78
10
2.5
3.0
3.5
4.0
4.5
5.0
Particle Diameter (ϕ)

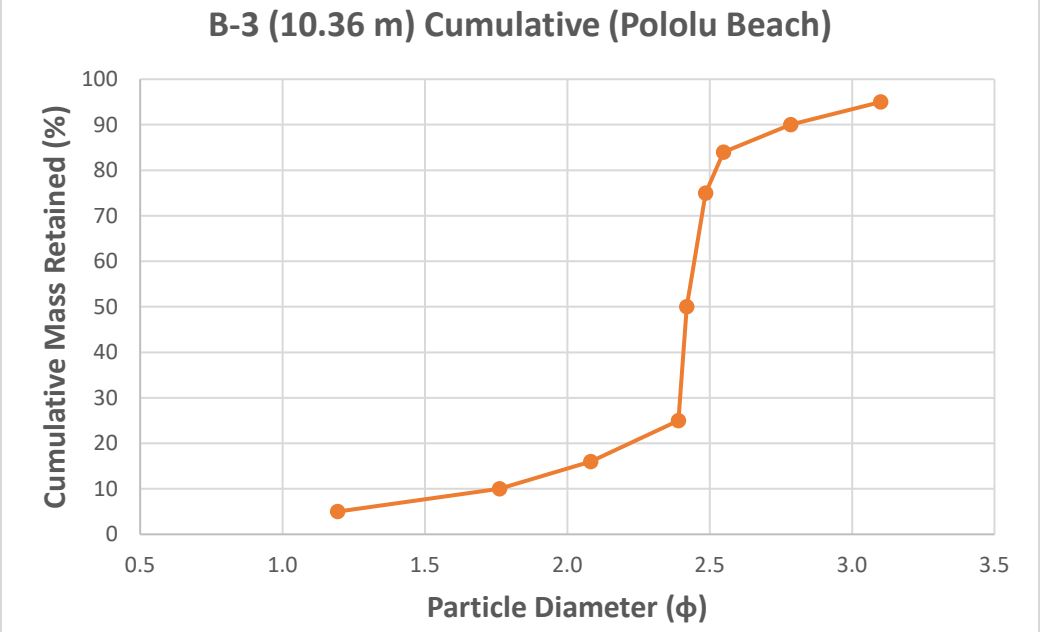
B-3 (10.36 m) Cumulative (Pololu Beach)
Cumulative Mass Retained (%)
100
90
80
70
60
50
40
30
20
10
0
0.5
1.0
1.5
2.0
2.5
3.0
3.5
Particle Diameter (ϕ)

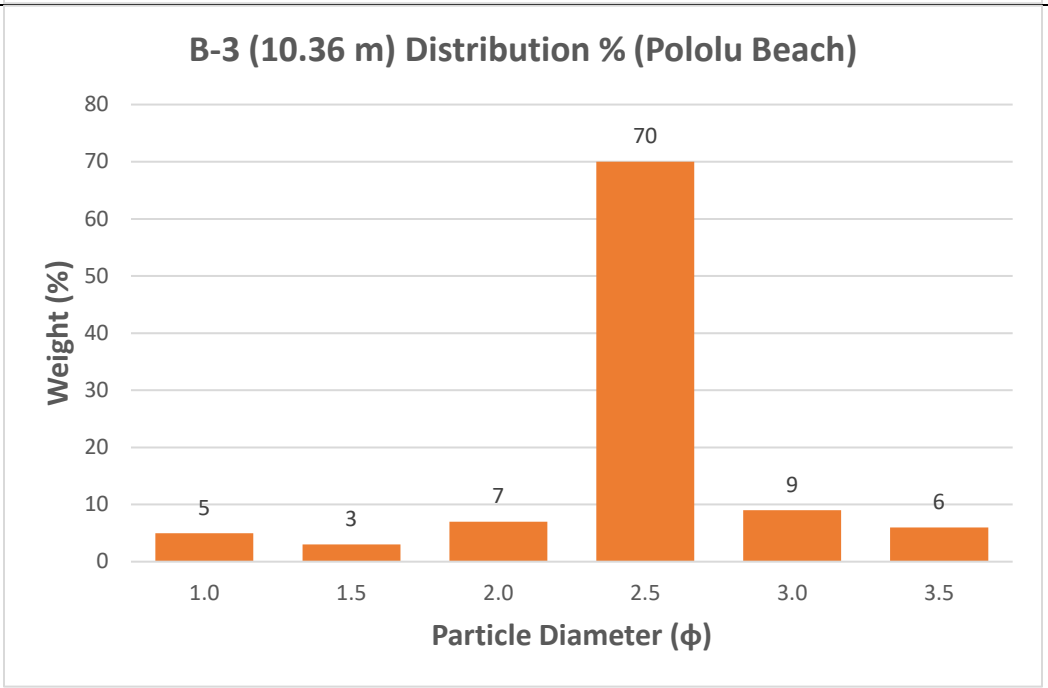
B-3 (10.36 m) Distribution % (Pololu Beach)
Weight (%)
80
70
60
50
40
30
20
10
0
5
3
7
70
9
6
1.0
1.5
2.0
2.5
3.0
3.5
Particle Diameter (ϕ)

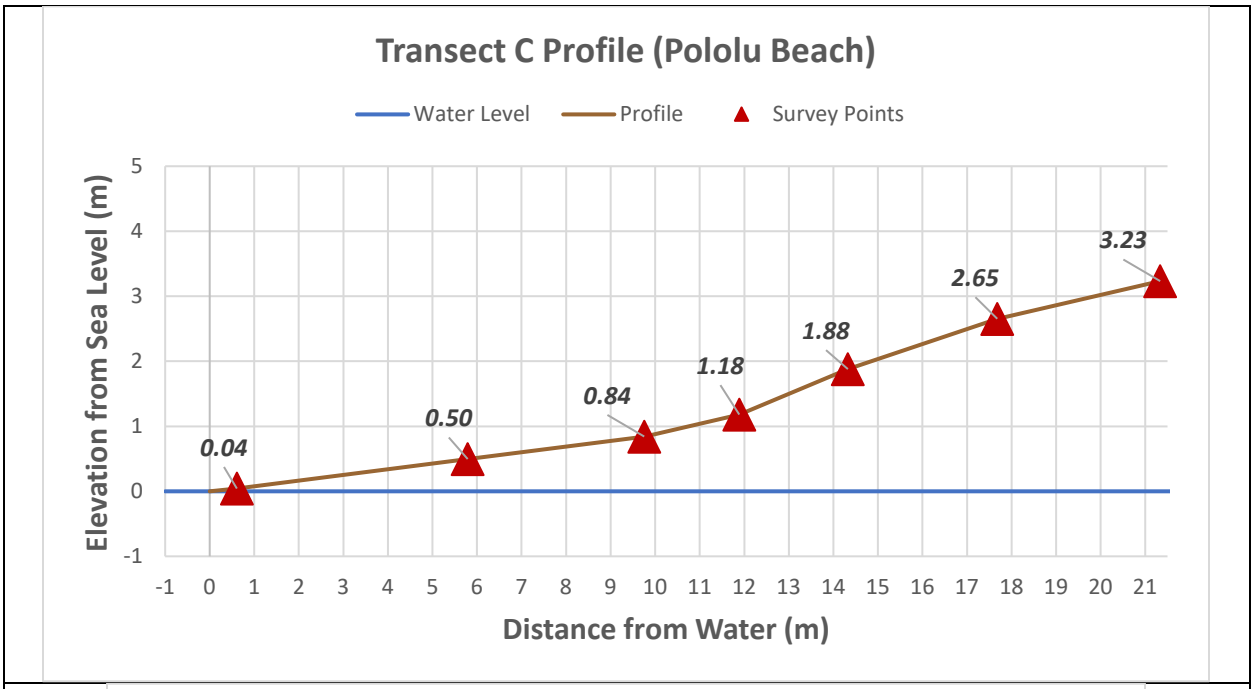
Transect C Profile (Pololu Beach)
Water Level
Profile
Survey Points
Elevation from Sea Level (m)
Distance from Water (m)
0.04
0.50
0.84
1.18
1.88
2.65
3.23

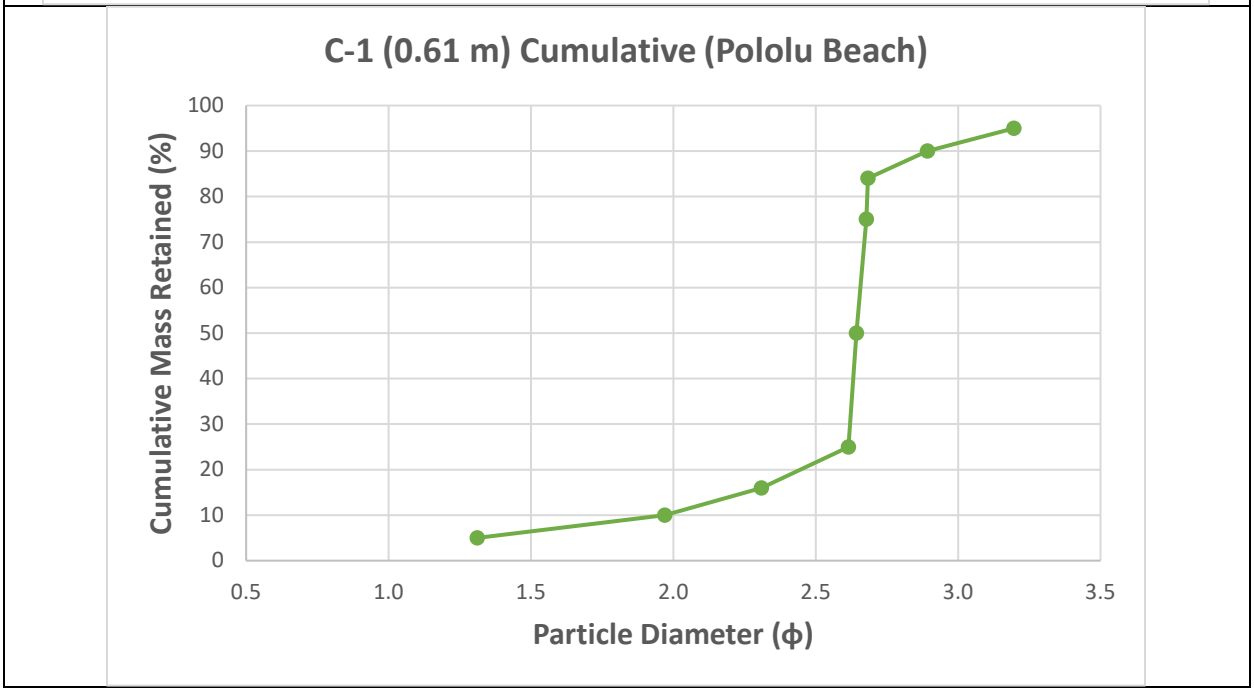
C-1 (0.61 m) Cumulative (Pololu Beach)
Cumulative Mass Retained (%)
Particle Diameter (ϕ)

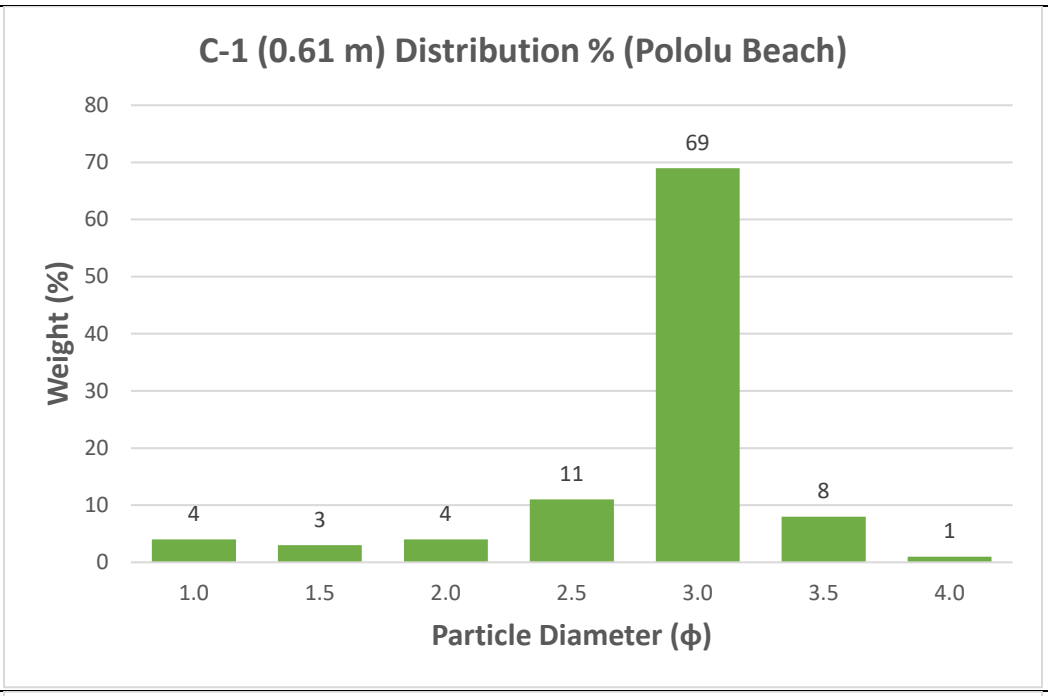
C-1 (0.61 m) Distribution % (Pololu Beach)
Weight (%)
80
70
60
50
40
30
20
10
0
4
3
4
11
69
8
1
1.0
1.5
2.0
2.5
3.0
3.5
4.0
Particle Diameter (ϕ)

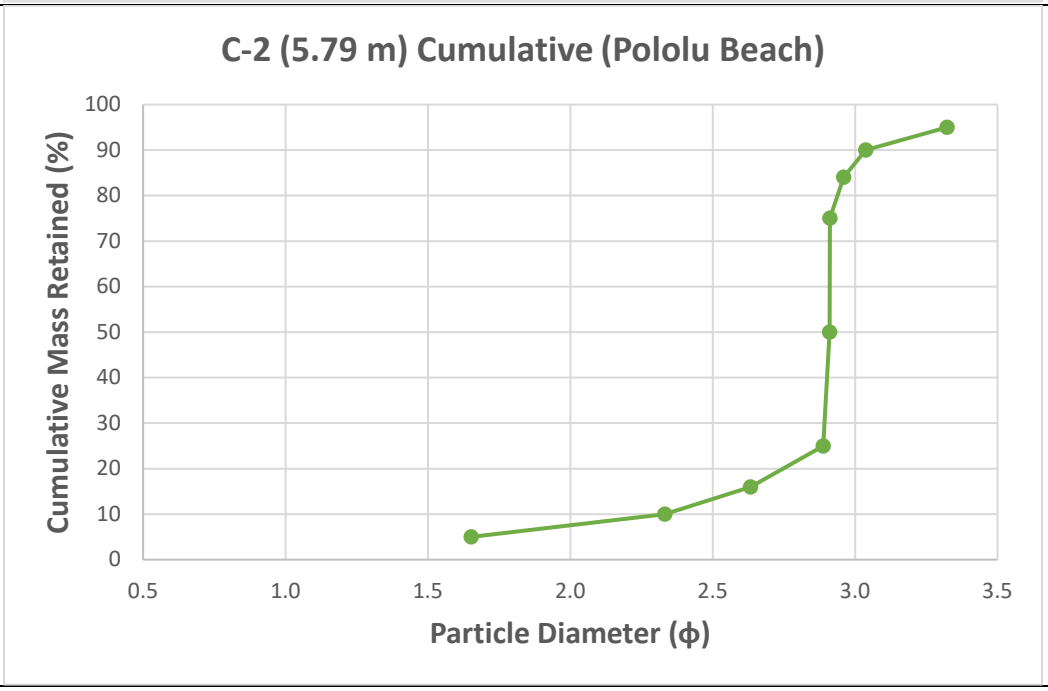
C-2 (5.79 m) Cumulative (Pololu Beach)
Cumulative Mass Retained (%)
100
90
80
70
60
50
40
30
20
10
0
0.5
1.0
1.5
2.0
2.5
3.0
3.5
Particle Diameter (ϕ)

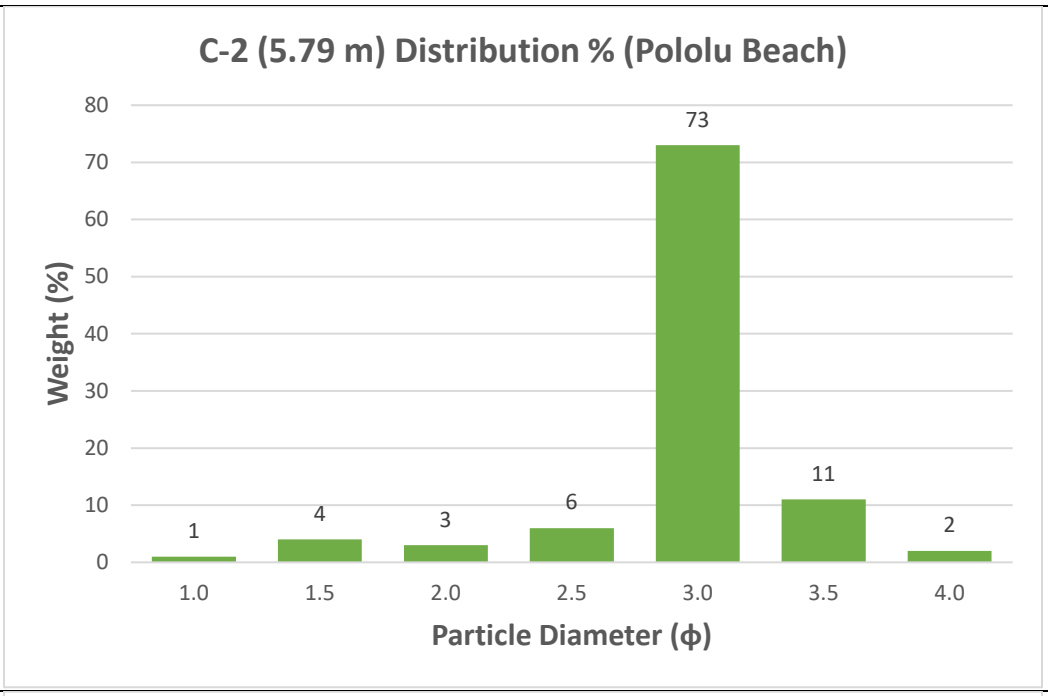
C-2 (5.79 m) Distribution % (Pololu Beach)
Weight (%)
80
70
60
50
40
30
20
10
0
1
4
3
6
73
11
2
1.0
1.5
2.0
2.5
3.0
3.5
4.0
Particle Diameter (ϕ)

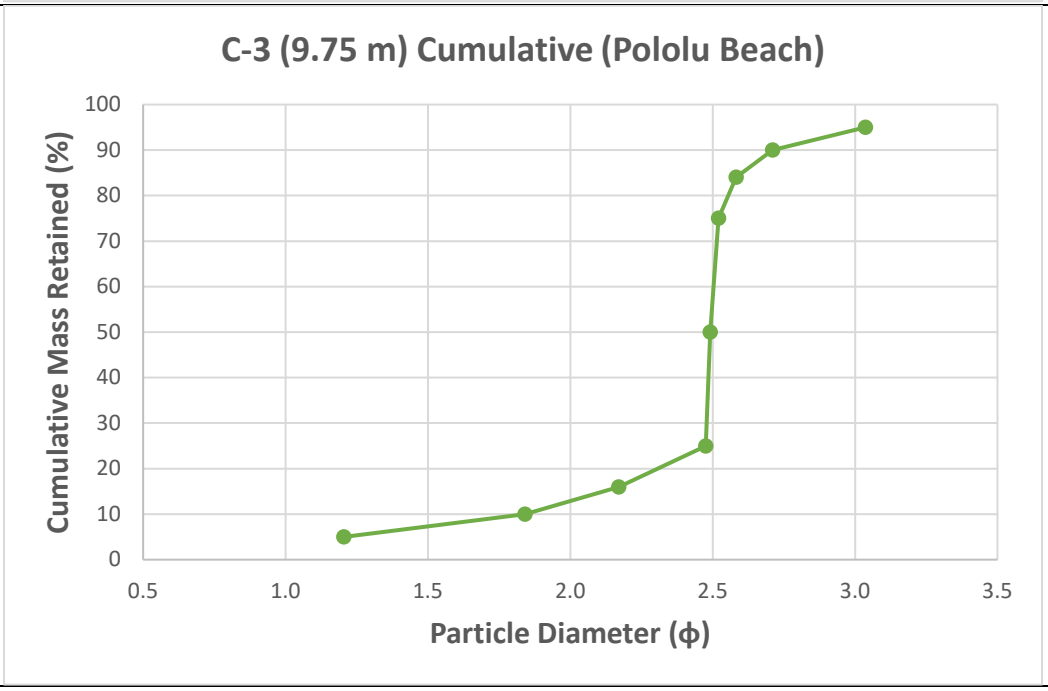
C-3 (9.75 m) Cumulative (Pololu Beach)
Cumulative Mass Retained (%)
100
90
80
70
60
50
40
30
20
10
0
0.5
1.0
1.5
2.0
2.5
3.0
3.5
Particle Diameter (ϕ)

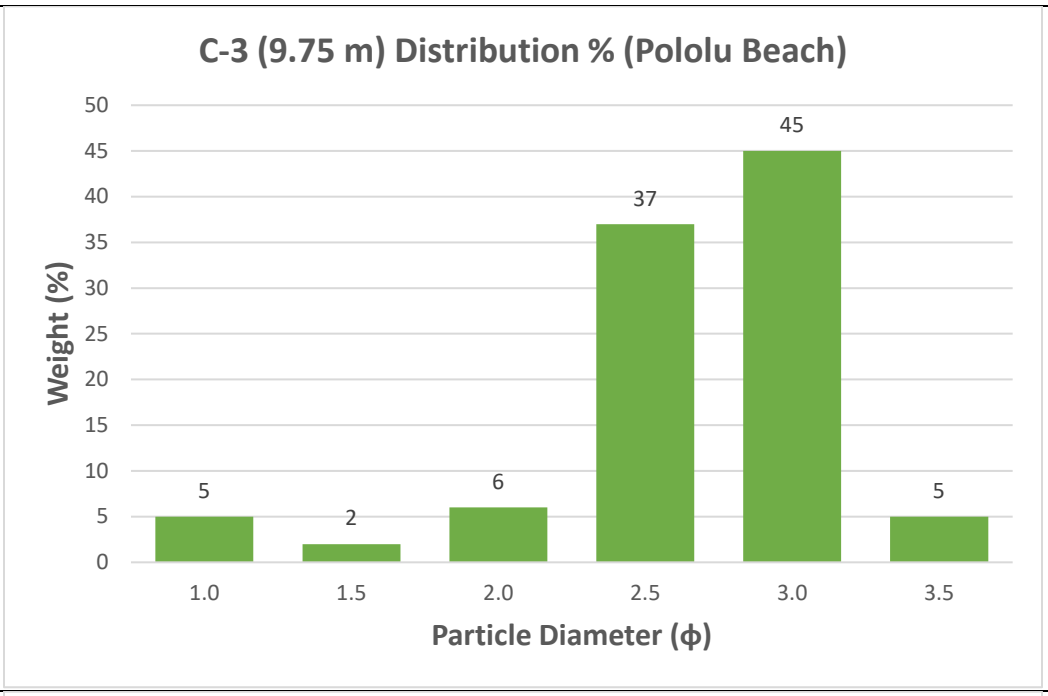
C-3 (9.75 m) Distribution % (Pololu Beach)
Weight (%)
50
45
40
35
30
25
20
15
10
5
0
5
2
6
37
45
5
1.0
1.5
2.0
2.5
3.0
3.5
Particle Diameter (ϕ)

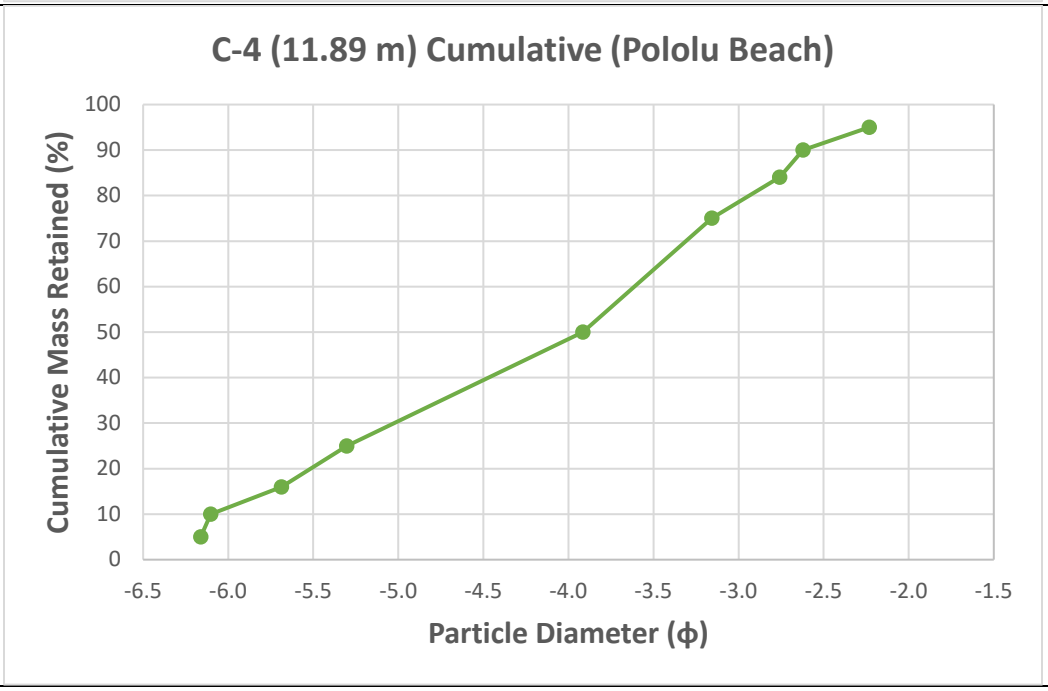
C-4 (11.89 m) Cumulative (Pololu Beach)
Cumulative Mass Retained (%)
100
90
80
70
60
50
40
30
20
10
0
-6.5
-6.0
-5.5
-5.0
-4.5
-4.0
-3.5
-3.0
-2.5
-2.0
-1.5
Particle Diameter (ϕ)

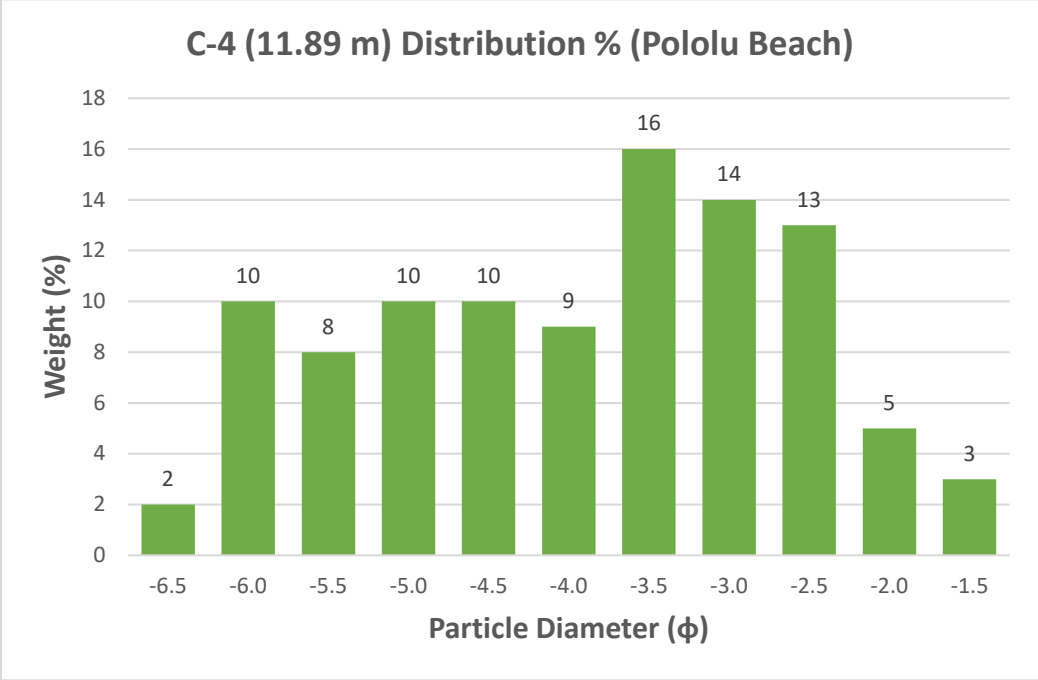
C-4 (11.89 m) Distribution % (Pololu Beach)
Weight (%)
18
16
14
12
10
8
6
4
2
0
2
10
8
10
10
9
16
14
13
5
3
-6.5
-6.0
-5.5
-5.0
-4.5
-4.0
-3.5
-3.0
-2.5
-2.0
-1.5
Particle Diameter (ϕ)

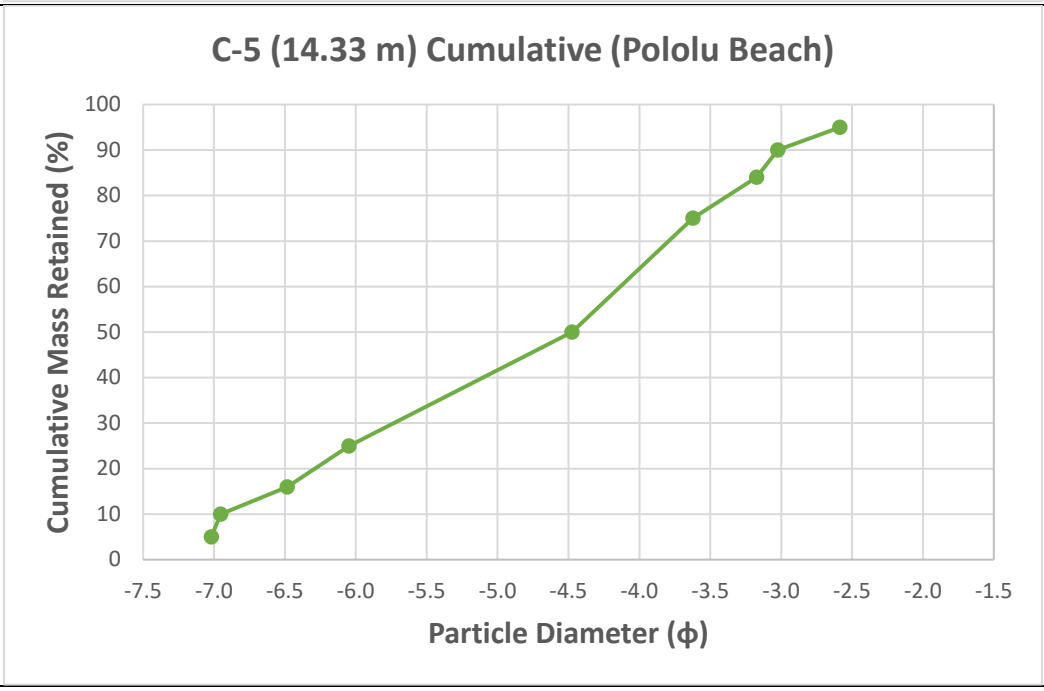
C-5 (14.33 m) Cumulative (Pololu Beach)
Cumulative Mass Retained (%)
100
90
80
70
60
50
40
30
20
10
0
-7.5
-7.0
-6.5
-6.0
-5.5
-5.0
-4.5
-4.0
-3.5
-3.0
-2.5
-2.0
-1.5
Particle Diameter (ϕ)

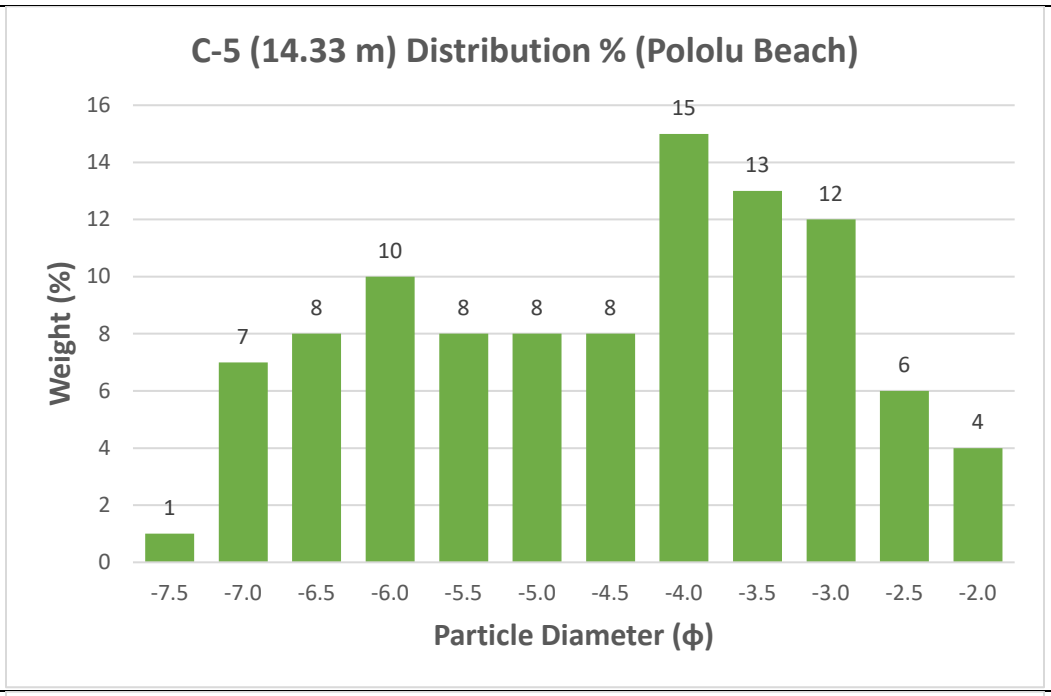
C-5 (14.33 m) Distribution % (Pololu Beach)
Weight (%)
16
14
12
10
8
6
4
2
0
1
7
8
10
8
8
8
15
13
12
6
4
-7.5
-7.0
-6.5
-6.0
-5.5
-5.0
-4.5
-4.0
-3.5
-3.0
-2.5
-2.0
Particle Diameter (ϕ)

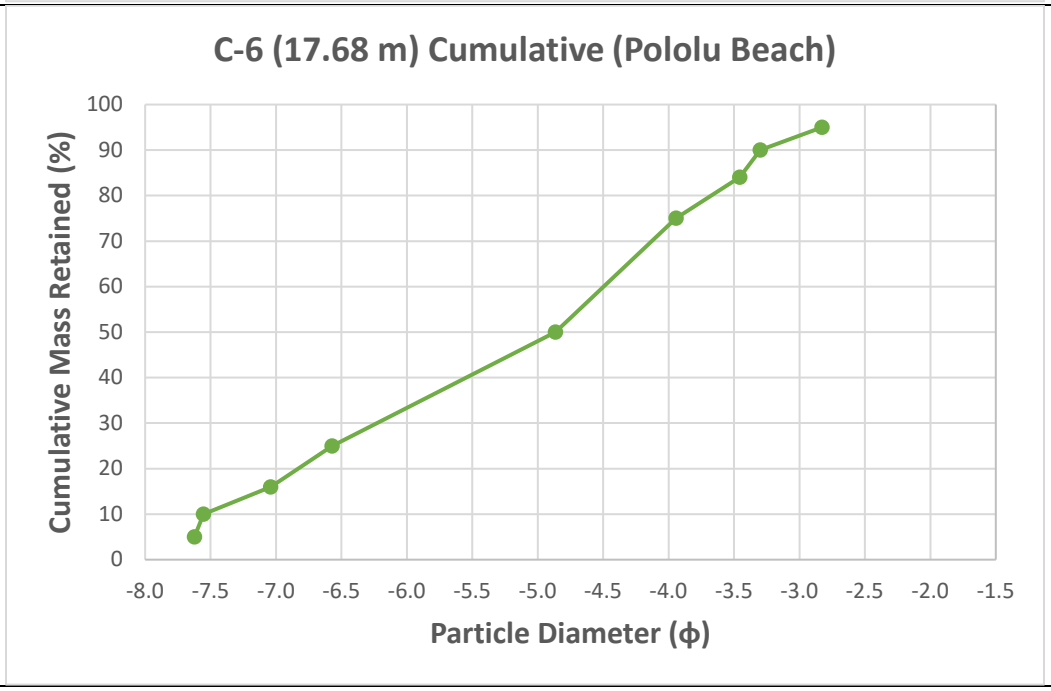
C-6 (17.68 m) Cumulative (Pololu Beach)
Cumulative Mass Retained (%)
100
90
80
70
60
50
40
30
20
10
0
-8.0
-7.5
-7.0
-6.5
-6.0
-5.5
-5.0
-4.5
-4.0
-3.5
-3.0
-2.5
-2.0
-1.5
Particle Diameter (ϕ)

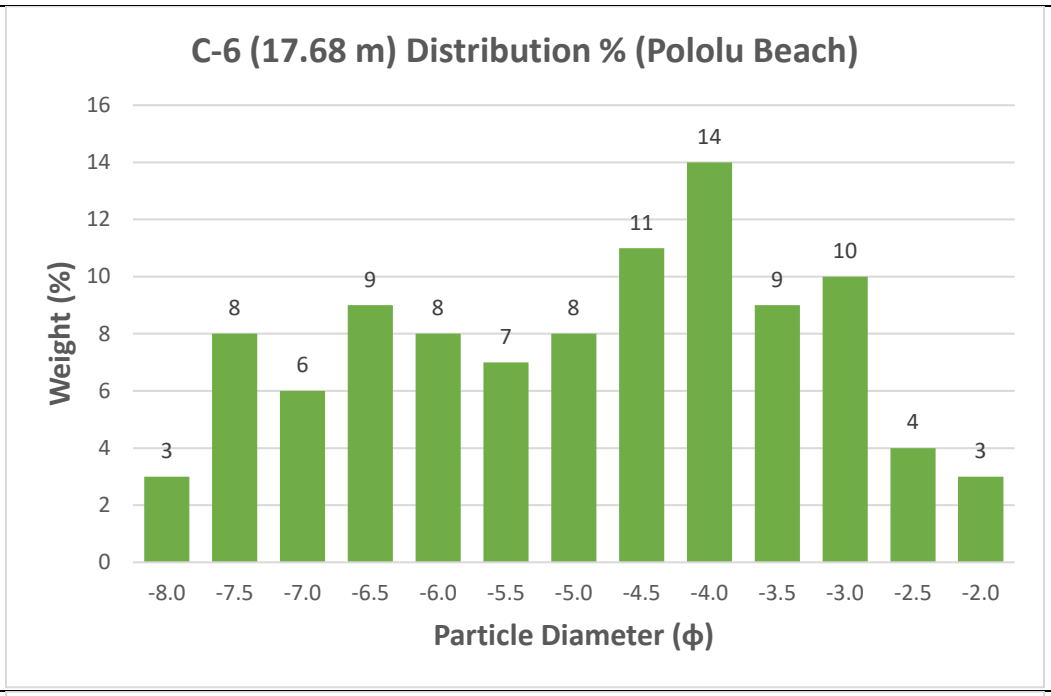
C-6 (17.68 m) Distribution % (Pololu Beach)
Weight (%)
16
14
12
10
8
6
4
2
0
3
8
6
9
8
7
8
11
14
9
10
4
3
-8.0
-7.5
-7.0
-6.5
-6.0
-5.5
-5.0
-4.5
-4.0
-3.5
-3.0
-2.5
-2.0
Particle Diameter (ϕ)

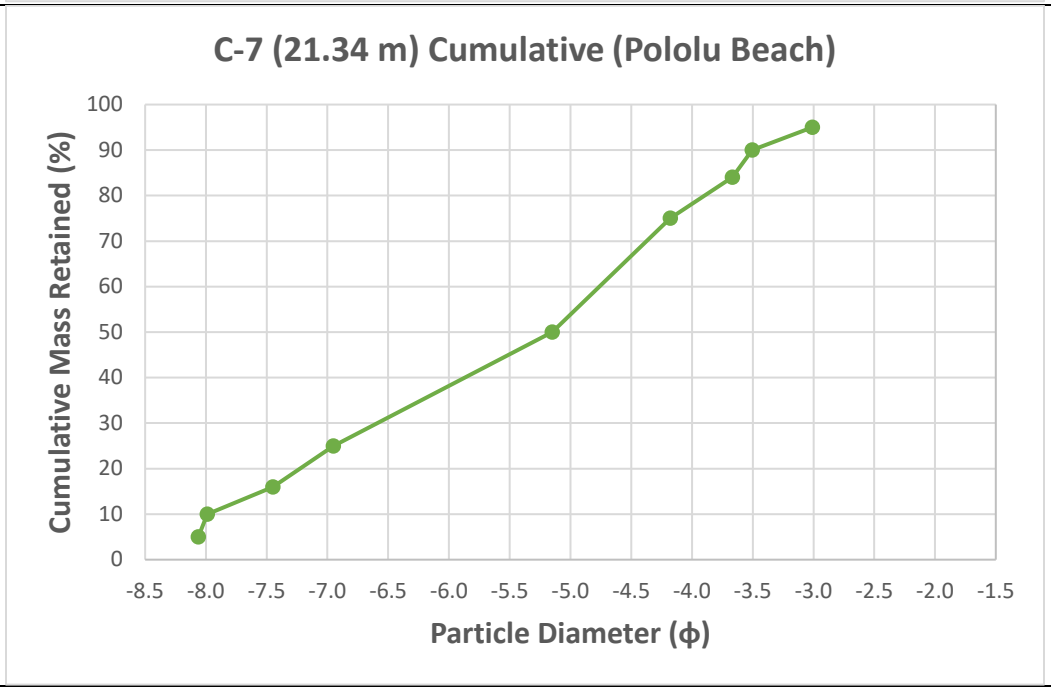
C-7 (21.34 m) Cumulative (Pololu Beach)
Cumulative Mass Retained (%)
100
90
80
70
60
50
40
30
20
10
0
-8.5
-8.0
-7.5
-7.0
-6.5
-6.0
-5.5
-5.0
-4.5
-4.0
-3.5
-3.0
-2.5
-2.0
-1.5
Particle Diameter (ϕ)

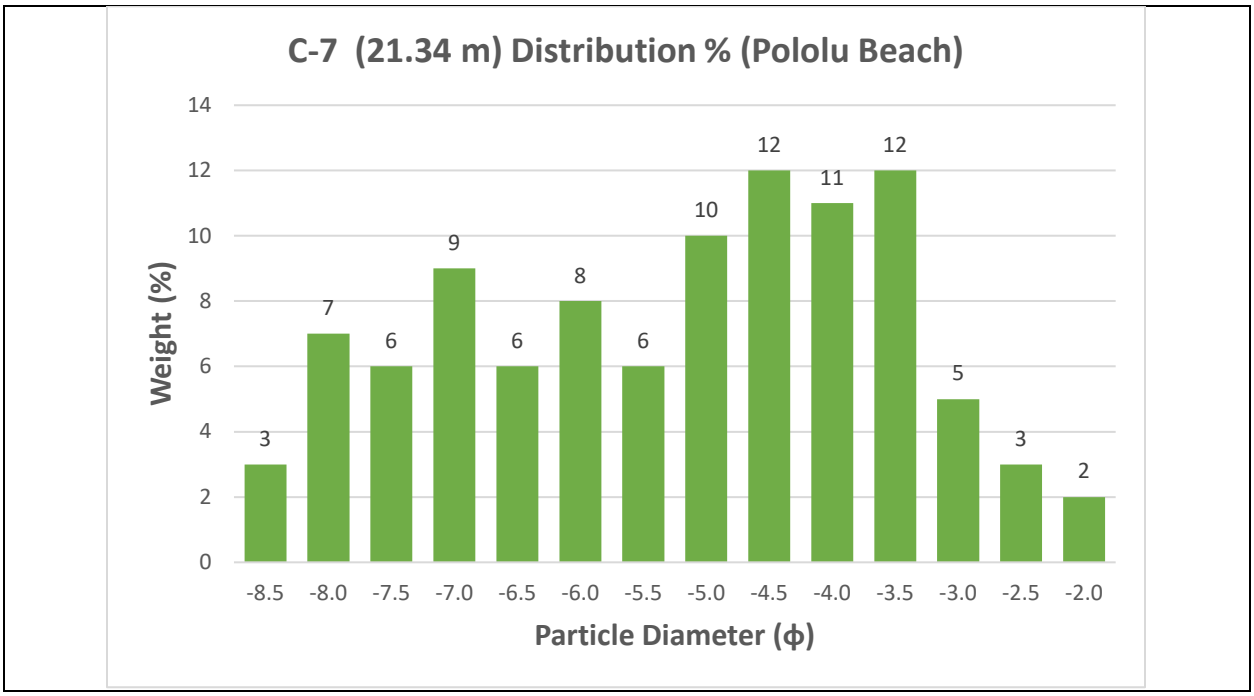
C-7 (21.34 m) Distribution % (Pololu Beach)
Weight (%)
0
2
4
6
8
10
12
14
3
7
6
9
6
8
6
10
12
11
12
5
3
2
-8.5
-8.0
-7.5
-7.0
-6.5
-6.0
-5.5
-5.0
-4.5
-4.0
-3.5
-3.0
-2.5
-2.0
Particle Diameter (ϕ)

Appendix E – Measured and Predicted mm and ϕ for the standards.

SAMPLE NAME	%	Measured		With "x" adjusted to 50th percentile		"x"
		MEASURED mm	MEASURED ϕ	PREDICTED mm	PREDICTED ϕ	
Browns Cay Bahamas	10	0.4063	1.299	0.580592177	0.784	-0.2
	50	0.2874	1.799	0.284181974	1.815	
	90	0.2016	2.31	0.126718109	2.980	
Santa Lucia	10	0.3744	1.471	0.559906532	0.837	-1.9
	50	0.221	2.178	0.222684367	2.167	
	90	0.1382	2.855	0.093047575	3.426	
Barbados	10	0.3452	1.535	0.556303076	0.846	-1.5
	50	0.2238	2.16	0.226423995	2.143	
	90	0.1451	2.784	0.105602929	3.243	
Yallahs	10	0.866	0.208	1.08499662	-0.118	-1.0
	50	0.4039	1.308	0.391338098	1.354	
	90	0.2296	2.123	0.140560656	2.831	
Galveston	10	0.2129	2.232	0.276949191	1.852	-3.0
	50	0.1395	2.842	0.13822894	2.855	
	90	0.09861	3.342	0.038341298	4.705	
San Juan	10	0.6327	0.66	0.731337706	0.451	-0.6
	50	0.3514	1.509	0.351420422	1.509	
	90	0.2214	2.175	0.140884692	2.827	
Mahaiula	10	3.0145	-1.592	1.296275467	-0.374	4.5
	50	1.3641	-0.448	1.157977995	-0.212	
	90	0.5886	0.765	0.858087149	0.221	
Nassau	10	0.6793	0.558	0.834950579	0.260	-0.6
	50	0.3721	1.426	0.368791056	1.439	
	90	0.2588	1.95	0.143022996	2.806	
Los Cabos	10	1.3134	-0.393	1.12556327	-0.171	0.6
	50	0.6955	0.524	0.694351234	0.526	
	90	0.3944	1.342	0.285079738	1.811	
Dry Tortugas	10	0.7889	0.342	1.116866656	-0.159	-0.5
	50	0.4196	1.253	0.421760711	1.246	
	90	0.281	1.831	0.148646309	2.750	
Hua Hin	10	0.4428	1.175	0.765433981	0.386	-1.4
	50	0.2337	2.098	0.243167086	2.040	
	90	0.1463	2.773	0.106849194	3.226	
Eritrea	10	0.4586	1.125	0.699839589	0.515	-1.1
	50	0.2771	1.851	0.276043618	1.857	
	90	0.1649	2.6	0.119713823	3.062	
Punaluu	10	0.9315	0.102	1.10746433	-0.147	0.8

	50	0.6519	0.617	0.649502009	0.623	
	90	0.4653	1.104	0.270146272	1.888	
Papakulea	10	0.4891	1.032	0.783400738	0.352	-0.7
	50	0.34	1.556	0.334395519	1.580	
	90	0.2181	2.197	0.12983663	2.945	
Algeria	10	0.1592	2.651	0.15233061	2.715	-6.3
	50	0.09289	3.428	0.092536815	3.434	
	90	0.05199	4.266	0.018507363	5.756	
White Sands	10	0.4631	1.111	0.85525436	0.226	-1.0
	50	0.3146	1.668	0.320526342	1.641	
	90	0.194	2.366	0.1235513	3.017	
Cancun	10	0.4693	1.091	0.794450742	0.332	-0.8
	50	0.3102	1.689	0.319382422	1.647	
	90	0.2124	2.235	0.132351584	2.918	
Bali	10	0.6725	0.572	0.816791453	0.292	-0.8
	50	0.3484	1.521	0.35300167	1.502	
	90	0.2191	2.19	0.139528531	2.841	
Newfoundland	10	1.5805	-0.66	1.209766467	-0.275	0.0
	50	0.6647	0.589	0.662218394	0.595	
	90	0.3992	1.325	0.235175991	2.088	
Isla Baru	10	0.2875	1.798	0.441054924	1.181	-2.0
	50	0.1777	2.492	0.178344268	2.487	
	90	0.1266	2.982	0.064919492	3.945	
KC - Punaluu	10	1.5656	-0.647	1.247536648	-0.319	2.2
	50	0.9544	0.067	0.955439544	0.066	
	90	0.5162	0.954	0.532401896	0.909	
KC - Mahai'ula	10	2.0142	-1.01	1.218365133	-0.285	6.0
	50	1.3191	-0.4	1.116923935	-0.160	
	90	0.6709	0.576	0.882451182	0.180	
KC - Spencer Beach	10	0.6508	0.602	0.975687539	0.036	-0.2
	50	0.466	1.102	0.470474136	1.088	
	90	0.3631	1.462	0.181906666	2.459	
KC - Mauna Kea	10	0.2803	1.835	0.435601816	1.199	-2.0
	50	0.1821	2.457	0.18937261	2.401	
	90	0.1329	2.912	0.081540601	3.616	
KC - Green Sand	10	0.624	0.68	0.908130151	0.139	-1.0
	50	0.347	1.527	0.343658269	1.541	
	90	0.1732	2.53	0.127293079	2.974	
KC - Pololu	10	0.2816	1.828	0.533093066	0.908	-1.5
	50	0.2032	2.299	0.207995688	2.265	
	90	0.1393	2.844	0.084055282	3.573	